NASA Contractor Report 159249

INTEGRATED APPLICATION OF ACTIVE CONTROLS (IAAC) TECHNOLOGY TO AN ADVANCED SUBSONIC TRANSPORT PROJECT– INITIAL ACT CONFIGURATION DESIGN STUDY

FINAL REPORT

BOEING COMMERCIAL AIRPLANE COMPANY
P.O. BOX 3707, SEATTLE, WASHINGTON 98124

CONTRACTS NAS1-14742 AND NAS1-15325
JULY 1980

NASA
National Aeronautics and Space Administration

Langley Research Center
Hampton Virginia 23665

FOREWORD

This document constitutes the final report of the Initial ACT Configuration Design that was begun under Contract NAS1-14742 and completed under Contract NAS1-15325.

NASA Technical Monitors for this subtask were D. B. Middleton and R. V. Hood of the Energy Efficient Transport Project Office at Langley Research Center.

The work was accomplished within the Preliminary Design Department of the Vice President-Engineering organization of the Boeing Commercial Airplane Company. Key contractor personnel who contributed were:

G. W. Hanks	Program Manager
H. A. Shomber	IAAC Project Manager
H. A. Dethman	Design Integration
L. B. Gratzer	Technology Integration
C. C. Flora	Task Manager (Initial ACT)
R. L. Sullivan	Aerodynamic Technology
G. E. Seidel	Configurations
A. Maeshiro	Flight Control Technology
C. E. Roth	Flight Control Technology
E. Heineman	Structures Design
J. F. Bueno-Varela	Structures Technology
M. T. McIntosh	Structures Technology
M. J. Omoth	Systems Technology
J. D. Brown	Weight Technology

During this study, principal measurements and calculations were in customary units and were converted to Standard International units for this document. The Initial ACT Configuration model number (768-103) appears in the lower right-hand corner of each illustration for ease in identification.

CONTENTS

CONTENTS (Continued)

CONTENTS (Continued)

CONTENTS (Concluded)

FIGURES

FIGURES (Continued)

PAGE

FIGURES (Continued)

PAGE

FIGURES (Continued)

PAGE

FIGURES (Continued)

PAGE

FIGURES (Continued)

PAGE

FIGURES (Continued)

PAGE

FIGURES (Concluded)

TABLES

TABLES (Concluded)

1.0 SUMMARY

1 0 SUMMARY

Page

1.0 SUMMARY

This report documents the first active controls configuration task of the "Integrated Application of Active Controls (IAAC) Technology to Advanced Subsonic Transports" Project. The performance and economic benefits of a constrained application of Active Controls Technology (ACT) are identified, and the approach to airplane design is established for subsequent steps leading to the development of a less constrained Final ACT Configuration. The active controls configurations are measured against the Conventional Baseline Configuration, a state-of-the-art transport selected and defined in a previous task, to determine whether the performance and economic changes resulting from ACT merit proceeding with the project. The technology established by the Conventional Baseline Configuration was held constant except for the addition of ACT. The wing, with the same planform, was moved forward on the Initial ACT Configuration to move the loading range aft relative to the wing mean aerodynamic chord. Wing trailing-edge surfaces and surface controls also were reconfigured for load alleviation and structural stabilization.

The pitch-augmented stability active controls function allowed the cruise center of gravity to be moved aft 10% and horizontal tail size to be reduced 45%. The fuel system and tank arrangement was revised to preclude flutter, yet the overall wing structure became lighter because of wing-load alleviation. The net effect of these changes was a 930 kg (2050 lb) reduction in airplane operational empty weight (OEW) and a 3.6% improvement in cruise aerodynamic efficiency. All required ACT functions were assumed available. The principal characteristics of the resulting airplane are shown in Figure 1.

The Initial ACT Configuration was not resized to the baseline mission. Consequently, there was a 13% increase in range at the same takeoff gross weight and payload as the Conventional Baseline Configuration. Adjusted to the 3590 km (1938 nmi) Baseline mission range, this becomes approximately a 6% reduction in block fuel and a 15.7% incremental return on investment (ΔROI); i.e., the incremental capital costs (based on factored cost data) for design, development, and installation of the equipment and configuration differences between the Initial ACT and Baseline Configurations. This 15.7% ΔROI corresponds to a \$0.1057/ℓ (\$0.40/gal) fuel cost, in 1978 dollars. Much larger return on investment may be expected if historical fuel inflation rates continue.

Configuration	
Passengers	197 mixed class, 207 all tourist
Containers	22 LD-2 or 11 LD 3
Engines	2 (CF6 6D2)
Design mission	
Cruise Mach	0 8
Range	4061 km (2193 nmi)
Takeoff field length	2118m (6950 ft)
Approach speed	68 6 m/s (133 4 kn)
Noise	FAR 36, Stage 3
Flying qualities	Current commercial transport practice
Airplane technology	Current commercial transport practice (aerodynamics, structural, propulsion, etc with the addition of active control functions)
Active control functions	
Pitch augmented stability	(PAS)
Maneuver load alleviation	(MLA) } Wing load alleviation (WLA)
Gust load alleviation	(GLA) } Wing load alleviation (WLA)
Flutter mode control	(FMC)
Angle-of-attack limiting	(AAL)

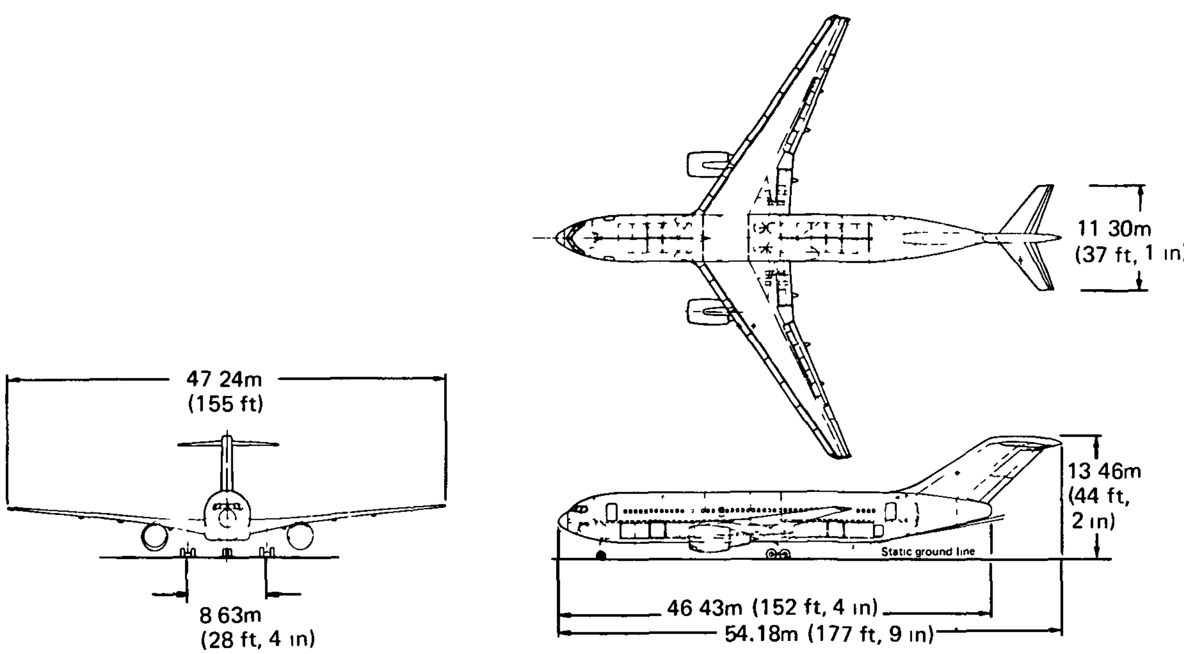

Figure 1. Initial ACT Configuration

The encouraging results of the Initial ACT Configuration design task clearly indicate that the IAAC Project should proceed to determine what further benefits may be achieved through wing planform changes and advanced ACT systems.

2.0 INTRODUCTION

2.0 INTRODUCTION

Page

2.0 INTRODUCTION

The principal objective of one of the projects under the NASA Energy Efficient Transport (EET) Program is to assess the benefits associated with a major application of Active Controls Technology (ACT) to the design of a modern, subsonic, commercial transport. This project, initially entitled "Maximum Benefit of ACT," is entitled "Integrated Application of Active Controls (IAAC) Technology to an Advanced Subsonic Transport." The IAAC Project has three major elements: the design of an airplane configuration and a related current ACT system; an examination of advanced technology implementation of ACT functions; and the testing and evaluation of selected elements of the proposed ACT system. A detailed discussion of the IAAC Project Plan is presented in Reference 1.

Figure 2 shows the makeup of the Configuration/ACT System Design Task. After the selection of a Conventional Baseline Configuration, described in Reference 2, the configuration design activity proceeded to the Initial ACT Configuration, which is a constrained application of ACT. The development of this Initial ACT Configuration, which is discussed in this document, was initiated under Contract NAS1-14742 and completed under Contract NAS1-15325.

2.1 OBJECTIVES

The objectives of the Initial ACT Configuration development task were to:

- Develop an airplane reconfigured to benefit from ACT functions, but constrained in external configuration for direct application of the Baseline aerodynamic data base

- Assess the performance and economic benefits of this constrained application of ACT

- Refine the analytical methodology and interdisciplinary relationships necessary for the development of transport airplanes configured with ACT

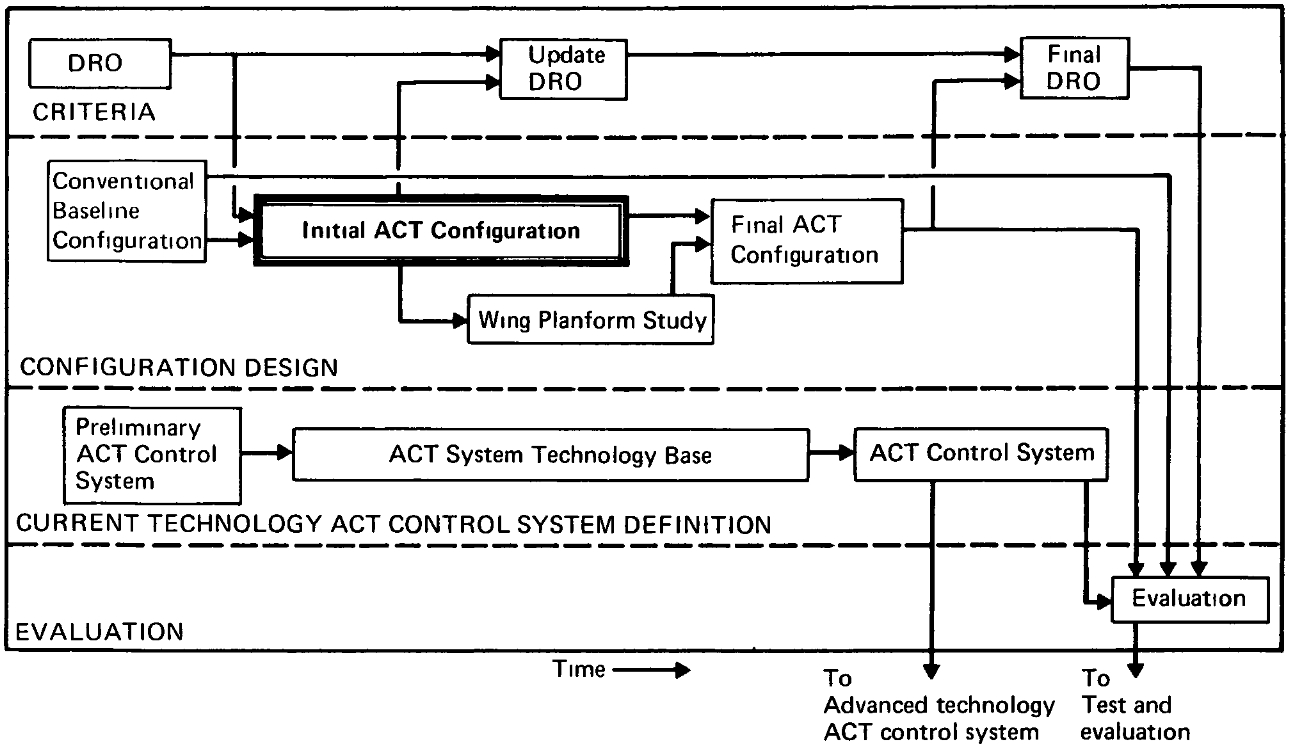

Figure 2. Configuration/ACT System Design and Evaluation Element

2.2 APPROACH

This study began with an airplane configuration for which Boeing had already accumulated substantial preliminary design background. The choice, data collection, and validation of this starting point constituted the Conventional Baseline Configuration Study. The Initial ACT Configuration evolved from the Baseline Configuration with the constraints that both the wing planform and the airplane size (i.e., the maximum takeoff weight) be unchanged. The range increase at constant payload was taken as the measure of improved performance. An advantage of this approach was that a reasonably thorough analysis could be made without reestimating aerodynamic characteristics for wing planform changes or detailed resizing to the design mission. Within these constraints, pitch-augmented stability and angle-of-attack limiting were used to rebalance the airplane and reduce the horizontal tail size to the minimum required for controllability. Wing trailing-edge surfaces and surface controls were reconfigured for load-alleviation and structural-stabilization ACT functions, which allowed structural weight to be removed from the wing. The reconfiguration assumed that all required ACT functions would be available and could be mechanized.

This assumption, which underlies the configuration development reported herein, cannot be accepted uncritically. The increased dependence of the airplane on active systems for controlled flight and for structural integrity demands careful consideration of the system's suitability, reliability, and interrelationship with the flight crew. A preliminary development effort in this area is the subject of the ACT System Technology Base task (fig. 2), which will be detailed in a separate report.

Previous studies (ref 3) have shown that wing planform changes, such as increased aspect ratio and reduced sweep, increase the aerodynamic efficiency. In conventional designs, this is counteracted by the effect of increased structural weight; however, ACT load alleviation and flutter stabilization should reduce the structural weight penalty associated with these planform changes. The next phase planned for the IAAC Project, therefore, is the Wing Planform Study.

2.3 SCOPE OF DOCUMENT

This document contains five major sections: 4.0 through 8.0. As described in Section 4.4 and illustrated in Figure 3, the design was derived from the Conventional Baseline Configuration.

Section 5.0 includes drawings showing the major components and payload capabilities of the Initial ACT Configuration. The illustrations comprise a general arrangement, inboard profile, body cross section, seating arrangement, cargo capability of the lower and upper lobes, and principal characteristics. Mission rules, speed schedules, performance and noise characteristics, design weight, and center-of-gravity management also are shown.

Detailed data on the design of the airframe, propulsion, and flight control systems constitutes Section 6.0. The major structures, components, and systems that will affect or be affected by an active controls system are described.

	Baseline Configuration	Initial ACT Configuration
Passengers		
Mixed class	197	
All tourist	207	
Containers		
LD 2 or LD 3	22 or 11	
Engines	(2) CF6 6D2	
Wing area m^2 (ft^2)	256 3[a] (2759)	
Maximum takeoff gross weight kg (lb)	122 470 (270 000)	
Operating empty weight kg (lb)	78 300 (172 610)	77 370 (170 560)
Design range km (nmi)	3590 (1938)	**4061 (2193)**
Takeoff field length m (ft)	2210 (7250)	2118 (6950)
Cruise Mach	0 8	

[a]Trapezoid geometry quoted, aero reference area—275 1 m^2 (2961 ft^2)

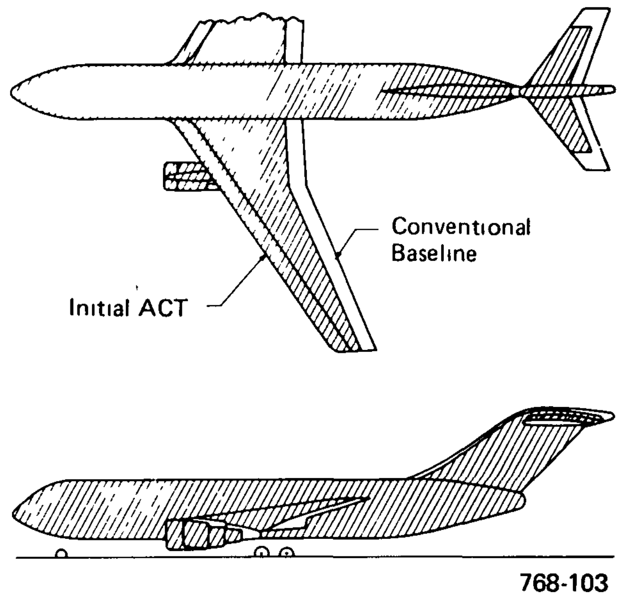

Figure 3. Initial ACT and Conventional Baseline Configuration Comparison

Section 7.0 describes a unified and substantially detailed program of structural, handling qualities, control system, and configuration development. This established the feasibility of the Initial ACT Configuration and the performance and economic benefits relative to the Baseline Configuration.

Section 8.0 contains the analyses of reliability, maintainability, and incremental costs of the ACT systems and their effect on overall airplane cost of ownership.

3.0 SYMBOLS AND ABBREVIATIONS

3.0 SYMBOLS AND ABBREVIATIONS

3.0 SYMBOLS AND ABBREVIATIONS

This section contains five subsections: Airplane Model Numbers, General Abbreviations, Subscripts, Symbols, and Axes and Sign Nomenclature. Each subsection is arranged in alphabetical order. For ease of reference, subsection 3.3 is further divided into three parts—coefficient subscripts (3.3.1), velocity and Mach number subscripts (3.3.2), and general subscripts (3.3.3).

3.1 AIRPLANE MODEL NUMBERS

768-102	Conventional Baseline Configuration
768-103	Initial ACT Configuration

3.2 GENERAL ABBREVIATIONS

a	lift curve slope
ac	alternating current
alt	altitude (same as H)
A	ampere
AAL	angle-of-attack limiter
ACEE	Aircraft Energy Efficiency (Program)
ACES	airline cost-estimating system (program)
ACT	Active Controls Technology
AFCS	automatic flight control system
Ah	ampere-hour
AIC	aerodynamic influence coefficient
AIL	aileron
AP	autopilot
APB	auxiliary power breaker
APU	auxiliary power unit

AR	aspect ratio
ARCS	Airborne Advanced Reconfigurable Computer System
ARINC	Aeronautical Radio Incorporated
ASN	assigned serial number
ATDP	air-turbine-driven pump
AWG	American Wire Gage
$\bar{A}$	gust response factor
b	wing reference span
BBL	body buttock line
BS	body station
BTB	bus tie breaker
BTWT	Boeing Transonic Wind Tunnel
BWL	body water line
c	chord
cg	center of gravity
cm	centimeter
cm^2	square centimeter
cm^3	cubic centimeter
c_T	tip chord
$\bar{c}$	mean aerodynamic chord (same as MAC)
C	Celsius
CARSRA	computer-aided redundant system reliability analysis
COO	cost of ownership
CPU	central processor unit
CY	calendar year
C_c	compressibility factor

d	differential quantity
dB	decibel
dc	direct current
deg	degree
D	drag
DADC	digital air data computer
DATCOM	U.S. Air Force Stability and Control Data Compendium
DRO	design requirements and objectives
ECS	environmental control system
EDP	engine-driven pump
EET	Energy Efficient Transport (Program)
EI	bending stiffness
ELEV	elevator
EMP	electric-motor-driven pump
fig.	figure
ft	feet
ft^2	square feet
f_k	multiplying factor for wing-load alleviation control effectiveness
f_v	flutter mode frequency
F	Fahrenheit; force
FAA	Federal Aviation Administration
FAR	Federal Aviation Regulations
FEL	flight envelope limiting
FH	flight hour
FMC	flutter mode control
FS	front spar

FWD	forward
F_s	stick force
F_w	wheel force
g	structural damping coefficient for neutral stability; acceleration due to gravity
gal	gallon
gen	generator
GAG	ground-air-ground (cycles)
GCB	generator contactor breaker
GJ	torsional stiffness
GLA	gust-load alleviation
GSE	ground service equipment
horiz	horizontal
hr	hour
H	altitude (same as alt)
HAA	high angle of attack
HSBL	horizontal stabilizer buttock line
Hz	hertz
i	imaginary number ($\sqrt{-1}$)
in	inch
in^2	square inch
I	airplane moment of inertia; input
IAAC	Integrated Application of Active Controls Technology to an Advanced Subsonic Transport Project
IAS	indicated airspeed
IDG	integrated drive generator
INBD	inboard

I/O	input/output
IRS	inertial reference system
kg	kilogram
kips	thousands of pounds (force)
km	kilometer
kn	knot
kPa	kilopascal
ksi	thousands of pounds per square inch (stress)
kVA	kilovoltampere
kW	kilowatt
K	thousand
KEAS	knots equivalent airspeed
KF	flutter-mode control gain
KG	gust-load alleviation gain
KMA	maneuver-load control aileron gain
KME	maneuver-load control elevator gain
KQ	pitch rate gain
KU	speed gain
lb	pound
lb/in	pounds per inch
ℓ	rolling moment; section lift; tail arm; liter
L	lift
LAS	lateral/directional-augmented stability
LAT	lateral
LD- (2,3)	lower deck containers (various sizes)
L/D	lift/drag

LE	leading edge
$\frac{LE}{LR}$	ratio of elastic lift to rigid lift
LRU	line replaceable unit
LVDT	linear variable differential transducer
L_{HT}	horizontal tail lift
L_T	tail lift
m	meter
m^2	square meter
max	maximum
min	minute
mm	millimeter
ms	millisecond
m/s	meters per second
M	Mach number
MAC	mean aerodynamic chord (same as $\bar{c}$)
MCU	modular control unit (ARINC dimension specification)
MG	main gear
MLC	maneuver load control
MLW	maximum design landing weight
MNP	maneuver neutral point
MOE	multiply occurring event
MS	margin of safety
MTBF	mean time between failures
MTOW	maximum design takeoff weight or maximum takeoff weight
MTW	maximum design taxi weight
MZFW	maximum design zero fuel weight

M_Y	bending moment about the Y axis
n	acceleration; normal load factor
nmi	nautical mile
n/α	normal acceleration per unit of angle of attack
n_y	side acceleration in g
n_z	vertical acceleration in g or load factor
N	newton; ultimate normal load factor
N/A	not applicable
NG	nose gear
Ni-cad	nickel-cadmium
N·m	newton meter
N/m	newtons per meter
No.	number
NPRM	Notice of Proposed Rule Making (FAA)
NWL	nacelle water line
N_o	characteristic frequency
O	output
OAI	outboard aileron (inboard section)
OEW	operational empty weight
OUTBD	outboard
psi	pounds per square inch
P	roll rate
$\hat{p}$	nondimensional roll rate
PAS	pitch-augmented stability
PCU	power control unit

PFC	primary flight controls
PROM	programmable read-only memory
PSD	power spectral density
q	dynamic pressure; incremental value of pitch rate
$\hat{q}$	nondimensional pitch rate (same as $\hat{Q}$)
Q	pitch rate
$\hat{Q}$	nondimensional pitch rate (same as $\hat{q}$)
QPA	quantity per aircraft
QSAE	quasistatic aeroelastic
rad	radian
ref	reference
rev	revision
rms	root mean square
R	yaw rate
RAM	random access memory
RAT	ram air turbine
RCV	receiver
ROI	return on investment
ROM	read-only memory
RS	rear spar
RSS	rear spar station; relaxed static stability
s	second (same as sec)
sec	second (same as s)
stab	stabilizer
subsec	subsection
S	area; Laplace variable

SAR	still air range
SL	sea level
SLST	sea level static thrust
SOB	side of body
SSFD	signal selection and failure detection
STA	station
S_v	vertical tail area
S_w	wing reference area
t/c	thickness ratio
$t_{h_{cross}}$	time to cross zero Δh for step pitch control input
$t_\phi =$	time-to-bank angle
TBD	to be determined
TBV	to be verified
TE	trailing edge
TOFL	takeoff field length
TOGW	takeoff gross weight
TP	tangent point
TR	taper ratio; thrust reverser
T-R	transformer-rectifier
TRU	transformer-rectifier unit
TX/RCV	transmitter receiver
T_{2x}	time to double amplitude
u	incremental value of forward-speed component
util	utility
U	forward-speed component
U_σ	true vertical gust velocity

V	velocity
VA	volt-ampere
V ac	volt alternating current
V dc	volt direct current
VOR	very high frequency omnidirectional radio range
VYRO	pitch-rate sensors (trade name)
V_1	takeoff decision speed
V_2	takeoff climb speed
$\bar{V}_H$	Volume coefficient: $\frac{S_H}{S_W}\ \frac{\ell_H}{\bar{c}_W}$ (horizontal tail)
$\bar{V}_V$	Volume coefficient: $\frac{S_V}{S_W}\ \frac{\ell_V}{b_W}$ (vertical tail)
w	incremental value of vertical-speed component
W	watt; vertical-speed component
WB	wing body
WBL	wing buttock line
WL	water line
WLA	wing-load alleviation
WRP	wing reference plane
$\ddot{Z}/\delta_{OAI}(S)$	outboard aileron to wing accelerometer transfer function

3.3 SUBSCRIPTS

3.3.1 Subscripts Related to Coefficient C

D	drag
HM	hinge moment

HM_δ	change in hinge moment due to control deflection
HM_0	hinge moment at zero deflection
HM_α	change in hinge moment due to angle of attack
HM_β	change in hinge moment due to sideslip
ℓ	rolling moment
ℓ_β	change in rolling moment with sideslip angle
ℓ_δ	change in rolling moment with control deflection
L	lift
$L_{\hat{q}}$	change in lift due to nondimensional pitch rate
L_R	"reference" value of lift
L_α	change in lift due to angle of attack
L_δ	change in lift due to control deflection
L_0	lift at zero angle of attack
m	pitching moment
$m_{\hat{q}}$	change in pitching moment due to nondimensional pitch rate
m_R	"reference" moment
m_T	pitching moment due to thrust
m_α	change in pitching moment due to angle of attack
m_δ	change in pitching moment due to control deflection
m_0	pitching moment at zero lift
n	yawing moment; section normal force
n_β	change in yawing moment due to sideslip
n_δ	change in yawing moment with control deflection
N	normal force

T	thrust
Y	side force

3.3.2 Subscripts Related to Velocity V or Mach Number M

APP	approach
B	gust penetration
C	cruise
D	dive
e	equivalent airspeed
g	gust
LO	lift-off
MCA	minimum control air
MCG	minimum control ground
MO	maximum operating
MU	minimum unstick
R	rotation
S	stall
T	true
X	crosswind
∞	infinity; free-stream value

3.3.3 General Subscripts

A	aileron (same as AIL)
AIL	aileron (same as A)
APP	approach
B	body

C	command (same as COM)
COL	control column
com	command (same as C)
E	elevator
EQV	equivalent
F	flap
H	horizontal tail
max	maximum
N	nacelle
OA	outboard aileron
OAI	outboard aileron (inboard section)
OAO	outboard aileron (outboard section)
P	phugoid
R	rudder
REF	reference
ss	steady state
SP	spoiler; short period
V	vertical tail
V_2	conditions at V_2 speed
W	wing
x,y,z	airplane reference axes defined in Figure 4

3.4 SYMBOLS

℄	centerline
α	angle of attack
α_{MU}	angle of attack (minimum unstick speed conditions)

β	sideslip angle
δ	control deflection
δ_w	control wheel deflection (lateral)
Δ	change in quantity
Δac	increment in aerodynamic center location
Δn	incremental normal load factor
Δ_U	change in forward speed
ζ	damping ratio
η	fraction of semispan (2 y/b)
θ	pitch attitude
$\ddot{\theta}$	pitch acceleration
λ	failure rate
Λ	sweep
σ	vertical tail sidewash angle
σ_w	root-mean-square vertical gust velocity
τ	time constant
ϕ	roll attitude
ψ	yaw attitude
ω	frequency
ω_C	command or crossover frequency
ω_n	natural frequency
$\cdot$	derivative with respect to time or rate of change (superscript)
$\cdot\cdot$	second derivative with respect to time or acceleration (superscript)

3.5 AXES AND SIGN NOMENCLATURE

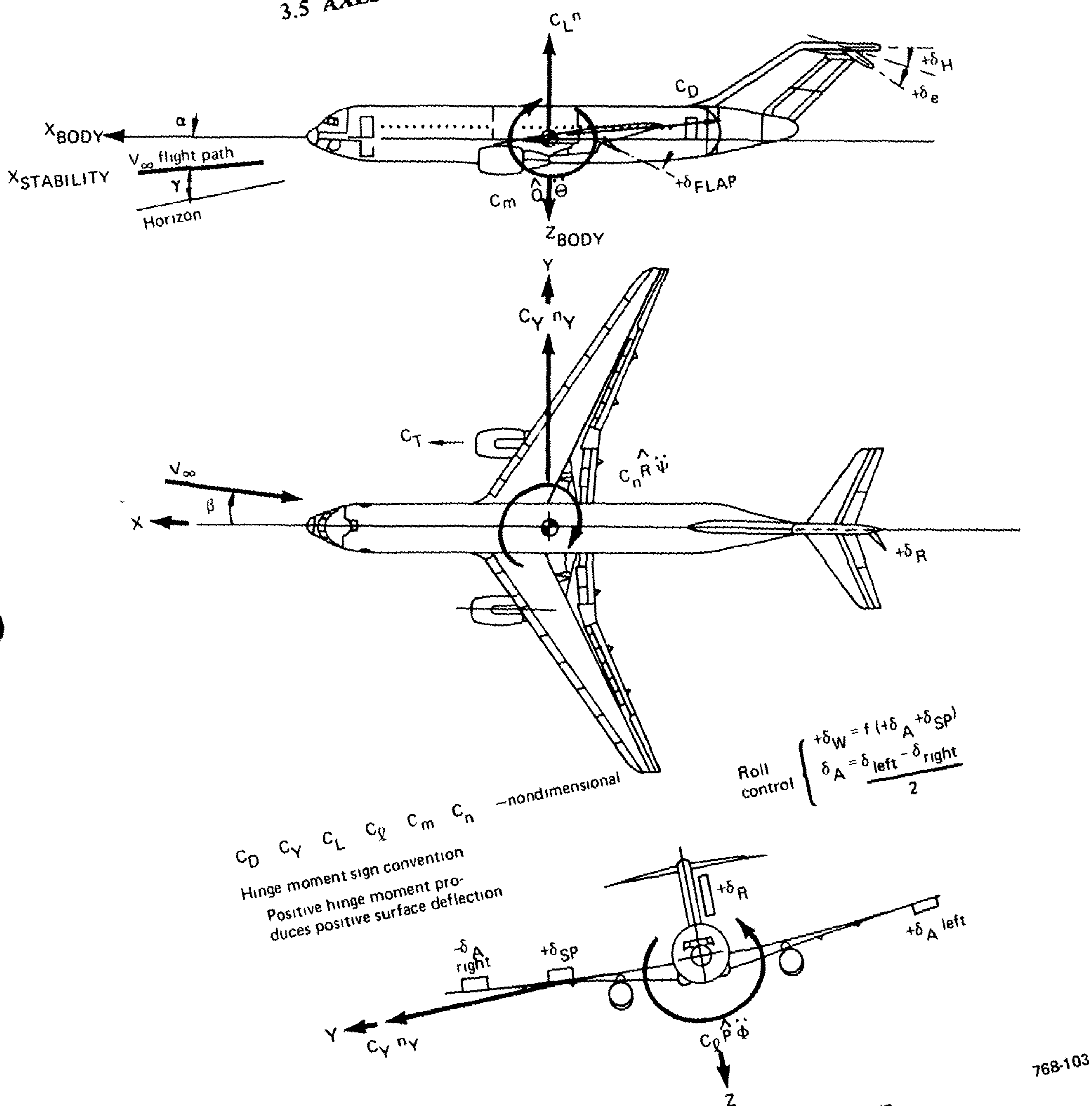

Figure 4. Axes and Sign Nomenclature

4.0 INITIAL ACT CONFIGURATION DEVELOPMENT

Page

4.0 INITIAL ACT CONFIGURATION DEVELOPMENT

4.0 INITIAL ACT CONFIGURATION DEVELOPMENT

Development of the ACT Configuration was preceded by definition of a Conventional Baseline Configuration (ref 2). The Baseline and Initial ACT Configurations have the same overall fuselage dimensions and the wing planform. However, they differ in wing location on the body, type of control surfaces on the wing and empennage, horizontal tail size, and main landing gear. The structure and systems of the Initial ACT Configuration are tailored to realize advantages of ACT. This section identifies study constraints, defines the design criteria and objectives that were influenced by ACT, and describes the resulting Initial ACT Configuration.

4.1 STUDY GROUND RULES AND CONSTRAINTS

Key ground rules and constraints adopted for this study are described in these subsections.

4.1.1 ACT FUNCTIONS

Selection of ACT functions for the Initial ACT Configuration was based on a preliminary assessment of the expected reduction in airplane weight or drag. No formal quantitative risk-versus-benefit evaluation was made before selection of these functions:

- Pitch-Augmented Stability (PAS)—The PAS function augments the airplane longitudinal stability to provide acceptable flying qualities. Both long-period (static stability) and short-period augmentation are included.

- Lateral/directional-Augmented Stability (LAS)—The LAS function is a conventional yaw damper identical to that of the Baseline Configuration. In the Baseline, the yaw damper is implemented in the analog control systems electronics unit, which is retained in the Initial ACT Configuration. Therefore, the LAS function is not considered part of the ACT system added in the Initial ACT Configuration.

- Angle-of-Attack Limiter (AAL)—The AAL function prevents the airplane from exceeding a limiting angle of attack, which is a small margin beyond that for maximum lift and allows a reduction in the horizontal tail size required to provide nose-down control margin for stall recovery.

- Wing-Load Alleviation (WLA)—The WLA function has two submodes composed of:

  - Maneuver-Load Control (MLC)—MLC reduces the wing vertical bending moment in longitudinal maneuvers by deflecting the outboard ailerons to redistribute the wing loads.

  - Gust-Load Alleviation (GLA)—GLA reduces the wing loads due to atmospheric disturbances by deflecting outboard ailerons to reduce and redistribute the induced loads.

- Flutter-Mode Control (FMC)—The FMC function stabilizes the wing critical flutter mode to the required speed margin $1.2V_D/M_D$ by sensing wing motion and commanding deflection of a small wing trailing-edge surface (the inboard segment of the outboard aileron).

4.1.2 CONFIGURATION CONSTRAINTS

To ensure close correlation between data base and performance of the Baseline and Initial ACT Configurations, definition of the Initial ACT Configuration followed this framework of constraints:

- Fuselage/Landing Gear—The 5.029m (198-in) diameter upper lobe and 5.410m (213 in) total depth through the lower lobe fuselage of the Baseline Configuration was maintained. Likewise, the same 54.178m (177 ft 9 in) fuselage length, the pilot compartment, the total 197 mixed-class passenger accommodations, and 22 LD-2 containers plus bulk cargo capacity were held constant. Passenger and cargo arrangements could vary if necessary; however, adequate service access, loading access, and escape provisions were mandatory. Fuselage structure could vary within the geometric constraints to accommodate final wing, empennage, and landing gear locations. Main landing gear would be selected as required for integrated design.

- Wing—The wing planform geometry used on the Baseline Configuration was maintained; i.e., a 47.24m (155-ft) total span, a 31.47-deg sweepback, and an 8.71 aspect ratio. The trailing-edge extension could be modified to accommodate the landing gear. The quantity, type, and location of control surfaces could change within the geometric constraints. Wing location, relative to the body, was constrained to increments of 0.56m (22 in), consistent with fuselage frame spacing and the requirement to accommodate 22 LD-2 containers.

- Empennage—The T-tail arrangement of the Baseline Configuration was retained; however, the sizes of the vertical and horizontal tails and of the control surfaces could be varied.

- Propulsion—Two CF6-6D2 engines, located at 33.6% of wing half-span, were the same as for the Baseline Configuration. Fuel containment and fuel systems were to be defined.

- Systems—Electric, electronic, hydraulic, and mechanical systems used on the Baseline Configuration could be modified to accommodate the ACT functions.

4.1.3 STUDY GROUND RULES

4.1.3.1 Operational Characteristics

Maximum and minimum operating characteristics, consistent with safe ground and flight operations provided by the Baseline Configuration, were maintained:

- Maximum takeoff field length (TOFL) at sea level = 2210m (7250 ft)

- Minimum cruise speed = 0.80 Mach number

- Maximum cruise altitude = 12 800m (42 000 ft)
- Maximum approach speed = 70 m/s (136 kn)
- Minimum cruise range with design payload = 3590 km (1938 nmi)

4.1.3.2 Technology Application

Except for the control system, current state-of-the-art technologies applied to the Baseline Configuration were maintained. Structural materials included advanced aluminum alloys and limited use of composites in secondary structure. General Electric CF6-6D2 engines and wing aerodynamic technology (i.e., type of airfoil, sweep, and thickness-to-chord ratio) were maintained. Wing thickness and twist could be locally tailored to accommodate ACT.

4.1.3.3 Performance Evaluation

The 122 470 kg (270 000 lb) maximum takeoff weight (MTOW) of the Baseline Configuration was held constant. The design payload of 17 891 kg (39 400 lb) of the Baseline Configuration also remained constant so ACT performance could be evaluated in increments of mission range.

4.1.3.4 Economic Evaluation

Economic evaluation was limited to determining the incremental return on investment (ROI) that would accrue considering the cost and consequent benefits of applying ACT.

4.2 DESIGN REQUIREMENTS AND OBJECTIVES

A comprehensive review was made to determine how design requirements and objectives applicable to a conventional (non-ACT) transport should change for a transport design that includes ACT. Because structural design and handling qualities were affected most, with relatively minor effects on other design areas, this section highlights the form they would take for a transport airplane. These design requirements and objectives (DRO) are discussed in more detail in Appendix A.

4.2.1 STRUCTURES

4.2.1.1 Configurations For Structural Design

In selecting the configurations for structural design, the effects of active controls will be considered:

- For flaps up, any control surface used for an active control function
- For flaps down, any control surface used for an active control function during landing approach or takeoff

4.2.1.2 Gust Loads

Gust loads will be established using power spectral techniques. Effects of the automatic flight control system will be included.

When a stability augmentation system is included in the analysis, the effect of system nonlinearities at limit load level will be realistically or conservatively accounted for.

4.2.1.3 Flutter

If FMC systems are installed, the airplane will be:

- Flutter free to $1.2V_D/M_D$ with:
  - Normal operation within limits of ± 6 dB gain and ± 45 deg phase
  - Normal operation with sensor location tolerances of $\pm 5\%$ semispan and $\pm 5\%$ local chord
  - Normal system operation but with one hydraulic system off

- Flutter free to V_D/M_D with:
  - The FMC system off
  - The FMC system operating within limits of ± 12 dB gain and ± 60 deg phase, including the effects of fail-safe structure
  - Any FMC system failure not shown to be extremely improbable
  - Normal system operation but with one hydraulic system off, including the effects of fail-safe structure
- Flutter free to V_{MO}/M_{MO} with fail-safe structure and with:
  - The flutter-suppression system off
  - Any flutter-suppression system failure not shown to be extremely improbable

4.2.2 FLYING QUALITIES

Flying qualities requirements are quantified wherever possible, following the format of Reference 4. In particular, quantitative requirements for longitudinal and lateral/directional dynamics are given as design information, in contrast to the qualitative minimum safe certification requirements of Federal Aviation Regulations (FAR) Part 25 (ref 5).

4.2.3 FLIGHT CONTROL SYSTEMS

The ACT system should enhance airplane safety by improving flight handling and ride and by reducing the loads imposed on the airframe. System failures must be considered, and the overall operation of the ACT system, including the probability of system failures, must not reduce the safety below that of conventional, contemporary, transport airplanes.

The safety impact of failure of any ACT function depends on its necessity for continued safe flight or its function criticality levels:

- Flight crucial—complete loss of function results in an immediate, unconditional hazard to safe and continued flight

- Flight critical—complete loss of function results in a potential hazard to safe, continued flight; i.e., appropriate flight crew action can avert the hazard

- Nonflight critical—complete loss of function may result in increased crew workload or passenger discomfort but does not result in hazard to safe, continued flight.

Table 1 relates criticality levels to reliability and redundancy levels required for the ACT systems. The PAS short-period system was designed to be flight crucial; other ACT functions are flight critical.

Table 1. Relationship of Reliability and Redundancy to Criticality Levels

Criticality level	Failure probability objective, per flight hour
Crucial	$< 1 \times 10^{-9}$
Critical	$< 1 \times 10^{-7}$
Noncritical	$< 1 \times 10^{-3}$

768-103

4.3 CONVENTIONAL BASELINE CONFIGURATION

As the first task on the Integrated Application of Active Controls (IAAC) Project, a comprehensive data base was established for a modern Mach 0.8 transport design.

The following paragraphs are excerpts from the Conventional Baseline Configuration Study document (ref 2). Characteristics of the U.S. domestic fleet were evaluated to determine the mission characteristics that would have the most impact on future U.S. transport fuel use. Selection of a 197-passenger (plus cargo) configuration with a mission of about 3590 km (1938 nmi) allowed Boeing to apply considerable analytical and test data that had been derived during earlier preliminary design efforts.

The existing data base was reviewed, and additional analyses were conducted to complete the technical descriptions. Significant characteristics of the resulting Baseline Configuration are shown in Figure 5. The configuration has a double-lobe, but nearly circular, body with seven-abreast seating. Externally, it has an 8.71 aspect ratio 31.5 deg sweep wing, a T-tail empennage, and a dual CF6-6D2, wing-mounted engine arrangement. The lower lobe can accommodate 22 LD-2 or 11 LD-3 containers plus bulk cargo. Passenger/cargo loading, servicing, taxi/takeoff speeds, and field length characteristics are compatible with accepted airline operations and regulations.

The Baseline Configuration construction is conventional aluminum structure except for use of advanced alumimum alloys and a limited amount of graphite epoxy secondary structure. It uses advanced guidance, navigation, and controls systems, which emphasize application of digital electronics and advanced displays.

This initial task of the IAAC Project resulted in a well defined Baseline Configuration that provided a firm base for definition and evaluation of the benefits offered by configurations that use ACT.

4.4 RESULTING INITIAL ACT CONFIGURATION

The Initial ACT Configuration (fig. 1) also carries 197 mixed-class passengers, over a range of 4061 km (2193 nmi) at a cruise speed of Mach 0.8. The TOFL is 2118m (6950 ft), and the approach speed is 68.6 m/s (133.4 kn). As the Baseline Configuration, the Initial ACT Configuration uses a double-lobe, but nearly circular, body with seven-abreast seating. External characteristics, as in the Baseline, feature an 8.71 aspect ratio 31.5 deg sweep wing, a T-tail empennage, and a dual CF6-6D2, wing-mounted engine arrangement. The lower lobe can accommodate 22 LD-2 or 11 LD-3 containers, plus bulk cargo. Passenger/cargo loading, servicing, taxi/takeoff speeds, and field length characteristics are compatible with accepted airline operations and regulations. Significant characteristics of the Initial ACT and the Baseline Configurations are compared in Figure 3, Section 2.3.

Configuration	
Passengers	197 mixed class, 207 all tourist
Containers	22 LD-2, or 11 LD-3
Engines	2 (CF6-6D2)
Design mission	
Cruise Mach	0.8
Range	3590 km (1938 nmi)
Takeoff field length	2210m (7250 ft)
Approach speed	70 m/s (136 kn)
Noise	FAR 36, Stage 3
Flying qualities	Current commercial transport practice
Airplane technology	Current commercial transport practice (aerodynamics, structural, propulsion, etc)

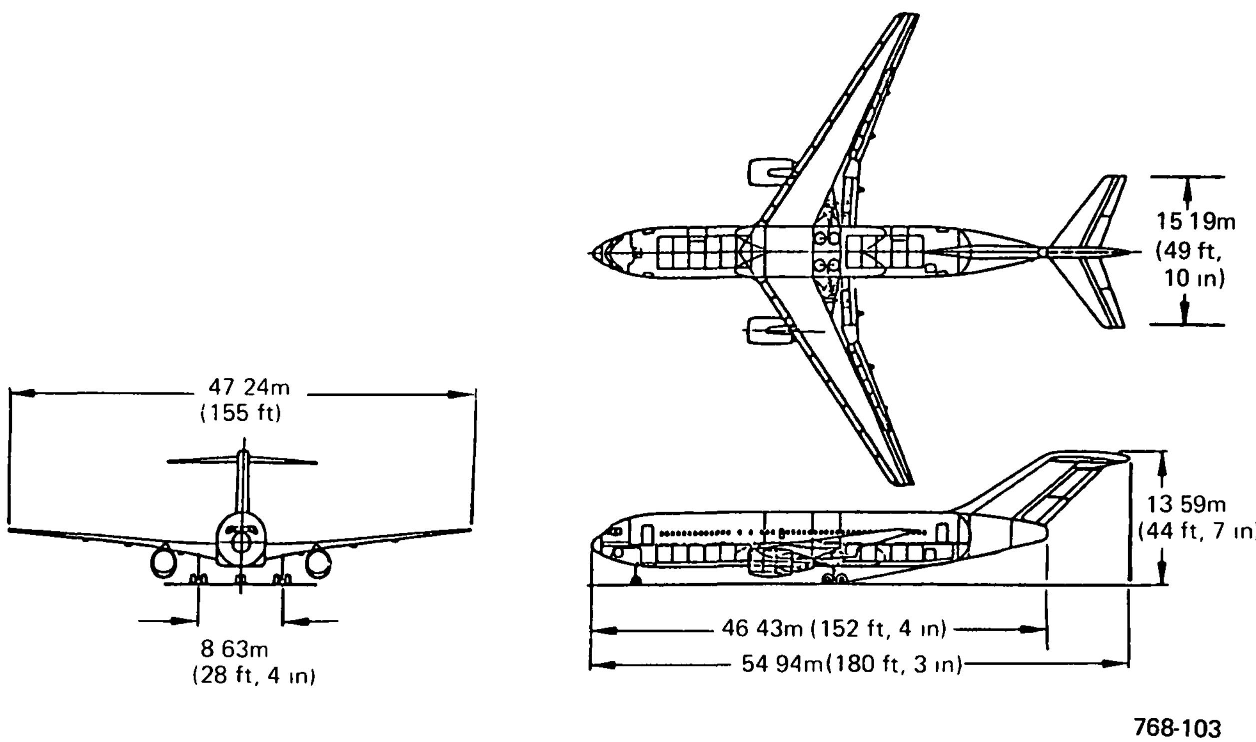

Figure 5. Baseline Configuration

The Initial ACT Configuration construction, as the Baseline Configuration, consists of conventional aluminum structure, except for advanced aluminum alloys and a limited amount of graphite epoxy secondary structure. Modern systems used, in addition to the ACT system, include advanced guidance, navigation, and controls provisions, which emphasize application of digital electronics and advanced displays.

The Initial ACT Configuration was established with the constraint that the wing planform would be the same as that of the Baseline Configuration, with a well defined airplane and data base substantiated by considerable analysis, design, and testing. The Initial ACT Configuration was designed to approximately neutral longitudinal stability with the horizontal tail size determined by controllability considerations. Wing trailing-edge surfaces and surface controls were reconfigured for load alleviation and structural stabilization. All required ACT functions were assumed available and mechanized. The resulting Initial ACT Configuration (fig. 1) has the wing positioned forward on the body and the horizontal tail size reduced relative to the Baseline Configuration.

The airplane was not resized for constant payload/range, so the block fuel at the Baseline design range and the range increase at constant takeoff gross weight were taken as measures of improved performance. Since the airplane was not resized, the propulsion system was unchanged from the Baseline Configuration. The Initial ACT Configuration has slightly improved sea-level takeoff and landing field performance; noise characteristics improved so little that they were not considered in this analysis. The resulting ACT airplane exhibits improved cruise aerodynamic efficiency of 3.6% (subsec 5.3.2, table 3), a 1.19% reduction in empty weight at constant takeoff gross weight, and increased range of 13% at constant payload.

5.0 AIRPLANE DESCRIPTION

Page

5.0 AIRPLANE DESCRIPTION

5.0 AIRPLANE DESCRIPTION

This section briefly describes the evolution of the Initial ACT Configuration by application of ACT functions to the Baseline Configuration, then it describes the associated modifications.

Illustrations of the general arrangement, major components, and payload capabilities are supplemented by descriptions of principal configuration characteristics. Also presented are the mission rules, speed schedules, performance and noise characteristics, design weights, and center-of-gravity (cg) management.

5.1 CONFIGURATION EVOLUTION

Two major decision stages were involved in developing the Initial ACT Configuration:

- Selection of the ACT functions
- Design of a realistic airplane, combining the ACT functions with a feasible general arrangement, structure, systems, and constant payload provisions

The most significant configuration changes were:

- A new wing location
- A new cg location aft of the previous cg range
- Reduced empennage size

5.1.1 ACT FUNCTIONS

The application of ACT functions was intended to improve the airplane performance through reduced drag and/or weight. These objectives were achieved by: (1) relying upon pitch augmentation and rebalancing the airplane with the cg range farther aft, and (2) reducing structural design loads and/or airframe structural stiffness requirements. The ACT functions that make these changes possible are:

- Pitch-augmented stability (PAS) system
    - Short-period pitch rate
    - Long-period speed

- Angle-of-attack limiter (AAL)
    - Alpha-limiting only

- Wing-load alleviation (WLA)
    - Maneuver-load control (MLC)
    - Gust-load alleviation (GLA)

- Flutter-mode control (FMC)

Figure 6 shows the aerodynamic surfaces used to implement these functions. WLA and FMC do not result in changes to the exterior lines or drag of the airplane; therefore, they are discussed in Subsection 7.2 (Structural Analysis), Subsection 7.3 (Control System Analysis), and Subsection 7.5 (Weight Analysis).

5.1.2 GENERAL ARRANGEMENT

The Initial ACT Configuration wing was moved forward on the fuselage, relative to the Conventional Baseline Configuration, and the main landing gear was moved aft relative to the wing to accommodate the new cg range. When combined with the reduced empennage size, these changes better aligned the cg ranges of the empty airplane, payload, and fuel, resulting in a reduction in required loading range for the same loading flexibility.

Wing forward movement was limited by the size of the wing trailing-edge extension needed to accommodate the main landing gear. In the early stage of selecting the Initial ACT Configuration, a qualitative conceptual study explored various landing gear designs and structural supports that were less dependent on the wing location. Five alternatives to the Conventional Baseline main landing gear (fig. 7) had landing-gear-footprint centroid farther aft, with respect to the wing:

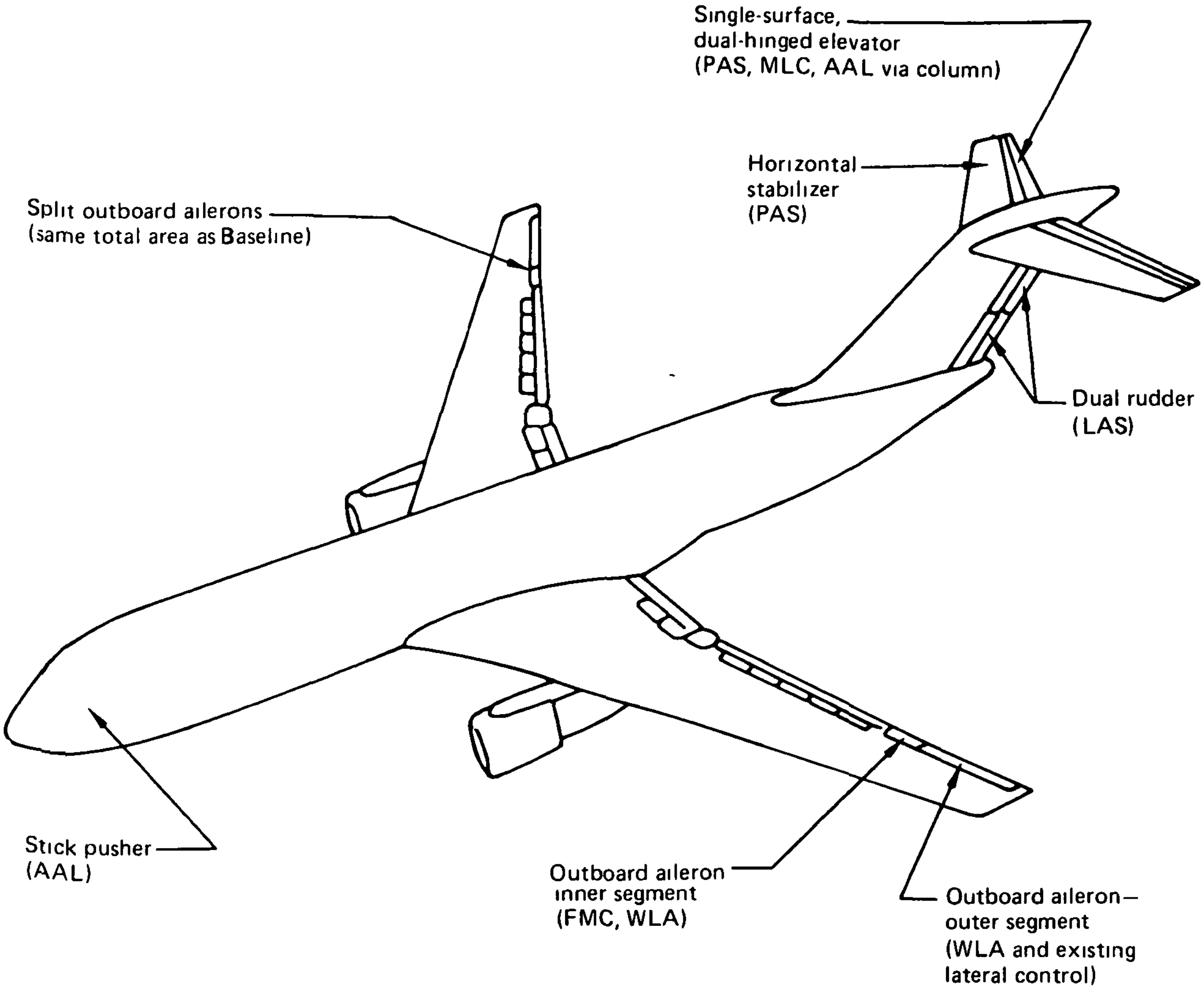

ACT function	Control
PAS (short period)	Elevator
PAS (speed)	Elevator and stabilizer
LAS	Rudder
AAL	Column/elevator

ACT function		Control
WLA	MLC	Outboard aileron Elevator (through PAS command)
	GLA	Outboard aileron
FMC		Outboard aileron (inner segment)

768-103

Figure 6. ACT Control System Surfaces

Option No.	Wing planform	Landing gear	cg range, percent MAC	Aft cg limit, percent MAC	Advantages	Disadvantages		
Reference	Baseline	2-post, 4-wheel truck	28	38	Largest amount of available information and data	No cg shift possible	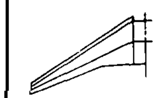	
1	Baseline	3- or 4-post, 2-wheel, wing-mounted and body-mounted	28	46	Large cg shift possible	Increased mechanical complexity and structural weight in landing gear and body (major body revision)	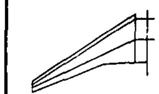	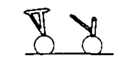
2	Inboard wing planform revision	Model 768-102	28	46	Structural and mechanical complexity similar to reference; large cg shift possible	Larger, heavier wing with more drag, possibly heavier landing gear beam, aerodynamics may differ from reference	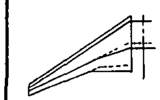	
3	Baseline	2-post, pod-mounted 6-wheel truck	28	46	Large cg shift possible	Large increase in weight and drag; pod interferes with required ACT control surfaces and high-lift system	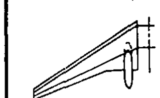	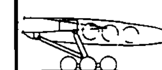
4	Baseline	Revised, pivoted post, radius arm	28	46	Provides increased cg shift	Increased cg shift without loss of cargo space or TE extension requires development of a less conventional landing gear		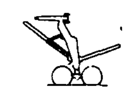
5	Baseline	Body-mounted, 2-post, 4-wheel truck	28	46	Large cg shift possible; wing shape unconstrained by landing gear	Major body revision required, probable body weight increase		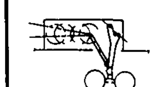
6	Baseline	Baseline	Unknown, forward cg limited by fuel management using existing tankage and/or body-installed tanks	38	Provides effect of cg shift; reduces cg range	Fuel management alternative; increased fuel system complexity		

768-103

Figure 7. Main Landing Gear Concept Study

- A combination of wing-mounted and fuselage-mounted landing gears, similar to the 747, with a total of three or four posts. The three-post arrangement was ruled out because external and internal loads could not be determined with available resources. The four-post design appeared feasible yet complex for an airplane of this size and it occupied more fuselage volume (Option 1).

- Wing-mounted gear with an extreme trailing-edge extension, which seemed unreasonable (Option 2).

- A six-wheel, wing-pod-mounted truck, with smaller wheels to reduce the pod frontal area. Large increases of weight and drag, as well as interference with the trailing-edge devices used for ACT functions, were likely (Option 3).

- Wing-mounted gear with maximum trail behind the trunnion. This arrangement appeared most feasible (Option 4).

- Body-mounted gear, retracting forward. The wide-track LaGuardia flotation requirement was difficult to reconcile with a skewed trunnion support of reasonable dimensions and weight. Option 5 also occupied more fuselage volume.

As an additional way to deal with the required cg range, Option 6 consisted of fuel management (i.e., the transfer of fuel betweeen tanks).

The qualitative evaluation resulted in selecting a version of Option 4, which is described in Subsection 5.1.3. Options 1 and 6 would merit consideration if the wing relocation forward on the body were not restricted by other ground rules, including:

- The same payload and number of seats as on the Baseline Configuration

- Whole increments of LD-2 containers in the lower lobe

- Sufficient space for access and cargo doors for the upper and lower decks in front of the wing

- Minimum horizontal stabilizer size for balance (moving the wing farther forward would increase tail size, weight, and friction drag, but would reduce the trim drag)

Solving for the required minimum horizontal tail size reduced the required loading range by 3%, which, in turn, further reduced the required horizontal stabilizer size. These changes were accomplished by shifting the wing forward (relative to the fuselage) 1.676m (66 in). Figure 8 illustrates the resulting cg range and location relative to the stability and control criteria. Specific configuration details are discussed in the following subsections.

5.1.2.1 Horizontal Tail

The AAL and PAS allow the airplane to be rebalanced with a more aft cg range and a smaller horizontal tail. The factors determining the horizontal tail volume coefficient ($\bar{V}_H$) as a function of airplane cg location (fig. 8) are critical for aft cg locations. For example, minimum longitudinal stability or nose-down control margins result in lines defining an aft cg limit and increasing $\bar{V}_H$ as the cg goes aft. Conversely, requirements for nose-up control margins result in lines defining a forward cg limit and increasing $\bar{V}_H$ as the cg goes forward. Ideally, the minimum tail size would result from simultaneously satisfying the most restrictive forward and aft limiting stability or controllability cases for the required cg range. However, the required cg range also varies as the airplane is reconfigured, and, although it is closely approximated, the ideal of minimum tail size is seldom completely achieved.

Using a double-hinged elevator, the Initial ACT Configuration requires a $\bar{V}_H$ of 0.55. In combination with the increased moment arm due to the wing shift, this reduces horizontal tail area 45% to 32.0 m^2 (344 ft^2) from the 57.6 m^2 (620 ft^2) tail area of the Baseline. The relation of the selected $\bar{V}_H$ and cg range to the various criteria in Figure 8 is highlighted below:

- Tail size for landing stall recovery is the critical case and requires an alpha-limiting system and a double-hinged elevator.

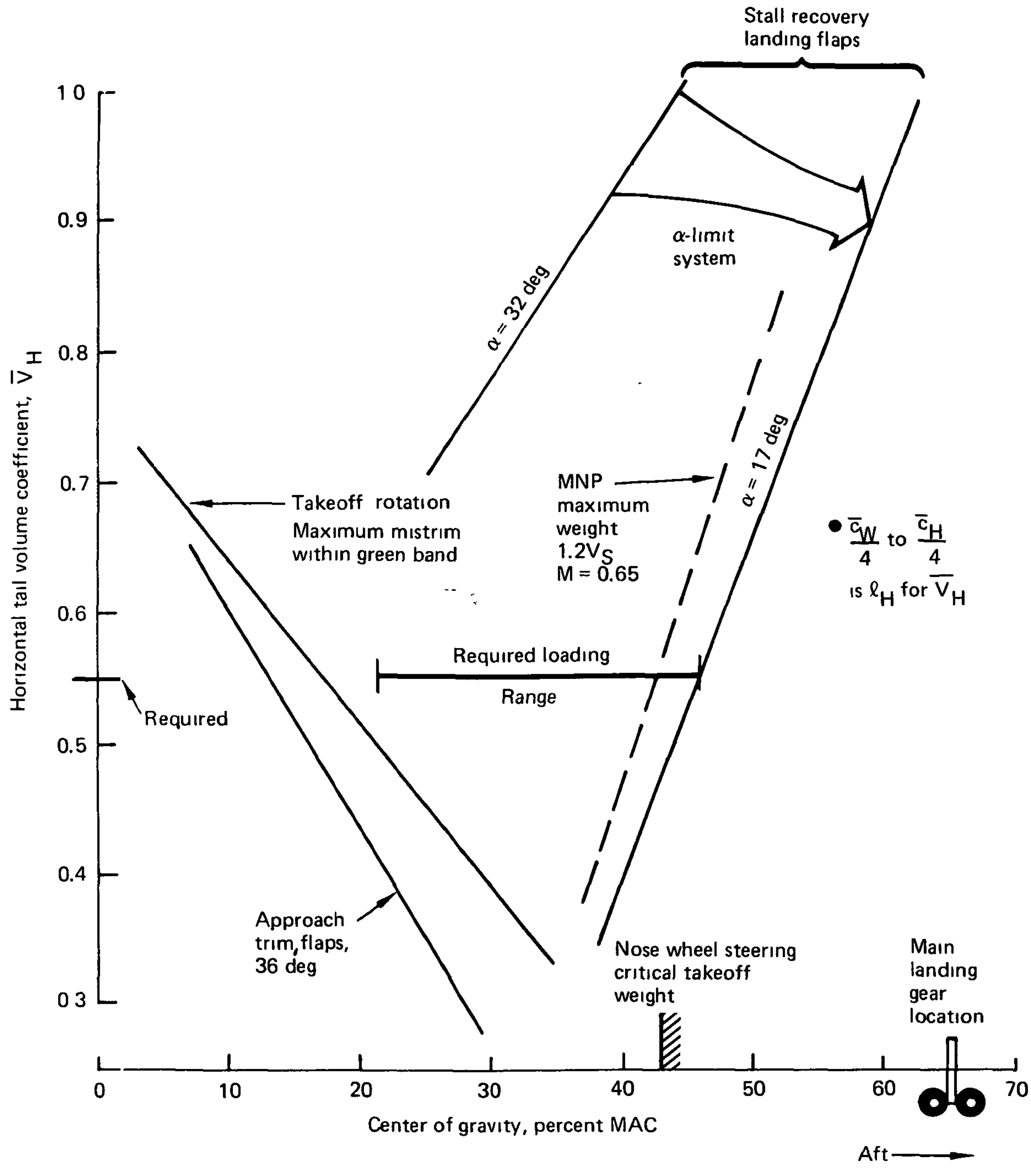

768-103

Figure 8. Horizontal Tail Size Requirements

- Maneuver neutral point (MNP) is shown for reference, indicating an unstable airplane requiring PAS.
- Normal and mistrimmed takeoff rotations illustrate that a "green-band" system is required to limit the trim range for takeoff.
- Landing approach trim does not define a limiting case.
- The nose-wheel steering limit, shown for the most critical aft loading condition, is defined by a dynamic condition at takeoff brake release where the nose-wheel load may not decrease below the limits set by adequate steering response.
- The main landing gear had to be relocated from 56% to 65% mean aerodynamic chord (MAC).

5.1.2.2 Vertical Tail

The vertical tail volume coefficient, $\bar{V}_V$, is the same as that of the Baseline Configuration, referenced to the aft cg limit; it is determined by the requirements for engine-out control on the ground (V_{MCG}). Due to the wing forward shift and resulting increased moment arm, the vertical tail area was decreased 6% to 54.0 m^2 (581 ft^2) from the 57.4 m^2 (618 ft^2) of the Baseline Configuration.

The tail size leads to low Dutch roll damping, similar to that with Boeing's Model 727, and requires a yaw damper as on the Baseline Configuration. Neither airplane needs lateral (roll) stability augmentation.

On both the Initial ACT and the Baseline Configurations, the lateral controls were sized for tameness, here defined as a static engine-out trim requirement using lateral control. This required the addition of a wing spoiler panel on each wing for the Initial ACT Configuration, because part of the outboard aileron was used for ACT functions, to yield about the same total roll control as the Baseline Configuration.

5.1.3 INTERNAL ARRANGEMENT AND LANDING GEAR

This subsection summarizes integration of wing, fuselage, and main landing gear in the rebalanced Initial ACT Configuration. The wing was shifted forward consistent with the fuselage frame spacing of 0.559m (22 in) and multiples thereof, and increments of whole lower lobe cargo containers at 1.53m (60.4 in) length. This resulted in a wing shift of 1.676m (66 in) forward.

The escape hatches on the body above the wing were moved accordingly. The passenger seating arrangement was maintained, and the provisions for the upper lobe cargo door were at the same stations as on the Baseline Configuration. The optional upper deck cargo door location remained compatible with ground cargo loading equipment with respect to engine nacelle clearance. The provisions for the large cargo door option in the lower deck were shifted to the aft compartment, which had the larger volume.

The design of the main landing gear differs from that of the Baseline Configuration, as explained in Subsection 5.1.2. The wing shape, including the trailing-edge extension, was maintained. The 9% $\bar{c}_w$ aft shift of the landing gear required by the more aft loading range was accomplished by a new design that has 0.533m (21 in) more trail between the trunnion and the footprint. The gear and its support are described in Section 6.1.5.

The deck height is the same as for the Baseline Configuration. The wing shift reduces the takeoff maximum rotation angle by 1.0 deg. Figure 9 illustrates the pertinent differences between the center sections of Initial ACT and Baseline Configurations.

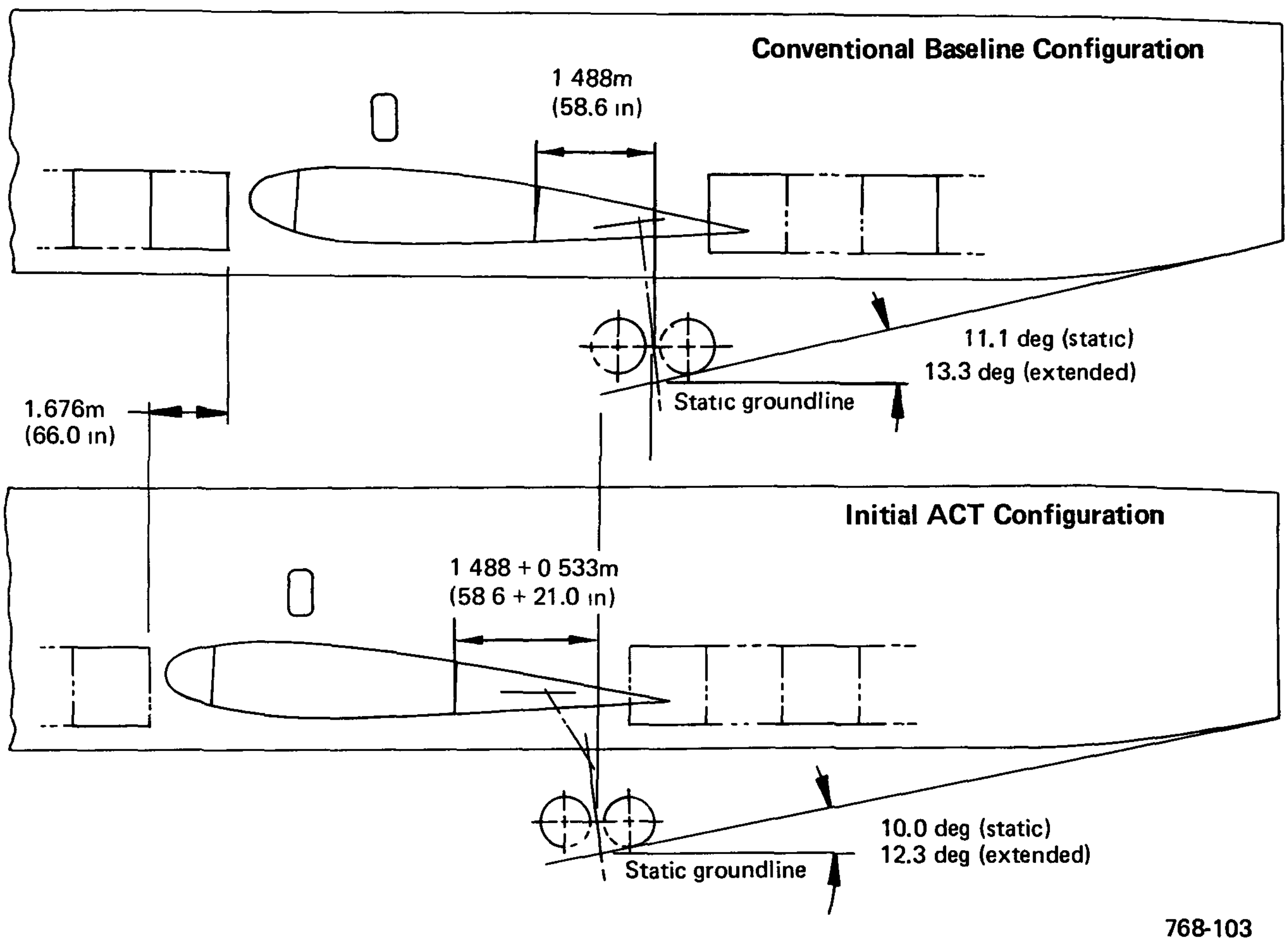

Figure 9. Airplane Center Fuselage Geometry Comparison

5.2 CONFIGURATION

5.2 CONFIGURATION

This section describes physical data, both geometric and characteristic for the Initial ACT Configuration. The external shape of the airplane and the major internal views (systems, passengers, and cargo) are shown. The geometric data are supplemented by pertinent characteristics of engines, fuel capacity, and flight crew.

5.2.1 GENERAL ARRANGEMENT

The principal dimensions and general arrangement of the Initial ACT Configuration resulting from the study are shown in Figure 10. This twin-engine, low-wing, land-based commercial transport airplane is sized for a design range of 4061 km (2193 nmi), a payload of 197 passengers in mixed-class accommodations, and 22 LD-2 containers of other types up to 2.44m (96 in) wide. General Electric CF6-6D2 engines in wing-pylon-mounted nacelles power the airplane. Structural materials and design are conventional, using aluminum alloy for the primary structure, with a limited amount of graphite epoxy secondary structure and other materials, such as high-strength steel, for landing gear components.

The wing has an additional outboard spoiler, and the 0.25 MAC is located at body station 23.44m (922.68 in), 1.68m (66 in) forward of that on the Baseline Configuration. The horizontal tail is a trimmable stabilizer with a single 30% chord double-hinged elevator on each semispan. The stabilizer area is 31.96 m^2 (344 ft^2), which is approximately 55% of that of the Baseline Configuration. The reduced tail area is permitted by PAS and, to some extent, by the increased moment arm resulting from the comparatively forward wing postition. The vertical tail area of 53.98 m^2 (581 ft^2) is approximately 94% of that of the Baseline Configuration, a reduction also permitted by the wing-position/moment-arm relationship. A two-segment, double-hinged rudder is sized by engine-out control requirements.

5.2.2 EQUIPMENT

An inboard profile drawing (fig. 11) of the airplane shows the locations of the major body components including passenger seats, cargo containers, electric and electronic

Geometry

Body cross section, m (in)			
Shape	Vertical double lobe		
Maximum width	5 029 (198 00)		
Maximum height	5 410 (213 00)		
Landing gear	Nose	Main	
Type	Dual	Truck	
Location, m (in)	BS 6 896 (271 50)	64 7% MAC	
Spacing, m (in)	0 609 (24)	1 143 x 1 422 (45 x 56)	
Tire size, m (in)	0 939 x 0 330–0 406 (37 x 13–16)	1 092 x 0 393–0 508 (43 x 15 5–20)	
Oleo stroke, m (in)	0 381 (15)	0 508 (20)	
Aerodynamic surfaces	Wing	Vertical tail	Horizontal tail
Area, m^2 (ft^2)	256 3 (2759)[a]	54 0 (581)	32 0 (344)
Aspect ratio	8 71[a]	0 67	4 00
Taper ratio	0 267[a]	0 700	0 400
Sweep at c/4, deg	31 5[a]	55 0	35 0
Incidence SOB, deg	3 8[a]	–	–
Dihedral deg	6 0[a]	–	-3 0
Root t/c, percent	15 1	12 0	11 0
Tip t/c, percent	10 3	12 0	9 0
Root chord, m (in)	8 567 (337 30)[a]	10 558 (415 74)	4 038 (158 98)
Tip chord, m (in)	2 286 (90 0)[a]	7 392 (291 01)	1 615 (63 59)
MAC, m (in)	6 031 (237 47)[a]	9 070 (357 07)	3 000 (118 10)
Span m (in)	47 244 (1860 0)	6 014 (236 76)	11 306 (445 13)
Tail arm, m (in)	–	21 679 (853 50)	28 633 (1127 28)
Tail volume coefficient		0 090	0 551

Engine toe-in angle = 1 deg to a BBL
Nacelle incidence = 2 625 deg to a BWL
Wing upper surface at SOB rib at WL 4 940m (194 5 in)

[a]Trapezoid geometry quoted aero reference area = 275 1 m^2 (2961 ft^2)

[b]Based on aero reference area

Passenger accommodations	Passengers	Abreast	Pitch
First class	18	6	0 965m (38 in)
Tourist	179	7	0 864m (34 in)
Cargo and baggage, m^3 (ft^3)			
Containers	22 LD 2	or	11 LD 3
Forward	33 98 (1200)		22 37 (790)
Aft	40 78 (1440)		26 85 (948)
Bulk cargo (aft only)	11 33 (400)		11 33 (400)
Total	86 09 (3040)		60 55 (2138)

Weights, kg (lb)

TOGW	122 470 (270 000)
OEW	77 370 (170 560)
MLW	111 640 (246 110)

Propulsion Two CF6-6D2

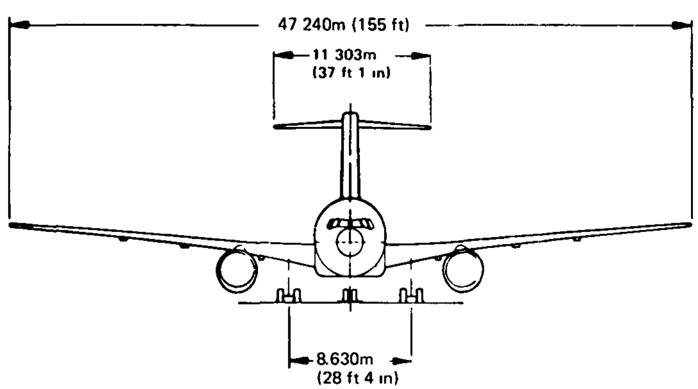

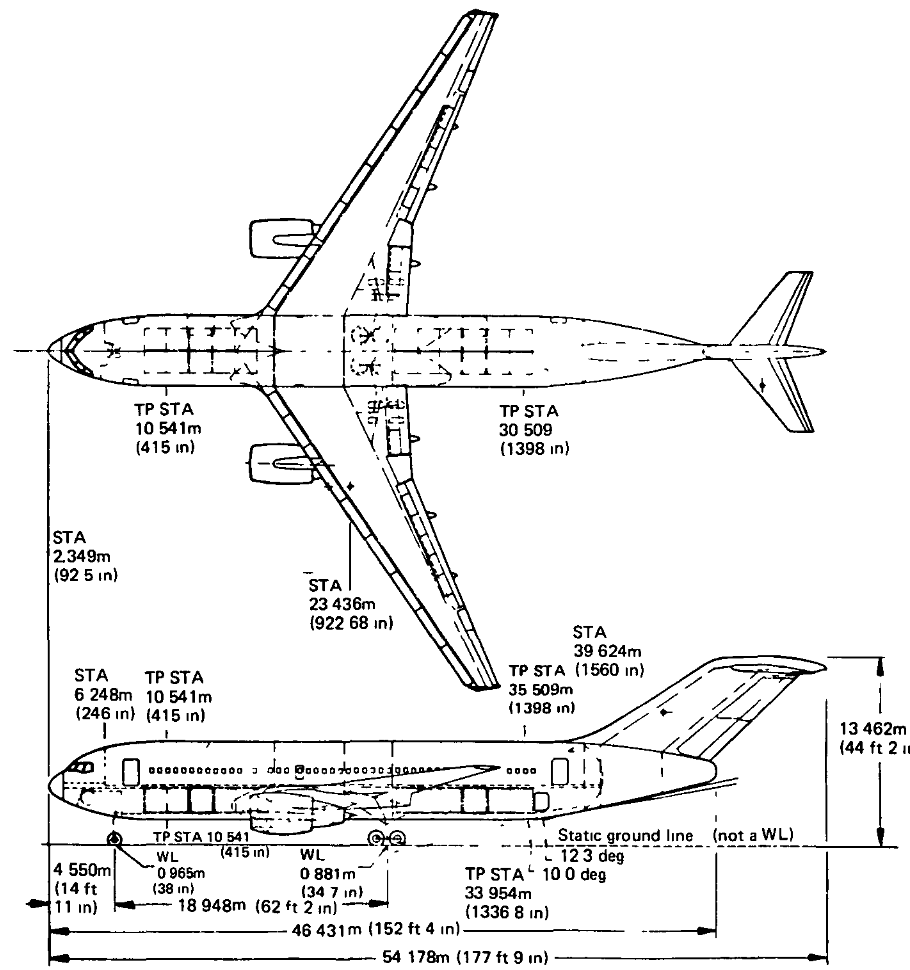

Figure 10. Initial ACT Configuration General Arrangement

768-103

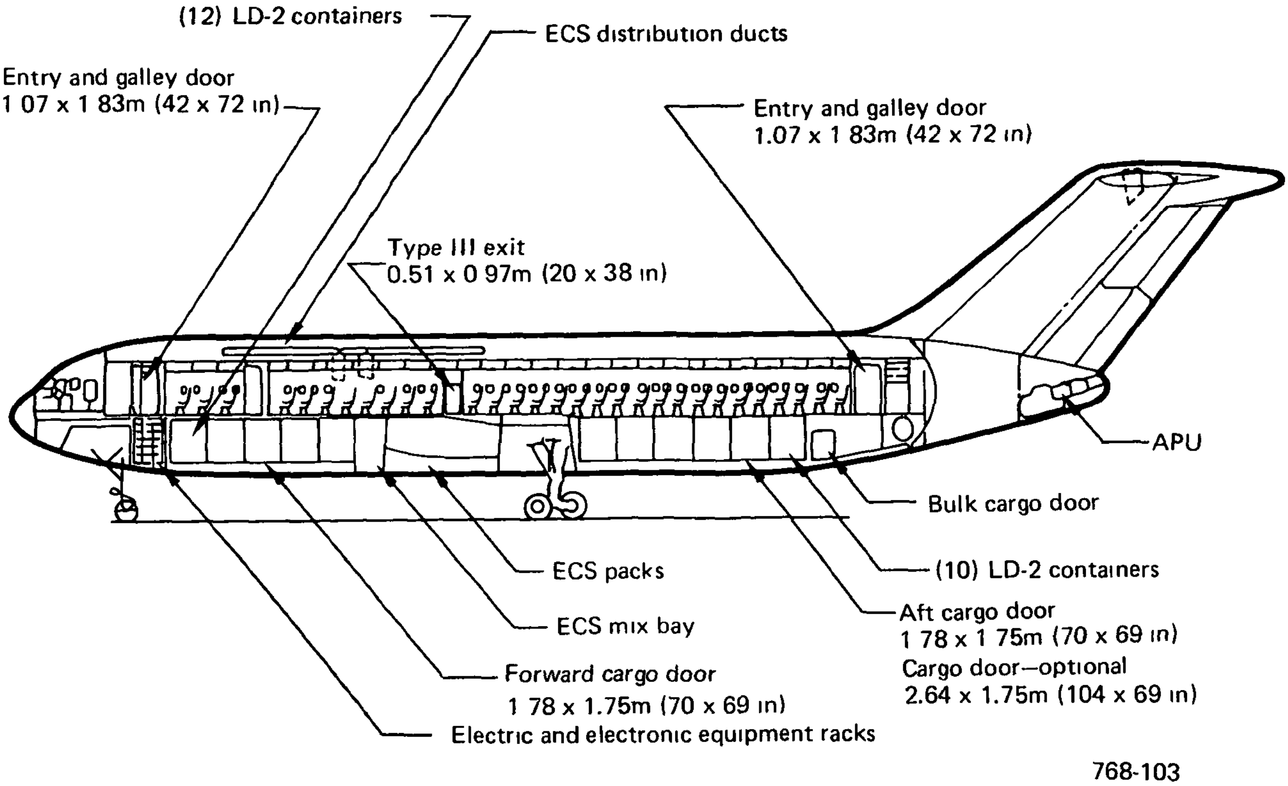

Figure 11. Inboard Profile

bays, environmental control packs and mixing bays, and landing gear. Doors for passenger entry, galley, emergency escape, and cargo also are shown.

5.2.3 BODY CROSS SECTION

In the body cross section, Figure 12, the upper lobe measures 5.03m (198 in) in diameter and provides 4.67m (184 in) seating width. The seven-abreast tourist-class seating is shown in the cross section. Low-density, first-class seating and high-density, inclusive-tour seating are shown as options (fig. 12). The lower lobe, sized for containers with bases 2.44m (96 in) wide, has a diameter of 4.92m (193.6 in). The total section height is 5.41m (213 in).

5.2.4 SEATING ARRANGEMENT

The upper part of Figure 13 shows seating arrangements for the basic two-class, 197-passenger version, including the locations of galleys, lavatories, cabin attendants'

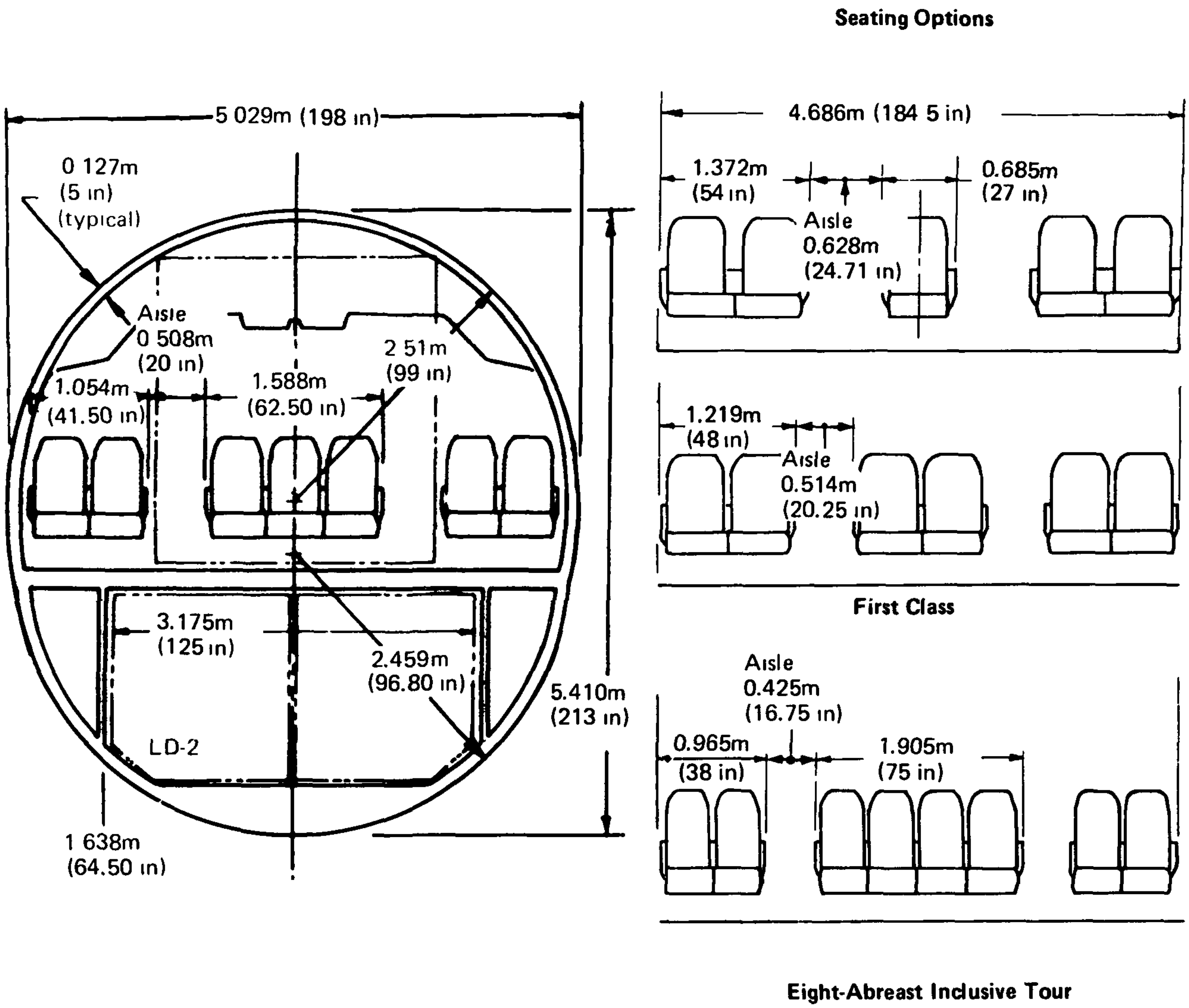

- Perimeter = 16.502m (649.70 in)
- Area = 21.6 m^2 (232 556 ft^2)

768-103

Figure 12. Body Cross Section

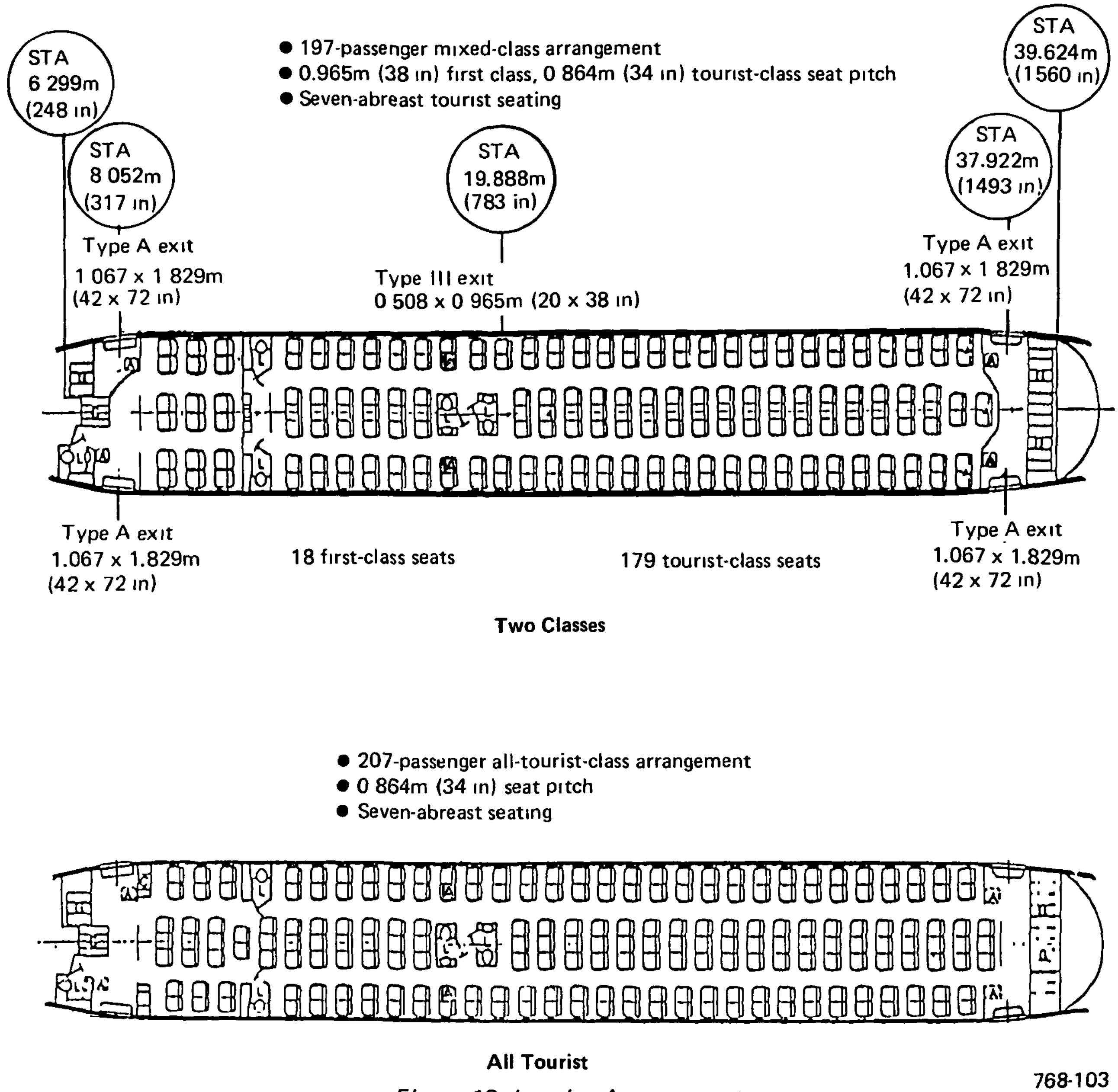

Figure 13. Interior Arrangement

seats, and cabin doors. The all-tourist version accommodates 207 passengers sitting seven-abreast with two aisles and seats spaced at 0.86m (34 in) pitch (lower part of fig. 13). Figure 12 shows additional seating options for first class and inclusive tour.

5.2.5 CARGO CAPABILITY (LOWER LOBE)

In the lower lobe, two compartments for containerized and bulk cargo will accommodate a dual row of LD-2 containers or a single row of LD-3 containers. The aft cargo compartment will also accommodate three pallets, each with a base 2.44m (96 in) wide and 3.18m (125 in) long, plus bulk cargo. The lower lobe cargo system and cargo volumes are shown in Figure 14. Container dimensions and volumes are illustrated in Figure 15.

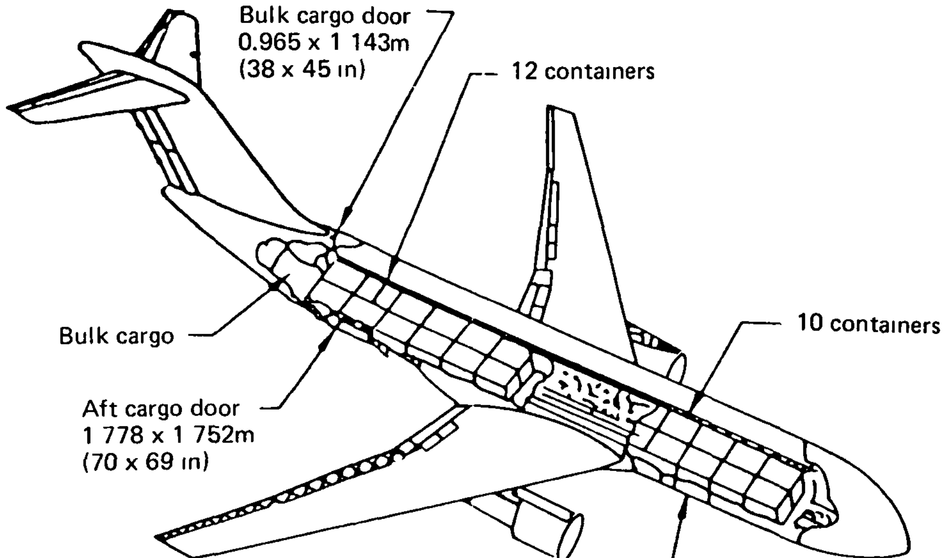

Volume, m^3 (ft^3)										
Forward compartment			Aft compartment				Total containerized			Total bulk
LD-2	LD-8	LD-3	LD-2	LD-8	LD-3	Bulk	LD-2	LD-8	LD-3	Bulk
33.98	34.55	22 37	40.78	41 46	26.85	11.33	74.76	76.01	49.22	11 33
(1200)	(1220)	(790)	(1440)	(1464)	(948)	(400)	(2640)	(2684)	(1738)	(400)

768-103

Figure 14. Lower Deck Cargo

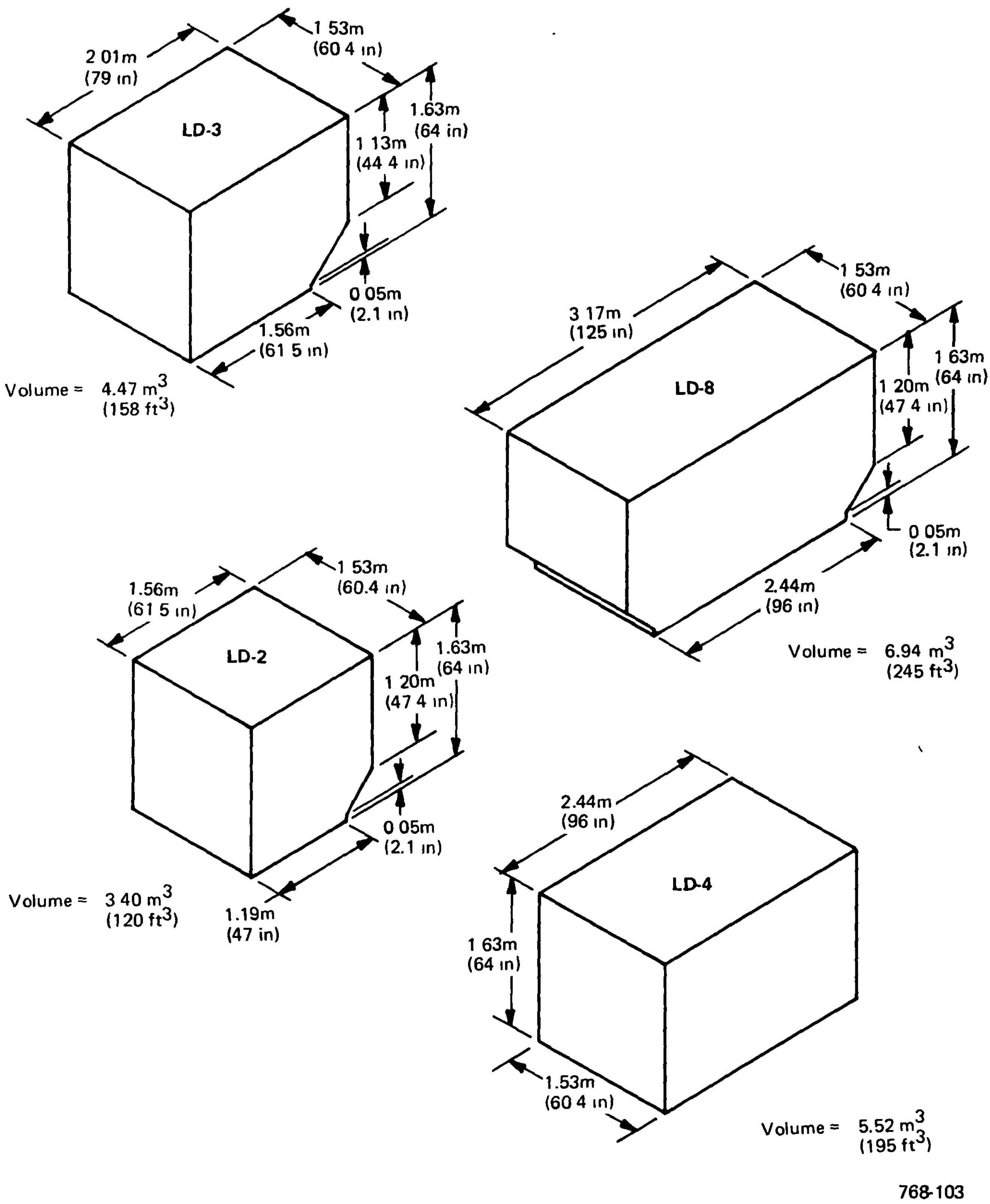

Figure 15. Cargo Containers

5.2.6 CARGO CAPABILITY (UPPER LOBE)

In all-cargo or in passenger/cargo combination versions, the upper lobe of the body will accommodate cargo containers that are 2.44m (8 ft) wide by 2.44m (8 ft) high by 3.05m (10 ft) long. Cargo pallets on a 2.44m (96 in) wide by 3.18m (125 in) long base also can be carried. A large forward cargo door, 2.57m (101 in) high by 3.40m (134 in) long, enables these cargo containers and/or pallets to be loaded. Although this feature is optional, space for installing this door has been provided in the Initial ACT Configuration.

5.2.7 PRIMARY FLIGHT CONTROL SYSTEM

The primary flight control system is similar to the Baseline Airplane System, except for the changes required for ACT, as described in Section 6.2.2.

5.2.8 PRINCIPAL CHARACTERISTICS

Principal characteristics of the Initial ACT Configuration are listed in Table 2.

Table 2. Initial ACT Configuration Principal Characteristics

Airplane size	
Maximum takeoff weight, kg (lb)	122 470 (270 000)
Wing area, m^2 (ft^2)	275.1 (2961) (aero reference area)
Wing span/sweep, m/deg (ft, in/deg)	47.24/31.47 (155, 0/31.47)
Location on body, percent body length	45.4
Location—engine pod on wind, percent b/2	33.6
Trailing-edge flaps	Single slot
Leading-edge devices	Slats
Horizontal tail area/$\overline{V}_H$, m^2 (ft^2)	32.0/0 551 (344/0.551)
Sweep, deg	35
AR/taper	4.0/0.40
Vertical tail area/$\overline{V}_V$, m^2 (ft^2)	54.0/0.090 (581/0.090)
Sweep, deg	55
AR/taper	0 67/0.70
Body cross section, m (in)	5.03W/5.41H (198 0W/213.0H)
Body length/overall length, m (ft, in)	46.43/54.18 (152, 4/177, 9)
Cabin length, m (in)	33.38 (1314)
Doors, number, type, size, m (in)	4, type A, 1.07 x 1.83 (42 x 72)
	2, type III, 0.51 x 0.97 (20 x 38)
Systems	
Engine number/type	2/CF6-6D2
Engine thrust (SLST), N (lb)	182 377N (41 000)
Nacelle and acoustic treatment	FAR 36 stage 3
Fuel capacity	
Wing tanks, m^3 (gal)	42.550 (11 240)
Center tanks, m^3 (gal)	Dry
Total, m^3 (gal)	42 550 (11 240)
Main gear wheelbase/track, m (in)	1 42/1 14 (56 0/45 0)
Location, percent MAC	64.9
Stroke/extended length, m (in)	0 51/3 18 (20/125)
Tire size wheel size, m (in)	1.09 x 0.39-0 51 (43 x 15.5-20)
Nose gear type/tire spacing, m (in)	Dual/0 61 (dual/24)
Stroke/extended length, m (in)	0.38/2.18 (15/86.0)
Tire size· wheel size, m (in)	0.94 x 0.33-0.41 (37 x 13-16)
Payload	
Flight crew/attendants	3/6
Mixed class passengers/split	197/9% first class, 91% tourist
All tourist passengers	207
Containers number/type	
Cargo	(22) LD-2 — (11) LD-3
Containerized, m^3 (ft^3)	74 76 (2640) — 49.22 (1738)
Bulk, m^3 (ft^3)	11.33 (400) — 11.33 (400)
Total, m^3 (ft^3)	86.09 (3040) — 60 55 (2138)
Center of gravity location	
Forward, percent MAC	21.0
Average cruise, percent MAC	31.8

768-103

5.3 PERFORMANCE

5.3 PERFORMANCE

Estimated performance data for the Baseline and Initial ACT Configuration are discussed in this section, with comparisons to the Baseline.

5.3.1 MISSION RULES

The mission is flown with a step-cruise procedure beginning at 10.7 km (35,000 ft) altitude, a cruise Mach number of 0.8, and standard day cruise conditions. Air Transport Association 1967 domestic reserves with a 370 km (200 nmi) alternate are used for determining range capability, which is quoted for a typical U.S. domestic mission profile (fig. 16) with full passenger payload and nominal performance.

5.3.2 PERFORMANCE CHARACTERISTICS

The Initial ACT and Baseline Configurations have the same gross weight, engine size, wing area, and payload. Performance comparison showed that in addition to cruise performance improvement, takeoff and landing performance were improved due to reduced trim drag with the cg about 11% farther aft. These improvements are realized despite a 1 deg loss in lift-off angle of attack at some takeoff flap conditions and a reduced tail clearance angle from 4 to 3 deg at touchdown.

Performance improvements for the Initial ACT Configuration are shown in Table 3. The improved cruise range resulted from reduced drag and reduced OEW. A 3.6% drag improvement, 2.4% due to a smaller empennage and 1.2% due to lower trim drag (with a farther aft cruise cg), increased the range about 204 km (110 nmi). This included the benefit of increased midcruise step weight; i.e., the 1219m (4000 ft) step in cruise altitude was made earlier at a higher weight. The reduced OEW and reserve fuel added 270 km (145 nmi) for a total improvement of approximately 13% or 474 km (255 nmi) still air range (SAR).

The takeoff performance of the Initial ACT Configuration improved primarily due to the reduced trim drag with a farther aft forward cg limit (0.10 to 0.21 MAC) and longer tail arm. However, for the leading edge in the slotted position and the trailing edge at moderate flap angle settings, the airplane was geometry-limited. Although

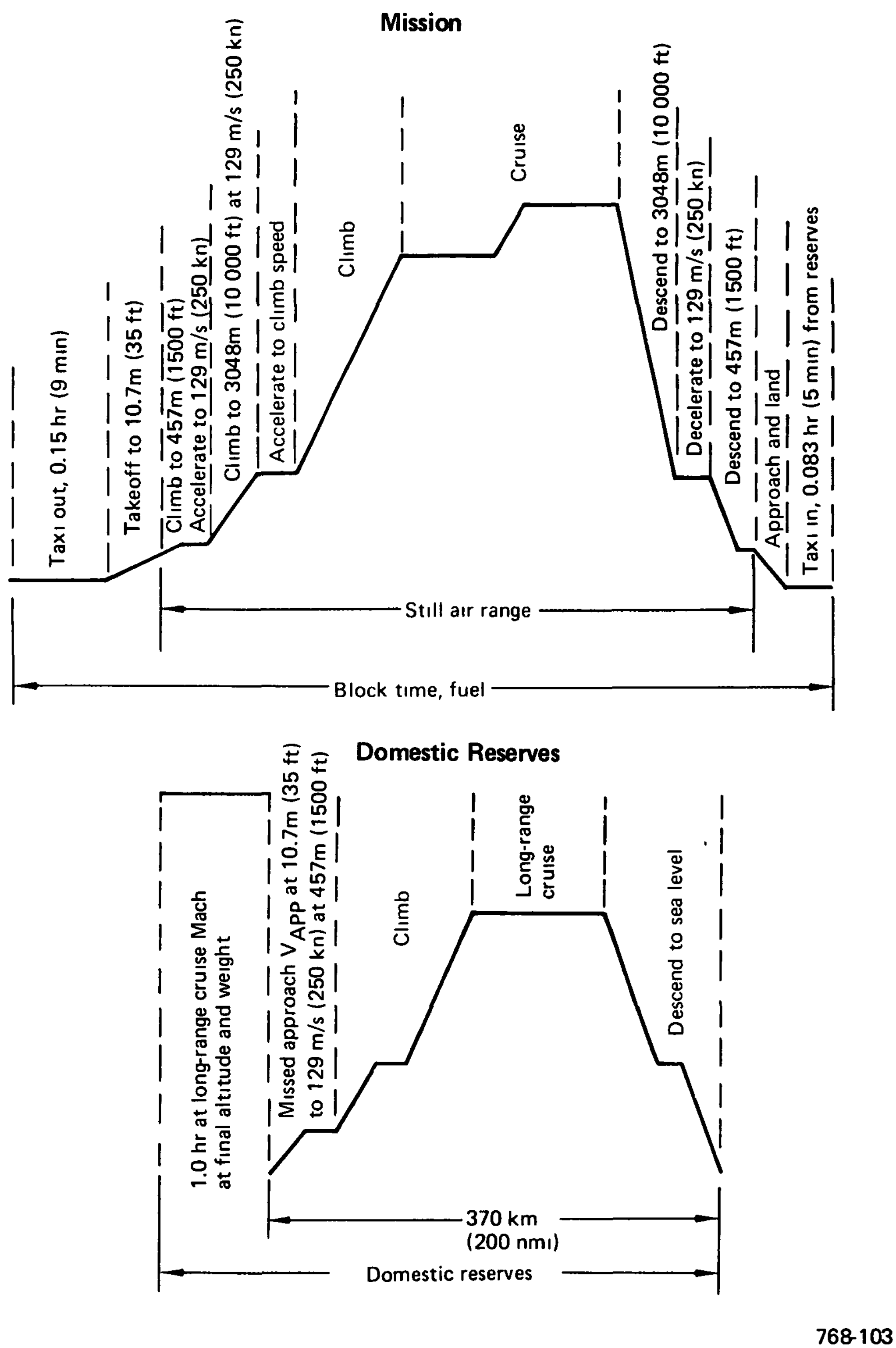

Figure 16. Typical Mission Profile

Table 3. Conventional Baseline and Initial ACT Performance Comparison

	Baseline	Initial ACT	Δ
MTW, kg (lb)	122 920 (271 000)	122 920 (271 000)	---
TOGW, kg (lb)	122 470 (270 000)	122 470 (270 000)	---
MZFW, kg (lb)	104 400 (230 160)	103 470 (228 110)	-930 (-2050)
MLW, kg (lb)	112 570 (248 160)	111 640 (246 110)	-930 (-2050)
OEW, kg (lb)	78 300 (172 610)	77 370 (170 560)	-930 (-2050)
Forward center of gravity, percent MAC	10 0	21 0	+11 0
Average cruise center of gravity, percent MAC	20 5	31 8	(+11.3)
Cruise L/D, (M = 0 8, C_L = 0.45)	Base	(+3 6)	(+3.6)
SAR, km (nmi)	3 589 (1 938)	4 061 (2 193)	+472 (+255)
TOFL, (SL 29°C (84°F) m (ft)	2 210 (7 250)	2 118 (6 950)	-92 (-300)
V_{APP} at maximum landing weight, m/s (kn)	70.0 (136.1)	68.6 (133 4)	-1 4 (-2 7)
Landing field length, sea level, dry, at maximum landing weight, m (ft)	1 443 (4 735)	1 402 (4 600)	-41 (-135)

768-103

the Initial ACT Configuration gear was canted aft 7 deg, with the wing moved forward 1.68m (66 in), the overall rotation capability decreased approximately 1 deg (from 13.0 to 12.0 deg). The α_{MU} limit increased takeoff field length (TOFL) at sea level, and 29°C (84°F), by approximately 45.7m (150 ft) relative to that set by a $1.2V_S$ reference speed. The overall TOFL improvement of 91.4m (300 ft) at sea level and 29°C (84°F) maximum takeoff gross weight (TOGW) conditions included the geometry-limited condition.

Relative to the Baseline, the approach speed of the Initial ACT Configuration decreased 1.4 m/s (2.7 kn). Tail clearance angle at touchdown decreased from 4 deg to 3 deg. The block fuel and block time data for the Baseline and Initial ACT Airplanes are compared in Figure 17. A net fuel saving trend versus mission SAR is shown in Figure 18. At the average mission stage length of 863 km (466 nmi), 3.3% block fuel,

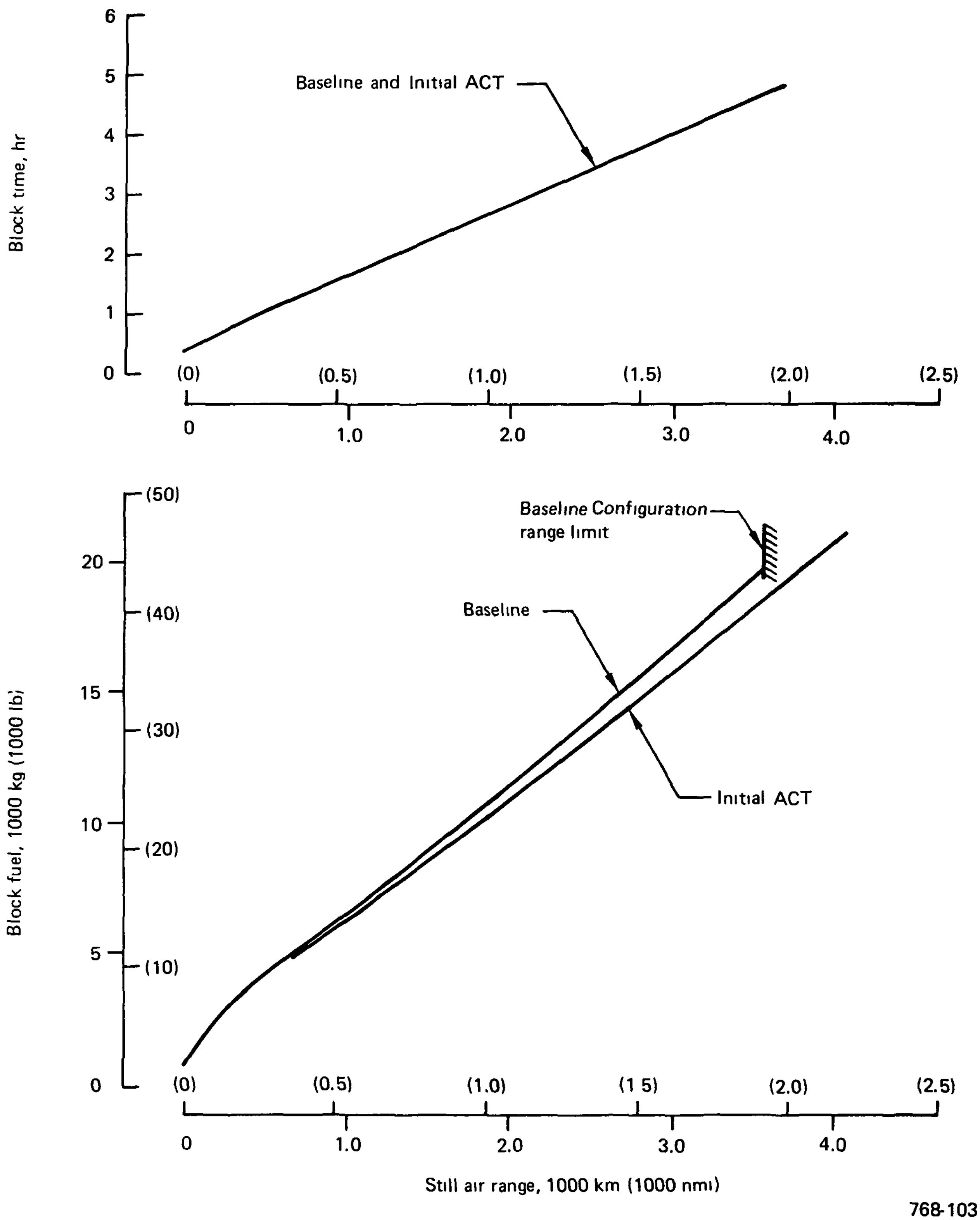

Figure 17. Block Fuel and Block Time Data for Conventional Baseline and Initial ACT Configurations

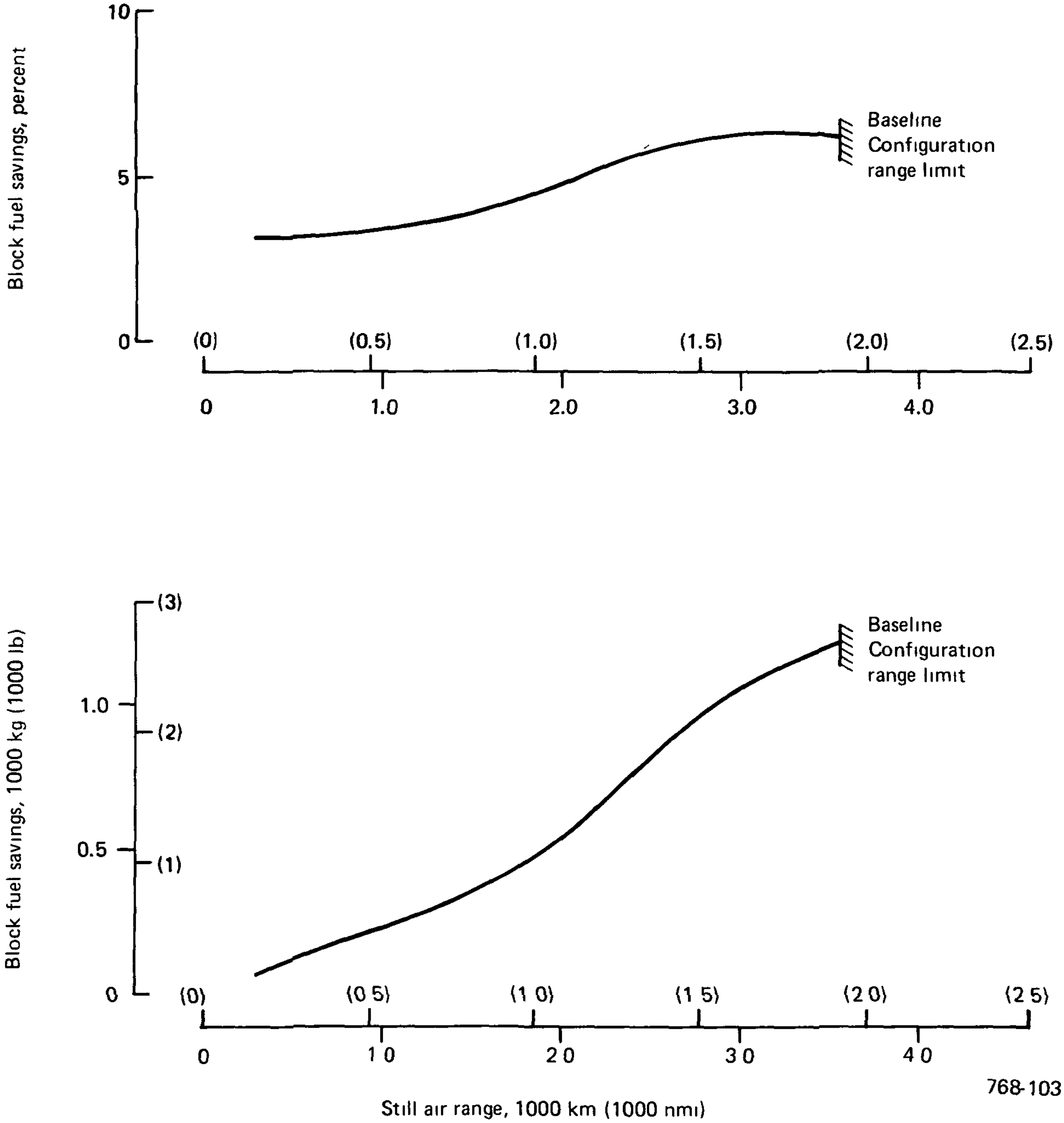

Figure 18. Fuel Usage Savings

180 kg (400 lb) were saved with the Initial ACT Configuration. At the Baseline range limit the fuel savings is about 6%. For a fixed design TOGW of 122 470 kg (270 000 lb), the reduced drag (9.2 counts) and OEW of 930 kg (2050 lb) increased SAR by 472 km (255 nmi).

In summary, the Initial ACT Configuration with the same gross weight, payload, engine, and wing size as the Baseline Configuration offered these performance benefits:

- Increased range = 13%
- Reduced block fuel = 6% (at Baseline range limit)
- Reduced takeoff field length = 4% (sea level)
- Reduced landing approach speed = 2%

Further performance benefits may be realized for missions where payload is limited by takeoff performance. For example, at Denver on a hot day, payload may be increased due to reduced OEW and a higher TOGW that satisfies both TOFL and climb gradient requirements. Rough estimates indicated a 2268 kg (5000 lb) increased Denver TOGW. This added effect of increasing payload or range could, for some route segments, increase profitability far more than the reduced fuel burned at a given payload/range.

5.3.3 NOISE

Since the propulsion system and the low-speed performance characteristics of the Initial ACT Configuration are so little changed from the Baseline, a specific noise analysis was not undertaken. The changes are all expected to be small improvements. Therefore, the Initial ACT Configuration noise characteristics are conservatively considered to be the same as the Baseline.

5.4 WEIGHT, BALANCE, AND INERTIA

Page

5.4 WEIGHT, BALANCE, AND INERTIA

5.4.1 FUNCTIONAL WEIGHT ASSESSMENT

A functional weight assessment provides visibility of the increments comprising the net benefit of active controls. Table 4 presents sequential weight increments for the ACT functions and systems as they were incorporated on the Initial ACT Configuration. The sequence is that which was followed for the structural loads and sizing analysis. Deviation from this sequence would result in differences in functional weight increments attributed to each ACT function and accumulative OEW increments.

Balance considerations for moving the cg range aft, such as maneuver and stability margins, are discussed in Subsection 7.1, "Flying Qualities." Analysis sequence of the active controls functions is described in Subsection 7.2, "Structural Analyses."

5.4.2 DESIGN WEIGHTS

Design weights used for structural loads analysis are listed in Table 5.

5.4.3 AIRPLANE MOMENTS OF INERTIA

Airplane moments of inertia for the Initial ACT Configuration about the three airplane reference axes and the product of inertia, I_{XZ}, are shown in Figures 19 through 22. Two critical gross weight conditions and the maximum inertias that resulted from distributed payload loading are shown versus cg.

5.4.4 CENTER-OF-GRAVITY MANAGEMENT

A cg management (loadability) diagram is presented in Figure 23. In determining the required cg loading range, a tolerance (+3% to -4% MAC) is applied to the nominal OEW cg (34% MAC) to account for manufacturing variations and airline options, such as increased cargo accommodations and engine substitution. The aft payload envelope is critical for 197 mixed-class passengers (18/179), establishing the aft cg envelope for payload. The forward envelope is critical for 207 tourist-class passengers and establishes the forward cg limit required for payload.

Table 4. Weight Assessment of Active Controls

Active control function/system	OEW increment from Baseline Configuration		Cumulative subtotal OEW increment[a]	
	kg	lb	kg	lb
Relaxed static stability (RSS)	**-414**	**-913**	**-414**	**-913**
Move center of gravity aft limit aft from 38% MAC to 46% MAC Included in the data are the effects of shifting the wing 1 68m (66 in) forward on the body				
Reduce body primary structure due to reduced horizontal tail loads	-122	-270		
Reduce wing box primary structure due to reduced horizontal tail loads	-73	-160		
Move main landing gear aft from 56% MAC to 64.9% MAC (reduced design loads)	-77	-170		
Change main landing gear design concept from conventional to swinging arm				
Landing gear structure	+281	+620		
Body structure and cargo handling system	+195	+430		
Reduce horizontal tail area from 57.6 to 32.0 m^2 (620 to 344 ft^2); substitute double-hinged versus single-hinged elevator	-482	-1063		
Reduce vertical tail area from 57.4 to 54 0 m^2 (618 to 581 ft^2)	-257	-566		
Add pitch augmentation system	+121	+266		
Add angle-of-attack limiter (AAL)	b	b		
Wing load alleviation (WLA)	**-659**	**-1452**	**-1073**	**-2365**
Reduce wing box primary structure due to reduced gust and maneuver loads	-780	-1720		
Add systems components accelerometers, computer changes, and electric wiring	+122	+268		
Flutter mode control (FMC)	**+143**	**+315**	**-930**	**-2050**
Reduce wing box structure for FMC off flutter speed = V_D	-82	-180		
Segment outboard aileron	+64	+140		
Add flutter suppression system components (provide flutter speed capability = 1 2V_D)	+25	+55		
Add one spoiler panel per side (five versus four)	+32	+70		
Add outboard structural reserve fuel tank	+104	+230		

[a]Subtotals are applicable only for the active control functional sequence shown

[b]Stick pusher [24 kg or (53 lb)] was included in the weight definition of the Baseline Configuration Normally, this feature is added with the RSS function.

768-103

Table 5. Design Weights for Structural Loads Analysis

Weight	kg	(lb)
Operational empty weight (OEW)	77 370	(170 560)
Maximum design zero fuel weight (MZFW)	103 470	(228 110)
Maximum design zero fuel weight with structural reserve fuel	106 420	(234 610)
Maximum design landing weight (MLW)	111 640	(246 110)
Maximum design takeoff weight (MTOW)	122 470	(270 000)
Maximum design taxi weight (MTW)	122 920	(271 000)

768-103

The forward and aft cargo compartment cargo moment vectors are based on 22 LD-2 containers at 105 kg/m^3 (6.58 lb/ft^3) density. Adding vectors for the bulk cargo compartment completes the loading envelope for the zero fuel weight airplane. Maximum design zero fuel weight (MZFW) establishes the maximum allowable payload.

The fuel system includes one main tank and one structural reserve tank per side. The structural reserve tanks, incorporated into the outboard wing for flutter stability, have a capacity of 1406 kg (3100 lb) per airplane. Normal operational speeds and speed margins are available only with this tank full. Transfer of fuel from the structural reserve tank would normally occur when the total airplane fuel is 3180 kg (7000 lb) or less, in combination with a reduction in operational and limit speeds to retain appropriate speed margins.

The forward and aft required operating center-of-gravity limits must allow the loading of full containerized cargo, with or without bulk, with any passenger load, (assuming seating order is window, aisle, then remaining seats). The aft flight limit is established aft of the aft operating limit by a moment margin that covers in-flight movements of passengers and crew, control surface deflections, landing gear movements, and fuel vector moment difference. The forward operating limit is established by the center-of-gravity range required for payload loadability. The 21%

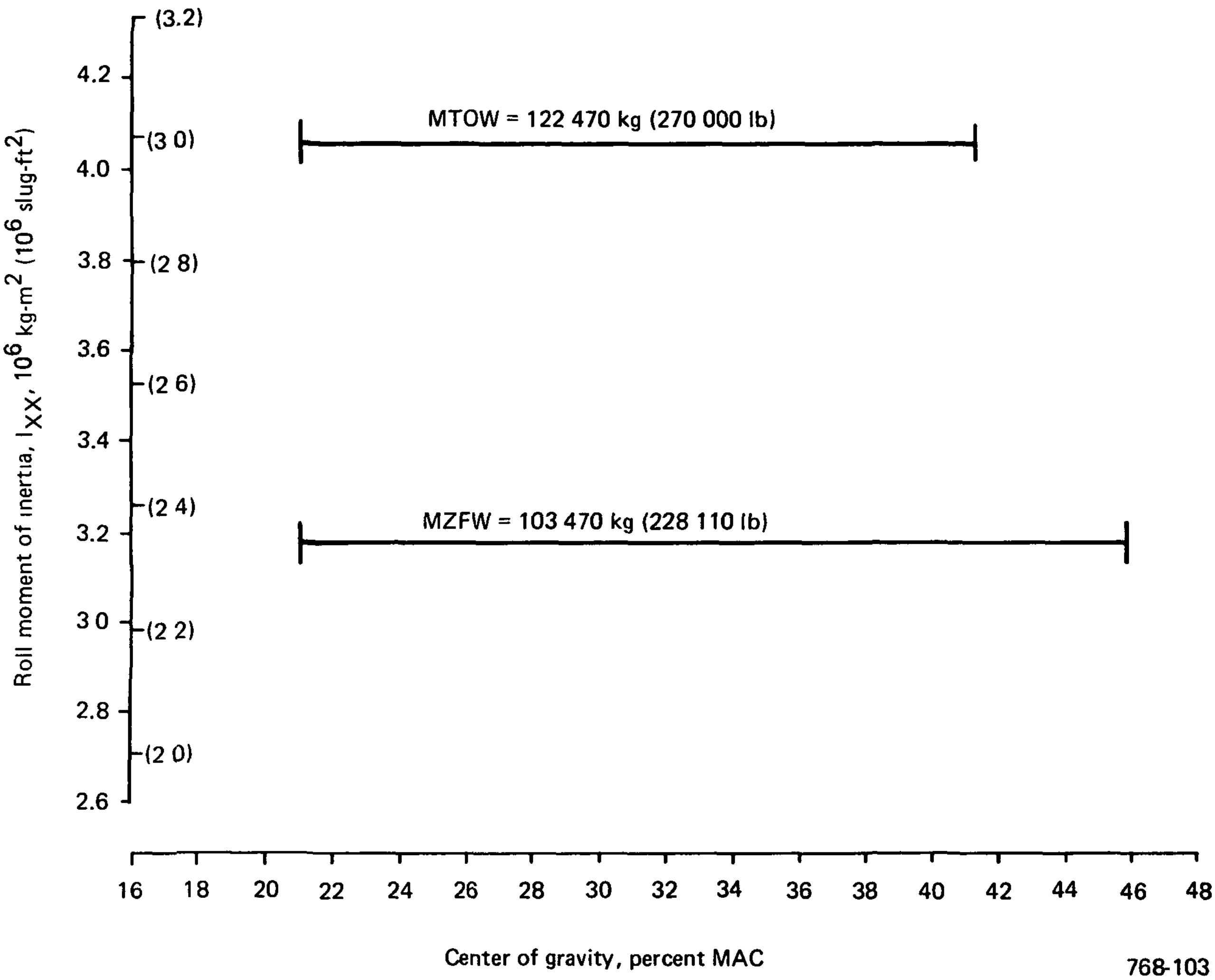

Figure 19. Roll Moment of Inertia

MAC forward required flight limit, then, clears the forward operating limit by a similar margin for in-flight movement and fuel moment difference (footnote a, fig. 23).

The typical cruise center of gravity is based on a payload definition consistent with the performance analysis ground rules used for a typical airline customer.

For the Initial ACT Configuration, the 46% MAC aft required flight limit is slightly exceeded by the extreme aft loading distribution of passengers plus cargo payload. A

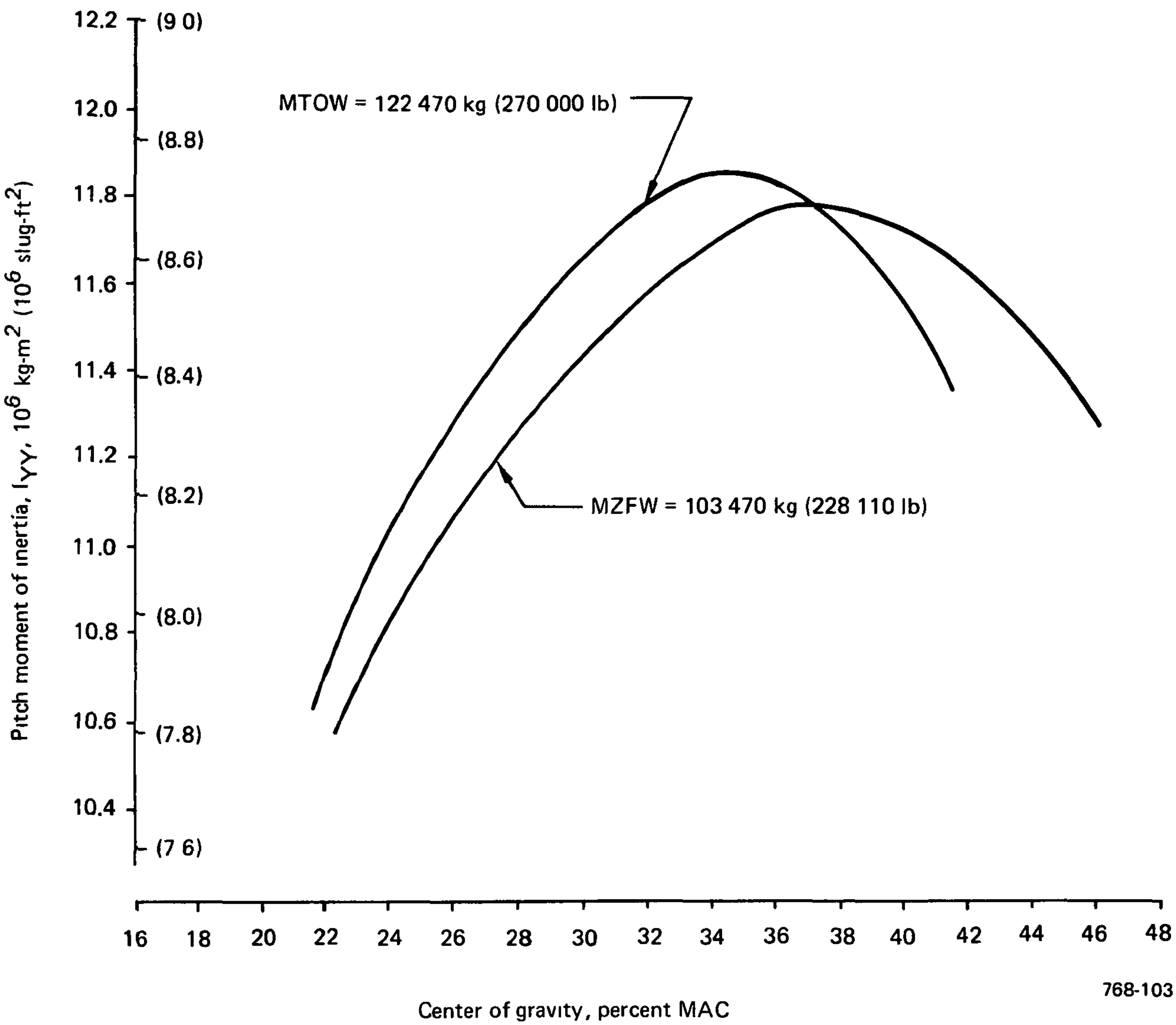

Figure 20. Pitch Moment of Inertia

ballast of 272 kg (600 lb) would be required in the nose-gear wheel well to stay within the design center-of-gravity envelope. However, a wing shift aft of approximately 0.051m (2 in) would eliminate this aft center-of-gravity problem with minor weight changes. Resources and time were not available to recycle the configuration. No ballast weight is included in the Initial ACT OEW, thus compatibility with the Conventional Baseline airplane and subsequent IAAC study configurations is maintained.

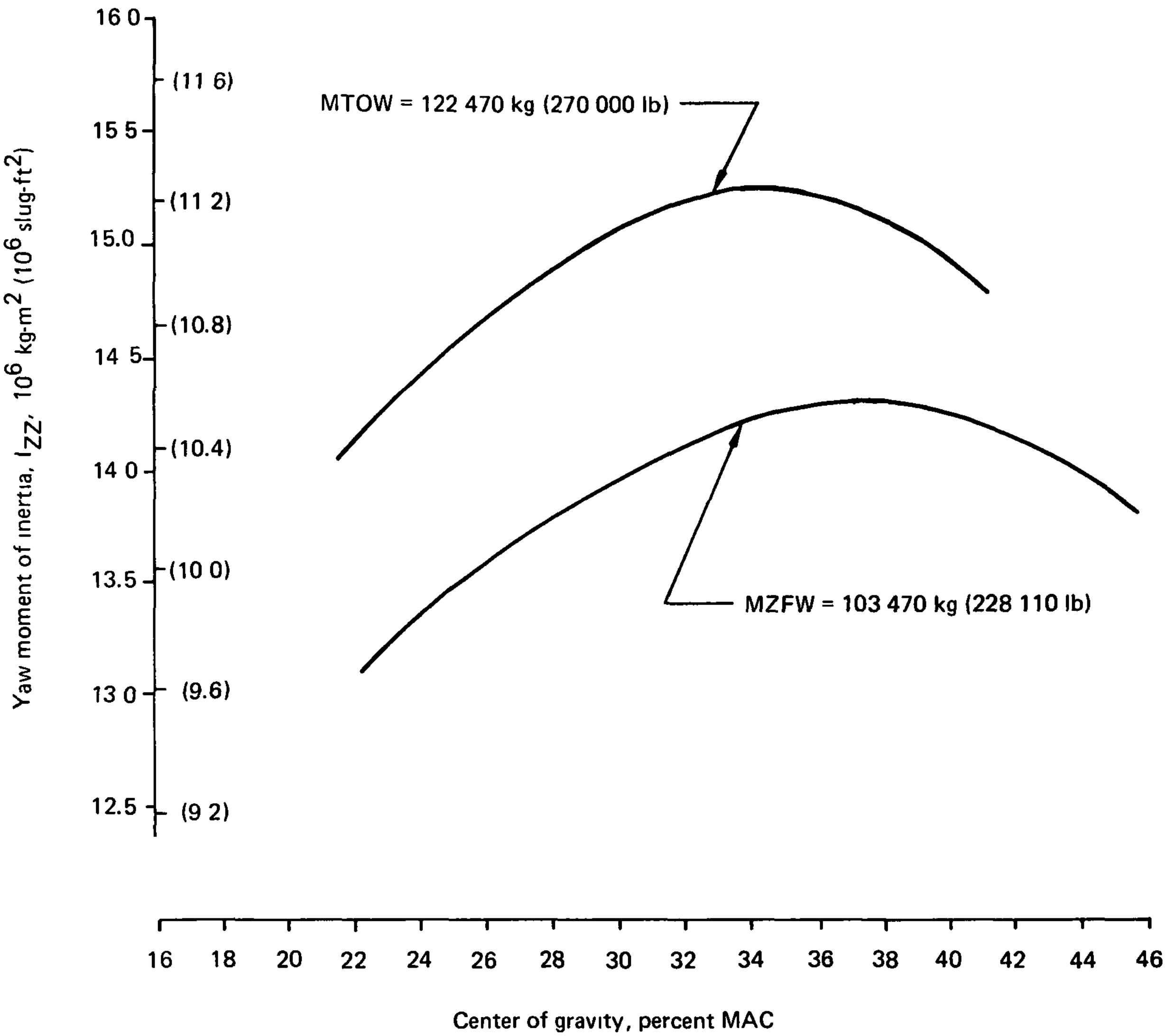

Figure 21. Yaw Moment of Inertia 768-103

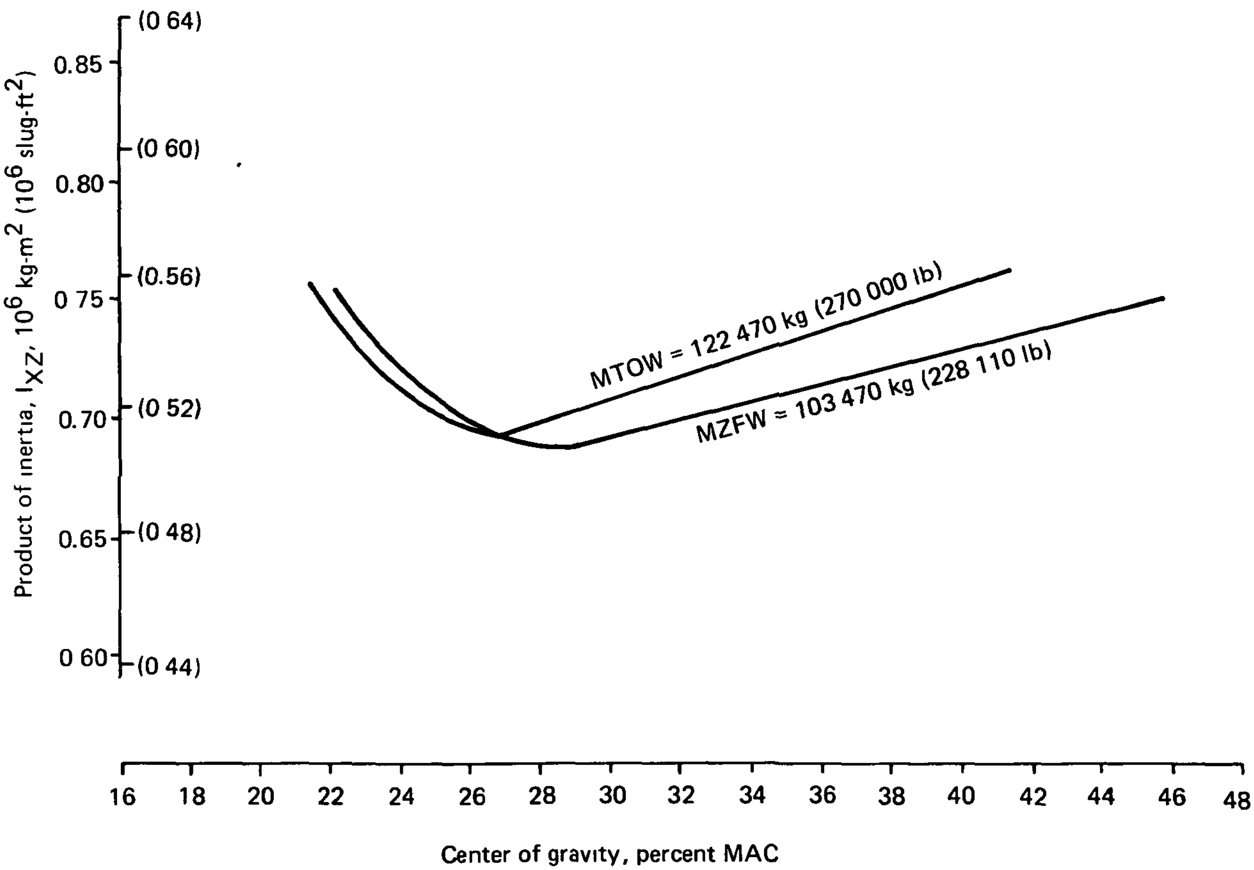

Figure 22. Product of Inertia

768-103

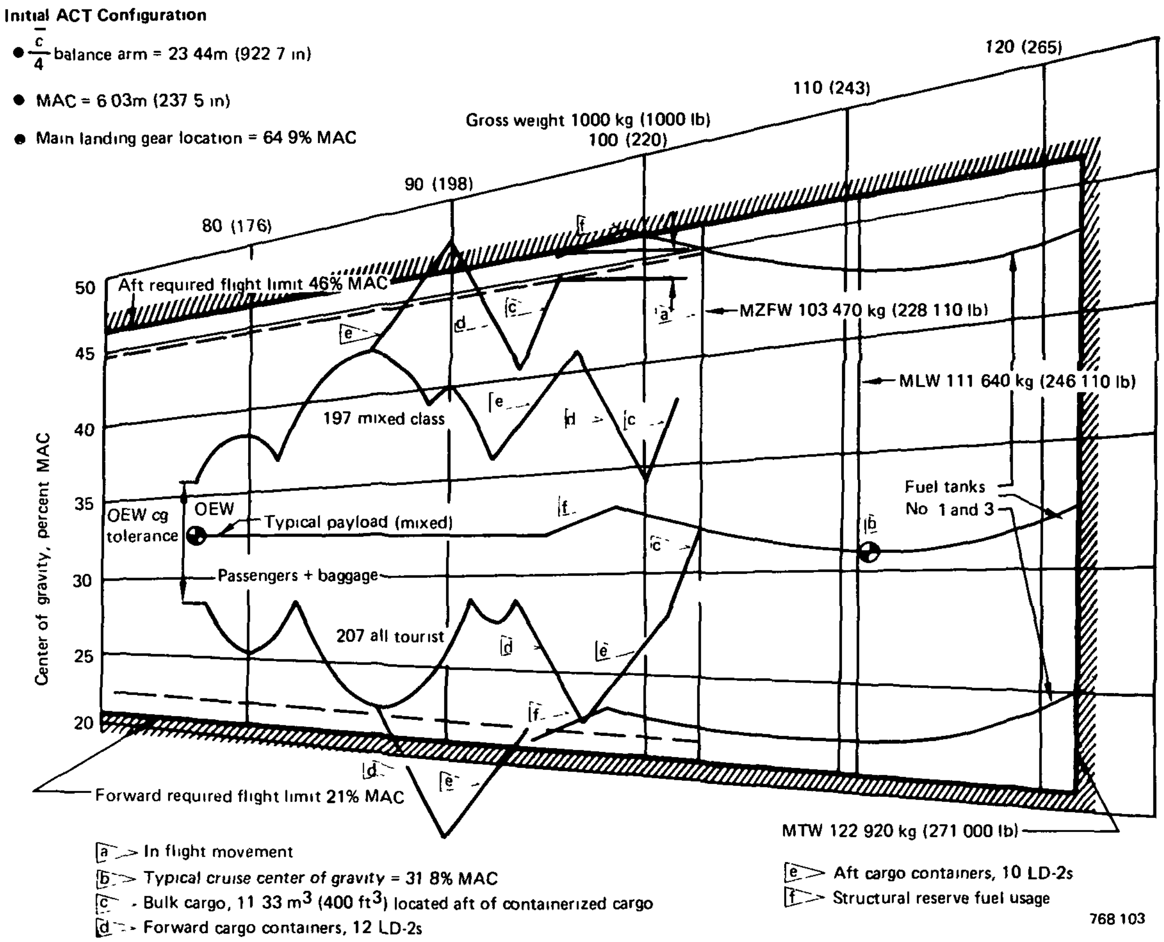

Figure 23. Center-of-Gravity Management

6.0 DESIGN DATA

The design details of the Initial ACT Configuration, described in Section 5.0, are discussed in this section. Design and analysis necessarily interact to arrive at a validated final configuration. The data presented in this section represent the status of this configuration at the end of the Initial ACT task. Supporting analysis is presented in the following section.

A structures description of the major airplane components is presented in Subsection 6.1, followed by a description of the major airplane systems that will affect, or be affected by, ACT systems (subsec 6.2).

6.1 AIRPLANE STRUCTURE

The airplane structure is presented in five major elements, which are described in the following subsections:

- Wing (6.1.1)
- Body (6.1.2)
- Horizontal tail (6.1.3)
- Vertical tail (6.1.4)
- Main landing gear (6.1.5)

Although these elements are similiar to those of the Baseline Configuration (ref 1), some details differ. Elements identical to the Baseline are not discussed in this section.

Conventional materials and construction are used in the design and fabrication of the airframe, except for a limited amount of graphite epoxy composite secondary structure. The airframe consists primarily of aluminum alloys, including advanced alloys selected to offer a high degree of structural reliability for the operational requirements and service life of the airplane. Highly stressed landing gear components are fabricated from high-strength vacuum melt steel.

6.1.1 WING

The wing structure basically duplicates that of the Baseline Configuration. It consists of left and right main outboard sections, joined to a wing center section through the body (fig. 24). The outboard sections include the wing box, the fixed leading- and trailing-edge structures, leading-edge slats and trailing-edge flaps, ailerons, spoilers, and wing tip. The wing-box structure is of conventional two-spar construction. The outboard wing-box structure, joined to the center section at the side-of-body rib, consists of stringer-stiffened upper and lower panels and build-up spars and ribs. The lower panel side-of-body splice is a double-shear design to reduce eccentricity and to improve durability. The spars consist of upper- and lower-machined chords; machined webs with pads around cutouts; and machined, extruded web stiffeners. The intermediate ribs are built up with extruded chords, stiffeners, and sheet webs.

Special ribs at engine- and landing-gear supports, trailing-edge flap supports, and the side-of-body joint incorporate backup and terminal fittings and skin panel shear ties as required. Chords and stiffeners are machined extrusions; webs are machined plate. Pin joints attach the landing gear support beam to the rear spar and fuselage. The space between the front and rear spars and between upper and lower wing panels of the outboard wing sections is liquid-vapor sealed to provide fuel storage. The volume is divided as required for fuel system requirements by tank-end ribs. Baffles control fuel movement.

The wing center section structure consists of stringer-stiffened upper and lower panels; built-up front and rear spars; three spanwise, full-depth beams; and a centerline rib. Fore and aft internal intercostals on the lower surface provide fixity for the lower surface stiffeners. External fore and aft floor beams on the upper surfaces provide fixity for the upper surface stiffeners. The center section is a dry bay area, but it includes fuel seal planes and structural provisions for an integral fuel tank.

The wing leading-edge slats consist of eight three-position slat assemblies per side. Each slat is supported by two machined tracks, programmed by two auxiliary tracks, and actuated by a ball-screw actuator. An additional two-position slat, sealed to the

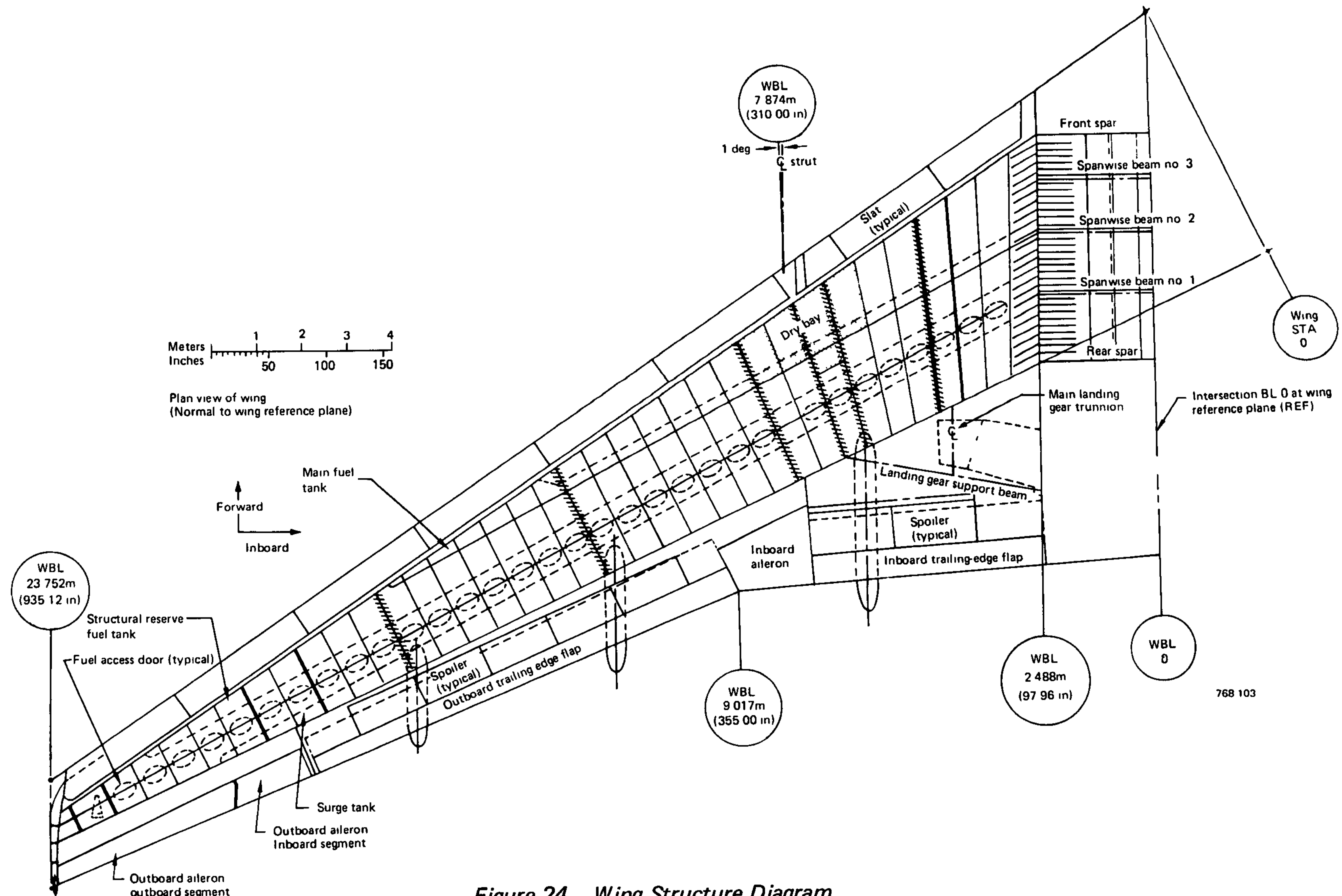

Figure 24. Wing Structure Diagram

inboard side of the nacelle strut in the extended position, is supported by two machined tracks and actuated by a rotary gear box and a linkage mechanism.

The single-slotted trailing-edge flaps consist of one inboard and one outboard section. The flaps are supported and extended by chordwise-oriented linkage mechanisms actuated by rotary gear boxes. A portion of each flap support mechanism extends below wing contour and is enclosed in streamwise fairings.

Each inboard and outboard aileron is hydraulically actuated and is attached to the rear spar on self-aligning bearings. The outboard aileron is divided into two segments.

Seven hydraulically operated flush spoilers are provided in the upper surface of each wing aft of the rear spar (fig. 24). The five outboard spoilers on the left and right wing are identical. The two inboard spoilers on the left wing are opposite handed to the two on the right wing.

6.1.2 BODY

The body consists of permanently joined major subsection assemblies, with a double-lobe cross section formed by upper and lower radii faired together with a second-degree curve. The basic body structure, of aluminum alloy, is of semimonocoque construction with formed hat section longitudinal stiffeners attached to the skin panels. Basic body frames are pitched at 0.559m (22 in). The body aft of the aft pressure bulkhead is constructed like the pressurized area except for the additional machined bulkheads, firewalls, and vertical tail attachment fittings. Support structure for mounting the auxiliary power unit (APU) equipment is also in this section.

The wing/body joint is designed so that the full body depth is effective in the vertical bending mode in the area of the wing center section. Machined fittings, which attach the main body bulkheads to the front and rear spars, and the body skin, which attaches to the wing upper surface "plus" chord, comprise the wing/body joint. The intermediate frames attach to the wing at the side-of-body rib and to the outboard longitudinal floor beams. A centerline diagram of the body structure is shown in Figure 25.

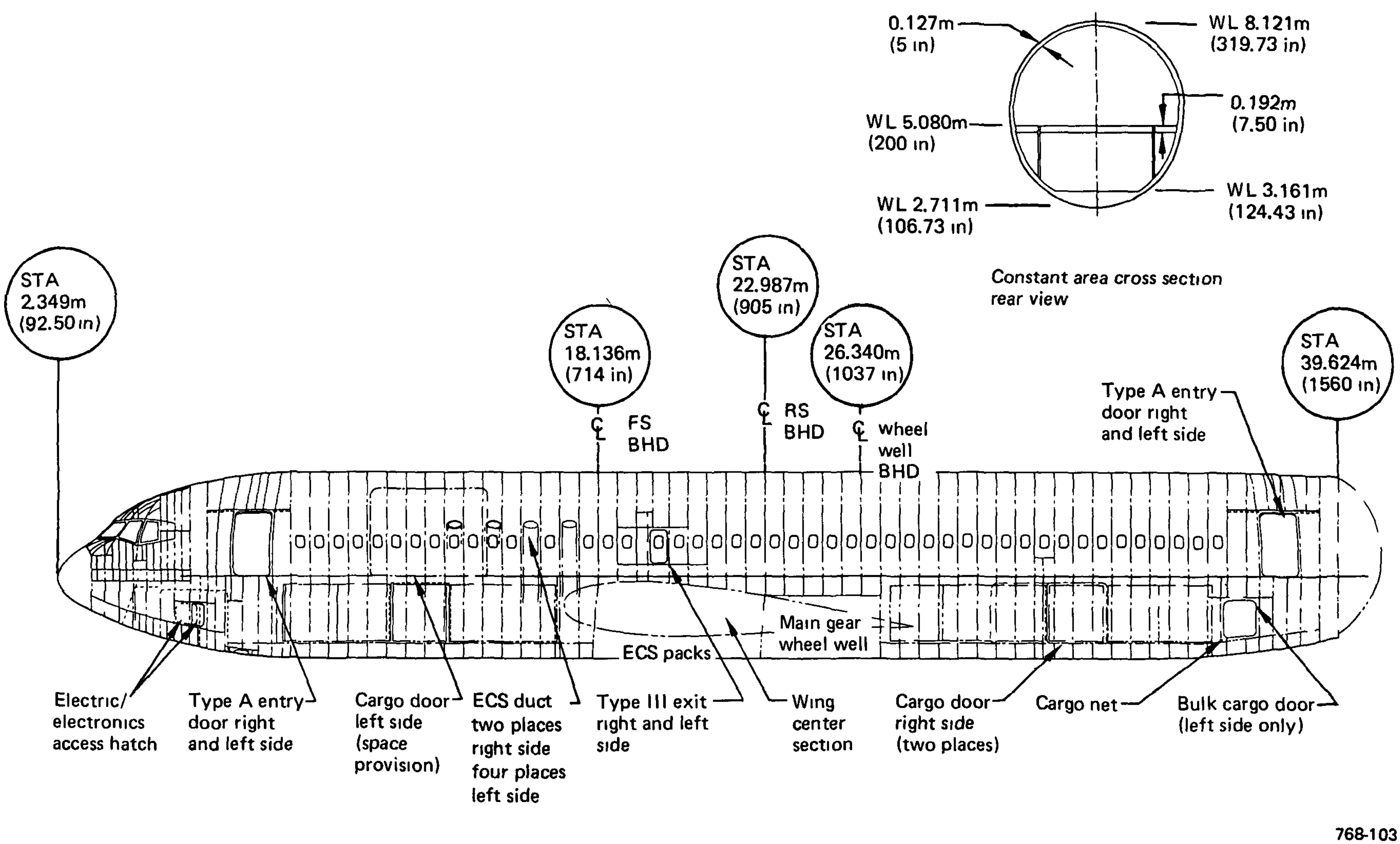

Figure 25. Body Centerline Diagram

6.1.3 HORIZONTAL TAIL

The horizontal tail is adjustable for airplane pitch trim and is actuated by a fail-safe jack-screw actuator. Elevator hinges are supported at the rear spar. The horizontal tail primary structure consists of a torque box from the side-of-fairing rib to the tip rib. The torque box is constructed of stiffened panels supported by built-up ribs and spars. The center section consists of the front and rear spars. The leading edge is a removable assembly of skin and closely spaced sheet-metal ribs. The double-hinged elevator, controlled by hydraulic actuators, is removable at the actuators and hinges. The horizontal tail tapers in thickness and width. Space for logo lights is provided. A centerline diagram of the horizontal tail structure is shown in Figure 26.

6.1.4 VERTICAL TAIL

The vertical tail supports the horizontal tail. The rudder-hinge ribs are attached to its rear spar. The rudder consists of an upper and lower double-hinged segment controlled by hydraulic actuators. The rudders are removable at the actuators and hinges. The vertical tail tapers in thickness and width. Space for a very high frequency omnidirectional radio range (VOR) antenna is provided.

The vertical tail primary structure is a full-span torque box of stiffened panels supported by built-up ribs and spars, with fixed attachments to the aft body. The leading edge consists of a forward removable assembly supported by closely spaced sheet-metal ribs. A centerline diagram of the vertical tail structure is shown in Figure 27.

6.1.5 MAIN LANDING GEAR

The swing arm, double-post main-landing-gear arrangement (fig. 28) is mounted from the wing rear spar and auxilliary beam and is stowed in the body. Compliance with balance requirements and the relatively forward position of the wing caused the main gear installation to be one of the major design problems of the Initial ACT Configuration, as described in Subsection 5.1.2.

- Dimensions
  - Area = 31.96 m^2 (344 ft^2)
  - AR = 4 00
  - TR = 0 40
  - Λ (0.25c) = 35 deg
  - t/c = 0 11 (root), 0 09 (tip)
  - MAC = 3.000m (118 10 in)
  - Span = 11 306m (445 13 in)
  - Anhedral = 3 deg
  - Trim limits = 4 deg up, 14 deg down
  - Elevator travel = 28 deg up, 20 deg down
  - Tab travel = 28 deg up, 20 deg down (relative to elevator)

Note Dimensions in figure are in plane of the surface

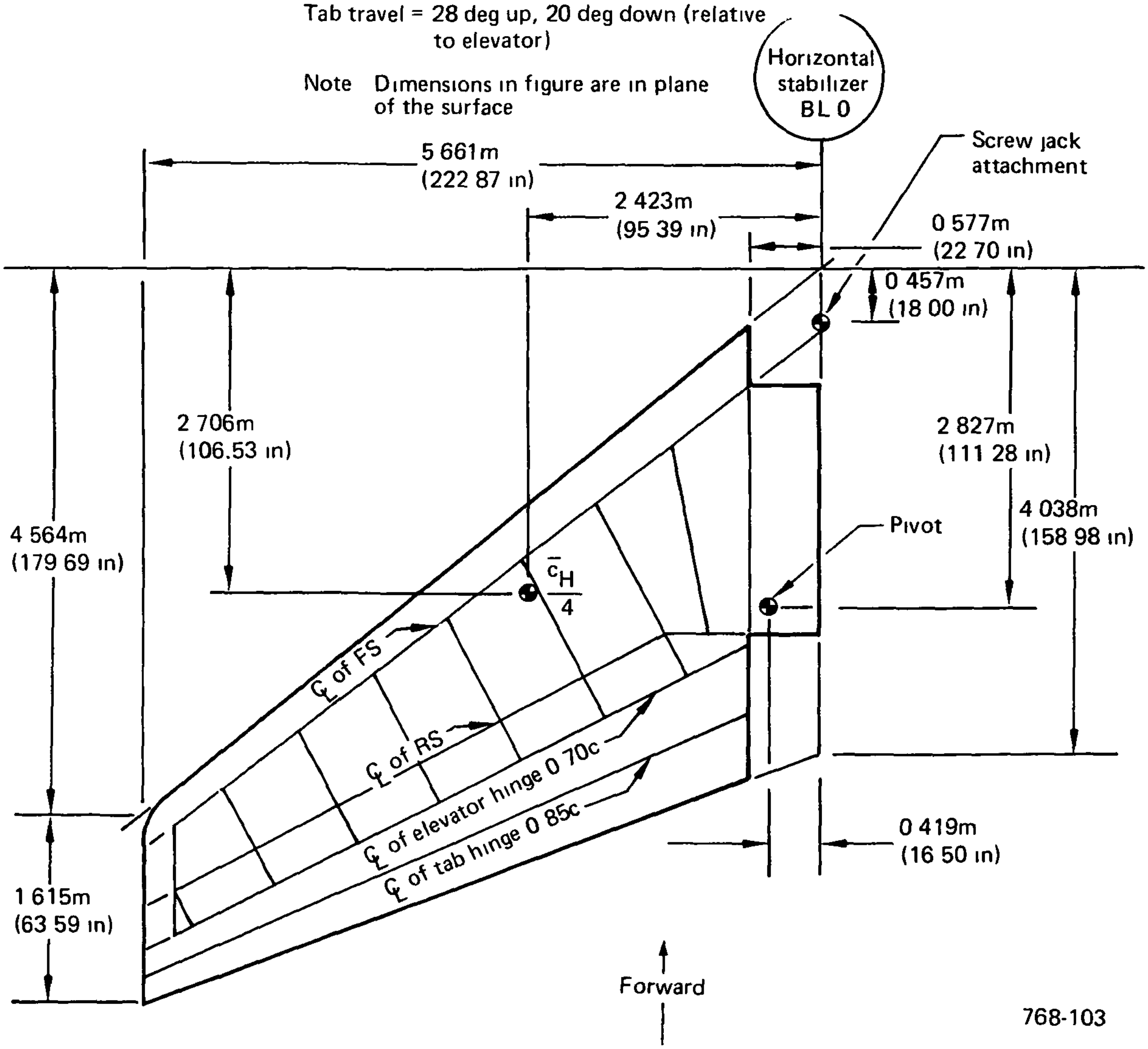

Figure 26. Horizontal Stabilizer Geometry, Plan View

- Dimensions
  - Area = 53 98 m^2 (581 ft^2)
  - AR = 0 67
  - TR = 0 700
  - Λ (0 25c) = 55 deg
  - t/c = 0 12
  - Root chord = 10 560m (415 74 in)
  - Tip chord = 7.392m (291 01in)
  - MAC = 9 069m (357 05 in)
  - Span = 6 014m (236.76 in)
  - Rudder travel = ±25 deg
  - Tab travel = ±25 deg (relative to rudder)

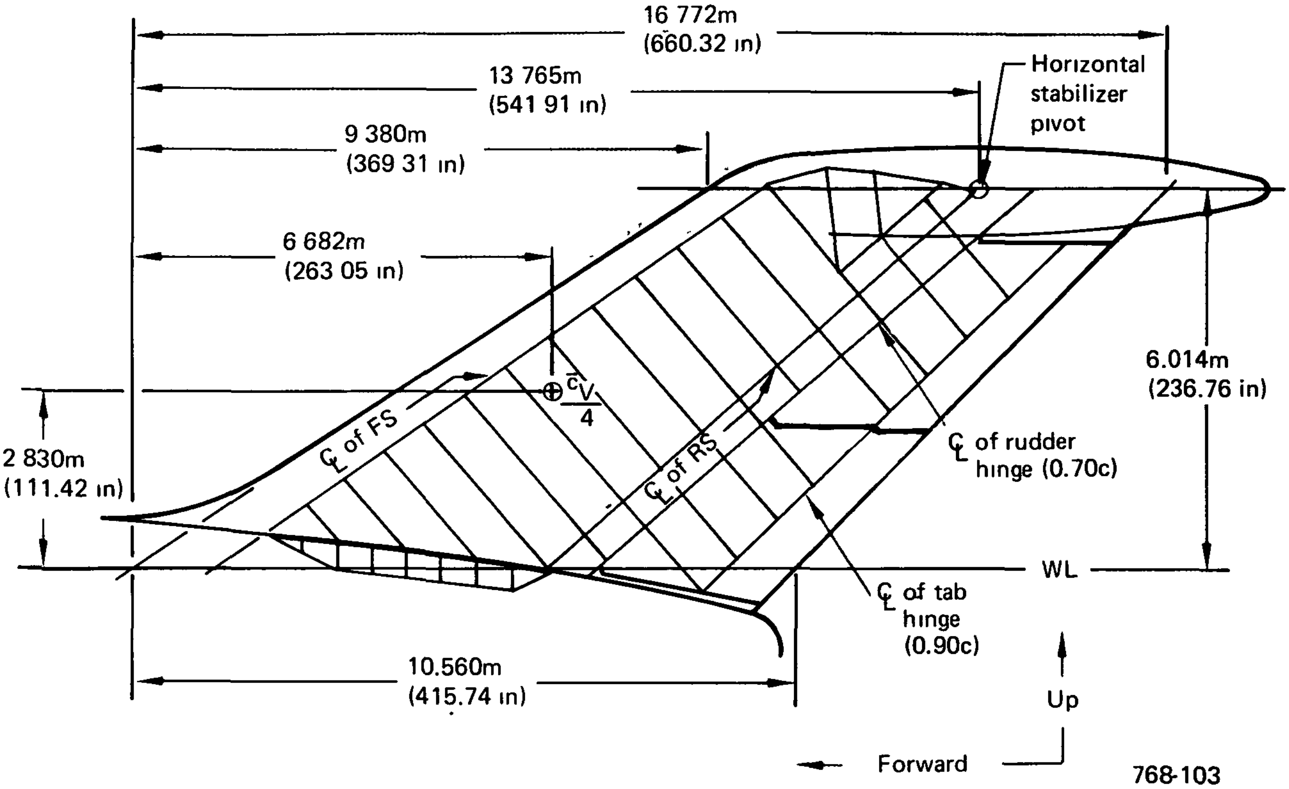

Figure 27. Vertical Stabilizer Geometry, Left-Hand Side View

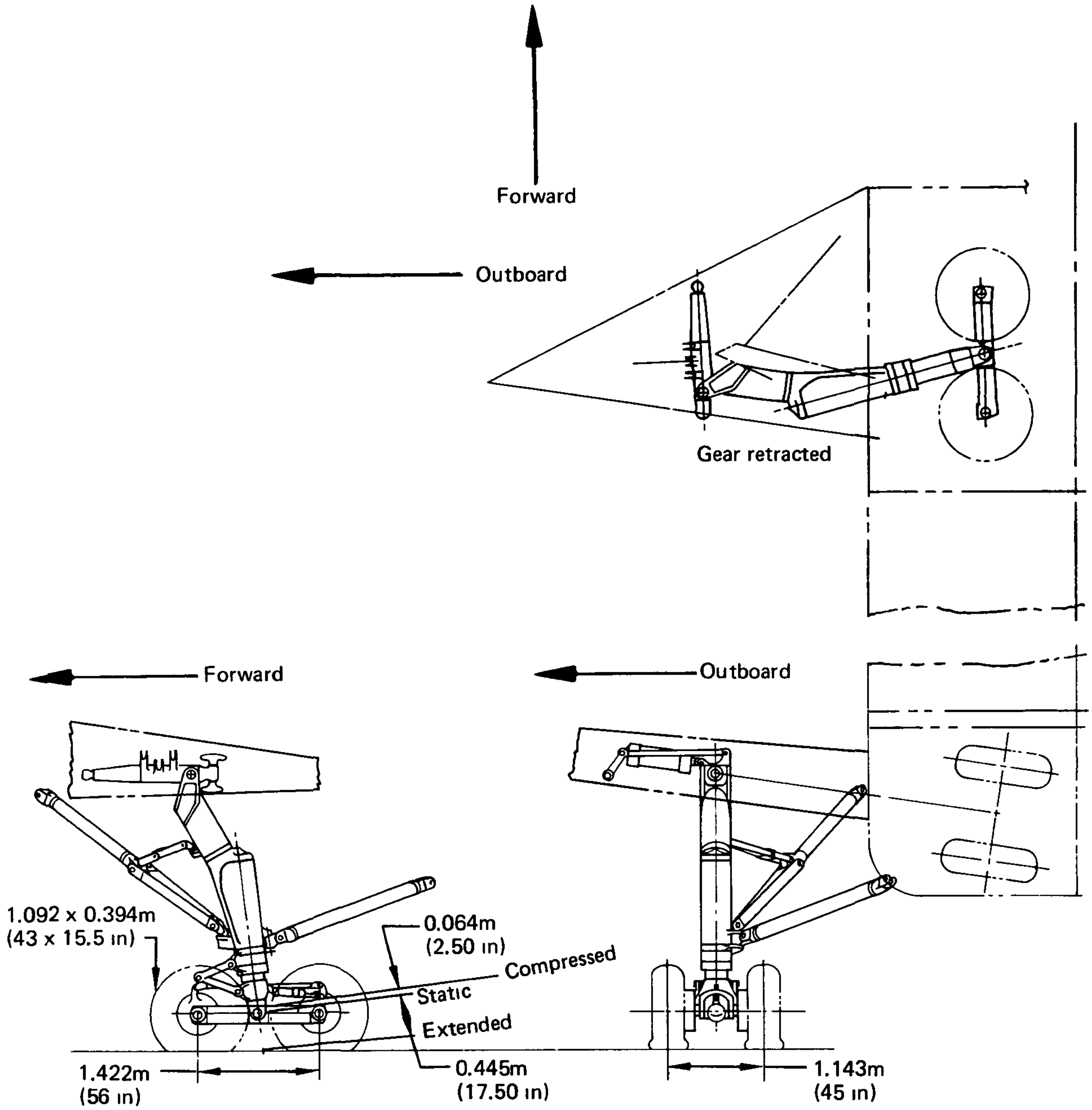

Figure 28. Main Landing Gear

The landing-gear primary structure is steel, and the brakes have steel heat sinks. Wheels are forged aluminum alloy with space for structural carbon brakes. Sleeve bearings are aluminum-nickel-bronze. All structural joints (static or dynamic) are bushed and lubricated. Structural and space provisions are incorporated for a weight-and-balance system and for a brake temperature monitor system.

6. AIRPLANE SYSTEMS

6.2 AIRPLANE SYSTEMS

This section describes the Initial ACT systems, including propulsion (subsec 6.2.1), flight controls (subsec 6.2.2), hydraulic power (subsec 6.2.3), and electric power (subsec 6.2.4). Current proven state-of-the-art concepts are used in defining and evaluating the systems for the ACT configurations.

6.2.1 PROPULSION SYSTEM

The propulsion system is identical to that of the Conventional Baseline (ref 1).

6.2.2 FLIGHT CONTROL SYSTEM

The flight control surfaces of the Initial ACT airplane are similar to those of the Baseline. Operation of the primary controls is unchanged from the Baseline; changes in surface size and some features of surface design are described in the following subsections. Mechanical features of the secondary flight control system are the same as the Baseline; some stabilizer trim commands originate in the ACT system. Only one new surface pair, the inboard section of the outboard ailerons, is introduced to serve ACT functions alone. This fast-response surface works primarily in flutter-mode control (FMC), but also receives wing-load alleviation (WLA) inputs.

Figure 29 shows the location of all control surfaces. Only those control surfaces associated with the active controls are described in detail.

6.2.2.1 Elevator Control Surface

The elevator control surface and actuator installation (figs. 30 and 31) use two single-segment, double-hinged elevators for longitudinal control. Each elevator is powered by three side-by-side primary actuators. The ACT electric signals command the secondary actuators that are series-summed with the pilot's mechanical input. To meet the pitch-augmented stability (PAS) redundancy requirement, three side-by-side force-summed secondary actuators provide dual fail operational capability. In the remote chance that one secondary actuator jams, the combined force of the other two

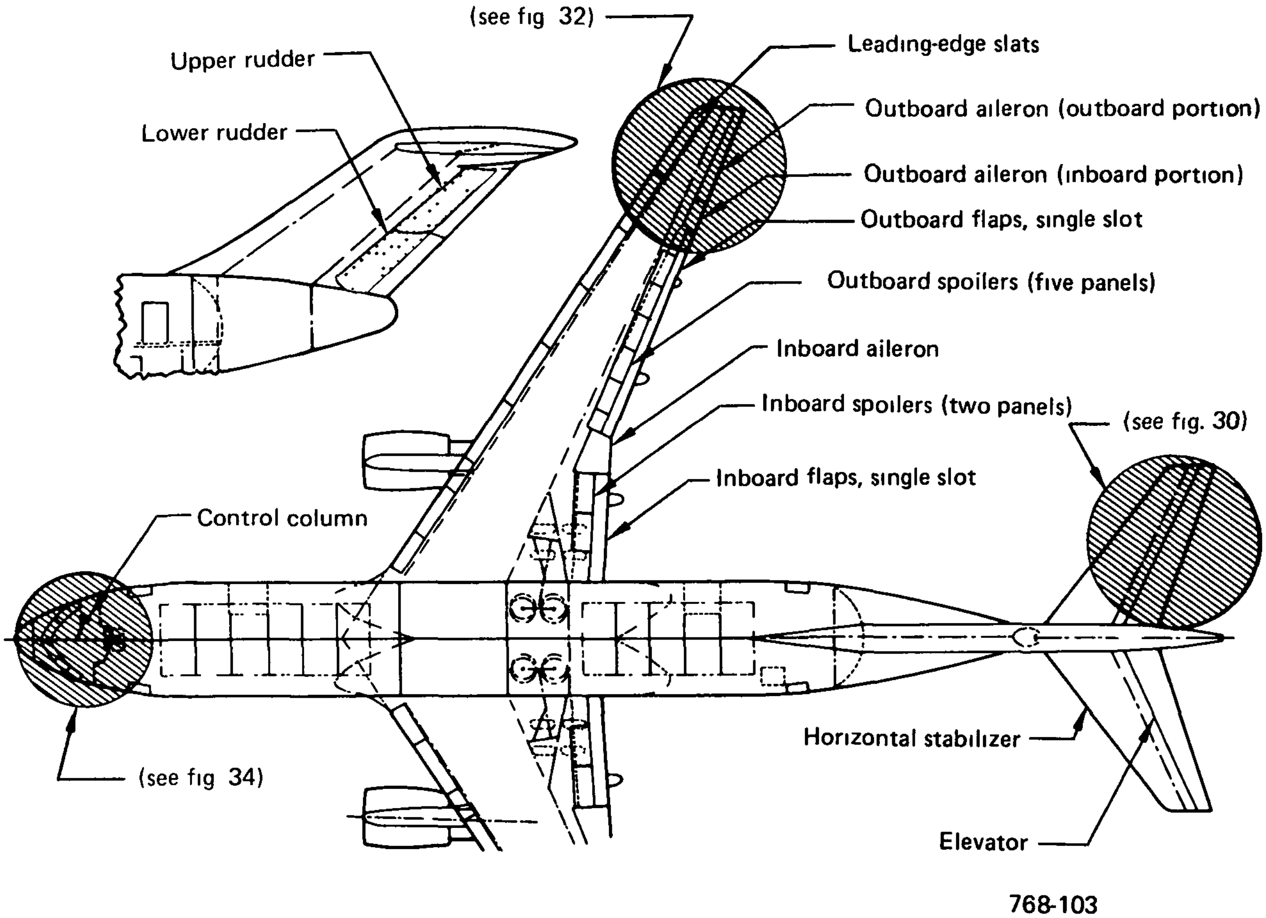

Figure 29. Flight Control Surfaces

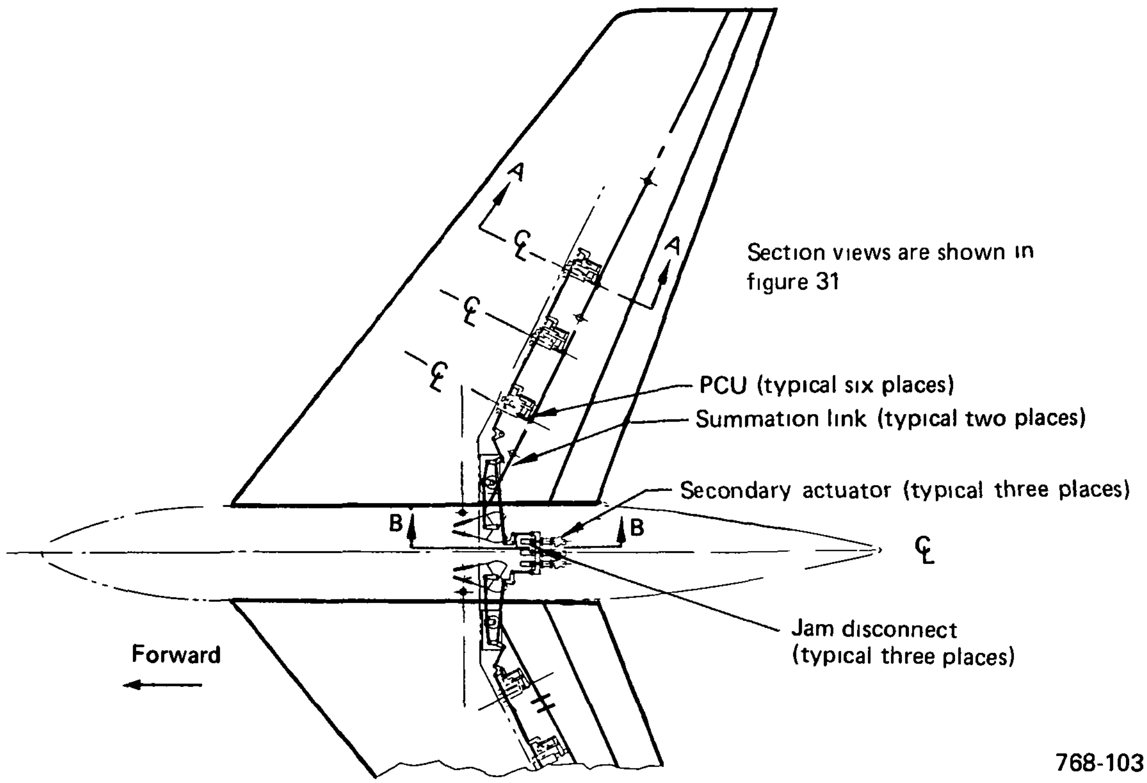

Plan View of Horizontal Stabilizer

Figure 30. Flight Control Surfaces—Horizontal Stabilizer Actuation Installation

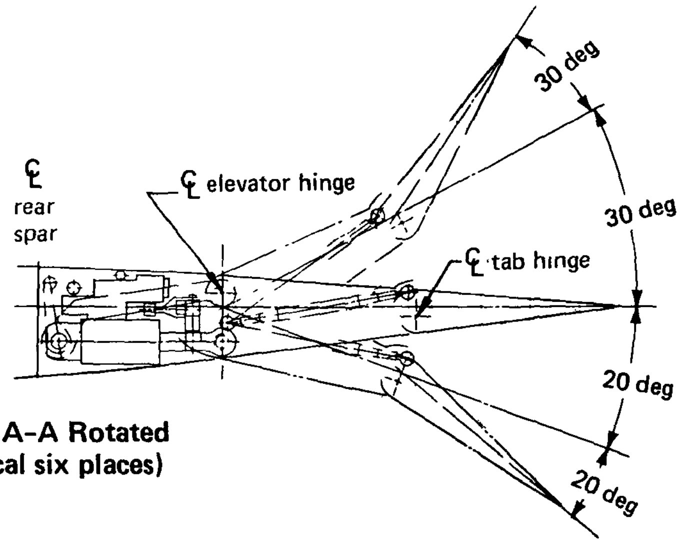

View A-A Rotated
(typical six places)

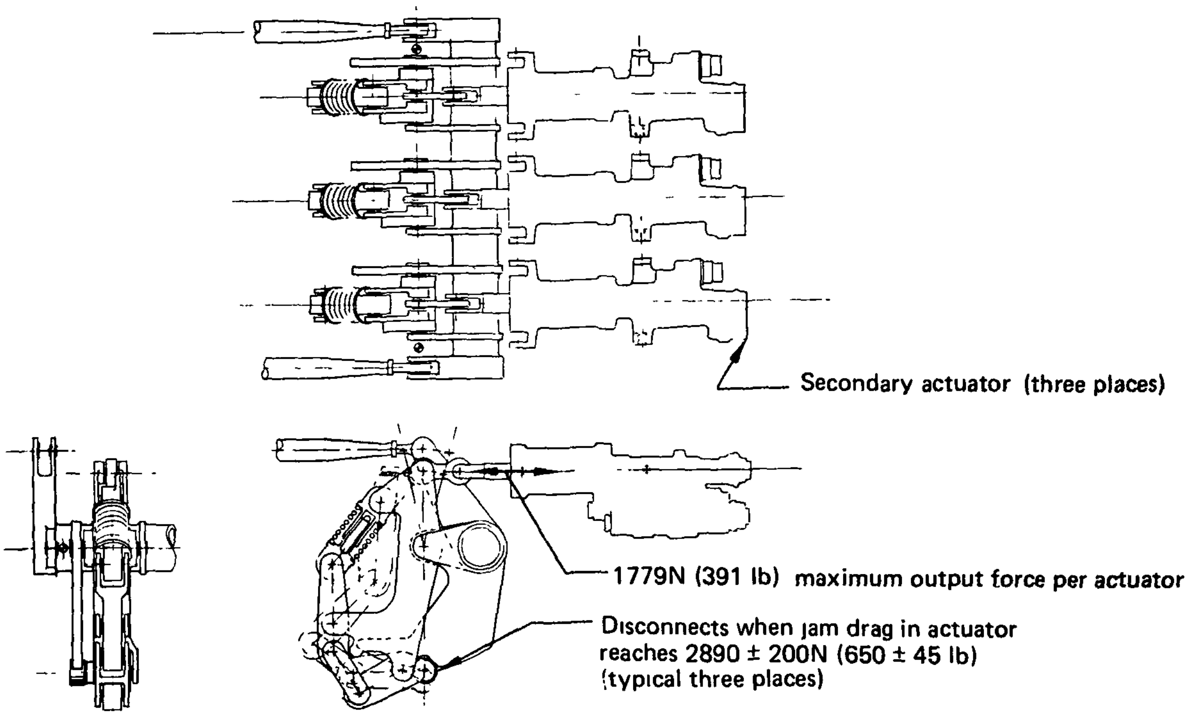

View B-B Secondary Actuator and Jam Disconnect Assembly

768-103

Figure 31. Flight Control Surfaces and Actuator Details—Elevator

secondary actuators would open the jammed actuator's disconnect assembly, and the system would be fail operational. View BB of Figure 30 (shown in fig. 31) shows a jam/disconnect assembly.

6.2.2.2 Outboard Aileron Control Surface

In the outboard aileron control surface and actuator installation (figs. 32 and 33), the outboard aileron is split. The inboard portion (roughly one-third of the total area) is used for FMC. The pilot's mechanical input is not connected to these power actuators; instead, the ACT electric signals feed directly to the dual-tandem actuator. The outboard portion of the outboard aileron is used for low-speed roll control, as well as for maneuver-load control (MLC) and gust-load alleviation (GLA). ACT control signals are fed through two force-summed secondary actuators and are series-summed with the pilot's mechanical input.

6.2.2.3 Pilot's Control Column

A dual-tandem pneumatic floating actuator on the pilot's control column provides an angle-of-attack limiter (AAL) function, which is fail operational. When pressurized on either end or both ends, the actuator will exert the same amount of forward force to the control column and that force continuously decreases as the column travels forward (see the chart on fig. 34).

6.2.3 HYDRAULIC POWER SYSTEM

The hydraulic power and distribution systems (figs. 35 and 36) are the same as for the Baseline Configuration, with additional lines added to the ACT hydraulic equipment.

Hydraulic power is generated by three continuous-duty 20 685 kPa (3000 psi) systems identified as A, B, and C, that use phosphate ester fluid. Systems A and C are functionally similar, with hydraulic power generated by an engine-driven pump (EDP) in parallel with an electric-motor-driven pump (EMP). System B generates power by two ac EMPs and one air-turbine-driven pump (ATDP). The bleed-air start mainfold serves as the pneumatic source, and emergency hydraulic power is furnished by

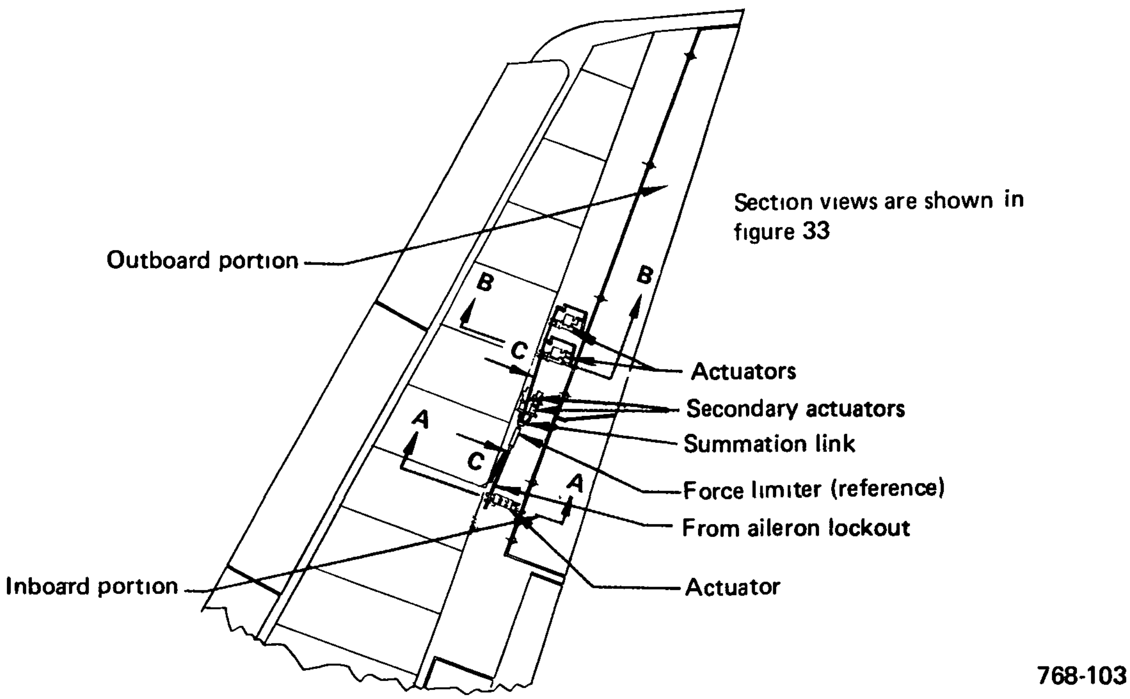

Plan View of Outboard Aileron, Right-Hand Wing (Left-Hand Wing Similar)

Figure 32. Flight Control Surfaces—Outboard Aileron Actuation Installation

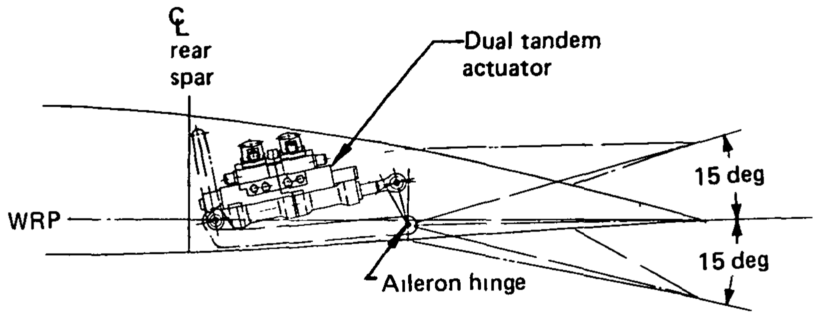

View A-A Rotated

Inboard Portion of Outboard Aileron

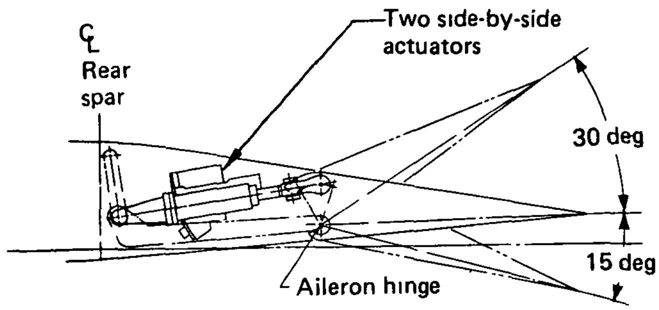

View B-B Rotated

Outboard Portion of Outboard Aileron

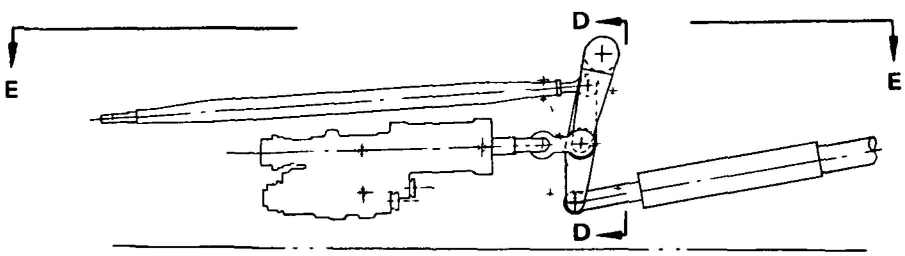

View C-C Rotated

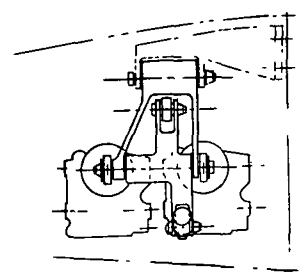

View D-D

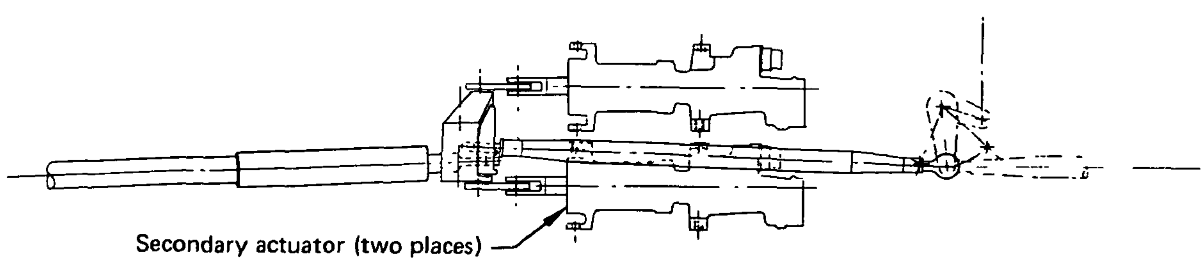

View E-E

768-103

Figure 33. Flight Control Surfaces and Actuator Details—Outboard Aileron

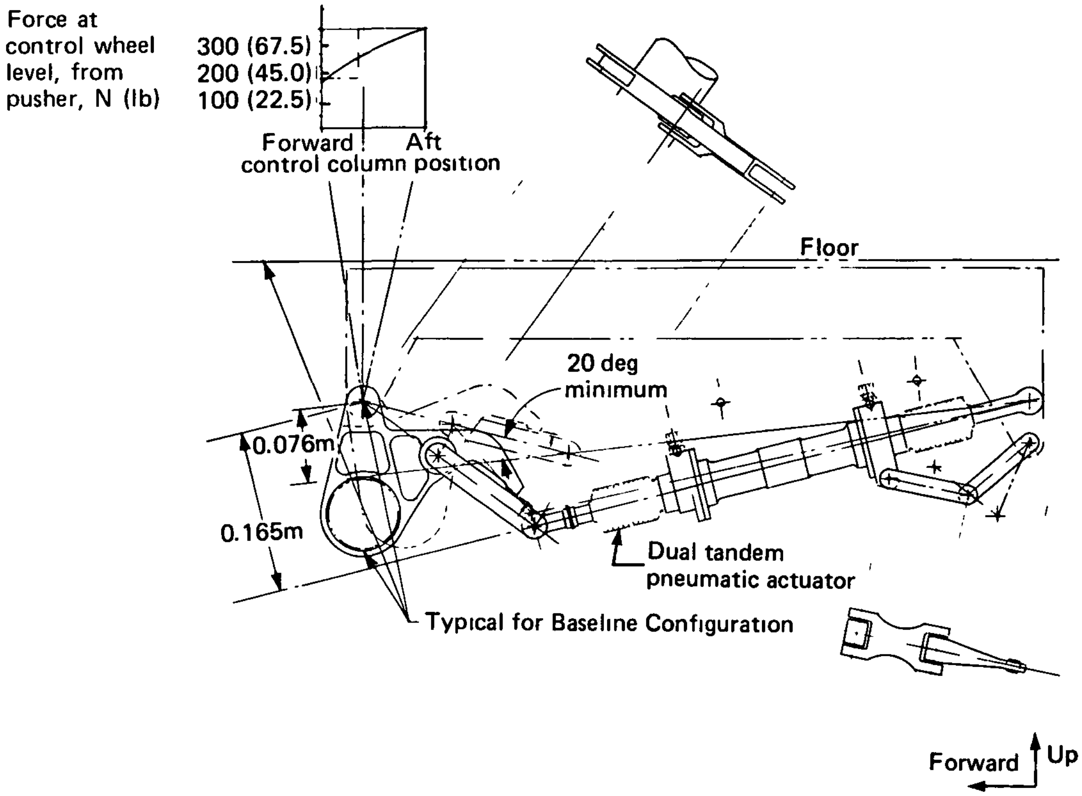

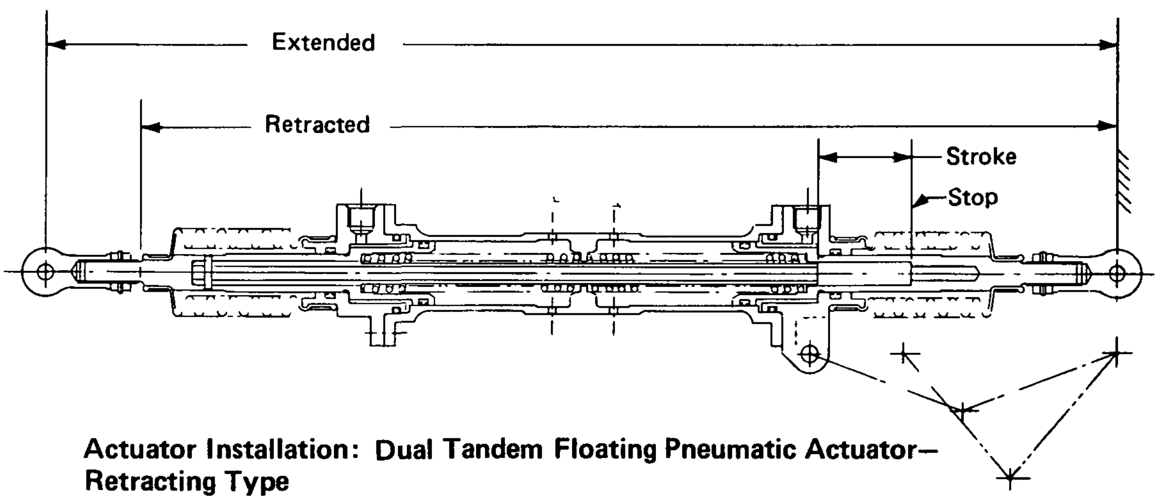

Actuator Installation: Dual Tandem Floating Pneumatic Actuator–Retracting Type

768-103

Figure 34. Control Surfaces—Stick Pusher

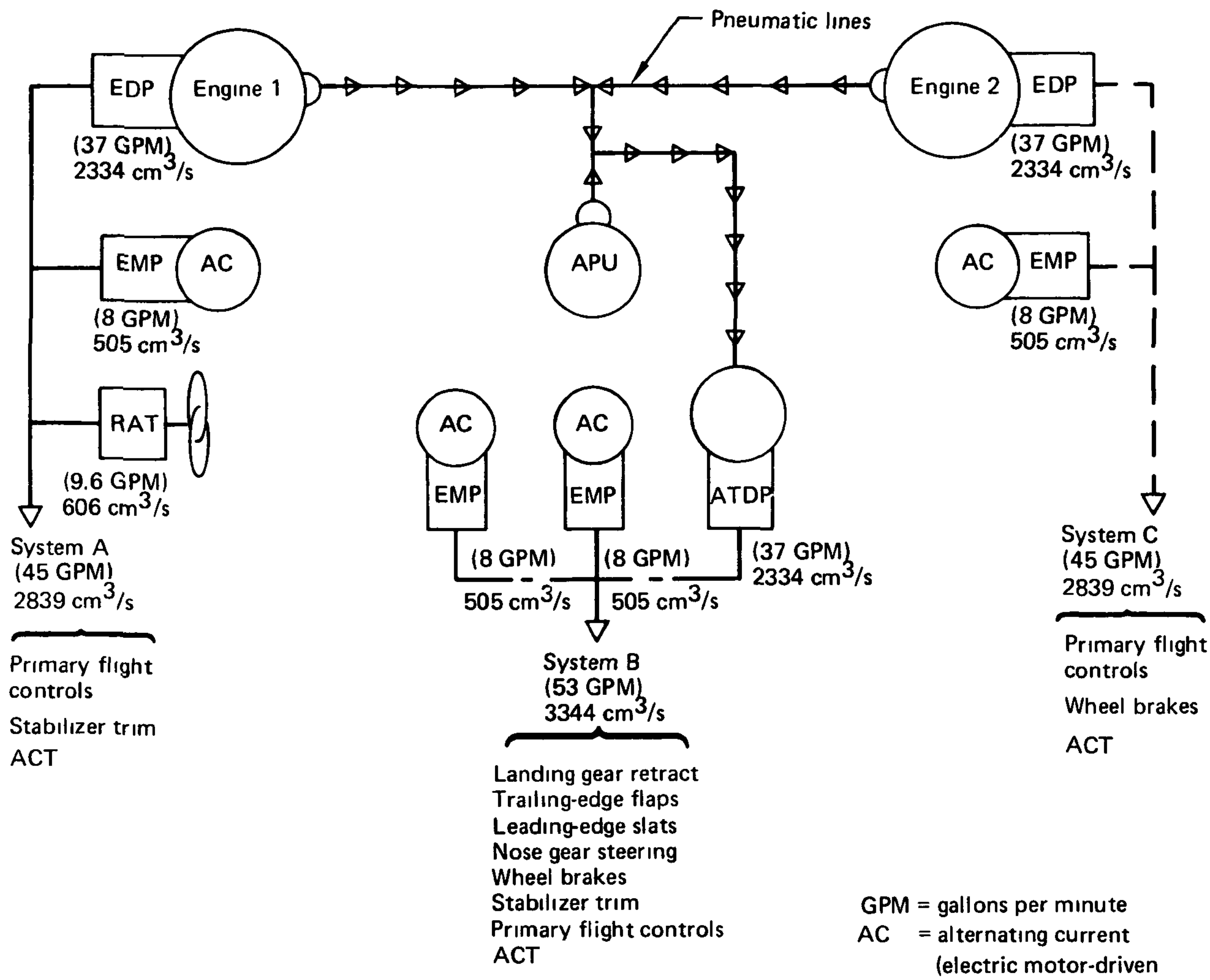

GPM = gallons per minute
AC = alternating current (electric motor-driven pump)

Figure 35. Hydraulic Power System

768-103

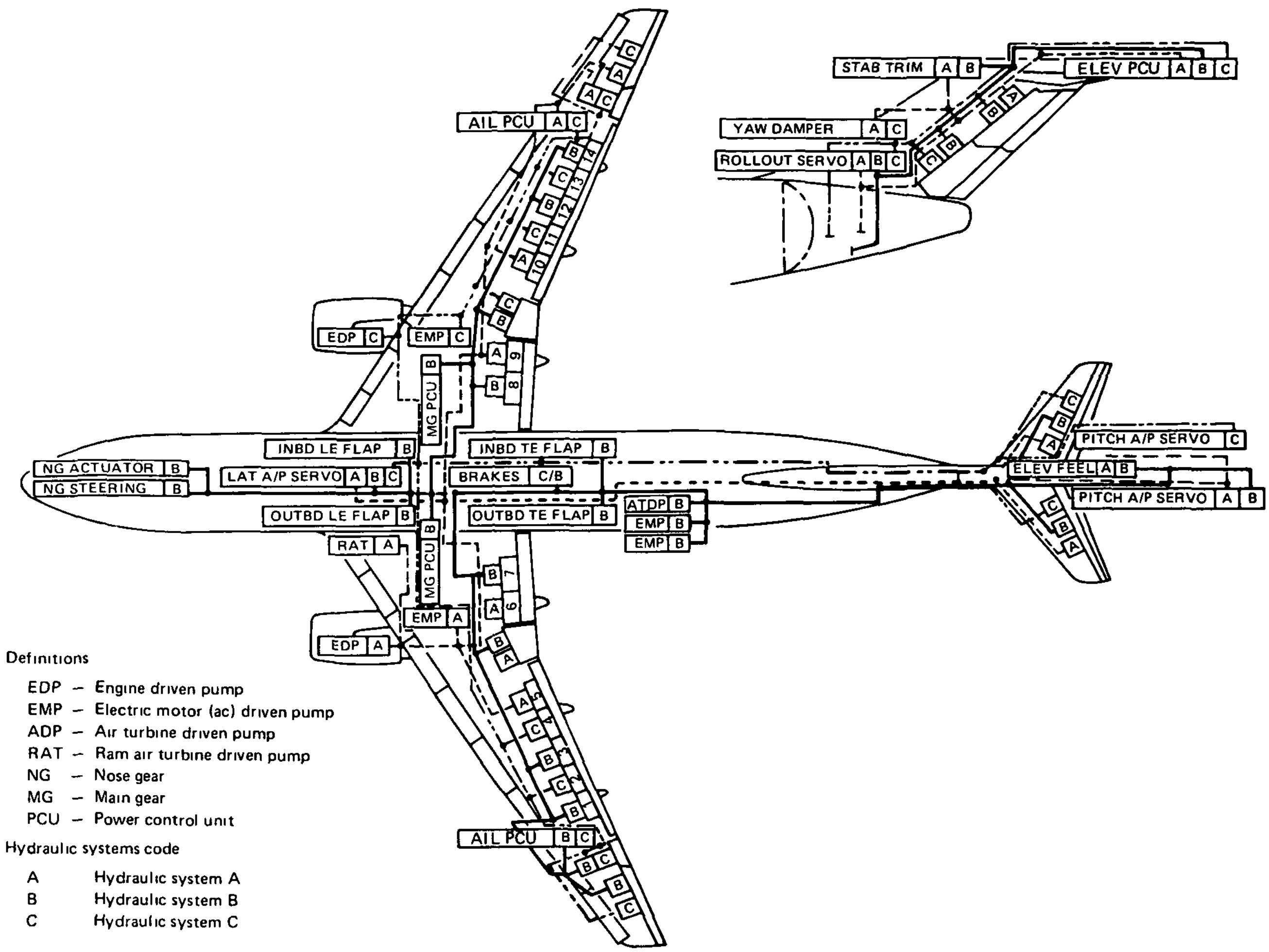

Figure 36. Hydraulic System Distribution 768-103

windmilling engines rotating the EDPs. System A is also augmented by a ram-air turbine (RAT) hydraulic pump. Ground hydraulic power is available either from the ATDP, powered by the APU, or from a pneumatic ground cart; the EMPs can also be energized by a ground cart, the APU, or an external hydraulic power supply. Flight deck controls and displays consist of depressurization switches for the EDPs, shutoff switches for the ATDPs and the EMPs, low-pressure and low-fluid warning lights, and selectable readout for system pressure and fluid quantity.

The hydraulic flow load analysis indicated that each Baseline system will have only 63 to 126 cm^3/s (1 to 2 gal/min) additional leakage (i.e., flow-through valves and actuators with no input signal) from the added ACT functions. In the low-speed range where normal demands are high, the ACT additions tend to only increase the leakage due to additional servo valves. This additional leakage can be accommodated by the Baseline systems. In the high-speed range, the hydraulic systems have adequate capacity to handle ACT activities. Since additional capacity or redundancy is not required, the hydraulic systems are the same as the Baseline Configuration systems.

6.2.4 ELECTRIC POWER SYSTEM

Crucial and critical systems with multiple levels of redundancy, such as the ACT systems, require power sources with the same degree of redundancy to avoid losing more than one channel if a single power source fails. Furthermore, the power sources must be at least two or three orders of magnitude more reliable than the power utilization systems if the overall reliability is not to be determined by the power sources. The electric system for the Initial ACT Configuration was designed to meet these requirements.

6.2.4.1 Primary Electric Power

Primary three-phase, 115V, 400 Hz power is supplied by two engine-driven 90 kVA integrated drive generators (IDG) that cannot be paralleled, so the system operates as two isolated channels. A third 90 kVA APU-driven generator is provided for ground maintenance operations and for in-flight backup to the two main engine-driven generators. The APU can be started at any altitude up to 7620m (25 000 ft) and can provide full electric power up to 10 670m (35 000 ft). The APU generator control unit is interchangeable with those used for the engine-driven generators. Any single generator can supply all essential flight loads. Two of the three generators must be operative for airplane dispatch with no load reduction or for a Category III landing.

During ground operations, electric power can be provided from either the APU generator or from a ground power cart through the 90 kVA external power receptacle. Ground power can be used to energize all main power buses or only those electric loads required for normal maintenance, servicing, and cargo handling. On the ground or in flight, utility and galley loads will be automatically shed when the system is overloaded.

Airplane 28V dc power is provided by two 120A unregulated transformer-rectifier (T-R) units. Each of the two main ac buses supplies its own T-R unit. The dc system operates isolated only. If a T-R unit fails, an automatic dc bus tie contactor enables the remaining T-R unit to supply both main dc buses. During ground operation, a 20A T-R unit provides dc power from ground ac power.

A T-R unit normally starts the APU when ac power is available from either the main generators or external power. When ac power is not available, a dedicated APU battery is used; a dedicated APU battery charger operates from either the main buses or external power.

6.2.4.2 Standby Electric Power

Backup power to flight-critical loads is supplied by a 40 Ah nickel-cadmium battery and a 1000-VA static inverter. A battery charger provides controlled recharge of the battery and operates as a T-R unit to supply the standby loads if the main dc source is lost but ac power is still available. Standby bus transfer is automatic.

As a third power source for the Category III autoland system, the standby battery and the battery charger (in the T-R mode) will supply the third channel autoland dc loads. Autoland ac loads will be supplied from the standby inverter.

6.2.4.3 Modifications for the Initial ACT Configuration—ACT System Power Supply Configuration

The electric system is modified to provide quadruple-redundant power for the quadruple-redundant ACT channels, with two power sources to each channel.

The electric system for the Initial ACT Configuration (figs. 37 and 38) includes a second standby battery, with charger, to provide the necessary redundancy to support the ACT system. The standby battery capacity required for the Initial ACT Configuration is approximately double that in the Baseline Configuration. Therefore, the additional standby battery has the same capacity as that in the Baseline. Battery No. 1 supplies Channels A and B, and Battery No. 2 supplies Channels C and D. For

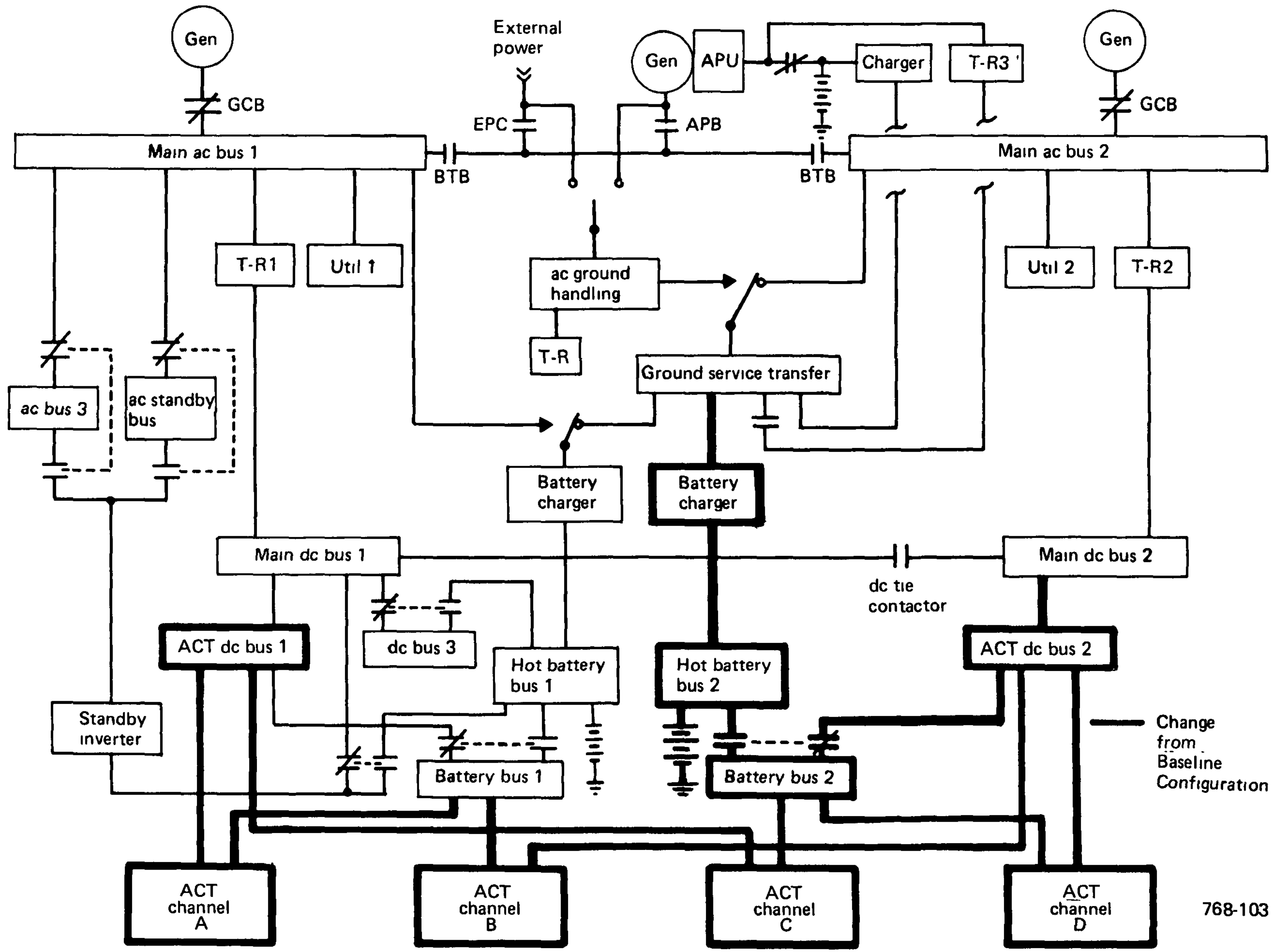

Figure 37. Electric Power System

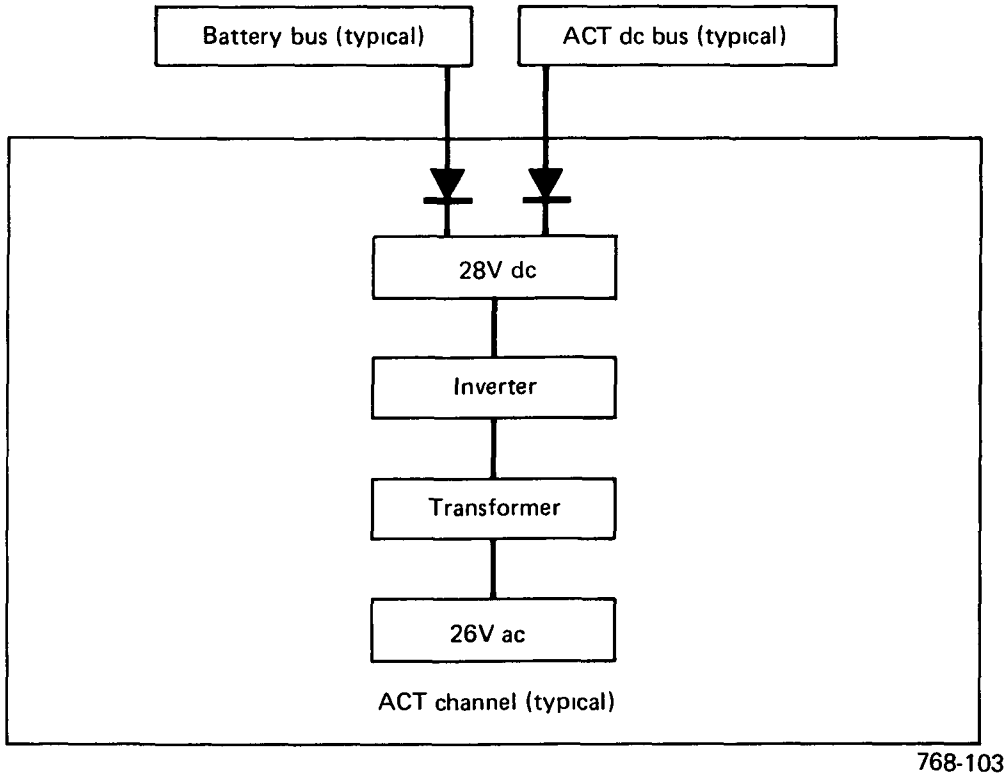

Figure 38. Detail of ACT Channel Power Supply (Typical)

dissimilar redundancy, no two buses share the same T-R and battery. Thus, T-R1 supplies Buses A and C, while T-R2 supplies Buses B and D (fig. 37 and 38). Assuming that standby battery load for the Baseline Configuration can be redistributed between the two ACT battery buses, each battery has approximately an equal load. The individual T-R and battery loads are listed in Table 6.

Assuming the total ACT battery load (crucial and critical) and the basic standby loads all are supplied by the batteries for 30 min during emergency operation, the battery energy requirements are:

- Battery 1--41.4A x 0.5 hr = 20.7 Ah
- Battery 2--43.0A x 0.5 hr = 21.5 Ah

Table 6. Individual T-R and Battery Loads

Power supply	Channels	Amperes		
		ACT system	Baseline	Total
T-R 1	A and C	9.6 + 8 5	44	62 1
T-R 2	B and D	11 8 + 9 5	44	65 3
Battery 1	A and B	9.6 + 11 8	20	41 4
Battery 2	C and D	8.5 + 9 5	25	43 0

768-103

The Baseline Configuration standby and APU starting batteries are 40 Ah units. To maintain commonality between standby and APU batteries, the same 40 Ah battery size is used for both functions.

The 120A T-R used in the Baseline Configuration is too small to absorb the ACT electric loads and still retain sufficient reserve capacity to supply all loads with one T-R inoperative. In the Initial ACT Configuration, the 120A T-Rs are replaced with 150A T-Rs that supply both the main dc buses and the ACT system dc buses. In effect, the ACT system dc buses are extensions of the main dc buses (fig. 37).

Each ACT electric channel has a small 400 Hz power requirement. To maintain the redundancy of the ACT channels, each channel must have an independent power supply, including conversion equipment. Therefore, a static inverter was added for each ACT channel, and the Baseline inverter was retained as part of the ac standby bus emergency power source.

The ACT 400 Hz loads are all at 26V. The inverter and 115/26V transformer capacity requirements (in VA) and the T-R and battery loads (in A at 28V dc) are summarized in Table 7. One 100 VA inverter and one 100 VA transformer for each ACT channel will supply the 26V ac power.

Table 7. Electric System Capacity Requirements

Channel	A	B	C	D
Inverter and 115/26V transformer capacity, VA				
Crucial ac loads	13 0	13.0	13.0	6 5
Critical ac loads	26 0	39 0	26 0	39 0
Total ACT system	39.0	52.0	39.0	45.5
T-R and battery loads, A at 28V dc				
ACT system T-R loads	9.6	11.8	8 5	9.5
Battery dc loads	6.7	8.0	5 6	6.1
Inverter input	2 9	3 9	2.9	3 4
Total battery loads	9 6	11 8	8.5	9 5
Battery	21.4 No. 1		18.0 No. 2	

768-103

The ACT electric load totals on each power source are summarized in Table 8. Table 9 identifies the equipment to be added for the Initial ACT airplane electric system to support the ACT function.

Table 8. ACT Load Totals for Each Power Source

T-Rs operating			T-Rs not operating			
TRU	Channel	A	Battery	Channel	A	Ah[a]
1	A and C	18 1	1	A and B	21.4	10.7
2	B and D	21.3	2	C and D	18.0	9.0

[a]30 minutes

768-103

Table 9. ACT Power Supply Equipment

Item	IAAC		Baseline	
	Number	Rating	Number	Rating
Battery	2	40 Ah	1	40 Ah
Battery charger	2		1	
Transformer-rectifier	2	150A	2	120A
Static inverter	4	100 VA		
Transformer, 115/26V	4	100 VA		

768-103

7 0 ANALYSES AND
CHARACTERISTICS

7.0 ANALYSES AND CHARACTERISTICS

Airplane design is an iterative process that involves most of the engineering disciplines in parallel or simultaneous tasks. Each discipline needs data from, or provides data to, other disciplines. Thus, to accomplish the design process, some work must begin with preliminary analyses that are updated as more complete data become available.

The principal objective of this section is to provide sufficient detail from the design process to validate the improved performance of the Initial ACT Configuration relative to the Baseline Configuration. In describing the analysis and design work that led to and supports the Initial ACT Configuration described in Section 4.0, this section presents, by implication, the design methodology and interdisciplinary communication that was necessary for the ACT design process.

Subsections 7.1 through 7.5 describe the individual analyses and data that were developed as part of the Initial ACT Configuration Design Task. These various analyses culminate in an aerodynamic drag estimate (subsec 7.4) and airplane weight and balance (subsec 7.5), which are the foundations for performance analysis.

7.1 FLYING QUALITIES

This section describes the methods used to predict the flying-quality parameters. Trim, control, and stability characteristics are described in Subsections 7.1.2, 7.1.3, and 7.1.4, respectively. Each subsection discusses the longitudinal axis, then the lateral/directional axes, and emphasizes the flight characteristics that are critical, relative either to controllability limits or to other criteria such as minimum safe levels of stability. These flight characteristics were predicted from static wind tunnel data (app. B), estimates of aerodynamic damping, and quasistatic-aeroelastic (QSAE) correction factors. Also, the stability augmentation requirements for control law and ACT system design are defined, and the flying qualities are evaluated with a preliminary control law design.

Figure 39 shows the high- and low-speed flight envelopes for two gross weights, which represent extremes for flying qualities. The design mission takeoff weight is about 122 470 kg (270 000 lb), and the end-of-cruise and descent and landing weights are

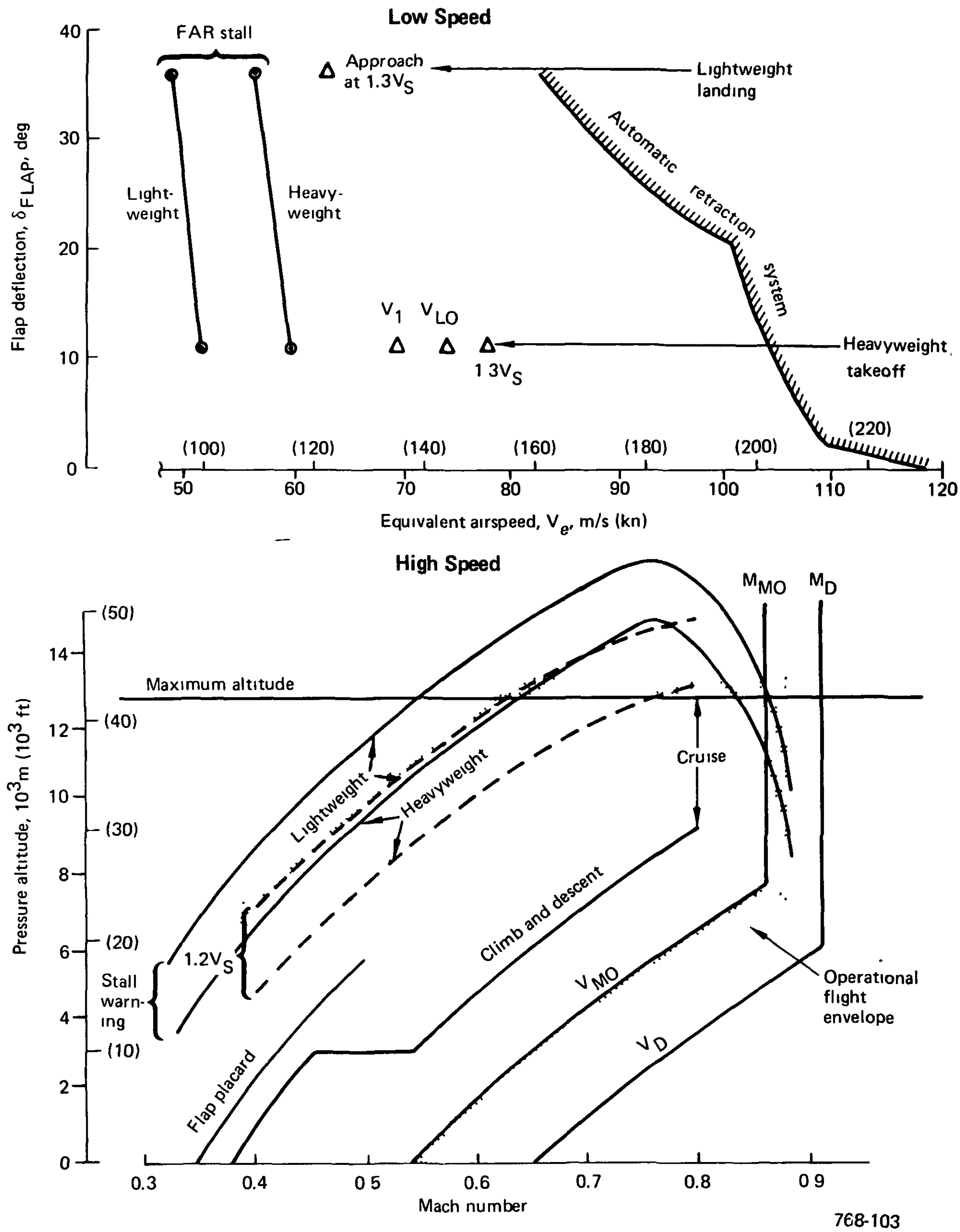

Figure 39. Speed and Altitude Flight Envelopes

about 90 720 kg (200 000 lb). The operational flight envelope is defined by V_{MO}/M_{MO}, $1.2V_S$ and a maximum altitude of 12 800m (42 000 ft). A design envelope for emergency flight is provided by V_D/M_D/flap placard and stall warning speeds. Figure 39 illustrates that $1.2V_S$ and stall-warning limits depend on airplane weight; however, the high-speed limits of V_D = 221.2 m/s (430 kn) calibrated airspeed, V_{MO} = 185.2 m/s (360 kn) calibrated airspeed, flap placard = 118.3 m/s (230 kn) equivalent airspeed, and the climb/descent speed schedule at 128.6 m/s (250 kn) calibrated airspeed below 3048m (10 000 ft) altitude, 154.3 m/s (300 kn) calibrated airspeed to 9144m (30 000 ft) altitude are independent of airplane weight. Generally, good flying qualities are required within the operational flight envelope, while the extremities of the design flight envelope must provide minimum safe flying qualities.

The flying-quality characteristics presented in this section emphasize the extremities of these flight envelopes for critical heavy or light weight and for forward or aft center-of-gravity (cg) limit location. Also, the critical moments of inertia used may represent unusual, but possible, payload-fuel distributions.

Engine-out, mistrim, hydraulic system failures, and ACT system failures also affect flight characteristics and are presented to emphasize the critical conditions. For example, critical control or trim conditions are presented in Figure 40 for various combinations of hydraulic systems. ACT functions on the Baseline and Initial ACT Configurations are compared in Table 10.

Baseline horizontal tail and elevator were sized for deep-stall recovery at the critical aft cg landing configuration; however, the Initial ACT Configuration uses an alpha-limiting device that allows the horizontal tail to be sized for recovery pitching moments at the stall lift coefficient. The critical aft cg landing condition is the same for both airplanes. The vertical tail and rudder were sized at the aft cg for engine-out control on the ground (V_{MCG}) for both the Baseline and Initial ACT Configurations. The lateral control for both configurations was determined by an engine-out trim requirement.

The Initial ACT airplane loading range did not result in a forward cg that was control critical for the horizontal tail. However, a green band, similar to that used in other

● Available control is greater at speeds less than those noted.

Critical for control

Critical for trim

Minimum percent of normal control remaining:

One system out

	Failed System: System A	System B	System C
Elevators $V_e > 133.8$ m/s (260 kn)	75	75	50
Speed brake C_m $V_e > 179.0$ m/s (348 kn)	100	50	50
Spoiler/brakes $V_e > 179.0$ m/s (348 kn)	67	67	67
Ailerons $V_e >$ 87 5 m/s (170 kn)	50	75	75
Rudders (with ratio changer) $V_e > 72.0$ m/s (140 kn)	90	80	90

Two systems out

	Failed Systems: AB	AC	BC
Elevators $V_e >$ 13 8 m/s (260 kn)	50	25	25
Speed brake C_m $V_e > 179.0$ m/s (348 kn)	50	50	0
Spoilers/brakes $V_e > 179.0$ m/s (348 kn)	33	33	33
Ailerons $V_e > 87.5$ m/s (170 kn)	25	25	50
Rudders (with ratio changer) $V_e > 72.0$ m/s (140 kn)	40	80	40

768-103

Figure 40. Control Power After Hydraulic System Failure

Table 10. ACT System Functions

Functions	Baseline	Initial ACT
Yaw damper	Three systems	Same
Multiple green band for takeoff	Pilot warning	Simplified
Stall	Pilot warning	Alpha limiting Two systems Fail passive
Pitch augmentation	None	Four systems
Speed augmentation	None (Mach trim)	Three systems Fail passive
Longitudinal feel augmentation	Yes	Yes, but simpler system than Baseline
Wing load alleviation	None	Three systems Fail passive
Flutter suppression	None	Three systems Fail passive
Ride qualities	Unknown	Unknown

768-103

Boeing airplanes, is required to preclude excessive takeoff mistrim at the extremes of the loading range. Without this system, additional pitch control would be needed.

Stability characteristics are such that the Baseline Configuration needed a yaw damper and longitudinal feel system augmentation. The Initial ACT vertical fin size and balance are such that virtually the same lateral/directional characteristics as the Baseline Configuration result, and the same yaw damper was used. Table 10 compares other ACT functions for the two configurations. The pitch and speed augmentation employed by the Initial ACT Configuration results in more uniform flying qualities than the Baseline Configuration and simplifies the longitudinal feel system design. Longitudinal feel system design was not detailed on the Initial ACT Configuration.

7.1.1 METHODOLOGY

This subsection describes the methods used to predict the flying-quality parameters and defines control law design requirements for stability augmentation. The design parameters (including static stability trim and control, steady maneuvers, and dynamic roots and responses) were used to design the flight control system. These methods are used throughout the IAAC Project to ensure design consistency. They are described in terms of the equations and variables used to estimate the design parameters to illustrate the level of design detail. Basic inputs to the methods were static wind tunnel force data, linear QSAE corrections, and damping estimates. These data were combined to form longitudinal and lateral/directional linear QSAE models composed of static and damping derivatives. The QSAE models were, in turn, used to estimate the design parameters related to the flying-quality requirements, to define stability augmentation requirements, and to design the control laws. Figure 41 illustrates the QSAE flying-quality analysis.

In Figures 42 and 43, illustrating the QSAE force and moment buildup, wind tunnel data were linearized for the tail-off configuration, tail input, and control effectiveness to incorporate the aeroelastic corrections. The rigid longitudinal derivatives were determined for several alpha regions between zero and initial buffet for three flap settings and 12 Mach numbers; the rigid lateral/directional derivatives were input at several specific alphas for three flap settings and 10 Mach numbers. These derivatives, along with the geometric and thrust constants, aeroelastic corrections, and damping constants, were input to the computer to form the QSAE models. Taping these characteristics facilitated editing for tail area, cg range, aeroelastic corrections, etc., to reflect design or configuration changes (see fig. 41).

Aeroelastic derivatives result from partial differentiation of each force or moment (figs. 42 and 43) with respect to the motions, including Mach number and dynamic pressure. The Mach derivatives were used to build up the speed derivatives, which, with the tail-off rotary or damping derivatives, were calculated from auxilary equations (not shown). The calculations, similar to the methods of the US Air Force Data Compendium (DATCOM), also include aeroelastic corrections. The pilot lateral control wheel derivatives (fig. 43) were actually modeled as eight individual surfaces representing spoilers and ailerons.

Both derivative programs (fig. 41) contain altitude models so the analysis can be made for any flight condition at the data-defined Mach number (or flap setting). A data region for longitudinal trim is selected for executing the computer program; if the

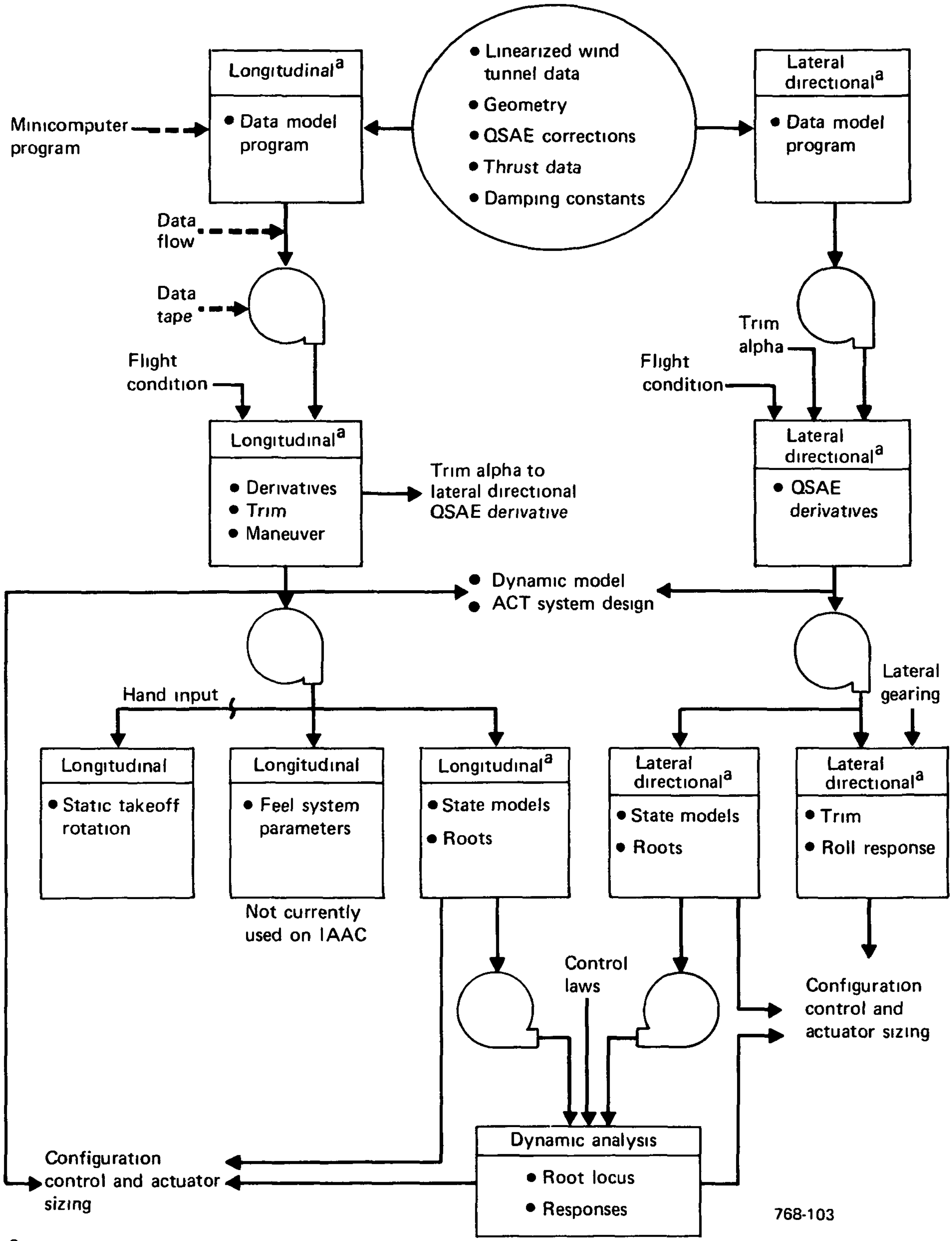

[a]IAAC development

Figure 41. QSAE Flying Quality Analysis Flow Chart

Lift

$$C_L = C_{L_o}^{WB} + \Delta C_{L_o} + \left(\frac{LE}{LR}\right)^W C_{L_\alpha}^{WB}\,\alpha + C_{L_{\hat{Q}}}^{WB}\,\hat{Q} + C_{L_{\hat{u}}}^{WB}\,\hat{u} + C_{L_n}^{W}\,n + \frac{S_T}{S_W}\,C_L^T$$

Pitching moment

$$C_m = C_{m_o}^{WB} + \Delta C_{m_o} + \left[C_{L_o}^{WB} + \Delta C_{L_o} + \left(\frac{LE}{LR}\right)^W C_{L_\alpha}^{WB}\,\alpha\right]\left[cg - ac^{WB} - \Delta ac^{W}\right]$$

$$+ C_{m_{\hat{Q}}}^{WB}\,\hat{Q} + C_{m_{\hat{u}}}^{WB}\,\hat{u} + C_{m_n}^{W}\,n - \bar{V}_H\,C_L^T$$

Drag

$$C_D = C_{D_o}^{WB} + K_W\left(\alpha - \alpha_o\right)^2 + C_{D_{\hat{u}}}^{WB}\,\hat{u} + \frac{ST}{SW}\left[C_{D_o}^T + K_T\left(C_L^T - C_{L_o}\right)^2\right]$$

Tail lift

$$C_L^T = (a_t\eta_t)\,K_{BB}\left(\frac{LE}{LR}\right)^T\left[\left(1 - \epsilon_\alpha\right)\alpha - \epsilon_o + K_\delta\,\delta_H + \left(\frac{LE}{LR}\right)^e K_\delta\,K_e\,\delta_e + 57.3\left(\frac{d\alpha}{dn}\right)^T n\right.$$

$$\left. + 57.3\left(\frac{d\alpha}{d\ddot{\theta}}\right)^T \ddot{\theta} + (2)\,57.3\,\frac{\ell_H}{\bar{c}}\,\hat{Q} + (2)\,57.3\,\frac{X_T}{\bar{c}}\,\epsilon_\alpha\,\dot{\hat{\alpha}}\right] + C_{L_{\hat{u}}}^T\,\hat{u}$$

Where: $$K_{BB} = \frac{1}{1 - \left(\frac{d\alpha}{dL}\right)^T q\;S_T\,(a_t\eta_t)\;57.3\left(\frac{LE}{LR}\right)^T}$$

Thrust

$$C_T = \frac{1}{qSW}\left[A + B\,(Alt) + C\,(Mach) + D\,(Alt)\,(Mach) + E\,(Alt)^2\right] + \frac{\partial C_T}{\partial \hat{u}}\,\hat{u}$$

Where: the constants A, B, C, D, and E are different above and below 11 000m (36 089 ft)

768-103

Figure 42. Longitudinal QSAE Force and Moment Buildup

Side force

$$C_Y = C^{WB}_{Y_\beta}\,\beta + C^{WB}_{Y_{\hat{P}}}\,\hat{P} + C^{WB}_{Y_{\hat{R}}}\,\hat{R} + C_{Y_{\delta W}}\,\delta W + \frac{S_V}{S_w}\left[C^{v}_{Y} + \left(\frac{LE}{LR}\right)^{R} K_{BR}\, C_{Y_{\delta_R}}\,\delta_R\right]$$

Yawing moment

$$C_n = \left(C^{WB}_{n_\beta}\right)_{REF}\beta + C^{WB}_{Y_\beta}\,\beta\,[CG - REF]\,\frac{\bar{c}}{b} + C^{WB}_{n_{\hat{P}}}\,\hat{P} + C^{WB}_{n_{\hat{R}}}\,\hat{R}$$

$$+ C_{n_{\delta W}}\,\delta W - \overline{V}_v\left[C^{V}_{Y} + \left(\frac{LE}{LR}\right)^{R} K_{BR}\, C_{Y_{\delta_R}}\,\delta_R\right]$$

Rolling moment

$$C_\ell = C^{WB}_{\ell_\beta}\,\beta + C^{W}_{\ell_{\ddot{\phi}}}\,\ddot{\phi} + C^{WB}_{\ell_{\hat{P}}}\,\hat{P} +$$

$$C^{WB}_{\ell_{\hat{R}}}\,\hat{R} + \left(\frac{RE}{RR}\right)^{W} C_{\ell_{\delta W}}\,\delta W + \frac{S_V}{S_w}\,\frac{Z_v}{b}\left[C^{v}_{Y} - \left(\frac{LE}{LR}\right)^{v} K_{BR}\, C_{Y_{\delta_R}}\,\delta_R\right]$$

Fin lift

$$C^{V}_{Y} = (a_v n_v)\, K_{B\beta}\left(\frac{LE}{LR}\right)^{V}\left[\left(1 + \frac{d\sigma}{d\beta}\right)(-\beta) - (2)\;57.3\,\frac{Z_v}{b}\,\hat{P} + 2\,(57.3)\,\frac{\ell_v}{b}\,\hat{R}\right.$$

$$\left. + \frac{1}{K_{B_\beta}}\left(\frac{d\alpha}{d\ddot{\psi}}\right)^{V}\ddot{\psi} + \frac{1}{K_{B_\beta}}\left(\frac{d\alpha}{dn_y}\right)^{V} n_y + 2\,(57.3)\,\frac{d\sigma}{d\beta}\,\frac{\ell_v}{b}\,\hat{\dot{\beta}}\right]$$

Where: $$K_{B\beta} = \frac{1}{1 - (a_v n_v)\left(\frac{d\alpha}{dL}\right)^{V} q\,S_V\left(\frac{LE}{LR}\right)^{V}}$$

$$K_{BR} = \frac{1}{1 - (a_v n_v)\left(\frac{d\alpha_V}{dL_R}\right) q\,S_V\left(\frac{LE}{LR}\right)^{R}}$$

768-103

Figure 43. Lateral Directional QSAE Force and Moment Buildup

resulting three-dimensional static trim is outside the applicable alpha range, the program is rerun with a different data region until trim is compatible with the linear data region. The output for a specified flight condition includes trim characteristics, QSAE derivatives, and steady-state stability parameters, such as neutral point and elevator deflection gradients for a constant speed pullup or for 1g trim versus airspeed. Figure 41 illustrates how these data interface with other analyses.

The lateral/directional QSAE model requires the trim alpha to interpolate for the rigid derivatives. Elastic, static, and damping derivatives are then calculated from the equations on Figure 41 to form the QSAE model. The trim program employs a lateral gearing relationship, specified by the user, for in-flight sideslip, crosswind, engine-out trim, and a one-dimensional roll response analysis.

The QSAE characteristics were incorporated into small pertubation equations of motion, converted to state variable form, and evaluated for unaugmented characteristic roots. Finally, Figure 41 illustrates that the QSAE state models can be optionally combined with control laws and analyzed in either time or frequency domain. This last step may be used to develop or evaluate control laws at any flight condition for which the QSAE model is defined.

The pitch-augmented stability (PAS) control law was designed with a preliminary QSAE model of the Initial ACT Configuration; however, the flying qualities presented here reflect the updated structure and evaluation of the preliminary control laws. Therefore, augmented stability characteristics presented here do not meet all flying-quality criteria and may not meet system criteria (e.g., gain and phase margins). The results do illustrate that the control laws are feasible and that only small additional modifications would be required.

The discussion of the QSAE model illustrates that most of the design parameters related to flying qualities are determined with computer programs. Other analytical methods are used for takeoff, stall recovery, and high-speed pitchup evaluation, but they employ QSAE inputs.

Design of the Baseline Configuration used a dynamic analysis for takeoff to determine cg limits for nose-wheel steering, rotation, and engine-out control. Those methods used landing gear characteristics, engine dynamic characteristics, and pilot reaction models to size elevators and rudders. The Initial ACT Program approximated those dynamic methods with static analyses and elastic corrections to the wind tunnel aerodynamic data, using the computer programs shown in Figure 41.

Stall recovery and high-speed pitchup were evaluated semiempirically with QSAE inputs. Nonlinear pitching moment can be characterized by linear data regions to initial buffet or stall. Trim, stability, and small maneuvers for the linear data regions were evaluated with QSAE analysis, while large amplitude maneuvers were analyzed by modifying the linear analysis to reflect the nonlinear moment characteristics. Stall recovery was determined by establishing stabilizer and thrust for trim and the aeroelastic effect on elevator power from QSAE solutions, then determining the pitch acceleration at the stall recovery condition.

Hinge moments for actuator sizing were determined from estimates of control surface hinge moments (app. B) and from the trim and control deflection requirements.

7.1.2 TRIM

The longitudinal and lateral/directional trim characteristics are important for establishing the required trim system authorities and for understanding the flight envelopes and control characteristics. Specifically, longitudinal trim is described in terms of angle-of-attack and stabilizer position, while rudder and wheel positions are shown for sideslip and engine-out trim.

Figure 44 illustrates the extremities of trimmed angle of attack within which flight characteristics are to be presented. The angle-of-attack margin between cruise and stall warning provides an incremental load factor of approximately 0.75g. The corresponding margin between the minimum speed operational limit, defined by $1.2V_S$ or 12 802m (42 000 ft), and stall warning is about 0.33g to M = 0.63, but that margin depends on weight at higher Mach number.

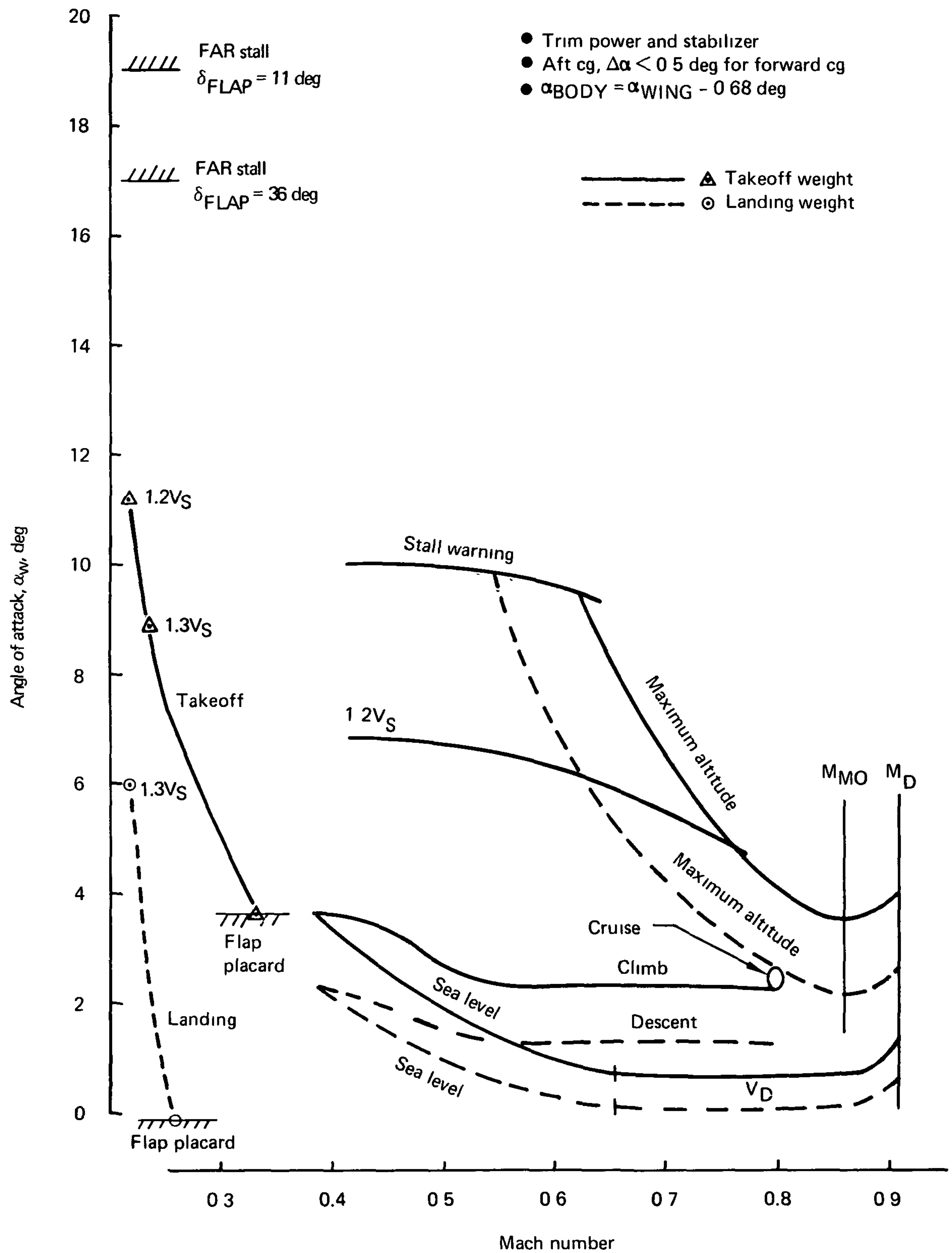

Figure 44. Angle of Attack for Trim

768-103

Stabilizer angle for longitudinal trim within the permissible operational flight envelope is shown in Figure 45. Normal trim gradient with speed (Mach number) is exhibited at forward cg but reversed at all aft cg flight conditions. The automatic trim followup function of the PAS will mask the trim reversal to the pilot; however, manual trim gradients are reversed at many flight conditions. Stabilizer trim limits were established by forward cg at landing, under icing conditions, and by aft cg at the flaps-up $1.2V_S$. The total trim range is about the same as for the Baseline Configuration, but about 1.5 deg more positive. The cruise trim range is about 1 deg greater than for the Baseline Configuration and also shifted about 1.5 deg more positive. This latter fact may mean that the wing camber/twist is not optimum for the Initial ACT Configuration.

If a passive trim failure occurs at cruise (+2.3 deg), then the -8.8 deg of stabilizer, normally used for landing trim, would require -13.3 deg of elevator for trim. Since ± 20 deg of equivalent elevator is available at the landing approach speed, adequate pitch control for maneuver and landing flare remains, even with one critical hydraulic system lost.

Takeoff mistrim can be illustrated in Figure 45. For example, normal takeoff conditions would employ -6.7 deg of stabilizer at the forward cg limit; however, if the trim were inadvertently set at the mechanical limit of +4.5 deg, rotation control would be compromised. The green band limits the trim range permitted for takeoff to prevent this situation. Subsection 7.1.3 describes normal and mistrim takeoff control.

Lateral and directional controls were sized for the Baseline and Initial ACT Configurations at the same flight conditions. This results in the same vertical tail volume coefficient about the aft cg for both configurations. The aft cg limits are 38% and 46% MAC, respectively. The lateral control surfaces of the two configurations differ in that the inboard segment of the outboard aileron is dedicated to ACT on the Initial ACT Configuration. The remaining portion of the outboard aileron is shared by wing-load alleviation (WLA) and lateral control, with the latter input taking priority over WLA commands. Both the Initial ACT and Baseline Configurations "lockout" lateral control signals to the outboard aileron at calibrated airspeeds above 128.7 m/s (250 kn). To compensate for the reduced low-speed roll control due to this change in

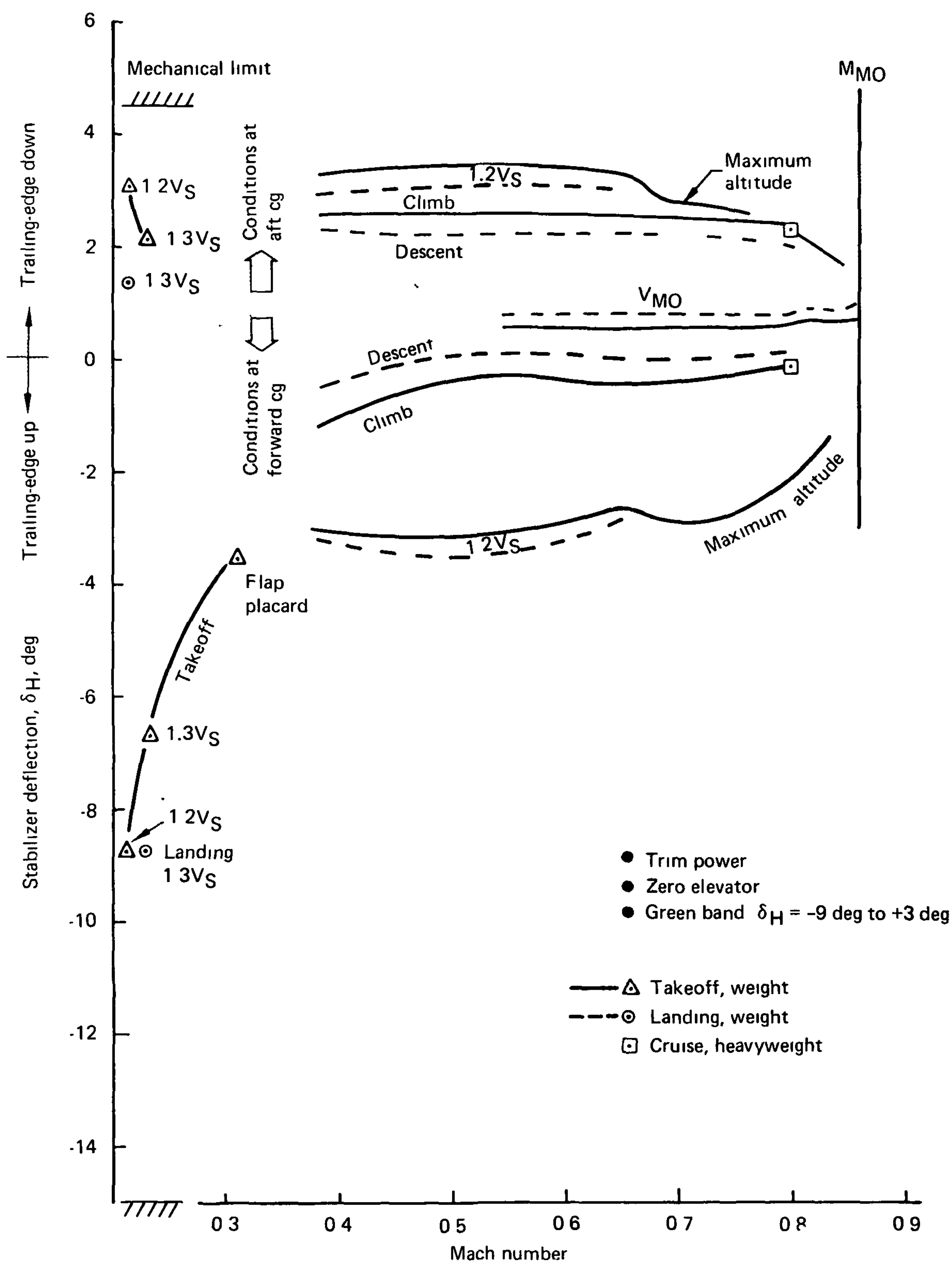

Figure 45. Stabilizer Angle for Trim

outboard aileron from the Baseline Configuration, an outboard spoiler panel was added to the Initial ACT Configuration, resulting in about 15% less maximum roll control; however, high-speed roll control is about 20% greater.

Yaw and roll control are adequate to trim an engine loss throughout the operational flight envelope (fig. 46). Only ailerons are used for engine out-trim at cruise, precluding spoiler drag.

Another lateral control criterion that is imposed by Boeing on commercial airplane design relates to pilot reaction to an engine failure during takeoff. It assumes that only lateral control is used for recovery and trim; this "tameness" is to be statically met with no more than two-thirds maximum wheel to allow for dynamic transients, gusts, and/or hydraulic system failure. The critical case, aft cg light-weight takeoff at $1.4V_S$, is the condition that sized the Baseline spoiler control system. Figure 46 shows that the Initial ACT Configuration, with its reduced low-speed lateral control relative to the Baseline Configuration, misses satisfying this criterion by about 6 deg wheel. However, the Initial ACT Configuration meets the criteria for minimum air and ground control speed, V_{MCA} and V_{MCG}, respectively (subsec 7.1.3), and additional spoiler control would have been excessive at high-speed flight, necessitating additional complex lockout mechanisms. For these reasons, the Initial ACT lateral control was not increased to meet the tameness criterion.

Figure 47 illustrates full rudder sideslip trim capability and required lateral trim. Foward cg leads to the smallest sideslip capability; however, aft cg requires the largest wheel for trim. Less than two-thirds lateral control is required to trim full-rudder sideslips throughout the operational flight envelope (fig. 47). Landing in a 30 kn crosswind at normal approach speed corresponds to a sideslip of 13.8 deg; however, with an allowable 4 deg crab, only 9.8 deg of sideslip are required. Rudder power available, even with one hydraulic system out, provides trim to 13.4 deg (fig. 47). Crosswind landing with 4 deg crab requires a rudder deflection of 18 deg and 50% of the lateral control at the critical aft cg.

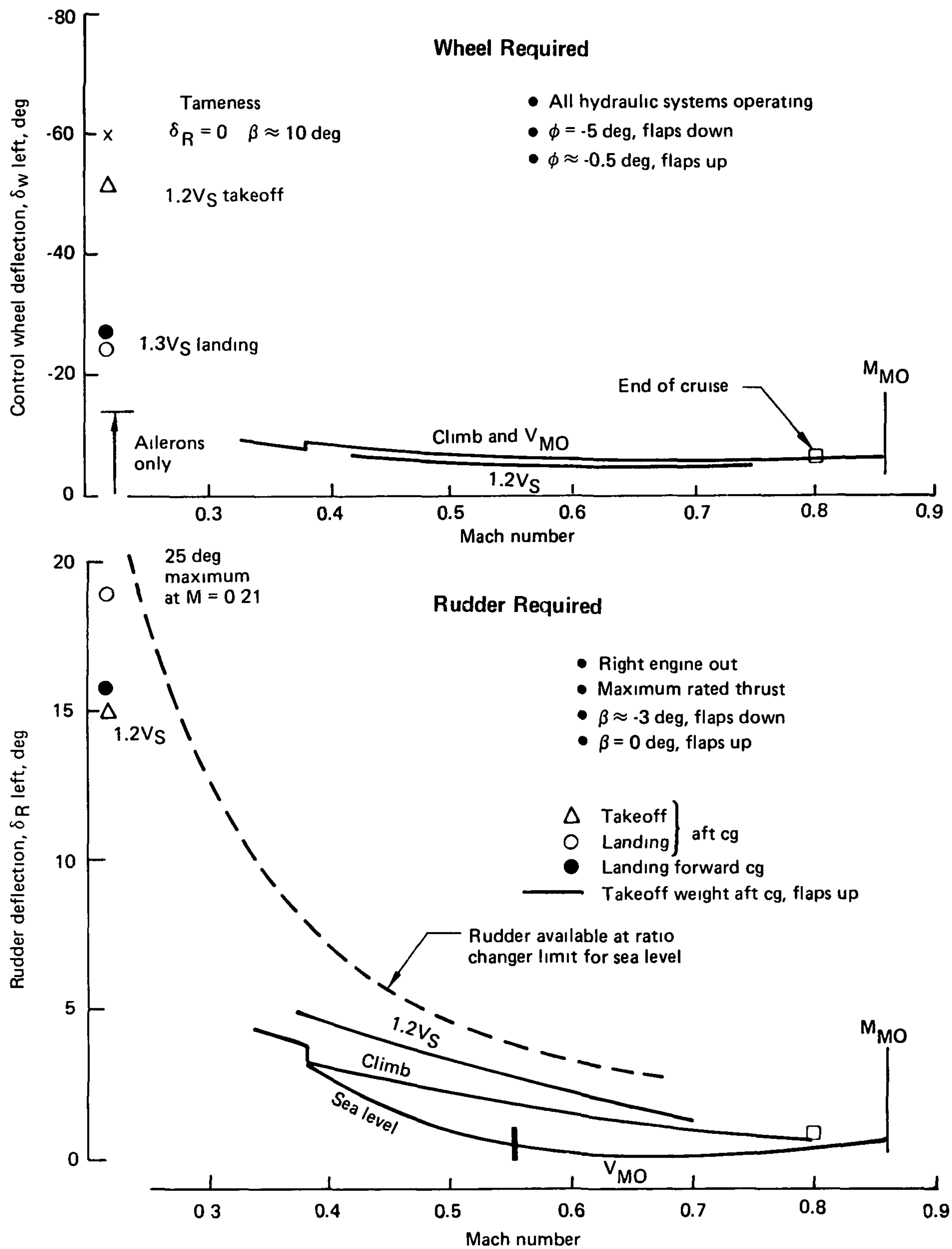

Figure 46. Engine-Out Trim

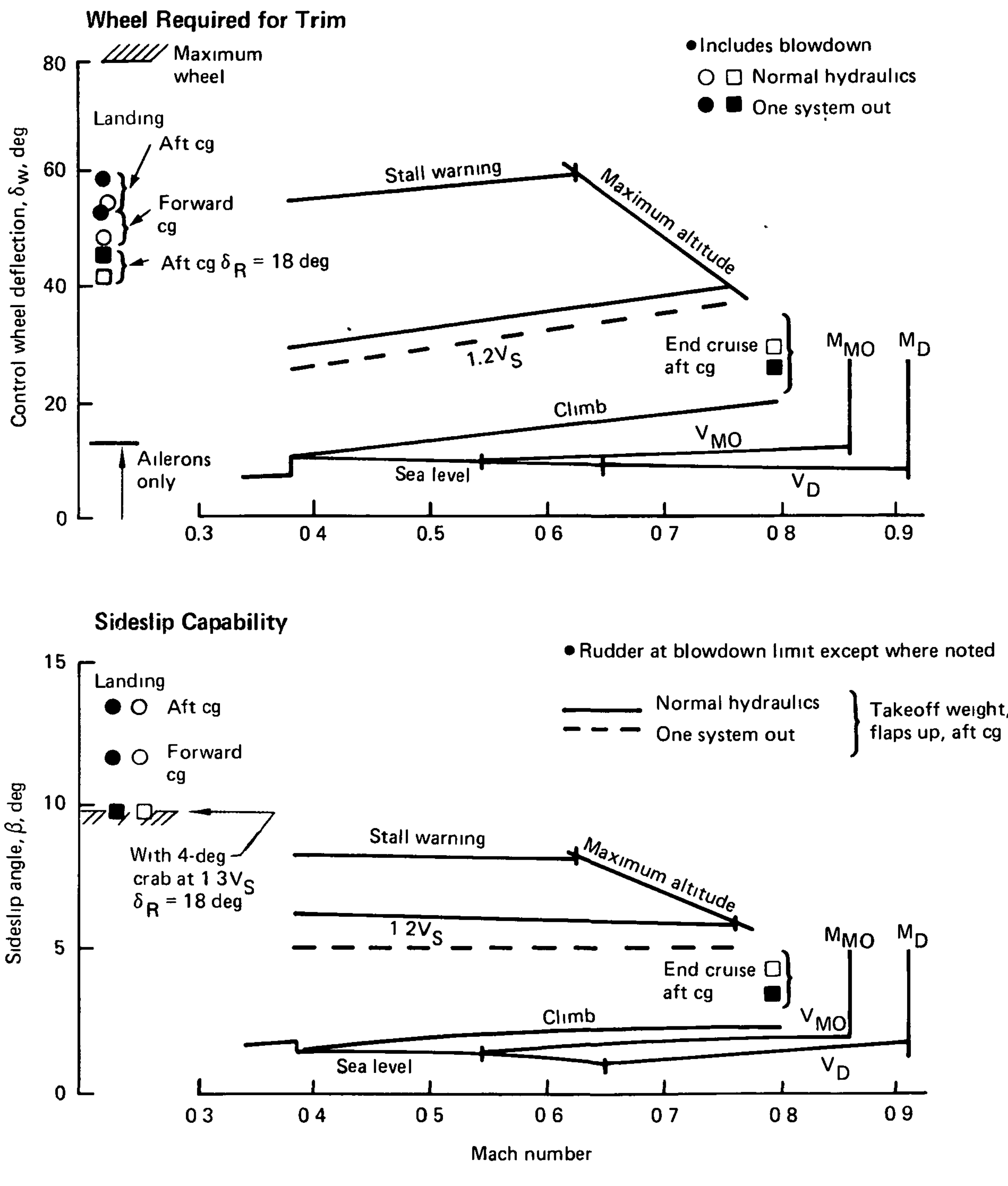

Figure 47. Sideslip Trim Capability

7.1.3 CONTROL

The longitudinal and lateral/directional control characteristics described are important for establishing balance limits for control and actuator sizing and for designing the feel systems. Specifically, control available and applicable requirements are shown for takeoff, landing, landing stall recovery, roll response, and longitudinal maneuvering. The latter is illustrated as the incremental elevator deflection required for constant speed pullup or pushover and for trimming a speed increase (1 kn), and they reflect basic airframe stability.

Takeoff control capability with loss of one critical hydraulic system is shown in Figure 48. Takeoff rotation capability, shown for normal trim set for climbout, provides control for rotation below the performance rotation speed. Full mechanical mistrim at the forward cg (at +4.5 deg stabilizer), however, cannot meet the performance rotation speed; and a green band will be incorporated to preclude full mechanical mistrim at takeoff. Because of the increased lift capability of the double-hinged elevator, the ability to control a full mistrim within a single green-band limit is possible.

Stall recovery is critical at landing and is illustrated for aft cg in Figure 49. The normal approach trim condition is stable and pitches up at about 25 deg alpha without natural recovery. The high angle-of-attack behavior, characteristic of T tails, and the requirement for nose-down control margin are the critical design conditions that size the horizontal tail and elevators. The Initial ACT Configuration uses an alpha-limiting device and a double-hinged elevator to reduce the horizontal tail size to meet stall recovery at the Federal Aviation Regulation (FAR) performance stall speed. An 0.08-rad/s^2 pitch control margin at stall with full positive elevator precludes angle-of-attack increases to locked-in stall (fig. 49). An alpha-sensing system will result in automatic elevator input at stall. Pitch augmentation will minimize the chance of inadvertently encountering stall.

A double-hinged elevator was not used on the Baseline Configuration because the stability and ground nose-wheel steering limitations would preclude significant tail size reduction or more aft balance. Furthermore, the tail input at deep stall is poor,

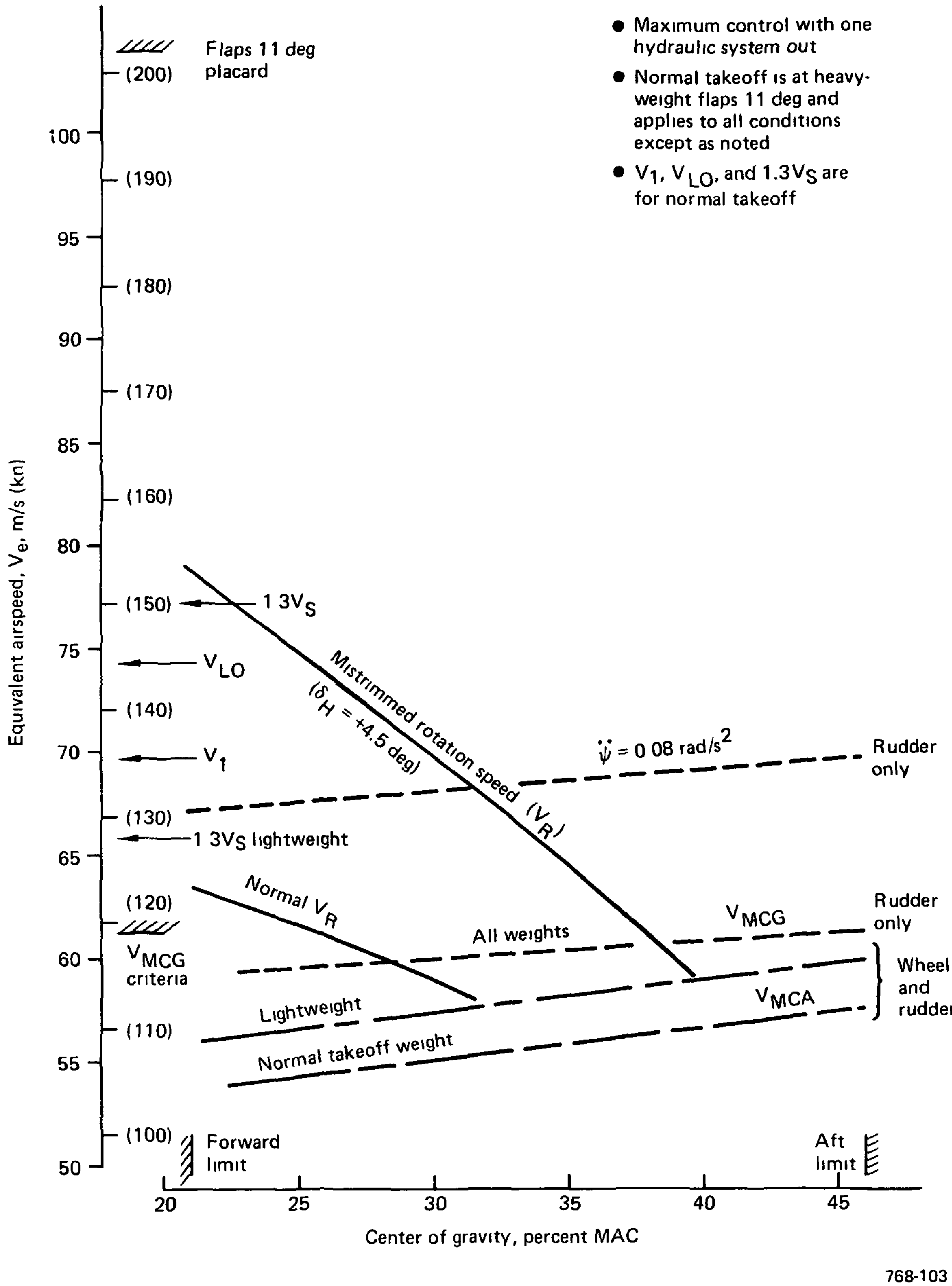

Figure 48. Takeoff Control

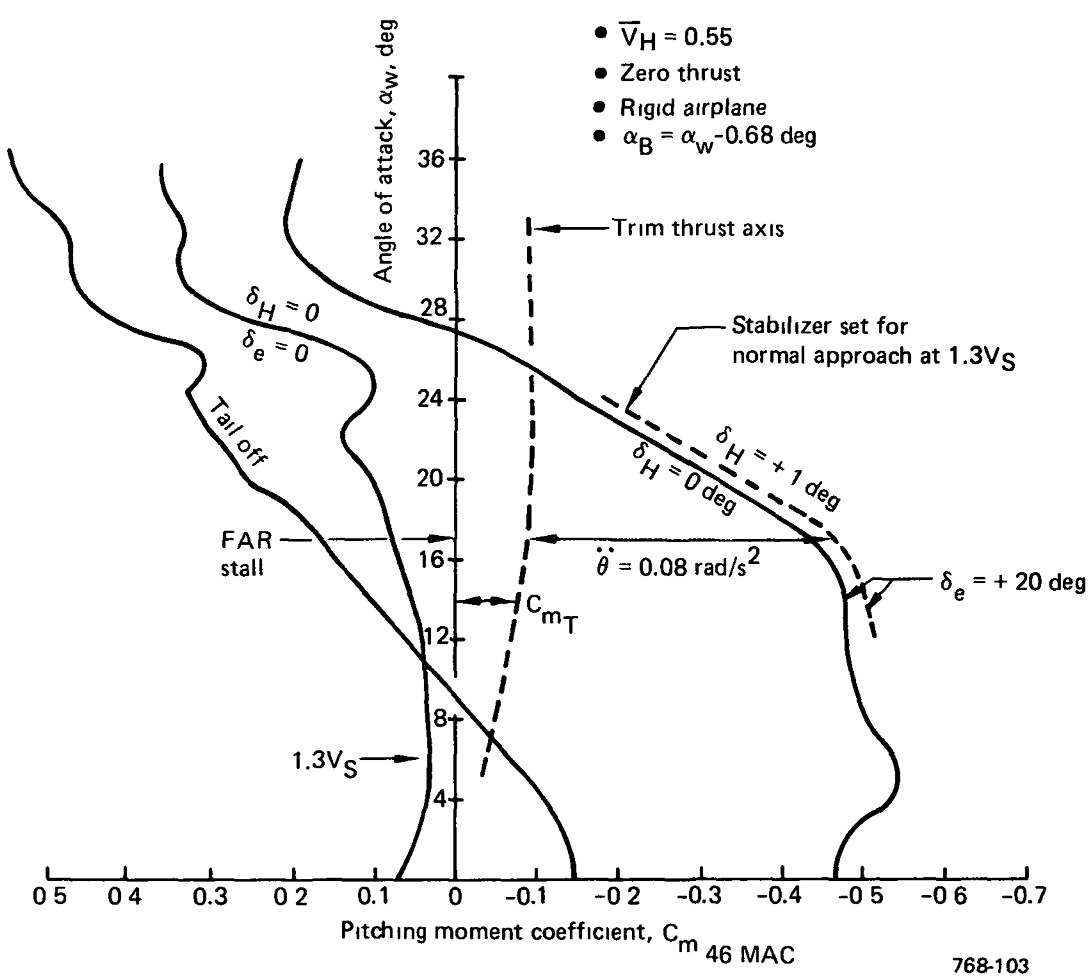

Figure 49. Landing Stall Recovery

and the payoff of a double-hinged over a conventional elevator probably does not warrant the complexity. However, the double-hinged elevator would preclude the need for the multiple green-band system on the Baseline Configuration.

The speed that provides 0.1 rad/s^2 pitch acceleration at landing is shown in Figure 50 for both normal approach trim and a mistrim, jammed at cruise. This pitch control capability is available at speeds well below the normal approach speed of 1.3V_S.

Minimum engine-out control speeds for the takeoff ground run and in free air (figs. 48 and 49) are based on a dynamic analysis that assumes a 0.6 sec reaction time before the pilot uses the rudder and wheel control. These capabilities exist with loss of one

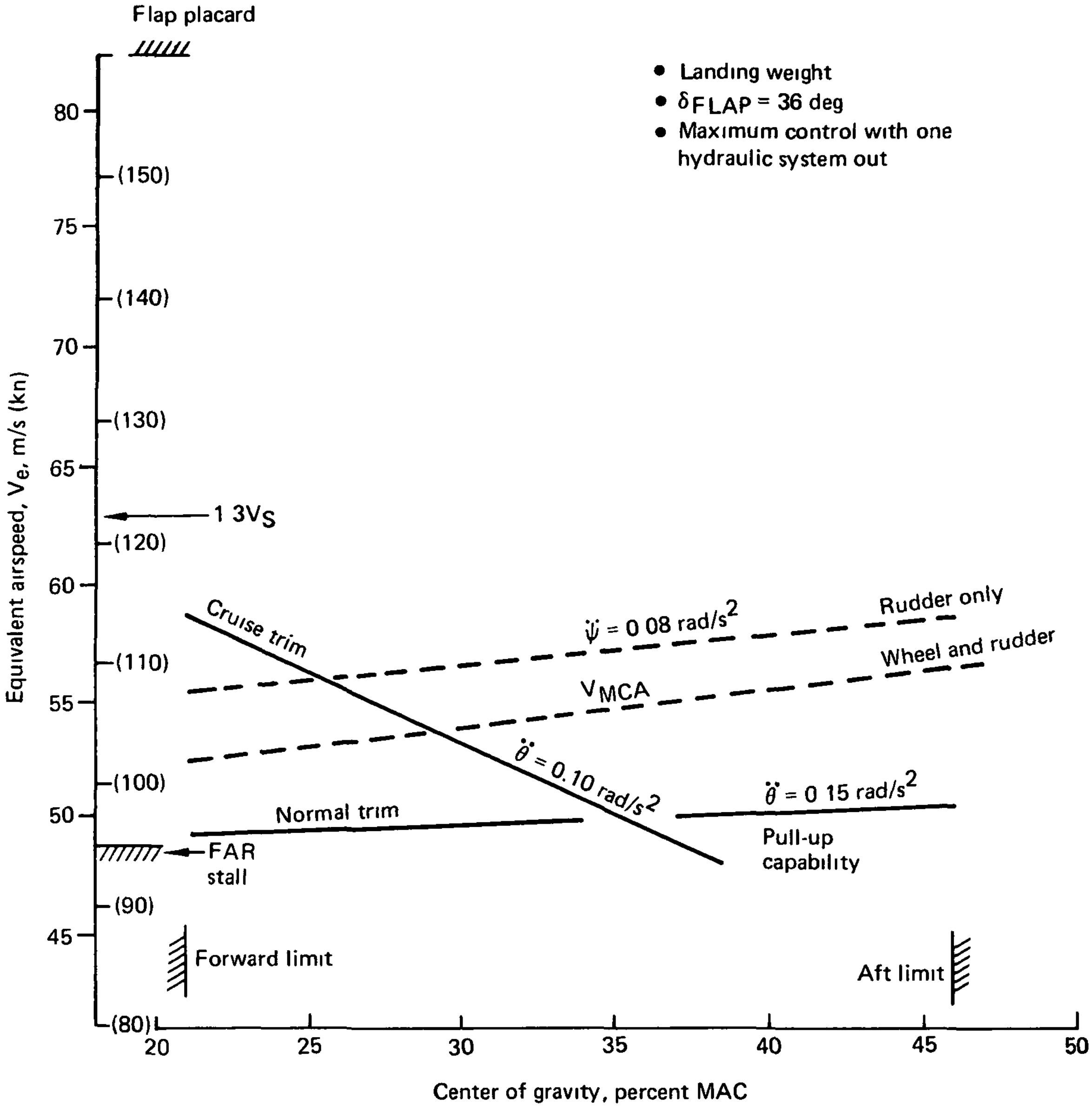

Figure 50. Landing Control

hydraulic system and are critical at light weight and aft cg. The V_{MCG} capability (fig. 48) is nearly identical for all takeoff weights and flap settings, but the criterion is most demanding at light takeoff weight. Figure 48 also shows that the V_{MCG} just meets the criterion and is the condition that sizes the vertical tail and rudders for both the Baseline and Initial ACT Configurations. Engine-out V_{MCA} capability (figs. 48 and 50) must be less than $1.3V_S$ minus 2.57 m/s (5 kn); the critical case is for light-weight takeoff and is less than this criterion by 4.37 m/s (8.5 kn) at aft cg.

Early in the Initial ACT Project, a rudder kicker activated by engine-out sensors was evaluated as a means of eliminating pilot reaction time and minimizing the effect of engine dynamics to reduce required vertical tail size. Preliminary assessment indicated that fin size could be reduced by 16% with engine-out control still sizing the fin and rudder. The system was not incorporated on the Initial ACT Configuration because the same system could apply to the Baseline Configuration and would not result in a benefit peculiar to ACT.

Rudder power capable of producing yaw acceleration of 0.08 rad/s^2 (figs. 48 and 50) is available to speeds well below normal takeoff and approach.

Roll response capability for takeoff and en route flight (fig. 51) reflects maximum roll inertia and full control wheel input as a 0.5 sec ramp. Takeoff capability, shown for all hydraulic systems operating and critical system failures (see fig. 40), illustrates that normal and two-system failure roll response capability are nearest their criteria requirements (Levels 1 and 3, respectively). Normal roll response at takeoff meets the Level 1 criteria down to about 18% above the stall speed, which is below the operational flight envelope. However, the two-system failure case exceeds the 4.5 sec to achieve 30 deg bank criteria at speeds less than about 23% above stall and is the critical case. Roll control is greater at increased flap settings; therefore, the landing condition exhibits better roll response than takeoff. Flaps-up roll response reflects the aileron lockout mechanism and shows that all criteria are met and that the critical case is normal hydraulic system operating just after roll control commands are eliminated to the outboard aileron (about 250 kn, calibrated airspeed). The Initial ACT Configuration roll inertia is about 7% greater than the Baseline due to outboard wing tanks. It has a reduced outboard aileron but one more spoiler panel per side. These differences result in about 20% more roll response capability at high speed when neither configuration uses the outboard aileron and about 13% less capability at takeoff when the aileron is unlocked. The two hydraulic systems failed condition at takeoff is critical for both configurations. The Baseline Configuration met this Level 3 criterion down to about 10% above stall speed, and both configurations were considered to have adequate roll response capability.

Unaugmented elevator angle per g (fig. 52) illustrates unstable short-period characteristics at flaps-up aft cg at low speeds or less than about $1.3V_S$ at takeoff.

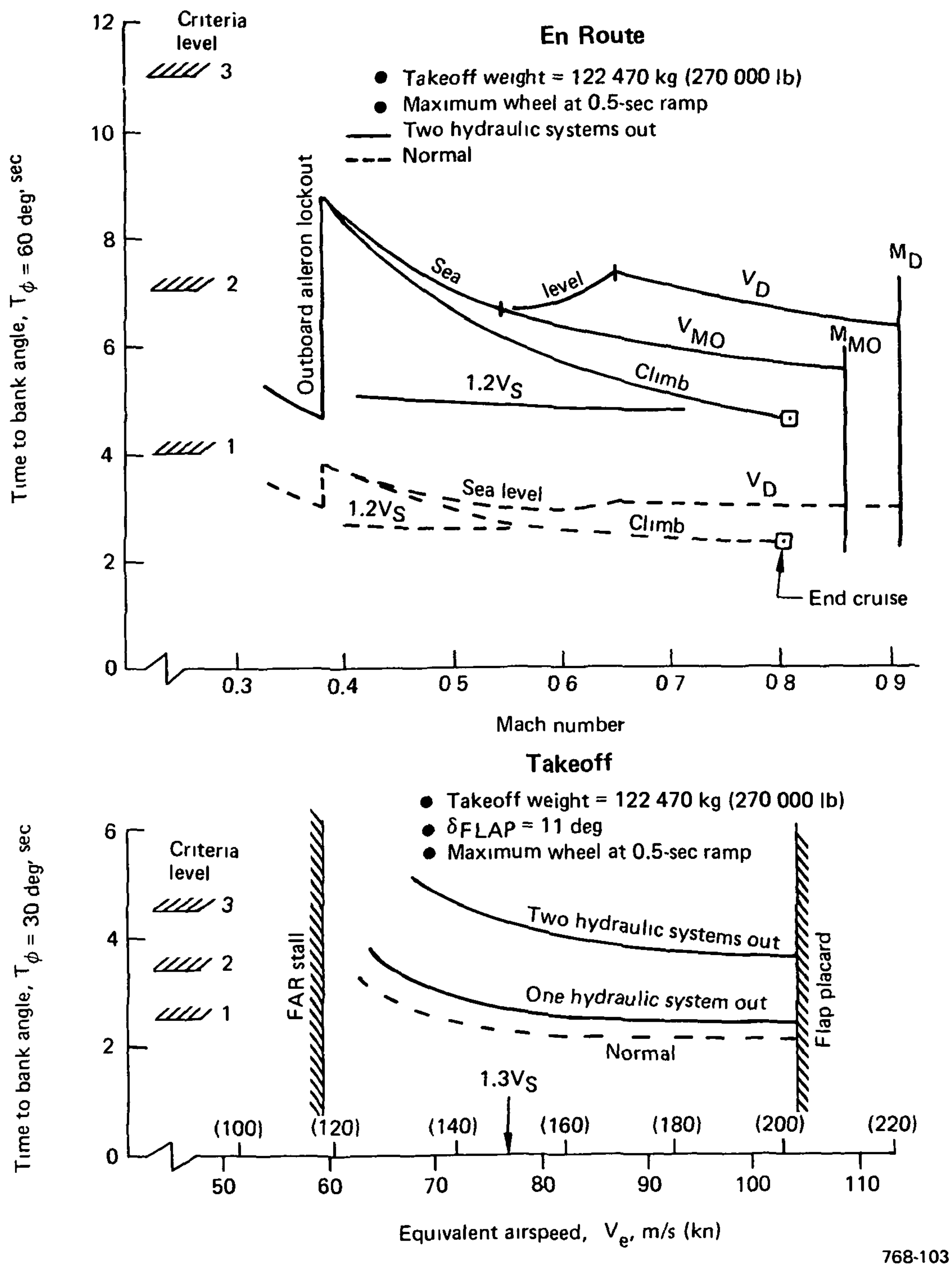

Figure 51. Roll Response Capability

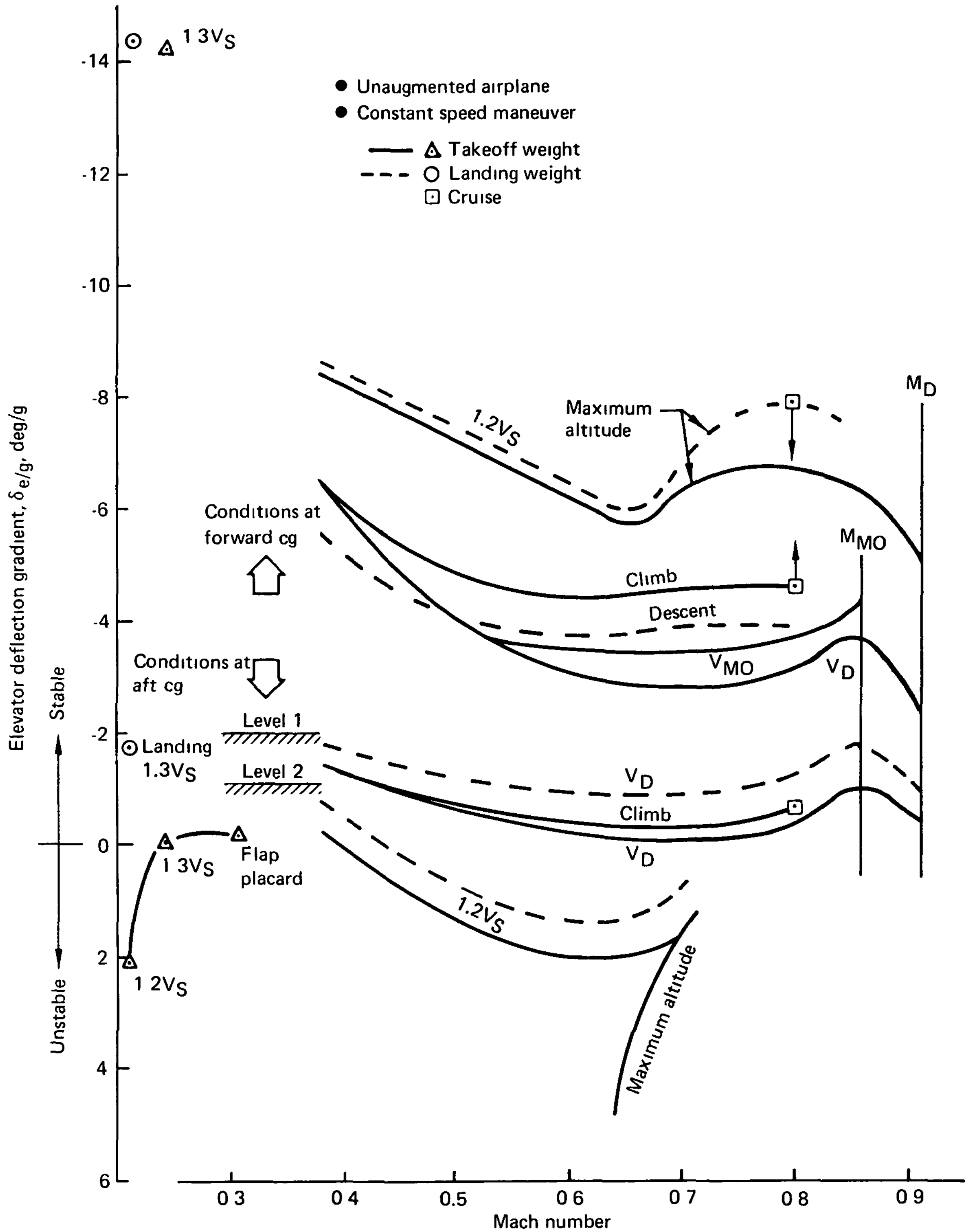

Figure 52. Elevator Angle per g

The critical pitch augmentation conditions will be M = 0.65 at $1.2V_S$ for Level 1 flying qualities and about M = 0.63 maximum altitude for Level 3. The latter condition is in the pitchup region, as illustrated in Subsection 7.1.4. In any event, stability agumentation will provide good elevator angle per g characteristics.

Figure 53 summarizes unaugmented speed stability characteristics as the elevator angle required to trim a 0.5144 m/s (1 kn) speed increases. Note that an unstable gradient exists throughout most of the design flight envelope and much of the operational flight envelope, reflecting an unstable phugoid mode that must be stabilized with the ACT system. The critical Level 1 design condition will be heavy weight, aft cg at $1.2V_S$ about M = 0.68; and the critical Level 3 control law design will occur in the pitchup region near maximum altitude at about M = 0.63. Feel system design, in conjunction with stability augmentation, will ensure that the stick force-speed gradient criteria will be met.

7.1.4 STABILITY

Basic airframe longitudinal stability is described in terms of static and maneuver margins, time to double amplitude, characteristic roots, and a time history response to an elevator input. These characteristics are used to define the critical flight conditions for design of control laws. Also, a preliminary set of control laws is evaluated in terms of augmented characteristic roots and elevator response. Lateral-directional stability is described in terms of static stability, Dutch roll damping, roll mode time constant, and spiral mode time to double amplitude.

The Initial ACT longitudinal unaugmented static margins are summarized in Figure 54 for cg = 0.46 MAC. The unstable aft cg conditions illustrate trim reversal through most of the flight envelope. The high-speed pitchup below M = 0.65 was exhibited in the basic aerodynamic data shown in Appendix B and in the elevator characteristics shown in the previous section.

Figure 55 illustrates rigid pitch characteristics with the Baseline tail size. The tail does not significantly change the pitchup tendency, which means that the wing is largely responsible for the pitchup shown in Figure 54. Wing development for

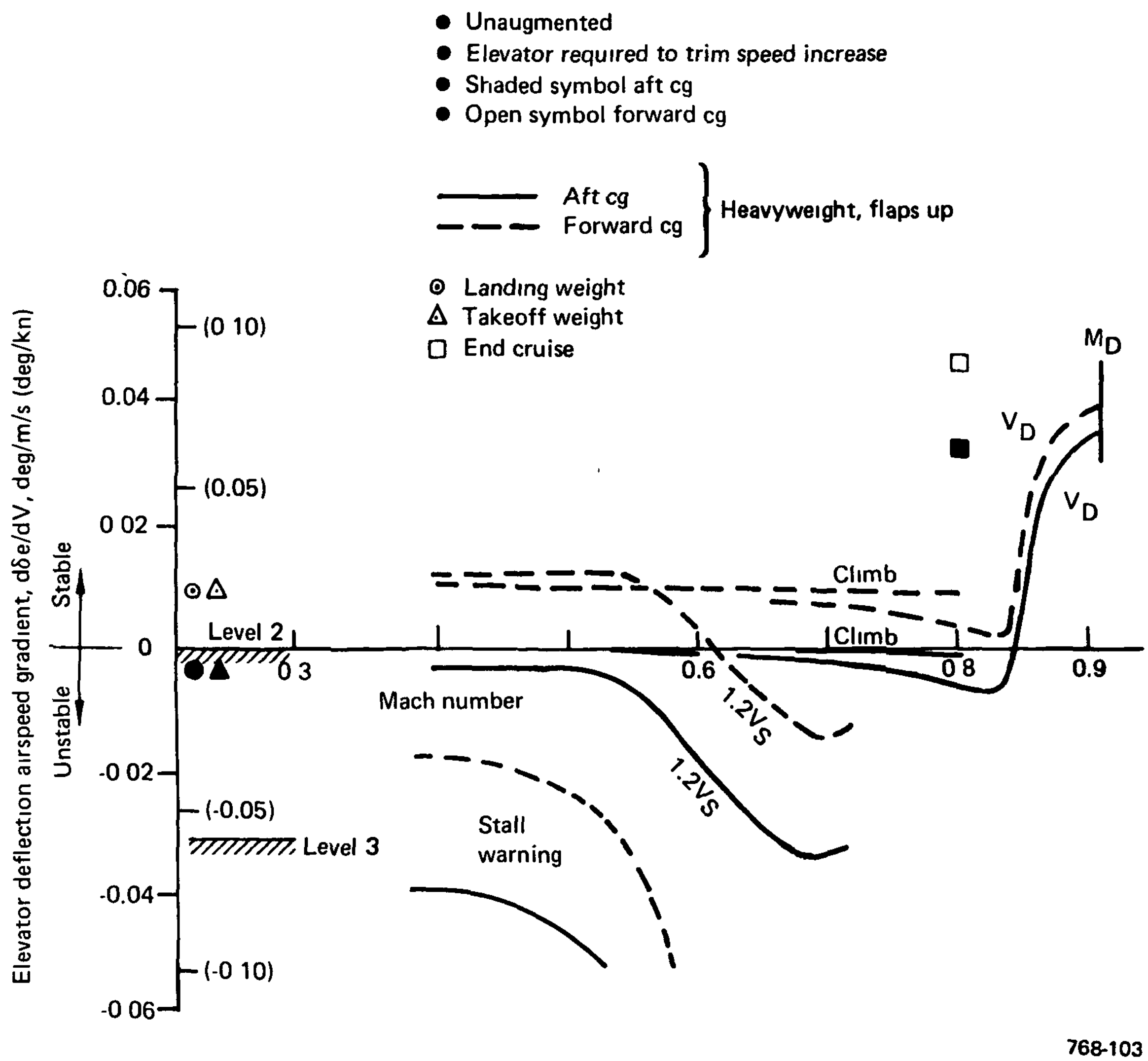

Figure 53. Speed Stability

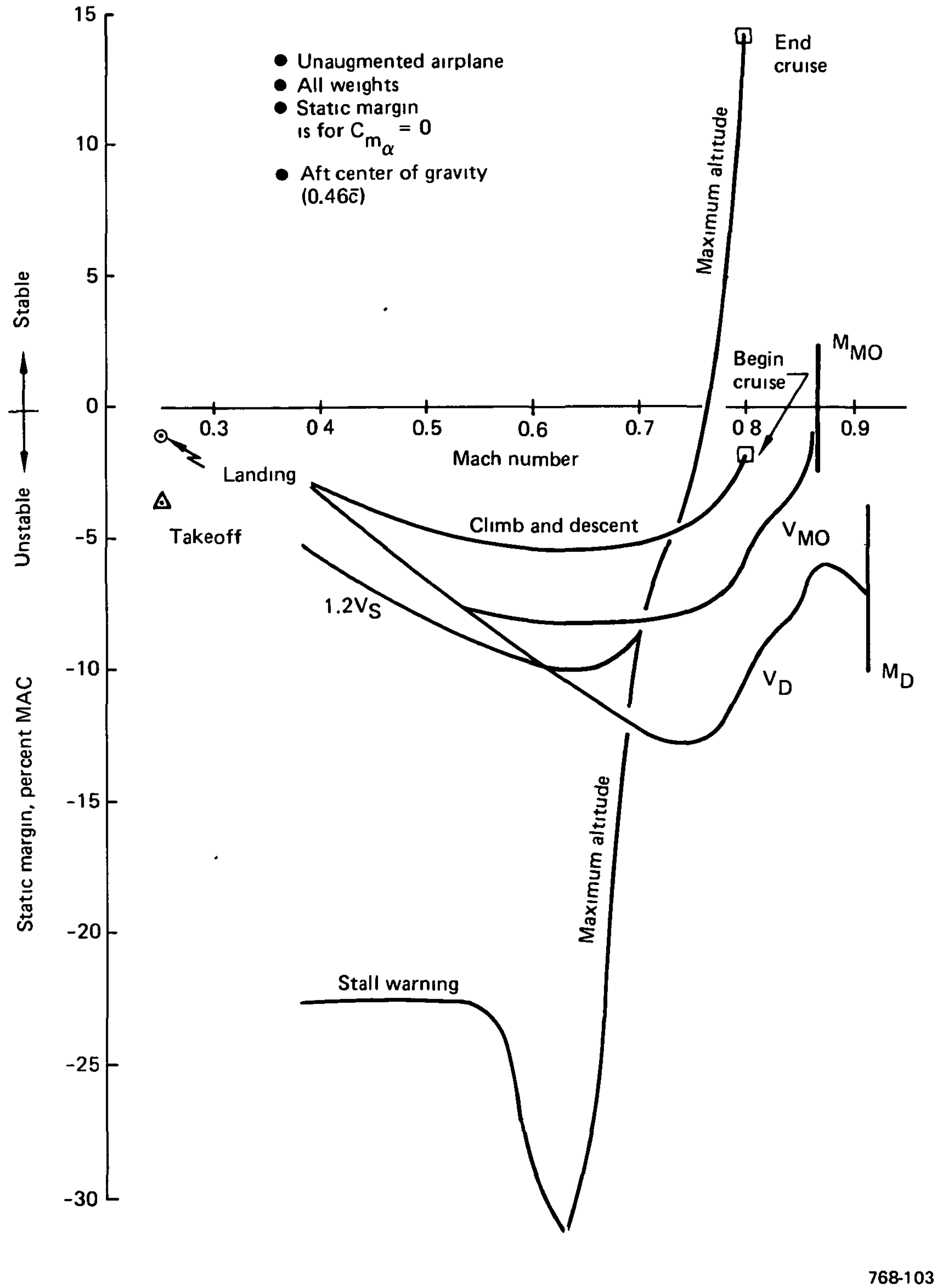

Figure 54. Static Margin at Aft Center of Gravity

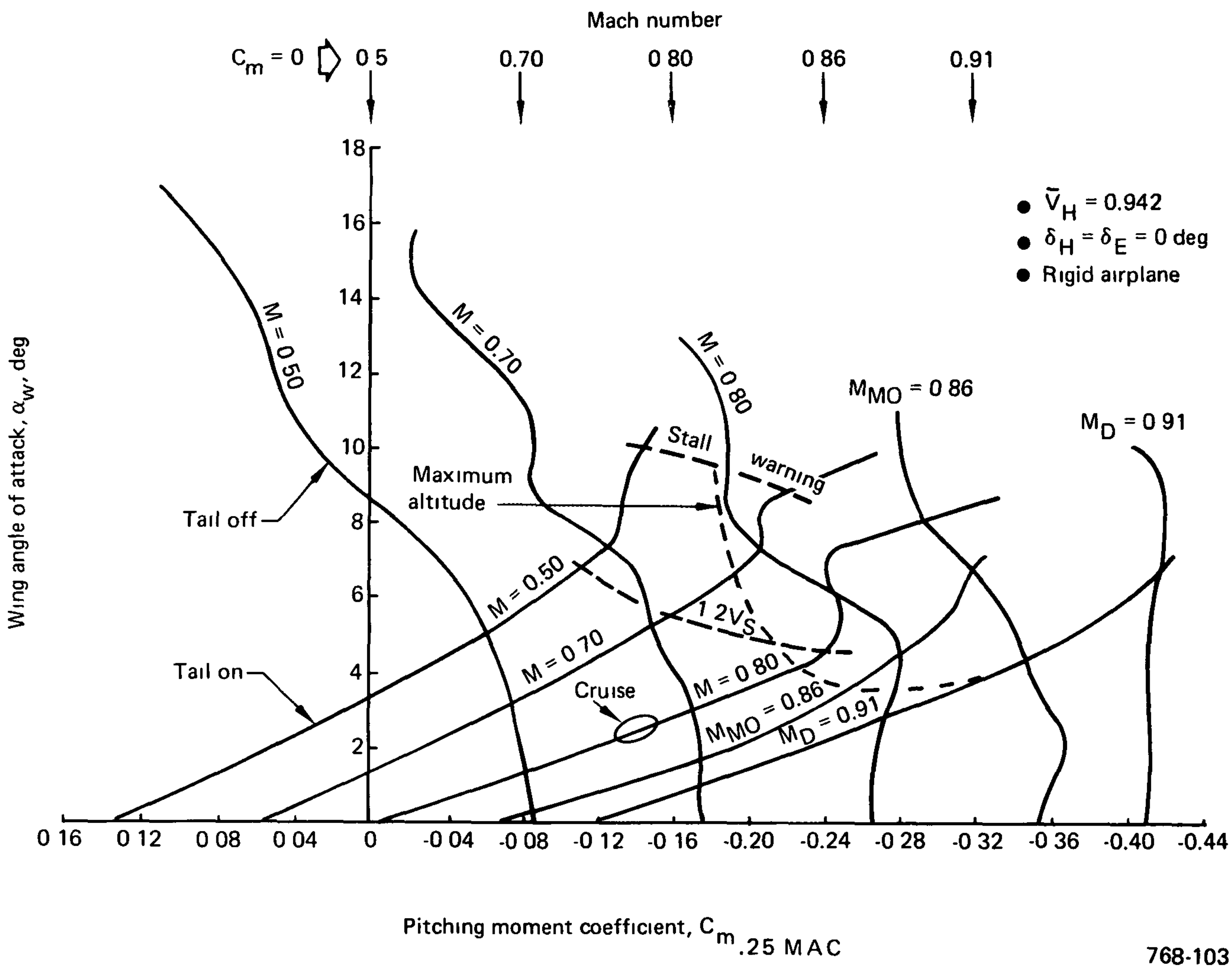

Figure 55. High-Speed Pitching Moment With Baseline Tail Size

conventional aircraft design is a compromise among performance, structural design, and pitchup. However, the pitch augmentation used on the Initial ACT Configuration should reduce the need to compromise wing design for pitchup. This potential performance benefit between the Baseline and Initial ACT Configurations has not been assessed. Finally, the stability augmentation should reduce the design effort and/or complexity of the feel system.

Unaugmented maneuver margin (fig. 56) reflects characteristics similar to the static margin and elevator angle per g. Note that maneuver stability exists at the aft cg for much of the operational envelope. This is confirmed by the short-period criteria for

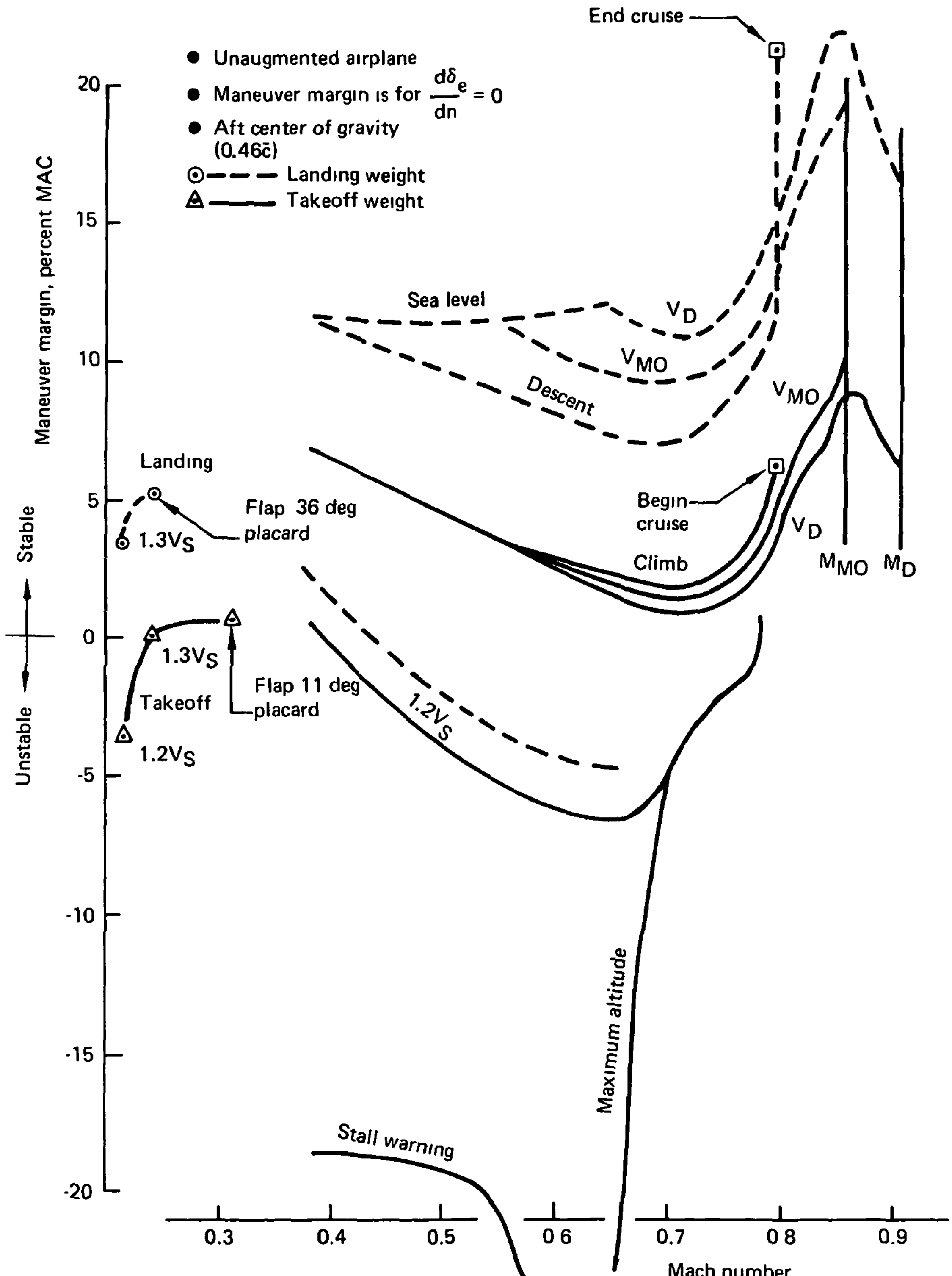

Figure 56. Maneuver Margin at Aft Center of Gravity

conventionally stable aircraft (fig. 57); however, the speed instability (phugoid mode) shown in Figure 53 is significant.

The Initial ACT PAS uses separate systems of pitch rate and speed feedback. These control laws were designed from a preliminary QSAE model (described in subsec 7.3), not the QSAE model reflected in the unaugmented characteristics described in this subsection. The following discussion illustrates the stabilizing effect of these preliminary control laws, with increased gains, on the final QSAE model. Results are shown in relation to unaugmented and augmented characteristic roots and elevator response. The WLA system does affect flying qualities; however, this system is excluded from the following assessment but is discussed in Subsection 5.5. Design conditions derived from Figures 52 through 58 are listed in Table 11; the stability and response criteria to be met are illustrated in Figures 57 through 61. The flight conditions (table 11) reflect lowest and best phugoid or short-period stability for the extremes of dynamic pressure. For example, Condition 61 is end of cruise; a stable, low dynamic pressure or speed condition in which the constant gain PAS should neither stabilize nor destabilize outside the Level 2 criteria. This flight condition is on the operational/design flight envelope boundary where Level 1 would be an objective, and it contrasts with Conditions 17, 99, and 97, which are definitely in the operational flight envelope.

Figures 59 and 60 illustrate basic and augmented stability in terms of characteristic root or pole locations. The constant gain control laws tend to stabilize the critically unstable conditions but to destabilize the naturally stable flight conditions. The latter cases are at end of cruise (Condition 61) and V_D (Conditions 67 and 69); however, no flying quality criteria are violated. The unstable high-speed conditions (36 and 107) were stabilized adequately, but the low-speed conditions (89, 58, 17, and 108) were not satisfactorily stabilized. For example, condition 89 in the pitchup region was not augmented to Level 3, while conditions 58 and 108 on the operational flight envelope boundary were only stabilized to about Level 2. As speed increases slightly to Condition 17, PAS performance becomes satisfactory.

Unaugmented and augmented elevator response is illustrated in Figure 61 for Flight Condition 58, which represents an unstable maneuver condition that was stabilized. In

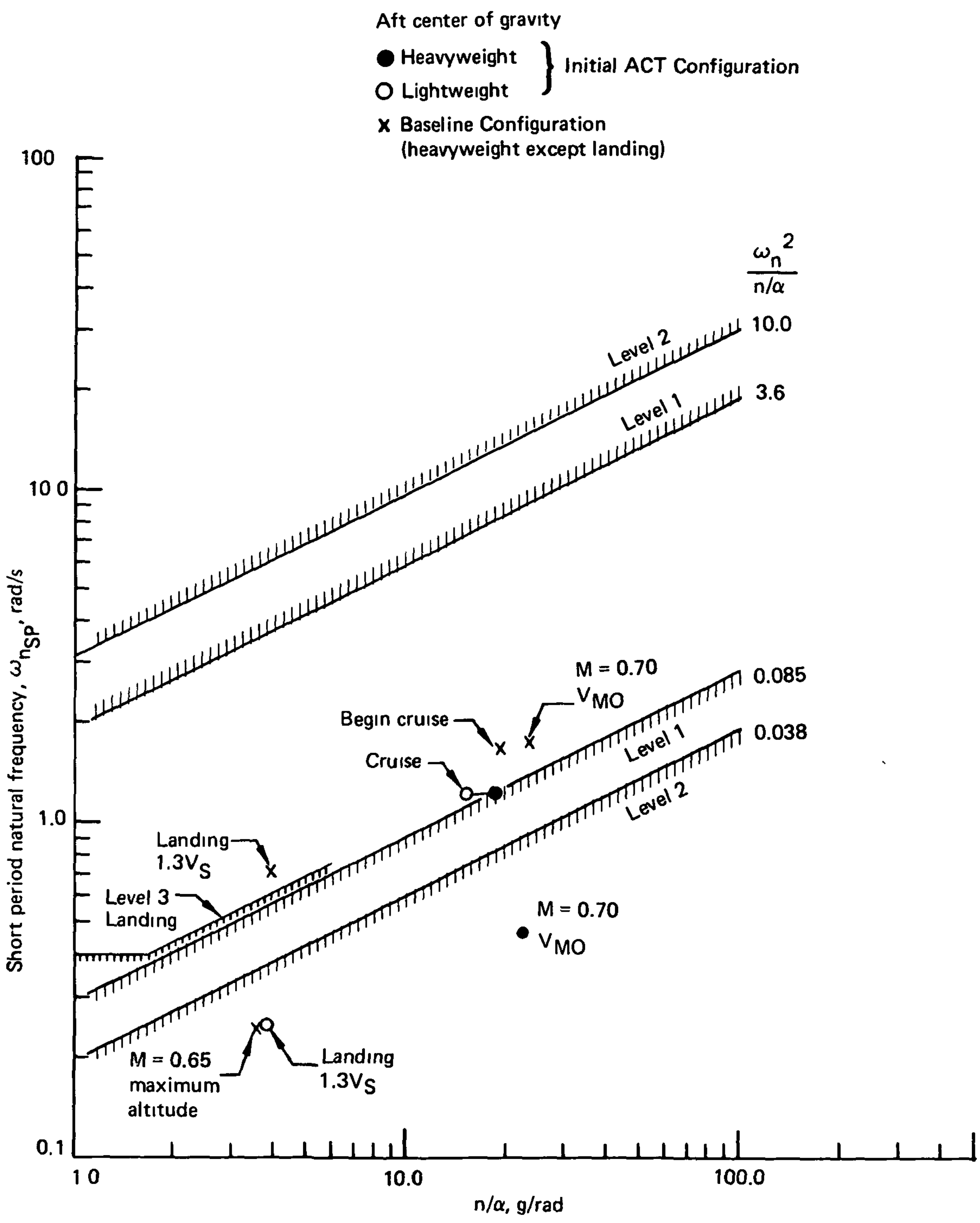

Figure 57. Unaugmented Short-Period Stability

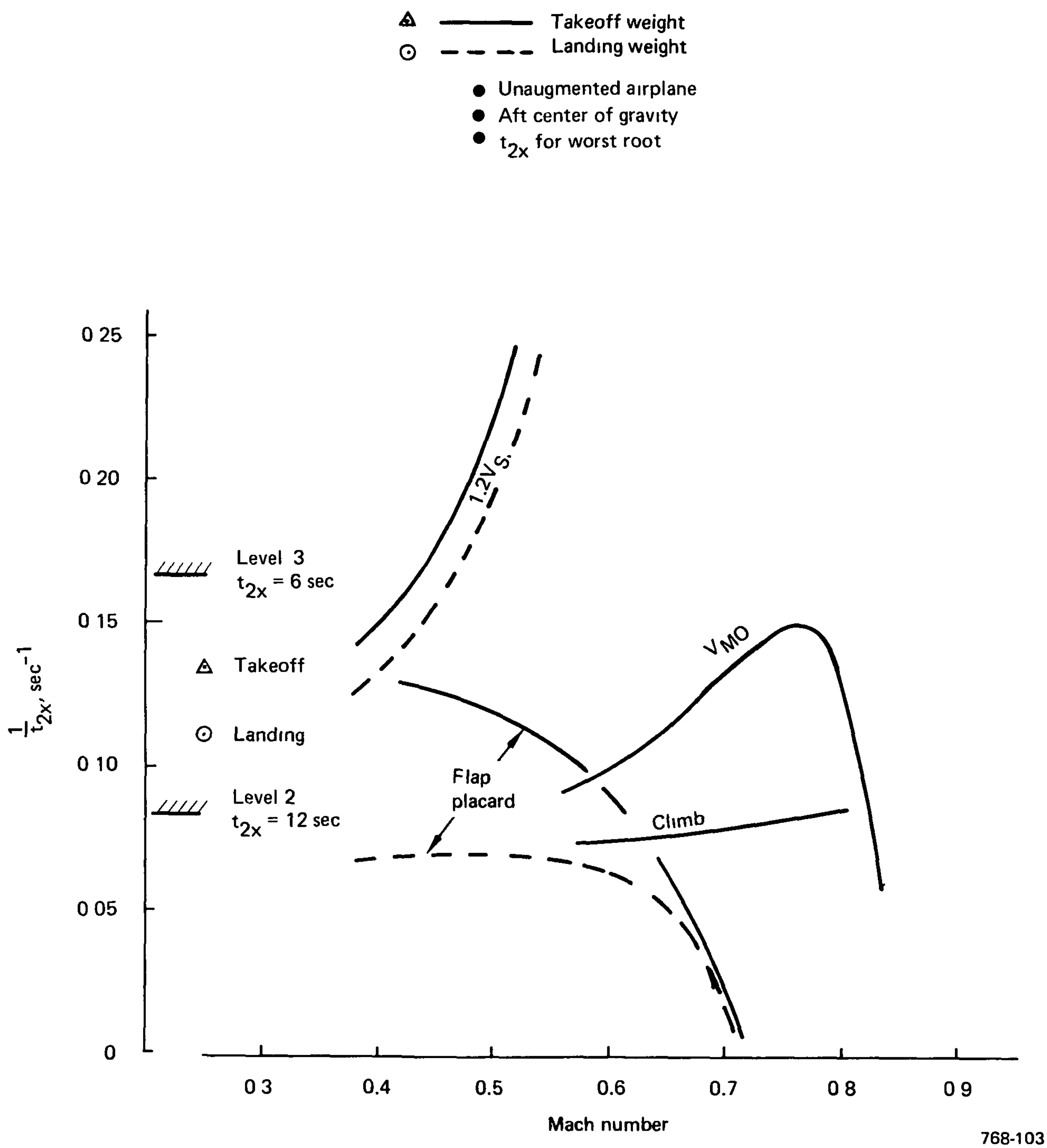

Figure 58. Time to Double Pitch Amplitude

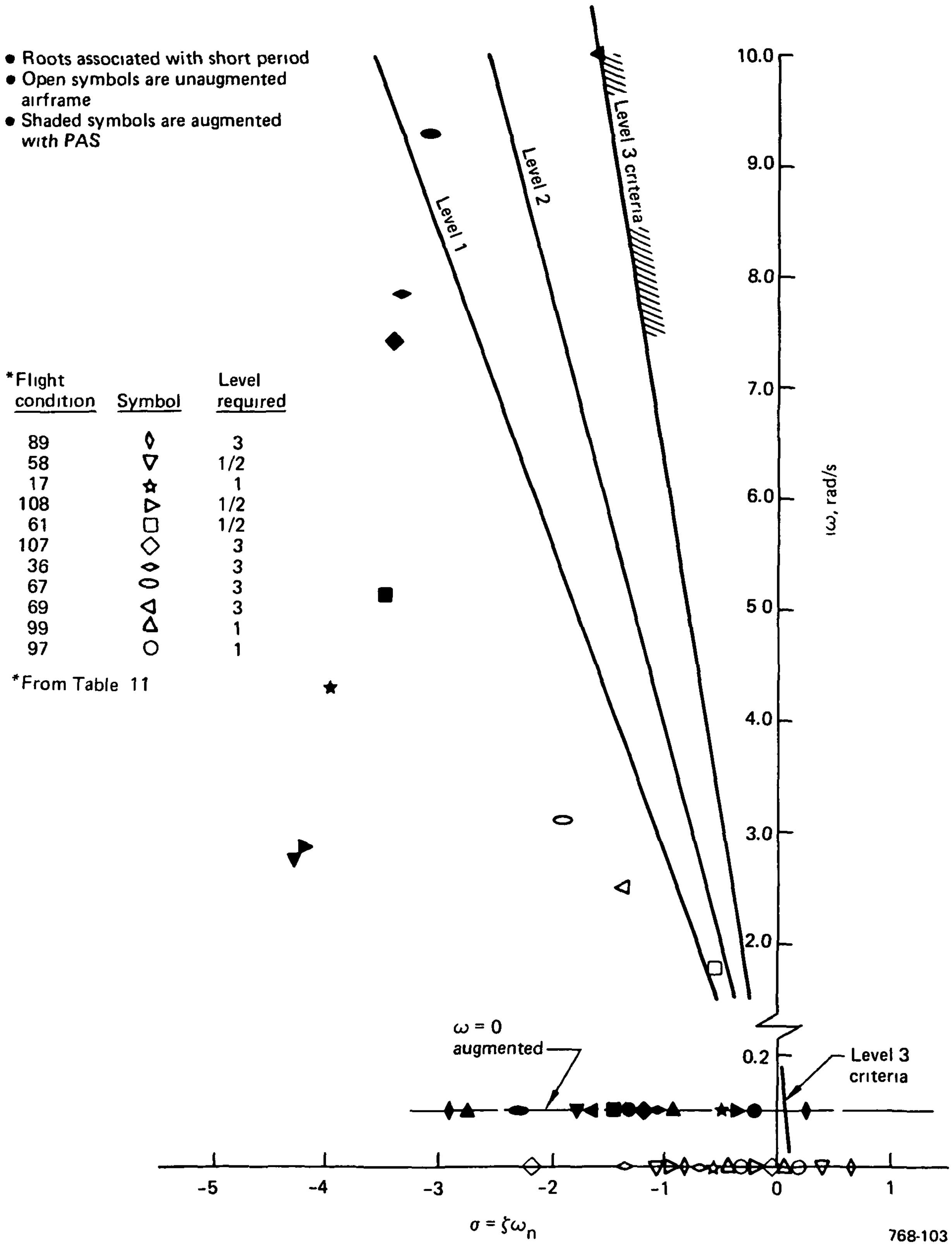

Figure 59. Short-Period Characteristic Roots

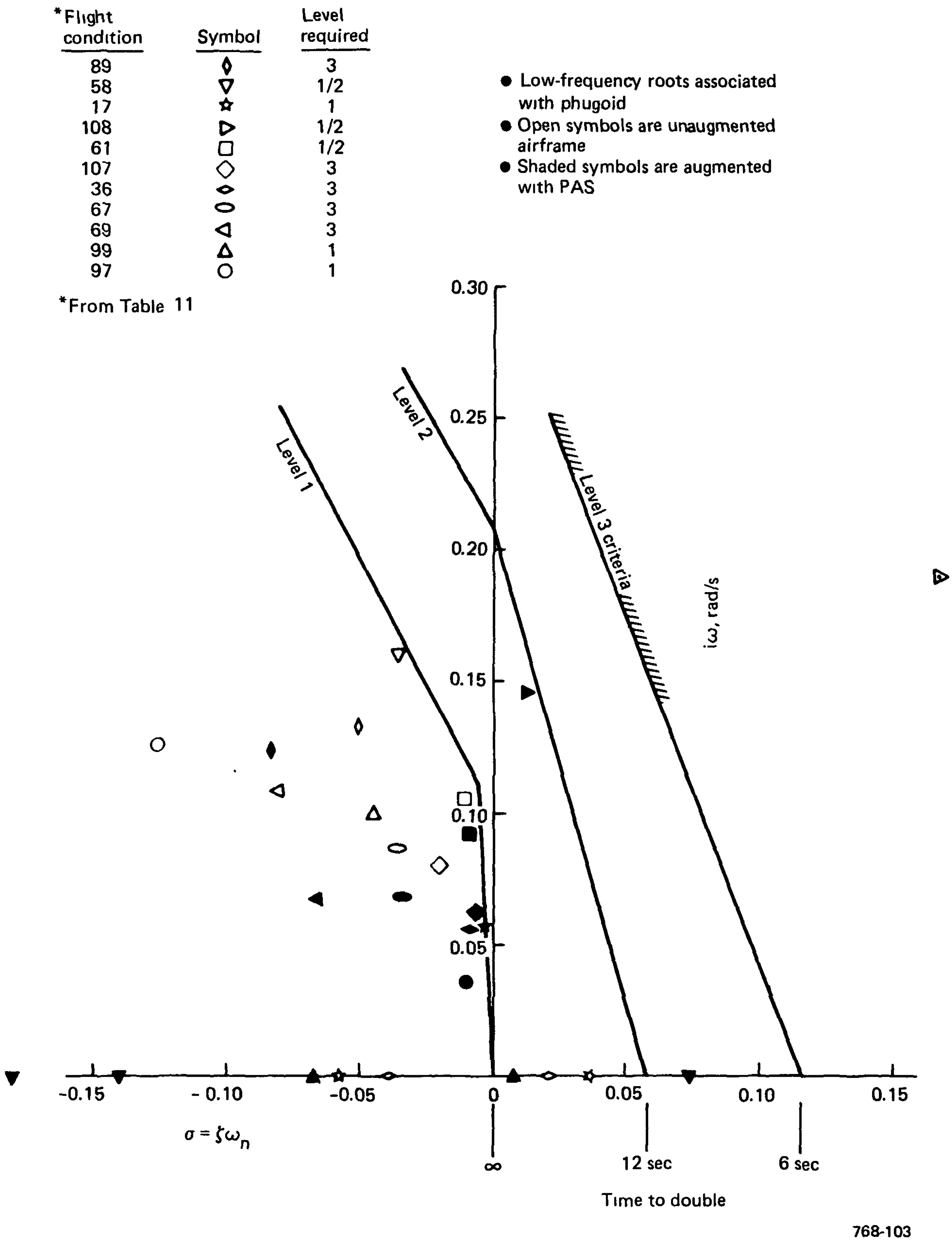

Figure 60. Phugoid Characteristic Roots

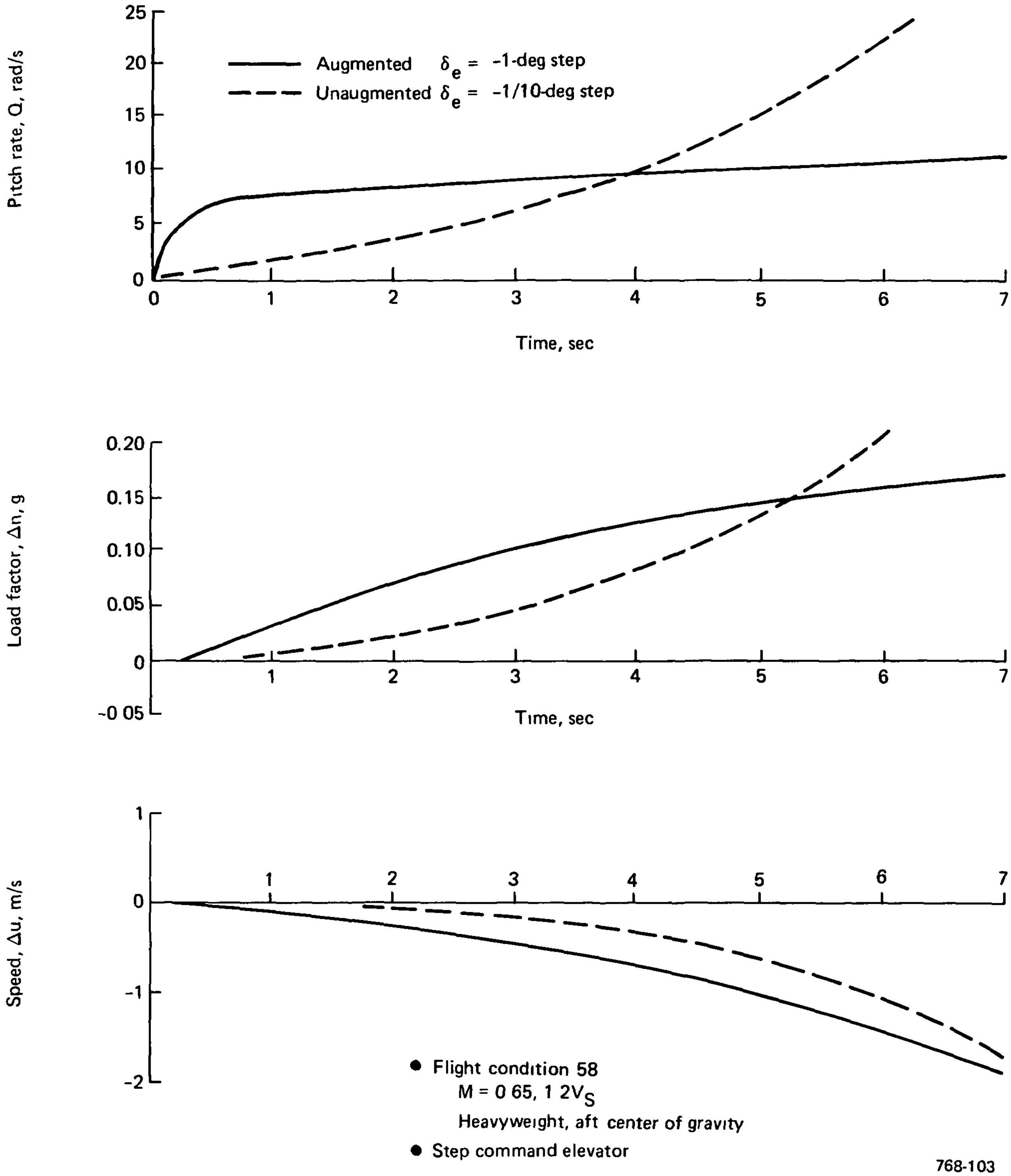

Figure 61. Elevator Response

Table 11. Design Conditions for Pitch Stability Augmentation

Flight condition	Mach No	Speed	Weight	Center of gravity	Required criteria level
89	0 65	Maximum altitude	Heavy	Aft	3
58	0 65	1 2V_S	Heavy	Aft	1 or 2
17	0 65	1 53V_S	Heavy	Aft	1
108	0 70	1 2V_S	Heavy	Aft	1 or 2
61	0 80	Maximum altitude	Light	Fwd	1 or 2
107	0 70	V_D	Heavy	Aft	3
36	0 82	V_D	Heavy	Aft	3
67	0 86	V_D	Light	Fwd	3
69	0.91	V_D	Light	Fwd	3
99	Takeoff	1.3V_S	Heavy	Aft	1
97	Landing	1 3V_S	Light	Aft	1

768-103

Figure 59, the unstable characteristic roots for the short-period exhibit a time to double of 1.8 sec, which is stabilized by the PAS to a damping ratio of 0.84 and frequency of 3.47 rad/s. These augmented characteristics meet Level 1 criteria. Figure 61 also shows the corresponding load factor responses to about a 1 deg elevator step command. This yields an approximate δ_e/g = -6.25 deg/g and is well within the conventional aircraft design value of -2 deg/g. The Level 1 criterion that pitch-rate overshoot should not exceed 2.5 times the steady-state value is met (fig. 61). Figure 60 and the speed response shown in Figure 61 show that the phugoid stability was degraded from a Level 1 value to an instability of 9.5 sec to double amplitude, which explains why the total augmented step response does not have a constant steady-state value.

Lateral/directional static stability, summarized in Figure 62, illustrates positive stability throughout the flight envelope for the critical heavy gross weight, aft cg. While these characteristics ensure conventional control deflection for trim and maneuver, the level of stability requires a yaw damper to increase Dutch roll damping. Lateral/directional stability at the aft cg is nearly identical to that of the Baseline Configuration.

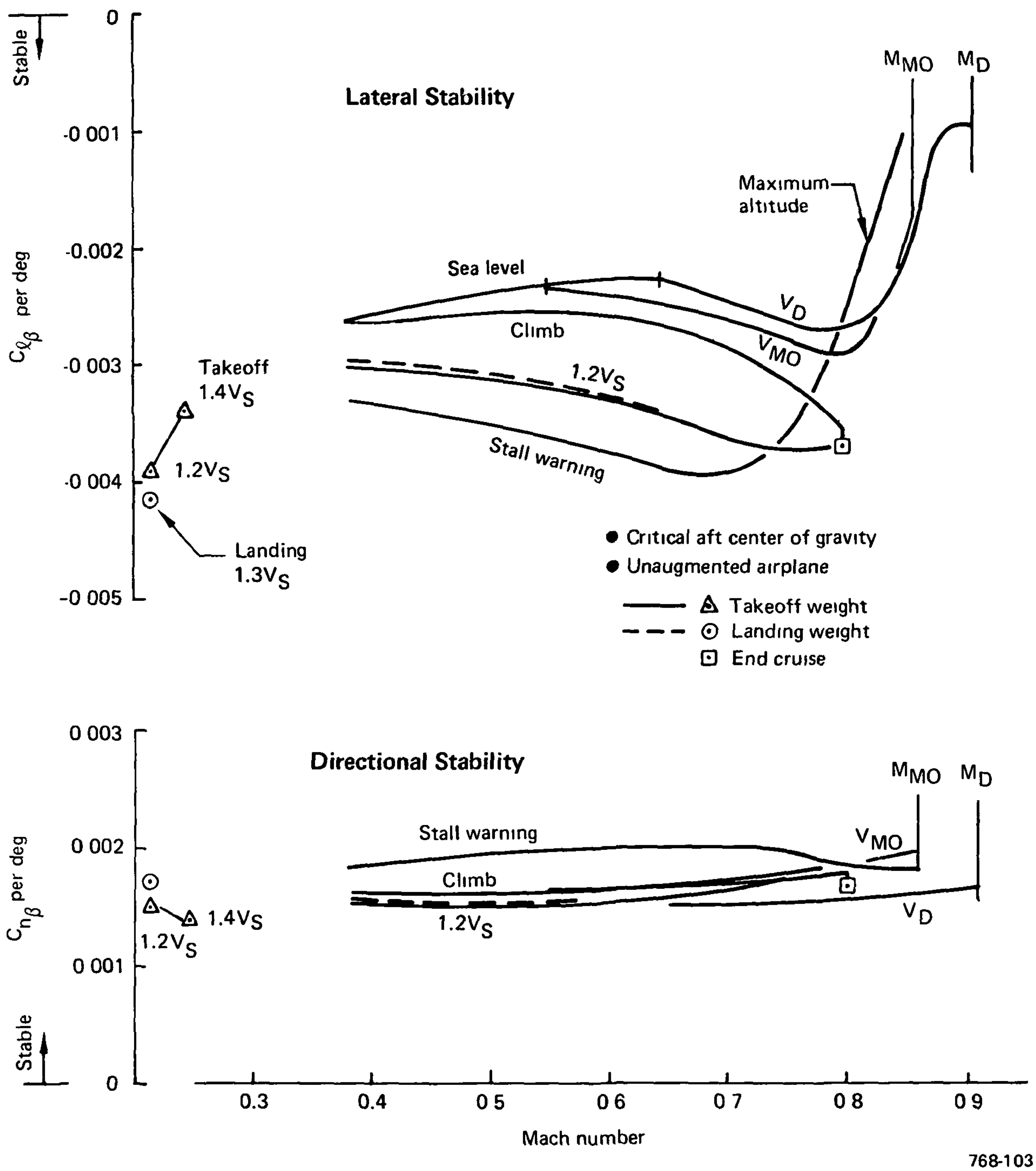

Figure 62. Lateral/Directional Static Stability

Figure 63 shows unaugmented Dutch roll damping characteristics and the design requirements for a yaw damper. The largest Dutch roll damping augmentation required is at the end of cruise where the damping ratio must be increased from 0.006 to at least 0.08 (Level 2) and, preferably, 0.20 for Level 1 flying qualities. The unaugmented characteristics do not meet Level 3 criteria (minimum safe). Therefore, the yaw damper must be triply redundant, and flight altitude must be restricted to about 10 668m (35 000 ft) after two failures. The additional damping required is about the same as that required for the 727 airplane, so the yaw damper probably would be a standard design concept. This yaw damper would provide good flying qualities and be identical for both the Baseline and Initial ACT Configurations, but it has not been designed. The Baseline Configuration has slightly less Dutch roll damping, primarily because the tail arm is about 8% smaller than on the Initial ACT Configuration and would be restricted to about 7620m (25 000 ft) flight altitude after two failures.

Basic spiral and roll mode characteristics (figs. 64 and 65) illustrate that Level 1 flying qualities are exhibited throughout the operational flight envelope and that lateral augmentation is not needed. However, the roll mode does deteriorate near stall warnings angle of attack at high Mach number, and it lightly couples with the spiral mode at this extremity of the design flight envelope. The Baseline Configuration exhibits a slightly better roll mode, primarily because it does not have the outboard wing fuel tank of the Initial ACT Configuration.

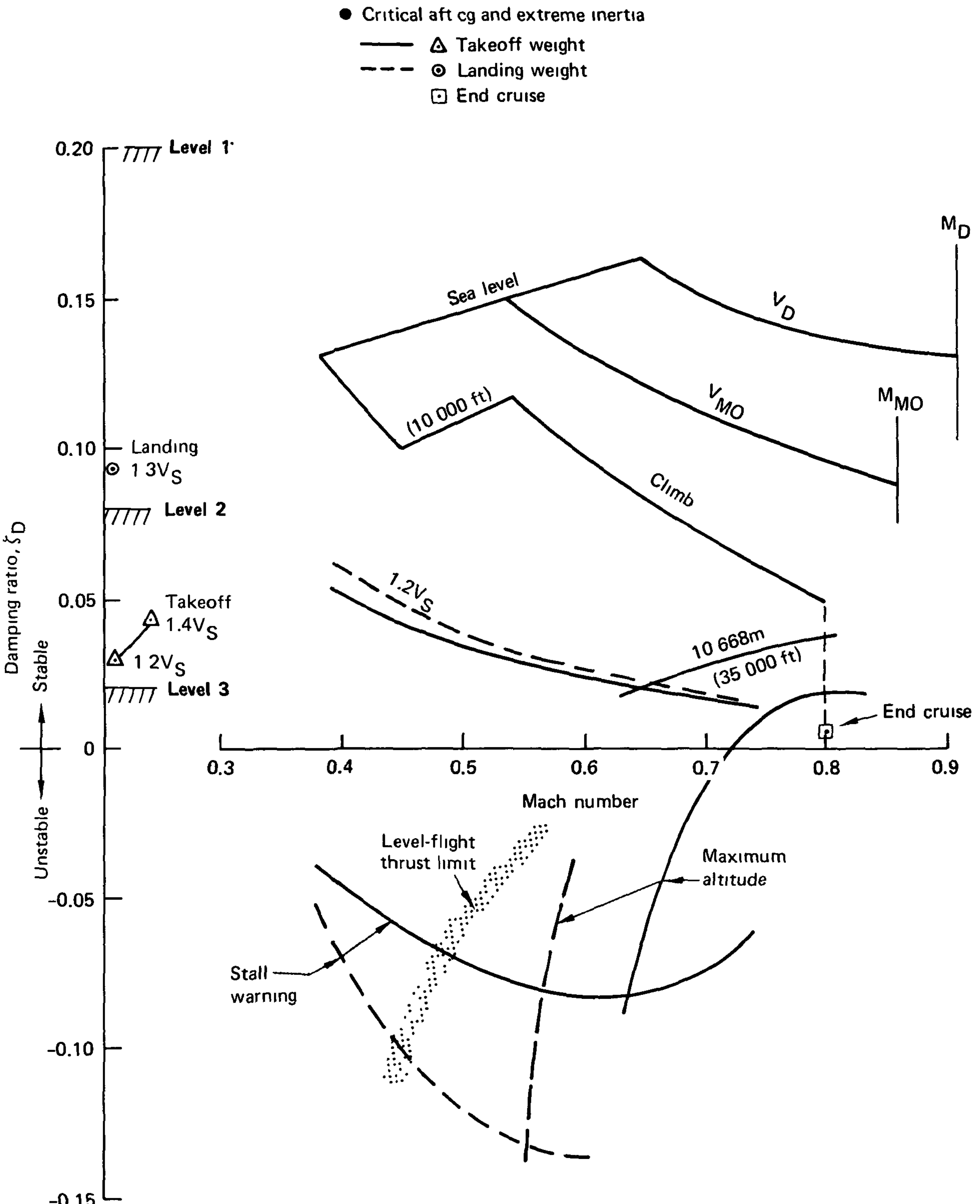

768-103

Figure 63. Dutch Roll Damping (Unaugmented)

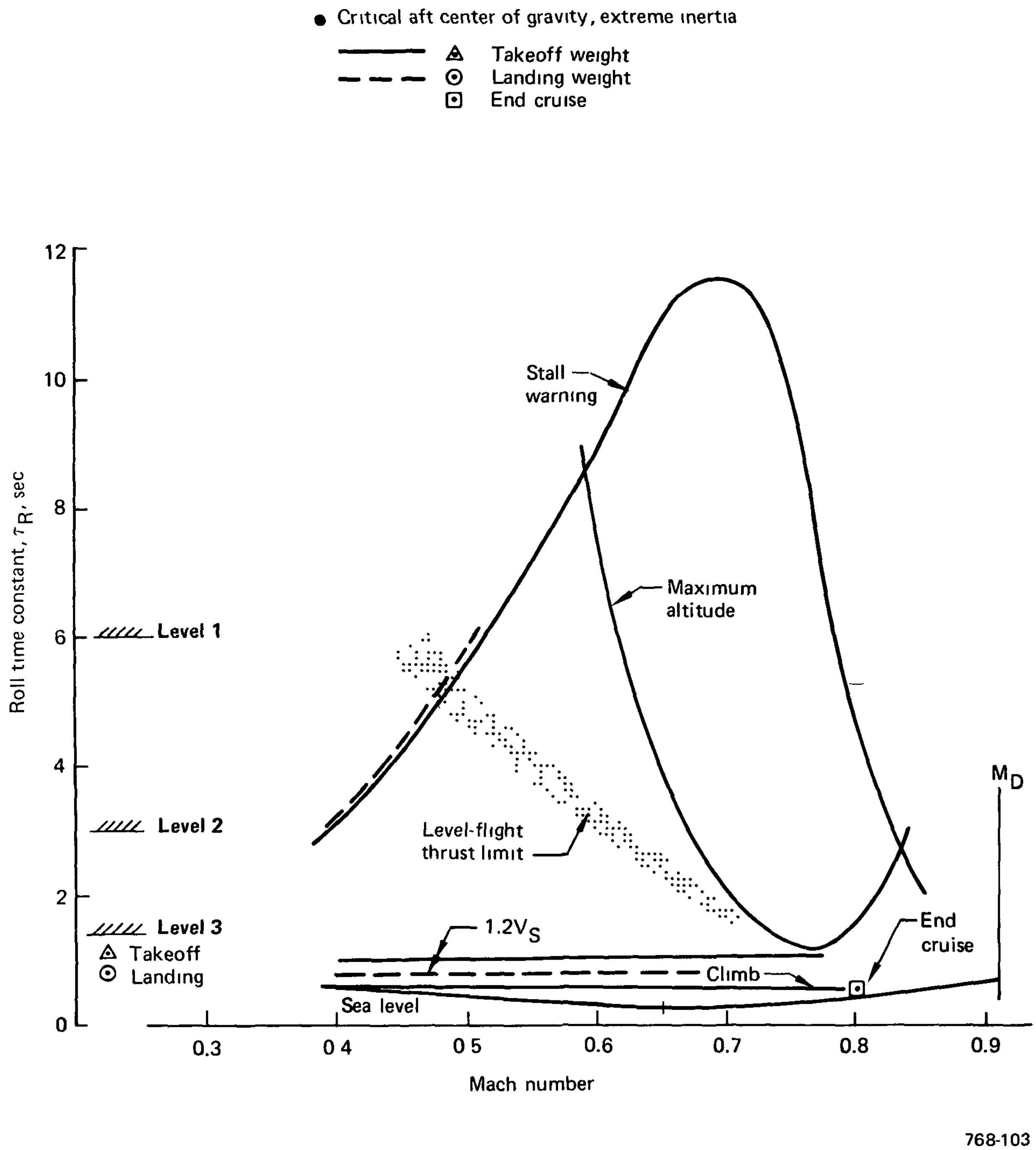

Figure 64. Roll Mode Time Constant

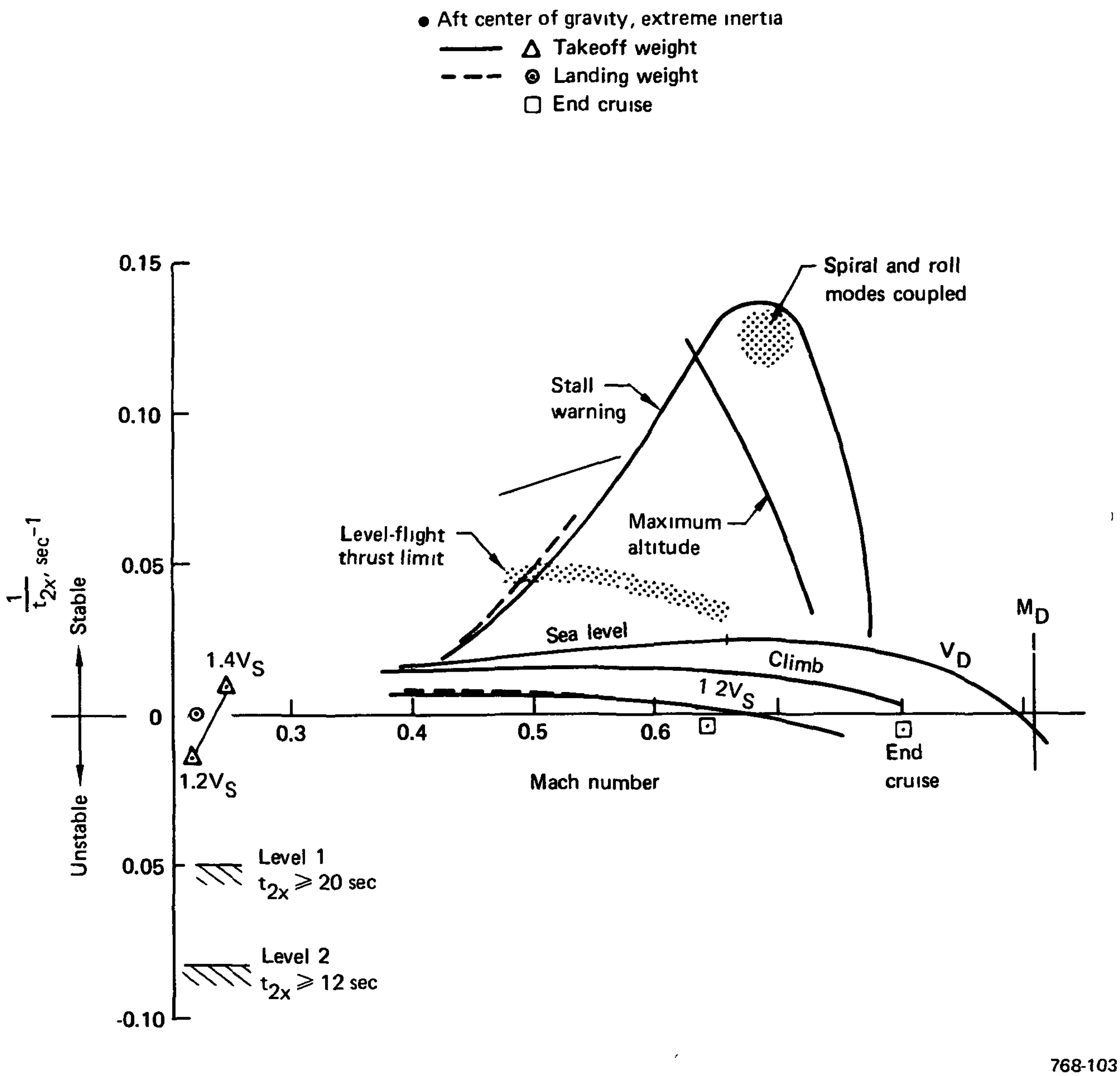

Figure 65. Spiral Mode Stability

7.2 STRUCTURAL ANALYSIS

7.2 STRUCTURAL ANALYSIS

This section contains the structural analysis results for the Initial ACT Configuration. The objectives of the analysis are:

- Evaluate the effect of ACT functions on structural material requirements

- Establish the structural characteristics of the dynamic model for control system design

- Validate the control laws for load alleviation, flutter-mode control, and fatigue reduction

The data base, methods, and criteria used for the analysis are consistent with those used for the Conventional Baseline Configuration except for the modifications required to include ACT functions. The major portion of the analysis involved establishing wing-box structural requirements. The horizontal tail structure was sized to provide a data base for weight assessment and to determine stiffness. The aft body was analyzed to assess the changes in stiffness and structural weight due to changes in horizontal tail loads.

A preliminary structural analysis was first performed to establish a design base (subsec 7.2.1) followed by a final structural analysis (subsec 7.2.2). A summary of the final wing-box structural sizing requirements showing the effects of the selected ACT functions is presented in Subsection 7.2.2.5.

As expected, the Initial ACT wing became more critical for flutter, fatigue, and dynamic gust conditions when WLA was used to lower basic strength requirements due to static maneuver and FAR gust formula conditions. The maximum reduction in structural material was achieved from a combination of ACT functions that provided design and fatigue load reduction and raised the flutter speed of the critical wing-flutter mode. A detailed weight assessment of the ACT functions is presented in Subsection 5.4.

7.2.1 PRELIMINARY WING

The preliminary structural analysis of the Initial ACT Configuration provided an initial determination of the structural sizing needed to meet strength, fatigue, and stiffness requirements. Potential benefits of ACT functions include:

- Wing-load alleviation (WLA) reduces loads due to maneuvers and gusts and allows lower structural material requirements for strength and fatigue

- Flutter-mode control (FMC) allows flutter margins at speeds in excess of V_D to be achieved with reduced structural requirements for added stiffness or mass

Control system characteristics required to achieve structural weight reductions are defined in this section. Preliminary control laws were developed and used to update the mathematical model for final control law synthesis.

The wing box for the configuration with relaxed static stability initially was sized to meet strength requirements without benefit of ACT devices for the wing. This structural design "base" was very close to the Baseline Configuration with similar stiffness requirements for flutter stability and with no allowance for fatigue material. The wing box was then resized to meet strength requirements using a WLA system that was developed to reduce wing loads for critical maneuver and gust conditions. The structural analysis was performed with the ORACLE integrated system computer code, which combines aeroelastic loads analysis (based on beam theory and lifting line aerodynamics), a simplified stress analysis (based on strength design), and weight analysis of the theoretical wing-box structure.

The wing section aerodynamic data for the Initial ACT Configuration are identical to those used for the Baseline Configuration. These data were derived from model pressure tests and are compatible with airplane aerodynamic data used for performance and stability analysis. Aileron and flaperon section aerodynamic data were derived from Boeing 747 wind tunnel test data adjusted for configuration differences. The structural allowables are the same as for the Baseline Configuration. They are representative of standard Boeing design practices and reflect the results of applicable structural tests. The mass data are preproduction quality and include adjustments to account for configuration differences between the Conventional Baseline and Initial ACT Configurations.

The wing with reduced structural material, permitted by introducing WLA, was used to conduct the preliminary fatigue, dynamic gust, and flutter analyses without active controls.

7.2.1.1 External Loads and Strength Sizing

External loads were analyzed for a combination of flight maneuver, gust, and ground conditions. These conditions were selected from previous design cycles as potential design conditions in the operating speed-altitude envelope of Figure 66.

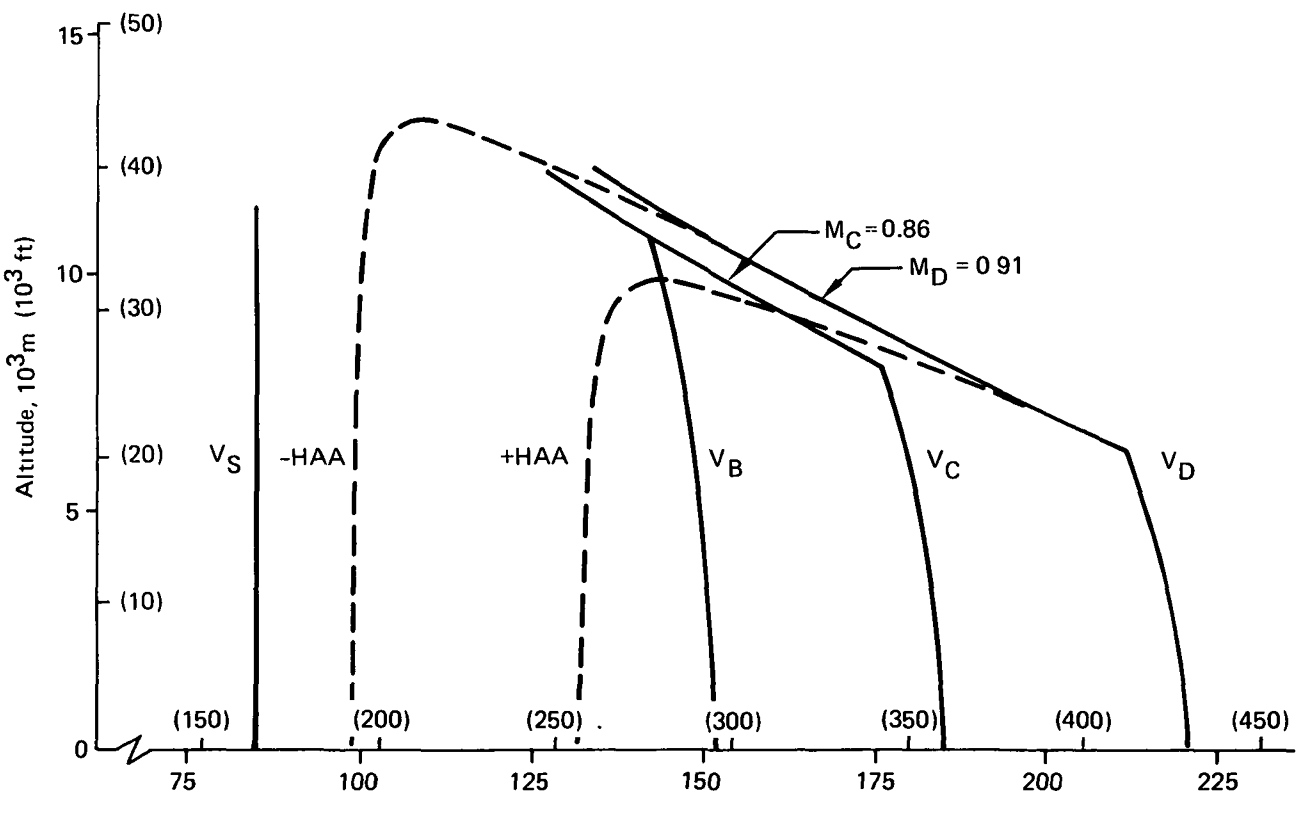

Figure 66. Speed-Altitude Envelope

The airloads were obtained by dividing the wing (fig. 67) into 12 streamwise aerodynamic panels, conveniently grouped to provide a good representation of regions where control surfaces are located. The stress analysis of the wing box was performed for the midpanel stations (fig. 67) on sections perpendicular to the load reference axis.

The maximum takeoff gross weight (TOGW) and payload of the Initial ACT Configuration are, by definition, identical to the Baseline Configuration. However,

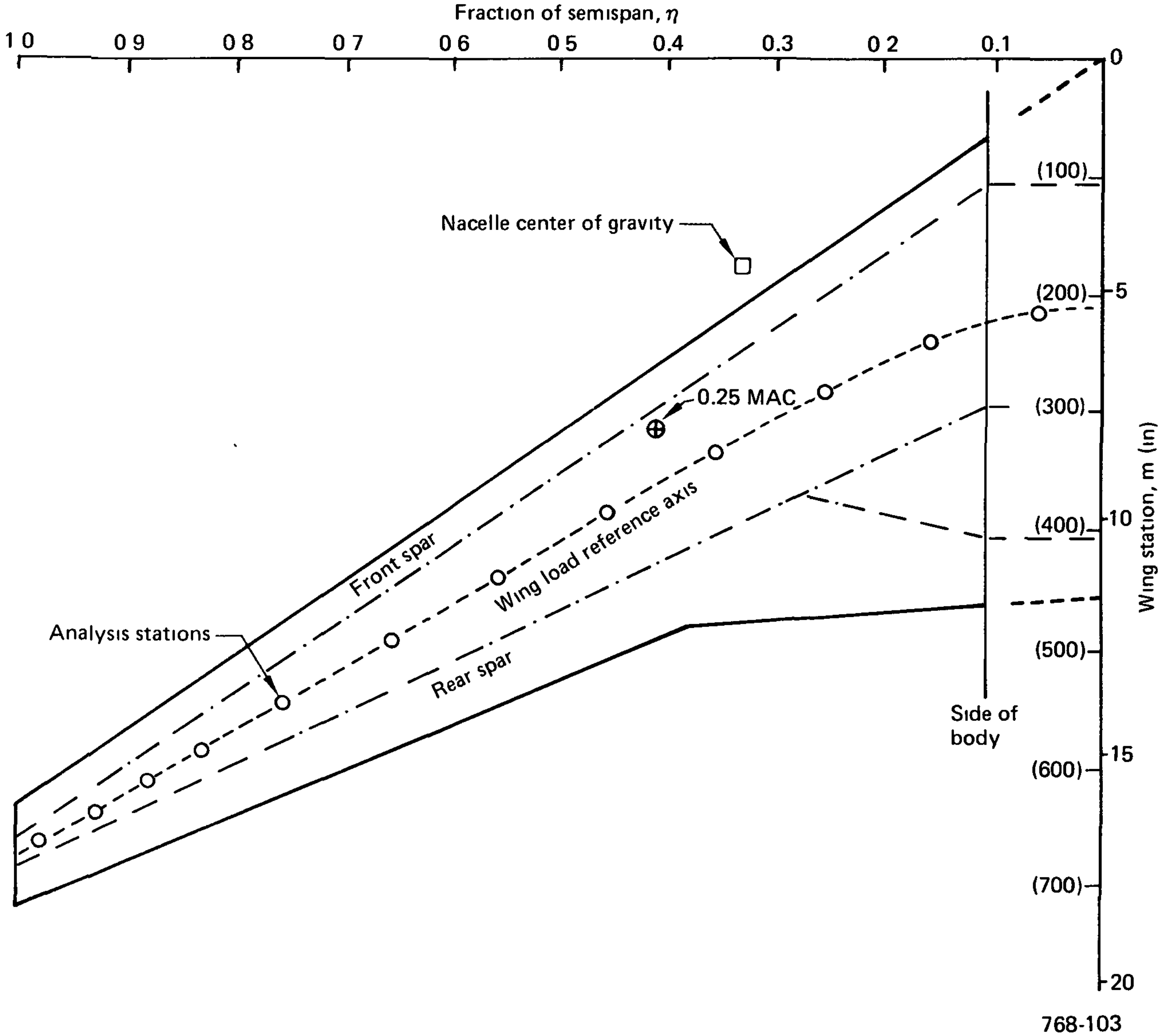

Figure 67. Wing Diagram for Structural Loads Analysis

lower weight conditions differ as a result of the reduction in operational empty weight (OEW) predicted for the Initial ACT Configuration. The wing-box strength sizing for the Initial ACT Configuration without WLA differs from the Baseline Configuration due to changes in cg limits and tail arm. The effects of flexibility on span loading are shown for two typical design conditions in Figure 68, and the positive design wing-box bending moment envelope is presented in Figure 69.

The wing is designed primarily by positive gust, based on the FAR gust formula with a 1.1 dynamic magnification factor; however, maneuver loads are within 3% of those due to the design gust condition. Ground conditions contribute to the design of spar webs. The theoretical structural material requirements for the strength-sized wing box are presented in Figure 70. These requirements form a base to assess benefits of selected ACT functions and to assess structural requirements for fatigue and flutter. For the structural analysis, the material requirements were represented by the upper and lower skins, stringers, spar caps, and spar webs. Distribution of material between skin and stringers was consistent with Boeing's current commercial design practices, including considerations for minimum gage.

7.2.1.2 Wing-Load Alleviation

A study was conducted to determine the effectiveness of two candidate WLA control surfaces shown in Figure 71; the outboard aileron (including its inboard segment) and the inboard aft flap segment. Wing design loads typically occur at speeds corresponding to high angle of attack for maneuvers. As speed increases, aeroelastic effects naturally shift the center of pressure inboard. However, torsion produced by control surface deflection increases with speed. Therefore, the gain of the control surface deflection should be adjusted as a function of dynamic pressure to avoid excessive torsional loading in the high-speed portion of the design envelope. In addition, control surface deflections should be adjusted as a function of load factor so that maximum control surface deflections are reached at, or a little above, the design load factors, either from maneuver or peak gusts. The control surface schedule used in this study is shown in Figure 72.

A dead zone corresponding to an incremental load factor of $\pm n_z$ = 0.5g was incorporated initially to avoid interference with normal cruise and autopilot operations. The

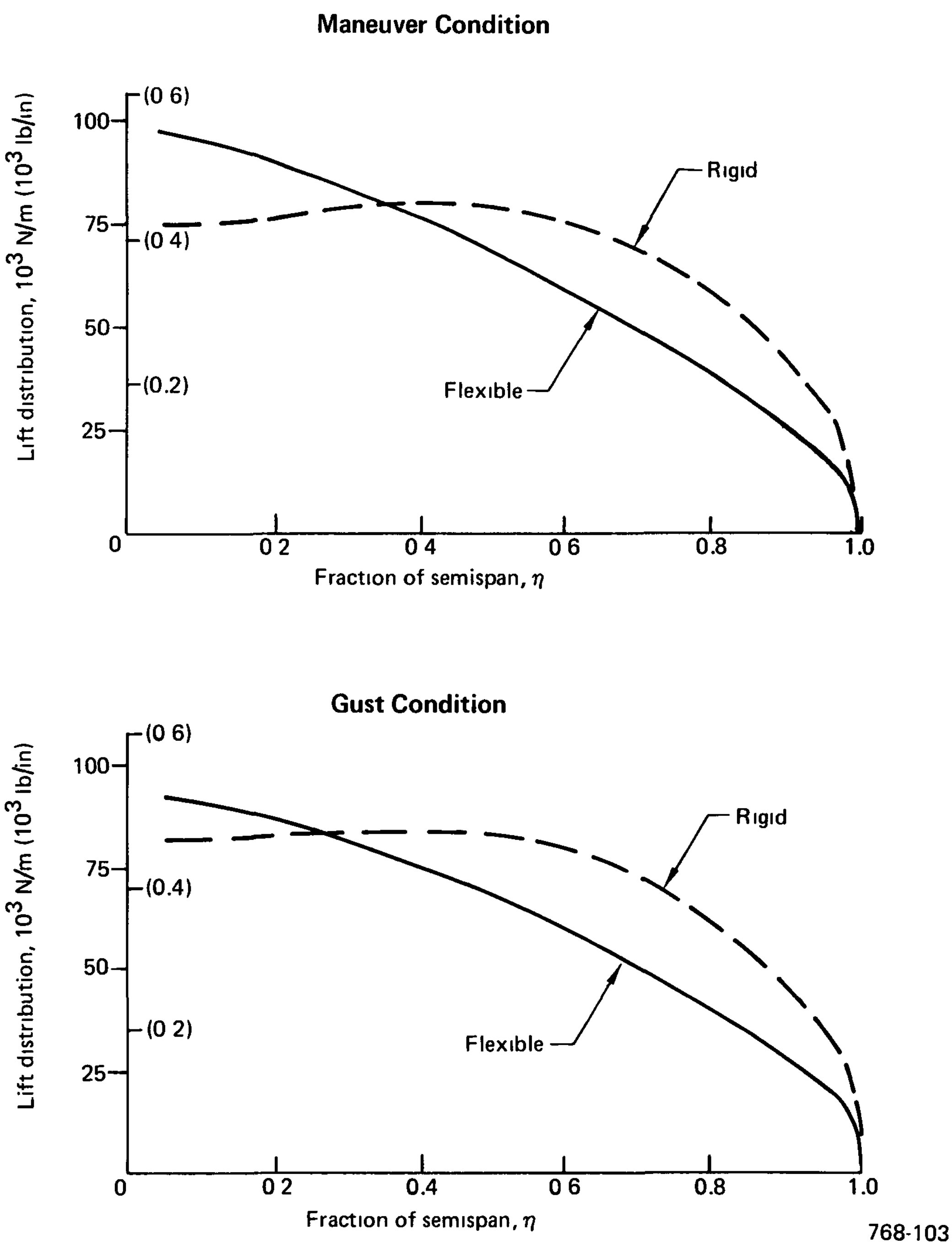

Figure 68. Typical Lift Distributions for Maneuver and Gust Conditions

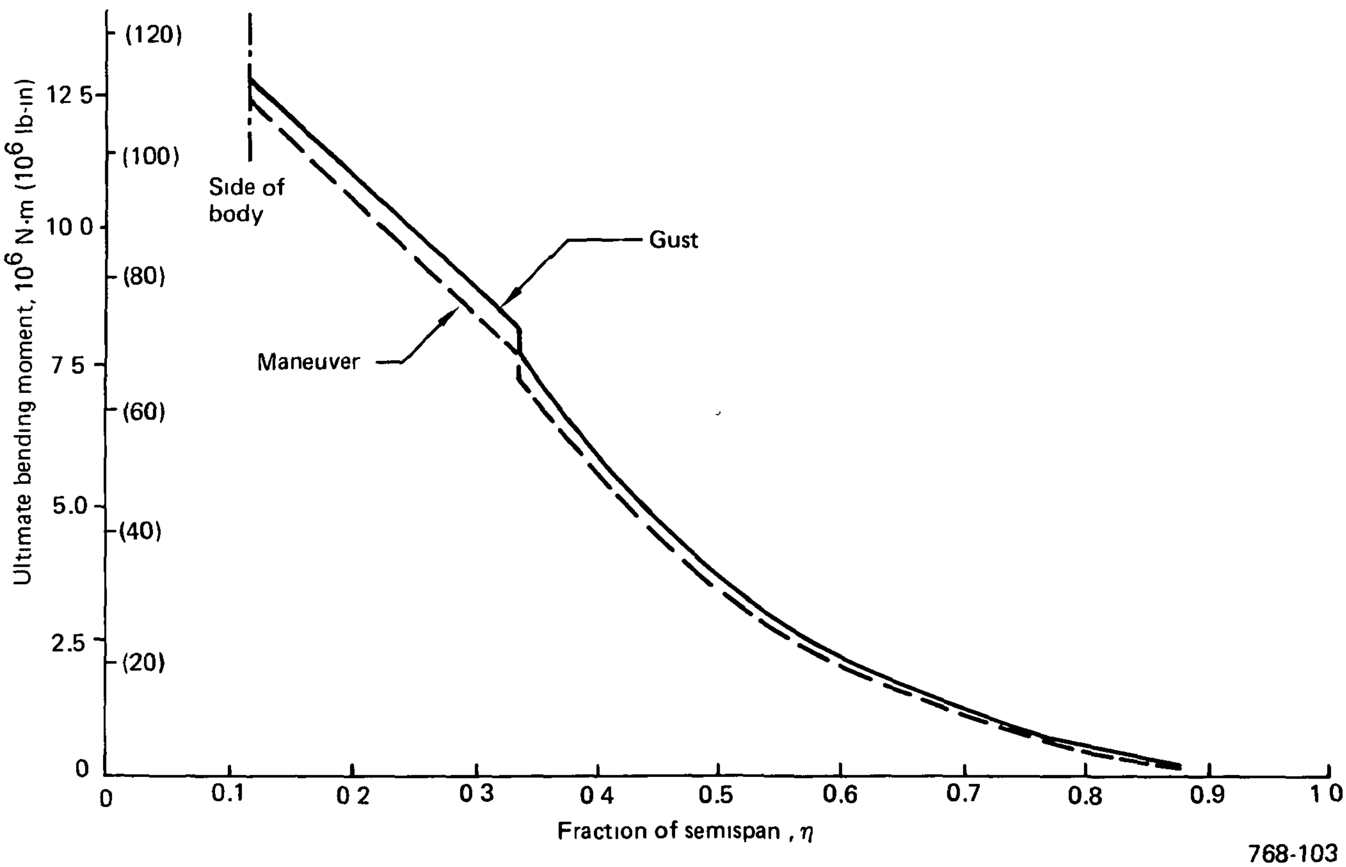

Figure 69. Positive Design Wing-Box Bending Moment Envelope—Full-Strength Wing at Start of Structural Design Cycle

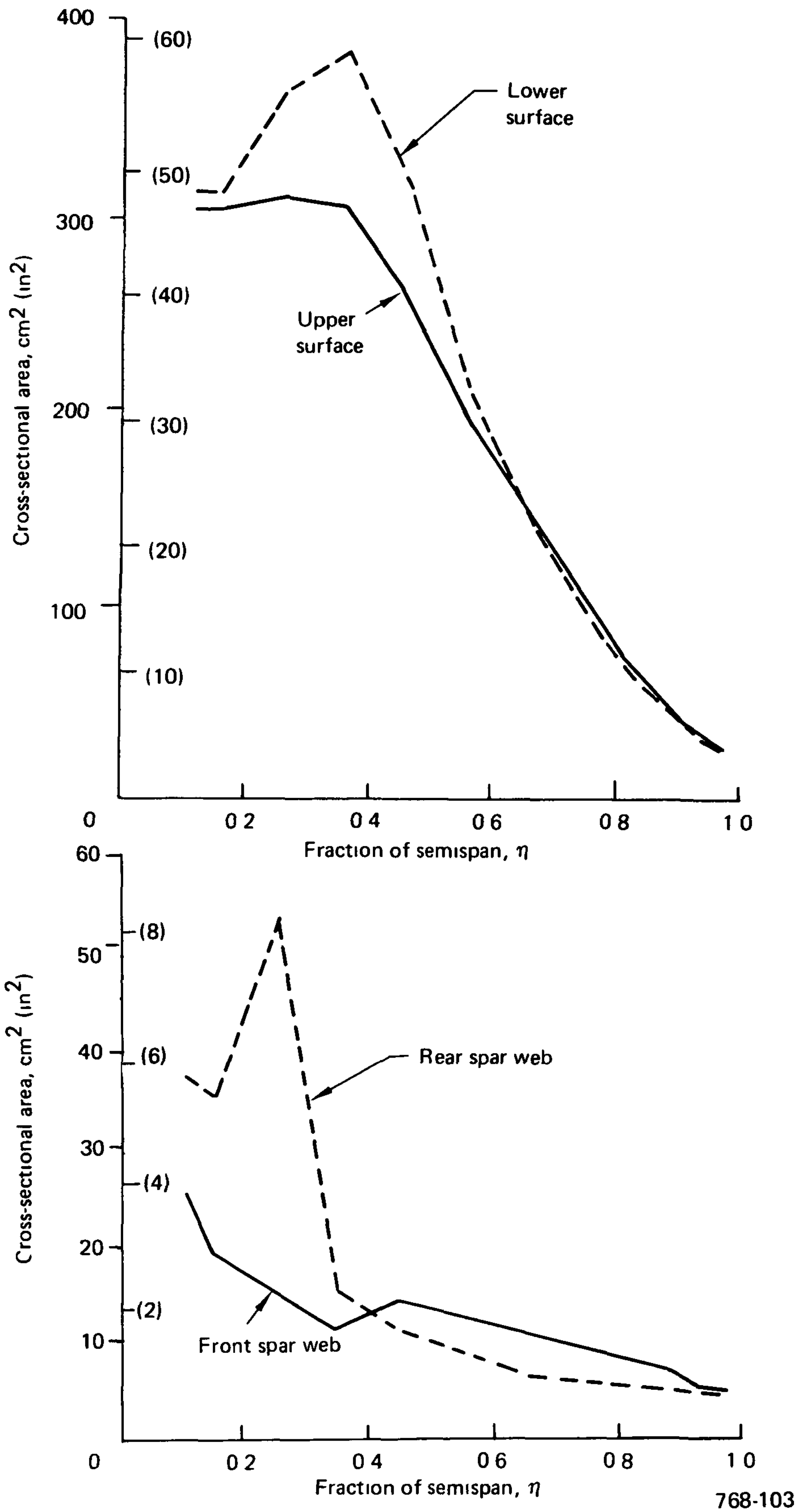

Figure 70. Theoretical Wing-Box Strength Material Requirements—Full-Strength Wing

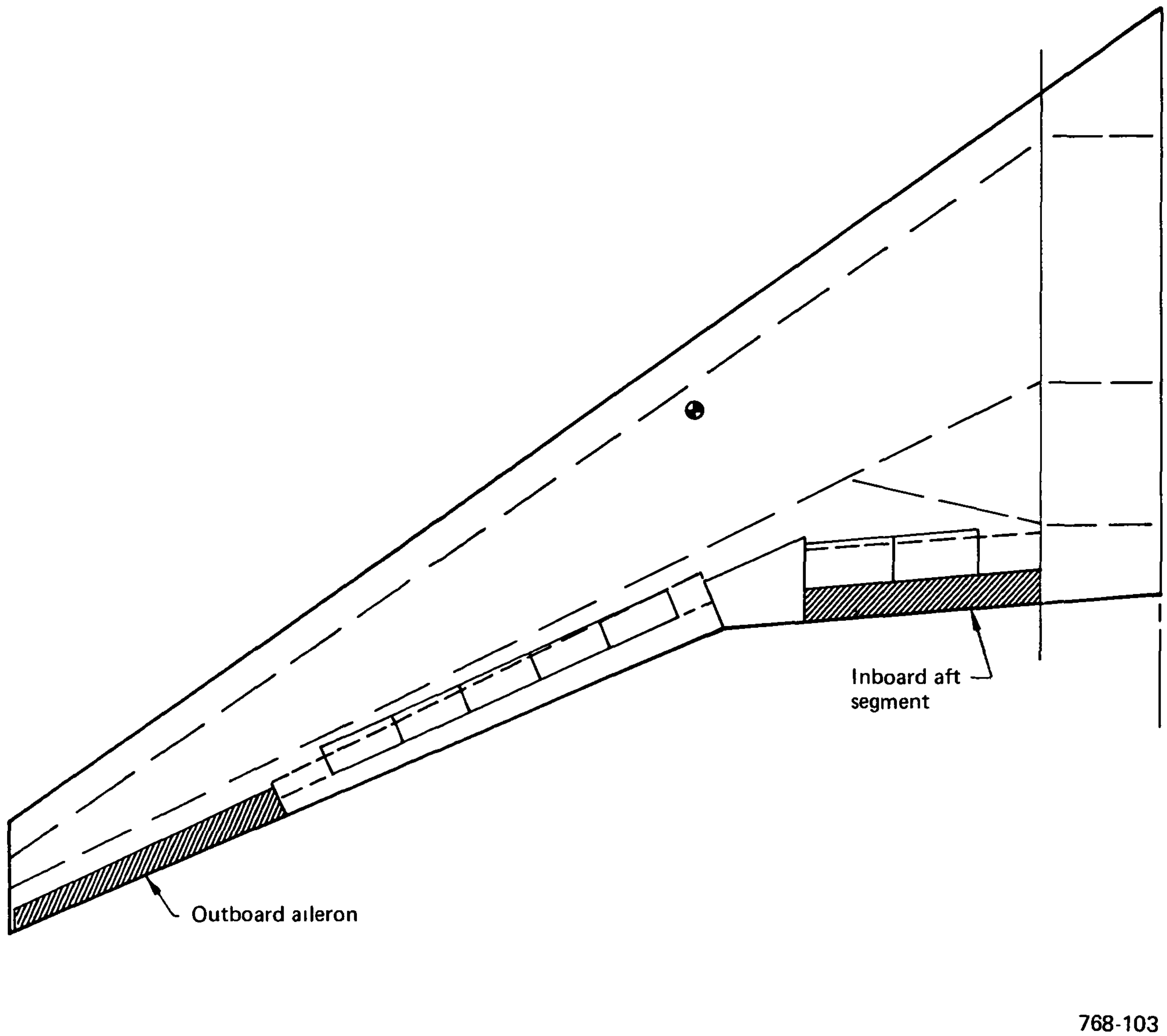

Figure 71. Candidate WLA Control Surfaces

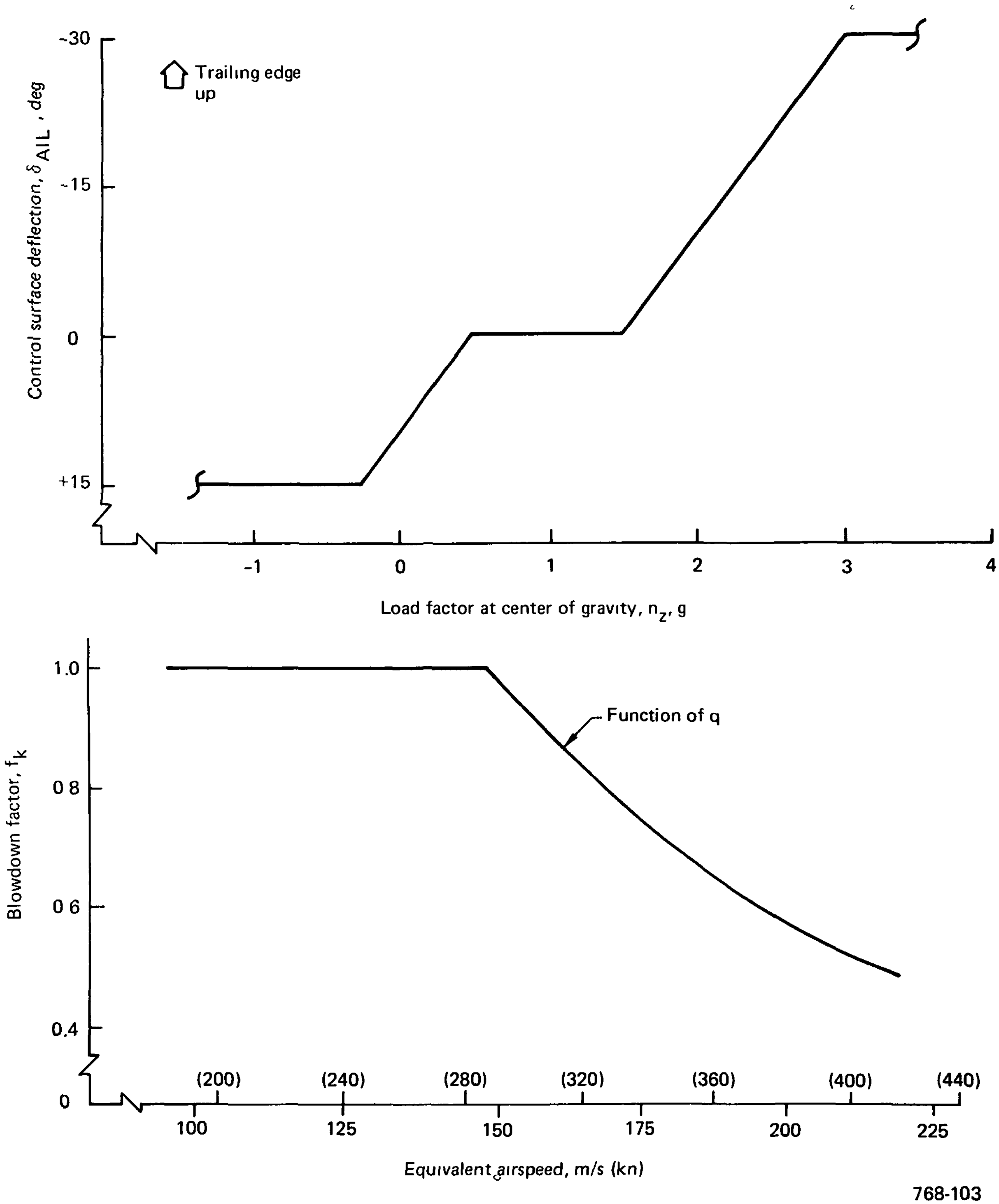

Figure 72. WLA Control Surface Inputs

feedback parameters were assumed to be cg acceleration and pitch rate. Elevator deflection was used to trim out unwanted pitching moment increments. This particular WLA system was designed to be effective for large load factor increments from maneuver and peak gusts. A bandpass filter decoupled the system from airplane excitation caused by low to nominal atmospheric turbulence or mild maneuvers.

The section aerodynamic data used to analyze the outboard aileron and inboard flap segment are shown in Figures B-7 and B-8 (app. B). These data provide typical aerodynamic lift and moment "reference coefficients." Previous studies have shown that the relative values of the incremental lift and pitching moments at a control surface determine its effectiveness as a WLA device in conjunction with its location, wing sweep, stiffness, etc. Because of these characteristics and because the true aerodynamic effectiveness of the reference control surfaces have not been verified by wind tunnel test, the reference lift and pitching moment characteristics were varied independently to provide better understanding of aerodynamic limitations and to determine a credible potential structural weight benefit.

Results of the study are shown in Figures 73 and 74. The incremental reductions in wing-box weight shown represent theoretical material of skin, stringers, spar caps, and webs. However, ribs, stiffeners, and nonoptimum weight contributions from material such as fasteners, joints, and padups are not included. Consequently, the weight increments shown are for comparison purposes only.

Typical airload distributions for maneuver and gust design conditions are shown in Figures 75 and 76 for outboard and inboard WLA systems on and off. Results for the outboard surface indicate that control surface lift is far more powerful than pitching moment for wing-box weight reduction, especially at high control surface gain, and that the current aileron surface appears quite effective compared to other control surfaces. Results for the inboard surface indicate that a down deflection (+) is effective in reducing loads for balanced maneuvers, but increases the severity of the FAR gust formula condition; a negative, up deflection is required to reduce gust loads. The control system mechanization would require a means of recognizing whether the airplane is maneuvered to realize these benefits. The modification to the lift distribution is inboard, with small leverage on the bending moment. The limiting

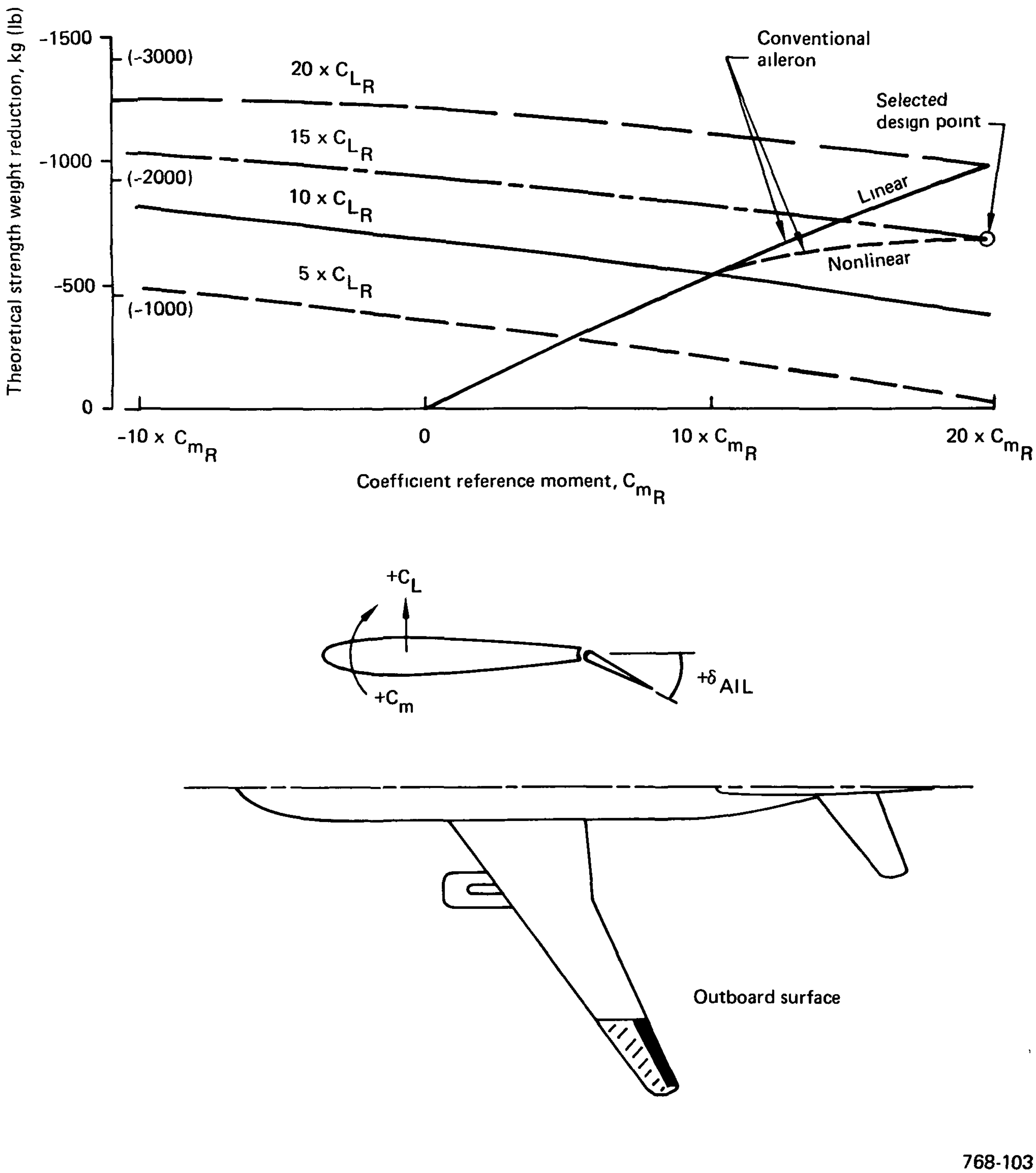

Figure 73. Potential Wing-Box Material Savings With Outboard Surface WLA System

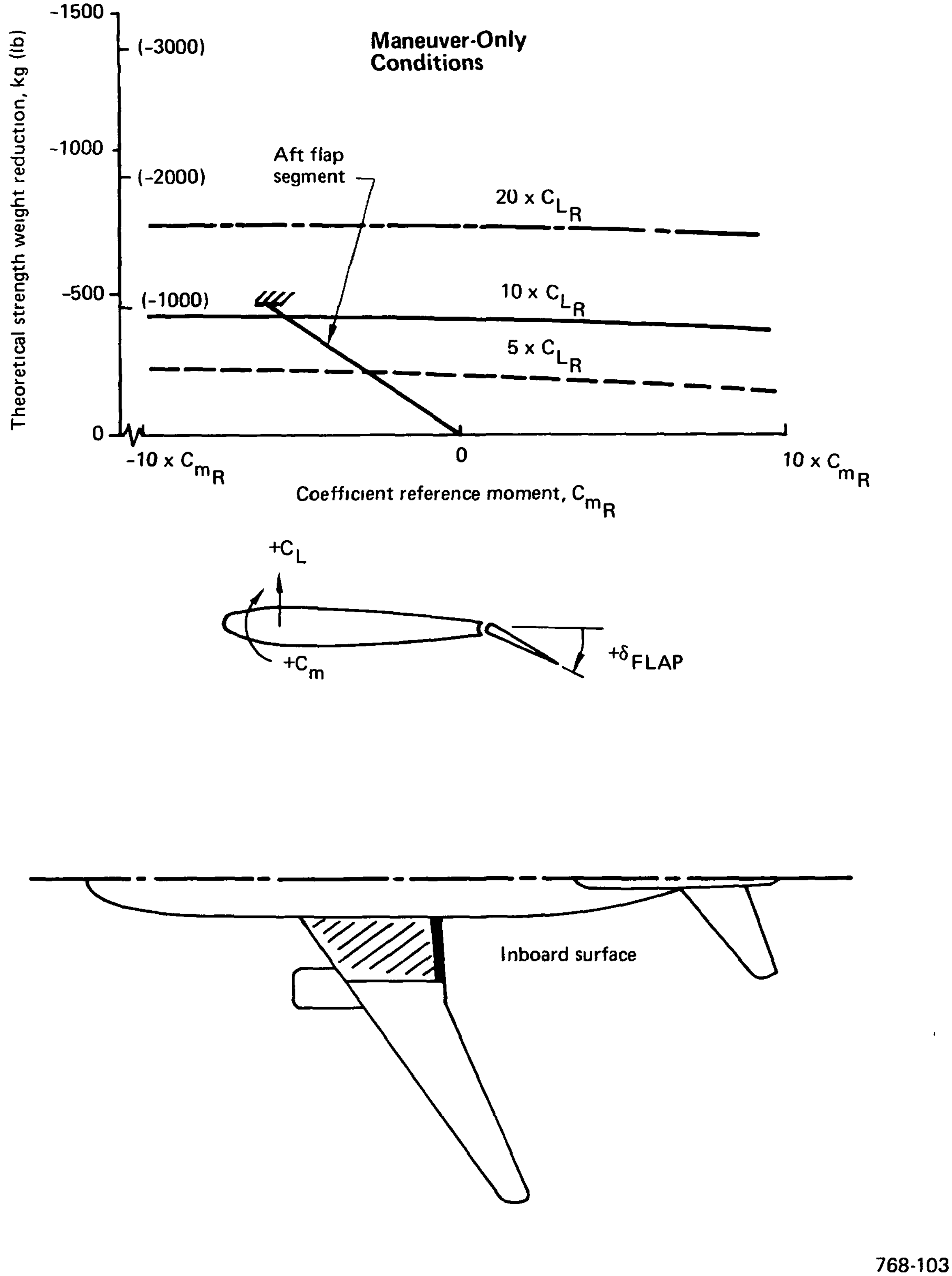

Figure 74. Potential Wing-Box Material Savings With Inboard Surface WLA System

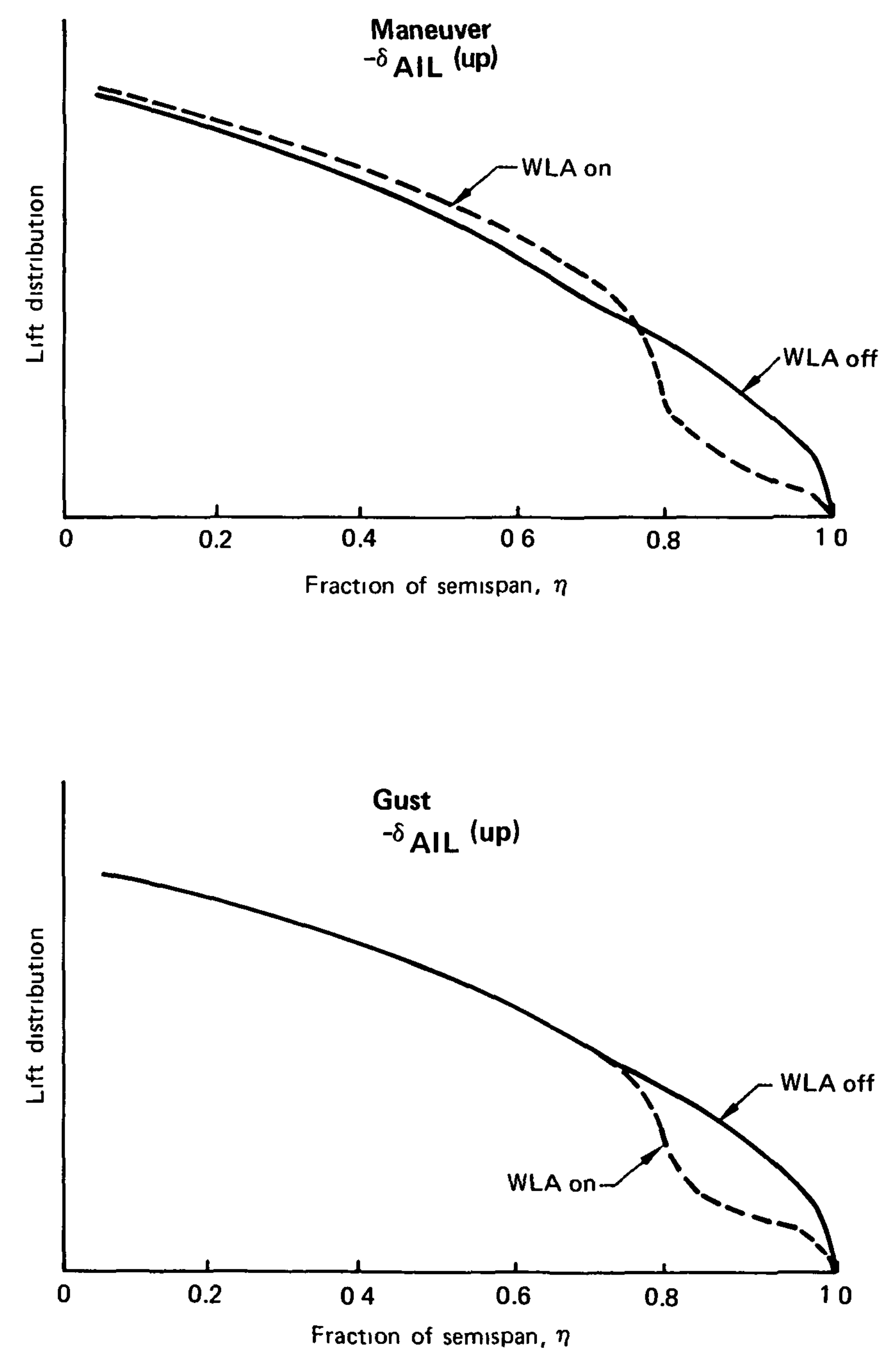

768-103

Figure 75. Typical Air Load Distributions—Outboard Aileron

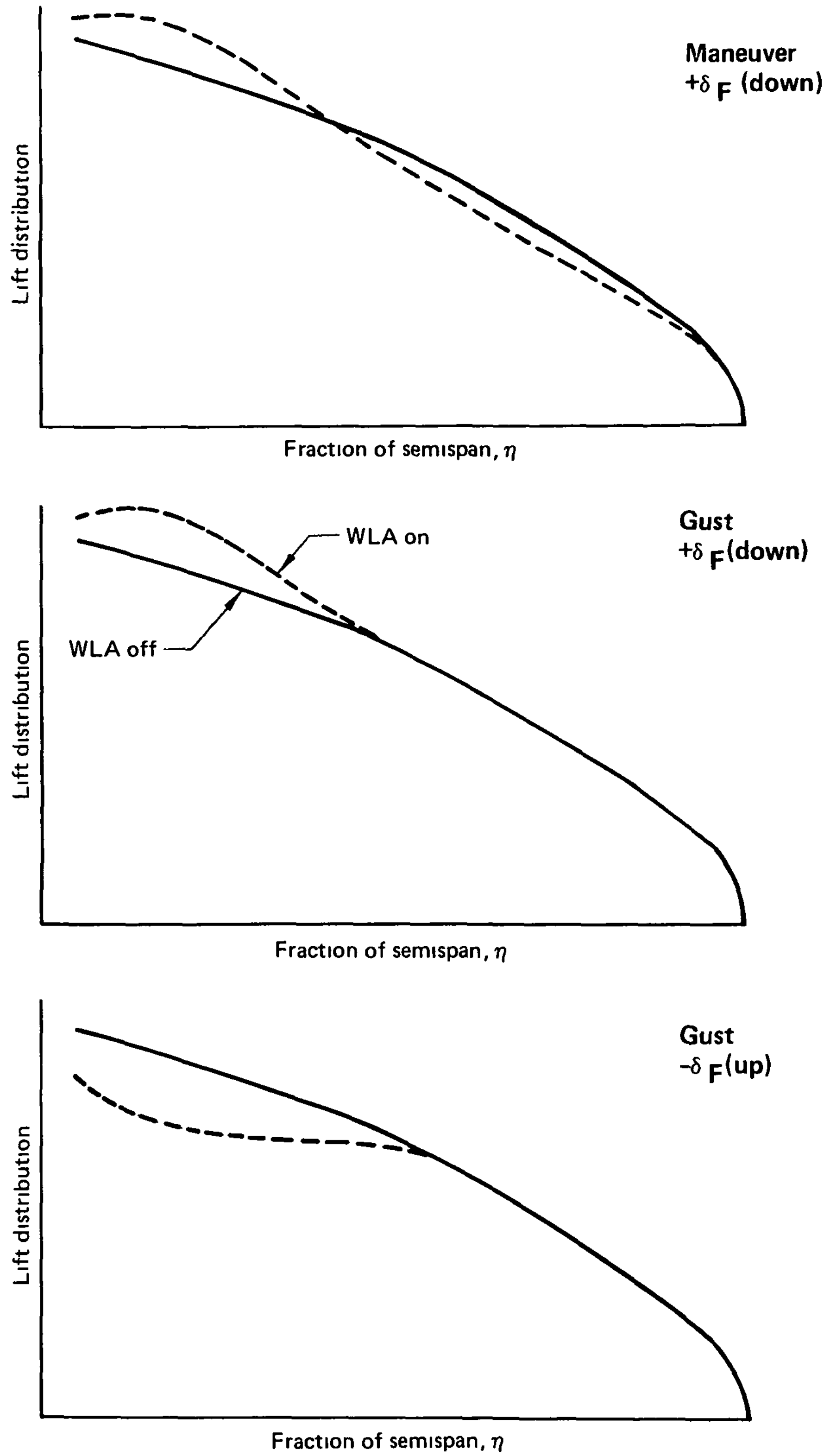

Figure 76. Typical Air Load Distributions—Inboard Flap Aft Segment

aerodynamic effectiveness of the "flaperon" is probably about $15 \times C_{L_R}$. Consequently, the potential benefits for the inboard surface are small, especially due to the problems of mechanizing this type of surface with sufficient support stiffness and the corresponding weight penalty.

A design point was selected from Figure 73 to represent the nonlinear aerodynamic effectiveness of the outboard aileron. The results of the structural analysis with the assumed WLA system were used to update the mathematical model and to define the desired characteristics of the system. The required control surface motion, as a function of speed and load factor and the related reduction in theoretical wing-box weight required for strength, are shown in Figures 72 and 77. The reduction in

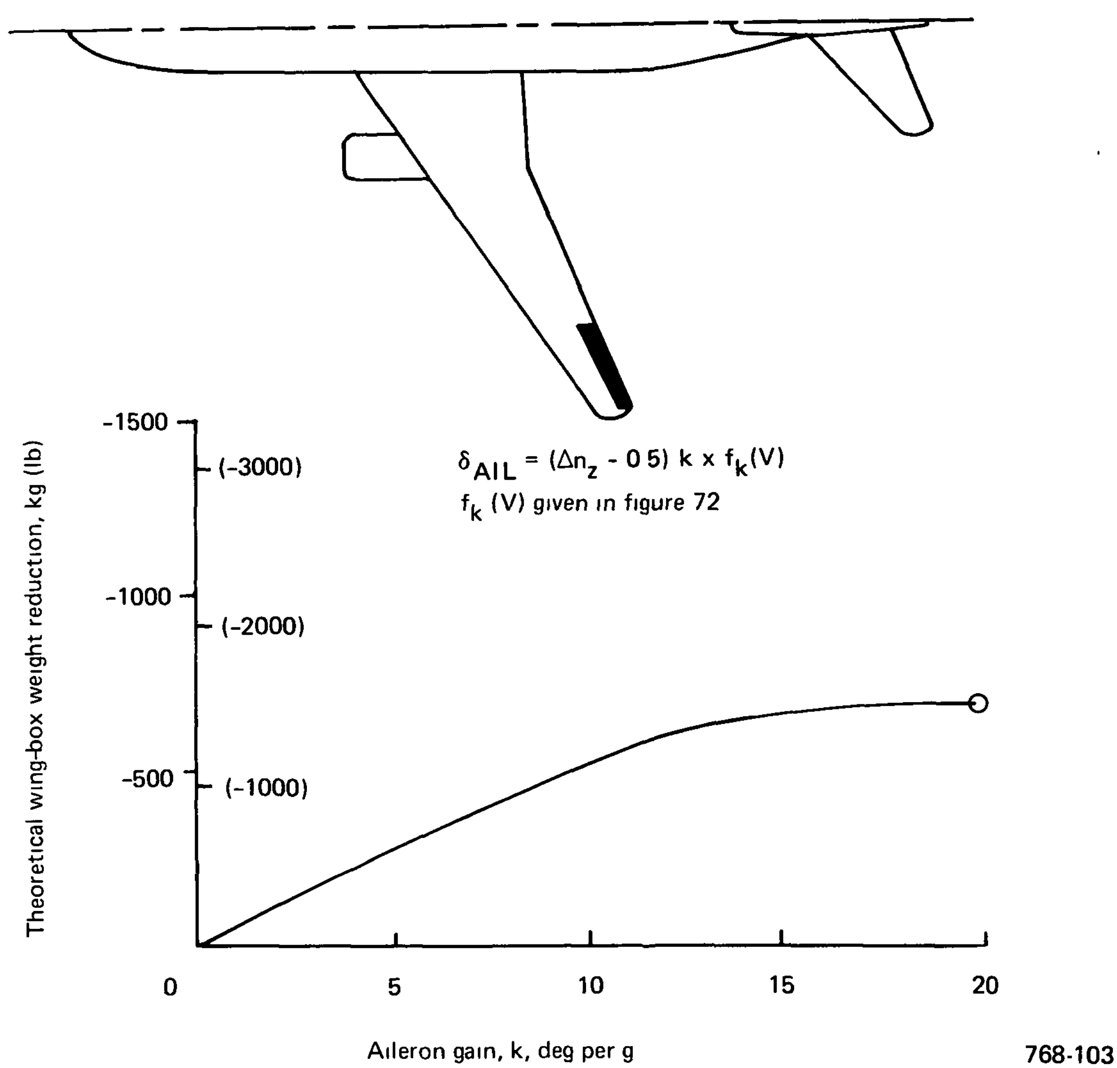

Figure 77. Control Surface Motion Related to Theoretical Wing-Box Weight Reduction

theoretical wing-box weight required for strength for the WLA design condition is 680 kg (1500 lb). The actual structural and net weight reductions, including system weight increment, are presented in Section 5.4, "Weight, Balance, and Inertia." The actual control law for the WLA system is presented in Section 7.3, "Control System Analysis."

The envelope of design wing-box moment, shear, and torsion (including the effects of the selected WLA system) is shown in Figures 78 through 80. As with the nonalleviated wing, the box is basically designed by the FAR gust formula with a 1.1 dynamic magnification factor. Comparing the wing-design bending moment with and without WLA (fig. 81) indicates an 8% reduction in bending moment at the side of body (SOB). The upper and lower surface material requirements for strength are compared in Figure 82. Although WLA reduces material requirements for most of the wing span,

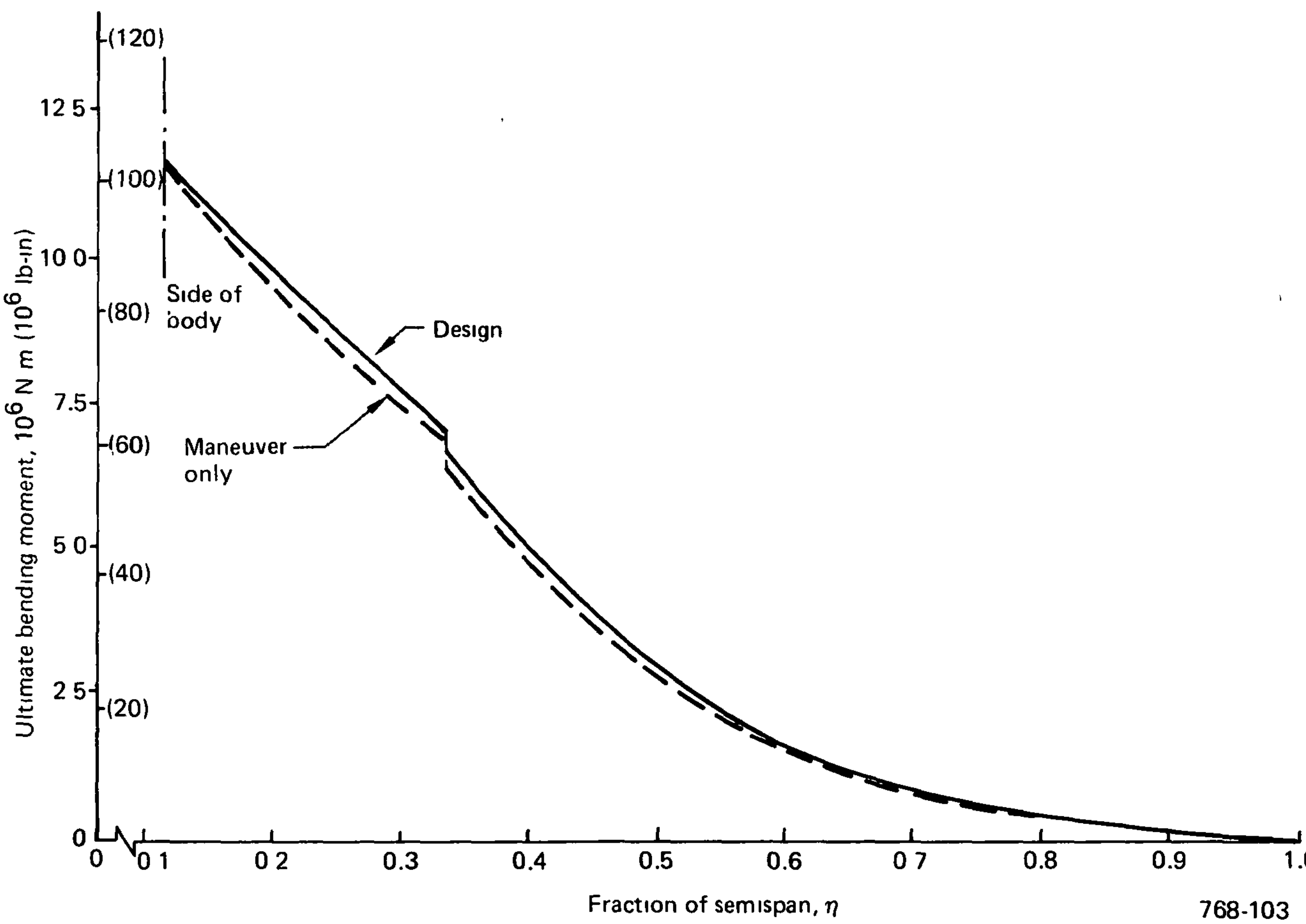

Figure 78. Wing Bending Moment Design Envelope—With WLA

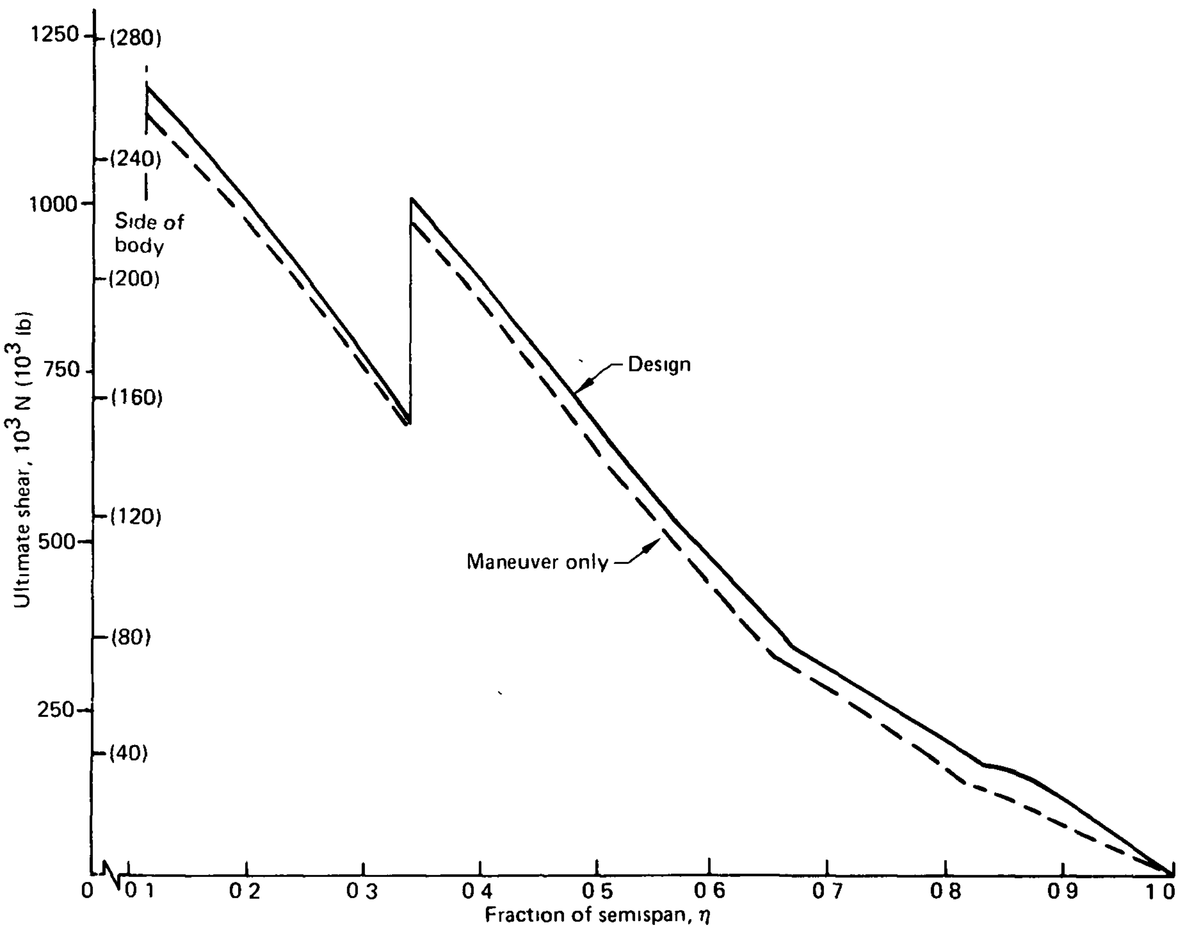

Figure 79. Wing Shear Design Envelope—With WLA

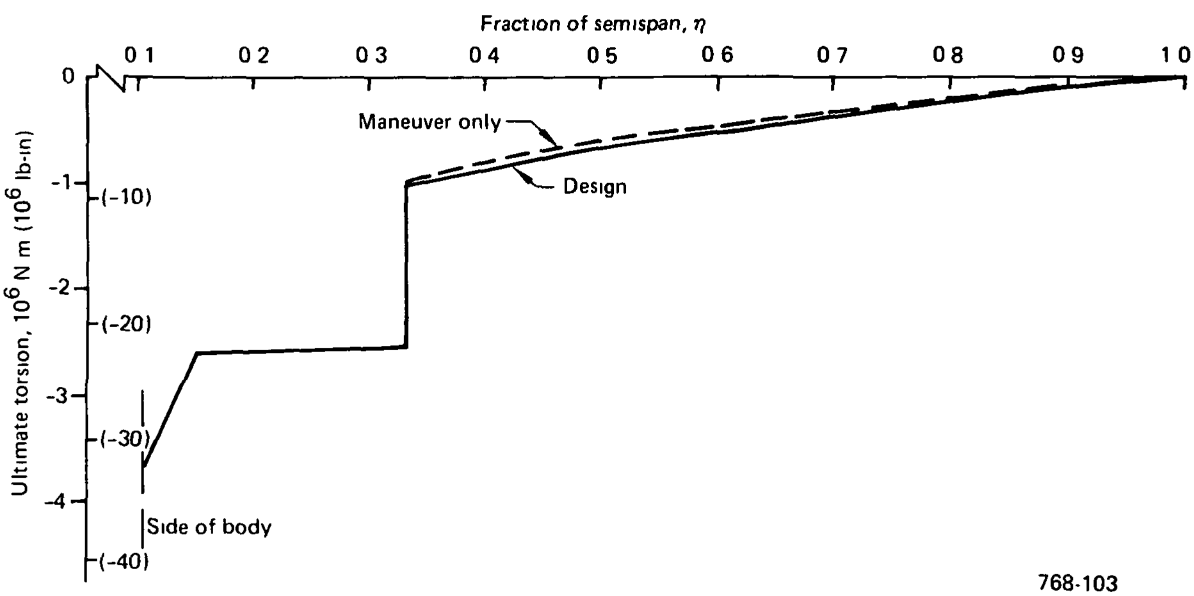

Figure 80. Wing Torsion Design Envelope—With WLA

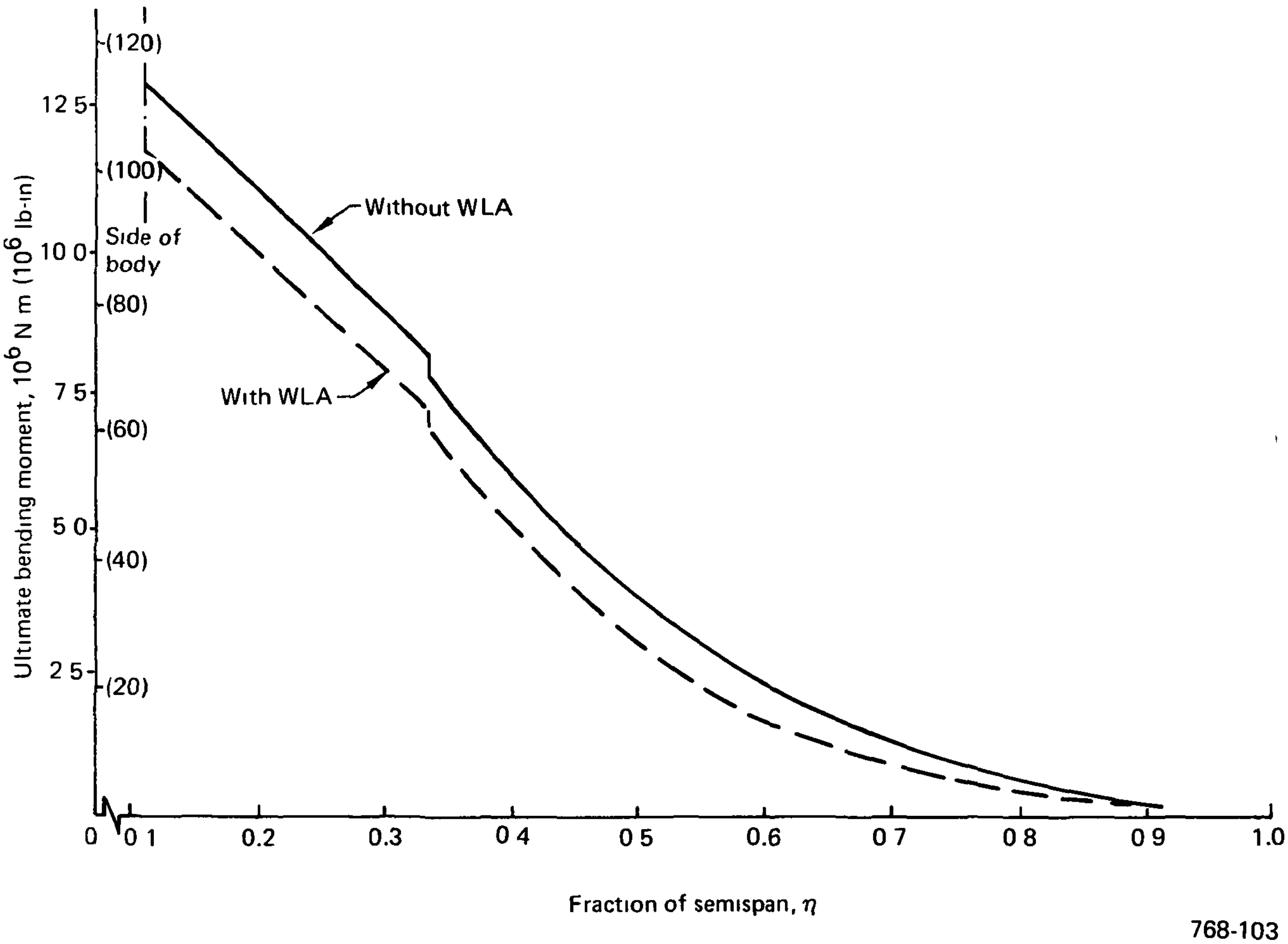

Figure 81. Wing Design Bending Moment Comparison—With and Without WLA

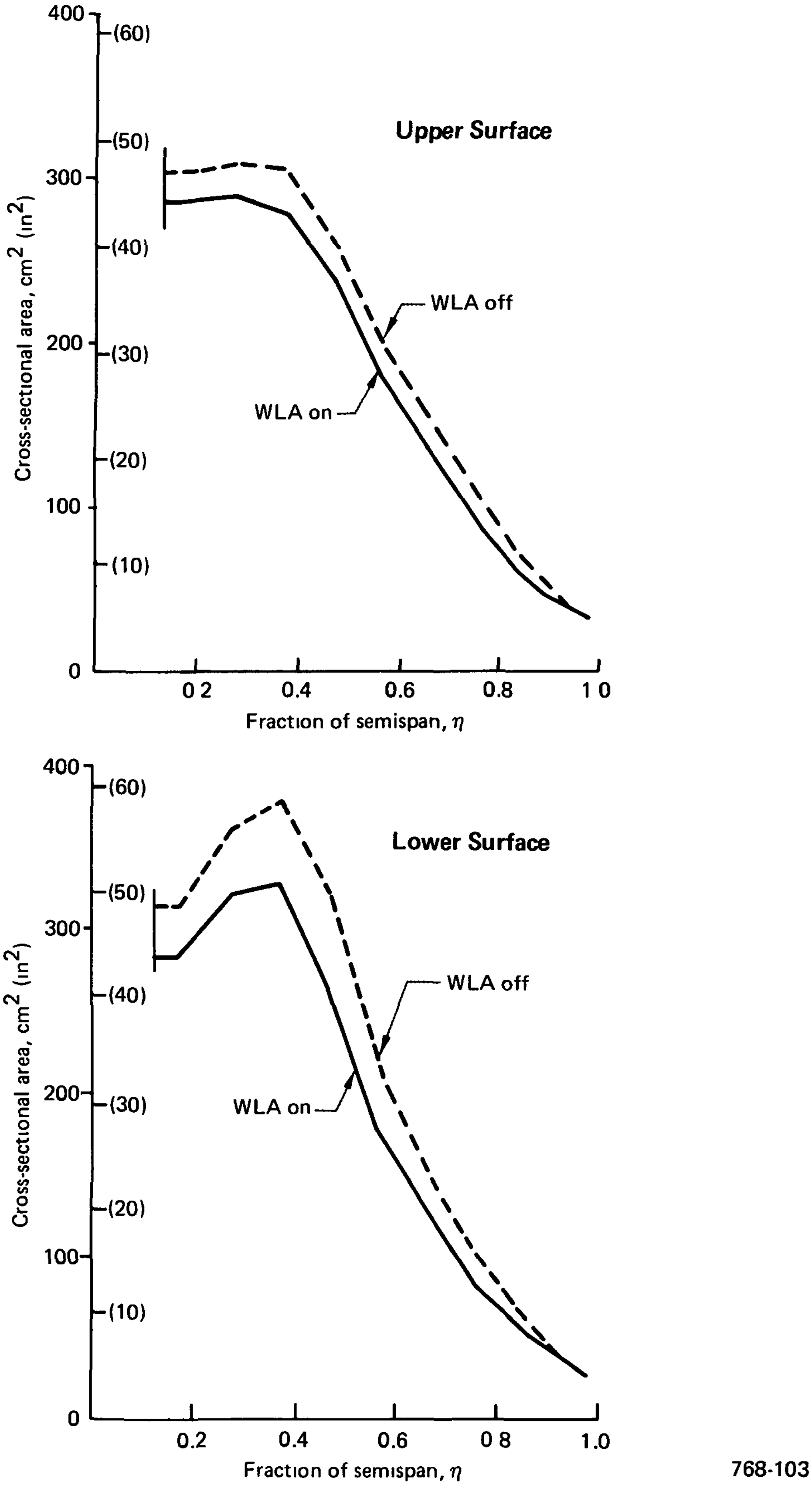

Figure 82. Comparison of Theoretical Wing-Box Strength Material Requirements

the major weight reduction is in the larger and heavy inboard portion of the wing box. The reduced wing-box stiffness shown in Figure 83 was used for the preliminary dynamic gust and flutter analysis.

7.2.1.3 Wing-Box Fatigue Requirement

The initial fatigue analysis objective was to determine if the wing-box structure of the Initial ACT Configuration was fatigue-critical when the selected WLA system was used to reduce the wing structural material required for strength. A similar analysis of the strength-designed Baseline Configuration indicated that no additional material was required for fatigue. Fatigue margins were analyzed for a design-life goal of 20 years. The flight segment distributions considered for design included:

- 62,000 short flights of 567 km (306 nmi)
- 40,500 medium flights of 954 km (515 nmi)
- 18,000 long flights of 3369 km (1819 nmi)

A comprehensive analysis performed during Boeing's new airplane program indicated that the short-flight segment was critical for fatigue. Consequently, the fatigue analyses for both the Baseline and the Initial ACT Configurations were performed for the short-flight segment.

The flight profile (fig. 84) was simplified by deleting conditions that did not contribute significant fatigue damage. The simplified profile, applied cycles, and load increments for the 567 km (306 nmi) flight are illustrated in Table 12.

Results indicated that the wing upper surface and spar webs have large positive fatigue margins; however, the wing lower surface showed negative fatigue margins of safety between SOB and 62% semispan. Preliminary stress and weight analysis indicated that approximately 227 kg (500 lb) of structural material, including nonoptimum factors, would be required to provide the required life goal in this portion of the wing box.

A second objective of the preliminary structural analysis of the Initial ACT Configuration was to define requirements for fatigue load reduction that would

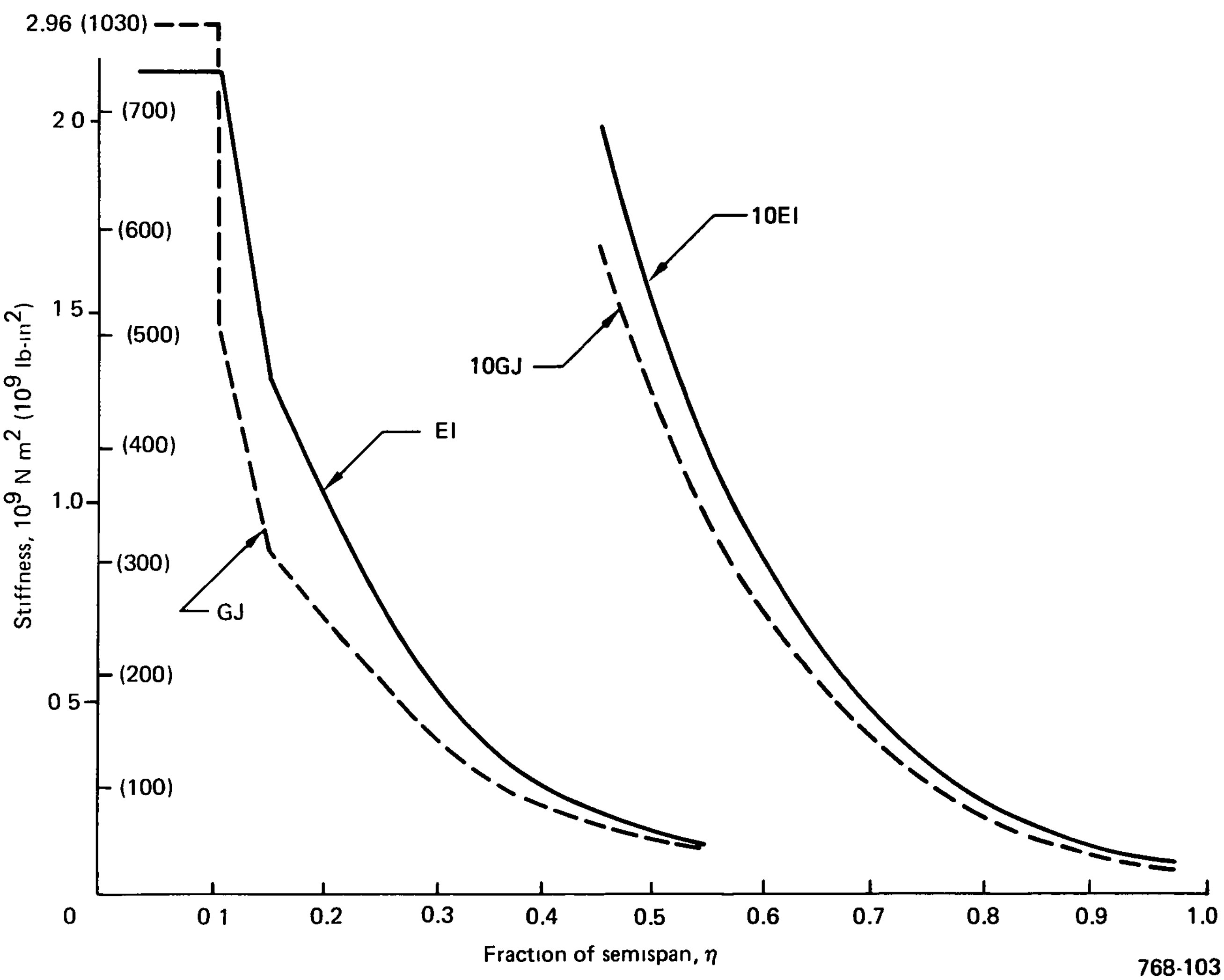

Figure 83. Wing-Box Stiffness (Strength Sizing, Preliminary Design Cycle)

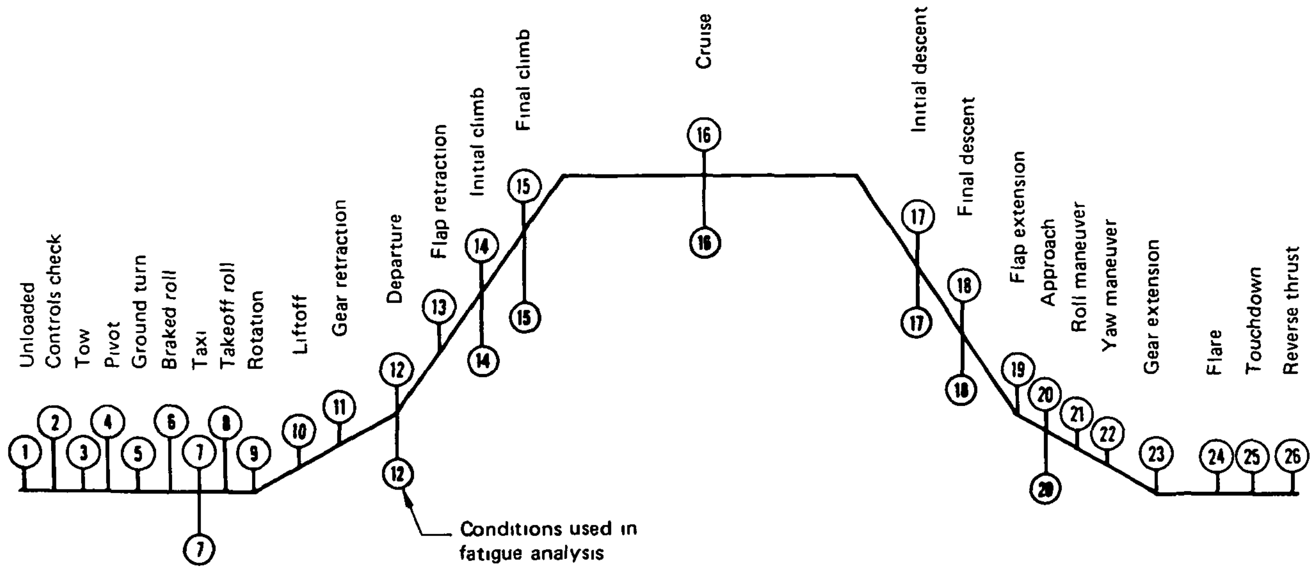

Figure 84. Flight Profile for Fatigue Analysis

Table 12. Fatigue Segment Distribution, Short Flight 567 km (306 nmi) Mission, Summary Calculation

Condition number	Segment	Length, km	(nmi)	Cycles/ flight	g or gust velocity
7	Taxi	0	0	8	1 ± 0.3g
12	Depart	0	0	2	1 ± 0.3g
14	Initial climb	15	(8)	2	± 3.05 m/s (± 10 ft/s)
15	Final climb	100	(54)	2	± 2 74 m/s (± 9 ft/s)
	Gust			3	± 3.05 m/s (± 10 ft/s)
16	Cruise	331	(179)		
	Maneuver			2	1 ± 0 3g
17	Initial descent	104	(56)	2	± 2 74 m/s (± 9 ft/s)
18	Final descent	17	(9)	2	± 3.05 m/s (± 10 ft/s)
20	Flaps down approach	0	0	2	1 ± 0 3g

768-103

eliminate the need to add structural material for fatigue. For this purpose the outboard aileron control surface inputs (fig. 72) were modified to a linear system eliminating the $\pm 0.5g$ dead zone as shown in Figure 85.

The results of the fatigue analysis shown in Figure 86 indicate the beneficial effects of an assumed 50% reduction in the alternating stresses caused by incremental gusts and maneuvers in the fatigue spectrum. The assumed reductions in the peak-to-peak ground-air-ground (GAG) stress cycle are illustrated in Figure 87 and Table 13. These results are an assessment of the potential benefits of fatigue load reduction assuming a 50% reduction in alternating stress. The final fatigue analysis for the Initial ACT Configuration is presented in Subsection 7.2.2.4.

7.2.1.4 Dynamic Gust Requirements

A preliminary gust analysis was conducted to evaluate the structural requirements for continuous turbulence criteria and to determine if a gust-load alleviation (GLA) system was needed to meet these requirements. The mathematical model for the preliminary dynamic gust analysis represented an airplane that did not satisfy flutter stability requirements, and the horizontal tail flexibiity was not representative of the model. However, the model was considered adequate to meet the study objectives.

Dynamic vertical gust loads caused by continuous atmospheric turbulence were calculated using random harmonic analysis methods based on the von Karman spectrum of atmospheric turbulence. The design criteria agree with the design requirements and objectives and with the recommendations of the Aerospace Industries Association. The dynamic gust analysis first was performed for a free airplane with no ACT system, then repeated with the active PAS. The preliminary PAS (fig. 88) uses pitch-rate feedback to control elevator motion. The reduced airplane short-period pitch response was expected to reduce wing loads.

Net wing bending moments from dynamic and static loads analyses are compared in Figure 89. In the static loads analysis, combined maneuver and gust conditions were considered for strength-sizing the wing. The gust conditions were based on the FAR formula including a dynamic magnification factor on incremental loads. This factor

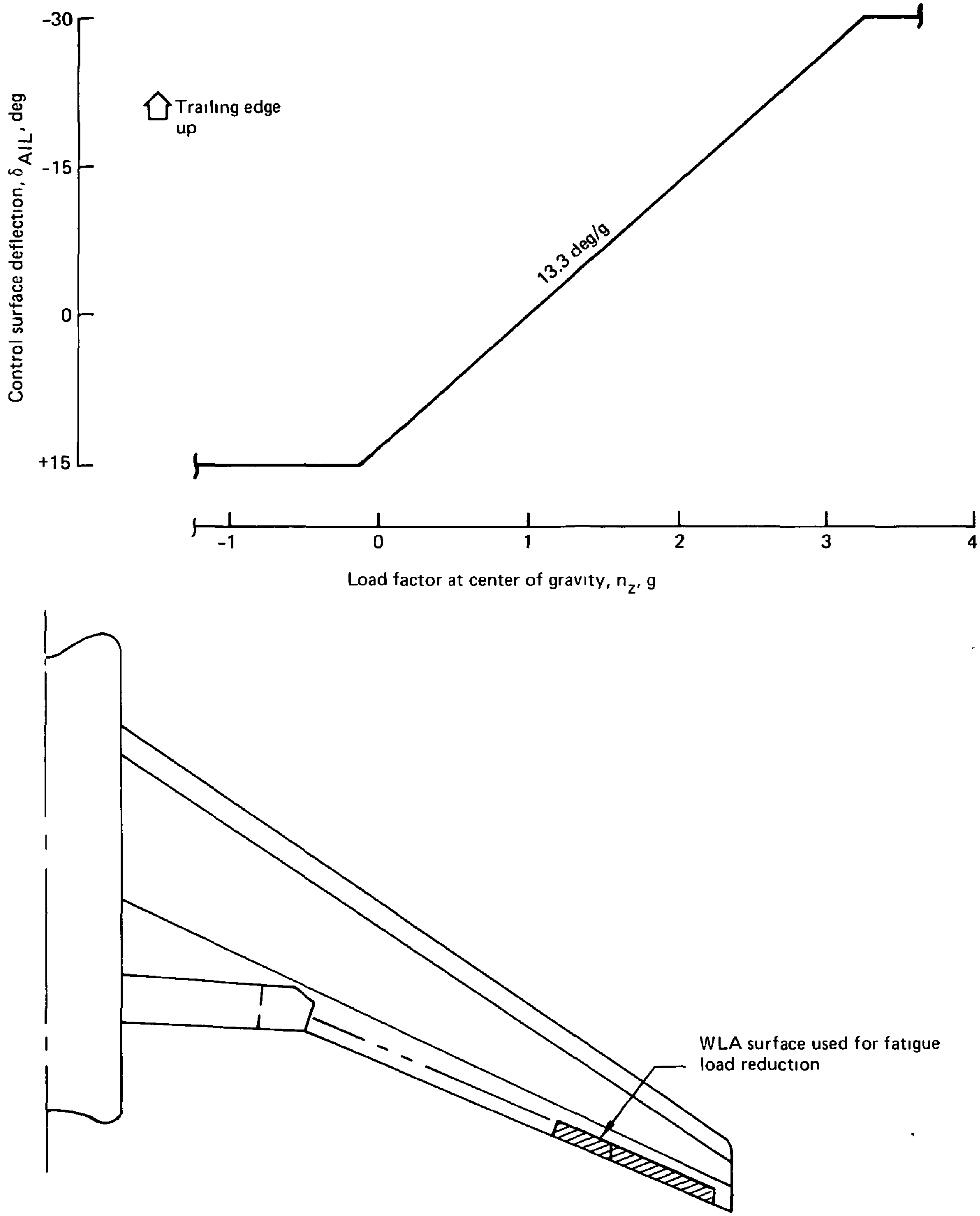

Figure 85. Control Surface Requirements for Fatigue Load Reduction 768-103

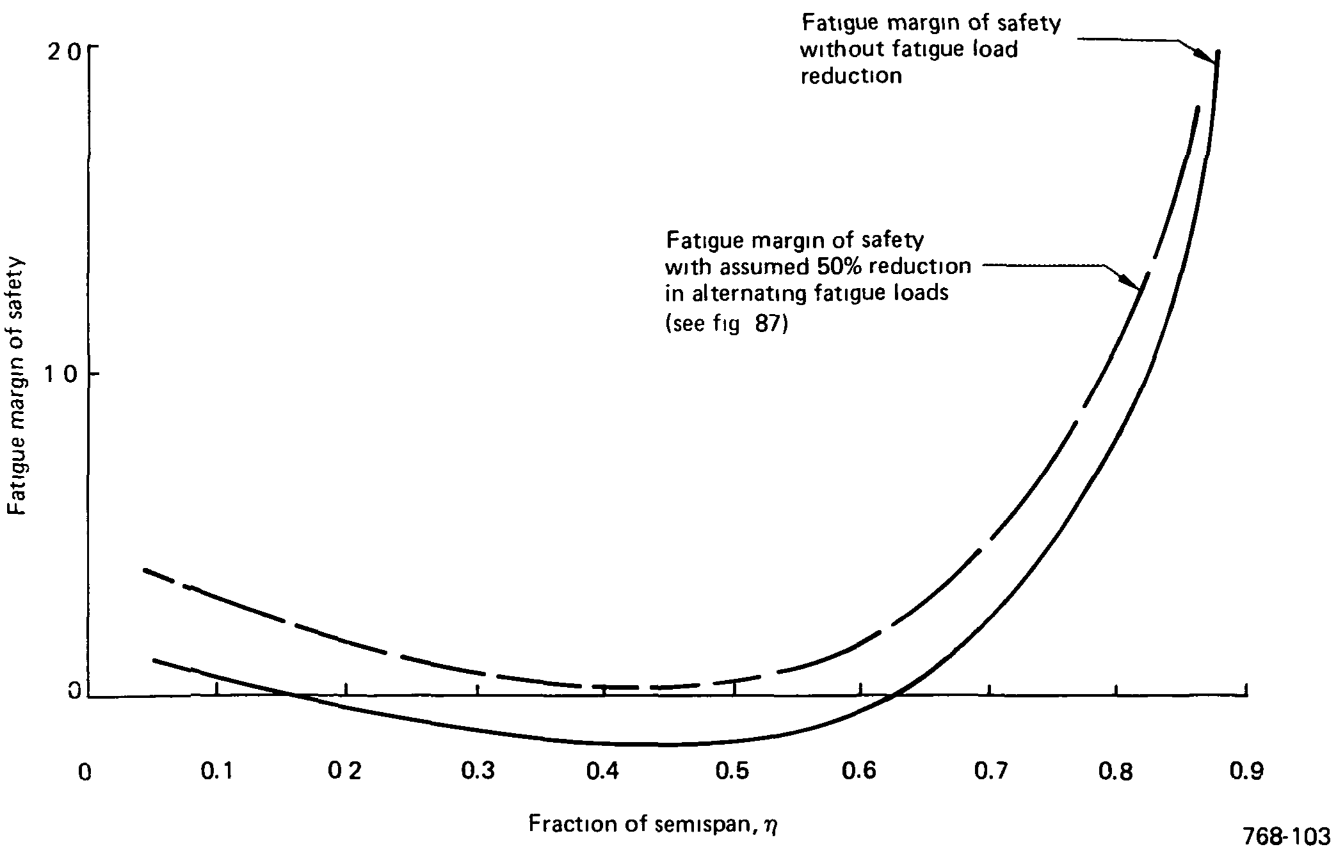

Figure 86. Initial ACT Airplane Minimum Fatigue Margin—Wing Lower Surface

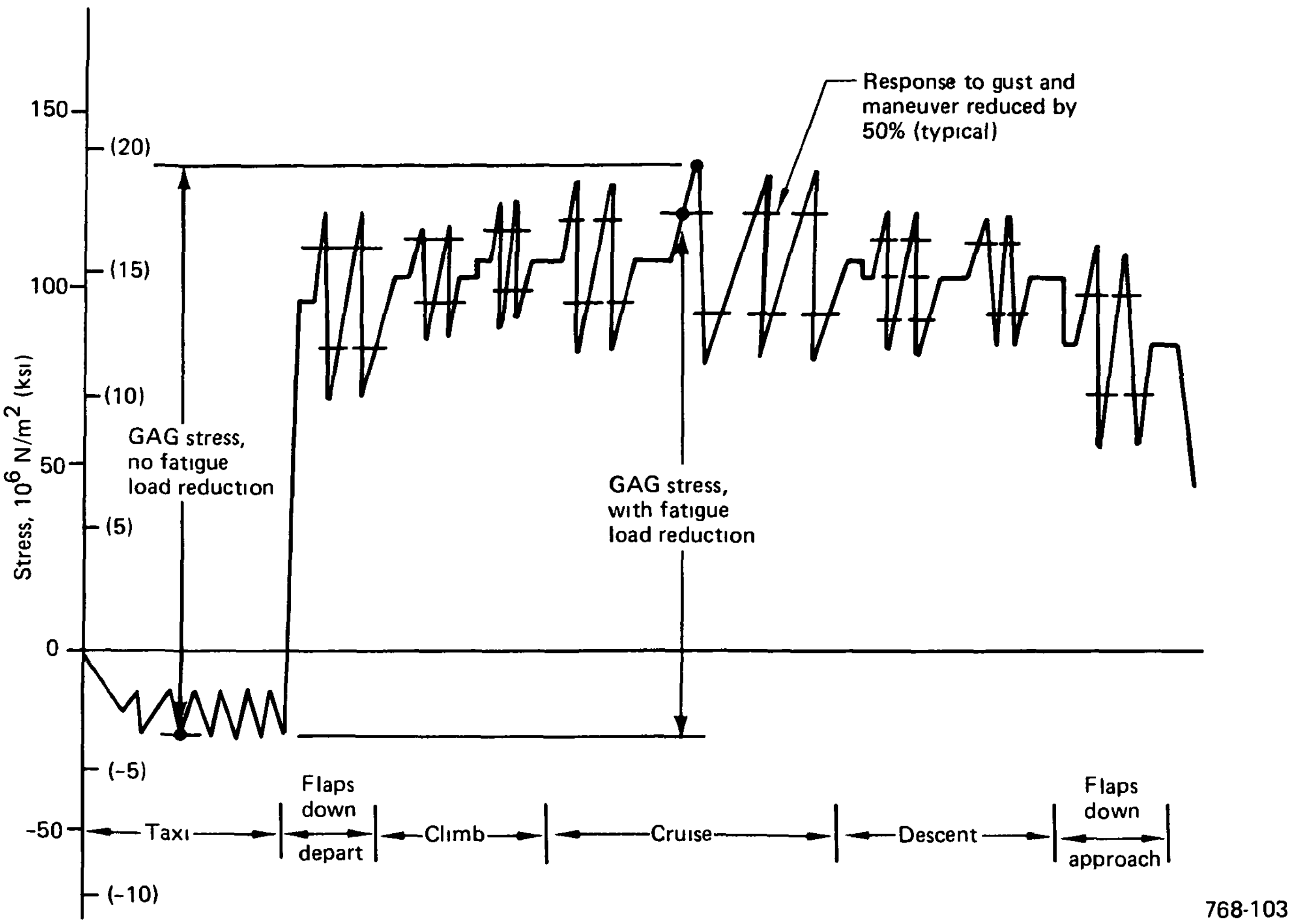

Figure 87. Typical Fatigue Profile—45% Semispan

Table 13. Effect of Linear WLA That Reduces Incremental Response to Gust and Maneuver by 50%, Typical

Example shown at 45% wing span		
GAG stress	No fatigue load reduction -24 1 to 133.7 10^6 N/m^2 (-3 5 to 19.4 ksi)	With fatigue load reduction -24 1 to 121.3 10^6 N/m^2 (-3.5 to 17.6 ksi)
Percent GAG	64	92
Fatigue margin of safety	-0.13	+0.02

768-103

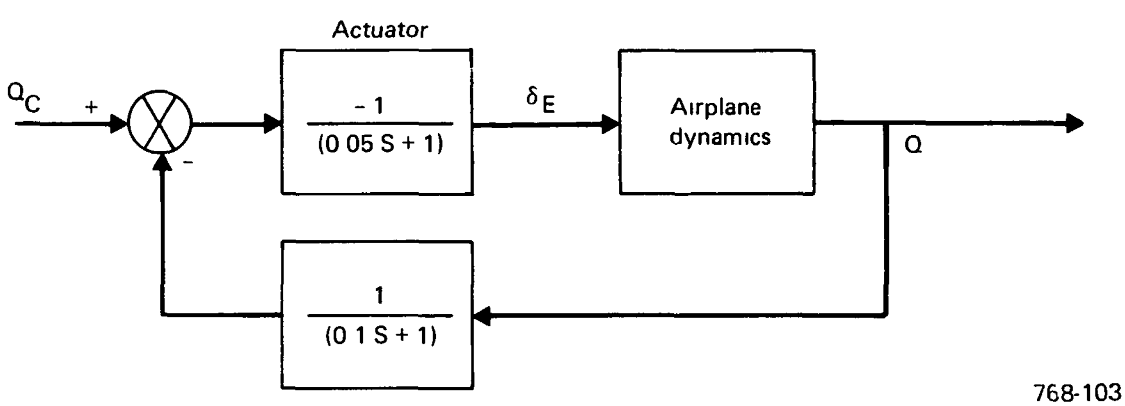

Figure 88. Preliminary Pitch-Augmented System (PAS)

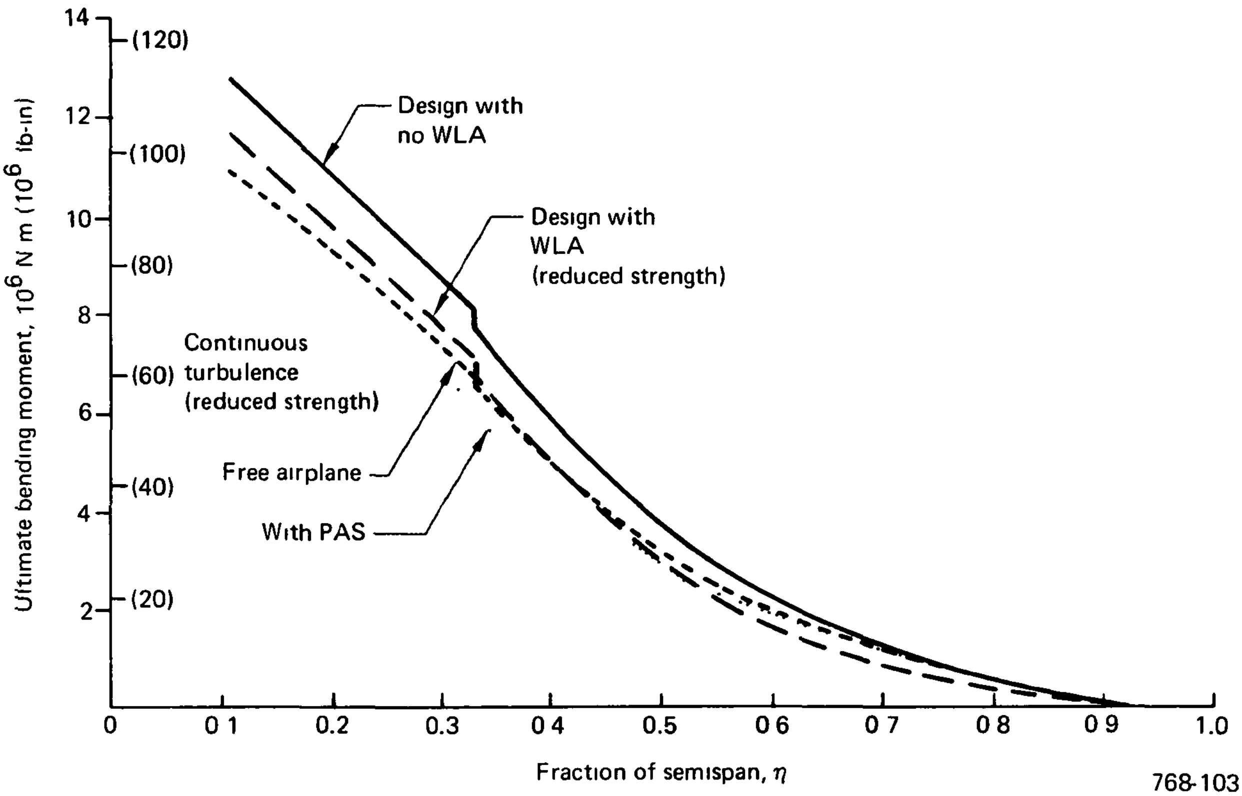

Figure 89. Wing Bending Moment Envelope Comparison

was developed in a previous analysis and has a magnitude of 1.1 for most of the wing span and increases gradually in the outboard 50% span. As expected, the PAS reduced bending moments all along the span, especially inboard. However, in the outboard 50% span, the reduced bending moments with PAS exceeded the strength-designed bending moments with WLA.

Critical bending moments in continuous turbulence occur at maximum flight gross weight for the inboard wing at the gust penetration speed (V_B) and for the outboard wing at the structural cruise speed (V_C). The load reduction caused by PAS effects on airplane short-period pitch response is evident in the typical output spectrums for wing bending moment shown for three analysis stations in Figures 90 through 92.

The results of the fatigue analysis in Subsection 7.2.1.3 and the bending moment comparison in Figure 89 suggest that, in addition to the PAS, a GLA system would be

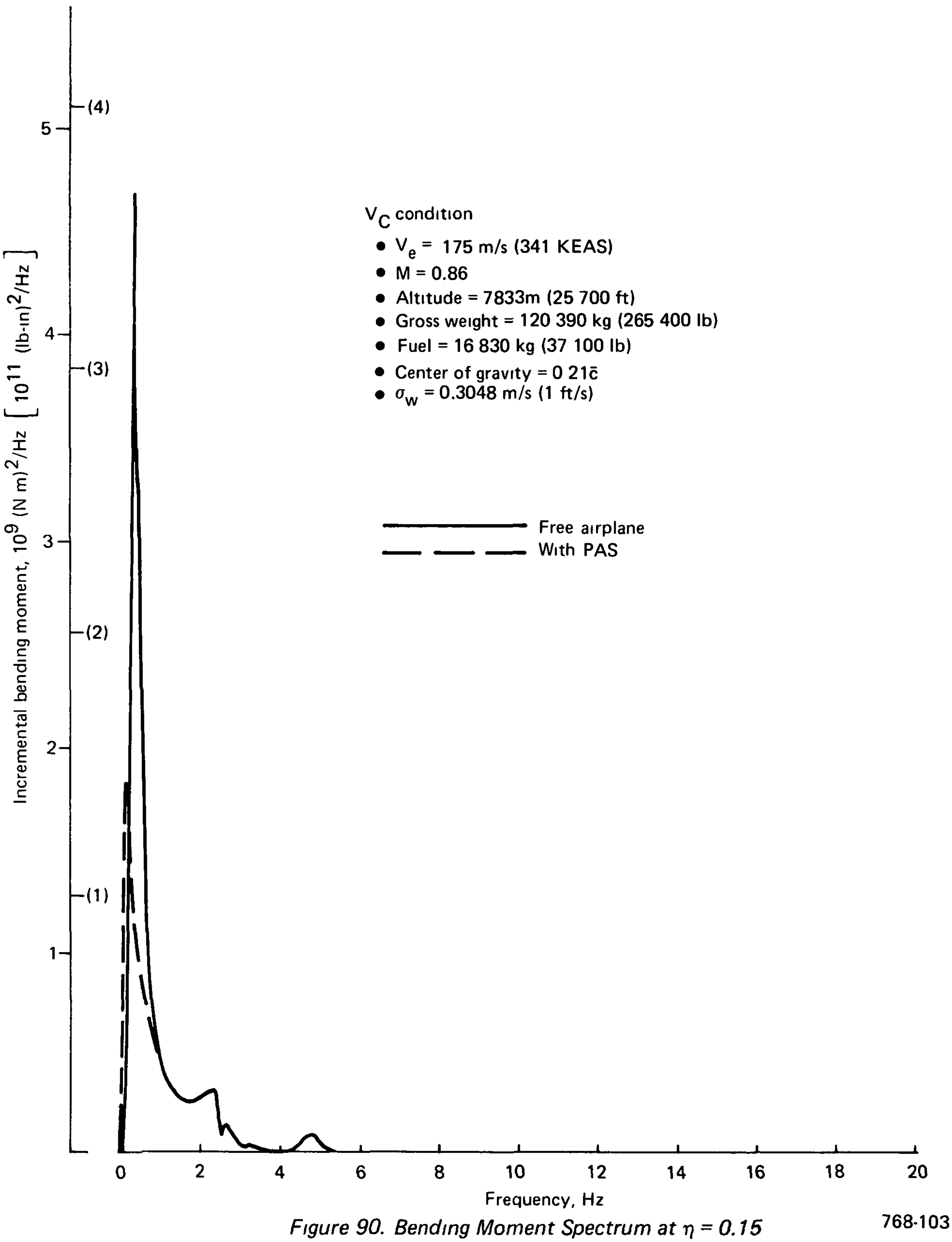

Figure 90. Bending Moment Spectrum at η = 0.15

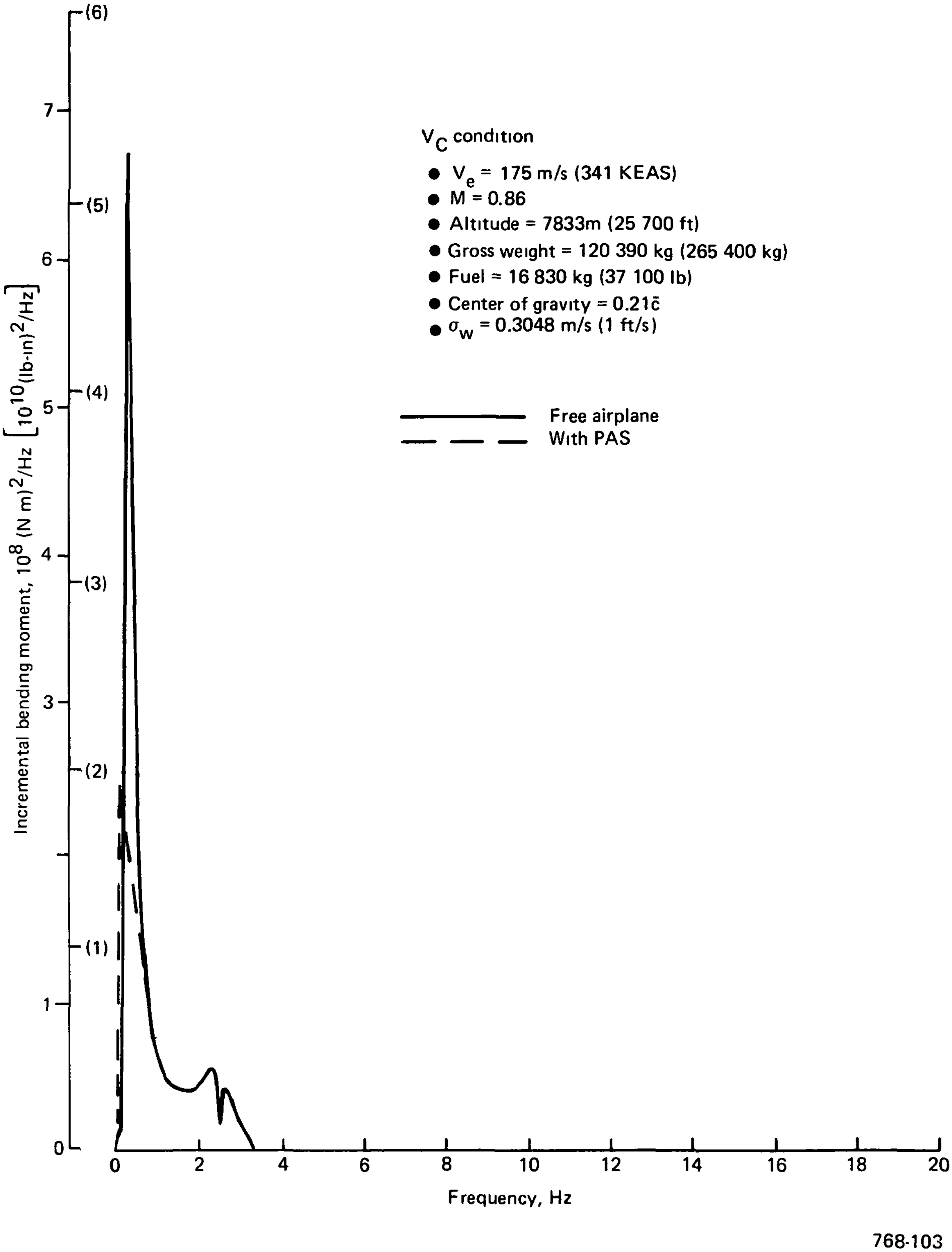

Figure 91. Bending Moment Spectrum at $\eta = 0.45$

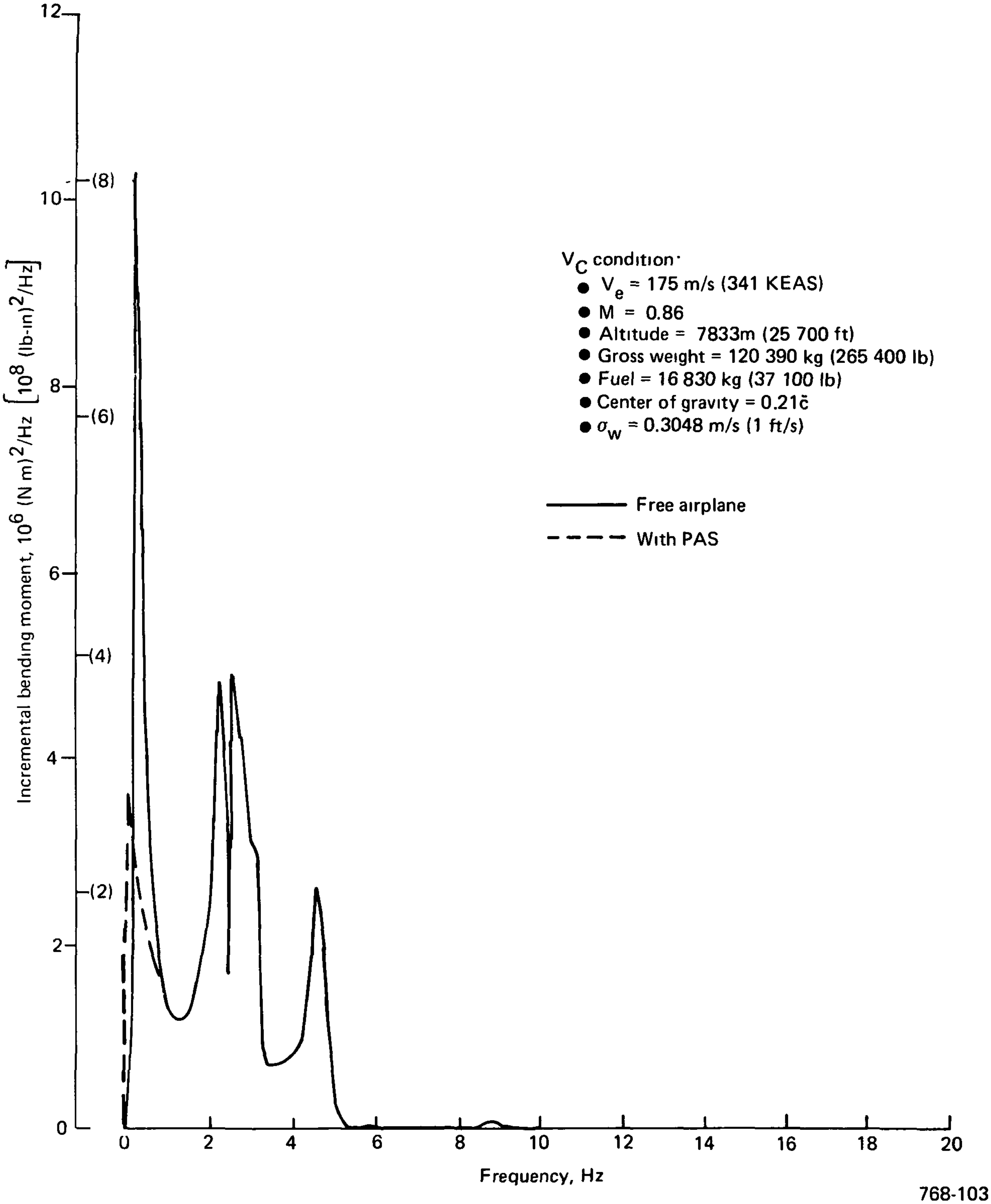

Figure 92. Bending Moment Spectrum at η = 0.75

desirable if it could further reduce inboard wing loads for improved fatigue life and further reduce outboard wing loads for lower strength requirements. These results further suggest that an outboard surface, such as the outboard aileron, would be most effective. The outboard aileron was therefore selected for further use as part of a GLA system to reduce gust loads in continuous turbulence.

7.2.1.5 Flutter Requirements

The preliminary flutter analysis of the Initial ACT Configuration was used to determine the flutter characteristics of the wing designed to satisfy strength requirements using the selected WLA system described in Subsection 7.2.1.2. Consequently, at this stage in the analysis it was assumed that active controls could be used to avoid adding material to meet fatigue life requirements (subsec 7.2.1.3) or continuous turbulence design requirements (subsec 7.2.1.4). Flutter speed sensitivities to variations in wing fuel distribution, nacelle strut flexibility, and aft body vertical bending frequency were investigated. However, for symmetric and antisymmetric conditions, the bulk of the analysis was performed for a nominal configuration known to be critical from previous studies:

- TOGW = 122 470 kg (270 000 lb)
- Fuel = 26 650 kg (58 760 lb), 80% maximum
- Payload = 19 120 kg (42 150 lb), aft loaded
- Center of gravity = 46% MAC, aft limit

The method of analysis was similar to that used for the Baseline Configuration. The development of the mathematical model of the airplane is described in Subsection 7.3.1.1, "Dynamic Model." (A schematic of the basic elements of the dynamic model is shown in Figure 127, Subsection 7.3.) The first three elements in the schematic were used in the flutter analysis to ensure conformity with the analyses used for control law development and stability and control verification. The resulting equations of motion were solved using the traditional V-g method for predicting flutter speeds and frequencies.

The conventional beam-lumped mass structural idealization for high aspect ratio wings was used for the vibration analysis. The airplane was modeled as an assemblage of cantilevered branches using the main surface elastic axes and control surface hinge lines as reference axes for the structural stiffness and panel masses. The branches considered in the analysis were: fore body, aft body, vertical tail, horizontal tail, wing, nacelle strut, outboard aileron, outboard flaperon, inboard aileron, double-hinged elevator, and split double-hinged rudders. The outboard aileron, outboard flaperon, and elevator were further subdivided to provide versatility in selecting candidate active control surfaces. The wing structural idealization and the structural nodes retained on the elastic axes and hinge lines are shown in Figure 93.

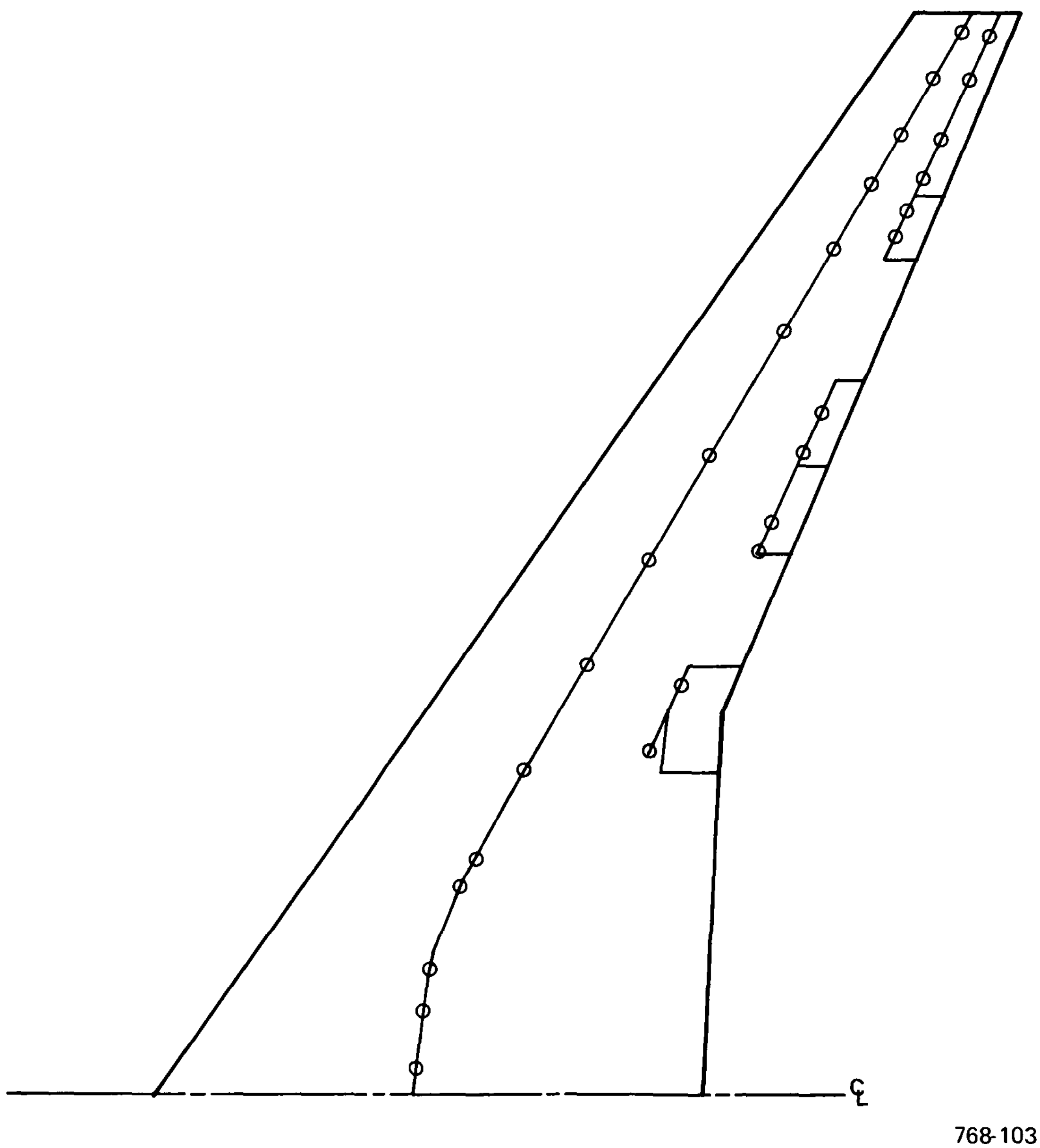

Figure 93. Wing Structural Idealization for Flutter Analysis

Conventional modal formulation was used to develop the equations of motion. The generalized coordinates used in the analysis were:

- Airplane rigid body modes
- Cantilevered coupled modes of:
    - Forebody
    - Aft body (rigid vertical and horizontal tail)
    - Vertical tail (rigid horizontal tail)
    - Horizontal tail
    - Wing (rigid nacelle strut)
    - Nacelle strut
- Rigid control surface rotation modes

The distributed stiffnesses along the elastic axes of the selected branches and the lumped masses used to calculate vibration modes were based on the structural sizing for strength. The nacelle strut modes used in the analysis were identical with those developed for the Baseline Configuration. Control surface flutter was not considered in the analysis; consequently, a hinge-line rotation mode with a high natural frequency of 30 Hz was selected to preclude coupling. The generalized coordinates used for the symmetric analysis of the nominal weight condition are listed in Table 14; however, the horizontal tail modes, which did not contribute significantly to wing flutter for the Baseline Configuration, were not included in the analysis.

The unsteady airloads were calculated with doublet-lattice lifting surface theory. The wing, including control surfaces and flaps, the horizontal tail with elevators, and the vertical tail with rudders, were modeled as lifting surfaces. The nacelles were represented by cruciform plates and the body by a flat plate. For the symmetric analysis, a total of 332 boxes were used; for the antisymmetric analysis, a total of 351 boxes were used. Figure 94 shows the aerodynamic model of the wing, nacelle, and part of the body. The generalized airforce matrices were calculated at zero Mach number with the pressures at aerodynamic boxes scaled to match wind tunnel static aerodynamic data (app. B).

Table 14. Generalized Coordinates for Symmetric Analysis (WLA Wing Stiffness, 80% Wing Fuel)

Branch	Frequency, Hz	Dominant modal description
Airplane	–0–	Rigid airplane fore/aft
	–0–	Rigid airplane plunge
	–0–	Rigid airplane pitch
Forebody	3 99	First vertical bending
Aftbody	2.06	First vertical bending
	6 66	Second vertical bending
Vertical tail	5.59	First vertical bending (in plane)
	28.09	Second vertical bending (in plane)
Horizontal tail	5 91	First vertical bending
	18 70	Second vertical bending
	23.94	First torsion bending
Wing	1 43	First vertical bending
	3.30	Second vertical bending
	3.70	First fore/aft bending (in plane)
	4.29	First torsion
	7 48	Third vertical bending
	9 19	Second fore/aft bending (in plane)
	11 37	Fourth vertical bending
	13 13	Second torsion
Nacelle	2 60	Side bending
	4 63	Vertical bending
	5.76	Roll/side bending
Control surfaces	30	Inboard elevator rotation
	30	Outboard elevator rotation
	30	Inboard aileron rotation
	30	Inboard flaperon rotation
	30	Outboard flaperon rotation
	30	Inboard of outboard aileron rotation
	30	Outboard of outboard aileron rotation

768-103

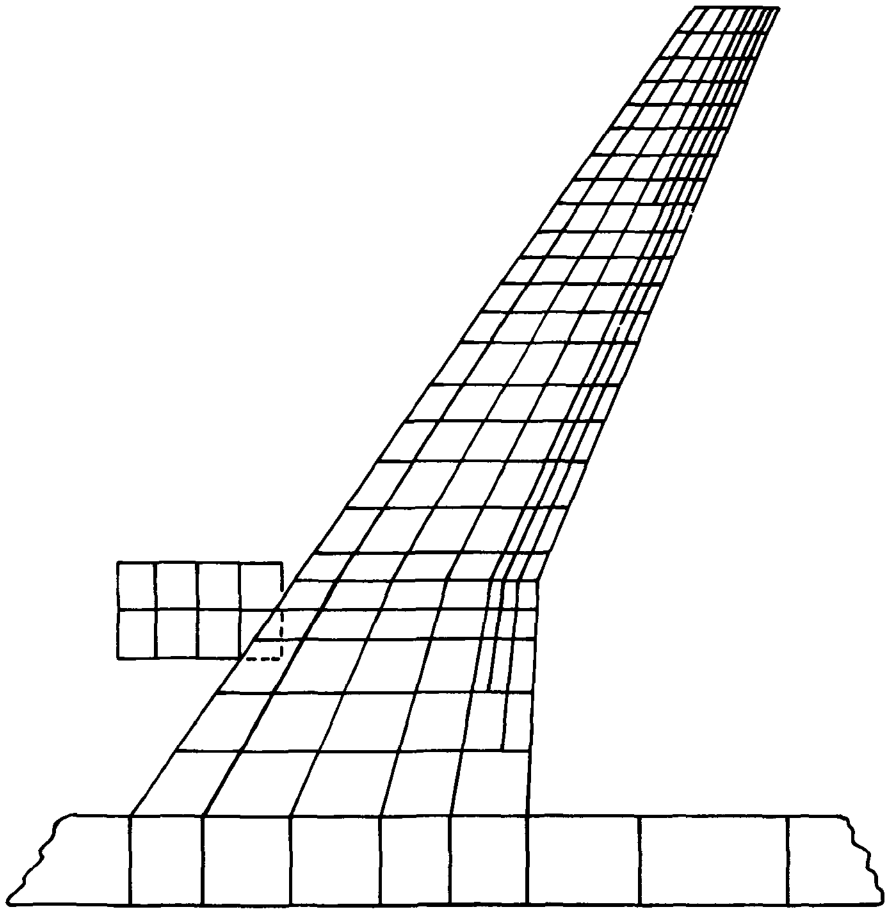

768-103

Figure 94. Doublet Lattice Aerodynamic Model

In the absence of experimental oscillatory aerodynamic data, the pressure scale factors determined from the rigid airplane static data also were used for the unsteady motion of the elastic airplane. The pressure scaling was done for two Mach numbers (0.4 and 0.86). At Mach 0.4, only the pressures at wing aerodynamic boxes were scaled and used in determining the conventional incompressible flutter speeds. A compressibility correction factor, C_c, was then applied to the incompressible flutter speeds at selected altitudes to derive the flutter boundary on the speed-altitude envelope. C_c is defined as the square root of the ratio of lift-curve slope at Mach 0.4 to lift-curve slope at the specific Mach number and is determined from the experimental aerodynamic data (app. B). The flutter boundary thus obtained always indicates that the most critical flutter condition occurs at the critical Mach number. Therefore, in the current IAAC study, control laws for flutter-mode control (FMC) were developed only at the critical Mach number of 0.86. Pressure scaling for all the aerodynamic boxes of the airplane at this critical Mach number is detailed in Subsection 7.3.1.1. The flutter analysis was performed for variations in altitude to determine a matched flutter point on the Mach 0.86 line of the speed-altitude envelope.

Symmetric and antisymmetric analyses at sea level were first performed for the nominal weight condition where wing fuel tanks are 80% full. Two distinct wing flutter modes were found for the symmetric case. The critical mode, designated herein as the "inboard wing flutter mode," is characterized as a soft flutter instability with a frequency of 3.2 Hz, caused mainly by coupling between wing vertical bending, wing torsion, and nacelle strut vertical bending. The V-g curve for this mode is shown in Figure 95. A second and more violent flutter mode occurs at a much higher speed with a 7.6 Hz frequency. This flutter mode consists mainly of outboard wing vertical bending and torsion and is designated herein as the "outboard wing flutter mode."

In the antisymmetric analysis, the outboard wing flutter mode was found to have nearly the same flutter speed and frequency as in the symmetric case. However, the 3.2 Hz antisymmetrical inboard wing mode (wing vertical bending/torsion and nacelle oscillation) was found to be stable with increasing speed (fig. 96).

Symmetric and antisymmetric flutter analyses at sea level were conducted for two additional fuel conditions, zero and full fuel. The wing flutter modes were similar for all fuel variations, except at full fuel where the symmetric inboard wing flutter mode became violent (fig. 95). The effects of wing fuel on flutter speed are shown in Figure 97. The most critical fuel distribution is 80% full for the symmetric case. For this critical case, the airplane was also analyzed at altitudes of 3048m (10 000 ft) and 6096m (20 000 ft) for Mach 0.4 and at altitudes of sea level, 3048m (10 000 ft), and 6096m (20 000 ft) for Mach 0.86. The flutter speed boundary (based on Mach 0.4 aerodynamic data and the compressibility correction factor) and the matched flutter point (based on Mach 0.86 aerodynamic data) are shown in Figure 98. The flutter speed boundary of the reduced-strength wing is clearly below V_D and, therefore, does not satisfy the design criteria requirements.

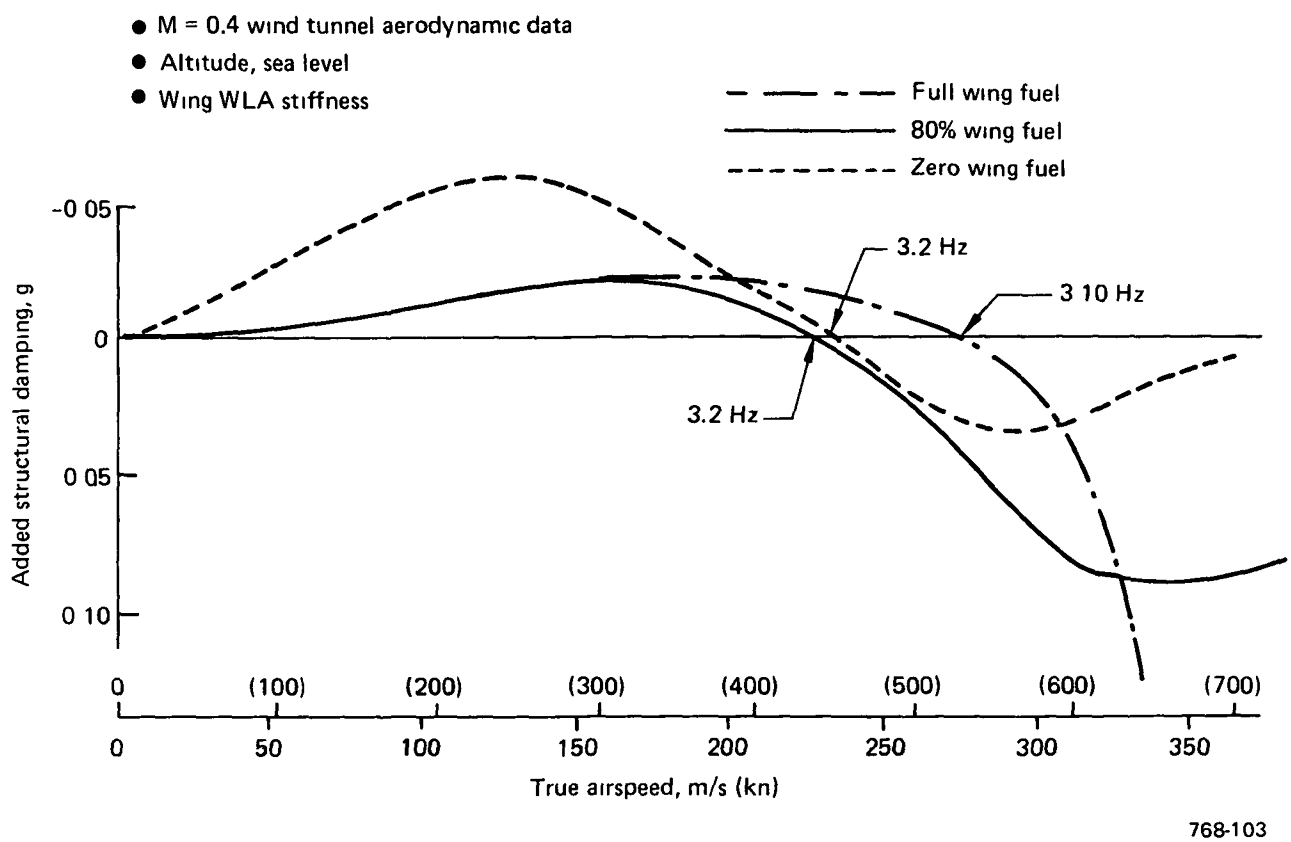

Figure 95. V-g Diagram for Airplane Symmetric Analysis—Inboard Wing Flutter Mode

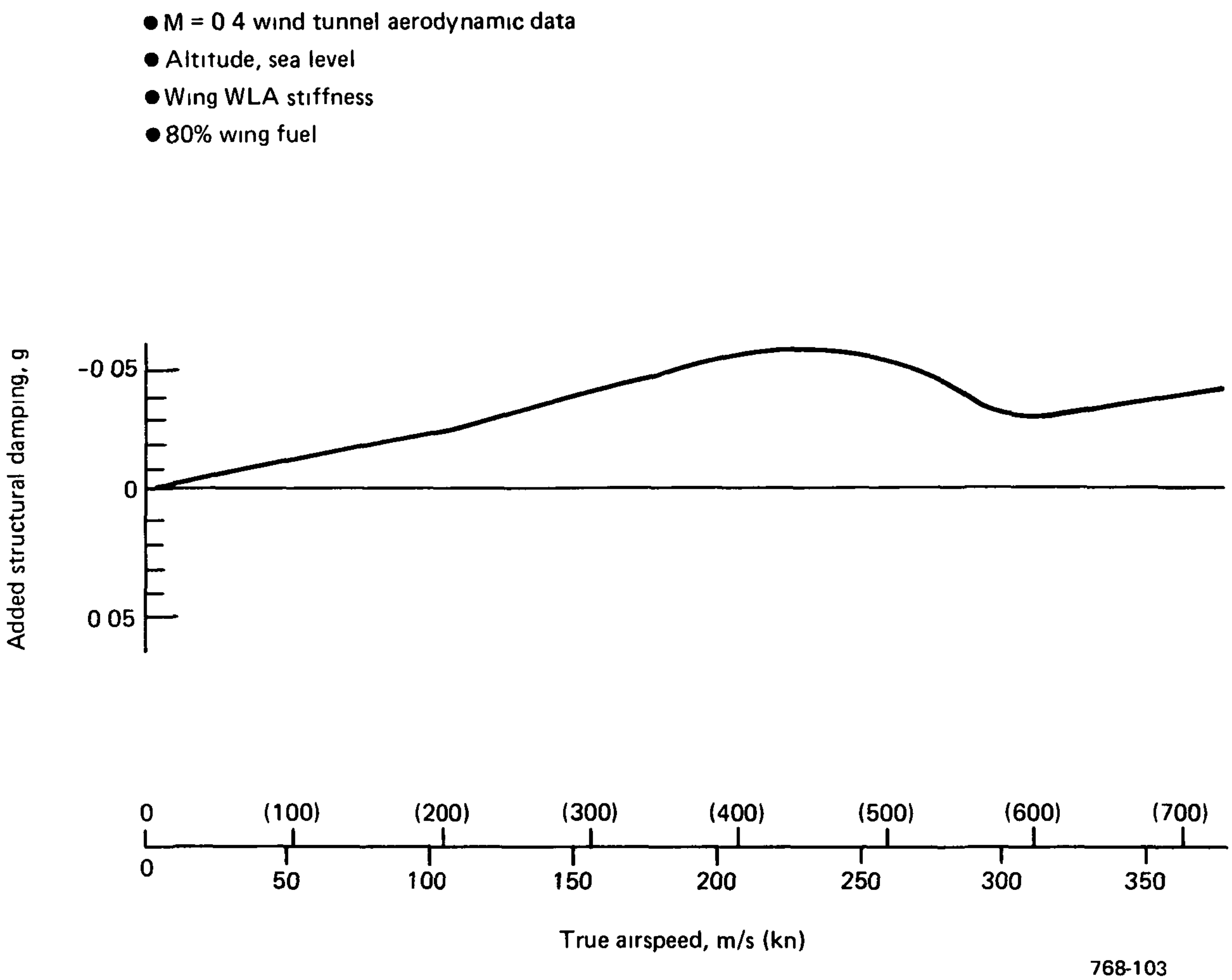

Figure 96. V-g Diagram for Airplane Antisymmetric Analysis—Inboard Wing Oscillation

- M = 0 4 wind tunnel aerodynamic data
- Altitude, sea level
- Zero structural damping

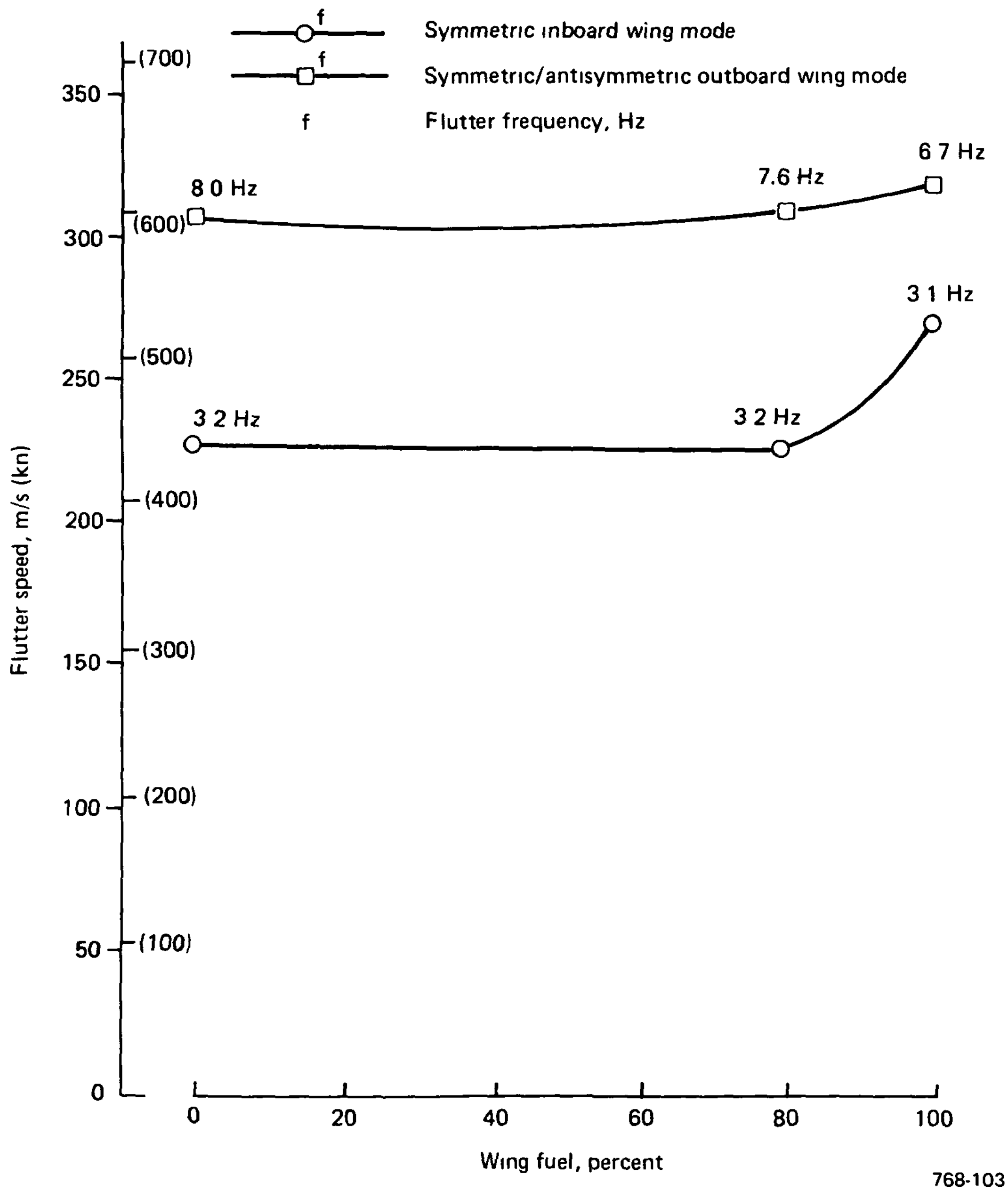

Figure 97. Effect of Wing Fuel on Flutter

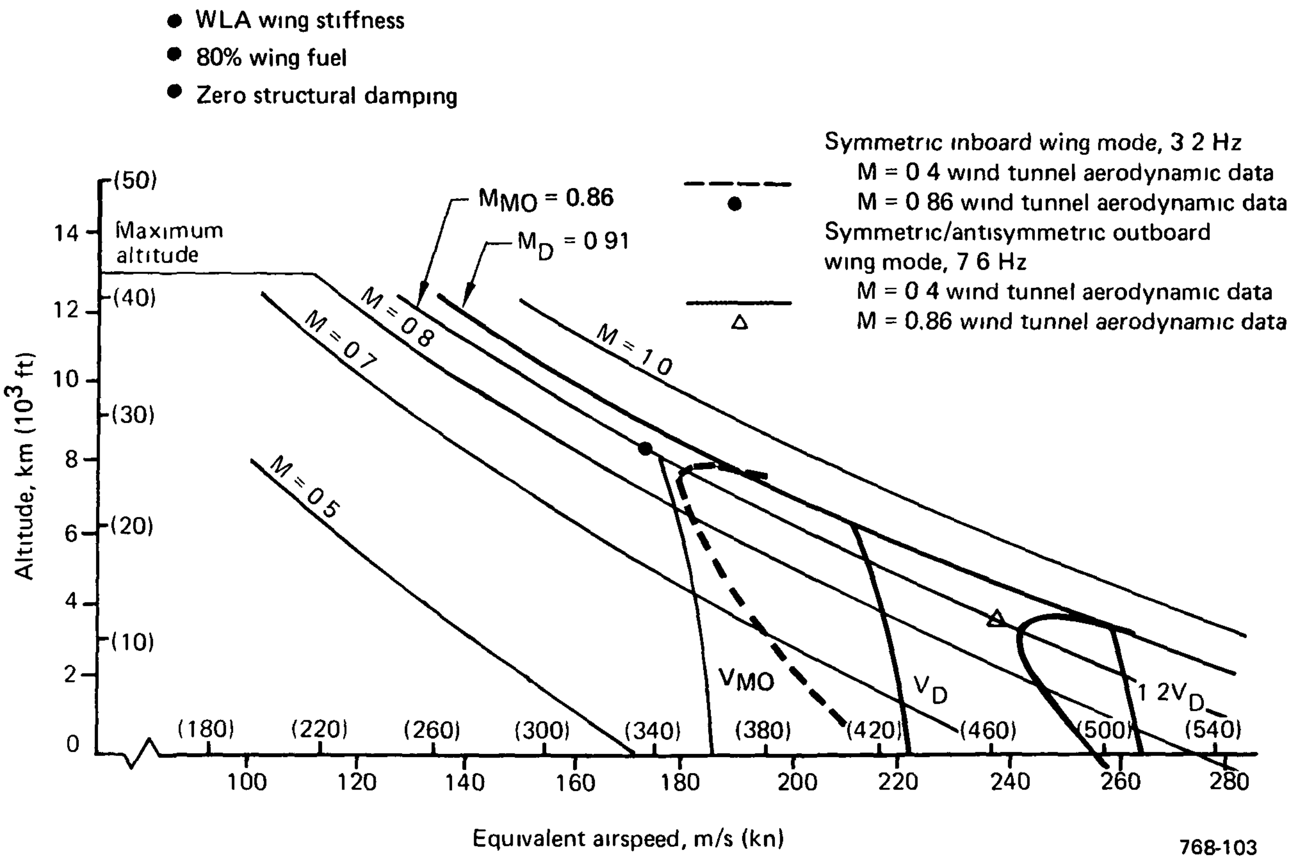

Figure 98. Symmetric Flutter Boundary

Flutter sensitivity studies based on the critical 80% fuel symmetric case were conducted to evaluate the effects of variations in nacelle strut vertical and side bending frequency and aft body vertical bending frequency. Through the range of nacelle vertical bending frequencies considered (3.2, 4.0, 4.2, nominal 4.63, 5.0, 5.5), the flutter speed was shown to have a maximum reduction of 19% at 3.2 Hz and a 2% increase at 5.5 Hz. Wing flutter speed did not decrease significantly when the nacelle strut side bending frequency was changed from the nominal 2.6 Hz to 3.0, 3.3, 3.65, and 4.0 Hz.

A 50% reduction of the nominal aft body vertical bending frequency of 2.06 Hz degraded wing flutter speed only 4% while a 70% increase of the frequency reduced wing flutter speed by 7%.

These studies indicated that minor variations from the nominal nacelle and aft body frequencies would not affect the conclusions from the flutter analysis for purposes of the Initial ACT study.

7.2.2 FINAL WING

The final structural analysis of the Initial ACT Configuration was used to establish the structural weight benefits associated with the selected ACT functions. The mathematical model was updated to include changes in mass and stiffness, and was expanded to include the control laws developed to meet the requirements established in the preliminary structural analysis.

The final structural analysis was directed toward an efficient solution of the structural design deficiencies uncovered in the preliminary design. Consequently, the first task was to provide a passive fix that would increase the flutter speeds to V_D. The mathematical model with the flutter fix was then used to validate ACT control laws to meet the remaining structural requirements for:

- Flutter clearance to $1.2V_D$ with an FMC system
- Outboard wing strength, by reducing design gust loads due to continuous turbulence with a GLA system
- Fatigue life on the inboard wing, by reducing incremental gust and maneuver loads using the GLA system and a WLA system with no dead zone

When all individual structural requirements were satisfied, a final wing structural sizing was performed to identify the benefits associated with the selected ACT systems.

7.2.2.1 Flutter Stability Design

The results of the flutter analysis presented in Subsection 7.2.1.5 indicated that the Initial ACT Configuration, with the wing structure sized to meet strength requirements using a WLA system, had a flutter speed boundary below V_D. The design criteria require that the airplane be free of flutter instabilities up to V_D without benefit of inherent structural damping or use of ACT devices and up to $1.2V_D$ including the effects of structural damping and ACT devices.

Three types of analyses are presented in this subsection. These include analyses to:

- Satisfy the flutter stability requirements to V_D with a passive fix

- Verify flutter stability to $1.2V_D$ with the active FMC system

- Assess the benefit of the FMC system by defining the weight penalty of a passive fix to increase the flutter speeds to $1.2V_D$, including the effect of structural damping

Design studies to provide flutter stability for V_D clearance on the Baseline Configuration indicated that a structurally efficient way to increase the wing-box torsional stiffness (GJ) was to increase the front and rear spar web thicknesses to match the smallest wing surface skin thicknesses. This increased stiffness is designated as GJ1. Flutter analysis of the Initial ACT Configuration, performed with the mathematical model updated to represent the additional wing structural weight and torsional stiffness, showed improved flutter speeds, but not enough to meet flutter stability requirements. Therefore, additional approaches to satisfy the flutter requirements were investigated using the critical symmetric condition with 80% wing fuel at 4960m (16 000 ft) and a reduced mathematical model with the fuselage and empennage idealized as rigid structure. This simplification was adopted for reasons of economy. It was considered adequate to define flutter trends, since the elastic freedoms of body and empennage had not been found to have a large influence on wing flutter characteristics. Three design features were investigated to improve the flutter stability: local wing torsional stiffness variations, mass balance and location trades, and an outboard wing reserve fuel tank.

Preliminary analysis indicated that changes in wing torsional stiffness inboard of the nacelle would have a larger effect on flutter speed of the inboard wing flutter mode than changes outboard of the nacelle. Further analysis indicated that a local torsional stiffness increase near 25% semispan was most effective. The approach finally selected was to increase torsional stiffness linearly from 15% semispan to a preselected maximum at 25% semispan then decrease torsional stiffness linearly to the original value at 35% semispan. The wing with this increased torsional stiffness had a soft, low-damped flutter mode similar to the base wing, and the unstable encroachment of the V-g curve was less severe as the added torsional stiffness increased. This method produced unreasonable weight penalties, however, since it required local torsional stiffness increases above 300% to clear V_D.

In the wing mass balance study, effects of varying the spanwise location of a 91 kg (200 lb) balance weight at constant 10% chord were evaluated. The most outboard location was found promising. The amount of balance weight at the outboard location was then increased, and the weight was gradually moved forward. Results of the analysis indicated that a balance weight of 91 kg (200 lb) located at 98.4% semispan and 1.83m (6 ft) forward of the wing leading edge would be required to increase flutter speed to V_D. This approach would require customer acceptance and proper design of a tuned support boom for the balance weight. However, the study showed the feasibility of increasing flutter speed in this way and the order of magnitude of the required balance weight was determined.

The third and most promising method involved implemention of an outboard wing reserve fuel tank. The resulting trend analysis indicated that reserve fuel in tanks from 82.5% to 97.50% semispan, holding 703 kg (1550 lb) of fuel per side was required to increase the flutter speed to V_D.

Symmetric and antisymmetric flutter analyses were conducted to confirm the results of the reserve fuel trend study. Three fuel distributions were considered: the critical 80% full, reserve fuel only, and zero fuel. The wing fuel distributions with reserve tank and a comparison with the base wing without reserve tanks at 80% full are shown in Figure 99.

For the critical 80% fuel condition, the antisymmetric inboard wing flutter mode, which consists mainly of wing vertical bending/torsion and nacelle vertical bending, remained stable as described in Subsection 7.2.1.5. The corresponding symmetric

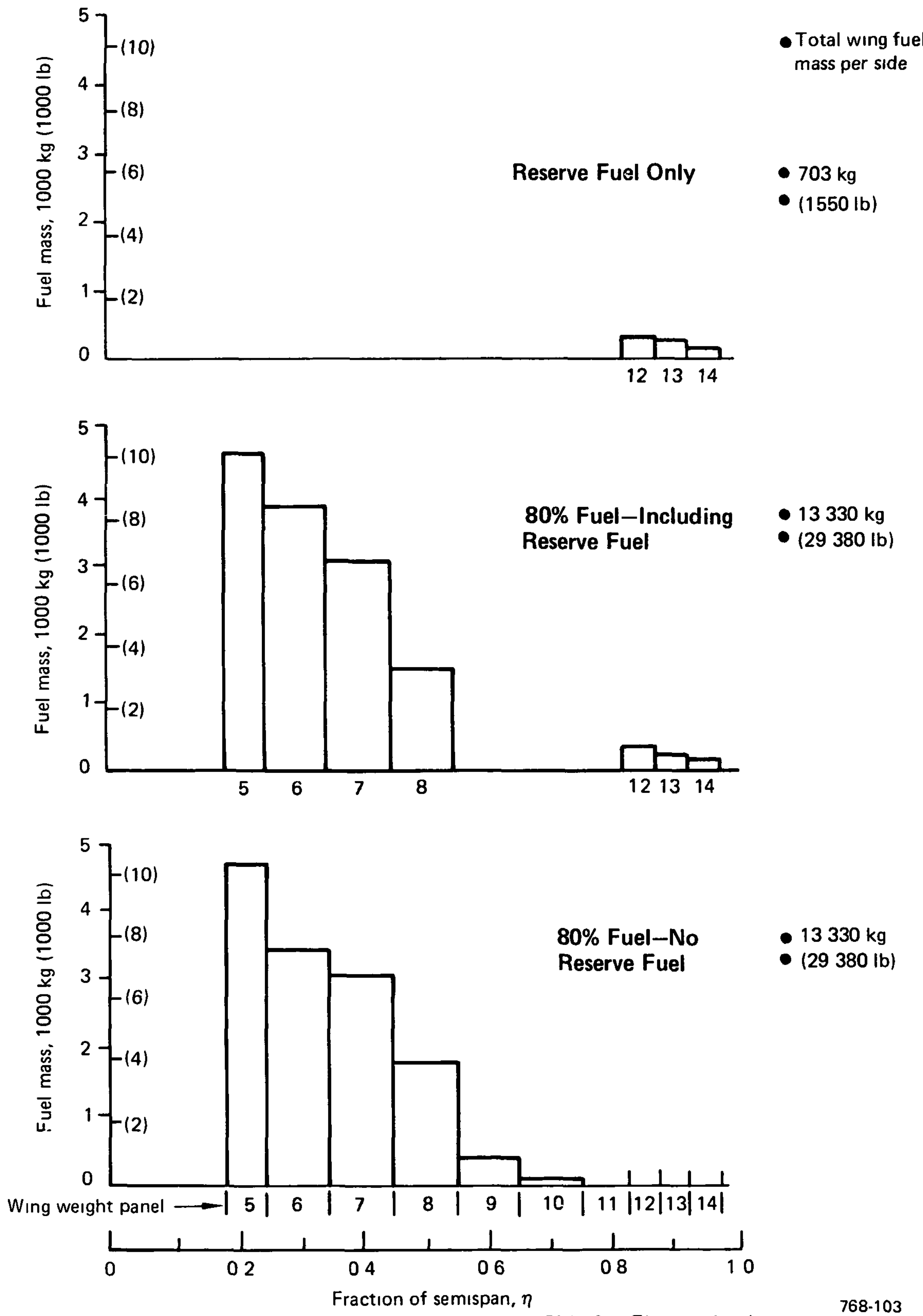

Figure 99. Wing Fuel Mass Distributions per Side for Flutter Analysis

flutter condition (with the outboard fuel reserve tank) occurred at a significantly higher speed (fig. 100) satisfying the requirement for flutter clearance to V_D.

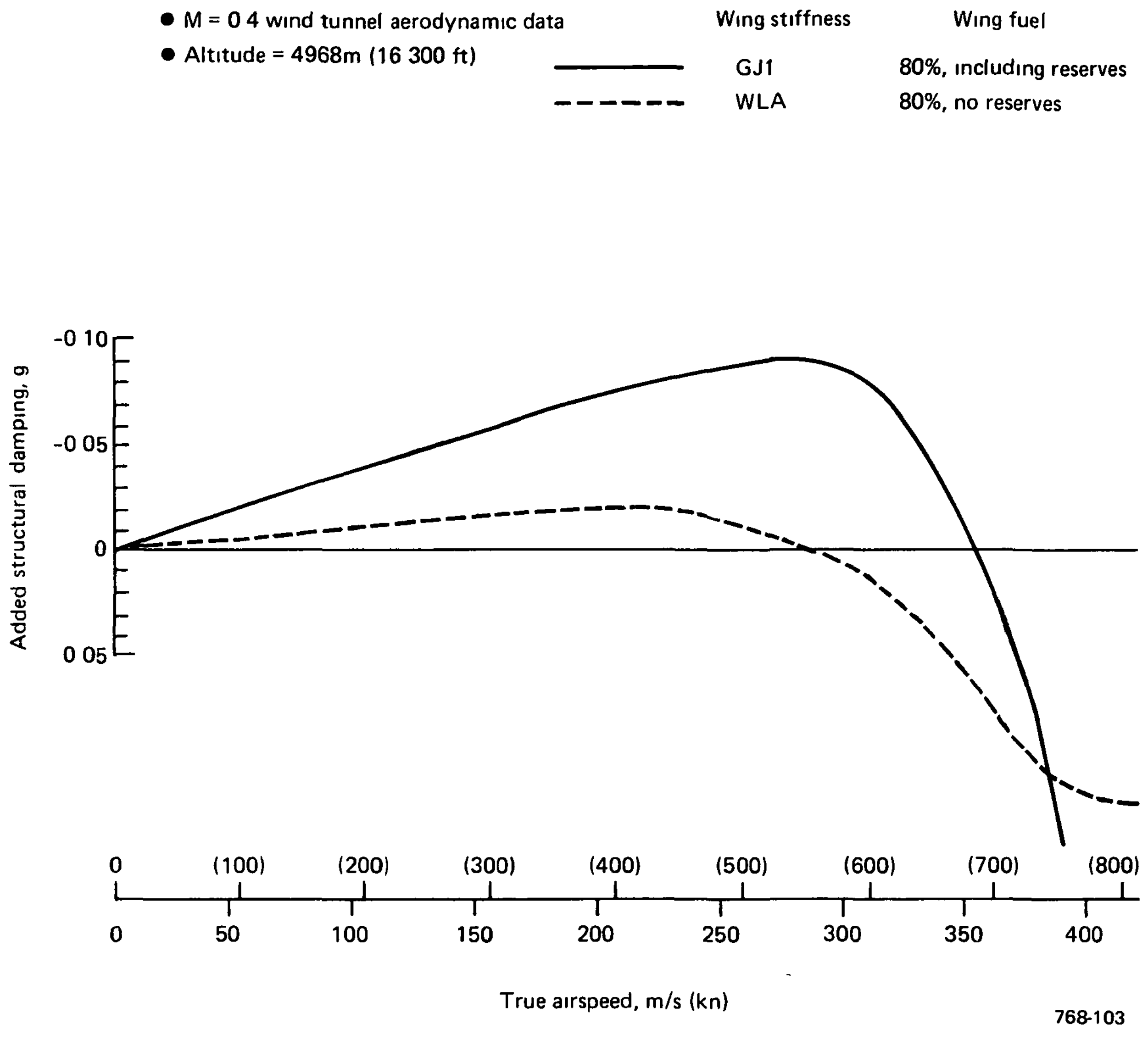

Figure 100. V-g Diagram for Symmetric Airplane—Inboard Wing Flutter Mode

For the case with reserve fuel only, flutter speeds were nearly the same as for the 80% fuel condition. For the zero fuel condition, the flutter speed was lower. Flutter boundaries for the critical symmetric inboard and outboard wing flutter modes at 80% fuel and zero fuel are shown in Figure 101. It is concluded from this figure that for all cases with fuel in the reserve tank the airplane is free from flutter up to V_D without structural damping. For emergency conditions requiring fuel transfer from the outboard tank, an airplane speed limitation would be imposed without significant effect on the airplane mission.

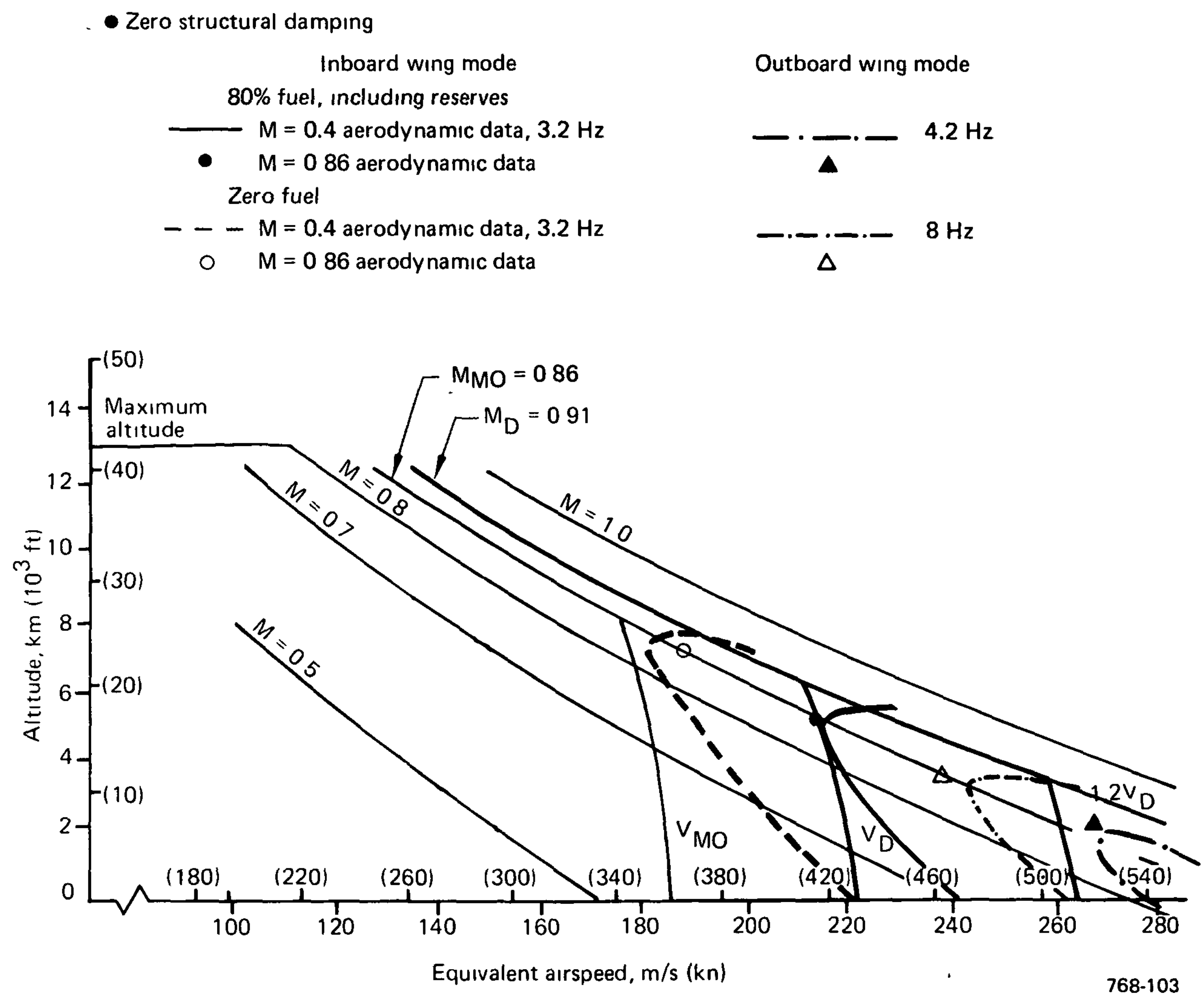

Figure 101. Symmetric Flutter Boundary, Increased Wing Torsional Stiffness

7.2.2.2 Flutter Stability Design For $1.2V_D$ Clearance

The flutter stability of the airplane to $1.2V_D$ using the FMC system described in Subsection 7.3.1 is verified in this section. The weight benefit of the system is also assessed.

In the development of the FMC system and the flutter verification, only the critical symmetric condition at Mach 0.86 for the 80% fuel distribution with reserve fuel was considered. Consequently, this study shows feasibility only and is not intended to represent a complete design verification.

The FMC system is documented in Subsection 7.3.1. The system uses the outboard ailerons to develop aerodynamic force in response to outboard wing acceleration at wing node 1417 (fig. 126). Figure 132 shows a functional block diagram of the FMC system control law and outboard aileron actuator model.

The dynamic model of the airplane was used to develop the control law characteristics. The frequency-dependent unsteady aerodynamic forces were transformed into the Laplace domain (S-plane) and the aileron hinge moments were zeroed out to represent a rigid aileron and supporting structure. Classic root locus methods were used to define the control law constants at four flight speeds: V_B, V_{MO}, V_D, and $1.2V_D$.

The resulting FMC transfer function is $KF \cdot S/\left[(S/15 + 1)\ (S/20 + 1)^2\right]$ and the associated aileron actuator model, which was also used for the maneuver-load control (MLC) and GLA systems, is $1/(S/40 + 1)$.

The FMC systen gain KF, which varies with equivalent airspeed, is specified for Mach = 0.86 in Table 22 (subsec 7.3.1.2).

To verify the FMC system, two flutter analyses were performed. The first analysis was conducted for the equations of motion with the frequency-dependent unsteady aerodynamic forces at Mach 0.86 transformed into the S-plane. At prescribed equivalent airspeeds and with the associated FMC gain values, the flutter damping ratios and frequencies were determined. The air density and speed were matched for Mach = 0.86. Results of this analysis are shown in Figure 102, which illustrates the effectiveness of the FMC system in controlling the flutter modes by increasing the critical speed at which neutral stability occurs.

Both the inboard and outboard wing flutter modes exhibit much higher damping values for speeds higher than 150 m/s (291 kn) and 200 m/s (389 kn). For the FMC system off, the coalescence of modes is well illustrated. However, with the FMC system operating, the wing first bending frequency starts to level off for speeds higher than 150 m/s (291 kn) and increases the stability of the flutter modes. Figure 102 also indicates that the critical inboard wing flutter mode clears $1.2V_D$ with FMC on and 3% structural damping added. Credit for this level of inherent structural damping is allowed by the design flutter criteria to clear $1.2V_D$.

In the second verification, the flutter speeds, frequencies, and associated structural damping requirements were determined directly with frequency-dependent unsteady air forces. This verification was necessary for consistency with the flutter speed predictions of the Baseline and the Initial ACT Configurations to V_D without active controls. The analysis was done for altitudes of 1890m (6200 ft) and 4968m (16 300 ft), corresponding to $1.2V_D$ and V_D, with the FMC system on and off (fig. 103). The performance of the FMC system is clearly illustrated and confirms the $1.2V_D$ clearance with the 3% structural damping added.

To assess the benefits of the FMC system, a flutter study was conducted at Mach = 0.86 to determine the weight penalty of a passive fix that would extend the flutter speed from V_D to $1.2V_D$, with 3% inherent structural damping included. The studies described in Subsection 7.2.2.1 indicated that the most efficient wing-span location for adding stiffness to increase flutter speed is from 15% to 35% semispan. The analysis reported in this section follows the guidelines of the previous study. However, the wing has the added torsional stiffness (provided by the increase in spar web thicknesses) and the reserve fuel that was required for the passive fix to V_D. The analysis was limited to an evaluation of the critical symmetric flutter oscillations for the 80% fuel condition. The torsional stiffness at the selected inboard region was gradually increased to establish the trend in flutter speed improvement. A 50%

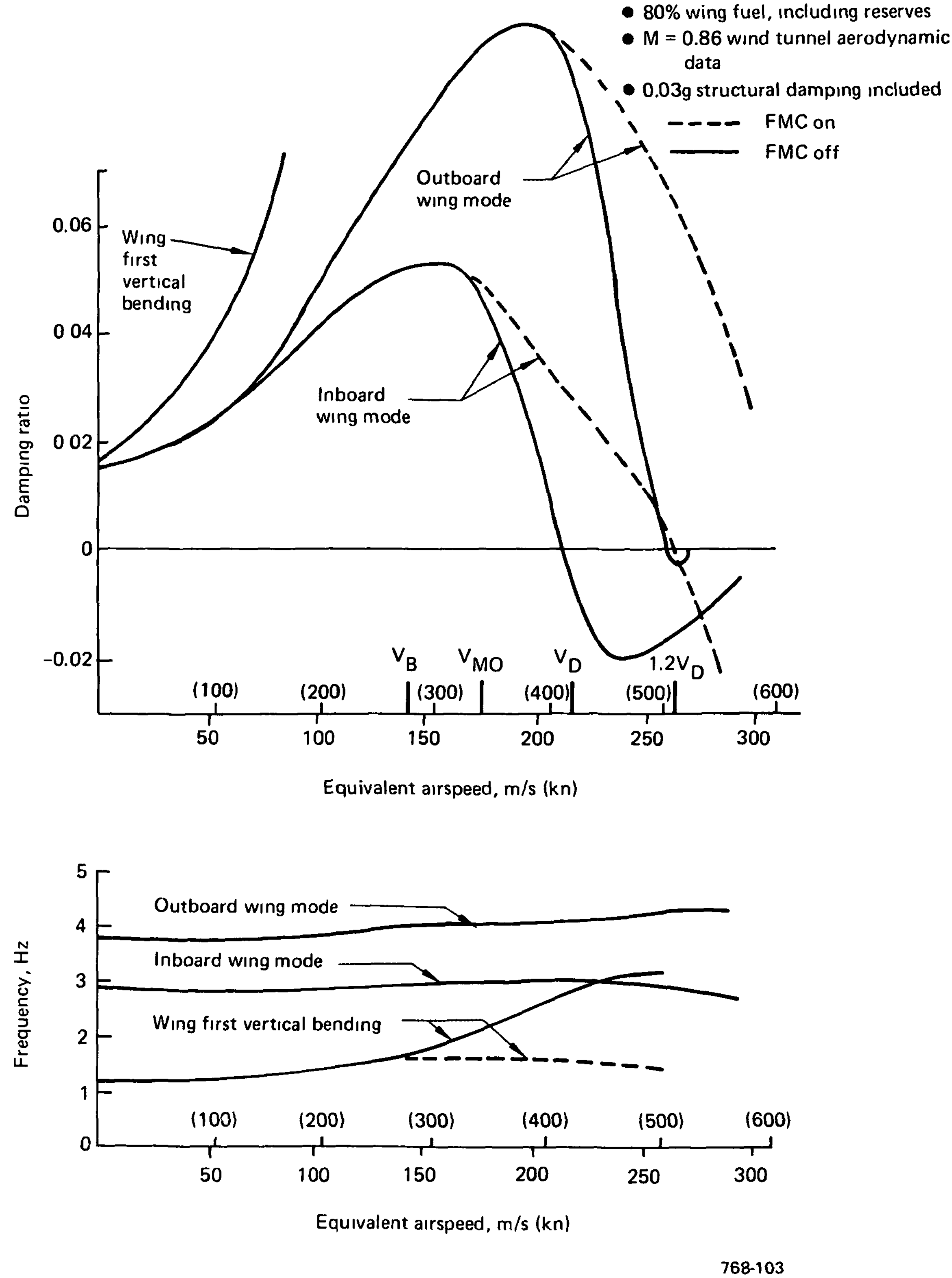

768-103

Figure 102. Symmetric Wing Flutter Modes Damping and Frequency

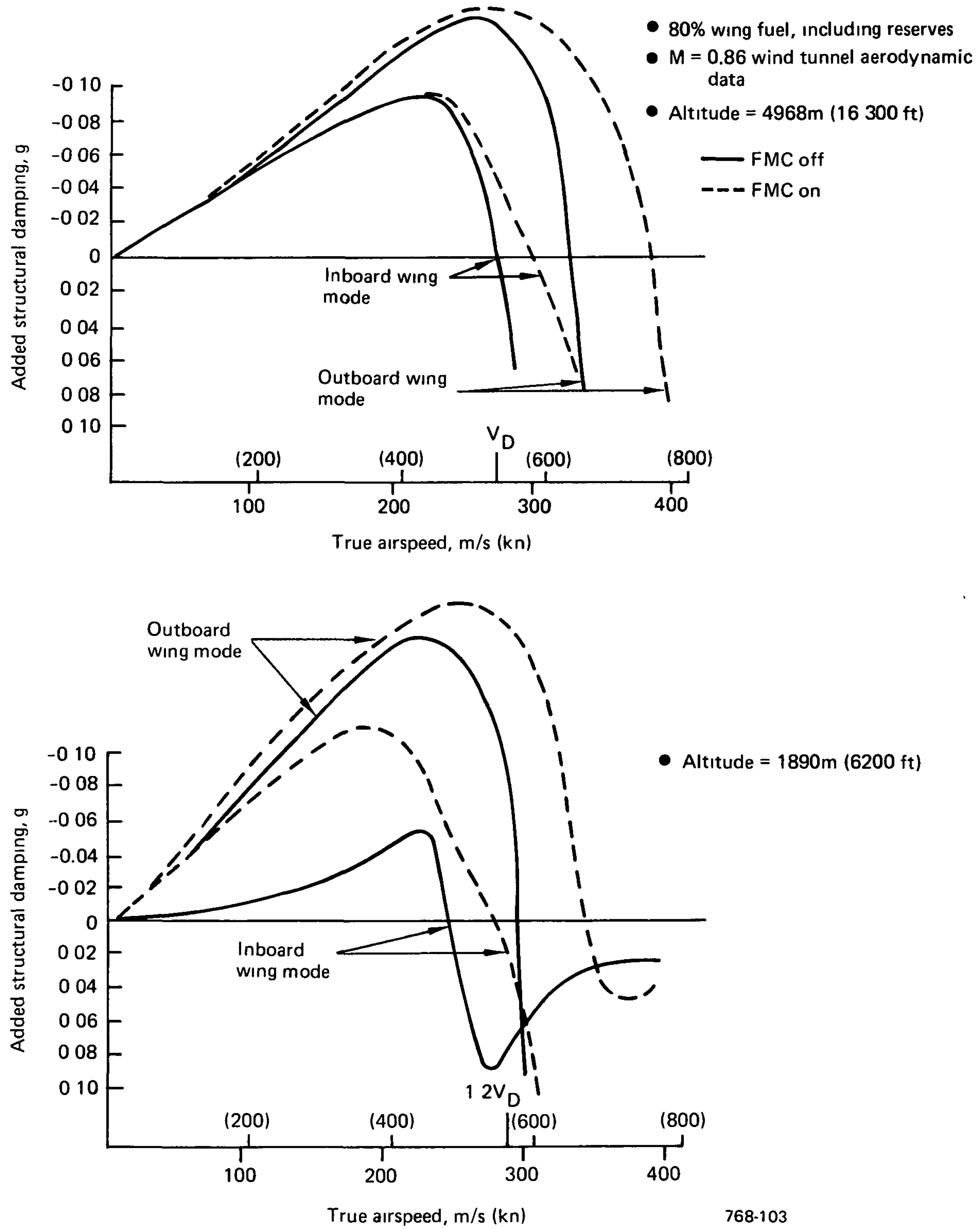

Figure 103. V-g Diagram—Symmetric Wing Flutter Modes

increase in the wing-box torsional stiffness at 25% semispan was required for flutter clearance to $1.2V_D$. The V-g diagram presented in Figure 104 shows the improved damping characteristics and the resulting increase in flutter speed. With 3% structural damping, the critical inboard wing flutter mode is stable at 1890m (6200 ft).

The matched-point flutter speeds, resulting from the flutter speed variation with altitude and the constant Mach ≈ 0.86 line, are shown in Figure 105. The matched points with no structural damping considered are shown for both the nominal stiffness and the added inboard torsional stiffness. Also shown is the variation of flutter speeds with altitude assuming 1% and 2% structural damping. In conjunction with at least 2% structural damping, the passive fix considered, clearly would provide flutter clearance to $1.2V_D$.

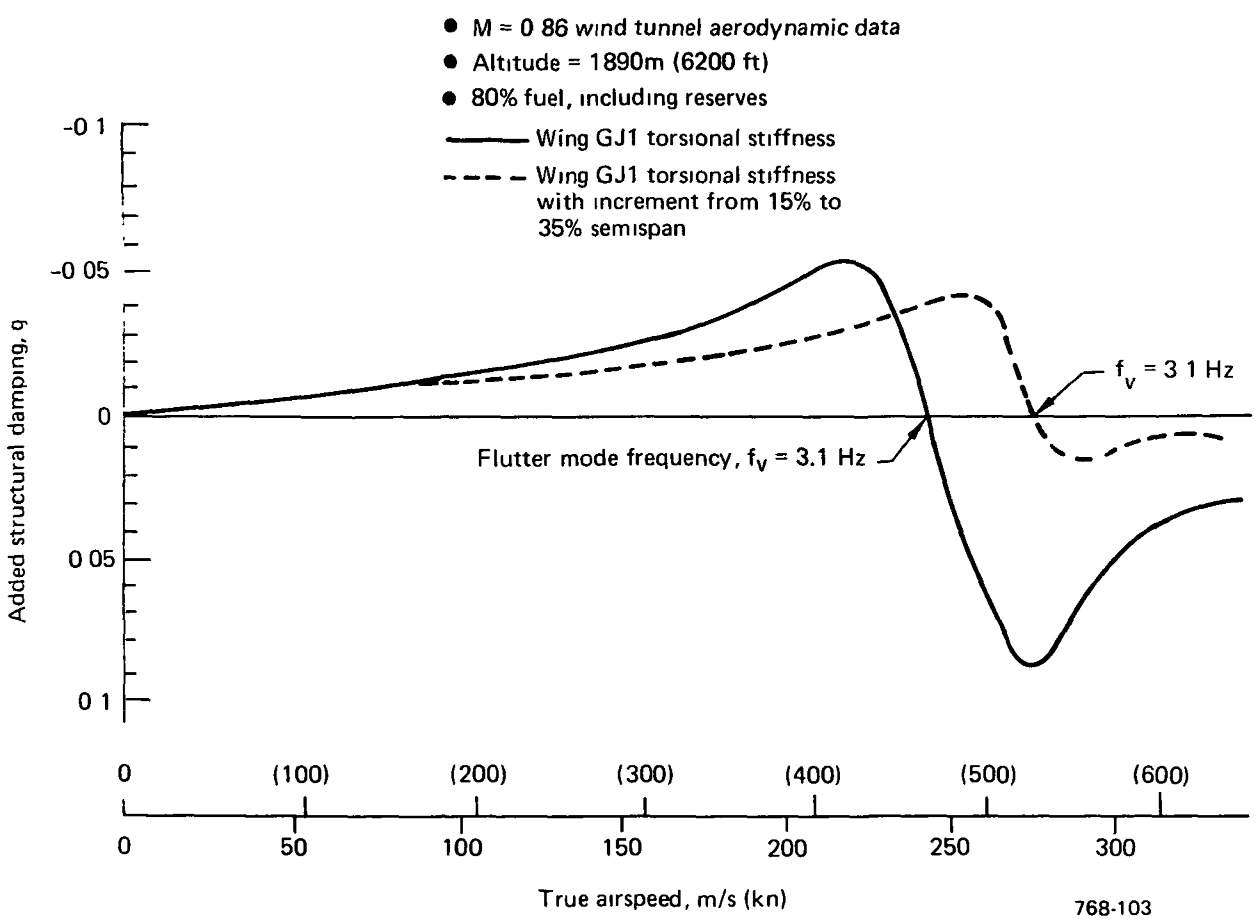

Figure 104. V-g Diagram for Symmetric Inboard Wing Mode

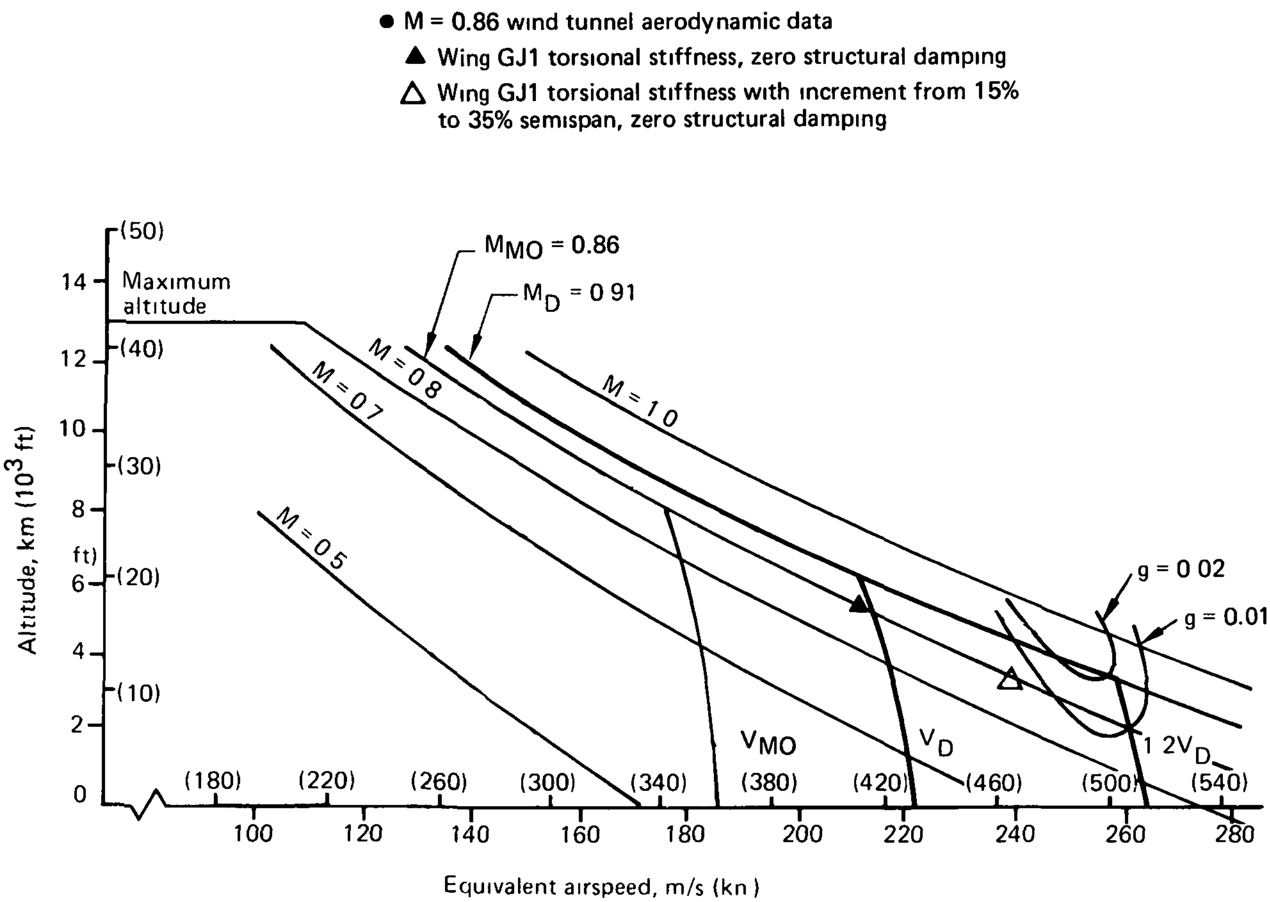

768-103

Figure 105. Symmetric Flutter Results, Inboard Wing Flutter Mode

The theoretical wing-box structural weight that provides the required stiffness increase was calculated to be 280 kg (620 lb). For this calculation the surface and spar gages were increased, at the 25% wing semispan station, to provide 50% increase in torsional stiffness, and were tapered to their nominal values at 15% and 35% semispan. The net weight increase, including nonoptimum structure, was calculated to be 358 kg (790 lb), which represents one measure of benefit for the FMC system.

7.2.2.3 Dynamic Gust Design

The final dynamic gust loads were calculated with the same methods described in Subsection 7.2.1.4; however, the mathematical model was updated to include the wing-mass distribution and structural stiffness needed to meet flutter requirements. The analysis includes the effect of the PAS, MLC, and GLA systems. These systems were derived using the dynamic model of the airplane as discussed in Subsection 7.3.1 and are illustrated in the functional block diagram (shown in fig. 132). The mathematical model for gust analysis incorporates all applicable portions of the dynamic model affecting vertical translation and pitch.

In Figure 106, the wing-design bending moment envelope from static maneuver and FAR gust formula conditions is compared with the bending moment envelope from continuous turbulence conditions. Loads from continuous turbulence are not critical for inboard wing strength design; however, they do design outboard wing structure. The combined active controls systems for PAS, MLC, and GLA are effective in

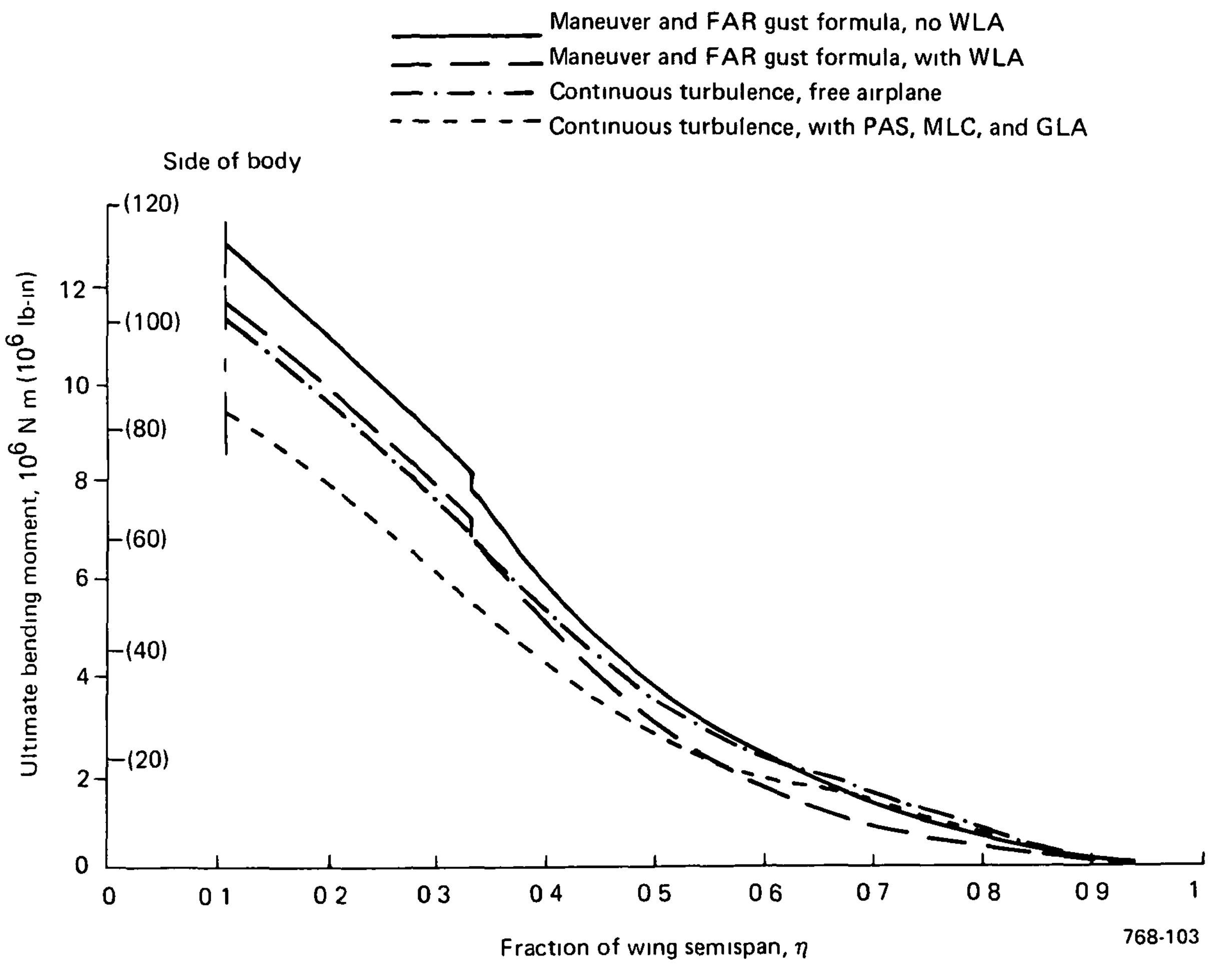

Figure 106. Wing Bending Moment Envelope

reducing the dynamic gust wing loads. However, the reduction in the dynamic gust loads is small in the outboard wing area compared to the reduction in static maneuver and gust formula loads.

A major portion of the reduction in the dynamic gust wing loads is due to the effects of the PAS on the airplane short-period longitudinal response. Figure 107 compares the reductions in wing bending moment from PAS and from the combined PAS, MLC, and GLA systems.

The power spectrum of wing bending moment at three wing analysis stations is shown in Figures 108 through 110. The large peak at 0.4 Hz corresponds to the airplane

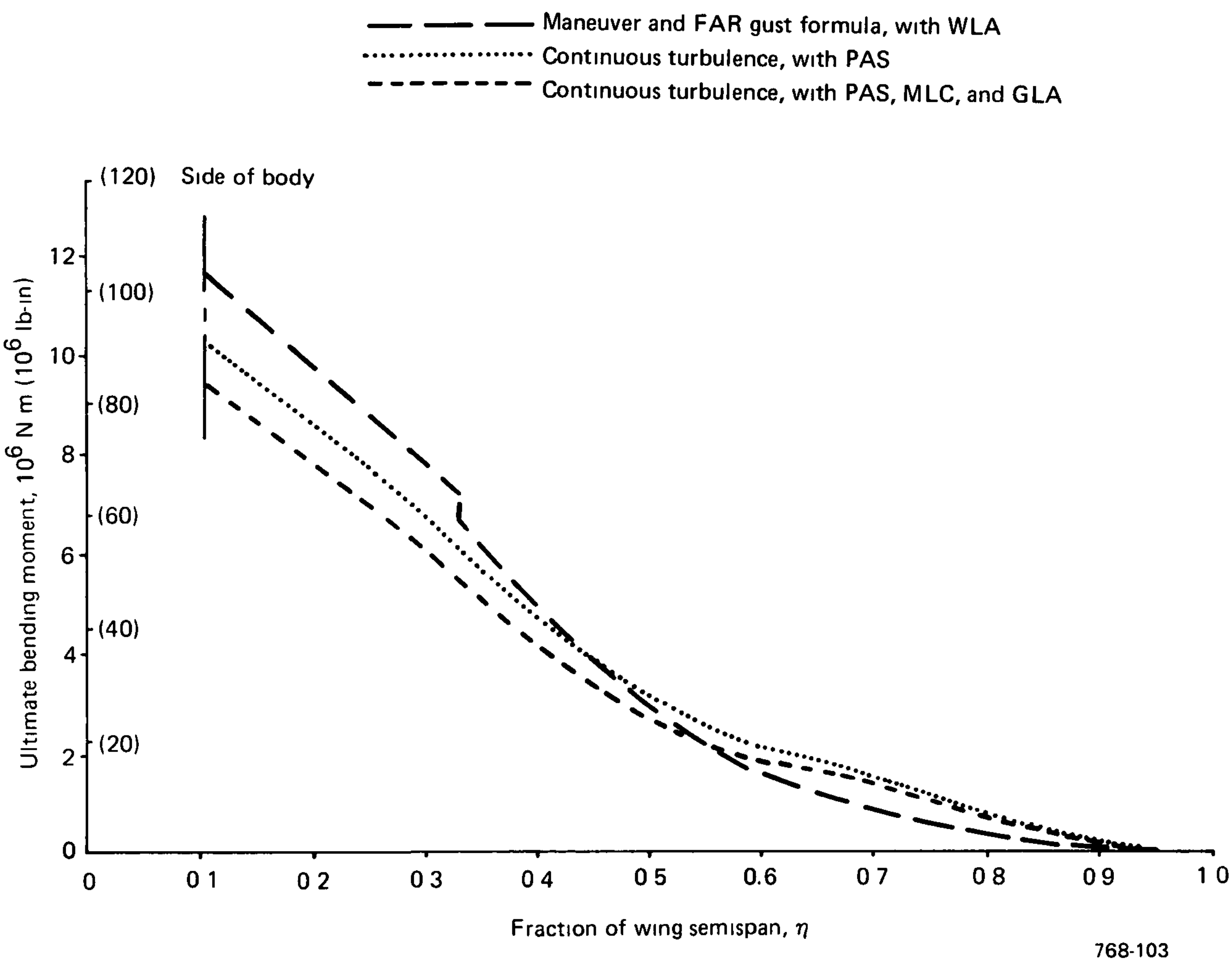

Figure 107. Effects of PAS, MLC, and GLA on Wing Bending Moment

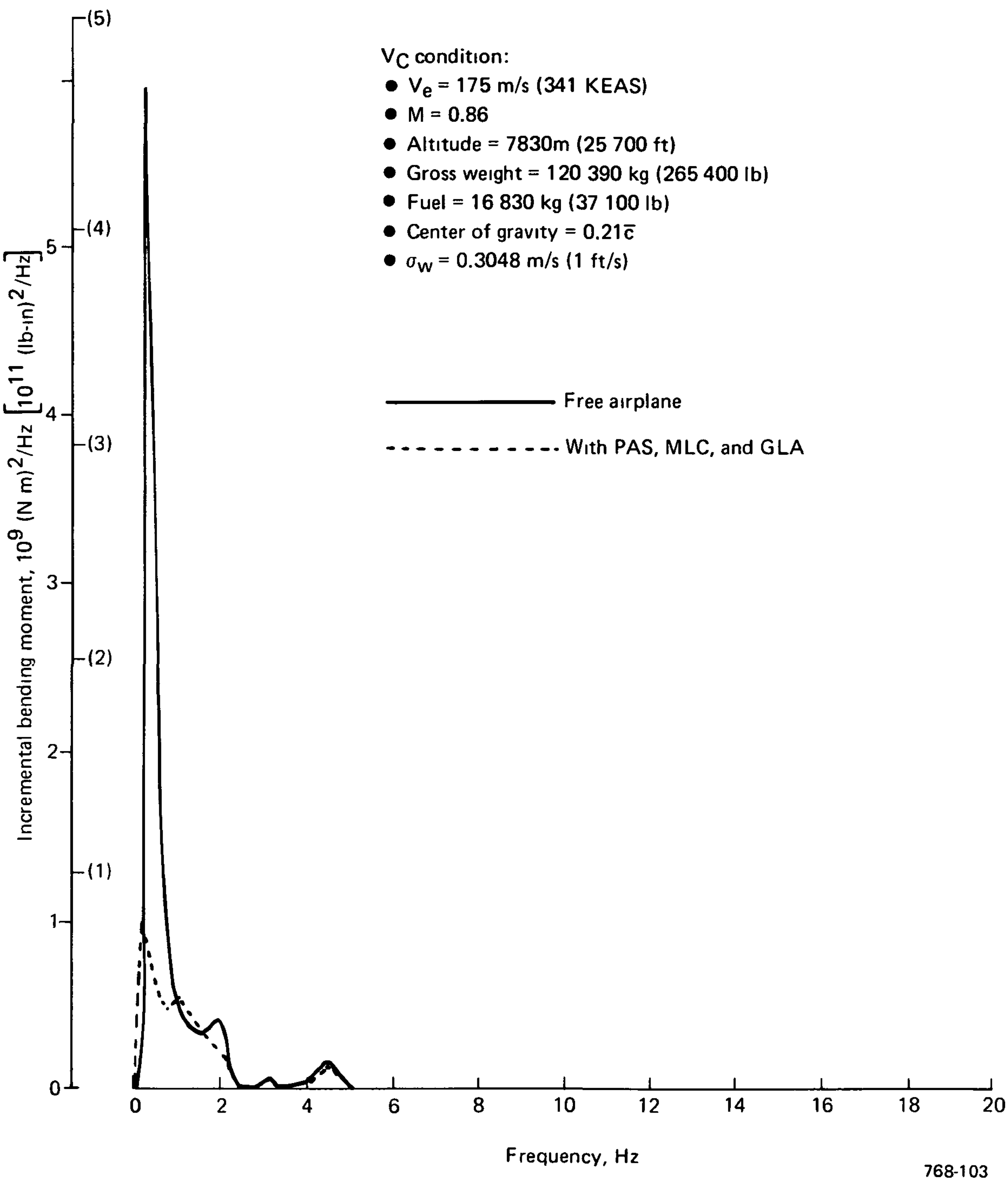

Figure 108 Bending Moment Spectrum at $\eta = 0.15$

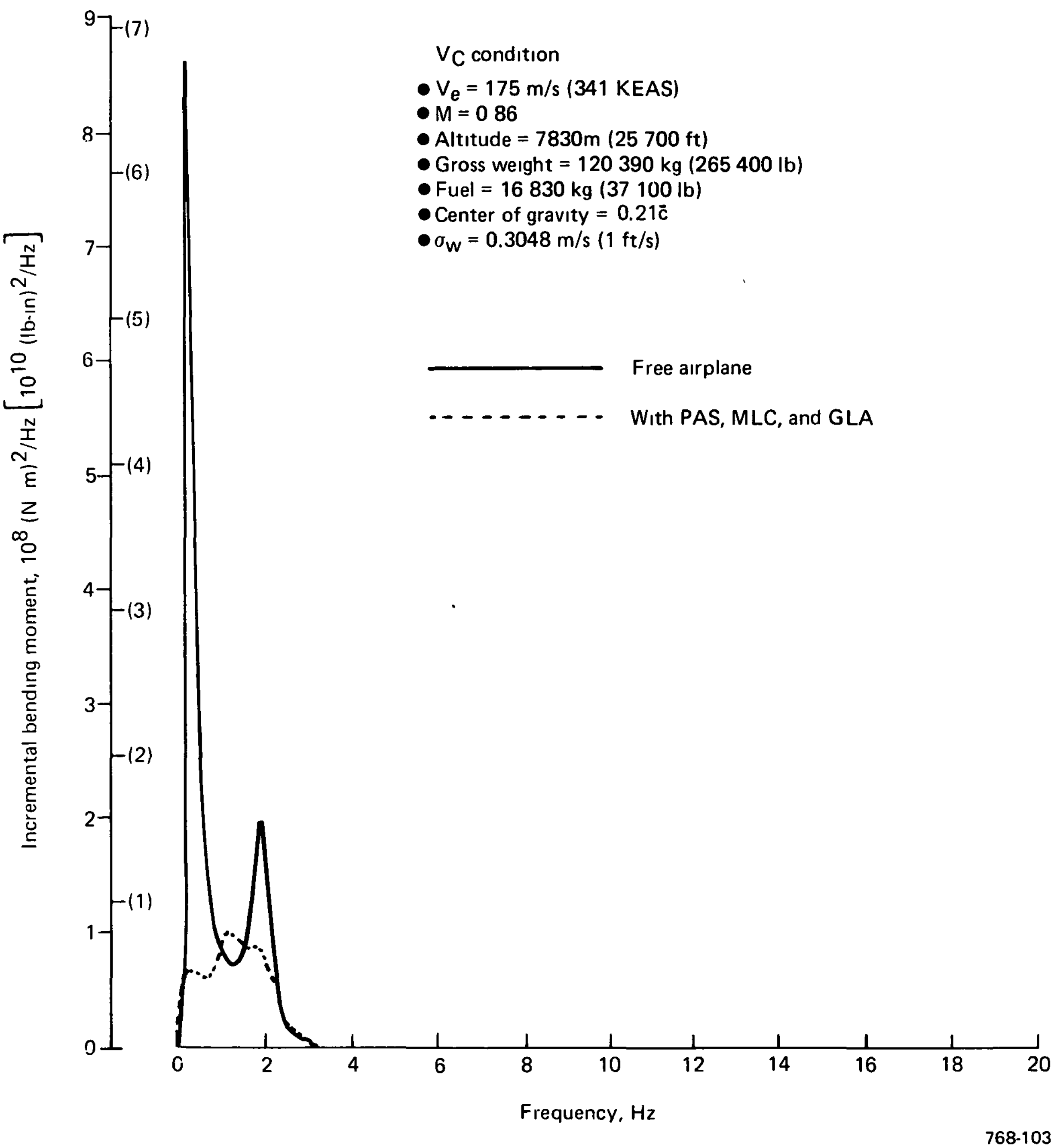

Figure 109. Bending Moment Spectrum at η = 0.45

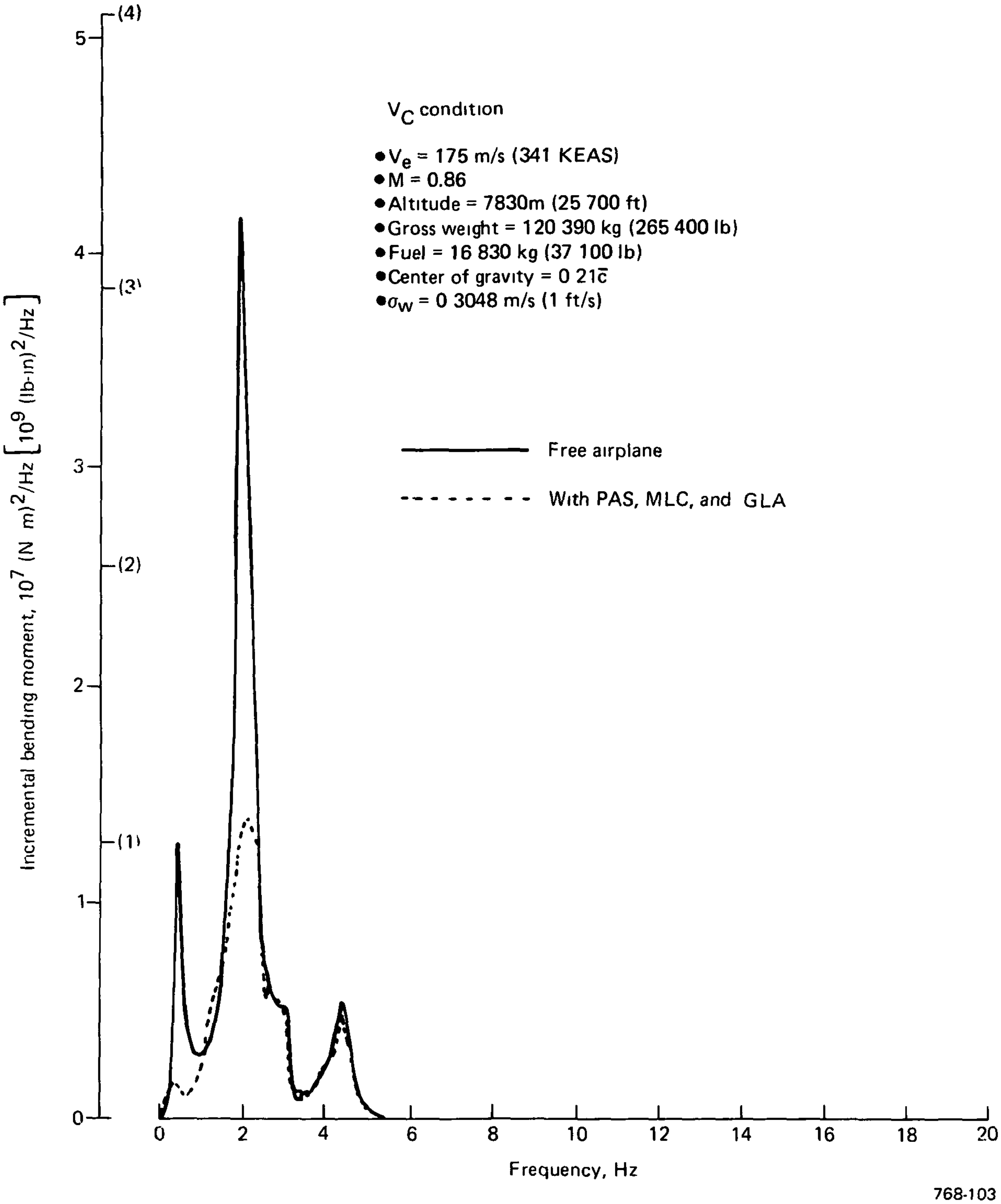

Figure 110. Bending Moment Spectrum at η = 0.75

short-period mode. The reduction in the short-period and elastic mode contribution with PAS, MLC, and GLA is evident.

Critical conditions in continuous turbulence occurred at maximum flight gross weight and forward cg. For the inboard wing, the gust penetration speed (V_B) is critical; Mach = 0.86 at 10 670m (35 000 ft) altitude. For the outboard wing, cruise speed (V_C) is critical; Mach = 0.86 at 7830m (25 700 ft) altitude.

The fatigue analysis described in Subsection 7.2.1.3 indicates a requirement to lower the alternating axial stresses in the inboard wing lower surface resulting from positive and negative gusts in continuous turbulence. Most fatigue damage due to gust occurs during cruise.

A dynamic gust analysis was conducted for a representative cruise flight condition with the PAS, MLC, and GLA systems on and off. The flight condition parameters are shown in Table 15. The gust response factors, $\bar{A}$, and the characteristic frequencies, N_0, from the power spectral density analyses were used to calculate the incremental wing bending moment exceedance curves shown in Figures 111 through 115. Results are shown only for the critical wing analysis stations. The incremental bending moments corresponding to a once-per-flight exceedance were read from the curves and used to calculate the reduction in bending moment due to the PAS, MLC, and GLA systems (table 16).

Table 15. Cruise Condition for Fatigue Analysis

Altitude = 7620m (25 000 ft)	Gross weight = 103 990 kg (229 250 lb)
Mach = 0 84	Fuel = 7600 kg (16 750 lb)
V_e = 174 m/s (388 KEAS)	Center of gravity = $0.30\bar{c}$
	Segment length = 332 km (179 nmi)

768-103

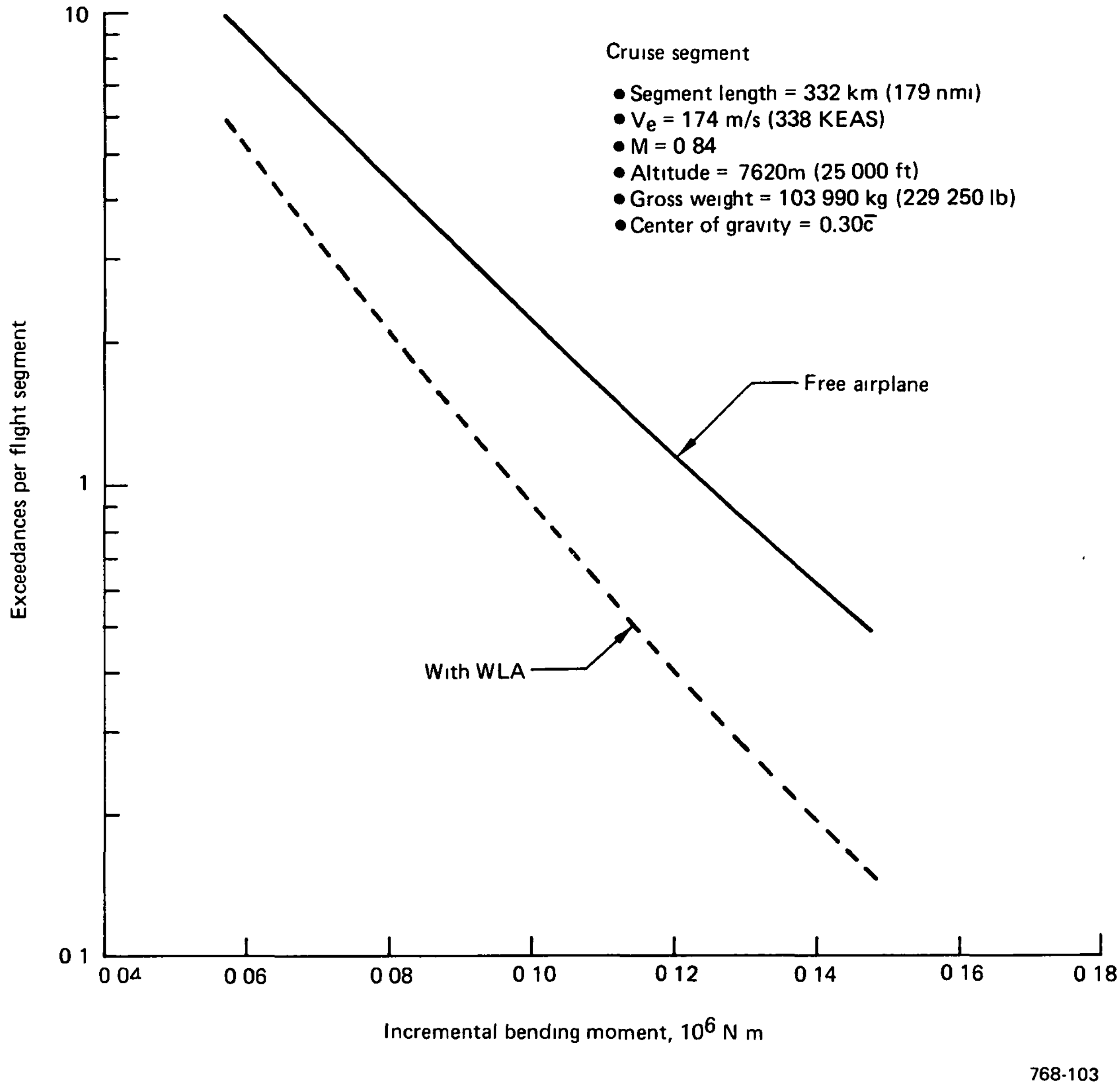

Figure 111. Wing Bending Moment Exceedance for η = 0.65

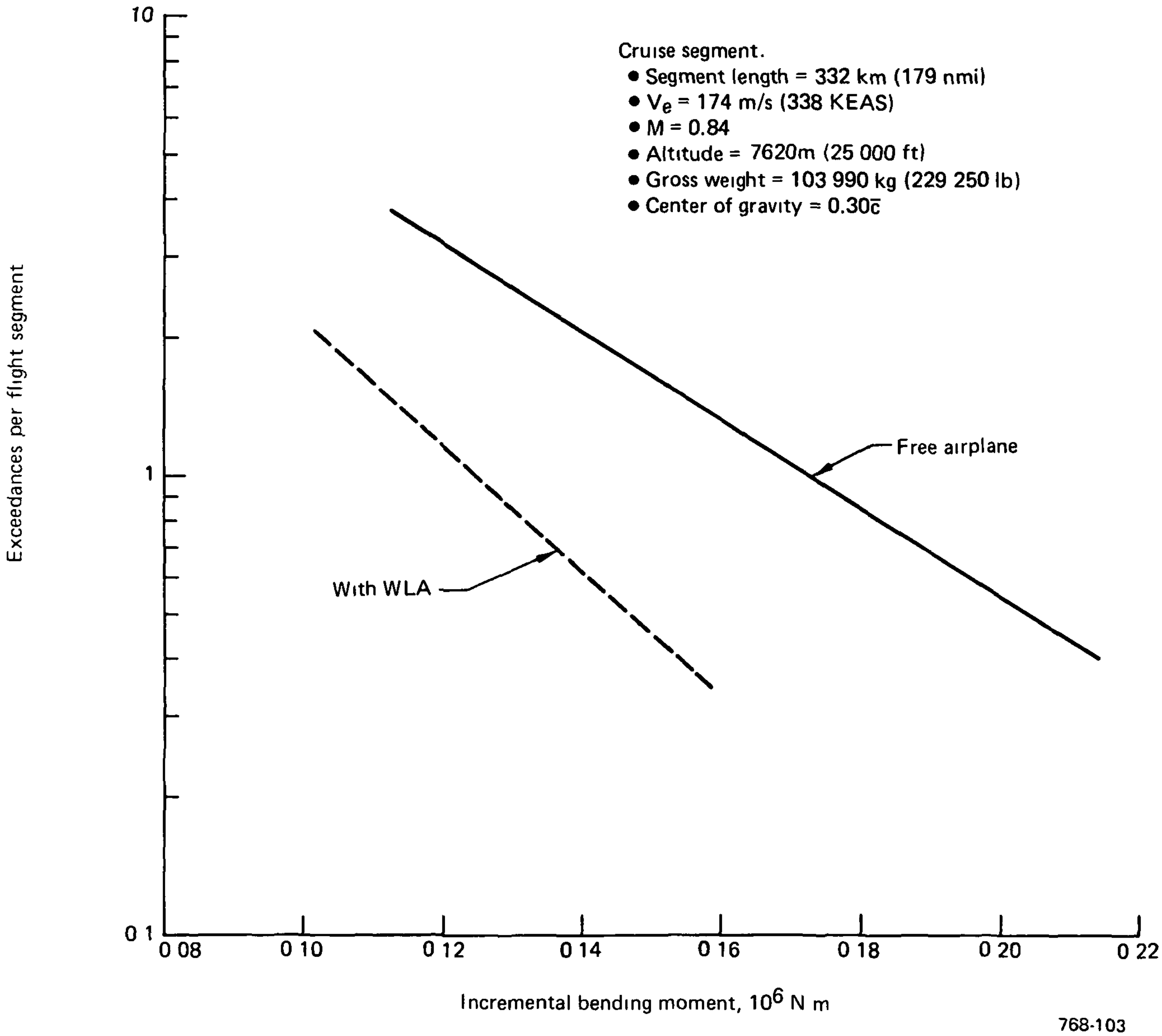

Figure 112. Wing Bending Moment Exceedance for η = 0.55

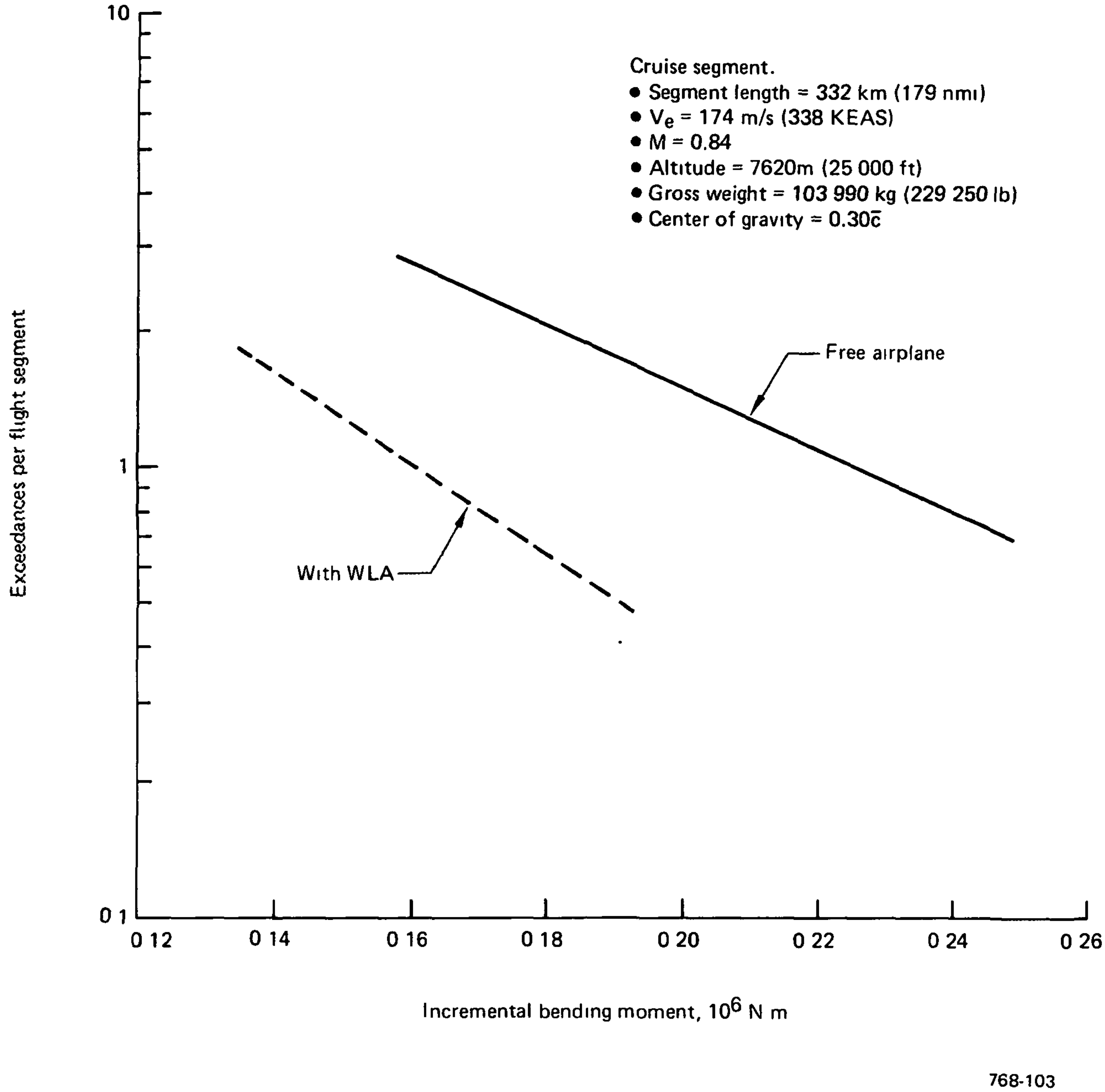

Figure 113. Wing Bending Moment Exceedance for η = 0 45

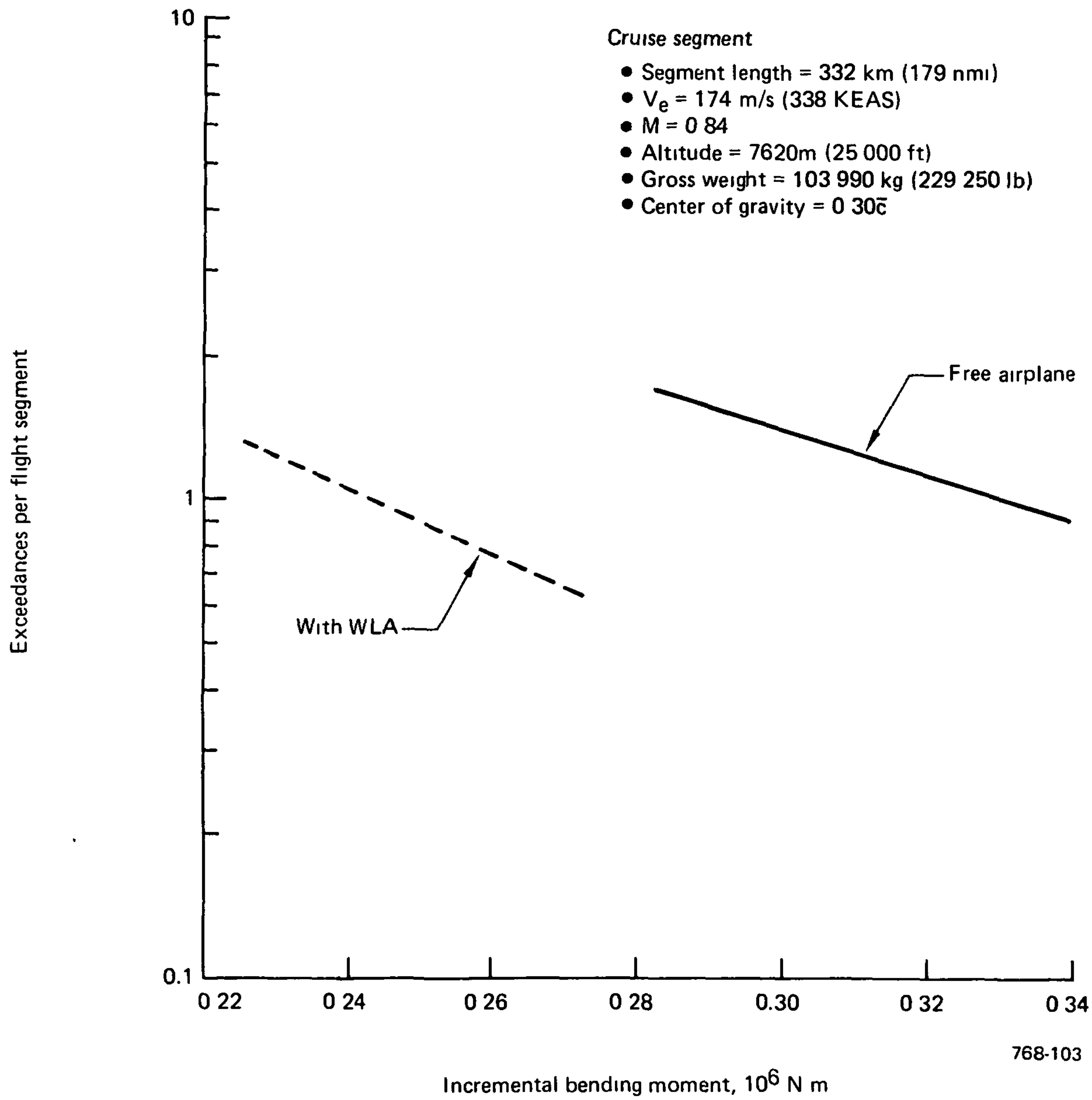

Figure 114. Wing Bending Moment Exceedance for η = 0.35

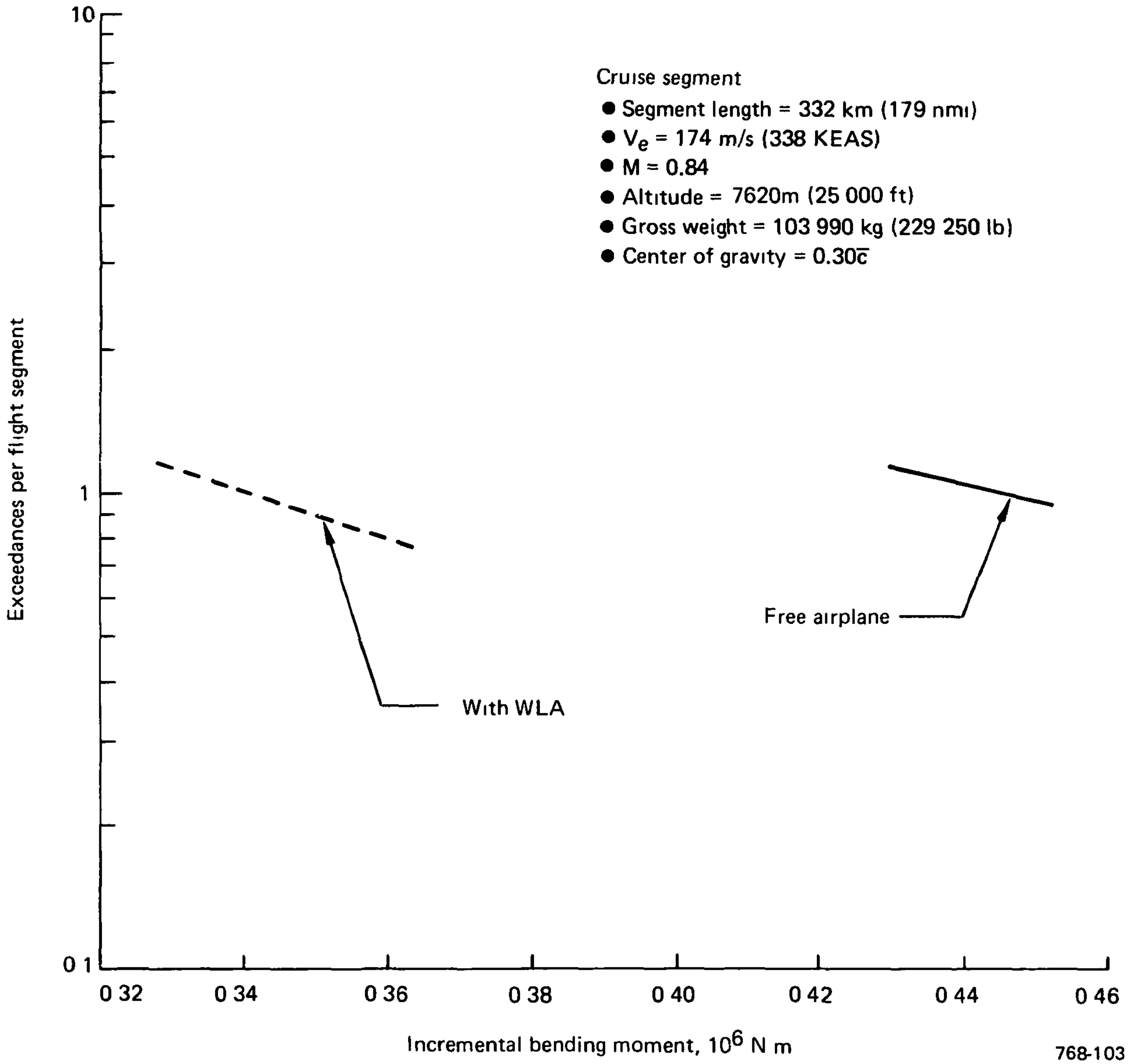

Figure 115. Wing Bending Moment Exceedance for η = 0.25

Table 16. Bending Moment Reduction Summary

Wing η station	Δ bending moment, 10^6 N m (10^6 lb-in)		Percent change in incremental bending moment	Bending moment at 1g, 10^6 N·m (10^6 lb-in)	Total bending moment, 10^6 N·m (10^6 lb-in)		Percent change in total bending moment
	WLA off	WLA on			WLA off	WLA on	
0 65	0 125 (1 11)	0 097 (0 86)	-23	0 354 (3 131)	0 479 (4 24)	0 451 (3 99)	-6
0 55	0 171 (1 51)	0 124 (1 10)	-27	0 659 (5 831)	0.830 (7 34)	0 783 (6 93)	-6
0 45	0 226 (2 00)	0 161 (1 42)	-29	1 100 (9.740)	1 326 (11 74)	1 261 (11 16)	-5
0 35	0 330 (2 92)	0 243 (2 15)	-26	1 721 (15 235)	2 051 (18 16)	1 964 (17 38)	-4
0 25	0 445 (3 94)	0 341 (3 02)	-23	2 413 (21 354)	2 858 (25 29)	2 754 (24 37)	-4

Note At cruise condition described in Table 15

768-103

The active PAS, MLC, and GLA systems reduced the incremental bending moments due to gusts from 23% to 29% and the total bending moments (1g + gust) from 4% to 6%. The reduction in axial stress in the wing-box surface was assumed to be the same as the reduction in the bending moment load. The final load reductions for maneuvers and gusts used for the fatigue analysis are shown in Figure 116. These load reductions were used to evaluate fatigue damage, systems on, in Subsection 7.2.2.4.

7.2.2.4 Fatigue Design

The final fatigue analysis was conducted to verify the fatigue design requirements for the critical wing-box lower surface. The alternating stresses from flight maneuvers and gust were reduced by the relieving effects of the selected ACT systems. The reduction in alternating stress, in turn, reduced the GAG peak stresses.

The wing spars and upper surface had large fatigue margins of safety in the initial fatigue analysis (subsec 7.2.1.3) and, therefore, were not considered in the final fatigue analysis.

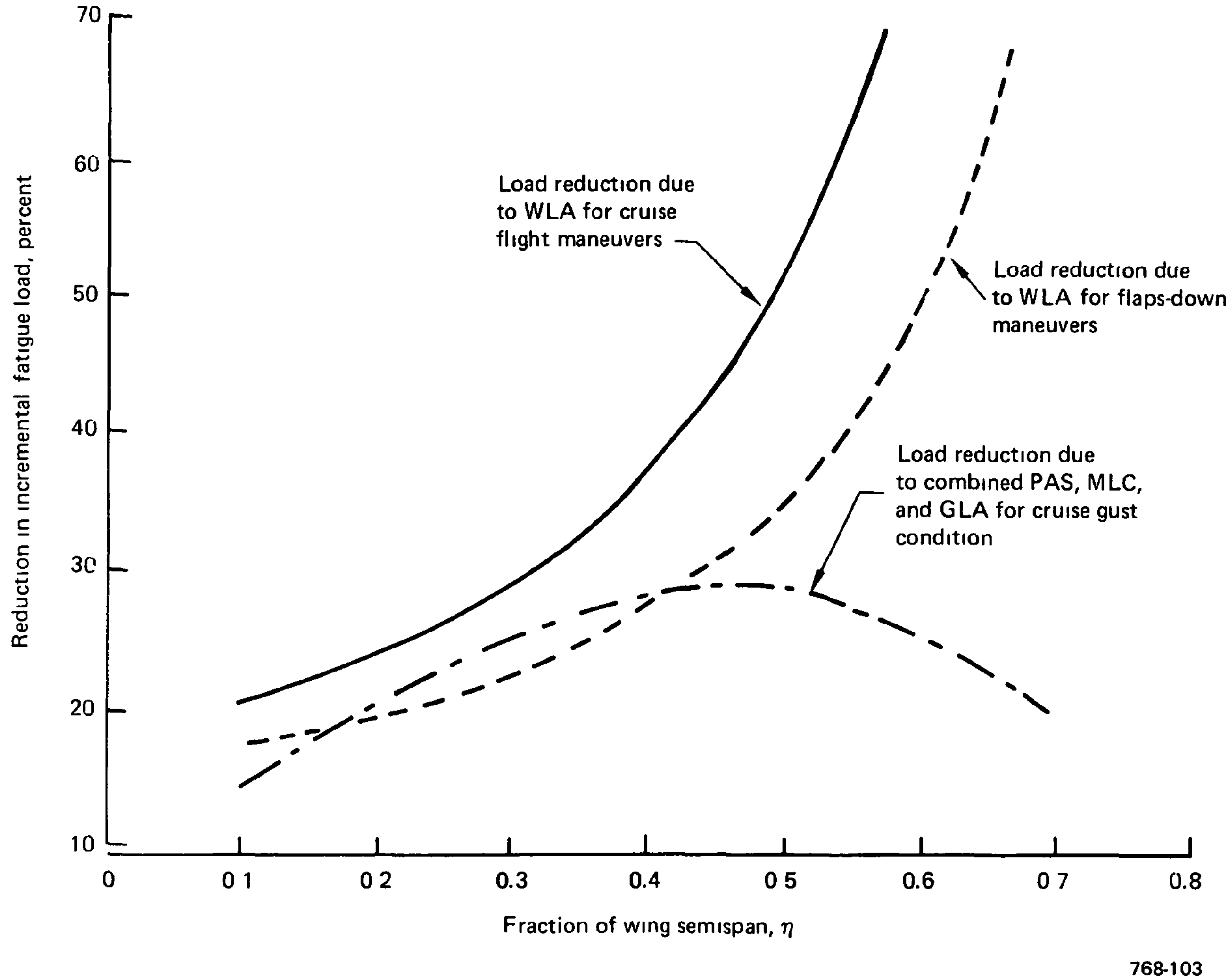

Figure 116. Fatigue Load Reduction due to Selected ACT Functions

The fatigue analysis method used for Boeing's production airplane programs was used to analyze the Baseline and Initial ACT Configurations. The method correlates well with operational experience and therefore provides credibility consistent with the state of the art. With this method, the fatigue load spectrum is represented by a specified number of "equivalent" maneuvers and gusts, and the fatigue stress spectrum and damage are represented by an equivalent set of GAG stress cycles and corresponding damage ratio.

For the Initial ACT Configuration, factors were developed to modify the fatigue stress profile for the unaugmented airplane to account for the effects of the selected ACT systems. For gust conditions, the factors were based on a power spectral density (PSD) analysis of airplane response with the PAS, MLC, and GLA systems on and off as shown in Subsection 7.2.2.3, "Dynamic Gust Design." For maneuver conditions, the fatigue stress reduction factors were based on the ratio of the incremental bending moments for ($\Delta n_z = 0.3g$) maneuvers, WLA system on to WLA system off. The resulting fatigue load reductions for maneuvers and gust are shown in Figure 116.

The results of the fatigue analysis are summarized in Figure 117. The small negative margins of safety at $\eta = 0.35$ (-0.01) and $\eta = 0.45$ (-0.02) theoretically require up to 2% increase in bending material at these stations. However, for the purposes of weight assessment it was assumed that this was close to the machining tolerance of a practical wing skin and that improvements in the selected ACT systems would probably provide the required positive margins. For evaluating the Initial ACT Configuration it was assumed, therefore, that no structural material was needed to satisfy life goal requirements.

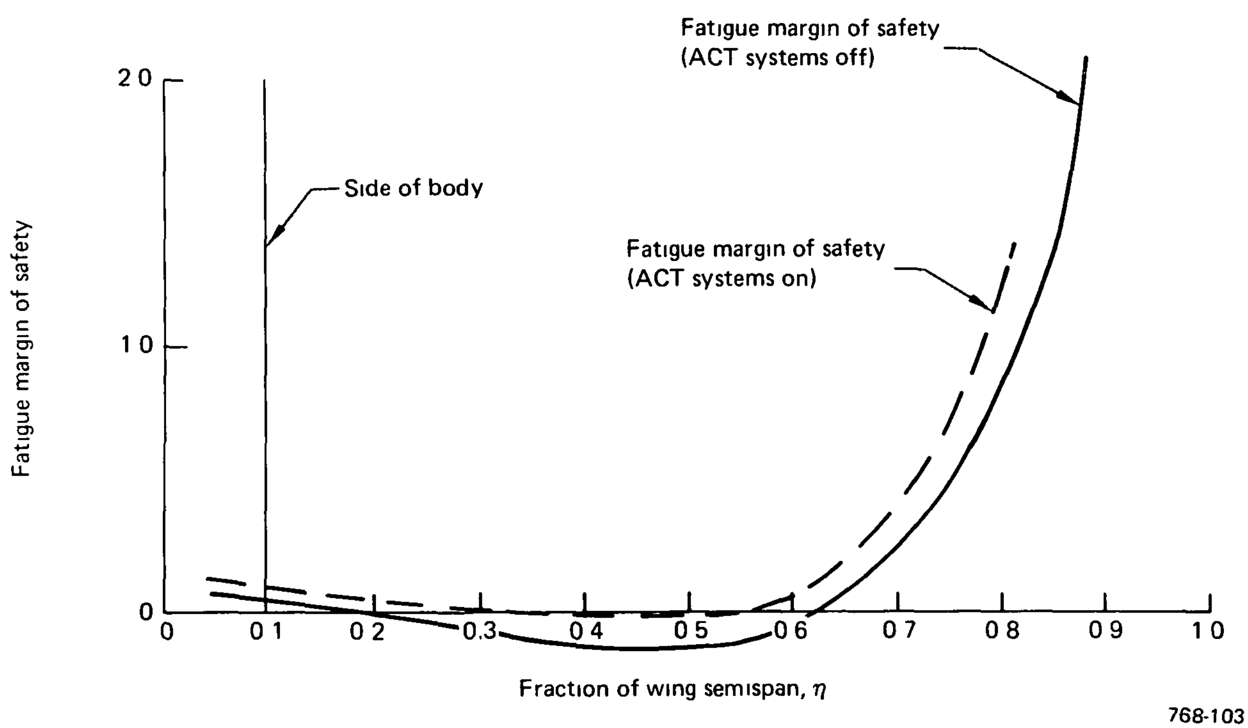

Figure 117. Initial ACT Airplane Minimum Fatigue Margins of Safety (Wing Lower Surface)

7.2.2.5 Final Wing Structural Sizing

This section summarizes the wing-box structural sizing requirements and highlights the structural benefits associated with the selected active controls functions. The ACT systems were not optimized; consequently, the results represent feasibility and order of magnitude levels. In addition, the mathematical models in the analyses did not benefit from final design data associated with production drawing release, static tests, vibration tests, etc. However, for the Initial ACT study, the potential benefits of ACT were adequately evaluated by conducting sensitivity studies on significant analysis parameters such as aileron aerodynamic effectiveness and body and nacelle structural frequencies. Additional experimental data such as wind tunnel pressure and flutter model test results would be required to further increase technical confidence in the evaluation of selected ACT functions.

The wing-box theoretical structural material that satisfied all basic structural requirements can be expressed in terms of the cross-sectional area perpendicular to the load reference axis (fig. 118). The effect of individual ACT functions on the wing-box structural requirements is shown in Figures 119 and 120.

The selected ACT functions were effective in reducing the structural material requirements for strength in the upper and lower surfaces due to static maneuver and FAR gust formula conditions. However, the effect on spar web material was negligible for the purposes of this study. The lower inboard surface was fatigue critical. Consequently, the initial WLA system was extended to provide fatigue load reduction by eliminating a dead zone in the control surface response at low load factors ($\Delta n_z = \pm 0.5g$) and by implementing a GLA system to further reduce gust loads due to continuous turbulence. The alternating fatigue stresses due to maneuvers and gusts were effectively reduced by the combined systems with the result that no structural material was required for fatigue. The combined PAS, MLC, and GLA systems were effective in reducing inboard wing loads due to continuous turbulence; however, the outboard wing loads, which were critical for design, were not significantly reduced. Additional refinements in the GLA system could probably improve the load reduction in this portion of the wing. However, the additional structural material required for strength was small, as indicated in Figure 119.

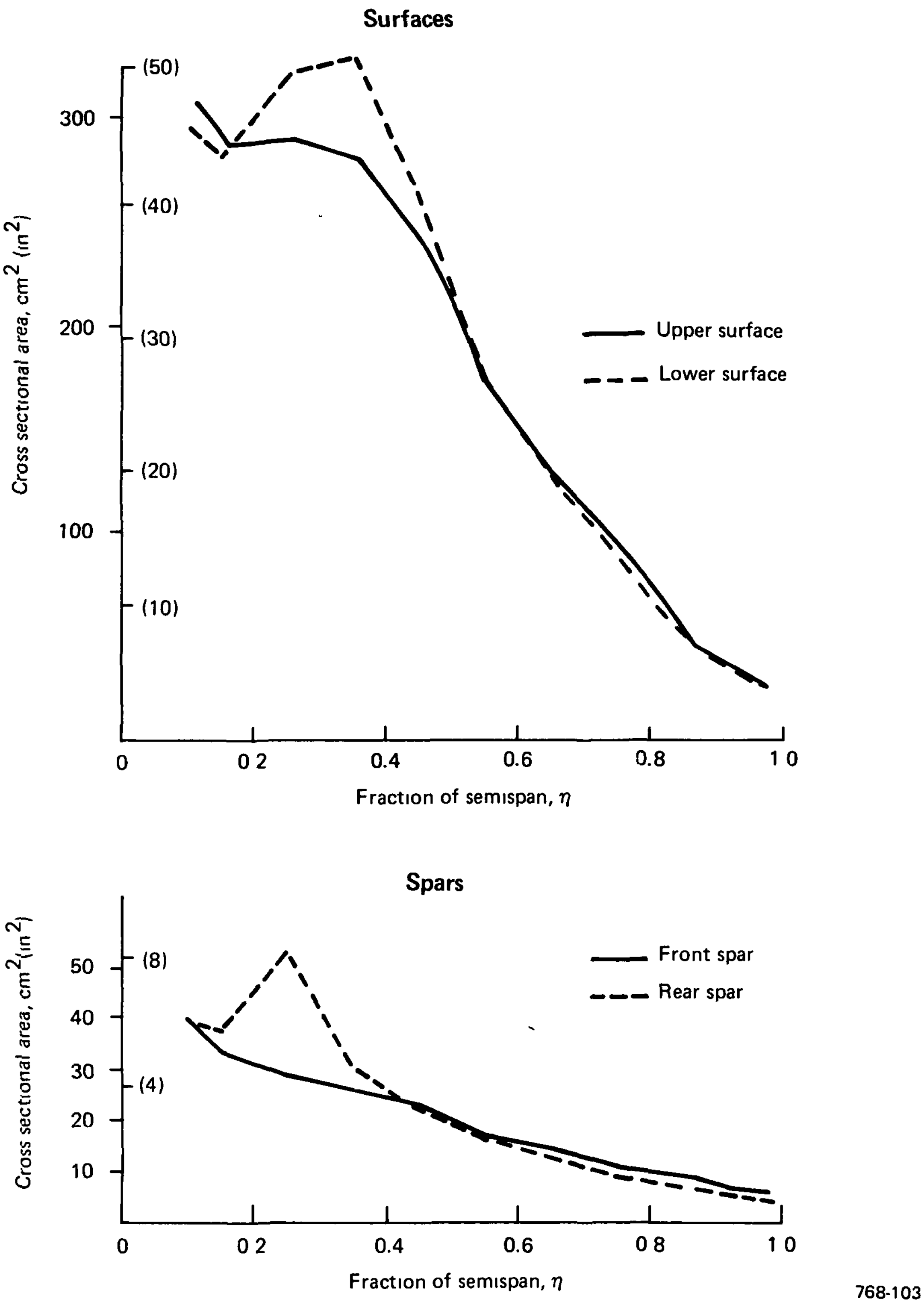

Figure 118. Final Wing-Box Structural Material Requirements, Including the Combined Effects of Selected ACT Functions

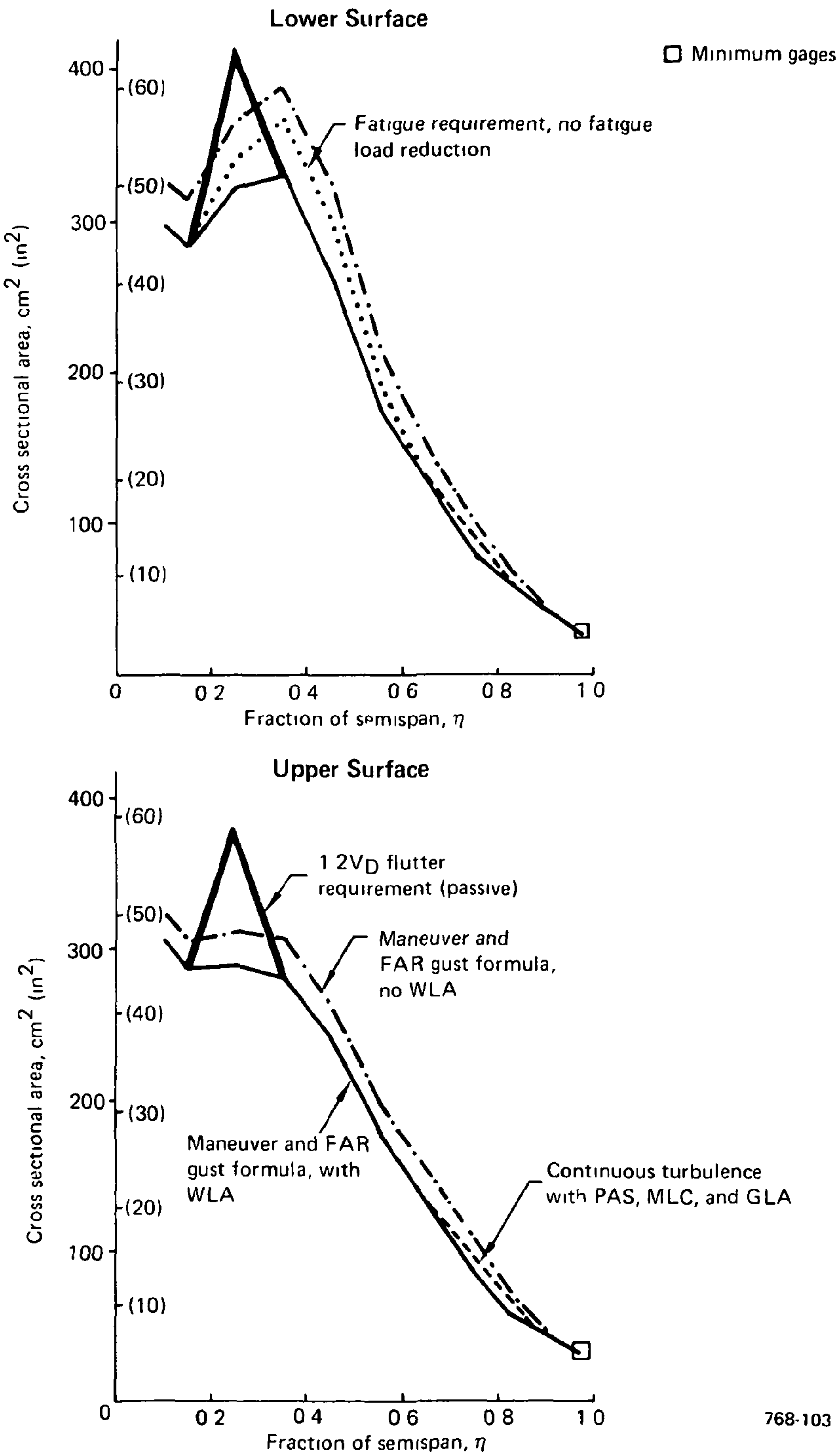

Figure 119. Effect of Individual Active Control Functions on Wing-Box Structural Material Requirements, Upper and Lower Surface

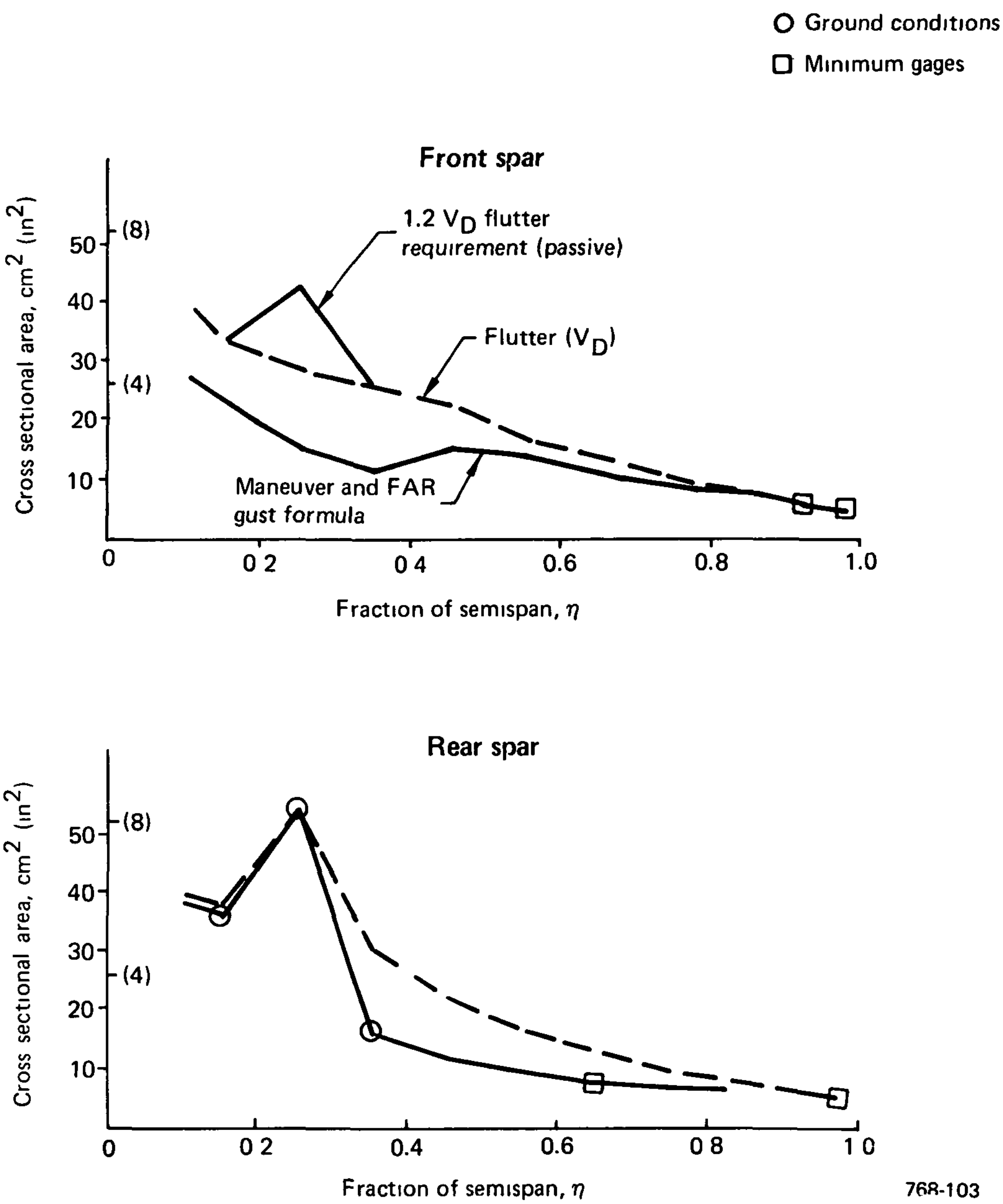

Figure 120. Effect of Individual Active Control Functions on Wing Box Structural Material Requirements, Front and Rear Spar

The flutter requirements, to V_D, were satisfied by increasing the spar web thicknesses and by adding an outboard fuel reserve tank. The flutter requirements between V_D and $1.2V_D$ were satisfied with a flutter-mode control system that was effective in providing increased stability in the critical inboard wing flutter mode. An alternative passive fix achieved by increasing the wing-box skins in the inboard wing section (η = 0.15 to 0.35) required a significant increase in structural material (fig. 119). This increase was avoided by using the FMC system.

7.2.3 HORIZONTAL TAIL

The basic objectives of the preliminary horizontal tail structural analysis were to calculate aeroelastic effects on elevator and tail aerodynamic derivatives and to assess the effects of tail load changes on aft body strength and stiffness. For these reasons, only significant design conditions were analyzed. Maximum tail loads were used for structural sizing and tail stiffness calculations. Balancing tail loads for aft body design conditions were calculated for input into the fuselage analysis.

The horizontal tail design load envelope is shown in Figure 121 and critical design conditions are listed in Table 17. The tail load differed from the Baseline Configuration primarily due to an increase in tail arm resulting from the 1.68m (66 in) forward wing shift in the Initial ACT Configuration and due to the change in stability resulting from a change in cg limits (from 9/39% MAC to 19.5/46.5% MAC).

The tail design loads for Initial ACT, with relaxed static stability, are lower than for the Baseline Configuration. However, since the horizontal tail area for the Initial ACT Configuration was reduced by 45%, the structural loading is increased from 12 200 N/m^2 (254.8 lb/ft^2) for the Baseline Configuration to 18 650 N/m^2 (389.5 lb/ft^2) for the Initial ACT Configuration. The horizontal tail stiffness is presented in Figures 122 and 123.

7.2.4 FUSELAGE

The fuselage structural assessment for the Initial ACT Configuration provided guidelines for incremental weight estimates resulting from changes in fuselage design

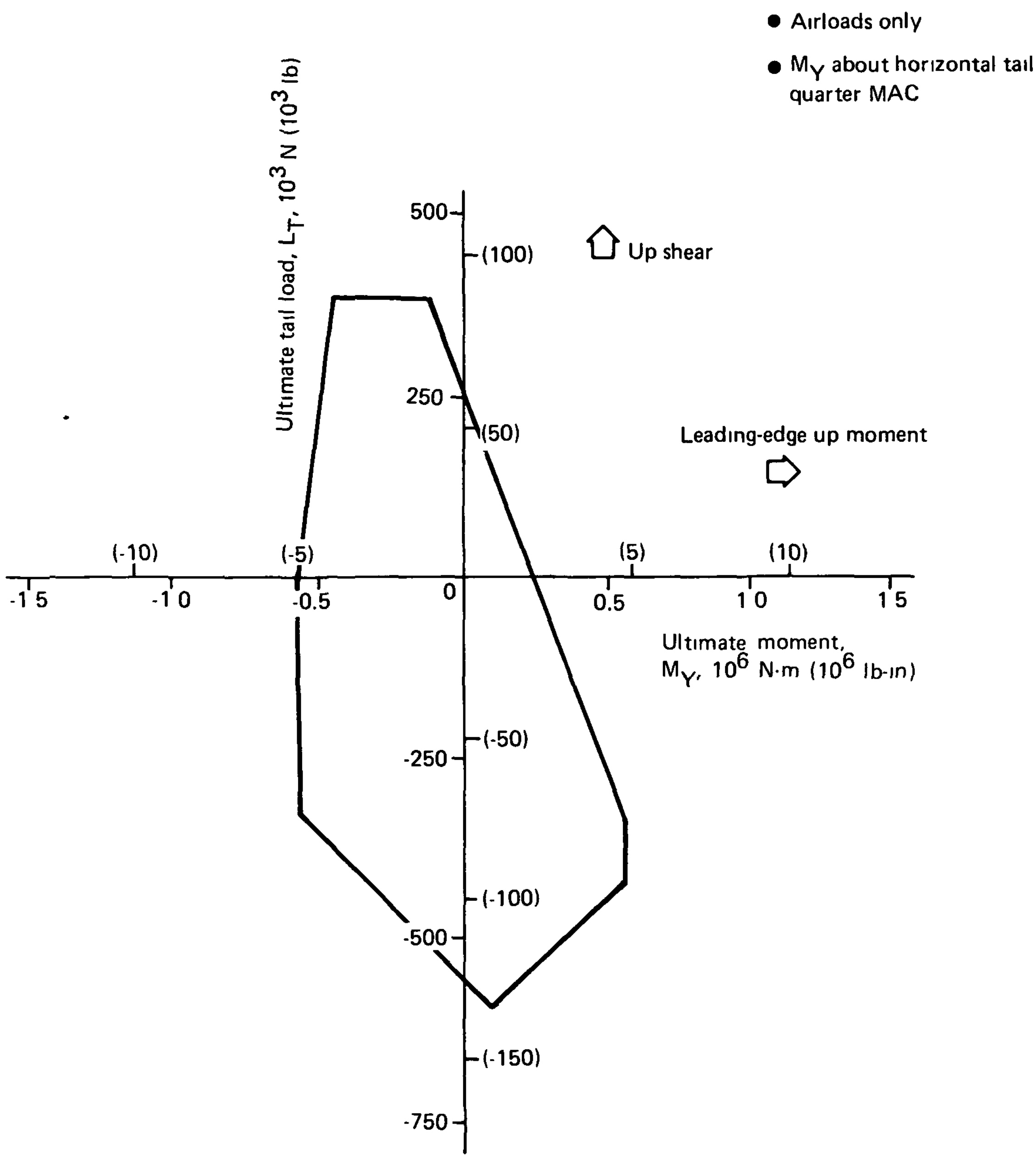

Figure 121. Horizontal Tail Design Load Envelope

Table 17. Summary of Horizontal Tail Design Loads

Condition	Direction	Altitude, m (ft)	V_e, m/s (KEAS)	Mach No	Weight, kg (kips)	cg, percent MAC	[1] n_z, g	$\ddot{\theta}$ rad/s^2
Balanced maneuver	Positive n_z	6065 (19 900)	211 (410)	0 91	119 8 (264.1)	0 09	2 5	0
	Zero n_z	6065 (19 900)	211 (410)	0.91	119 8 (264 1)	0 09	0	0
	Negative n_z	12 190 (40 000)	127 (246)	0 86	117 9 (260.0)	0 09	-1.0	0
Abrupt elevator	Up	6065 (19 900)	211 (410)	0 91	119 8 (264.1)	0.09	0 14	0 31
	Down	0 (0)	152 (295)	0 45	120.7 (266 1)	0.39	2 33	-0 51
Checkback	Positive	0 (0)	131 (255)	0.39	120 7 (266 1)	0 39	3 24	-0.28
	Negative	0 (0)	185 (360)	0.55	120.7 (266 1)	0 13	-2 5	0.54

[1] Balanced maneuver = n_z at center of gravity and $(\bar{c}/4)_{HT}$

Accelerated maneuvers = n_z at $(\bar{c}/4)_{HT}$ only

768-103

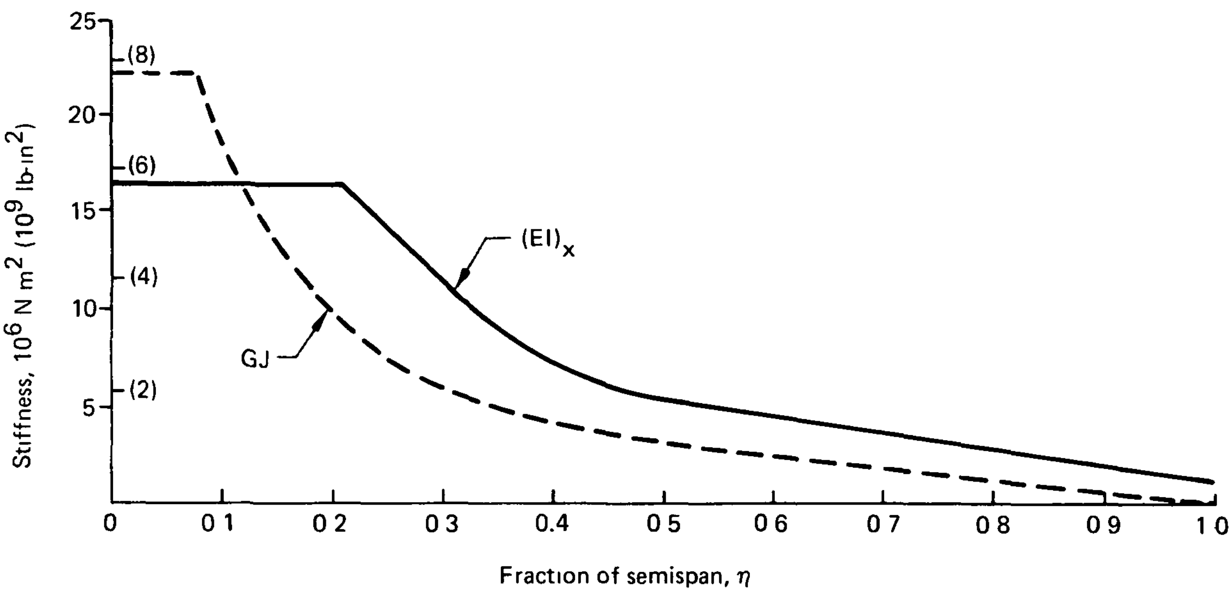

Figure 122. Horizontal Tail Stiffness

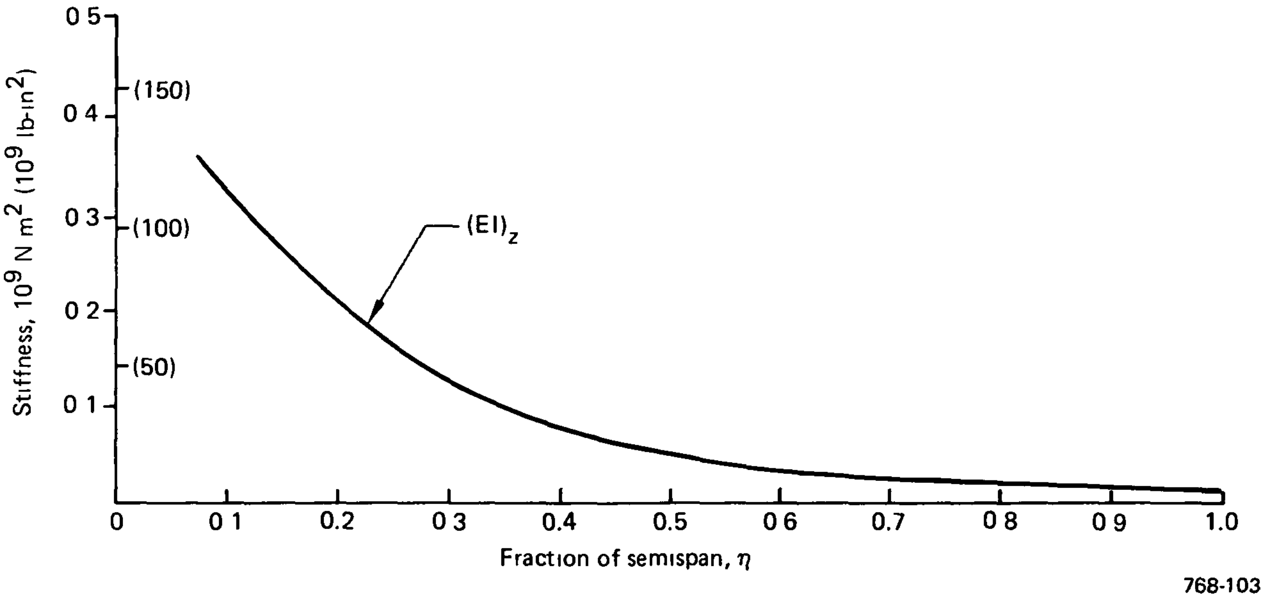

Figure 123. Horizontal Tail Stiffness in Horizontal Plane

loads and provided a basis for deriving aft body stiffnesses from the basic data for the Baseline Configuration.

The adjustment in aft body loads (fig. 124) reflects the reduced horizontal tail loads for the critical balanced maneuver and the 1.68m (66 in) forward shift of the wing. The forward body loads were adjusted only for the effects of wing shift. The resulting aft body stiffness used in the mathematical modeling of the Initial ACT Configuration is presented in Figure 125.

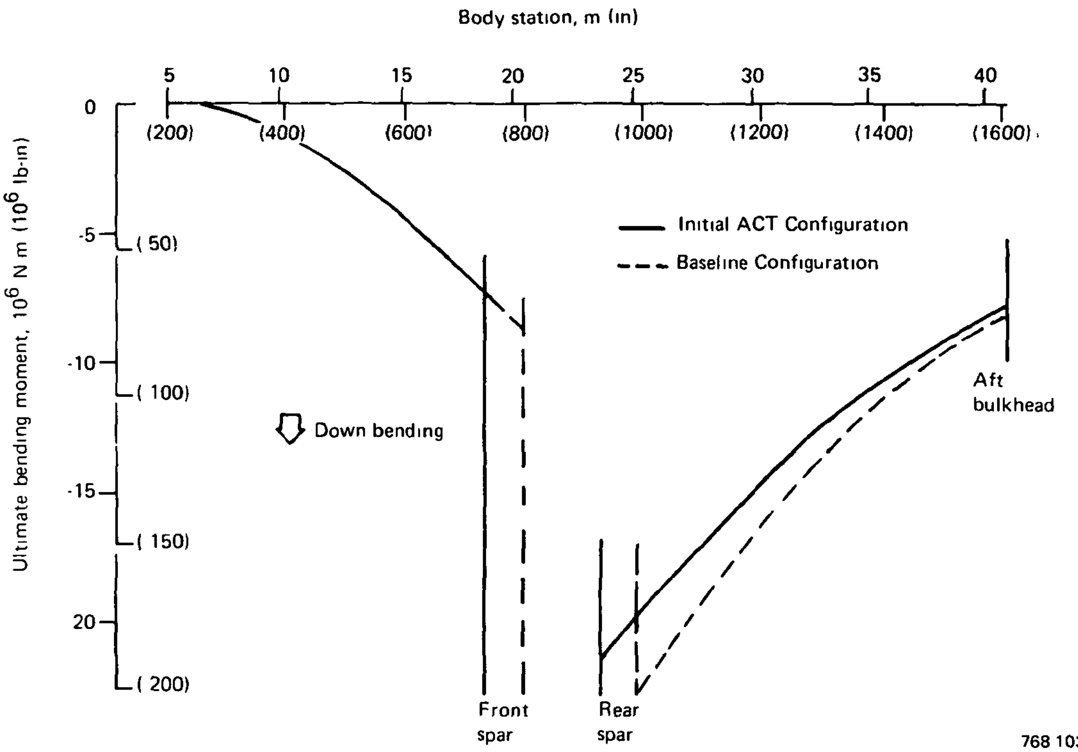

Figure 124. Aft Fuselage Design Vertical Bending Moment

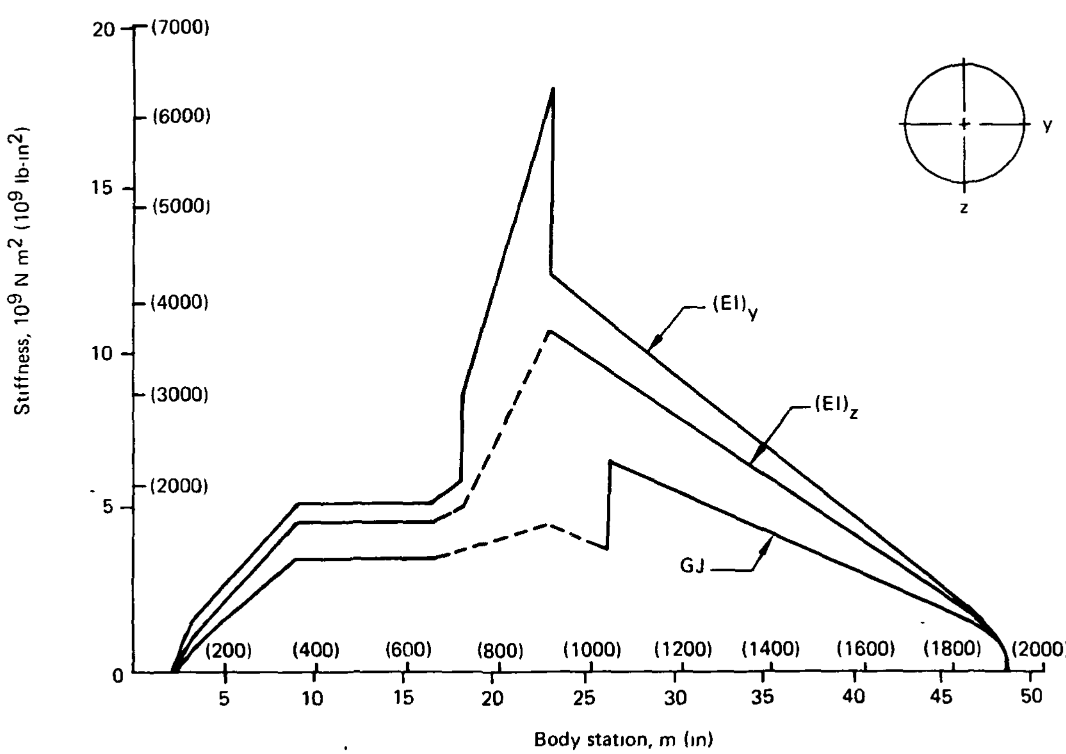

Figure 125. Fuselage Stiffness

7.3 CONTROL SYSTEM ANALYSIS

7.3 CONTROL SYSTEM ANALYSIS

The control system analysis and synthesis undertaken to support the Initial ACT Configuration is described in this section. The topics discussed are:

- The control system synthesis, which includes both the mathematical modeling of the airframe to define the "plant" or controlled element and the development of the control laws required to perform the ACT functions

- The mechanization of a control system (hardware and software) to execute these control functions with the required safety and reliability

7.3.1 CONTROL LAW SYNTHESIS

The IAAC control law synthesis and results described in the following sections were divided into low-frequency and high-frequency phases (or frequency bandwidths) related to the characteristic response modes of the airplane. The low-frequency phase included the dc or steady state, the phugoid, and the short-period modes of the airplane. The high-frequency phase enlarged the modal bandwidth characterizing airplane response to include the structural mode dynamics.

The control law loops are used to modify the basic airplane flying qualities, provide maneuver and gust load relief, and preclude wing flutter. The performance to be attained with a control loop is determined by the flying-qualities requirements (subsec 7.1) or by the structural requirements (subsec 7.2). These performance objectives were used as guidelines for control law development and were substantially fulfilled.

The low-frequency control law design phase used the QSAE mathematical model of the airplane (subsec 7.1).

The PAS and the MLC systems were synthesized in the low-frequency phase. The high-frequency control law design phase used the dynamic model of the airplane and synthesized the GLA and the FMC systems. Design of the GLA included active PAS and MLC systems, but no FMC system; whereas design of the FMC also included the

PAS and MLC systems, but no GLA. Subsequent analyses verified that the GLA and FMC were compatible with PAS and MLC at the two dynamic model flight conditions, V_B and V_{MO}. All synthesis work used traditional design techniques (i.e., root locus, Bode plots, power spectral density plots, and time response plots).

During the Initial ACT Configuration design process, two QSAE models were generated, a preliminary model used for the PAS and MLC synthesis and a "current" model that incorporated updated structural data. The latter was used in the flying-qualities description and for evaluation of the PAS control law synthesized using the preliminary QSAE model. Although the PAS is slightly deficient at two high-altitude, low-dynamic pressure flight conditions that were evaluated, the required changes appeared minimal and should not invalidate the general conclusions of the design study. Gain and phase margins for the PAS using the current QSAE model were not determined. It is intended that the PAS design will be recycled using this QSAE model of the Initial ACT Configuration. In this recycling, PAS performance will be evaluated, including gain and phase margins. This work will be done to provide a consistent initial PAS configuration for the development anticipated in the Wing Planform Study phase of the IAAC Project and will be reported in the documentation for that phase.

7.3.1.1 Dynamic Model

The dynamic mathematical model provided a single set of equations that may be used to develop control laws for multiple ACT functions operating over a wide frequency range. Conventional airplane design customarily carries out aeroelastic analysis for specialized design objectives by simplifying the general mathematical equations into categories such as steady, quasisteady (or static elastic), and dynamic. Techniques have evolved in each category that are not necessarily satisfactory for the others. For example, in structural dynamic response and flutter, the equations are usually simplified into modal form using Lagrange's equation. Quasisteady aeroelastic corrections, however, are calculated by direct influence coefficient methods. The simplification is achieved by neglecting the forces due to structural rates and accelerations. The assumption is that the interaction between those categories is small.

In addition, various aerodynamic theories and empirical correction techniques are used. Table 18 summarizes the approaches used on the Baseline and Initial ACT Configurations, and it shows the modeling features of four types of conventional analyses used on both configurations. The last column shows the features of the Initial ACT Configuration's dynamic model. Standard lumped-mass data and a statically determinate beam idealization of the structure, flexible in bending and torsion, were used in all cases. In the region of the wing/body junction where the structure is redundant, equivalent beam stiffnesses (based on experience with other airplanes) were used. Engine strut flexibility was calculated in a separate finite element analysis. In all the analyses (except gust loads, which used mean axes), the total motion was represented as the summation of rigid body motions and structural motions relative to the wing/body junction (cantilevered). The flying-qualities analysis used rigid wind tunnel force data modified by aeroelastic corrections calculated as in the maneuver loads analysis. Thus, the structural idealization is implicitly the same as the maneuver loads analysis. All analyses used wind tunnel pressure data for the rigid zero frequency distribution of lift and moment, and all used some means of modifying the theoretical aerodynamic influence coefficients (AIC) to force a match of rigid lift slope distribution. Lifting line theory was used for the loads analyses, with the unsteady aerodynamic influences represented by lift-growth functions, and AIC corrected by downwash (postmultiplication). The flutter analysis used an unsteady lifting surface theory (doublet lattice), and corrected AIC by pressure (premultiplication). Customarily body-fixed axes are used to analyze flying qualities and maneuver loads, while structural dynamic analyses use inertia axes.

In the design of a multifunction ACT control system, the interactions are apt to be significant, and a single mathematical model is needed. Such a dynamic model should:

- Include the essential characteristics of all relevant specialized aeroelastic models (quasisteady, static aeroelastic, and structural dynamics)
- Contain enough candidate control surfaces and sensors for determining the best practical combination
- Be able to accommodate linear, flexible, actuator models

Table 18 Comparison of Modeling Features

Modeling features	Analysis objective				
	Flying qualities	Maneuver loads	Gust loads	Flutter	Control law development[a]
Structure	Contained in aeroelastic corrections from maneuver loads analysis	Statically determinate beam (elastic axis)			
• Mass		Lumped	Lumped	Lumped	Lumped
• Stiffness		Bending and torsion	Bending and torsion	Bending and torsion	Bending and torsion
• Constraint		Cantilevered	Free-free (mean axis)	Cantilevered	Cantilevered
Aerodynamics		Modified theoretical technique			
• Theory		Lifting line with three-dimensional induction	Lifting line with three-dimensional induction	Lifting surface	Lifting surface
• Unsteady representation	Potential flow for low-frequency damping only	Quasi-steady	Quasi-steady with lift growth	Full unsteady (frequency dependent)	Full unsteady with S-plane approximation
• Empirical correction technique	Direct application of rigid wind tunnel data	Lift and moment distribution by downwash	Lift and moment distribution by downwash	Lift distribution by pressure	Lift distribution by pressure
• Empirical data source	Wind tunnel force model	Wind tunnel force and pressure model	Wind tunnel force and pressure model	Wind tunnel pressure model	Wind tunnel force and pressure model
Motion reference axes	Body-fixed	Body-fixed	Inertia	Inertia	Body-fixed
Load coefficient technique	–	Load summation	Load summation	–	Modal displacement

[a]Dynamic model

768-103

- Be in a form suitable for both classical and modern control theory; i.e., the equations should be constant coefficient linear differential equations solvable by Laplace transforms (S-plane)

- Be capable of predicting both airplane and structural responses to pilot command and gust

- Be constructed for enough weight (fuel and payload) and flight (Mach number and altitude) conditions to include the critical cases for the various ACT functions, including failure cases

To meet these objectives, the dynamic model was developed by adopting a modal formulation that used cantilevered branch-coupled modes chosen to include all significant structural dynamics up to 10 Hz and other high-frequency modes chosen to include the significant static flexibilities in the model. For example, horizontal tail torsion was included despite its natural frequency of 23.9 Hz. Including these high-frequency modes made it unnecessary to introduce the complication of residual flexibility. Modes included for one typical condition are listed in Table 19.

A constant amount (0.03g) of structural damping was included in the model. A fully unsteady lifting surface aerodynamic theory (doublet lattice) was selected in preference to a lifting line theory (see table 18) because it better predicts control surface forces, especially at high frequencies. The wing, horizontal tail, and vertical tail were idealized as lifting surfaces, the nacelles as cruciforms, and the body as a flat plate. The total number of aerodynamic boxes was 332 for the symmetric case and 351 for the antisymmetric case. Pressure scalers were introduced on the wing boxes to force a match with rigid angle-of-attack spanwise lift-slope distribution from pressure model data, on the tail boxes to force a match with rigid angle-of-attack total lift from force model data, and on the body boxes to force a match with total rigid tail-off angle-of-attack lift and moment from force model data. The nacelle boxes were not scaled. The equations were referred to body-fixed (body) axes rather than inertia axes.

As shown in Table 18, the flying-qualities equations of motion were built up by using rigid wind tunnel force data in the form of aerodynamic derivatives. They were then

Table 19. Modes Included in Symmetric Model
80% Wing Fuel, Aft Center of Gravity

Branch	Frequency, Hz	Dominant modal characteristic
Fore body	3 99	First vertical bending
Aft body	2 06	First vertical bending
	6 66	Second vertical bending
Vertical tail	5 59	First vertical bending (in plane)
	28 1	Second vertical bending (in plane)
Horizontal tail	5 91	First vertical bending
	18 7	Second vertical bending
	23 9	First torsion
Wing	1.14	First vertical bending
	3 12	Second vertical bending
	3 19	First fore/aft bending (in plane)
	4 34	First torsion
	7.05	Third vertical bending
	8 10	Second fore/aft bending (in plane)
	11 2	Fourth vertical bending
	12.6	Second torsion
Nacelle	2 60	Side bending
	4 63	Vertical bending
	5 76	Roll/side bending

768-103

modified for aeroelasticity by corrections that were calculated the same way as the maneuver loads. By performing a static-elastic reduction of the elastic modes, the dynamic model also yielded values for those derivatives. The two sets of derivatives were compared, and the rigid terms in the dynamic model were modified to force agreement.

Both the symmetric and antisymmetric models used seven control surfaces including the five wing-control surfaces in Figure 126. The symmetric model had both segments of a split double-hinged elevator while the antisymmetric had two (upper and lower) double-hinged rudders. Equations were included for the 20 sensors in Figure 126.

The dynamic model contained hinge-moment equations for use with linear flexible actuator models. Optionally, the hinge moment may be zeroed out for use with rigid

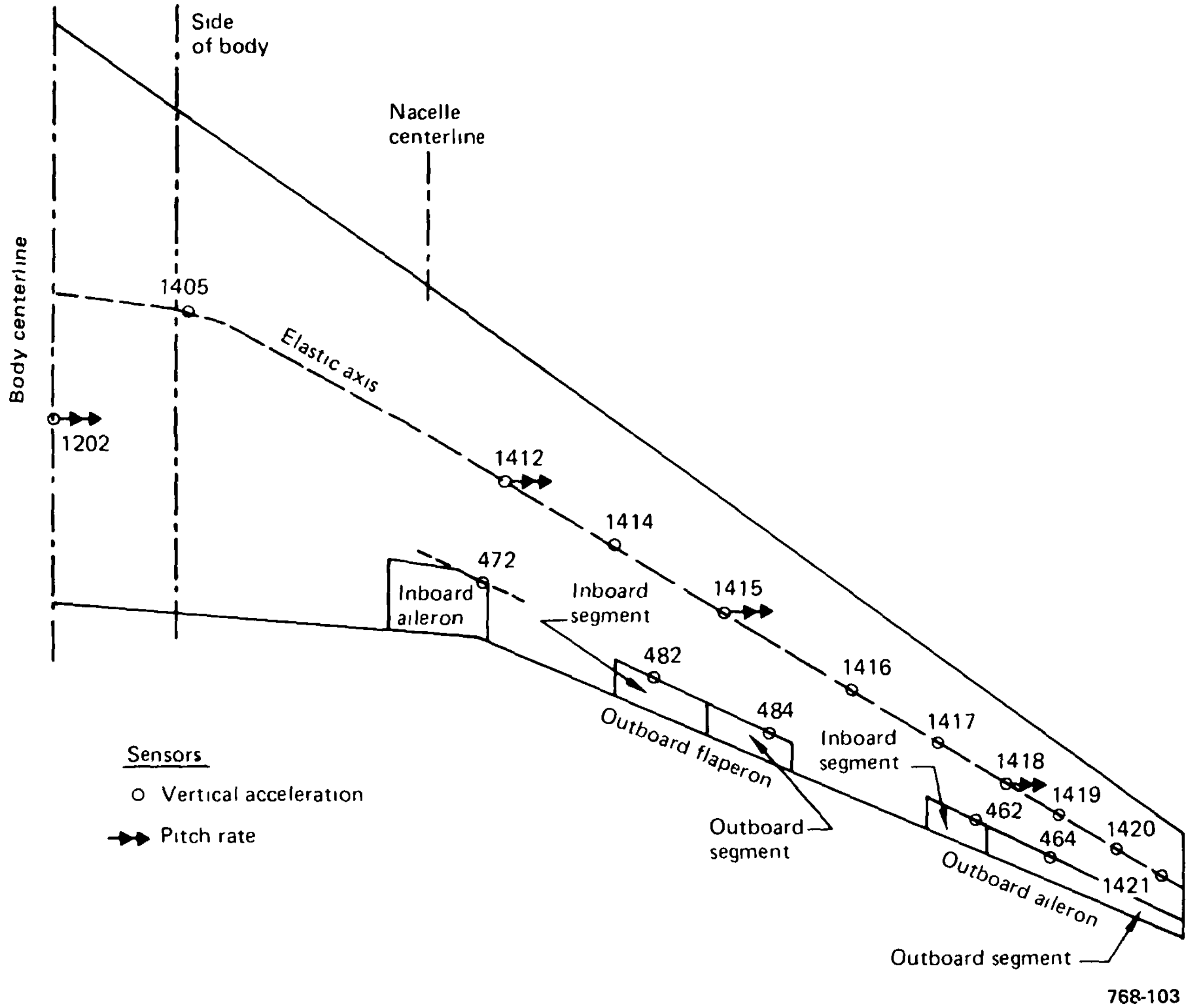

Figure 126. Modeled Wing Controls and Sensors

(first order lag) actuator idealizations. The Initial ACT control law development used rigid actuators, while a structural back-up spring was placed in series with a rigid actuator in the flutter analysis.

An unsteady lifting surface theory was used for the aerodynamic forces. The resulting equations contained frequency-dependent coefficients and were unsuitable for control law development, so they were transformed using a least-squares fit process to an assumed function in the Laplace variable S (assuming $S = i\omega$). A very simple function (a second-order polynomial) was assumed, resulting in a set of second-order differential equations suitable for control law development. The use of body-fixed axes ensured that the low-frequency (quasisteady) characteristics of the transformed equations were unaffected by the approximating procedure.

Gust-forcing vectors, representing vertical gust for the symmetric case and lateral gust for the antisymmetric case were added to the equations. For predicting load, a set of equations relating load to the equation variables was generated. The loads analyses (table 18) used a loads summation technique. In the dynamic model, load summation would require a way of transforming box pressure coefficients to the S-plane. Because such a means is not available, a modal displacement technique, in which the loads are determined from the structural displacements, was used.

The dynamic model concentrated on one Mach number. Most wing aeroelastic phenomena are critical at the Mach number where the wing lift curve slope is greatest. The wing fuel condition chosen was the 80% identified as critical for flutter. Payload was loaded to bring the total weight to maximum takeoff weight with the cg at the aft limit (46% MAC) to reflect the critical condition for flying qualities. Symmetric (longitudinal) and antisymmetric (lateral directional) equations were produced at four altitudes corresponding to V_B, V_{MO}, V_D, and $1.2V_D$. The conditions are listed in Table 20. A system of computer programs was developed to carry out the

Table 20. Symmetric and Antisymmetric Conditions

Flight condition	Mach No	Altitude, m (ft)	Pressure, N/m^2 (lb/ft^2)	Equivalent airspeed, m/s (kn)	Mass, kg (lb)	Center of gravity, percent MAC
V_B	0.86	10 668 (35 000)	12 344 (258)	142 (276)	122 470 (270 000)	46
V_{MO}	0 86	7 833 (25 700)	18 846 (394)	176 (341)	122 470 (270 000)	46
V_D	0 86	4 968 (16 300)	28 049 (586)	214 (416)	122 470 (270 000)	46
$1.2V_D$	0 86	1 890 (6 200)	41 887 (875)	262 (508)	122 470 (270 000)	46

768-103

procedure (fig. 127). The final form of the equations is schematically represented in Figure 128.

As pointed out, a simple technique was used to transform the frequency-dependent aerodynamic coefficients to the S-plane. This involves a numerical approximation involving a least-squares fit technique and a physical assumption that the form of the fitting function (a second-order polynomial) can be physically realized.

Figure 129 compares the structural eigenvalues (roots) computed using frequency-dependent aerodynamics and the polynomial approximation. Frequency and damping are plotted against true airspeed at a constant altitude assuming that the aerodynamic coefficients are invariant with Mach number in the manner of a conventional flutter solution.

Because the frequency-dependent case is a V-g solution and the polynomial case is a quadratic solution, g (added structural damping) is shown for the frequency-dependent case and ζ (damping ratio) for the polynomial case for comparison purposes. For small values $g = 2\zeta$. For clarity, Figure 129 shows only the potential flutter modes, and the correlation is good. Figure 130 shows the correlation of the critical flutter modes for a case that includes the FMC system; again, the correlation is reasonably good. The apparent discrepancy in frequency in mode 1 at high speeds is because frequencies calculated in a V-g solution and in a quadratic solution are equivalent only when the damping is small. Note that structural damping was not included for this comparison, but it is included in the dynamic model for control law development.

Using a polynomial form to transform the aerodynamic coefficients to the S-plane leads to a physically realizable form only if the polynomial is restricted to a quadratic order. A widely used alternative form is a series of lag functions that remain physically realizable no matter how many lags are included; however, this greatly complicates the resulting equations.

The lifting surface program does not compute in plane forces or forces due to in-plane motions, so it is necessary to read into the dynamic model forces derived from the QSAE. Also, as mentioned previously, a means was incorporated to increment the

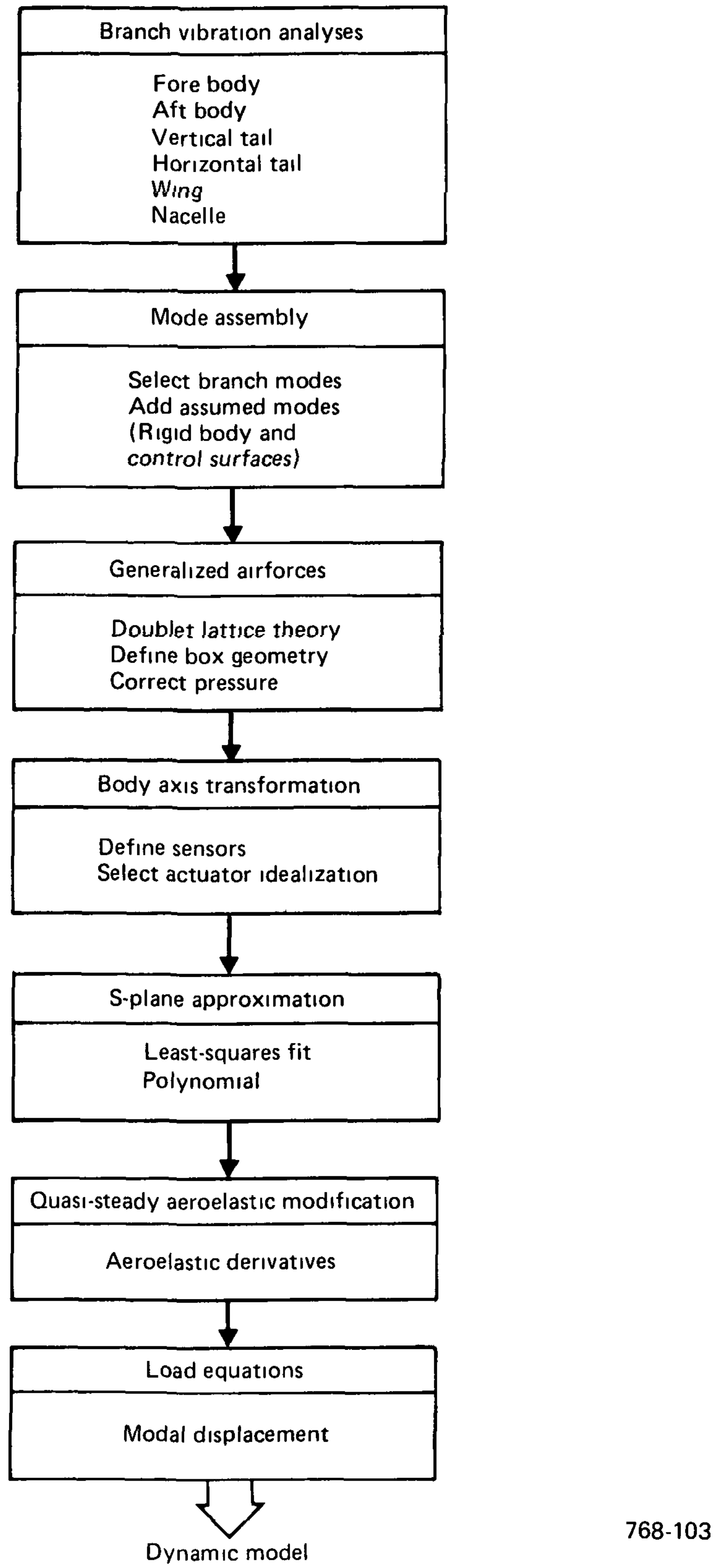

Figure 127. Dynamic Modeling Procedure

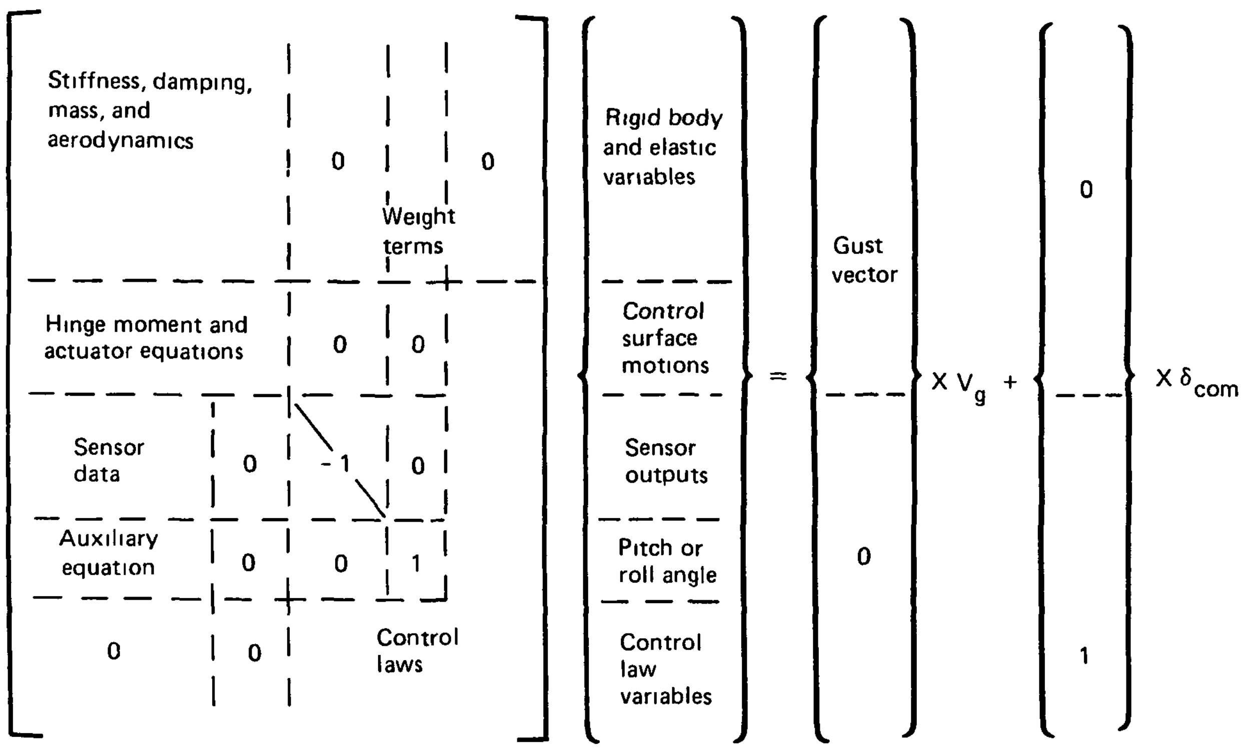

● V_g = gust velocity

● δ_{com} = pilot command

768-103

Figure 128. Matrix Form of Equations of Motion

- Symmetric modes
- 80% wing fuel
- Constant altitude of 4968m (16 300 ft)

V-g Solution.
Frequency-Dependent Aerodynamics

Quadratic Solution:
Polynomial Approximated Aerodynamics

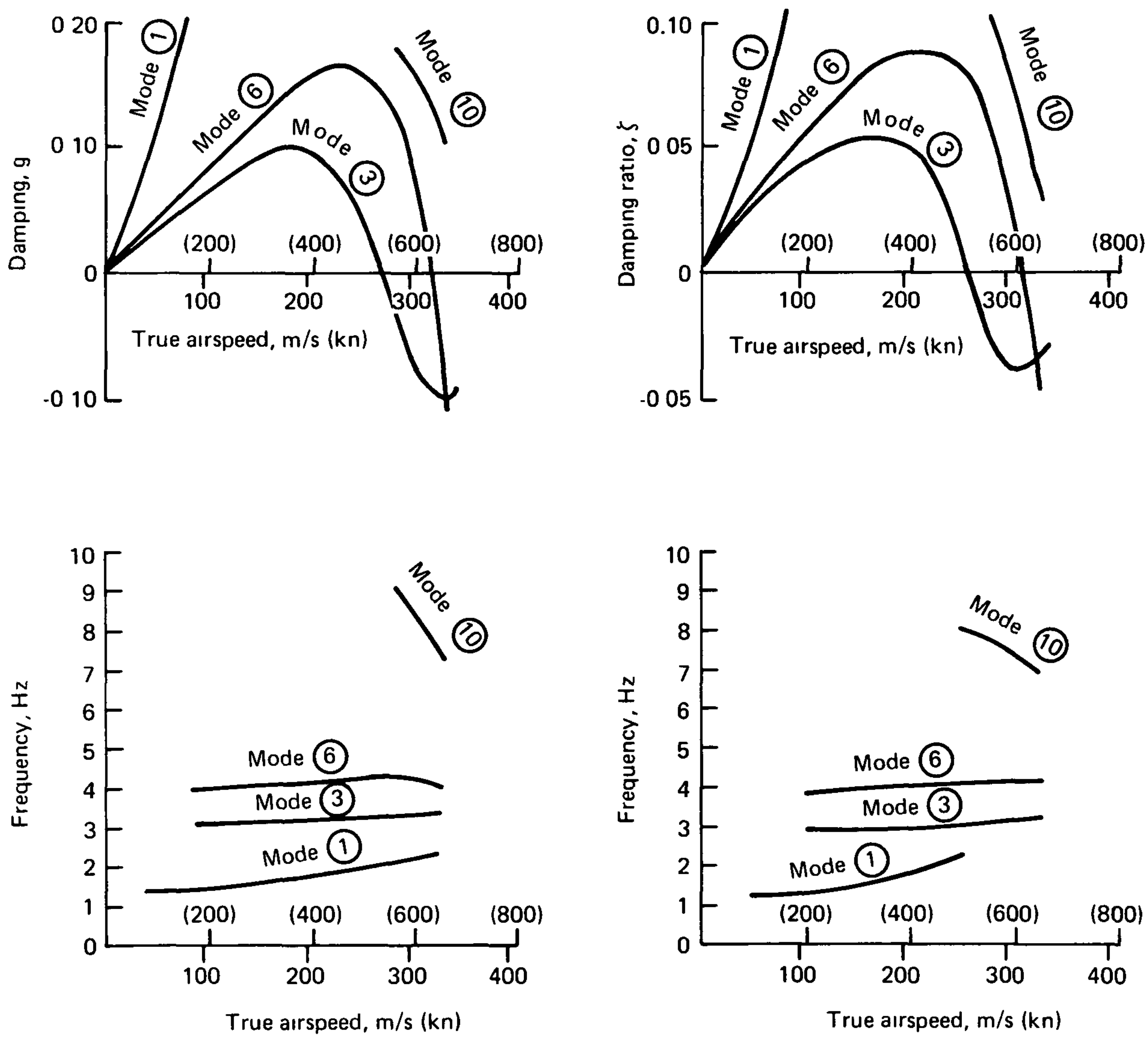

Figure 129. Flutter Solution Correlation

768-103

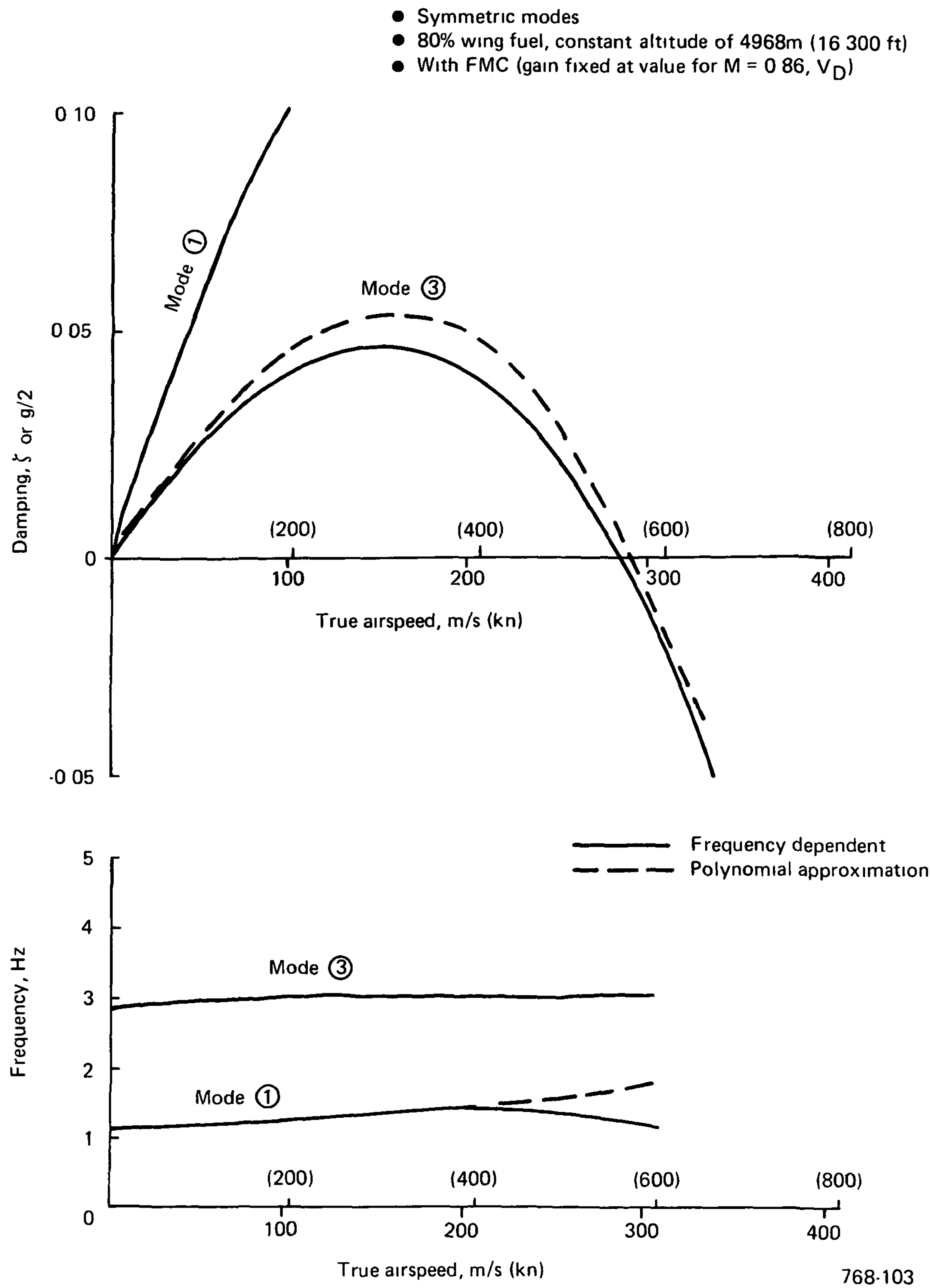

Figure 130. Flutter Solution Correlation, With FMC

dynamic model for differences between the QSAE derivatives from the flying-qualities analysis and those reduced from the dynamic model. A comparison for some longitudinal derivatives and the magnitude of the corrections involved shows good correlation at least for the more important derivatives (table 21). For this condition, note that the airplane is slightly statically unstable (i.e., C_{m_α} is positive). The relationship between control lift and pitching moment differs considerably between the dynamic model and the QSAE because, at the flight condition chosen, both control surfaces are near reversal speed. The lateral/directional derivatives show a similar good correlation.

The outboard aileron is used for load alleviation, and the effectiveness predicted by the aeroelastic analysis that was used for maneuver loads and aeroelastic corrections (see table 18) was compared to that predicted by the dynamic model. Figure 131 shows rolling moment (which has similar characteristics to wing root bending moment)

Table 21. Quasi-Steady Derivative Correlation—Longitudinal Derivatives

Derivative[a]	Force model data, modified by static aero-elastic corrections	Dynamic model static-elastic reduction of structural modes	Magnitude of correction, percent
C_{m_α}/deg	0.00122	0 00422	Δac = 3% MAC
C_{L_α}/deg	0 0916	0 0888	3
$C_{m_{\hat{q}}}$/rad	-21.7	-20.2	7
$C_{L_{\hat{q}}}$/rad	6 68	10.56	57
$C_{m_{\delta_E}}$/deg	-0 0189	-0.0184	2
$C_{L_{\delta_E}}$/deg	0 00413	0 00304	35
$C_{m_{\delta_A}}$/deg	-0 00211	-0.00175	17
$C_{L_{\delta_A}}$/deg	-0 00103	-0 00092	9

[a]No inertia relief
M = 0.86
Center of gravity = 0 46 MAC
Weight = 122 500 kg (270 000 lb)
$V = V_{MO}$ [175 m/s (341 KEAS)]

768-103

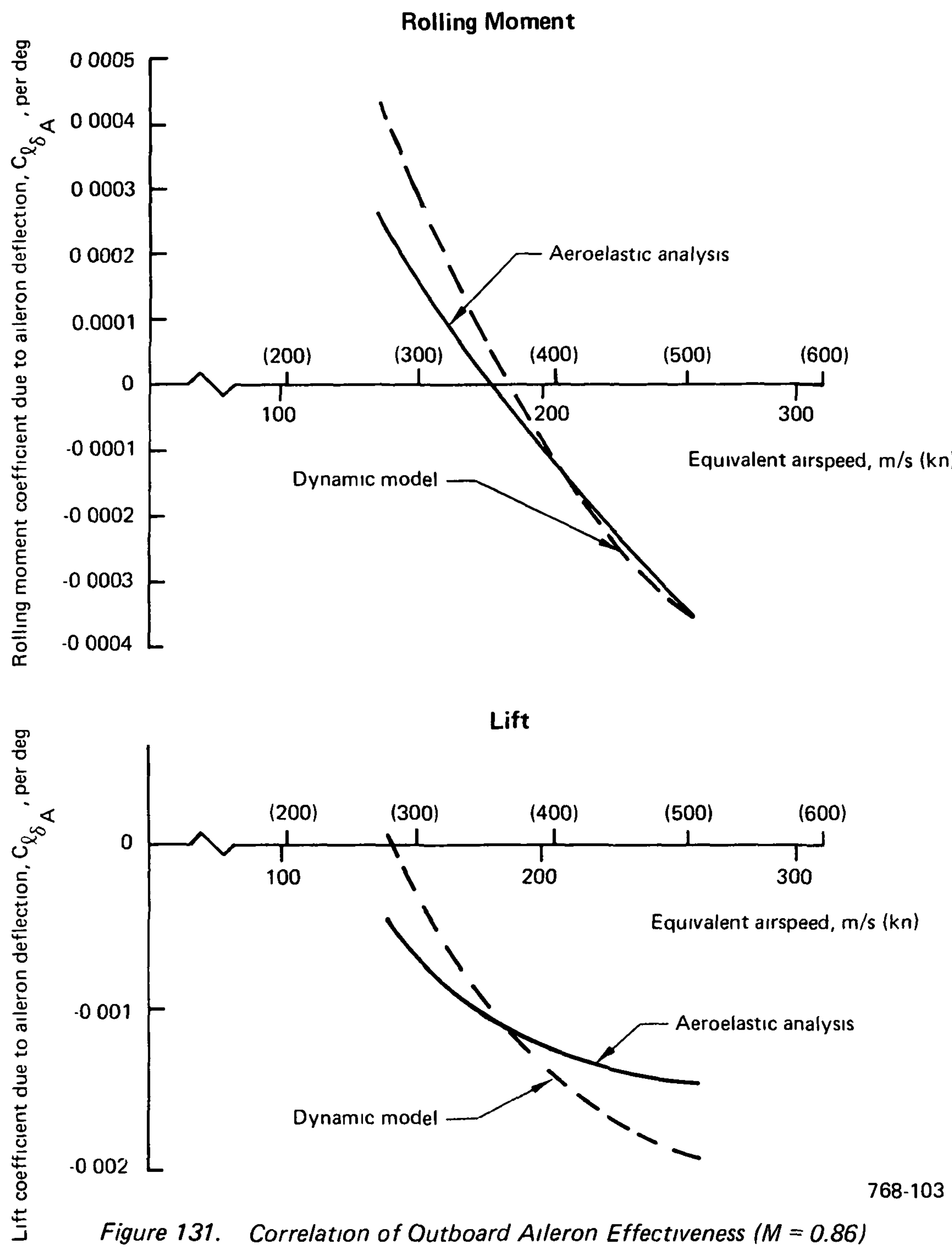

Figure 131. Correlation of Outboard Aileron Effectiveness (M = 0.86)

and lift plotted against equivalent airspeed. The correlation is reasonably good, showing about 20 m/s (40 kn) difference in reversal speed. However, note that at some speeds the two analyses show rolling moments that are small but of opposite sign.

As mentioned previously, load equations were provided for use with the dynamic model. By static-elastic reduction of the structural modes, equivalent steady-state wing-load coefficients were computed and compared to those computed in the maneuver-loads analysis. The results indicated that while the bending moments, due to angle of attack, correlated fairly well (up to 9% difference), shear and torsion were subject to very large differences; and the load, due to aileron, was subject to the same order of difference as the rolling moment in Figure 131. The dynamic model is built around the flutter analysis rather than either of the loads analyses (table 18). The most significant differences are in the aerodynamic theory used and the empirical correction techniques. The empirical correction technique used in the dynamic model was aimed at matching the rigid wing pressure data rather than control surface pressure data, and some additional development work is required on this subject.

The dynamic model, which showed good correlation with the flutter results and the flying-qualities analysis, was modified to match steady-state conditions exactly. It provided enough incremental loads information to guide the development of wing-load alleviation control laws. In the Initial ACT Project, such control laws performed adequately when evaluated by conventional analyses. Although most objectives of the dynamic modeling were met, further investigations and developments, as noted, are desired.

7.3.1.2 PAS Description

For maximum reliability, the PAS design was made as simple in concept as compatible with yielding an augmented airplane having acceptable flying qualities. As the block diagram of Figure 132 shows, this implementation augments the longitudinal short-period with a constant-gain, single-loop system using lag-filtered pitch-rate feedback.

The mathematical model of the airplane used for PAS synthesis was the preliminary QSAE representation of the airplane with the conventional longitudinal degrees-of-freedom. The PAS design process used airplane dynamics at eight flight conditions (table 22). The flight conditions are given in Table 22 and plotted on the airplane's speed and altitude envelope in Figure 133.

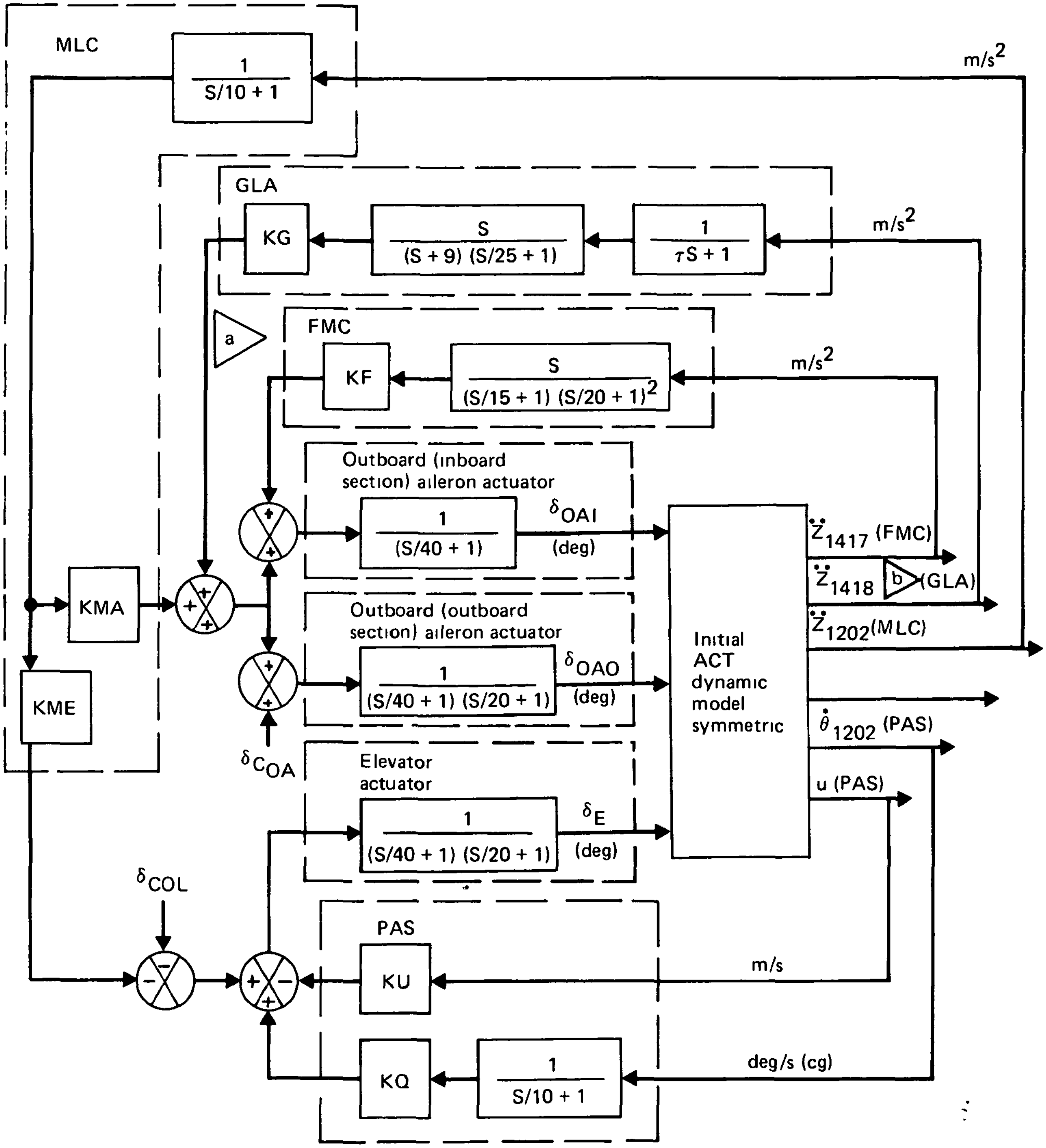

a Refer to table 22 for gain values

b Refer to figure 126 for sensor locations

768-103

Figure 132. Longitudinal-Pitch Stability Augmentation System—Functional Block Diagram

Table 22. PAS, MLC, GLA, and FMC Control Constants

	Flight condition (b)	Gains (a) KQ	KU	KMA $\ddot{Z}_{1202} < 0$	KMA $\ddot{Z}_{1202} > 0$	KME	KG	KF	GLA time constants, τ, sec
(c) Dynamic model	V_B	1 0	0 0226 (0 00688)	1 3596 (0 4144)	0 7648 (0 2331)	0 1168 (0 0356)	0 2257 (0 0688)	0 0377 (0 0115)	0.16
	V_{MO}			0 9791 (0 2984)	0 5509 (0 1679)		0.1129 (0 0344)	0 0377 (0 0115)	0.10
	V_D			0 6798 (0 2072)	0 3826 (0 1166)		—	0 1503 (0 0458)	—
	$1\ 2V_D$			0 4078 (0 1243)	0 2293 (0 0699)		—	0.4511 (0 1375)	—
(d) QSAE model	1			0.9791 (0 2984)	0 5509 (0 1679)		—	—	—
	1A			0.9791 (0.2984)	0 5509 (0 1679)		—	—	—
	2			1 3596 (0 4144)	0 7648 (0 2331)		—	—	—
	3			1 3596 (0 4144)	0 7648 (0 2331)		—	—	—
	4			0 9653 (0 2942)	0 5430 (0 1655)		—	—	—
	7			0 6431 (0 1960)	0 3619 (0 1103)		—	—	—
	8			1 3596 (0 4144)	0 7648 (0 2331)		—	—	—
	9			1 3596 (0 4144)	0.7648 (0.2331)		—	—	—

768-103

(a) Dimensions are in meters (feet), seconds and degrees

(b) For positive directions, X = forward, Y = right, and Z = down

(c) Refer to table 20

(d) Refer to table 23

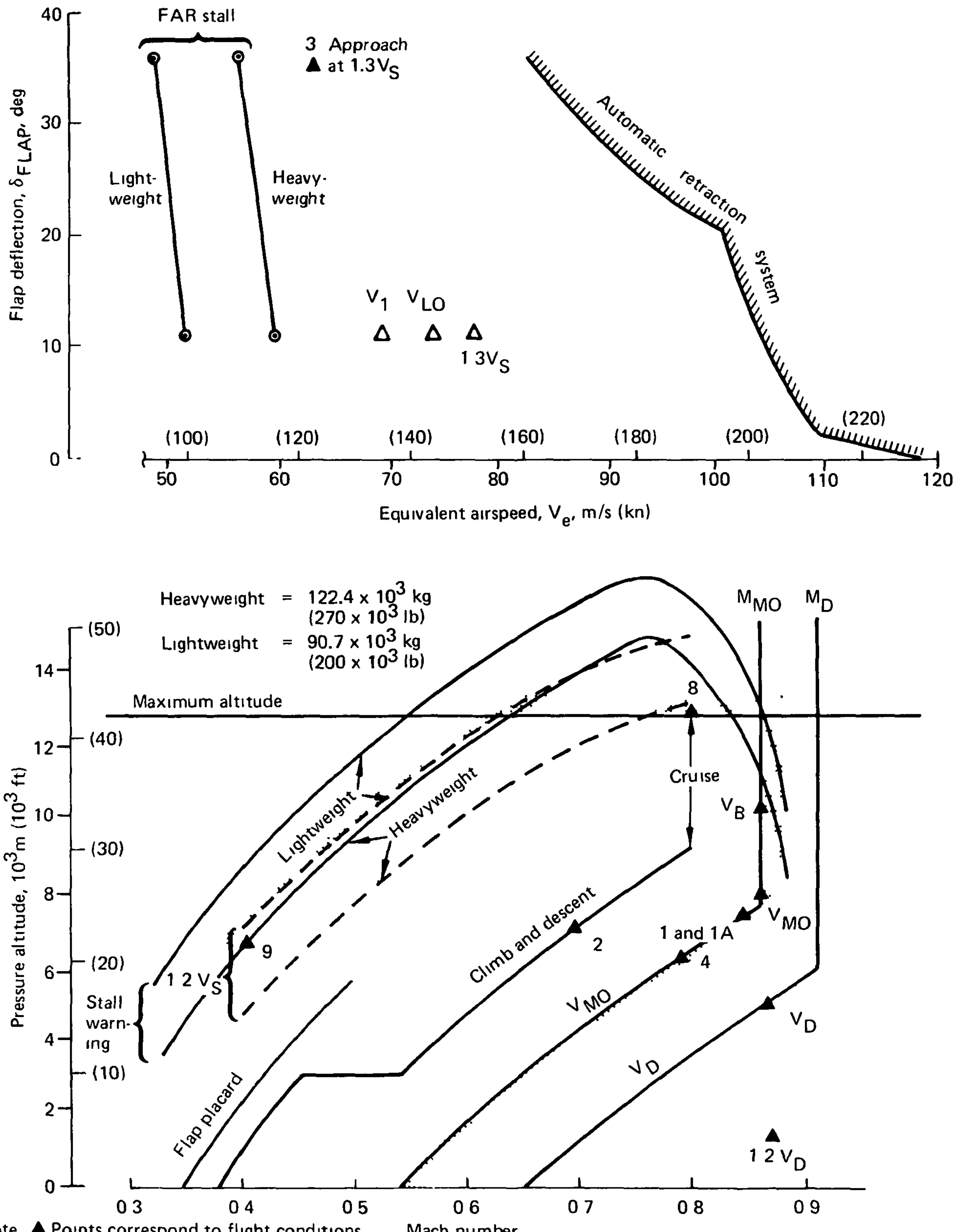

Note ▲ Points correspond to flight conditions shown in Table 23

768-103

Figure 133. Speed and Altitude Flight Envelopes

Synthesis Method—The root locus and system time response were the basic analytical tools used in the PAS design process. The root locus was used to determine system stability as a function of the lag filter time constant or loop gain. System time response plots were used to evaluate the flying qualities of the airplane with PAS. For several tabulated flight conditions, the unaugmented airplane dynamics exhibited a fast divergent mode characterized by a positive real root or pole.

Pitch-rate feedback to the elevator can reduce the divergence rate; however, due to the zero at the origin of the root locus plot in the pitch-rate/elevator transfer function, pitch-rate feedback alone cannot completely stabilize the airplane. To eliminate this remaining slow divergence, speed feedback to the elevator was required, as illustrated by the pitch rate and speed loop root loci for Flight Condition 1, Figure 134. The stabilizing effect of the PAS at this flight condition can be seen in Figure 135, which shows the response of the airplane (with and without PAS) to a pitch-rate command.

Verification of Stability and Flying Qualities—The design stability requirements for the augmented airplane are shown in Figure 136. With pitch-rate feedback only, the airplane exhibits Level 2 stability, but closure of the speed loop yields Level 1 stability. The design requirements on flying qualities are shown by the short-period versus n/α footprints in Figure 137. In addition, the ratio of maximum to steady-state pitch rate shall be less than:

- En route phase
    - Level 1 2.5
    - Level 2 3.5
    - Level 3 (not a requirement)
- Terminal phase
    - Level 1 2.0
    - Level 2 3.0

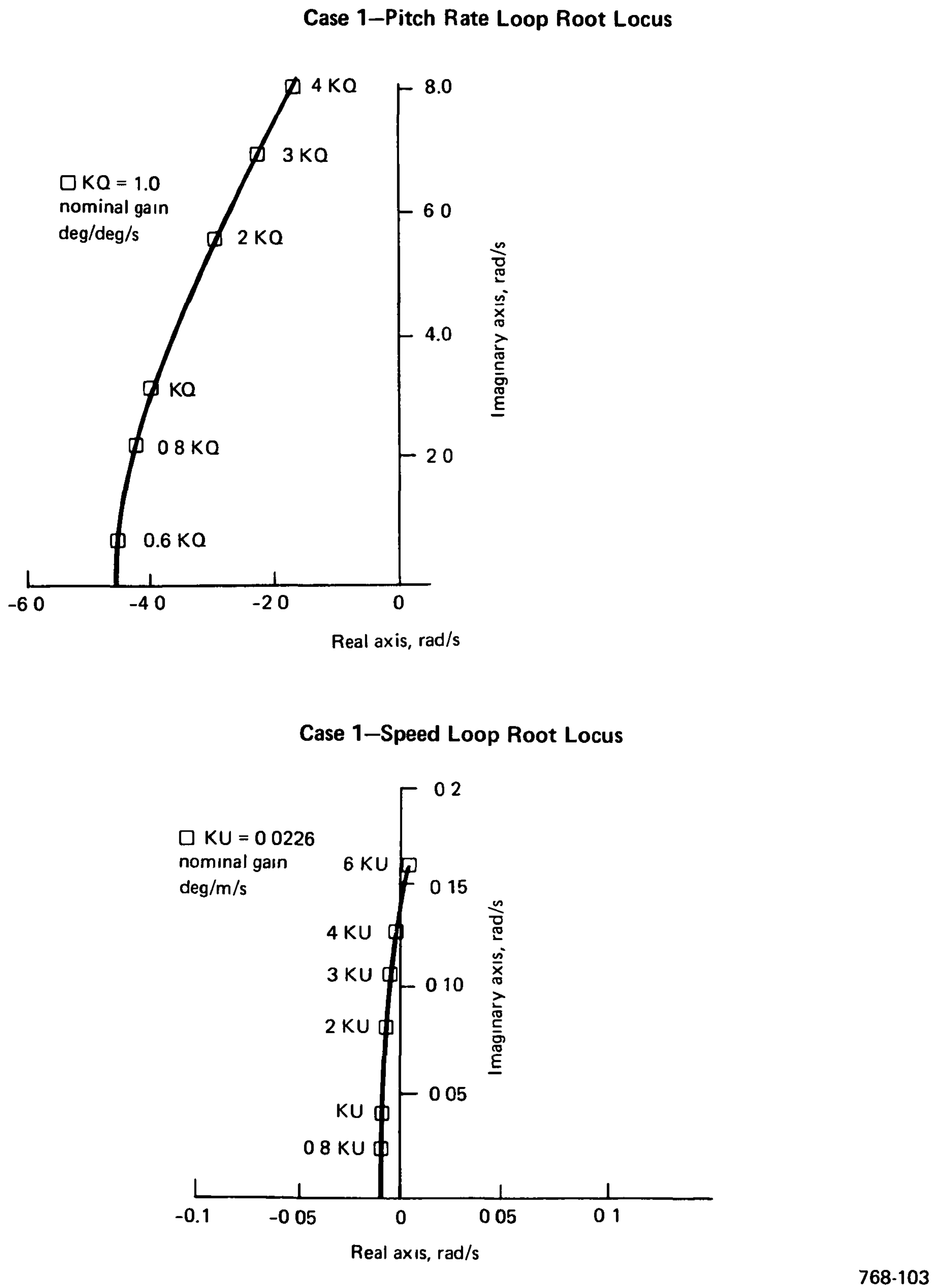

Figure 134. PAS Root Loci (Flight Condition 1)

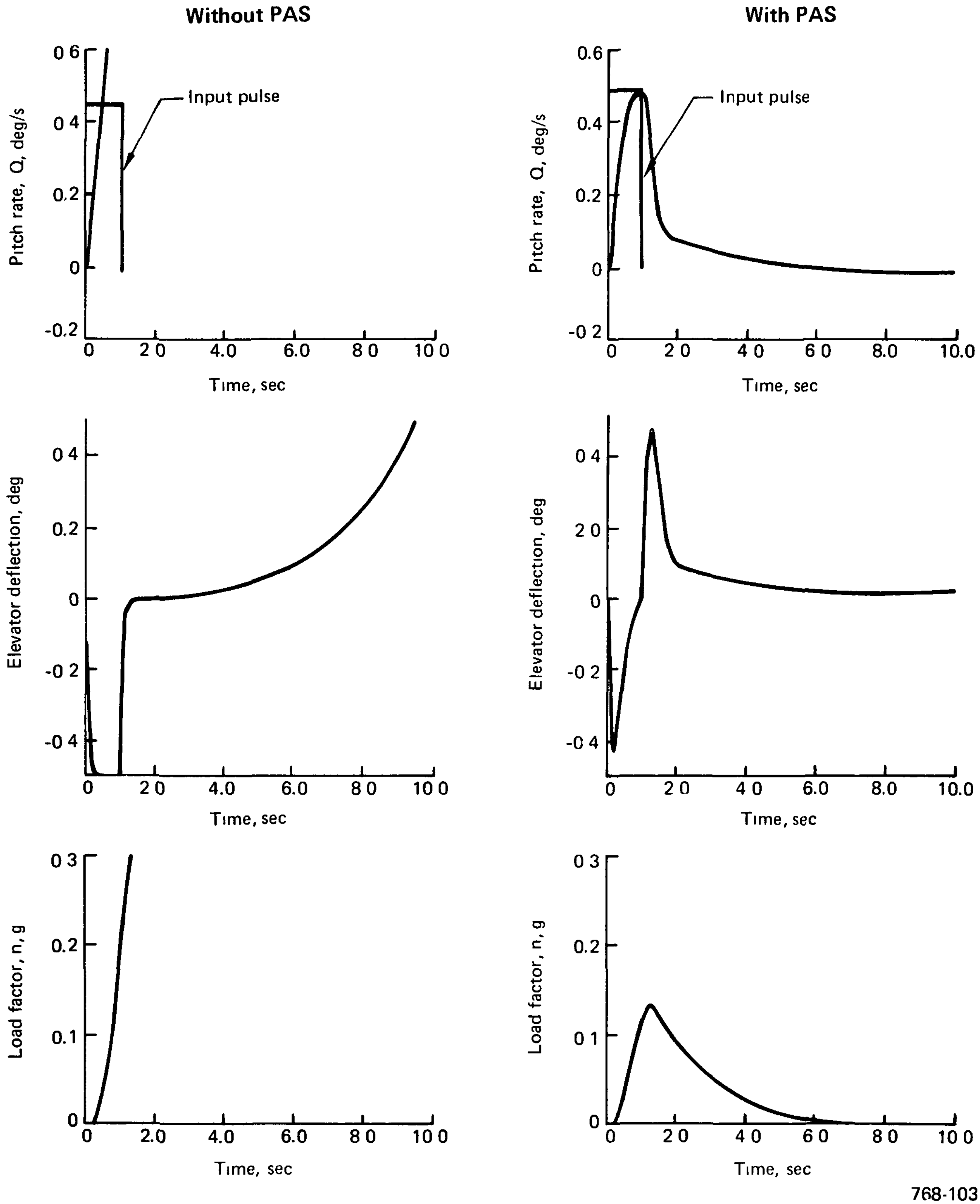

Figure 135. Case 1—Response Dynamics to a 1-sec, 0.5-deg/s Pitch Rate Command Pulse (Flight Condition 1)

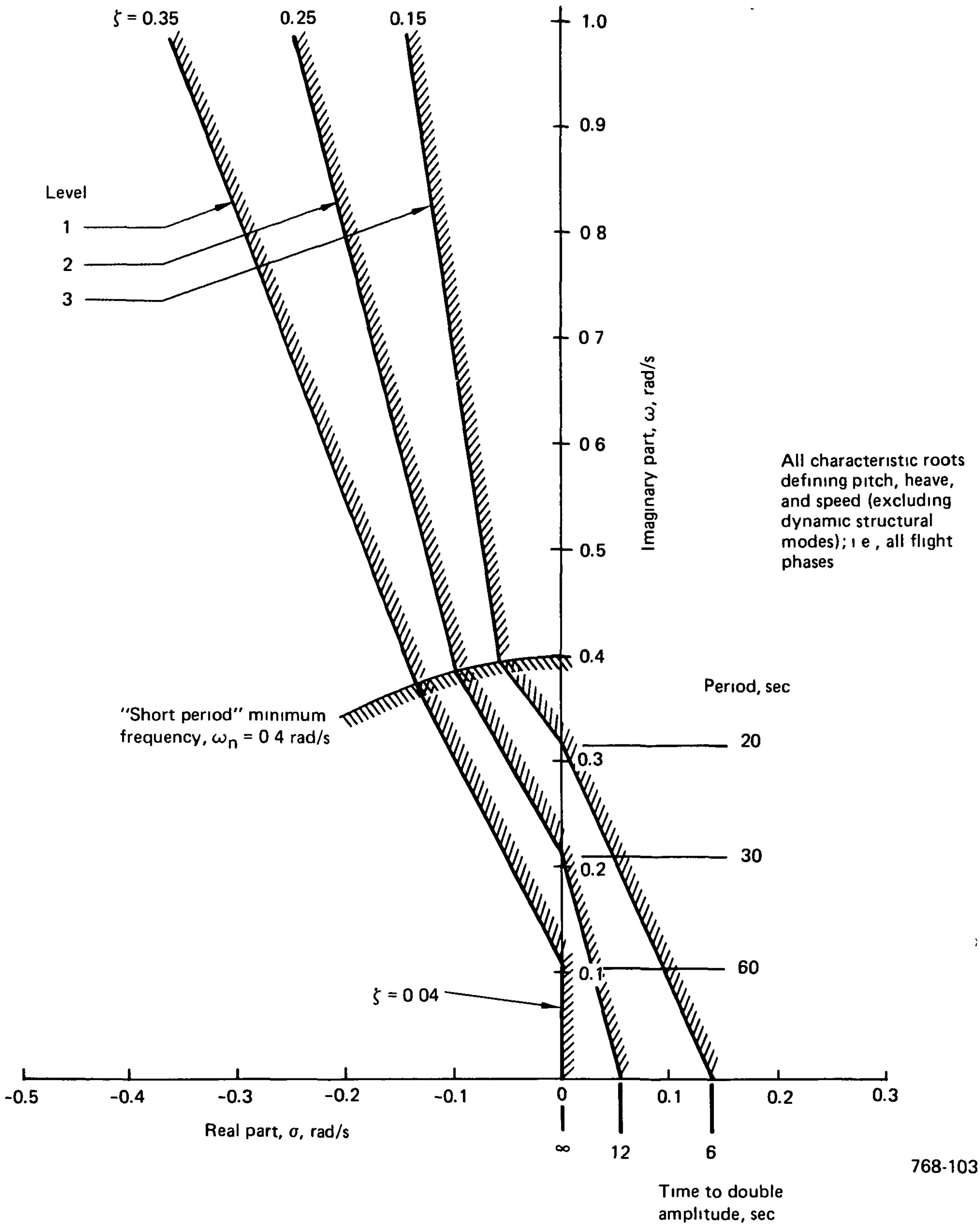

Figure 136. Minimum Damping Requirements—Longitudinal Roots

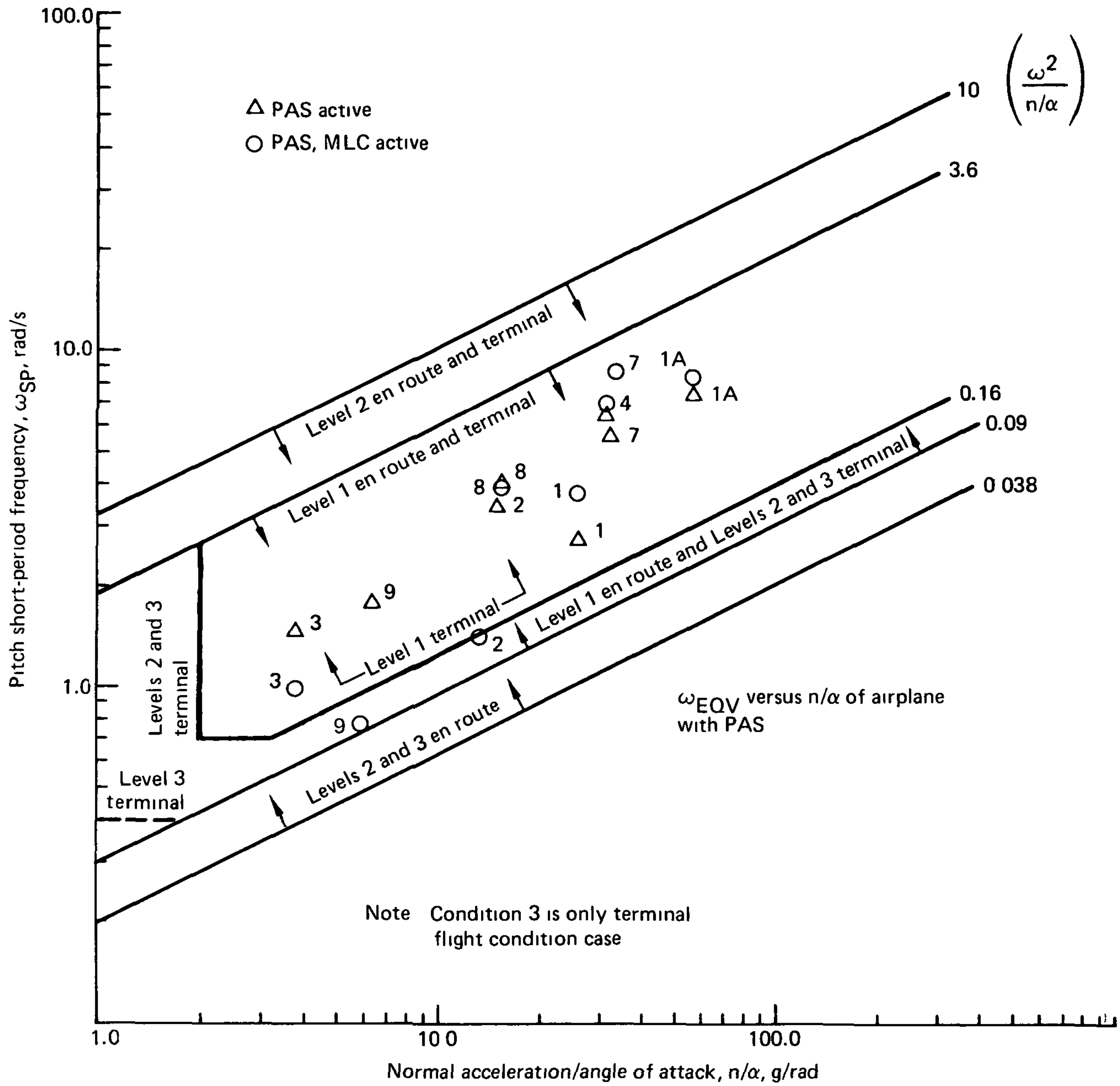

Figure 137. Flying Qualities Short-Period Requirements 768-103

The flying qualities at the several flight conditions were determined from the response of the augmented airplane to a pitch-rate step command. From the time response, the ratio of the maximum to steady-state pitch rates, Q_{max}/Q_{ss}, was determined, and $\omega = \omega_{EQV}$ was estimated for the short-period frequency value.

With the PAS loop closed, the short-term response characteristics of the airplane, as typified in Figure 138, are cubic, rather than second order having an explicit ω_{SP}. The frequency ω_{EQV} was obtained by fitting an appropriate second-order system step response to the cubic response. When this process was repeated for the eight flight conditions analyzed, all the ω_{EQV} were acceptable (Level 1) and are plotted on Figure 137; all Q_{max}/Q_{ss} also were acceptable.

7.3.1.3 Wing-Load Alleviation Control System

The WLA control system comprises a low-frequency MLC system and a high-frequency GLA system (table 23). The MLC was developed for the critical QSAE flight synthesized for the V_B and V_{MO} dynamic model flight conditions of Subsection 5.5.1.1. Classical synthesis methods of root locus and time and frequency responses were used while developing the WLA control law.

QSAE MLC Synthesis—The MLC system reduces wing bending moments resulting from pilot-initiated airplane maneuvers. The outboard ailerons are deflected symmetrically to shift the wing spanwise airload distribution inboard when a change in aircraft cg load factor is sensed (refer to fig. 75, subsec 7.2.1.2).

The MLC signal from the cg accelerometer to the ailerons was converted to a load factor and was gain-scheduled according to an actuator blowdown schedule (refer to fig. 72). The MLC load factor conversion was linearized for this development (no dead zone). The short-period dynamics of the aircraft also were augmented by the MLC signal that commands deflections of the elevators. The elevator response counteracts the increment of pitch rate caused by the deflection of the ailerons, and it preserves the same pitch characteristics that would be encountered with MLC off and the PAS active. The high-frequency content of the MLC signal was attenuated with a first-order lag filter (fig. 132).

The MLC control law was synthesized for the eight critical QSAE flight conditions (table 23) of the PAS development. The short-period stability requirement criteria of Figures 136 and 137 apply to both the MLC and the PAS. As with the PAS, the short period was not distinct, and an equivalent second-order frequency and damping were estimated. The equivalent results are presented in Table 23 and Figure 137. The PAS

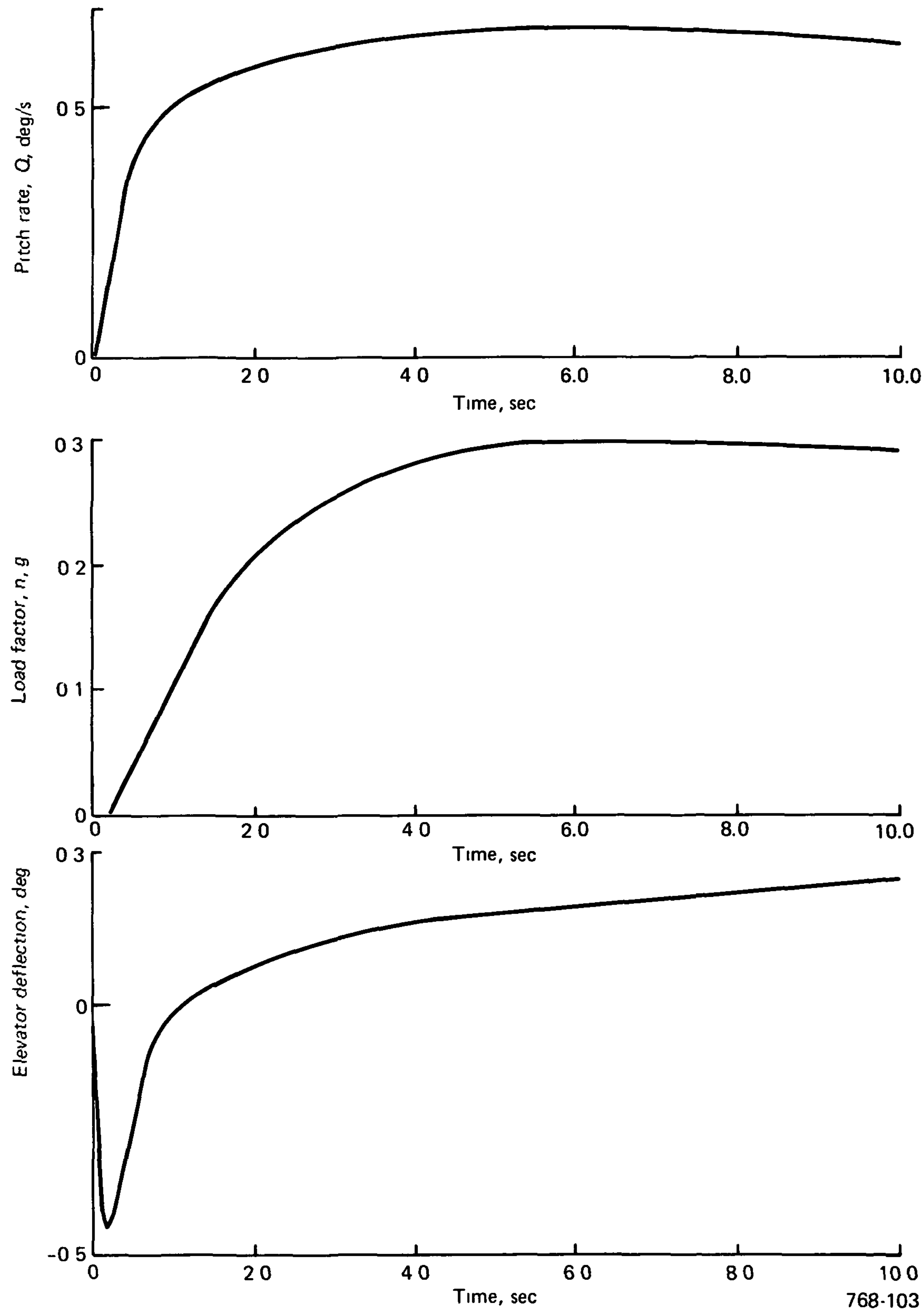

Figure 138. Case 1 PAS Response Dynamics to a 0.5-deg/s Pitch Rate Command Step

Table 23. PAS and MLC Verification Flight Conditions

Flight condition	1	1A	2	3	4	7	8	9
Weight, 10^3 kg (10^3 lb)	122 4 x 10^3 (270)	→	→	90.7 x 10^3 (200)	→	122.4 x 10^3 (270)	90.7 x 10^3 (200)	→
Mach number	0.84	0.84	0.65	0.185	0.78	0.65	0.80	0.378
q, 10^3 N/m2 (lb/ft2)	19.39 (405)	19.39 (405)	13.79 (288)	2.384 (49.8)	19.82 (414)	29 97 (626)	7.661 (160)	4.659 (97.3)
H, km (10^3 ft)	7.32 (24)	7 32 (24)	6.1 (20)	0 0	6.1 (20)	0 0	12.8 (42)	6 1 (20)
Center of gravity, percent	46	21	46	46	46	46	46	46
n/α	25 8	58.2	16 0	3.82	31.5	32.4	15.6	6.34

"Equivalent short period" and phugoid characteristics of airplane with PAS

ω_{EQV} rad/s	2 75	7.5	3.50	1.47	6.4	5.6	4 0	1.76
ζ_{EQV}	1.0	0.4	1.0	1 0	1.0	0.6	0 8	1.0
ω_P	0.043	0.081	0 053	0.082	0.043	0 063	0.013	0.054
ζ_P	0 26	0.133	0.065	0.61	0.046	0 080	0.37	0 17

"Equivalent short period" and phugoid characteristics with both PAS and MLC active

ω_{EQV} rad/s	3 79	8.12	1.56	0.93	6.6	8.23	4.01	0 75
ζ_{EQV}	1 0	0.5	1.0	1.0	1.0	0.8	0.9	1.0
ω_P rad/s	0 038	0.079	0.059	0.086	0.044	0 058	0 014	0.062
ζ_P	0 297	0.138	0.047	0.615	0.045	0 091	0.377	0.164

768-103

versus PAS-MLC equivalent results vary due to slightly different estimation procedures of the analysts involved. However, both system configurations meet Level 1 flying-quality requirements.

The sensitivity of the short-period characteristic roots to variations in the gains KMA (maneuver-load control aileron gain) and KME (maneuver-load control elevator gain) is illustrated in the root locus plots of Figures 139 and 140, respectively, which apply to QSAE Flight Condition 2 (table 23). While small gain changes do not appreciably affect the damping of the short period, the frequency is more sensitive to those changes.

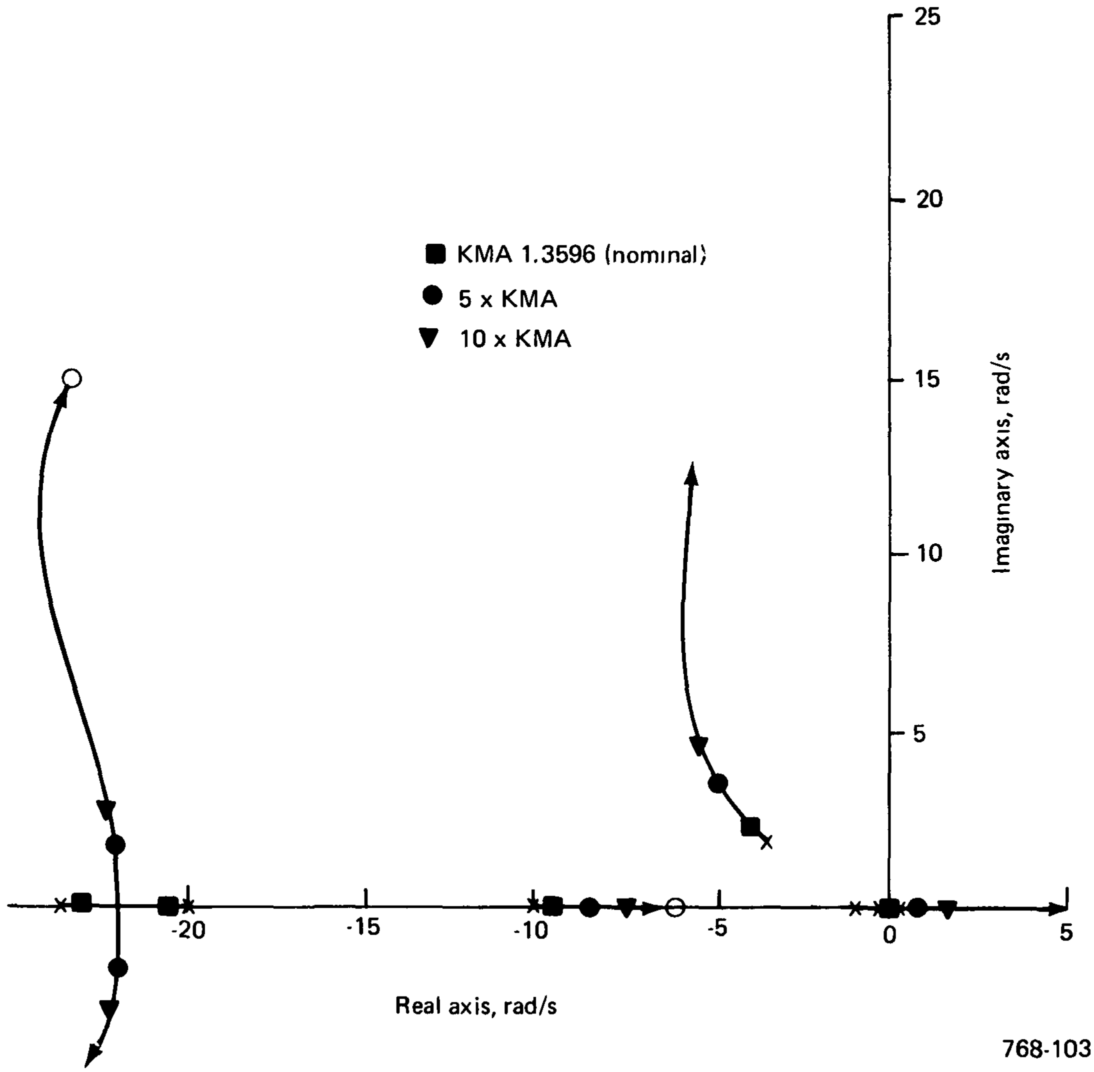

Figure 139. QSAE Model MLC, Root Locus on KMA (Flight Condition 2)

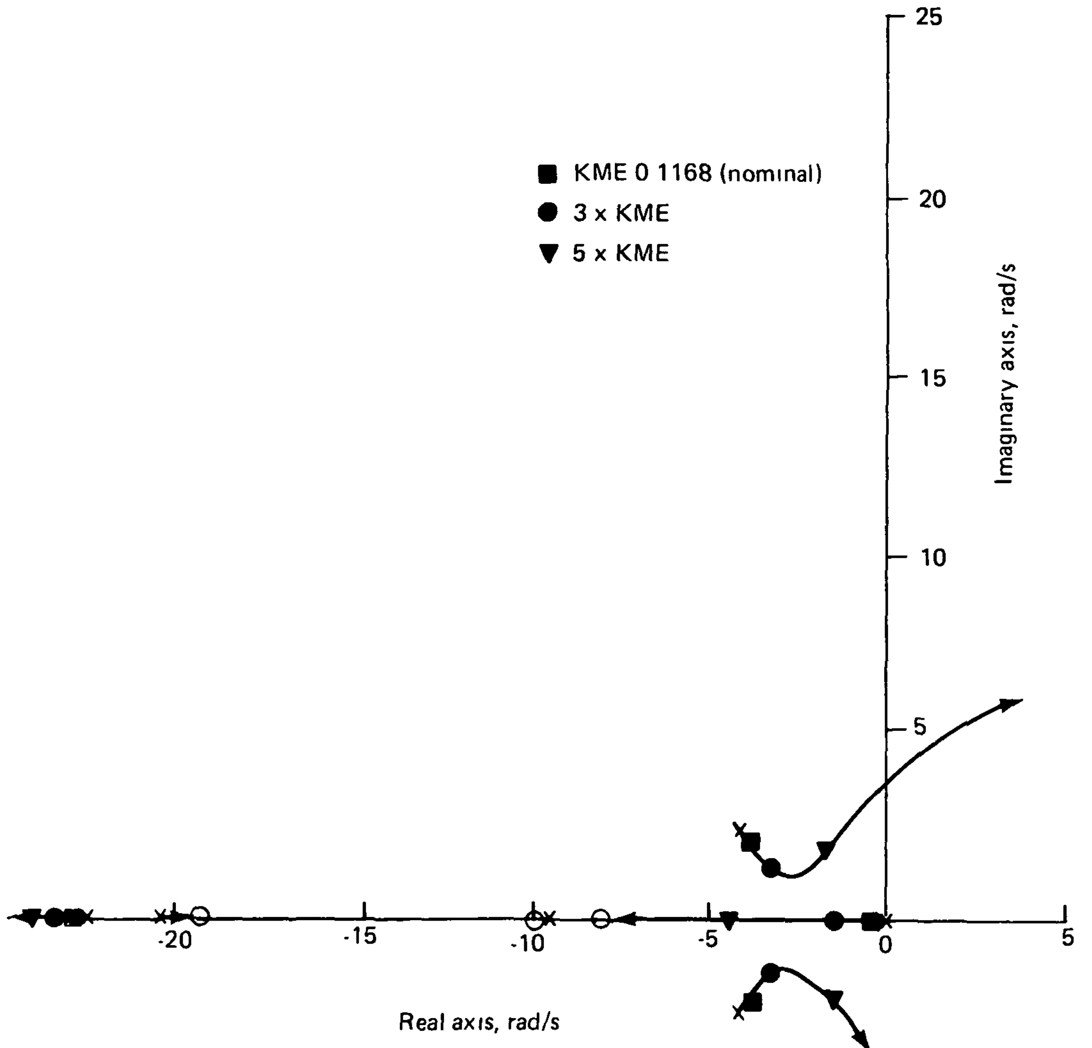

Figure 140. QSAE Model MLC, Root Locus on KME (Flight Condition 2)

Wing bending moment equations developed for the QSAE model were applied to this same Flight Condition 2. Those equations are a function of angle of attack, load factor, and aileron deflection. Responses were calculated at wing station $\eta = 0.25$ near the wing root and at wing station $\eta = 0.75$ near the control surface. Time responses for an incremental 1.5g load due to an elevator column pulse command are presented in Figure 141. The MLC significantly reduced the wing root bending moments during the 1.5g low-frequency input maneuver. The incremental bending moment near the controlling surface has been almost negated by the MLC.

Dynamic Model GLA Synthesis—The GLA system attenuates the dynamic response of the higher frequency wing bending modes when the aircraft is disturbed by sharp-edged gusts or continuous turbulence. The first wing bending mode is a main contributor to wing structural dynamic loading.

The GLA filter consists of a bandpass filter encompassing the frequency region of the first wing bending mode. The first mode frequency range was determined from a locus plot (fig. 142) of the open loop poles (PAS and MLC active) for each of the dynamic model flight conditions (table 23). The frequency range of the first wing bending mode ranged from 1.6 to 3.0 Hz. A filter bandwidth between 1.4 and 4.0 Hz was selected. The higher band limit includes some higher frequency wing modes including the 3.2 Hz flutter critical bending torsion mode; damping of that flutter mode was increased a small amount by this filter. The damping of the first wing mode was further improved by altering the phase of the feedback signal with a first-order lag filter (fig. 132).

The GLA employs the full-span outboard aileron in response to a wing vertical accelerometer output to reduce wing structural bending moments. The optimum wing accelerometer location was investigated by a zero locus technique as shown in Figure 143. The open loop zeros with respect to an aileron deflection were computed for six accelerometer locations along the elastic axis of the outboard portion of the wing (structural nodes 1416 through 1421 of fig. 126). This zero locus plot for flight condition V_B also includes the open loop poles. In placing the accelerometer, a location should be chosen where the associated transfer function has no right half-plane zeros. Further, the accelerometer location should place the zeros relative to the mode poles to offer the maximum potential for increasing critical mode damping.

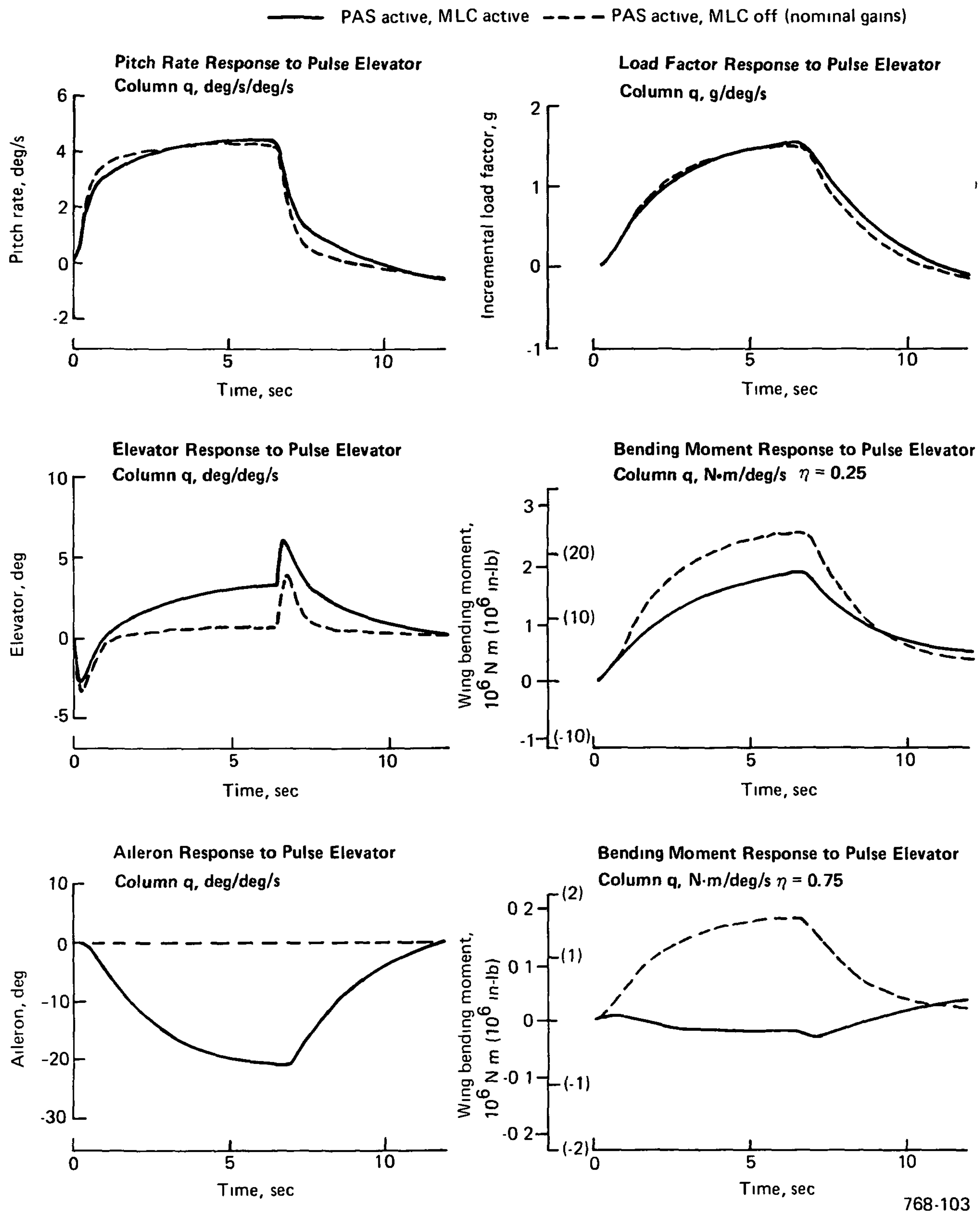

Figure 141. QSAE Model, 1.5g 6.5-sec Column Pulse Time Histories, MLC Control Law Synthesis (Flight Condition 2)

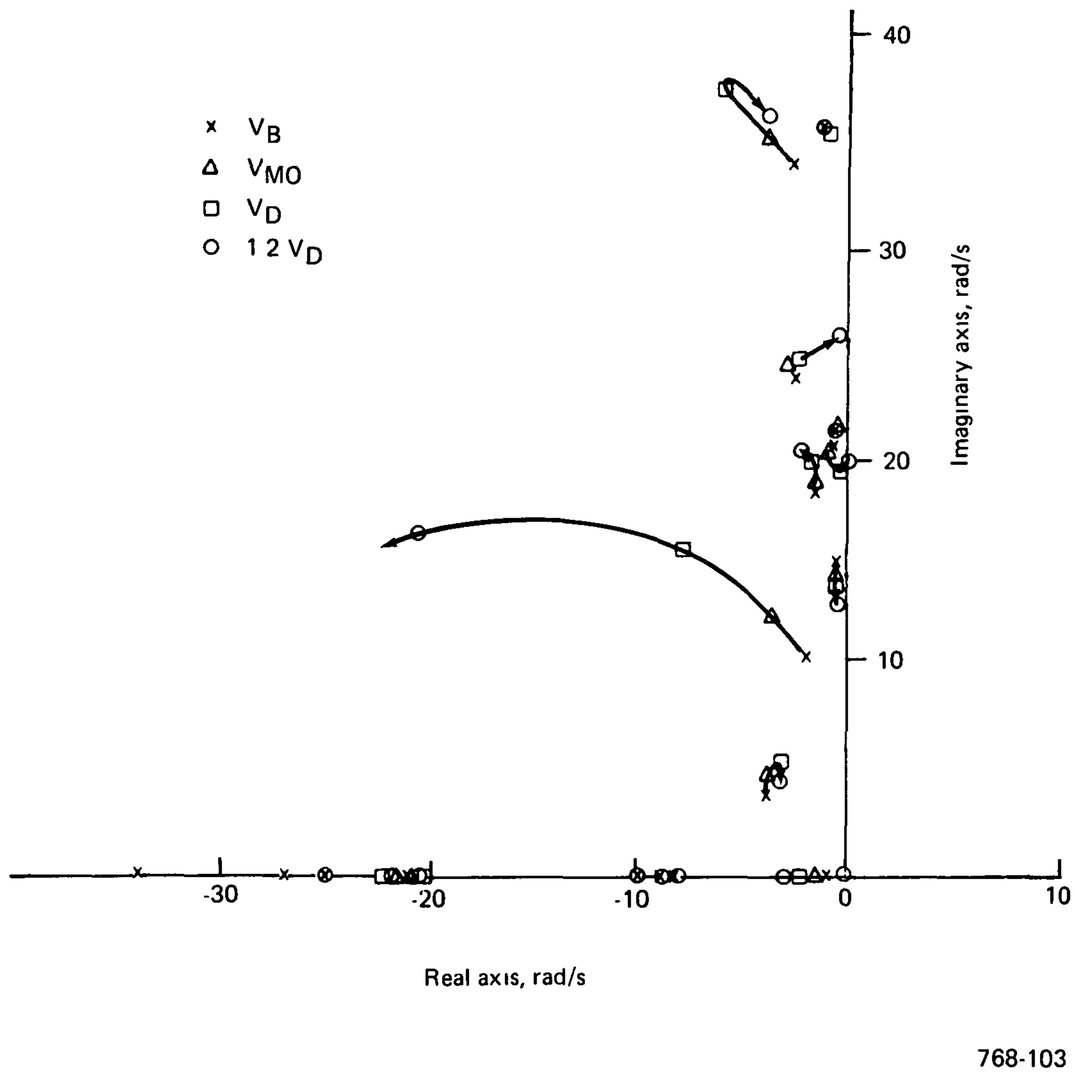

Figure 142. Dynamic Model, Pole Locus as a Function of Flight Condition (PAS MLC Active)

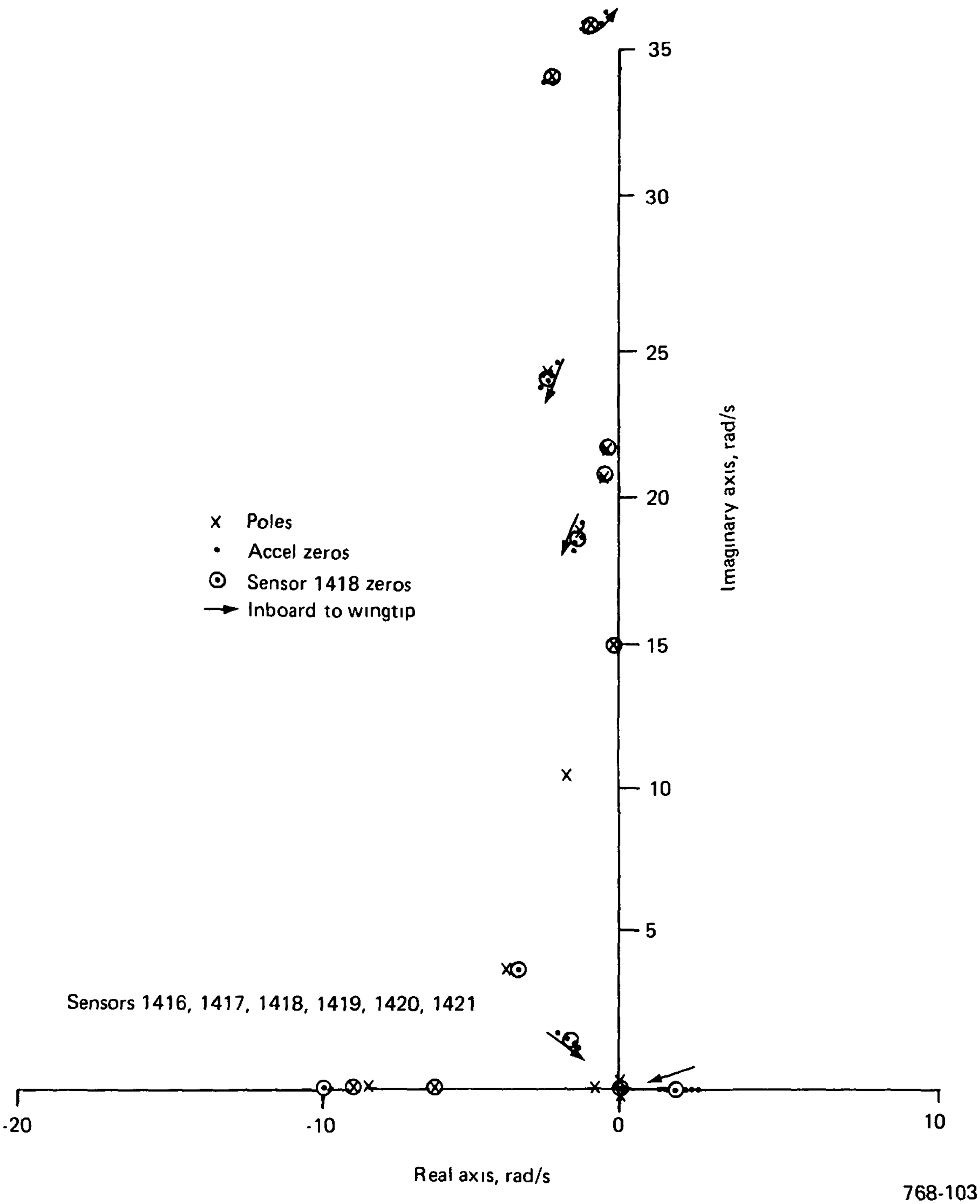

Figure 143. Dynamic Model, GLA Wing Accelerometer Zero Locus (Flight Condition V_B)

The zero locus shows that no close proximity zero is located near the first wing bending moment pole for an outboard aileron input. Other zeros are located close to the remaining higher frequency poles. Node 1418 was selected for the GLA vertical accelerometer location (fig. 126) because of its installation accessibility along the elastic axis in the outboard wing box.

The optimum values of the GLA gain KG and time constant τ of Figure 132 were extracted from root locus plots such as those of Figures 144 and 145. The final values corresponded to optimum damping of the first mode as shown for flight condition V_B. Gain scheduling of both constants with flight condition was necessary to retain optimum damping.

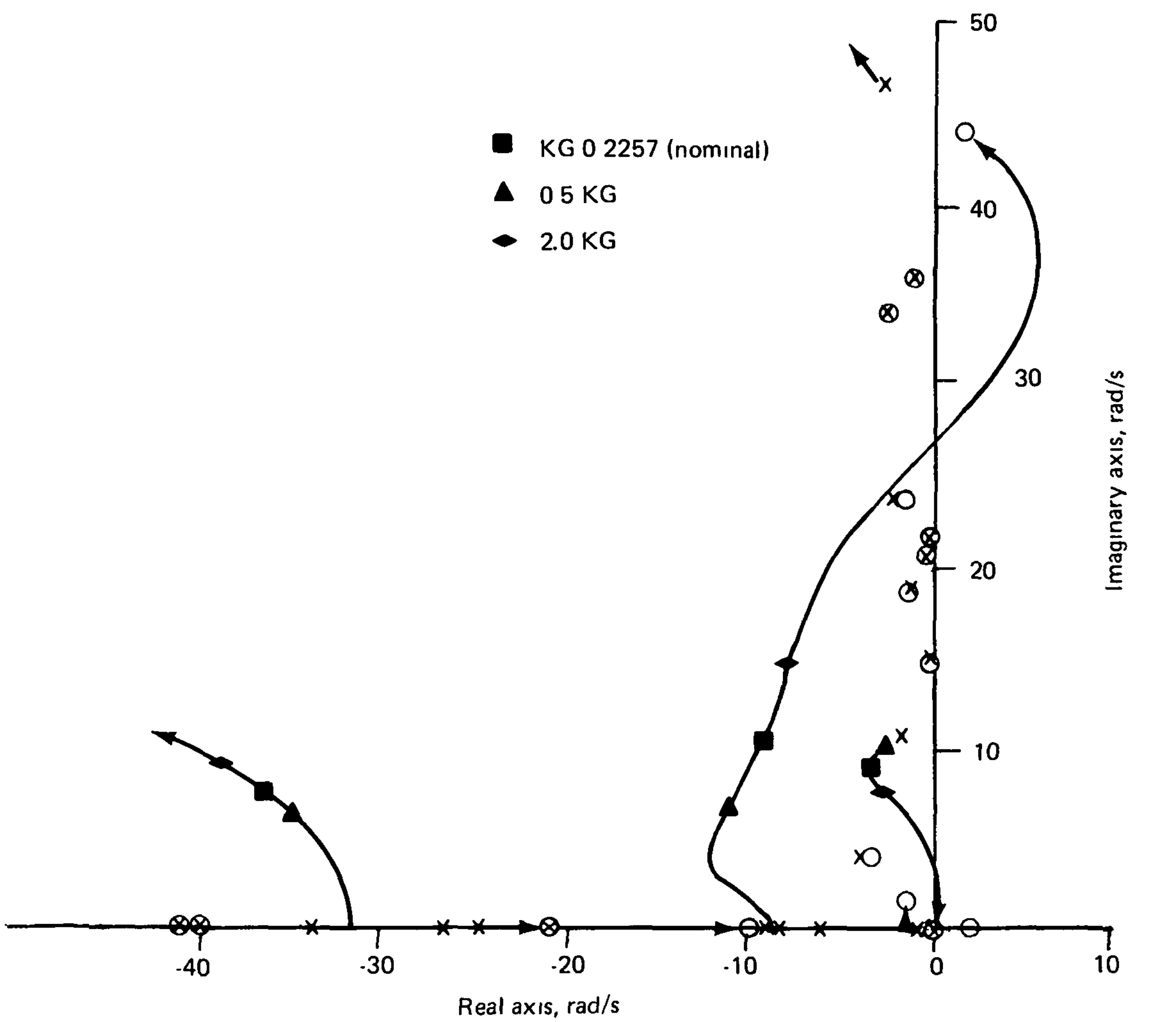

Figure 144 Dynamic Model, WLA Root Locus on KG (Flight Condition V_B)

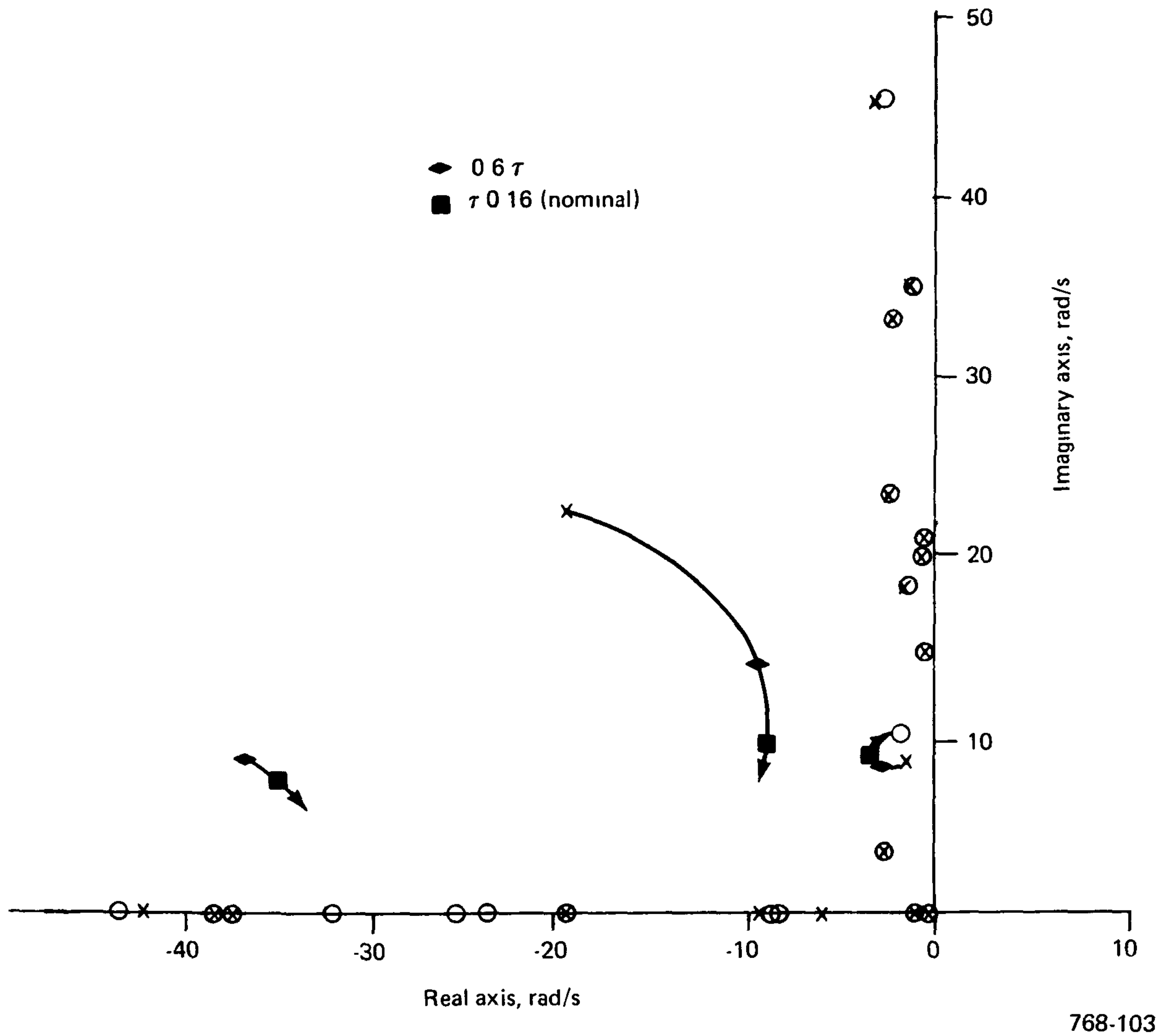

Figure 145. Dynamic Model, WLA Root Locus on τ (Flight Condition V_B)

The MLC control law was unchanged from the QSAE model synthesis. Figures 146 and 147 illustrate the effects of changing the gain constants KMA and KME, respectively, for flight condition V_B of the dynamic model. The higher frequency elastic modes were relatively unaffected by MLC gain changes.

Wing bending moment equations were generated for the dynamic model for the wing station $\eta = 0.25$ and wing station $\eta = 0.75$ (refer to subsec 7.3.1.1 for the equation description). Responses for a 1.5g incremental load due to an elevator column pulse

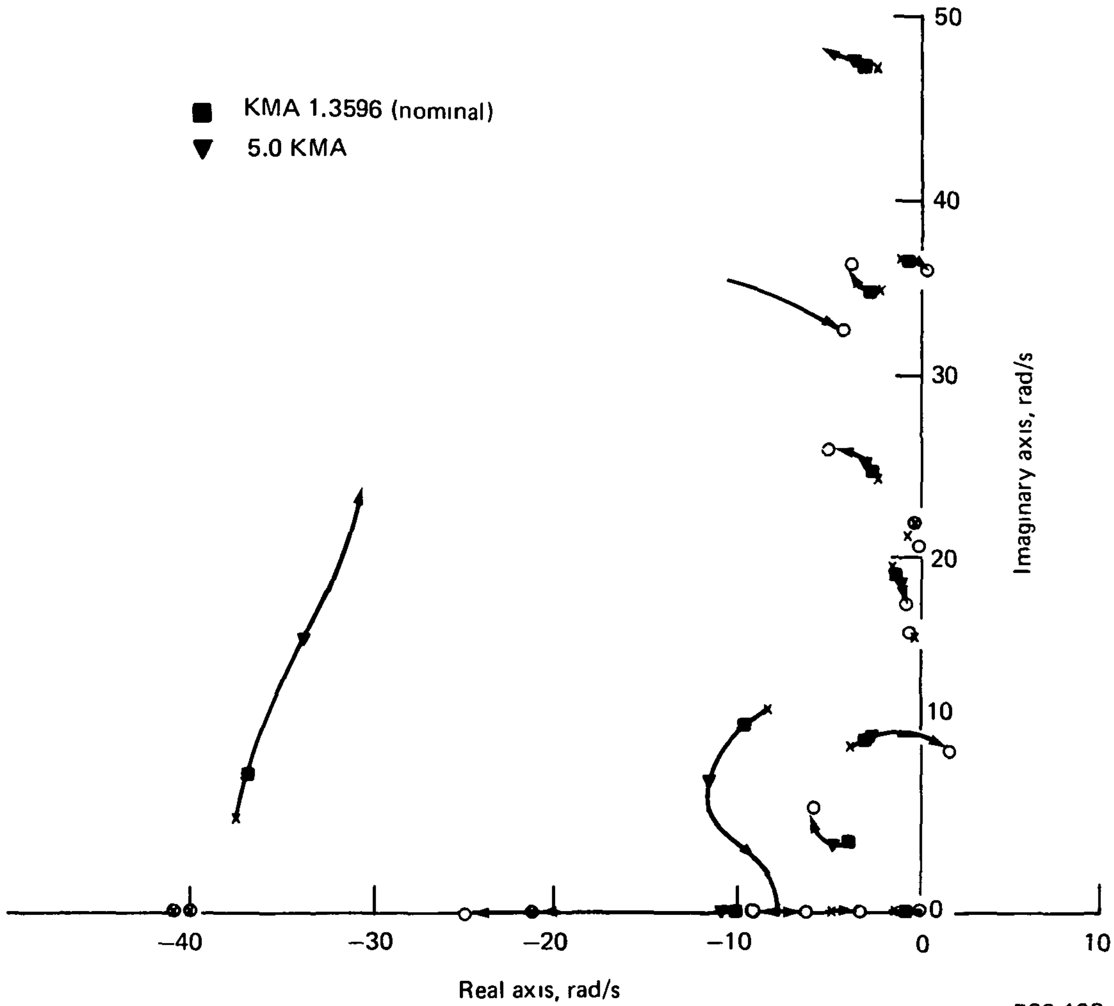

Figure 146. Dynamic Model, WLA Root Locus on KMA, WLA Control Law Synthesis, PAS MLC GLA Active (Flight Condition V_B)

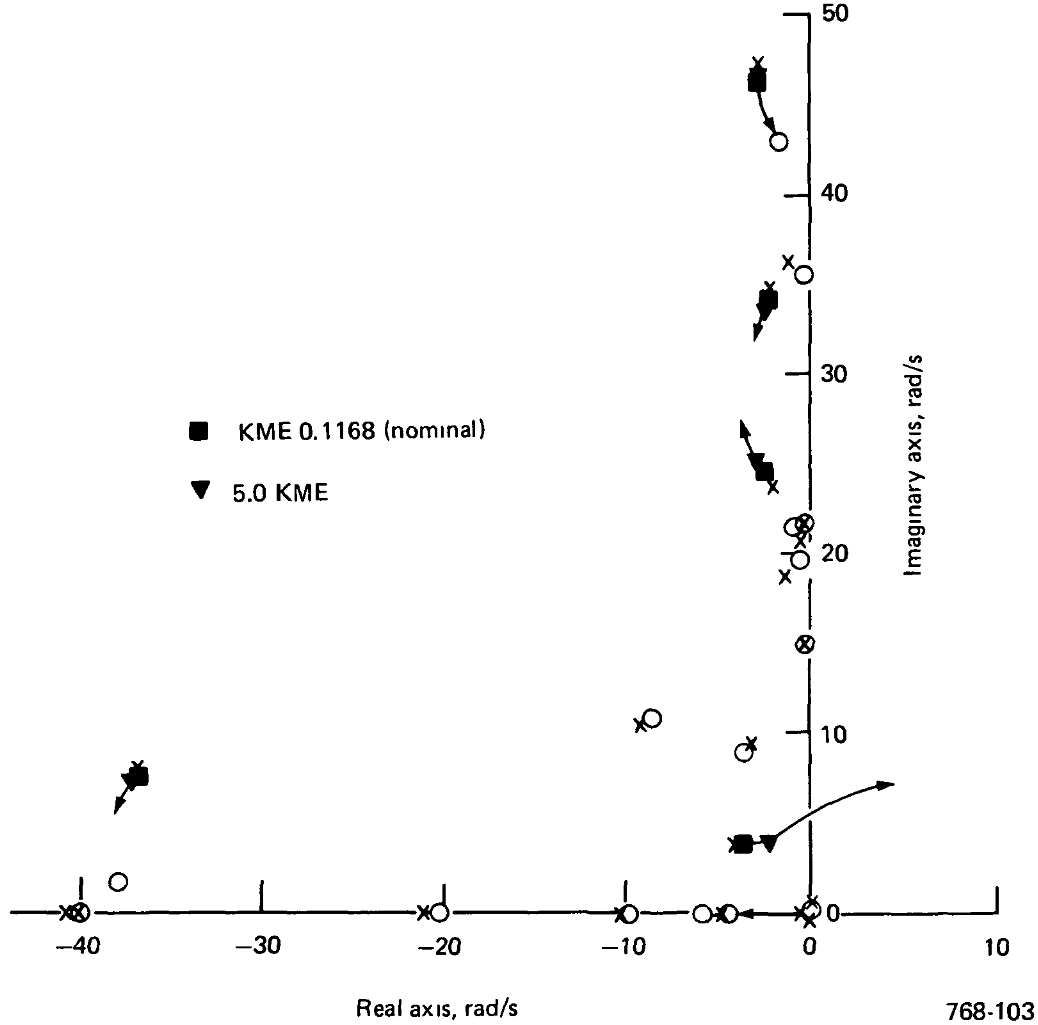

Figure 147. Dynamic Model, WLA Root Locus on KME (Flight Condition V_B)

command are shown in Figure 148 for flight condition V_B. For the low-frequency column input, reductions in incremental bending moment were similar to those reductions obtained with the QSAE model (fig. 141).

The effectiveness of the WLA was demonstrated by a power spectral density analysis when higher frequency gust excitation, in the form of von Karman vertical continuous turbulence, was encountered. A gust intensity of 0.3 m/s (1 ft/s) with an integral scale of 762m (2500 ft) was input.

The form of the von Karman vertical gust spectrum is

$$\phi(\omega) = 2K\,\sigma_Z^2 = \frac{\left(\frac{L}{V}\right)\left[1 + 4.7811\left(\frac{L}{V}\right)^2 \omega^2\right]}{\left[1 + 1.7929\left(\frac{L}{V}\right)^2 \omega^2\right]^{\frac{11}{6}}}$$

where

ϕ = gust spectrum in ($)^2$/Hz
σ_Z = root mean square (rms) turbulence level of gust
V = true airspeed
L = integral scale (characteristic length) of turbulence
ω = the frequency
K = arbitrary user constant

Bending moment decreased as first the MLC and then the GLA were activated (figs. 149 and 150). The MLC, active without the GLA, adversely increased the magnitude of the first wing bending mode response. However, the PAS-MLC-GLA combination demonstrated the effectiveness of the WLA design control laws. The GLA reduced the bending moment due to the first wing bending mode and, to a lesser extent, the higher frequency modes, as intended. At the inboard wing, η = 0.25 station, the greatest power was concentrated in the pitch short-period region. As shown, the MLC effectively attenuated the power in this frequency region at both wing stations. The PAS also significantly reduced the bending moments in this region. $\bar{A}$ rms bending moment values for the various ACT control law configurations are indicated on the figures.

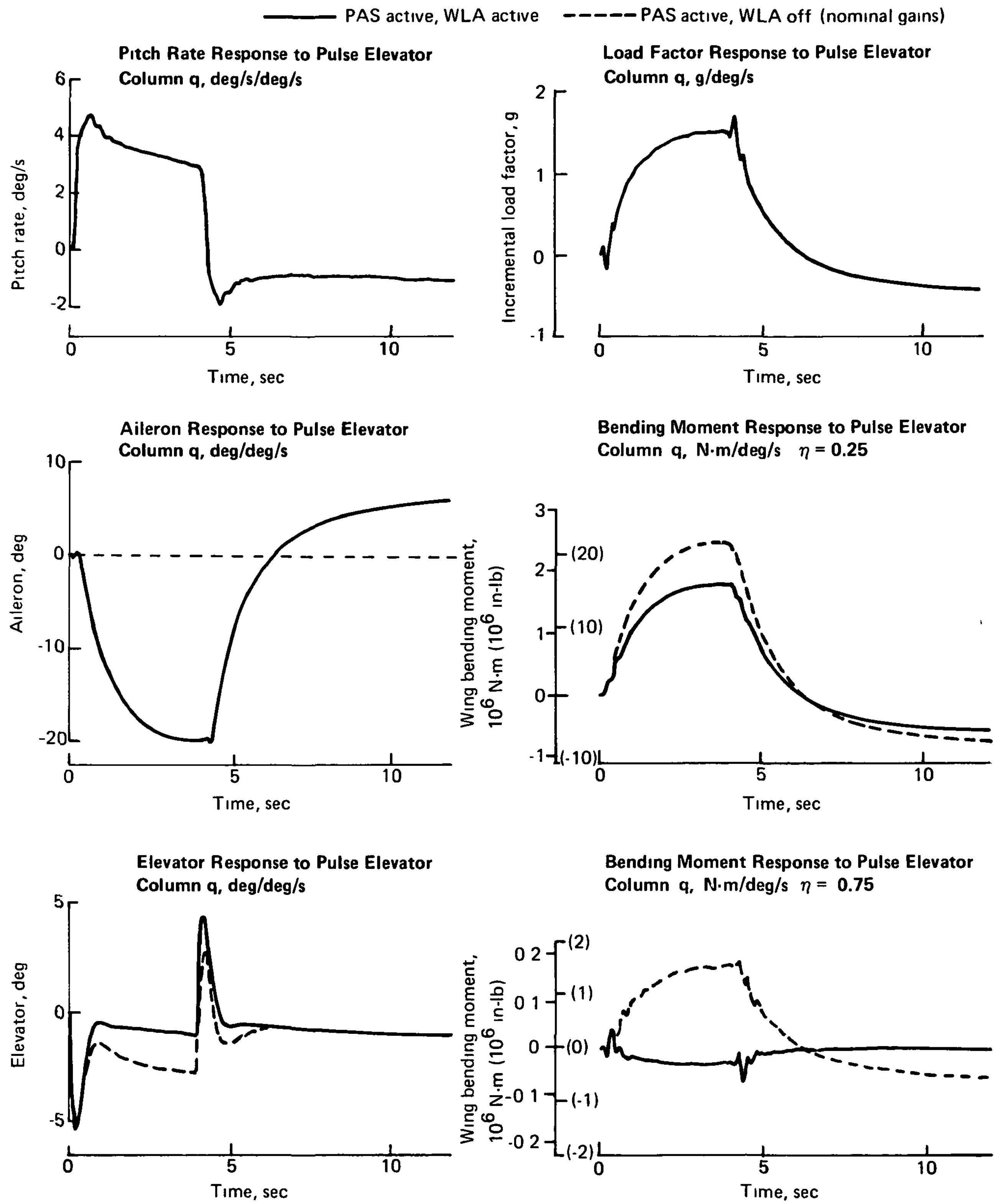

Figure 148. Dynamic Model, 1.5g 4.0-sec Column Pulse Time Histories, WLA Control Law Synthesis (Flight Condition V_B)

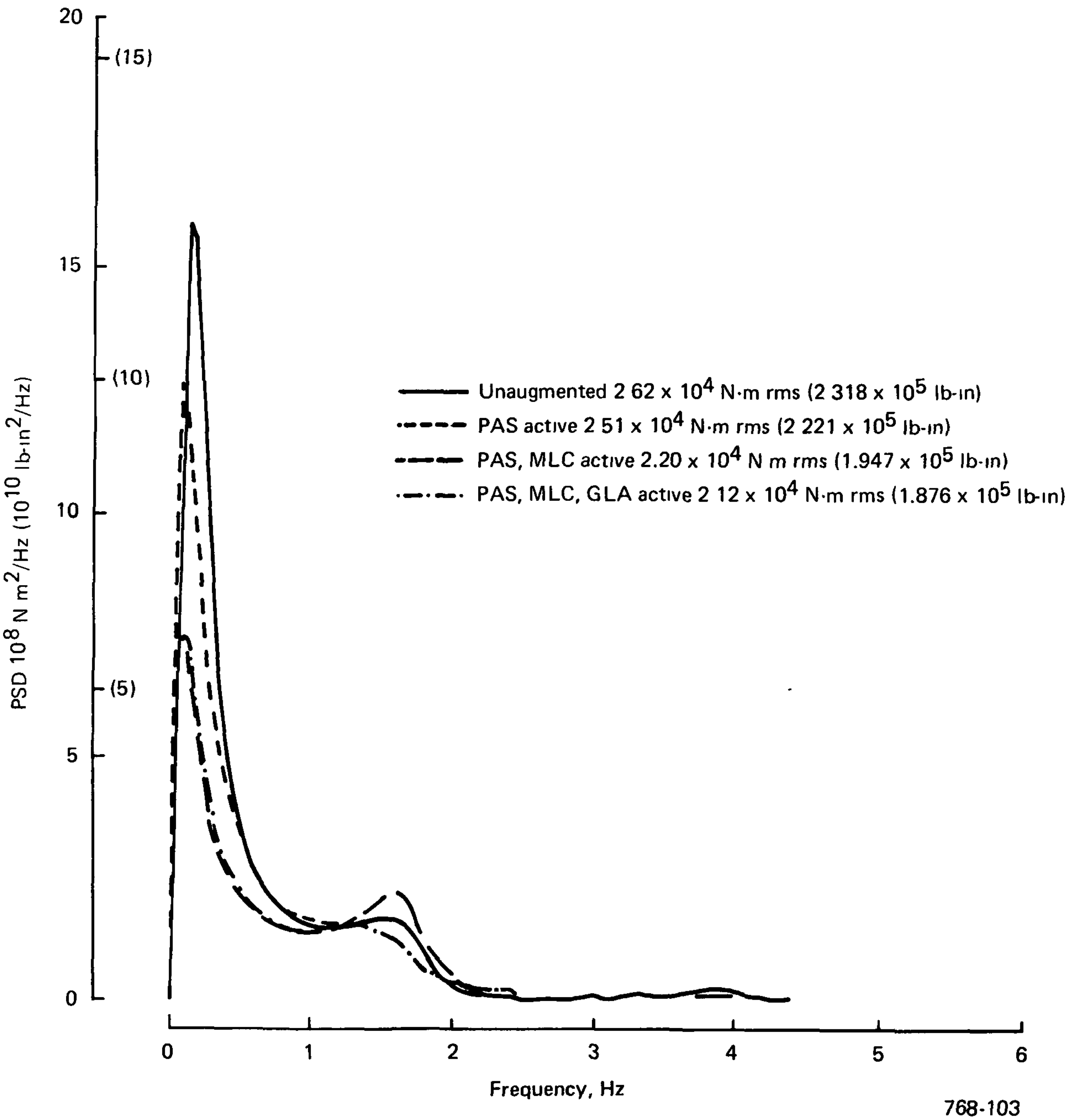

Figure 149. Initial ACT Symmetrical Dynamic Model, Bending Moment to 0.3 m/s von Karman Vertical Gust, PSD (N·m)^2/hz, η = 0.25 (Flight Condition V_B)

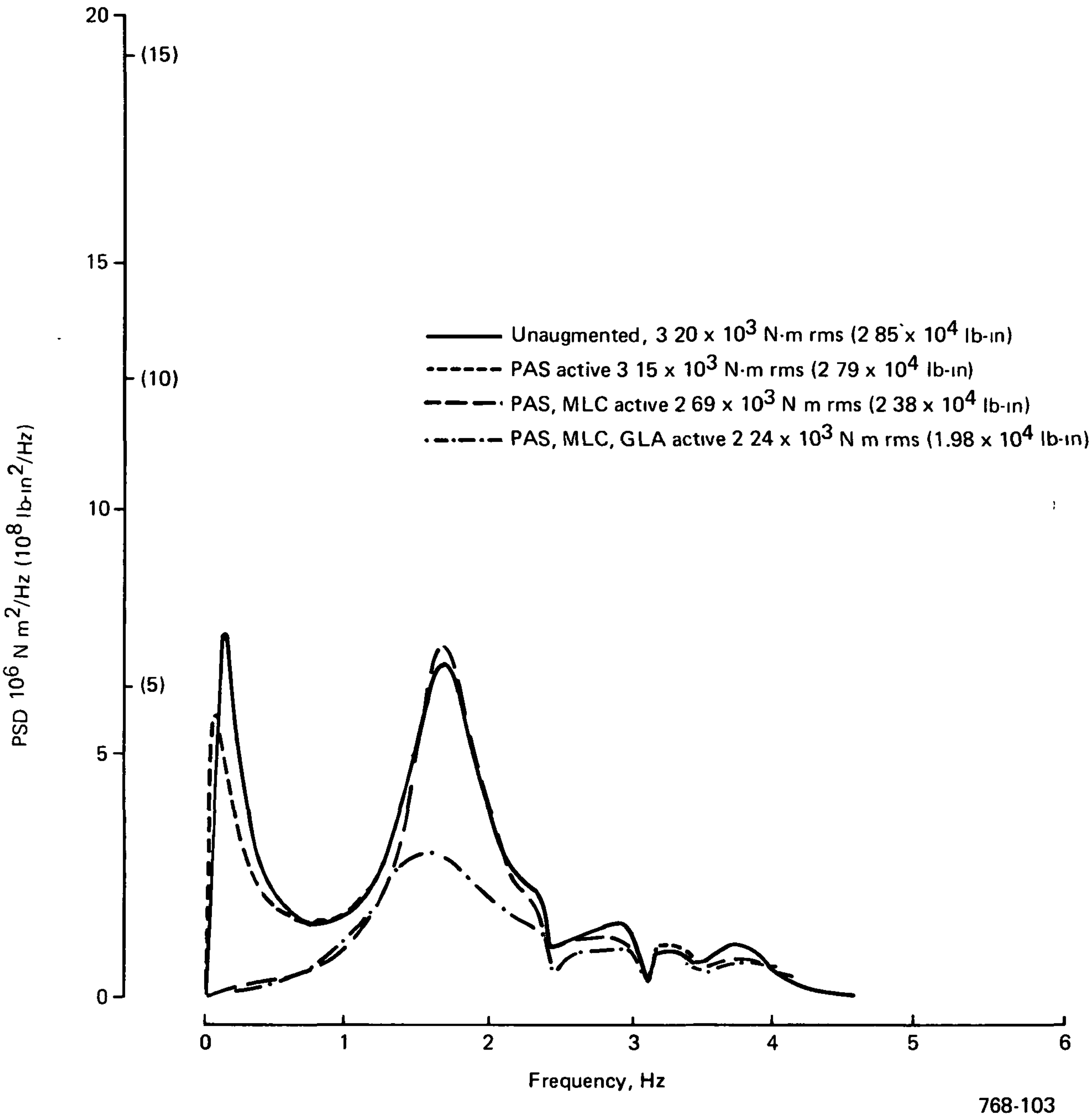

Figure 150. Dynamic Model, Bending Moment to 0.3 m/s von Karman Vertical Gust, PSD (N·m)^2/Hz, η = 0.75 (Flight Condition V_B)

The MLC and GLA meet the phase and gain margin requirements specified in the design requirements and objectives (DRO). The MLC stability margins were verified with both the "current" QSAE and dynamic models. The GLA margins were checked with the dynamic models.

7.3.1.4 FMC Description

The FMC uses the inboard section of the outboard aileron as the controller. Feedback is signaled from a single vertical acceleration sensor at wing location 1417 (fig. 126). The accelerometer signal is fed through a fixed bandpass filter.

The FMC was designed to provide, for any critical flutter mode, a damping coefficient $g \geq 0.03$ for all altitudes and speeds up to V_D and a $g \geq 0.0$ for all altitudes and speeds up to $1.2V_D$. In the present instance, the critical mode (No. 3 in fig. 102) had $g = 0$ at V_D and $g = 0.022$ at $1.2V_D$ without FMC. With FMC, $g = 0.074$ at V_D and $g = 0.044$ at $1.2V_D$. The FMC system cooperates with the MLC system but does not rely on it to provide the design damping.

The mathematical model of the airplane used for FMC synthesis incorporated elastic structural modes (subsec 7.3.1.1). The degrees of freedom were u, w, q, and the flexible modes ζ_1 through ζ_{19}.

The FMC was verified for the heavy-weight condition of the airplane at V_B, V_{MO}, V_D, and $1.2V_D$. The additional data are given in Table 20 and plotted on the airplane's speed and altitude envelope in Figure 133. The plots of the critical mode frequency and damping versus the equivalent airspeed (V_e) are shown in Figure 102 for the FMC on and off.

Synthesis Method—As the primary tool used in determining an appropriate FMC loop filter, the root locus was first used to help choose a "good" location on the wing planform for the accelerometer. With PAS and MLC active, the locus of zeros of the $\ddot{Z}/\delta_{OAI}(S)$, transfer function was determined as a function of wing location for the flight conditions V_B, V_{MO}, V_D, and $1.2V_D$. The accelerometer should be placed so that: (1) the associated $\ddot{Z}/\delta_{OAI}(S)$ transfer function has no right half-plane zeros and

(2) its zeros, relative to the critical flutter mode poles, offer the potential to maximize the critical mode damping.

The zero locus indicated the vicinity of location 1416 through 1420 (see subsec 4.6.1.1) as desirable. Figures 151 and 152 show the mode poles and the locus of zeros, at the V_D and $1.2V_D$ flight conditions, for accelerometer movement from location 1416 to locations 1417, 1418, and 1419. Evaluation of the zero loci indicated location 1417 as desirable for the FMC system. Interestingly, location 1414 had a right half-plane zero in the vicinity of the critical mode at the $1.2V_D$ flight condition.

For the proper loop phasing to damp the critical mode, the literature on flutter mode control suggested an FMC accelerometer filter of the form:

$$\frac{K \cdot S}{\left(\frac{S}{\omega_l} + 1\right)\left(\frac{S}{\omega_c} + 1\right)^2}$$

where ω_c is chosen to equal, or nearly equal, the critical mode frequency. The frequency ω_l may be equal to, or somewhat less, than ω_c. For the Initial ACT airplane, ω_c was taken to be 20 rad/s, and 15 rad/s was found to be an acceptable value for ω_l.

Figures 153 and 154 show the FMC root loci for the V_D and $1.2V_D$ flight conditions with PAS and MLC active. The improved damping of the critical mode at V_D is shown by comparing the vertical displacement (relative to the body) of the wing at the FMC sensor in response to a 10 deg, 0.5 sec wide pulse input at the FMC summing junction with the feedback loop open and closed (fig. 155).

Examination of these root loci show that, although the critical mode is stabilized, the first mode frequency and damping decreased by approximately 50%. This mode softening may adversely affect the performance of the GLA system. The time available for the Initial ACT design phase precluded examination of the performance of the FMC and GLA system operating together at the V_D and $1.2V_D$ flight conditions.

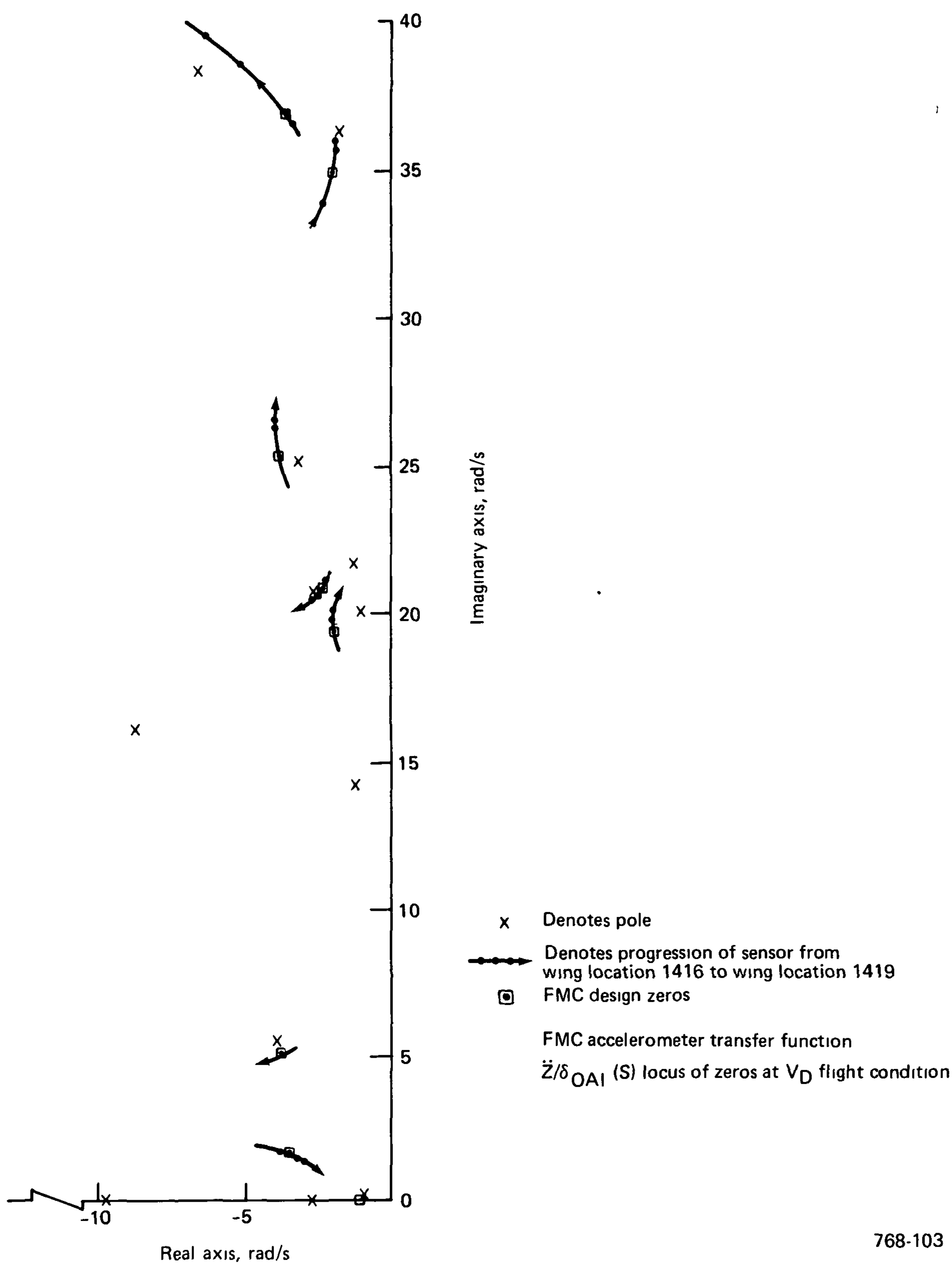

Figure 151. Dynamic Model, FMC Wing Accelerometer Zero Locus (Flight Condition V_D)

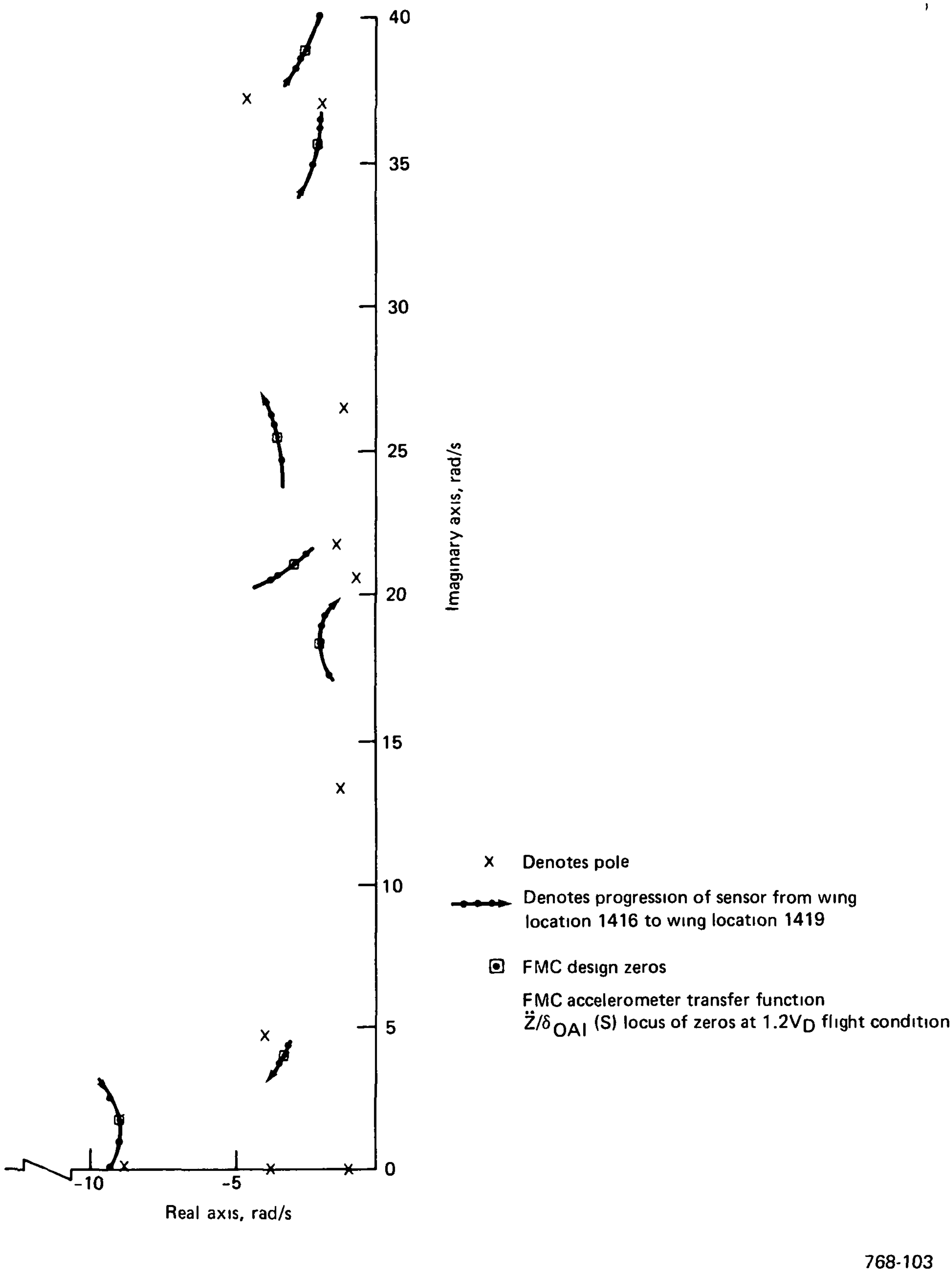

Figure 152 Dynamic Model, FMC Wing Accelerometer Zero Locus (Flight Condition $1.2V_D$)

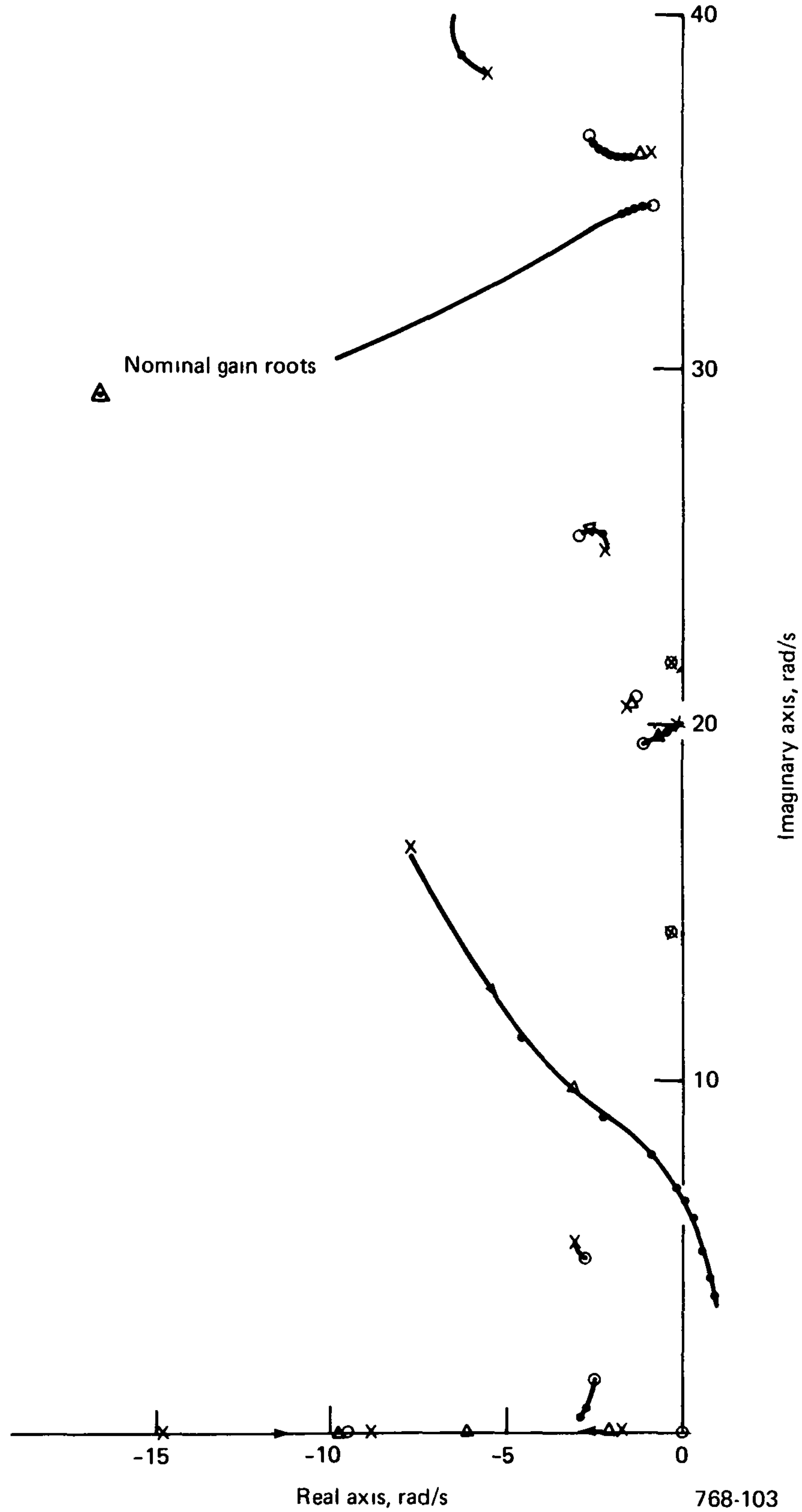

Figure 153. FMC Root Locus at V_D

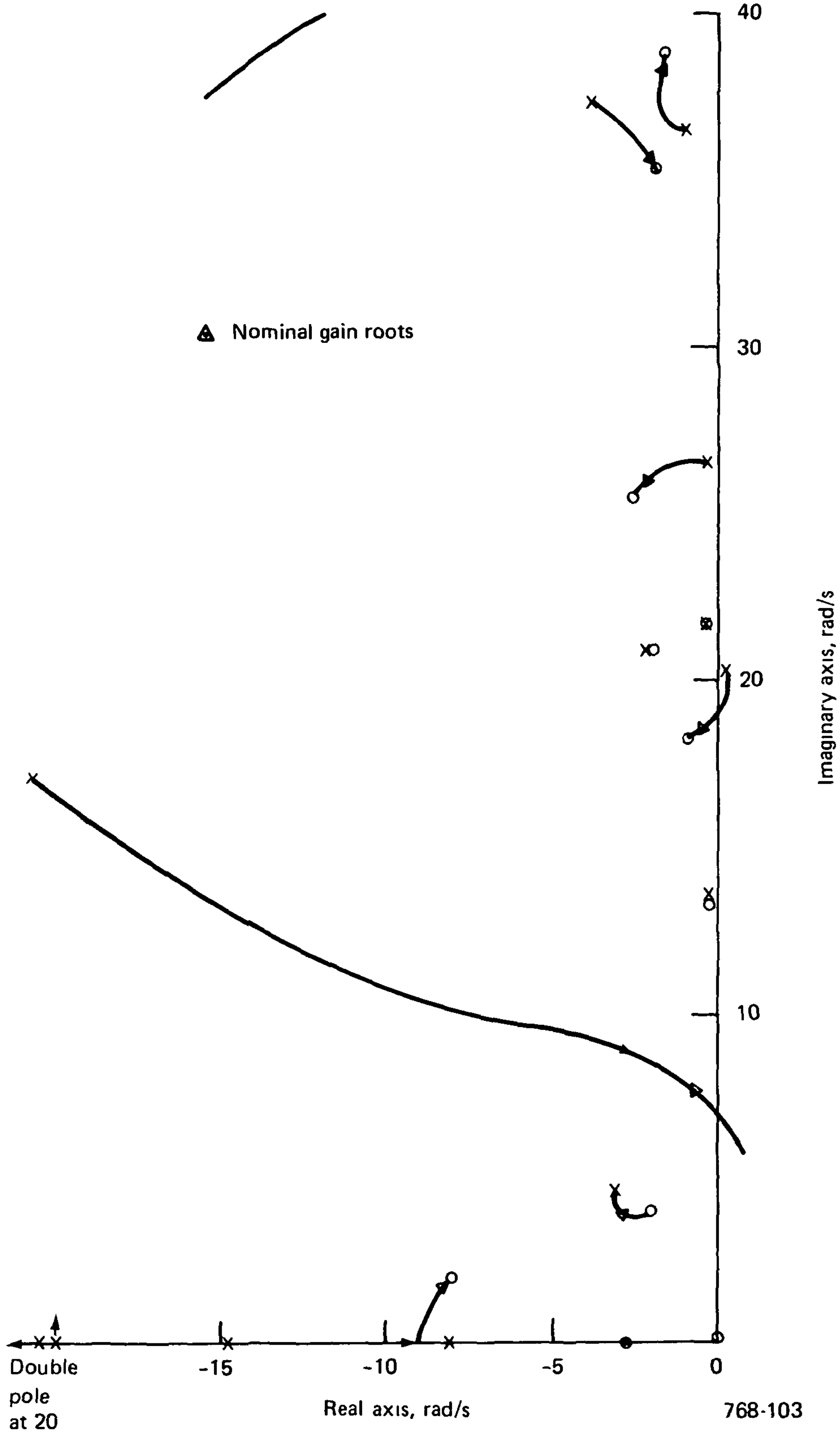

Figure 154. FMC Root Locus at 1.2V_D

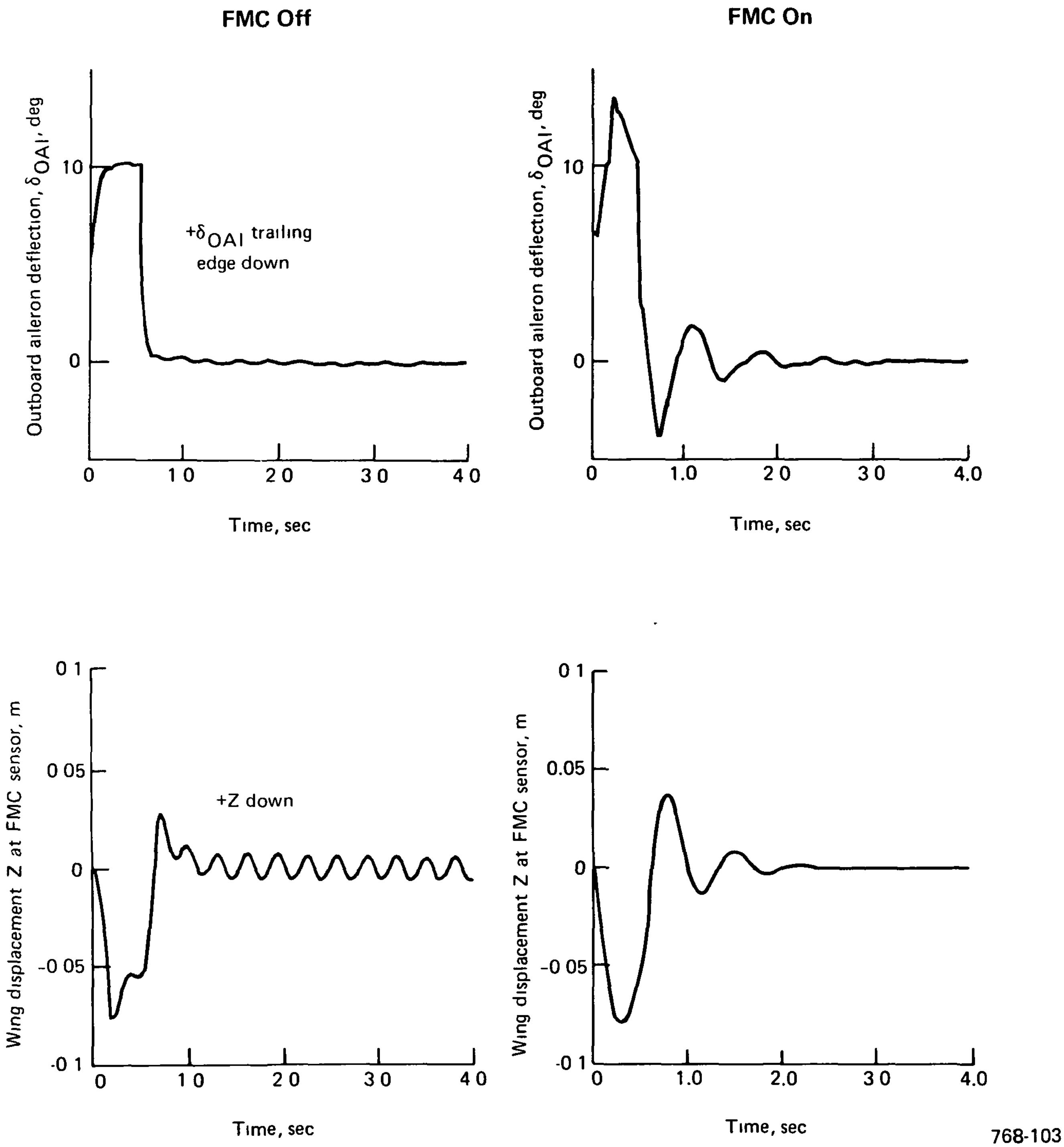

Figure 155. Response of Aileron and Wing Displacement at FMC Sensor to a 10-deg, 0.5-sec-Wide Pulse Input to the FMC Summing Junction

7.3.2 SYSTEM MECHANIZATION

7.3.2.1 ACT System Architecture

The Initial ACT system mechanizes four ACT functions, PAS, WLA, FMC, and angle-of-attack limiter (AAL). Figure 156 outlines the interface between major sensors, computers, and actuation systems. This control system shares sensors with the automatic flight control and avionics functions of the Baseline Configuration. Each computer receives signals directly from the sensors in the same channel, and the data from the sensors in other channels are transferred from the other computers over cross-channel links. These are dedicated one-way high-speed digital data buses that connect transmitters and receivers in the computers. This cross-channel data communication scheme has been used in the Baseline automatic flight controls system (AFCS) and other applications. The crucial ACT function (PAS) is mechanized in quadruple redundancy, and the critical functions (WLA, FMC, and AAL) are mechanized in triple redundancy. To minimize the probability of loss of all critical functions if two computers fail, the critical functions are distributed among the four computers, which have identical software for interchangeability.

Each computer consolidates all input signals (analog, digital, and discrete) in a signal selection and failure detection (SSFD) process. The SSFD process selects the most trustworthy of the redundant sensor inputs. Controlled by software, the process is necessarily varied because of differing signal character and use and differing levels of redundancy. Fundamentally, it uses midvalue selection for three input signals, and average derivation for two inputs. A four-sensor set is treated as three with an operating standby. The failure detection is a software-controlled logical comparison of inputs and selected signal to single out any value that is inordinately different from the others.

The SSFD provides essentially the same sensor signal in all computers for computation of the control laws. Since the ACT functions require different redundancy levels depending upon function criticality and failure conditions, the SSFD process is varied as necessary to handle the different types of sensor signal. The computers of the Initial ACT system are frame synchronized such that each simultaneously executes the

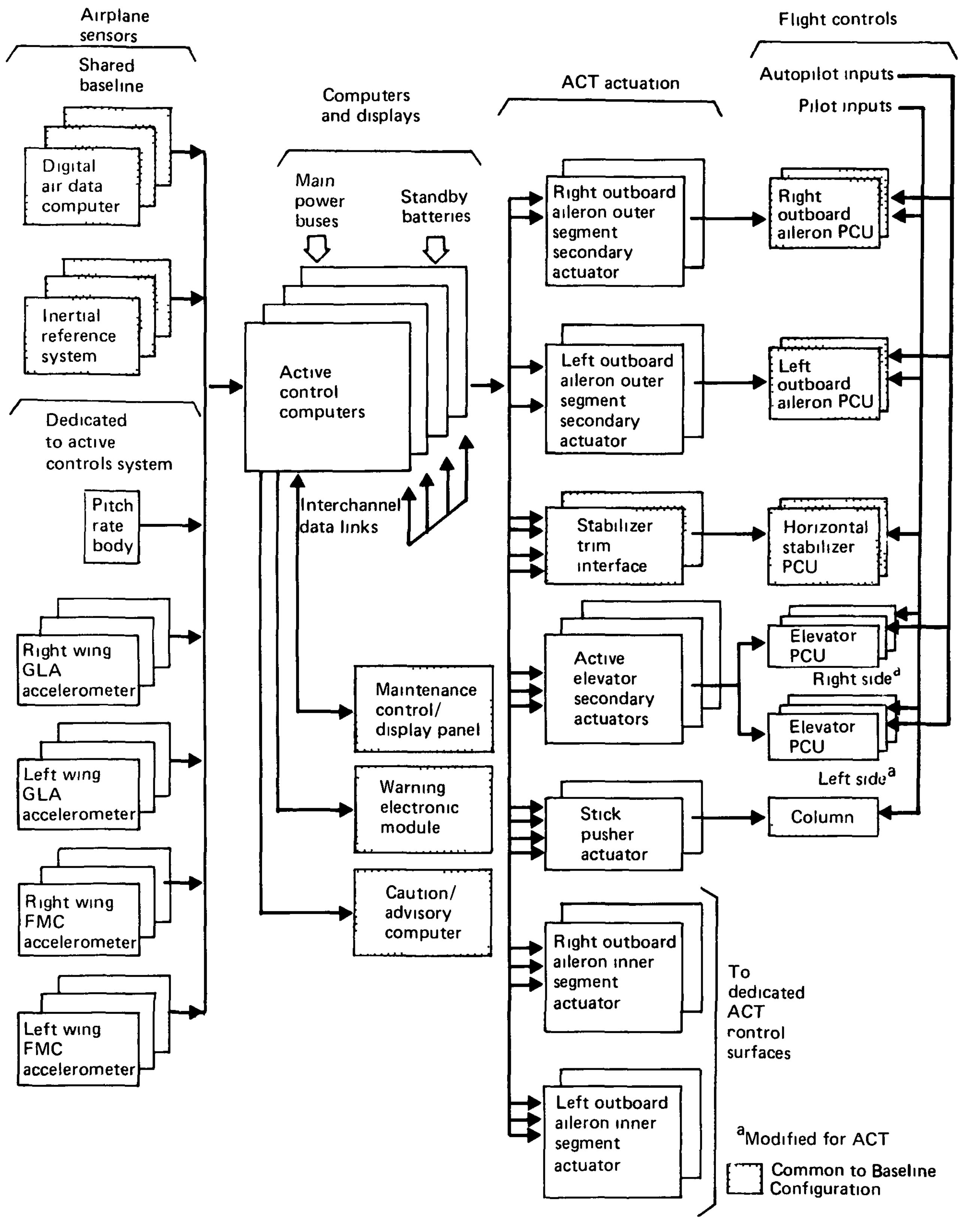

Figure 156. Initial ACT System Architecture

same computations. Using the SSFD process and frame synchronization, the four computers transmit identical command signals to the ACT actuators, reducing the need for actuator equalization, simplifying the design, and simplifying the failure detection algorithm for passive failures. The redundant ACT command signals sent to the actuators are consolidated at the actuator for use in a mechanical voting process.

Two basic concepts are used for the ACT actuator design. For the control surfaces driven by the pilot's mechanical signal and ACT signals, a force-summed multiple-channel actuation system converts the ACT electric signals into a mechanical signal that series-sums with the pilot's mechanical input. For the dedicated ACT control surfaces, the signal is fed directly to the ACT power control unit.

ACT Functions—The PAS function includes short-period and phugoid mode control. Figure 157 shows a block diagram of the redundant PAS and the elevator off-load functions. The short-period PAS is a crucial function that is implemented by quadruple sensors and computers and by triple actuators with mathematical models mechanized in the quadruple computers. The short-period control requires a fixed pitch-rate feedback gain, and the phugoid control requires an airspeed feedback to stabilize the airplane. The servo position signals are used to relieve a steady-state elevator trim deflection. This is achieved by trimming the horizontal stabilizer through the horizontal stabilizer trim interface (fig. 157).

The WLA function comprises the MLC and the GLA subfunctions. Figure 158 shows a block diagram of the WLA function. MLC reduces maneuver-induced wing vertical bending moment by sensing vertical acceleration at the airplane cg and by commanding the outboard aileron (both inner and outer sections). The feedback from the accelerometer at cg to the aileron destabilizes the short-period and phugoid modes, but cross-feeding the MLC command signal to the elevator compensates for the instability. The GLA function reduces wing loads induced by atmospheric disturbance by sensing vertical acceleration at both wings and commanding the outboard ailerons. For the outer section of the outboard aileron, force-summed secondary actuators convert the electric WLA command to a mechanical signal. The WLA and FMC electric command signals sum to drive the inner section of the outboard aileron dedicated to ACT control.

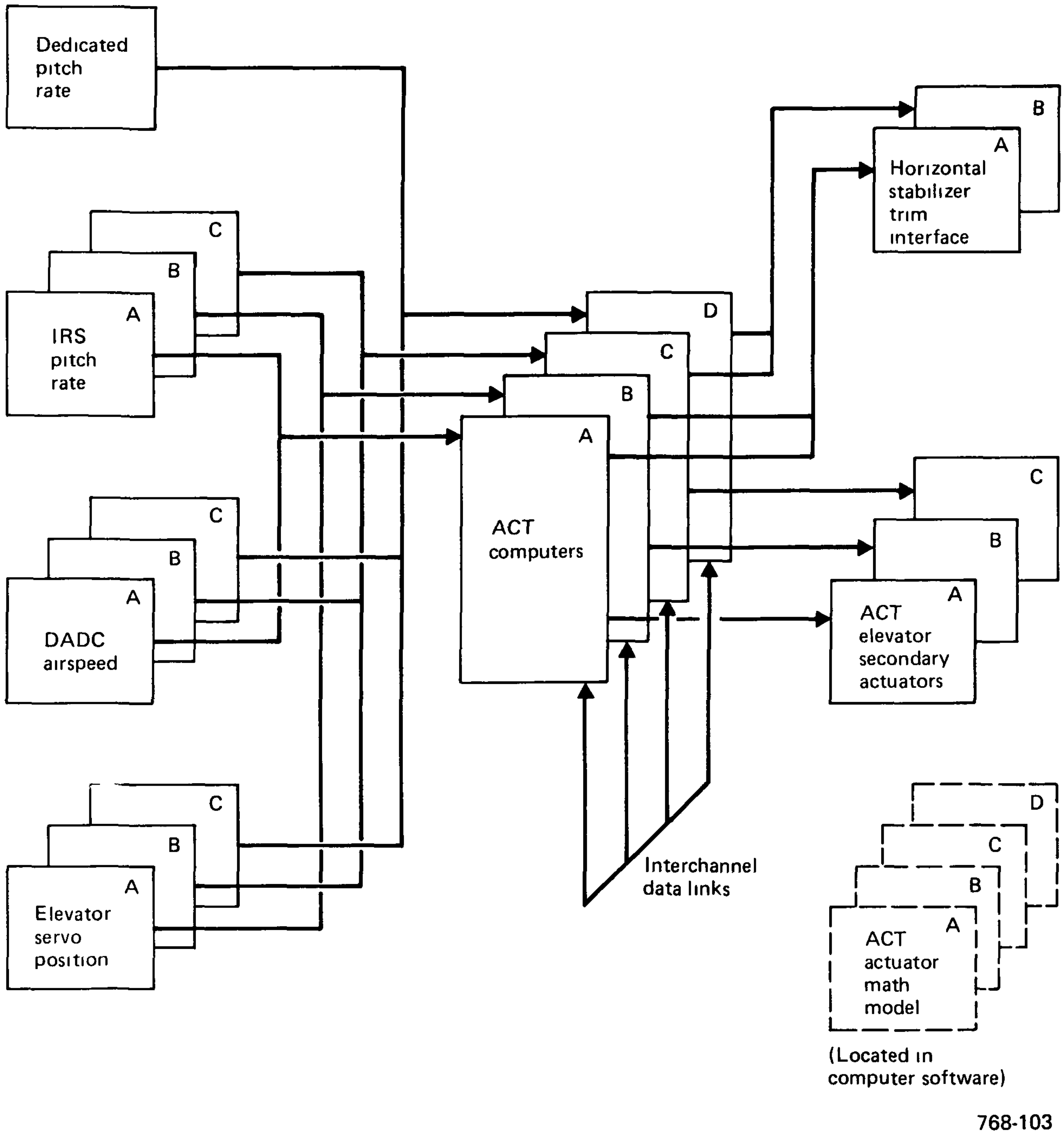

Figure 157. Pitch Augmented Stability (PAS)

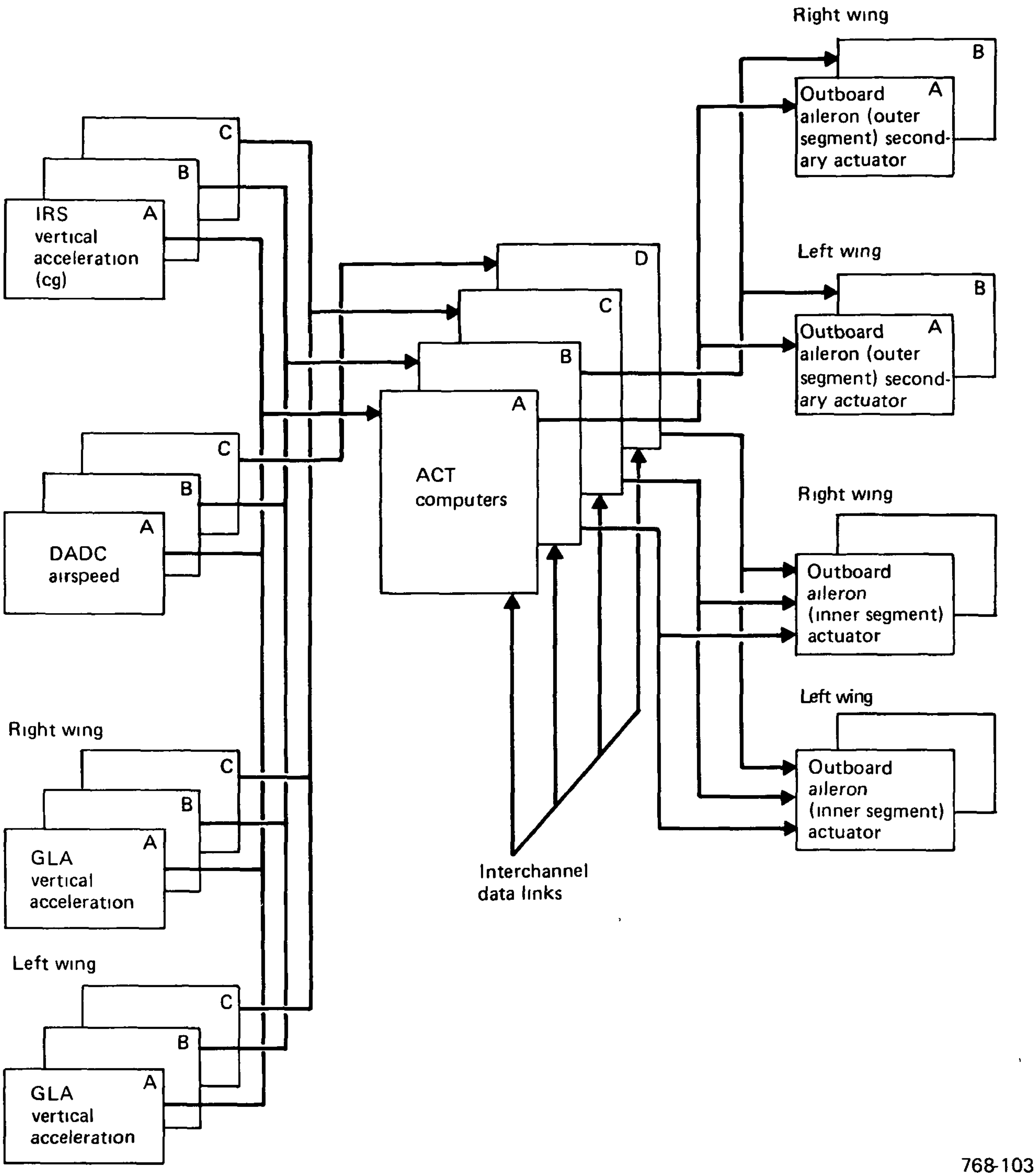

Figure 158. Wing Load Alleviation (WLA)

FMC senses wing acceleration and commands the outboard aileron (inner section) to extend the flutter-free speed margin up to $1.2V_D/M_D$ (the unaugmented flutter margin is V_D/M_D). Figure 159 shows a block diagram of the FMC function. The vertical

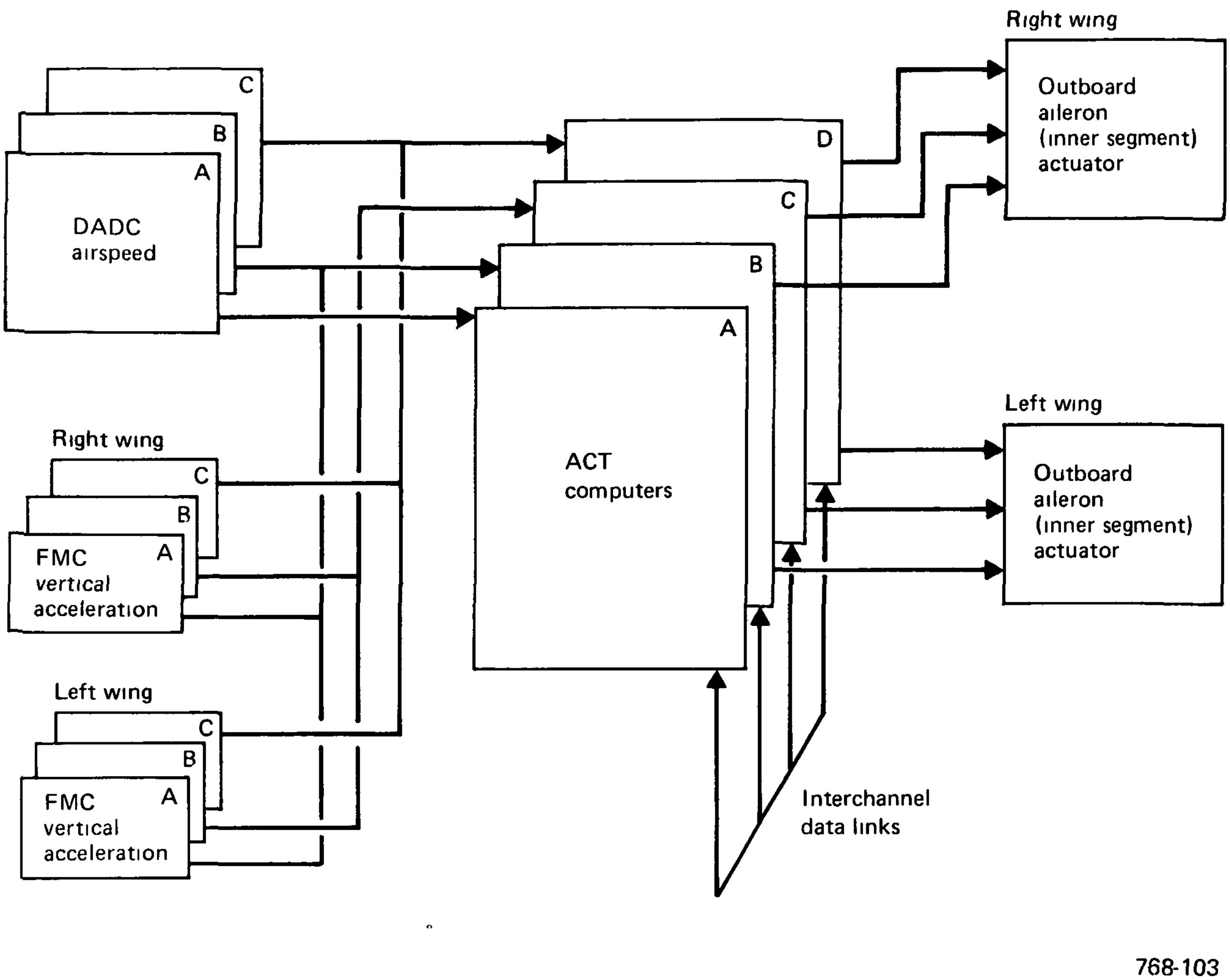

Figure 159. Flutter Mode Control (FMC)

acceleration signals from both wings are processed through shaping filters to generate the FMC command.

The AAL function prevents the ACT airplane from entering a deep stall by sensing angle of attack and pitch rate and commanding a forward (airplane nose-down) column deflection. Figure 160 is a block diagram of the AAL function. The pitch-rate signal is used to provide anticipation in the AAL control to prevent overshoot of the limiting angle-of-attack in rapid maneuvering.

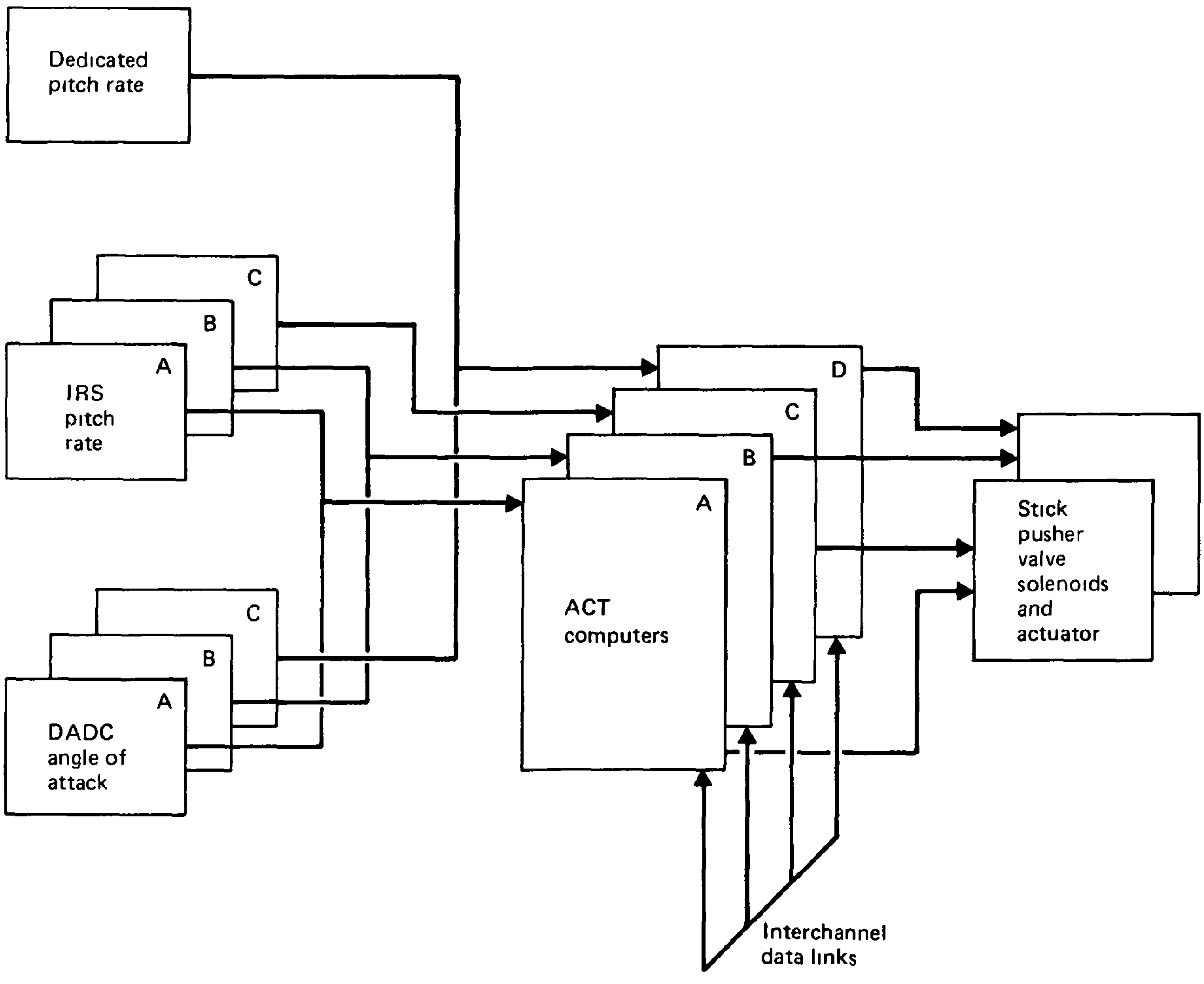

Figure 160. Angle-of-Attack Limiter (AAL)

7.3.2.2 Sensors

The Initial ACT system uses both shared and dedicated sensors to implement the various ACT functions. Figure 161 illustrates the general location of the major sensors. Many sensed parameters required for ACT are already in the Baseline Configuration inertial reference system (IRS) and the digital air data computer (DADC), both configured in triplex. These computers provide airspeed, Mach number, angle of attack, pitch rate, and vertical acceleration at the cg.

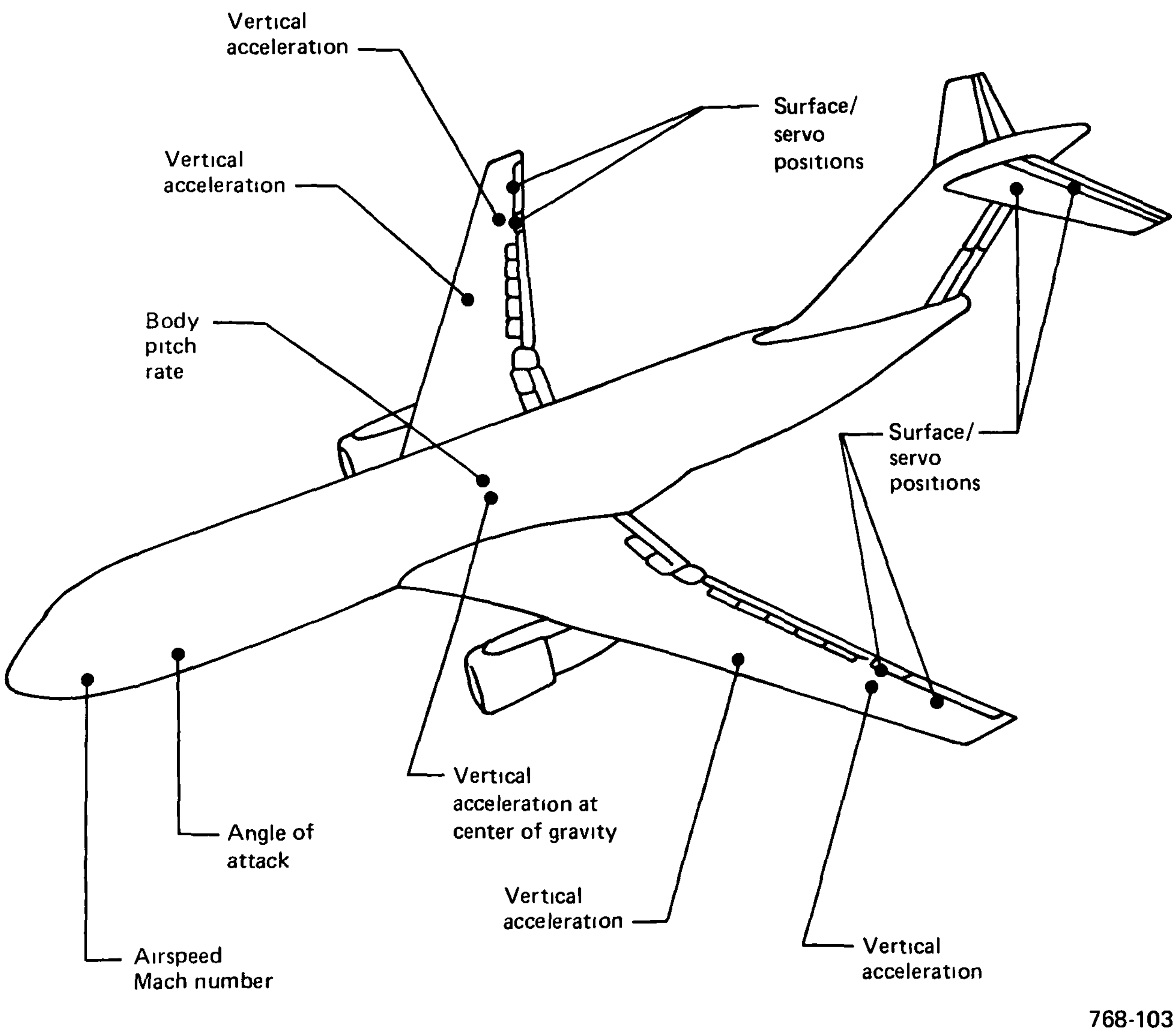

Figure 161. Initial ACT System Variable Sensors

The dedicated pitch-rate sensor, used in conjunction with the baseline airplane triplex IRS pitch-rate signal, serves to implement the quadruply redundant PAS function. The remaining dedicated sensors; i.e., vertical acceleration at several wing locations, are generally simple, triple-redundant packages. Sensors are dedicated to their respective digital ACT computers, where data are then transmitted cross-channel to satisfy the redundancy requirements. Table 24 relates the various sensors to the respective ACT control functions.

Table 24. ACT Variable Sensors

Initial ACT variable sensors	ACT functions					
	PAS		MLC	GLA	FMC	AAL
	Short	Long				
Pitch rate, body	X					X
Vertical acceleration at center of gravity			X			
Wing vertical acceleration—two locations				X	X	
Mach number					X	X
Airspeed		X	X	X	X	X
Angle of attack						X
Elevator secondary servo position	X	X	X			
Stabilizer position		X				
Outboard aileron, inboard segment position			X	X	X	
Outboard aileron, outboard segment secondary servo position			X	X		

768-103

7.3.2.3 ACT Computer

The ACT computer is the key element in the integrated control system concept as applied to the Initial ACT Configuration. This section presents the salient features of a candidate ACT computer that was based upon work described in the Airborne

Advanced Reconfigurable Computer System (ARCS) Program (ref 6). Data estimates for the ACT computer were derived from current technology production flight control hardware.

The ACT computer may be characterized by the following design features, which are responsive to the overall system requirements stated earlier:

- Digital implementation to facilitate a comprehensive and flexible design suitable for real-time control applications

- A computer architecture structured to handle flight safety crucial and critical ACT functions

- A highly fault-tolerant design, which implies the ability to withstand transient faults in the system and recover normal operation

- Extensive fault identification and fault storage capability, necessary to enhance maintainability of the overall system

Computer Architecture—The ACT computer (fig. 162) retains many of the ARCS architectural features, such as the bus-oriented structure, autonomous input/output (I/O) operations, and microprogrammed control processing. The basic change from the ARCS to the ACT application is in partitioning crucial and noncrucial functions; i.e., PAS is separated in both I/O and memory from noncrucial functions such as WLA and FMC. This change is essential because of the extremely high reliability required of the crucial function.

Each ACT computer in the parallel redundant system possesses identical hardware and software. Communication between computers is required to provide sensor data exchange and synchronous operation from duplex through quadruplex redundancy levels. The ACT computer consists of three major sections, central digital processing, I/O, and power supplies, communicating on a common bus structure. The central digital processing section is common to all processes and is therefore a critical element for all ACT functions. The I/O section is designed for flexibility and can be adapted to the computer application.

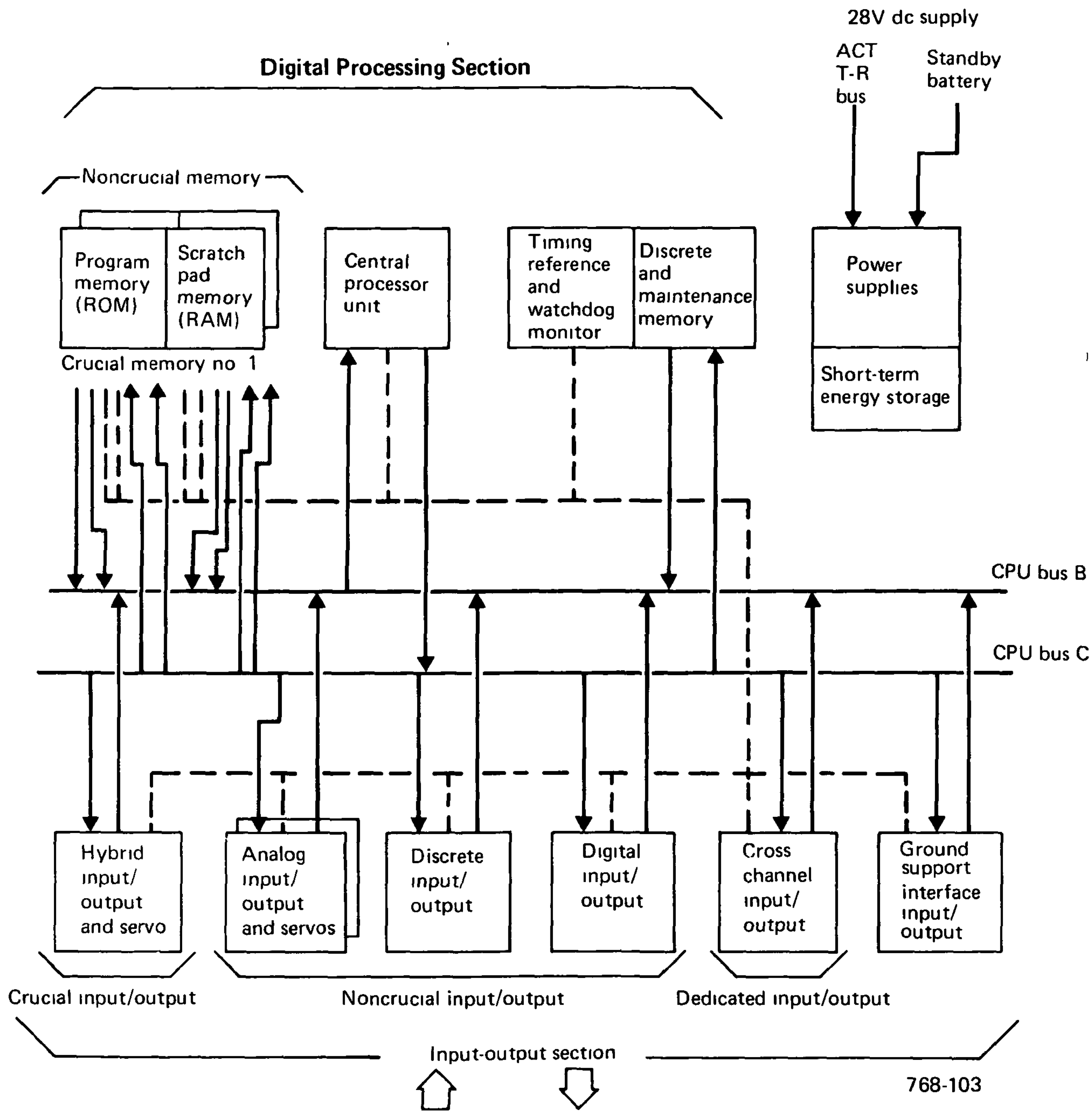

Figure 162. ACT Computer Block Diagram

The digital processing section contains the central processor unit, memory, and iteration timing reference/discrete modules fundamental to the processing of all ACT functions. All intracommunication is handled by the bus structure. The modules are:

- A central processor unit microprogrammed as a general purpose parallel processor

- Two main memories partitioned into flight-crucial and nonflight-crucial operations (physical memory mapping aligned to software module structure)

- A timing/discrete module for timing, monitoring, machine/system status, and nonvolatile maintenance data storage

The I/O section of each ACT computer consists of analog, digital, and discrete modules providing communication between the digital processing section and the external environment. All I/O modules interface directly with the bus structure, and each contains a dedicated memory addressed by the central processing section. The I/O modules are process oriented:

- A hybrid I/O dedicated to the flight crucial function and containing a mixture of analog/digital processing and servo drives

- An analog I/O partitioned into analog/digital signal conditioning, conversions, and servo output drives

- A discrete I/O that services system discretes at two logic levels

- A digital I/O providing serial digital ARINC 429 Digital Information Transfer System (standard) data communication between the ACT computer and system sensors, the maintenance control/display panel, and the flight deck caution system

- A cross-channel data link for high-speed data exchange between redundant ACT computers

- A ground support interface with line and shop maintenance support equipment

The power supply section for each computer accepts dual +28V dc aircraft bus power (main dc bus and standby battery bus). It conditions and generates output power for internal computer operations, discrete circuit excitation, and actuator shutdown logic. Except for the dedicated pitch-rate sensor, all sensor excitation in the integrated system configuration is derived from the aircraft power buses and not from the computer. The same excitation power is input to the computer for demodulation reference and power normalization. The computer power supplies contain monitor and protection circuitry for internal high/low dc-voltage tolerance monitors, short circuit, over voltage, and thermal overheat conditions. Computer power outputs can sustain a short circuit without causing failure to internal voltage supplies.

Computer Characteristics—Table 25 summarizes both functional and physical characteristics of the ACT computer. The computer timing is multirate structured to

Table 25. ACT Computer Characteristics

General	Digital, general purpose, stored program
Arithmetic	Binary, 2s complement fixed point, 16-bit data/instructions standard
Memory (main)	32K ROM, program/data constants 2K RAM, variable program 128-word, 8-bit nonvolatile, fail vector data
Input/output	16/5 analog 40/20 discrete 3/2 serial digital (ARINC 429) 3/1 digital (cross channel) 1 GSE interface
Timing	5-ms minor frame 20-ms major frame
Interrupts	8 priority level, software maskable
Power	Dual 28V dc, 100W dissipation
Volume	0 0164 m^3 (1000 in^3) (ARINC 600–8 MCUs)
Weight	12 kg (26 5 lb)
Reliability	6800 hr MTBF (inhabited, 40°C [104°F])

768-103

accommodate all the ACT function control law requirements. A minor time frame of 5 ms was selected to meet the FMC bandwidth requirements. Slowest control laws are executed at the major frame interval of 20 ms. Elimination of FMC would remove the 5 ms frame rate requirement and yield a small reduction of software and memory volume.

Memory sizing was estimated based on comparable digital automatic flight control computer programs for tasks similar to those required for ACT; these were capacity sizing estimates only and include a 50% growth allowance. I/O signal capacity reflects the integrated system configuration based on control laws chosen to fulfill the Initial ACT requirements. The physical characteristics summarize the size, weight, and packaging configuration typical of the new ARINC 600 standards for digital avionic equipment. Reliability estimates are consistent with new-generation digital flight control hardware used on the Baseline Configuration.

Redundancy Management—Redundancy management is an automatic process designed into the ACT computers to provide maximum functional survivability in the presence of transient or permanent fault conditions. Redundancy management is the heart of the fault-tolerant system and is based on the following strategy:

- Information exchange between the system-redundant channels, made through the ACT computers, is largely implemented in software.
- All system elements are monitored for faults by strategically placed failure detectors in the computer hardware and software.
- Faults declared hard failures are isolated under software control to prevent detrimental effect to the good signal outputs.
- The remaining good elements are then reconfigured to allow continued operation with normal or degraded performance.

The various processes that provide redundancy management are illustrated in Figure 163 and described in the following subsections.

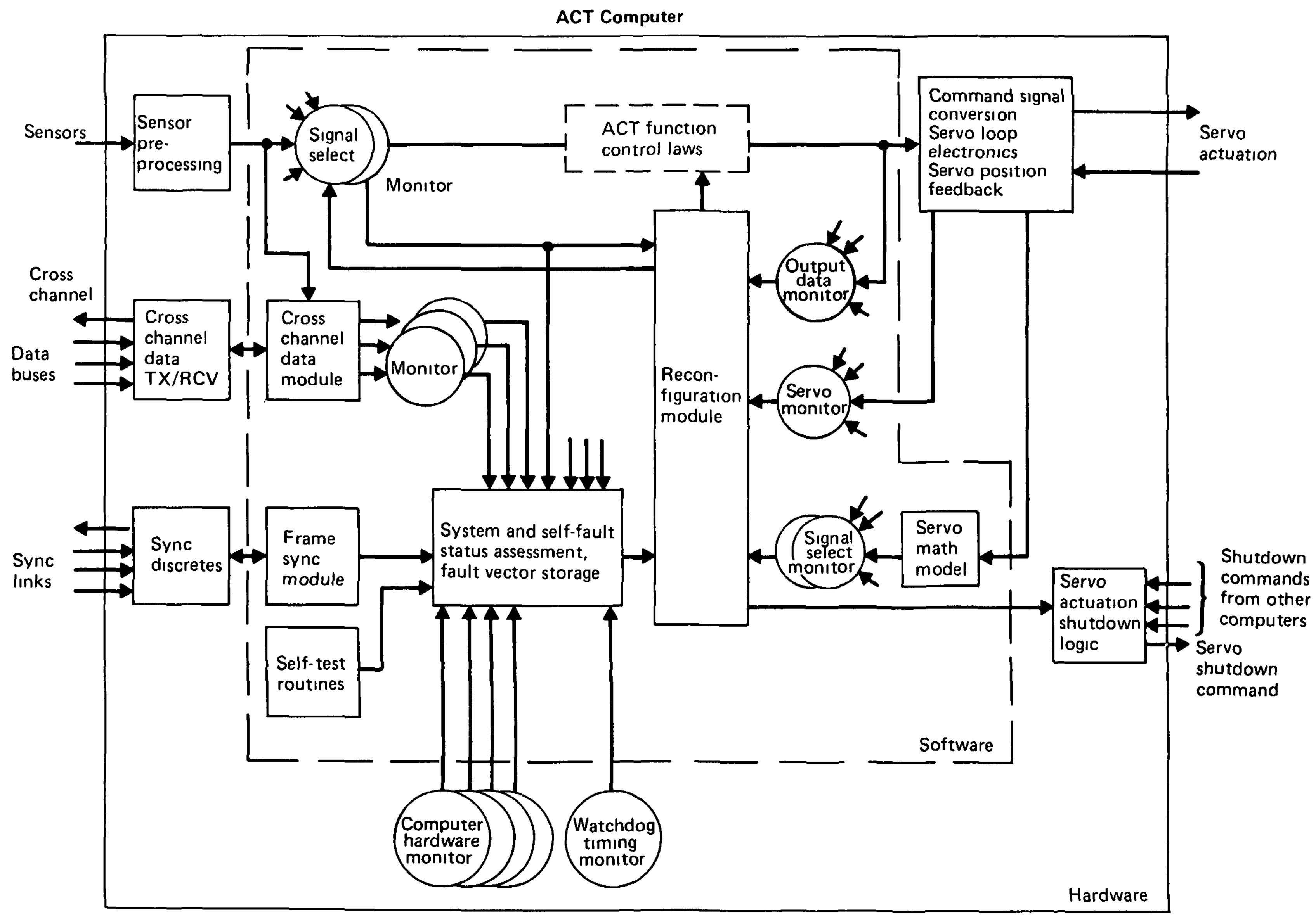

Figure 163. ACT Redundancy Management Process Overview

768-103

Synchronization—The ACT computer uses a software-controlled routine to establish and maintain major frame synchronous computations in all four channels. The synchronization concept is based on a "wait" algorithm, which requires that all computers be ready within a set time window with no detected failures before synchronization release is achieved. Lack of synchronization will not inhibit continued processing of any channel, but a fault notice will be stored for maintenance.

Signal Selection—The Integrated ACT system consolidates signals from redundant channels in two voting planes, one between the ACT sensors and the computers and another at the secondary actuators force-summed output.

Signal selection provides a point for consolidating the redundant sensor data so that all processors operate on identical data, and, therefore, perform identical processes with identical results. Such a voting plane provides additional fault tolerance to the system. A signal selection concept is chosen primarily for its ability to prevent sensor failures causing a hazardous airplane maneuver. It is anticipated that oscillatory and step modes will present the most severe conditions for ACT with regard to pitch stability and wing structural design.

The signal-selection process for the ACT system is implemented in the computer software. Sensor sets are dedicated to the computers (figs. 157 through 160), and the only interconnection between redundant channels is through the computer cross-channel data transfer link. Sensor data are, therefore, cross-communicated between computers ahead of the signal-selection voting plane.

The concept is based upon an active-standby method for quadruple-channel operation, with three inputs designated "active"; the fourth input, on "standby," switches into "active" status when the first "active" signal fails. Triplex sensor inputs are treated as quad inputs with a first failure. Upstream failure monitoring inhibits the signal selector from switching to a bad standby signal at the first failure of an active input. The median is selected for both normal and first-failure operation. Signals are averaged after a second input failure, operating in dual-channel mode.

Cross-Channel Data Link—Dedicated, high-speed, one-way digital data buses provide the cross-channel communication link between the redundant computers to achieve interchannel transfer of sensor data, synchronization of computations, and flow of necessary data to perform cross-channel signal monitoring and reconfiguration if failures occur. Redundant data must be transferred between channels and processed within the same minor time frame to minimize computation delays. Careful design is required to avoid propagating faults between redundant channels through the data links.

Failure Protection—Several methods of failure protection are incorporated into the ACT System to maximize survivability and minimize effects of failures on airplane performance. Figure 164 summarizes the overall failure protection design for the ACT system and illustrates the top-down structure for redundant channel operation. This is divided into failure detection by design and by monitoring. Failure detection by design includes such features as hydromechanical voting in the actuation concepts, redundant channels, physical and functional isolation, and computer architecture, hardware and software design. Failure detection by monitoring, accomplished within each ACT computer, is composed of system monitoring and computer self-monitoring.

System monitoring, largely a software process, uses cross-channel comparison by the computers to decide the level of redundant operations. Single-channel operation is unacceptable in the ACT design. To detect sensor faults, computer faults, and servo actuation faults, monitoring at three basic planes uses cross-comparison techniques in a continuous checking process associated with the real-time control activity.

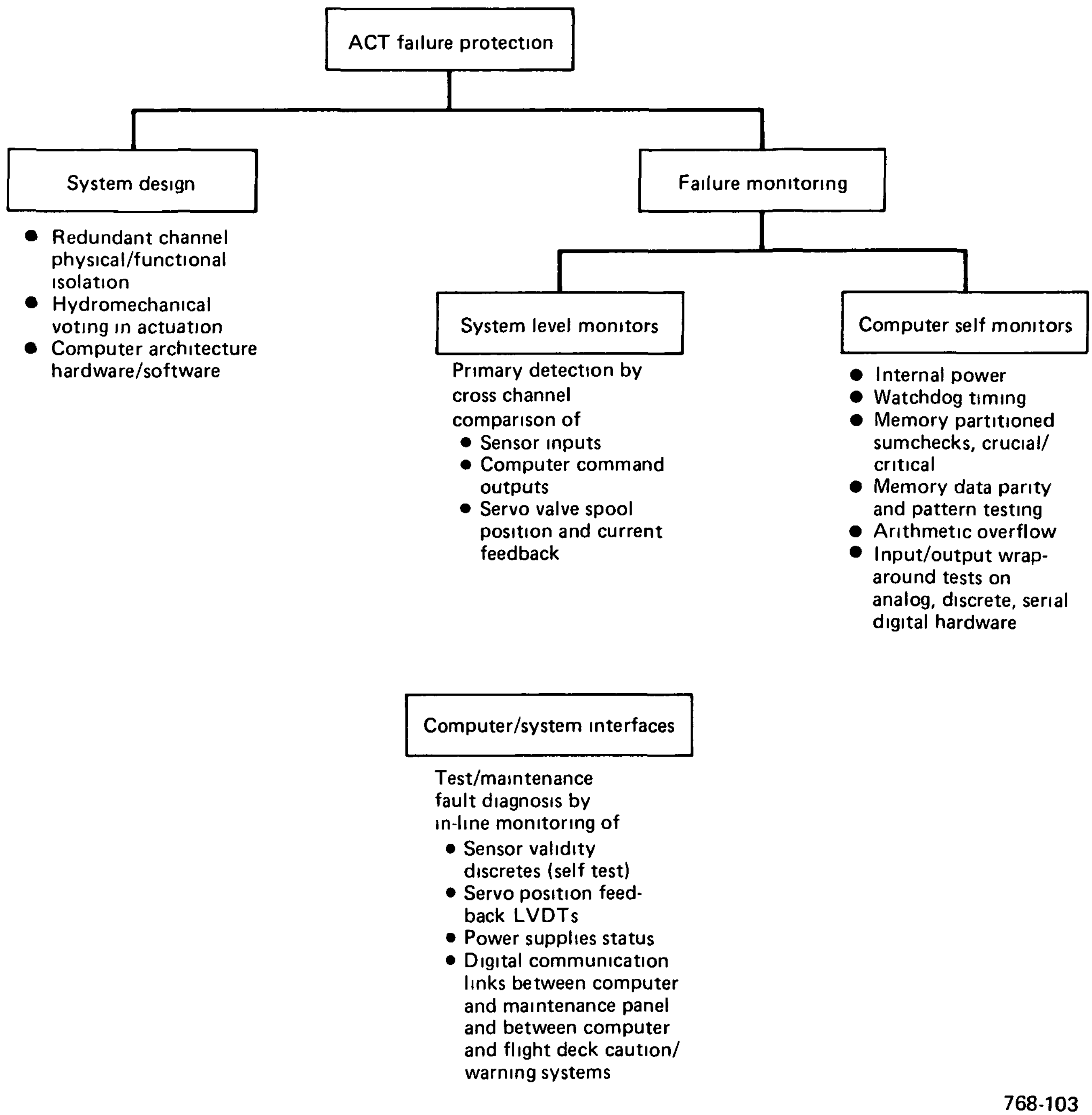

Figure 164 ACT Failure Protection Summary

Basic areas checked are:

- Internal power supplies
- Machine timing
- Processor capability, memory sum checks and parity, and invalid arithmetic operation
- Input/output, wraparound testing of all digital, discrete, and analog circuitry

Reconfiguration—The flight-critical nature of the ACT system dictates the need to maximize system survival through reconfiguration techniques. Since reconfiguration relies on fault detection by cross-channel monitoring, single channel operation cannot be guaranteed. Even current in-line monitoring techniques cannot totally ensure channel health.

Reconfiguration is defined as the process of attempting to tolerate a fault. Faults may be detected or go undetected. A detected fault may appear temporarily (transient) or become permanent, the basic distinction being time. Three possible outcomes result from such fault conditions within the ACT system:

- The system recovers normal operation
- The system survives with degraded capability
- The system fails and shutdown occurs

Degradation is defined as: (1) reduced system redundancy level, or (2) operation with simpler control laws and perhaps a penalty in airplane flying qualities or restricted operation. The latter accommodates sensor faults, presuming that alternate control laws exist. For example, WLA (fig. 158) uses airspeed as a gain schedule input. If a DADC fails, the system would be reduced to a two-channel operation. If a second DADC fails, a substitute control law could be activated using the flap position as an approximate airspeed indication.

Reconfiguration for ACT is divided into four areas: electric power, sensor inputs, computer functions, and servo outputs. The strategic monitoring points in the computer hardware and software (fig. 163) are basic to the reconfiguration process.

Electric Power—The ACT electric power system is organized on a per-channel basis, with airplane battery backup power available to each operating channel within 50 ms of detection of primary dc power loss. Each ACT computer would store sufficient energy to maintain the entire computer regulated power for a minimum of 50 ms, sufficient to overlap acquisition of main battery power. Therefore the computer software would not require special reconfiguration.

Sensor Inputs—The signal-selection failure monitoring algorithms handle the sensor inputs. Reconfiguration of an ACT function due to sensor faults at triplex or higher redundancy levels reduces redundancy by one level until recovery is achieved. The minimum redundancy level is duplex; no single-channel operation is permitted. The deviating signal is isolated until it recovers within the prescribed threshold detection bands and remains "good" for a prescribed time. The recovery time selection is influenced by several factors: type of sensor signal characteristics; risk of encountering a second, like failure during recovery; the concern for latent failures; and the possibility of false recoveries. In case the remaining signals disagree during recovery of the initial faulted signal, the latter is declared a permanent failure, and the recovery procedure is attempted on the second like occurrence. A total time-out period must be mechanized for the attempted recovery procedure to take care of a hardover failure; i.e., the signal exceeding threshold and never returning.

Computer Faults—These are defined as faults generated within the software processes; faults generated in the digital-to-analog output hardware are handled differently. Further assumptions are:

- The basic machine executive is not faulted, and the machine does have the ability to attempt recovery.

- The cross-channel data links are not faulted, and vital information appropriate to the monitoring process is transferred between redundant machines.

- Read-only memory (ROM) is not destroyed, such that program instructions and constants remain intact.

- An autonomous I/O exists.

If any of these assumptions does not apply, computer shutdown is indicated. The computer fault recovery mechanism is based upon cross-channel comparison for monitoring computed command outputs. Additionally, watchdog monitoring of individual machines indicates the local computer's ability to operate logically.

Methods proposed to reestablish the faulty processor computation through variable data exchange from other good processors include rollahead, rollback, coast, memory copy, and restart (see ref 6). A "warm restart" method was selected in which, upon detection of an output data fault, each operating computer determines the level of redundancy by checking its resident status table of permanent computer faults, then determines which computer is at fault by examining the output monitor table. When a fault occurs during three-computer redundant operations, the system attempts to recover the faulted computer. A fault occurring in duplex will result in a shutdown. The unfaulted computers will maintain normal operation, assuming that the faulted machine is operable until a permanent fail flag is set, which indicates the faulted machine's inability to recover.

Servo Outputs—Each servo actuator is directly commanded by the associated processor. Servo actuator faults are monitored and detected in the software of the associated processor. Each channel engagement is controlled by a voted hardware discrete issued by its associated command computer. Consent is required of the other channel computers for the local servo to remain engaged. If a failed computer does not disengage its servo channel, then disengagement is accomplished through the hardware voting mechanism.

Reconfiguration for servo actuation results from redundancy degradation upon faulting, with recovery after a prescribed number of iterations (wait time) after signals exceed the monitor threshold. The recovery delay time should be sufficient to avoid possible oscillatory actuator engage-disengage cycling. The local faulted machine first freezes its affected servo command outputs , then it attempts recovery. Meanwhile it still communicates with the unfaulted machines, and loss of synchronization will not cause shutdown. Recovery is not attempted if a fault occurs in duplex actuation in which the faulty actuator cannot be determined; in such case both actuator channels shut down.

The recovery mechanism, "warm restart," is a simplified power-up routine. Program variables are initiated once, and time is allowed for the command outputs to recover within the output tolerance of the operating computers. If the attempt is successful, the faulted machine will be permitted to release its affected servo commands. If the attempt is unsuccessful, the affected servos in the faulted channel will be permanently shut down, and the unfaulted computers will be reconfigured to recognize the faulted machine and reduce their respective machine status tables to reduce the monitor redundancy level.

7.3.2.4 Actuation

Three actuator configurations are used in the ACT system: ACT secondary actuation configuration, ACT dedicated actuation configuration, and stick-pusher actuation configuration.

ACT Secondary Actuator Configuration—A side-by-side, force-summed, secondary actuation concept was chosen to implement the PAS and WLA ACT functions, which use the primary flight control surfaces of the Initial ACT Configuration (fig. 165). ACT secondary actuator output is series-summed with the pilot's mechanical control signal to form a command input to the power control unit (PCU). Both PAS and WLA actuation concepts use a multichannel, side-by-side arrangement, selected on the basis of the installation envelope. The number of channels are compatible with the respective redundancy requirements of each ACT function. For reasons of weight, cost, reliability, and compatibility with the airplane's three hydraulic systems, the quadruple-channel PAS is implemented by three actuators and one mathematical model channel. The WLA actuation uses the same principle with two active channels and one model channel.

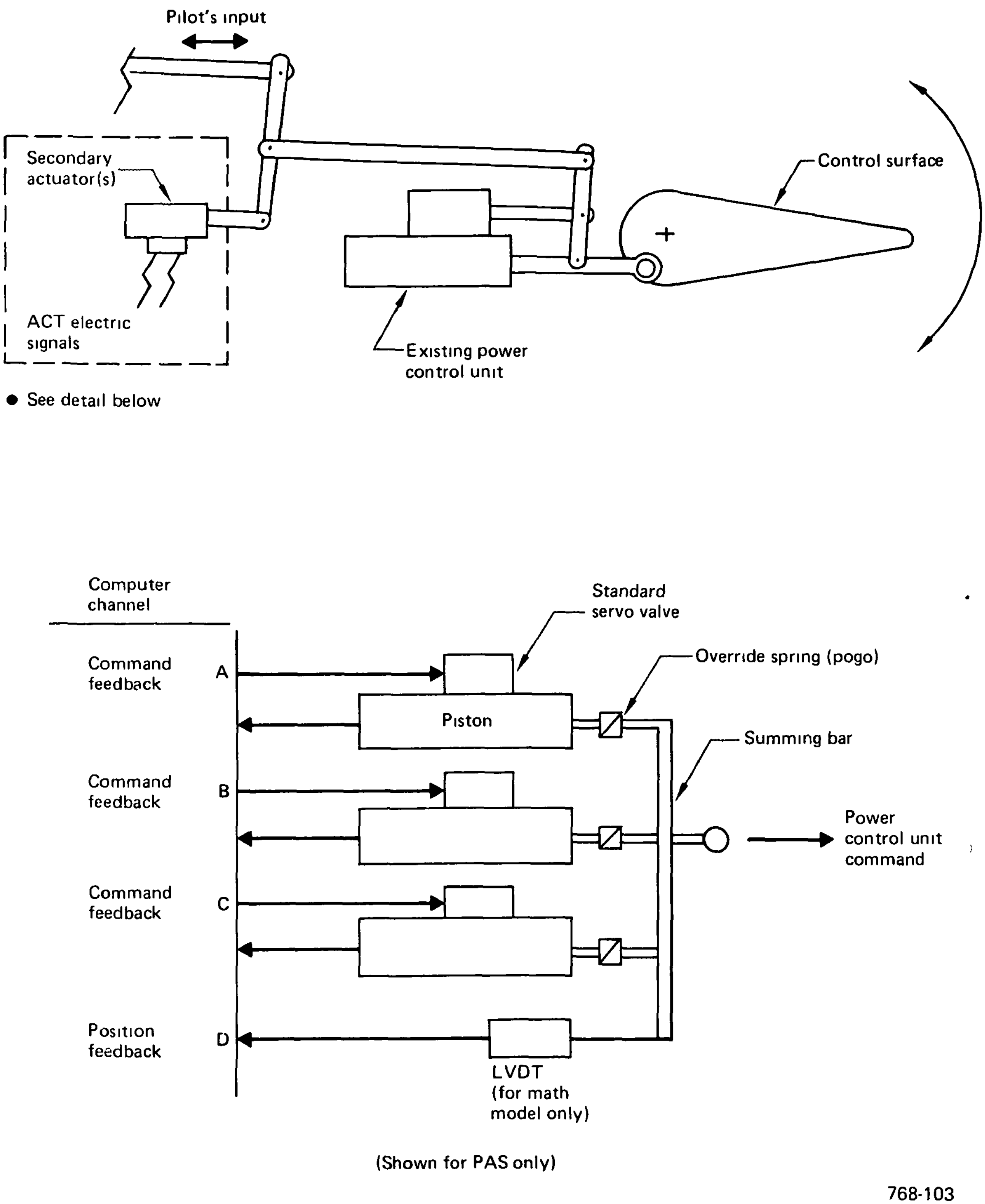

Figure 165. ACT Secondary Actuation Configuration

The selection of the force-summed concept was based upon the ability of the digital computer to produce essentially identical actuator command signals. Identical channel command signals depend on computer sensor selection and cross-channel synchronization.

Each channel of the concept has a conventional two-stage, low-pressure gain electrohydraulic servo valve operating a single ram. Valve spool and ram positions are fed back to each ACT computer for servo loop control and failure detection. The model channel in each computer receives the summed actuator ram position feedback and combines this with the command signal to compute servo valve position.

ACT Dedicated Actuation Configuration—The power control actuation configuration (fig. 166) was chosen to operate control surfaces dedicated to ACT functions. It was designed to remain fully operational with decreased dynamic peerformance after one electric and one hydraulic failure. The actuation configuration is a "fly-by-wire" implementation in that electric signals from the ACT computers directly command the control surface. Position command signals from each of three ACT computers are magnetically flux-summed in the four first-stage electrohydraulic servo valves, two per hydraulic system. Each group of two first-stage valve outputs is mechanically position-summed by a linkage. The second stage valve spool is controlled by force-summing the resultant mechanical output of each first-stage linkage. The second-stage-valve-to-main-output-ram power amplification is the same as for conventional dual-tandem actuation.

Stick-Pusher Actuator Configuration—The Baseline Configuration is equipped with a stick-shaker system that provides aural and tactile warning of an impending stall by sensing the angle of attack, computing the airplane stall margin, and operating two stick-shaker motors, one on each control column.

The Initial ACT Configuration AAL system uses a fail-operational stick-pusher actuation mechanism to follow up the stick-shaker system. It provides positive stall prevention by causing a large, rapid, forward motion of the control column at the stall recovery angle of attack if the pilots fail to act after the stall-warning system is activated.

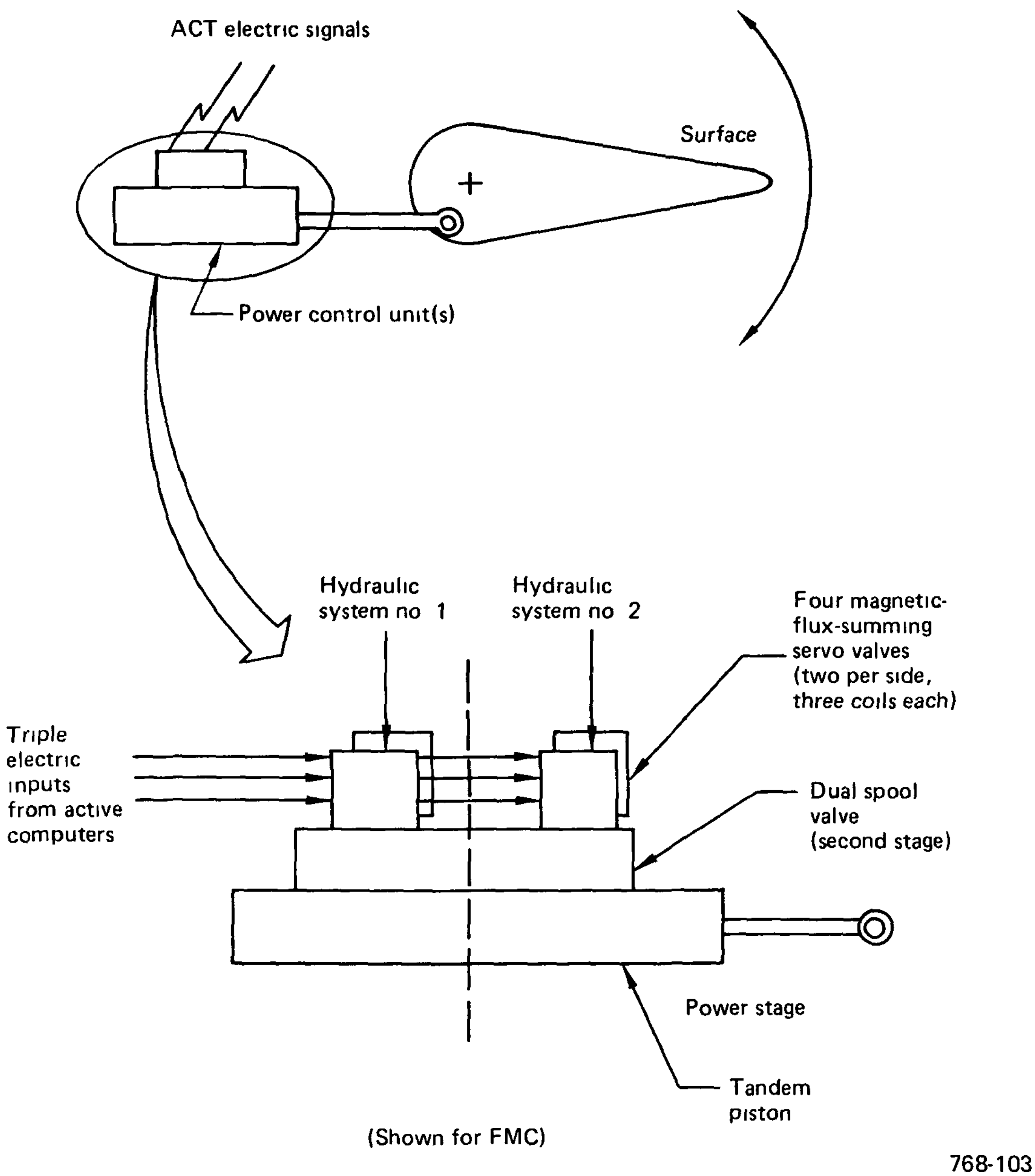

Figure 166. ACT Dedicated Actuation Configuration

The stick-pusher concept (fig. 167) uses three sensors, four computers, a dual-tandem floating actuator, and two pneumatic power sources. The actuator exerts the same force when pressurized by either one or both sides. The installation linkage is such that the force exerted on the control column continuously decreases as it travels forward; 356N (80 lb) exerted at the full aft position reduces to 178N (40 lb) at the full forward position. Each dual-pneumatic power source consists of a nitrogen bottle at 13 788 kPa (2000 psi) and a regulator that reduces the pressure to the 3447 kPa (500 psi) required for actuation. Two series solenoids, each signaled by an ACT computer, must be opened before the actuator will operate.

Actuation time is approximately 0.2 sec. When either command is removed, the actuator vents to ambient through the solenoid valve. The pilot may override the pusher at any time by exerting sufficient force on the column or by operating the manual dump valve, which directly vents the actuator to ambient. Operating the dump valve also actuates two switches that deenergize the solenoid valves and provide logic information to the computers.

7.3.2.5 Operational Status and Maintenance

The ACT system must inform the flight crew of system failure status and required procedural actions, and it must facilitate system preflight checkout and maintenance support activities. The system communicates with the flight crew through the flight deck caution and warning systems and with the ground crew through a maintenance control and display panel in the main electronics bay that also serves other flight systems. A dedicated ACT control and display panel, located at the flight engineer's station, could be considered for in-flight maintenance support. All these communication media, except the latter, are Baseline equipment. ACT digital processing offers extensive built-in test capability and decision logic necessary to implement these interface requirements.

In-flight Operation—Two levels of in-flight fault data are processed and transmitted by the ACT computers to the flight deck for appropriate crew actions. Information relevant to loss of ACT function capability is presented to the pilots through the respective warning and caution priority structure. Procedural actions normally listed

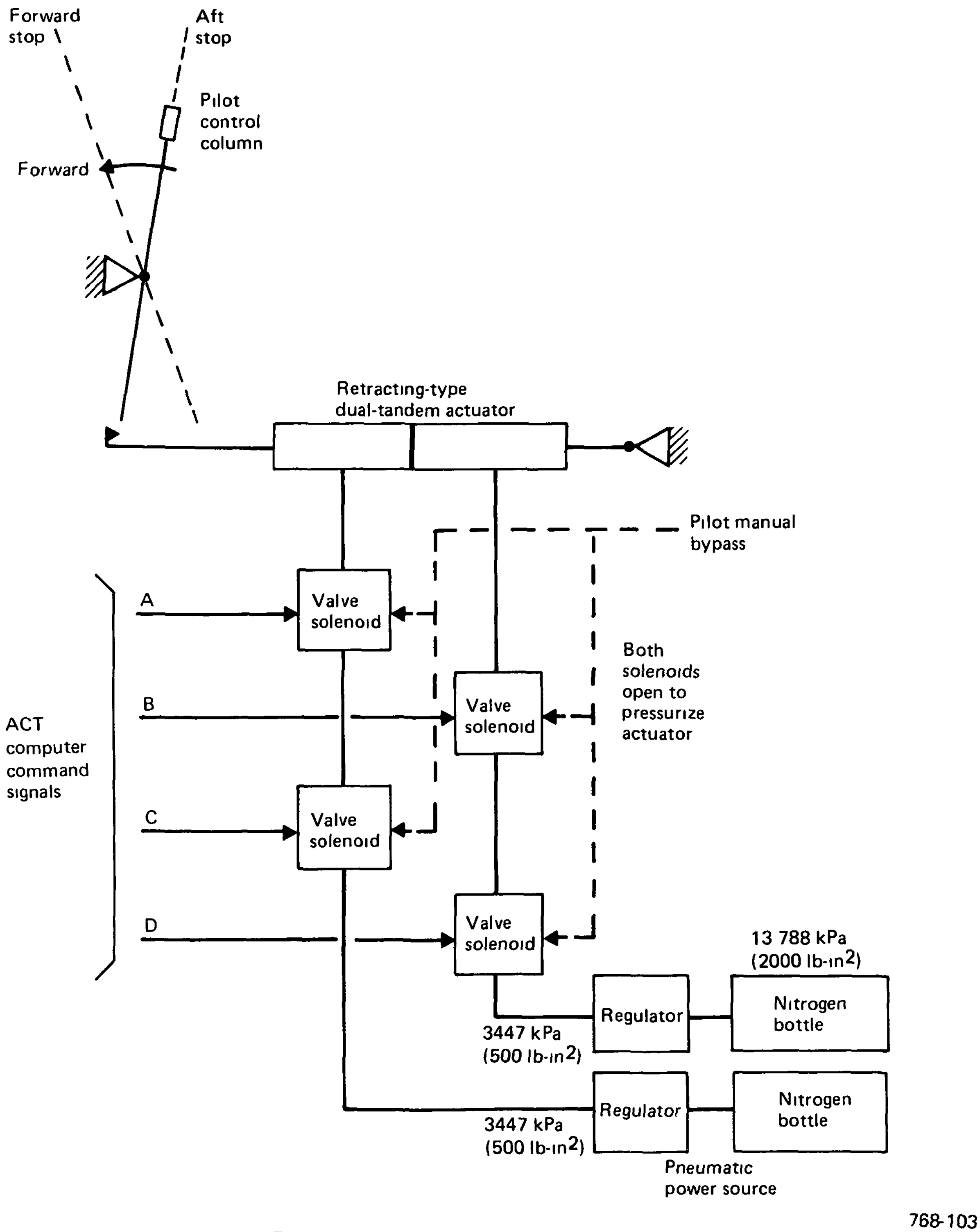

Figure 167. Stick Pusher Actuation Concept

in the flight operations manual (carried in the flight deck) are displayed on the caution system alphanumeric message display unit to aid pilot decision.

Information relevant to ACT equipment failures at the LRU level, which impacts flight dispatch, is presented at the flight engineer's station to permit maintenance support "call-ahead" action. The fault vector data from monitor detection outputs and the annunciated decisions are stored in the ACT computer's nonvolatile memory and transferred to the maintenance control and display panel at touchdown for appropriate ground crew actions.

Ground Operations—Two basic ground operations are defined for the ACT system. First, preflight testing is required to establish system integrity for both flight safety and airplane dispatch. Preflight testing must be fully automated, must be conducted with flight crew concurrence, and must conclude with a recommended decision as to whether the airplane may be dispatched normally, with operational restrictions, or not at all.

Second, maintenance activities associated with ACT must be consistent with other airplane flight control systems maintenance. That is, the system must be assumed operational and available for service unless preflight test indicates a failure or a flight squawk was generated in a previous flight. Through-flight maintenance will be restricted to changing components that are dispatch required, easily removable, and readily replaced with spares made available by the call-ahead procedure. Most system maintenance will be deferred to turnaround or overnight facilities with less impact upon flight operations.

System maintenance testing is structured to be an extension of preflight checkout with the capability to diagnose equipment problems to the LRU level. The in-flight stored fault data assist the gound crew toward this goal. An important objective in structuring the maintenance testing is to preserve the separation between flight-crucial and flight-critical functions to avoid extensive requalification of functions other than those repaired.

7.4 AERODYNAMIC DRAG

Page

7.4 AERODYNAMIC DRAG

The drag estimates for the Initial ACT and Baseline Configurations are compared to illustrate the effects of the reconfiguration made possible by ACT. Initial ACT drag improvements are due to reductions in trim and skin friction drag associated with the smaller horizontal tail, farther aft cg, and longer tail arm (wing shifted forward). Cruise lift/drag (L/D) is improved 3.6% and takeoff L/D is increased 2.3%.

The principal geometric charcteristics for both the Baseline and the Initial ACT Configurations are defined in Section 4.0 and listed in Table 26. Both airplanes have the same gross weight, engine size, wing area, and payload.

7.4.1 CRUISE DRAG COMPARISONS

Cruise drag polars for the Initial ACT and Baseline Configurations are based on wind tunnel test data of similar configurations, with empirical and analytical corrections for small geometric differences shown in Figure 168. Table 27 summarizes the cruise drag reduction at an average cruise condition (C_L = 0.45, Mach = 0.8). The 3.6% drag improvement for the Initial ACT configuration is due to a reduced skin friction drag from a smaller tail size (2.4%) and reduced trim drag. The trim drag improvement at cruise C_L = 0.45 is 3.2 counts or 1.2% (fig. 169), primarily due to the farther aft cruise cg position. Other factors influencing the trim drag improvements are the increased tail arm (beneficial) and the reduced tail size (detrimental).

The Initial ACT and Baseline Configurations share many design components such as engine, fuselage, and wing geometry. Differences between the two configurations affecting the high-speed lift and drag performance include the horizontal and vertical tail sizes, the wing location (longitudinal) on the fuselage, and the midcruise cg locations. Similarly, values of minimum parasite drag for the body, wing, engines, struts, and flap tracks and seals are identical to those for the Baseline Configuration. The incompressible drag polar shape (Mach = 0.7) and the compressibility drag at various Mach numbers (M = 0.7 to M = 0.84) are identical for the two configurations.

Table 26. Conventional Baseline and Initial ACT Configuration Comparison

Geometric characteristics	Conventional Baseline	Initial ACT[a]
Airplane size		
Maximum takeoff weight, kg (lb)	122 470 (270 000)	
Wing area, m^2 (ft^2)	275.1 (2961)	
Wing span/sweep, m/deg (ft, in/deg)	47.24/31.47 (155, 0/31 47)	
Location on body, percent body length	49 0	45.4
Location—engine pod on wing, percent b/2	33.6	
Trailing-edge flaps	Single slot	
Leading-edge devices	Slats	
Horizontal tail area/$\bar{V}_H$, m^2 (ft^2)	57.6/0.942 (620/0 942	31.97/0.551 (344/0 551)
Sweep, deg	35	
AR/taper	4.0/0.40	
Vertical tail area/$\bar{V}_V$, m^2 (ft^2)	57.4/0.88 (618/0.088)	53.97/0 090 (581/0 090)
Sweep, deg	55	
AR/taper	0 67/0 70	
Body cross section, m (in)	5 03W/5 410H (198.0W/213.0H)	
Body length/overall length, m (ft-in)	46.43/54.94 (152.4/180.3)	46.43/54.18 (152, 4/177, 9)
Cabin length, m (in)	33 38 (1314)	
Doors, number, type, size, m (in)	4, type A, 1.07 x 1.83 (42 x 72) 2, type III, 0.51 x 0 97 (20 x 38)	
Systems		
Engine number/type	2/CF6-6D2	
Engine thrust (SLST), N (lb)	182 377 (41 000)	
Nacelle and acoustic treatment	FAR 36, Stage 3	
Fuel capacity		
Wing tanks, m^3 (gal)	42 775 (11 300)	42 550 (11 240)
Center tanks, m^3 (gal)	Dry	
Total, m^3 (gal)	42 775 (11 300)	42.550 (11 240)
Main gear wheelbase/track, m (in)	1.42/1 14 (56 0/45.0)	
Location, percent MAC	56	64.9
Stroke/extended length, m (in)	0 46/3 18 (18/125)	0.51/3.18 (20/125)
Tire size wheel size, m (in)	1.09 x 0.39-0 51 (43 x 15.5-20)	
Nose gear type/tire spacing	Dual/0 61 (Dual/24)	
Stroke/extended length, m (in)	0.38/2.18 (15/86 0)	
Tire size wheel size, m (in)	0.94/0.33-0.41 (37 x 13-16)	
Payload		
Flight crew/attendants	3/6	
Mixed class passengers/split	197/9% first class, 91% tourist	
All tourist passengers	207	
Containers number/type	(22) LD-2 or (11) LD-3	
Cargo		
Containerized, m^3 (ft^3)	74 76 (2640) 49.22 (1738)	
Bulk, m^3 (ft^3)	11.33 (400) 11 33 (400)	
Total, m^3 (ft^3)	86.09 (3040) 60 55 (2138)	
Center of gravity location		
Forward, percent MAC	10 0	21 0
Average cruise, percent MAC	20 5	31.8

[a]Blank areas same as the Conventional Baseline

768-103

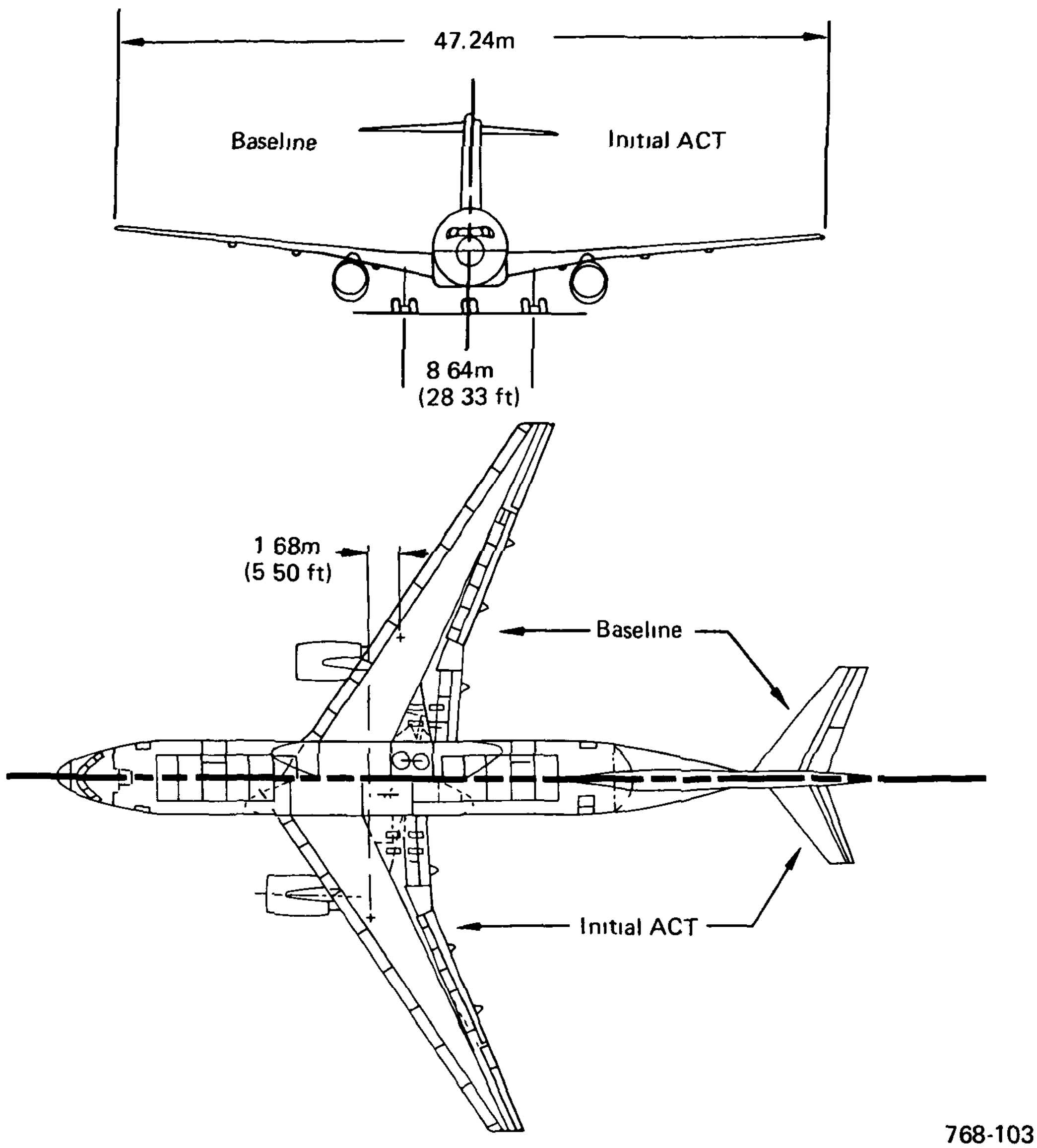

Figure 168. Conventional Baseline and Initial ACT Configuration Comparison

Table 27. Conventional Baseline Configuration and Initial ACT Configuration Cruise Drag Summary

Drag item	Drag difference Initial ACT Configuration relative to Baseline Configuration		
Parasite drag	ΔC_D	$\Delta C_{D_{total}}$, percent	Total, percent
Wing	0	0	0
Body	0	0	0
Horizontal tail	-0 00051	55	2 0
Vertical tail	-0 00004	5	0 2
Nacelles and struts	0	0	0
Flap tracks and seals	0	0	0
Excrescence	-0 00005	5	0 2
Drag rise and polar shape	0	0	0
Trim drag	-0.00032	35	1 2
Total ΔC_D	-0.00092	100%	3 6%

- Cruise drag, C_D at C_L = 0 45 (M = 0 80)

768-103

Baseline Configuration	0.02525	100%
Initial ACT Configuration	0 02433	96 4%
Total change	0.00092	-3.6%

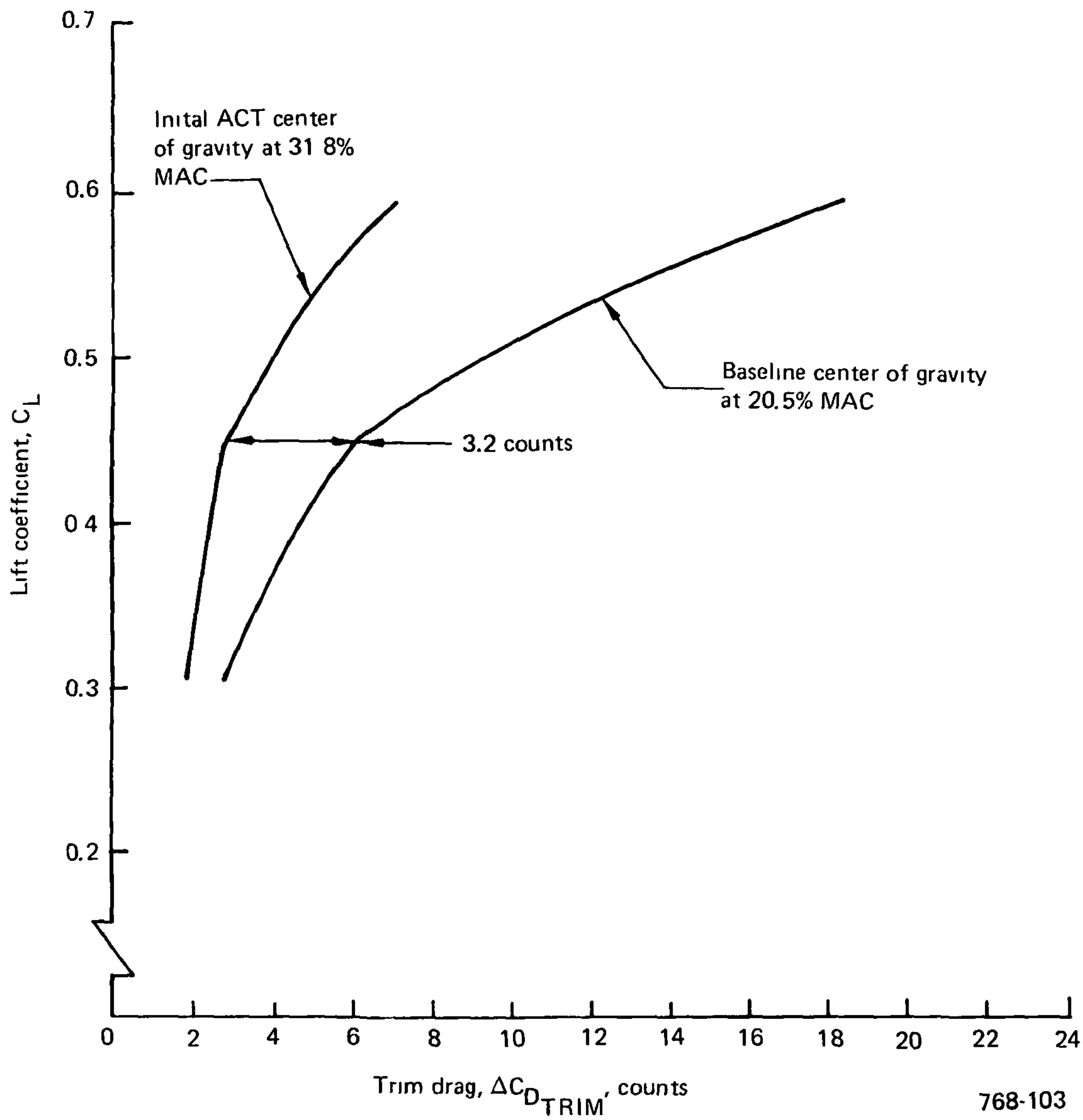

Figure 169. Trim Drag Comparison, M = 0.8

7.4.2 TAKEOFF AND LANDING DRAG COMPARISON

Estimated takeoff and landing lift-and-drag data for the Initial ACT and Baseline Configurations are presented in this subsection. Improvements of 2% to 9% in takeoff L/D and 3.3% in landing approach C_L are indicated for the Initial ACT Configuration, mainly the result of the farther aft location of the forward cg position. Because the Initial ACT Configuration has 1 deg less rotational capability than the Baseline

Configuration, it is slightly geometry-limited at intermediate takeoff flap settings and just meets the desired 3-deg tail clearance angle at touchdown.

Differences between the two configurations affecting the low-speed lift and drag performance result from changes to the horizontal and vertical tail sizes and the wing location (longitudinal) on the fuselage (table 28). The identical high-lift systems of these configurations consist of single-slotted trailing-edge flaps and full-span leading-edge slats with both sealed and slotted positions. The Initial ACT Configuration is geometry-limited for takeoff at α = 12.7 deg, a rotation capability 1 deg less than that of the Baseline Configuration, which is not geometry-limited for takeoff. The

Table 28. Low-Speed Configuration and Drag Comparison
S_{REF} = 275.1 m^2 (2961 ft^2)

Configuration	Baseline	Initial ACT		Improvement, percent
Forward center of gravity, percent MAC	10 0	21 0		—
Horizontal tail				
ℓ_H, m (ft)	27 14 (89 03)	28 6	(93 93)	—
S_H, m^2 (ft^2)	57.60 (620)	34 0	(344.0)	
$\overline{V}_H$	0.942	0.551		
Vertical tail				
ℓ_V, m (ft)	19 97 (65 5)	21 67	(71 10)	—
S_V, m^2 (ft^2)	57 41 (618)	54.0	(581)	
$\overline{V}_H$	0 088		(0.090)	
Takeoff climbout				
$C_{L_{V_2}}$	1.35	1 35		
L/D_{V_2} (all engines operating)	11 6	11 87[a]		+2 3[a]
Landing approach				
$C_{L_{APP}}$ (1 3V_S)	1 334	1 378		+3 3
L/D_{APP}	8 11	8 23		+1 5

[a]Includes effect of geometry limit on rotation capability for the Initial ACT Configuration

768-103

loss in rotation capability for the Initial ACT Configuration results from the more forward wing location on the fuselage with the same gear length. Clearance at landing touchdown is also reduced almost 1 deg for the Initial ACT Configuration. However, the Baseline Configuration had 1 deg more tail clearance than necessary for touchdown (4 deg versus 3 deg) because gear length was determined by nacelle clearance rather than aft body clearance. Thus, the Initial ACT Configuration appears acceptable. Lift-and-drag data (table 28) are from the low-speed aerodynamic prediction program, with adjustments based on recent wind tunnel tests on similar configurations.

Takeoff speed schedules and times for the Initial ACT Configuration are unchanged from those of the Baseline Configuration.

7.5 WEIGHT ANALYSIS

7.5 WEIGHT ANALYSIS

7.5.1 WEIGHT AND BALANCE

7.5.1.1 Weight Statement

A weight statement for the Initial ACT Configuration (table 29) shows a weight distribution within individual groups that is consistent with aerospace industry practice as defined in Reference 7.

7.5.1.2 Methods of Weight and Balance Analysis

The wing box was analyzed using a computerized beam analysis (ORACLE) to size "theoretical" structure, including upper and lower skins and stringers and front and rear spar webs (refer to subsec 7.2). Additional components required for an "installed" weight were applied, based on development experience with similar commercial airplane structures. These components consisted of manufacturing tolerance, feather material, pads, fasteners, spar web stiffeners, and ribs.

Wing secondary structure (leading and trailing edges) was based upon a reference airplane unit weight and was adjusted for loads and geometry. Main and nose landing gear weights were derived using a computer program, "GEARS," which is sensitive to design loads and configuration geometry. Body primary structure was adjusted for differences in horizontal tail load from the Baseline Configuration. Empennage weight represents the reference airplane unit weight adjusted for geometry and function.

Surface controls, hydraulics, electric, and electronic system components were defined in detail. A weight was calculated for each component/subsystem representative of the definition. Fixed equipment, other than these four airplane systems, was identical to the Baseline.

Conventional manual analysis was applied to the cg of detailed airplane components. Much of the data was obtained by incrementing the Baseline data.

Table 29. Weight and Balance Statement—Initial ACT Configuration

Functional group	Weight		Longitudinal center of gravity (body station)		
	kg	(lb)	m	(in)	Percent MAC
Wing	14 840	(32 720)	24 46	(963)	
Horizontal tail	1 070	(2 360)	52.73	(2 076)	
Vertical tail	1 751	(3 860)	47.47	(1 869)	
Body	15 622	(34 440)	23.80	(937)	
Main landing gear	6 437	(14 190)	24.71/25.35[a]	(973/998)[a]	
Nose landing gear	880	(1 940)	6.17/6.76[a]	(243/266)[a]	
Nacelle and strut	2 545	(5 610)	19.76	(778)	
Total structure	43 146	(95 120)	25 25/25 35[a]	(994/998)[a]	
Engine	7 951	(17 530)	20.04	(789)	
Engine accessories	100	(220)	16.99	(669)	
Engine controls	82	(180)	16.21	(638)	
Starting system	77	(170)	18.92	(745)	
Fuel system	644	(1 420)	24.66	(971)	
Thrust reverser	1 638	(3 610)	20.17	(794)	
Total propulsion system	10 492	(23 130)	20.28	(798)	
Instruments	488	(1 076)	11.10	(473)	
Surface controls	2 245	(4 950)	30.99	(1 220)	
Hydraulics	1 020	(2 248)	24.49	(964)	
Pneumatics	354	(780)	20.02	(788)	
Electric	1 042	(2 297)	13.26	(522)	
Electronics	775	(1 709)	12.04	(474)	
Flight provisions	417	(920)	4.90	(193)	
Passenger accommodations	6 681	(14 730)	22.30	(878)	
Cargo handling	1 229	(2 710)	23.39	(921)	
Emergency equipment	422	(930)	19.79	(779)	
Air conditioning	975	(2 150)	18.21	(717)	
Anti-icing	186	(410)	20.09	(791)	
Auxiliary power unit	676	(1 490)	42 80	(1 685)	
Total fixed equipment	16 510	(36 400)	22.35	(880)	
Exterior paint	68	(150)	23.04	(907)	
Options	907	(2 000)	23.95	(943)	
Manufacturer's empty weight	71 124	(156 800)	23.83/23 88[a]	(938/940)[a]	
Standard and operational items	6 241	(13 760)	25.60	(1 008)	
Operational empty weight	77 370	(170 560)	23.96/24 02[a]	(943/946)[a]	33 7/34 7[a]

[a]Gear up/gear down

768-103

7.5.2 MASS DISTRIBUTION AND MOMENTS OF INERTIA

In support of the mathematical model and structural loads analyses, mass distribution and moments of inertia of detailed components were analyzed. The resulting airplane mass and moment of inertia data are presented and documented in Subsection 5.4. Detailed components were subtotaled for the entire wing, body, horizontal tail, vertical tail, landing gear, and propulsion pod. Panel geometry definition for each of the major airplane components (wing, horizontal tail, vertical tail, body) are shown in Figures 170 through 173. Calculation methods were consistent with the computerized methods used on Boeing's commercial airplanes.

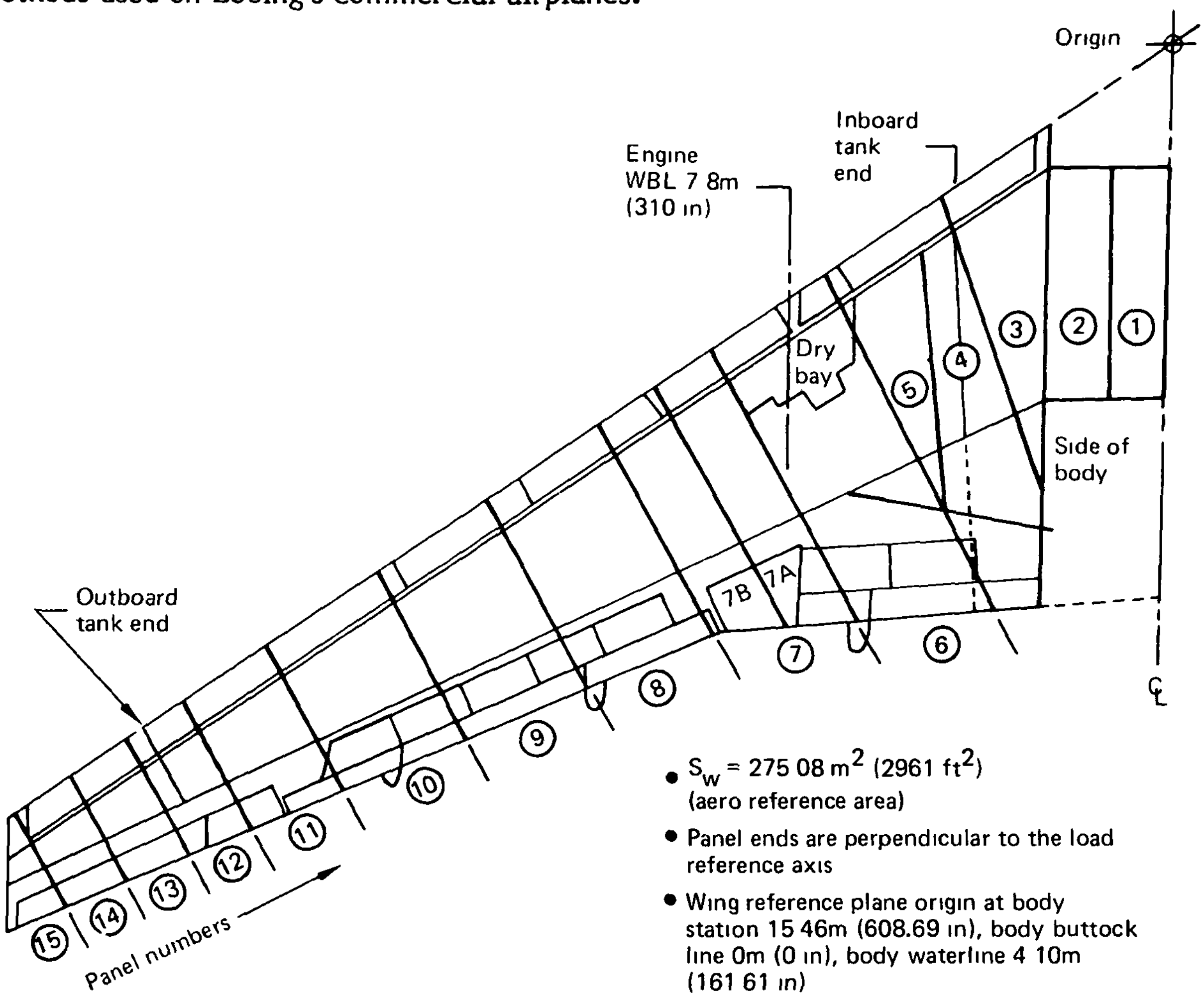

- S_W = 275 08 m^2 (2961 ft^2) (aero reference area)
- Panel ends are perpendicular to the load reference axis
- Wing reference plane origin at body station 15 46m (608.69 in), body buttock line 0m (0 in), body waterline 4 10m (161 61 in)
- Intersection of side of body and wing reference plane at body buttock line 2 47m (97.42 in), body waterline 4.10m (161 61 in)

768-103

Figure 170. Wing Mass Panel Definition

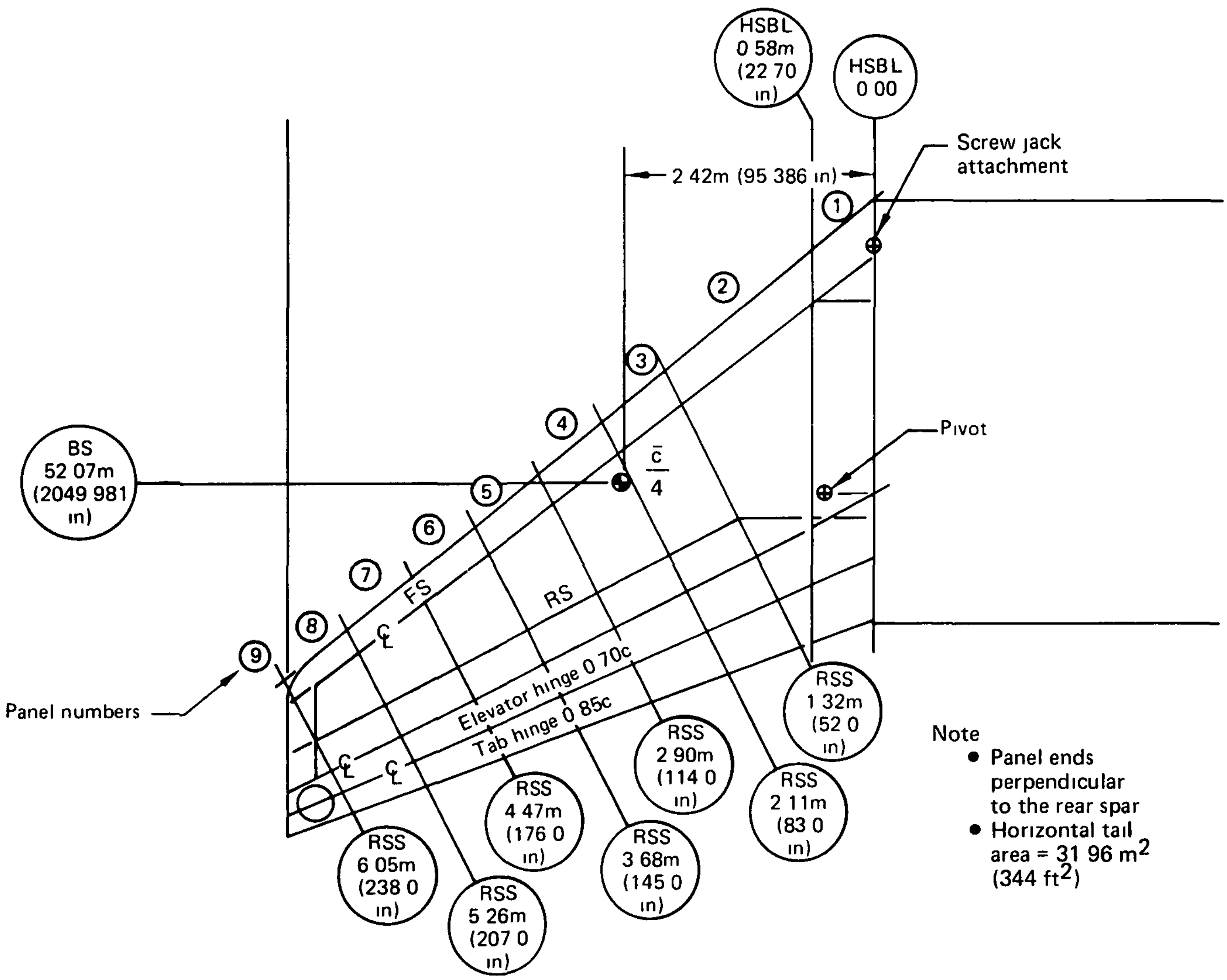

Figure 171. Horizontal Tail Mass Panel Definition

768-103

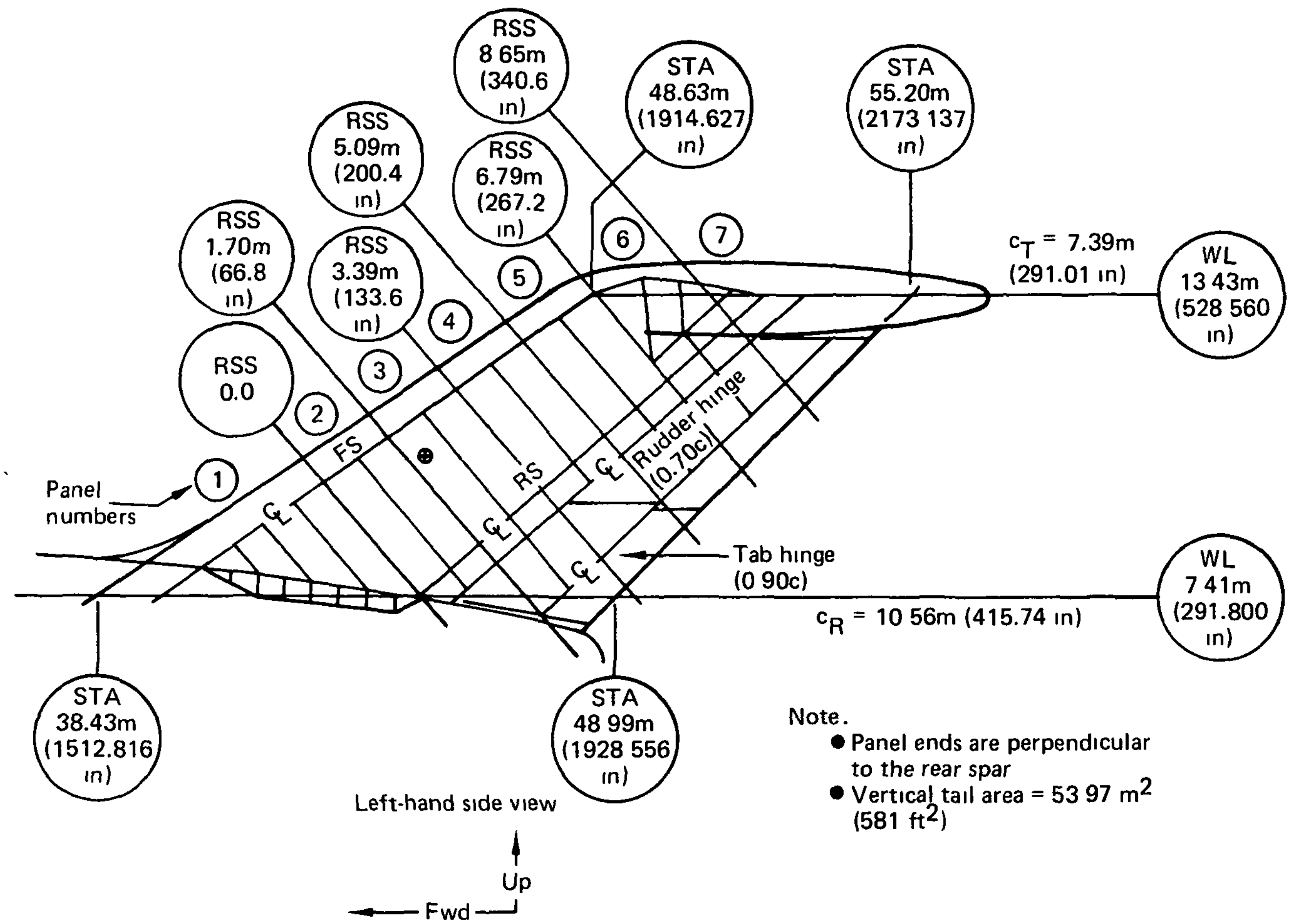

Figure 172. Vertical Tail Mass Panel Definition

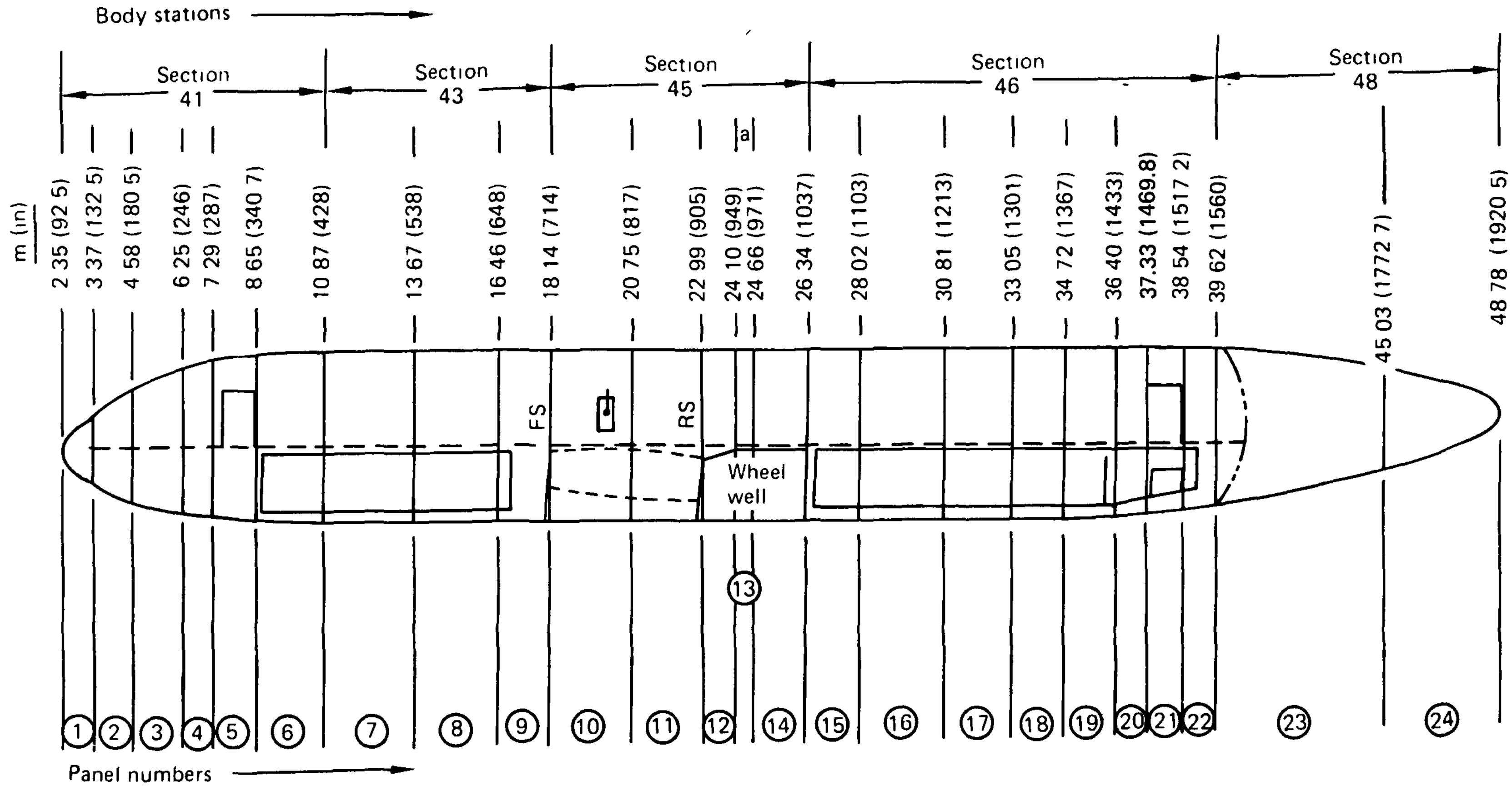

[a]Approximate gear uplock and beam reaction points

Figure 173. Body Mass Panel Definition

768-103

8.0 RELIABILITY, MAIN-TAINABILITY, AND COST OF OWNERSHIP

Page

8 0 RELIABILITY, MAIN-
TAINABILITY, AND
COST OF OWNERSHIP

8.0 RELIABILITY, MAINTAINABILITY, AND COST OF OWNERSHIP

Reliability of the Active Controls Technology (ACT) system is of utmost importance because loss of crucial ACT functions, such as short-period pitch-augmented stability (PAS), can cause aircraft loss. The probability that crucial functions will be lost must be less than 1×10^{-9} per flight hour (FH) (ref 8). Critical and noncritical functions have lower reliability requirements (subsec 4.2.3, table 1).

Once safety requirements are met, design considerations are focused on fuel efficiency, aircraft purchase cost, maintainability, maintenance cost, and schedule reliability.

Subsection 8.1 describes the reliability prediction methodology used in selecting the Initial ACT Configuration and in showing compliance with numerical requirements. Significant maintainability requirements from the IAAC Project design requirements and objectives (DRO) are discussed in Subsection 8.2. Maintenance costs expected for the Initial ACT Configuration are also addressed in that subsection. Subsection 8.3 describes the cost-of-ownership methodology and analysis results.

8.1 RELIABILITY

The reliability of the Initial ACT integrated systems, containing many multiple occurring events (MOE), was generally predicted using the computer-aided redundant system reliability analysis (CARSRA) model (ref 6). Failure rates were, where possible, based on commercial service experience.

Analysis showed that meeting extremely improbable failure criteria requires a minimum of four channels, but three or less channels are sufficient where safe retreat into a restricted flight envelope is possible. In the latter case, the redundancy should be selected based on cost-of-ownership analysis that trades the first cost and maintenance cost of additional redundant channels for the ability to dispatch with certain components down. However, since the crucial PAS made four channels mandatory for Initial ACT integrated systems, such trades were not considered necessary at this stage of design.

8.1.1 REQUIREMENTS

PAS short period, the crucial ACT system, meets the Federal Aviation Administration (FAA) requirements that any loss of function that can result in aircraft loss must be extremely improbable. FAA draft Advisory Circular, System Design Analysis (ref 8), advises that "extremely improbable" should be regarded as $< 1 \times 10^{-9}$ failures/FH. This same circular also establishes an upper limit of 1×10^{-3}/FH for functional failures that require the imposition of operational limitations. The latter limit is used for guidance concerning the allowable frequency of critical function failures that require flight envelope restrictions, provided that the failure rate does not exceed the failure rates (for similar functions) that past experience has shown acceptable to the airlines. Note that the major airlines, which provide mechanical flight schedule deviation data to Boeing, do not consider flight envelope restriction a mechanically caused flight schedule deviation, provided the airplane departs on time on the subsequent flight.

8.1.2 DATA AND DATA SOURCES

Failure rates generally have been based on the large data banks of service experience maintained by Boeing. Data specially obtained and researched by Boeing and reported under References 9 and 10 also were used. Where no airline service experience exists (on new technology equipment), vendor mean times between failures (MTBF) for similar equipment were used, or MIL-HDBK-217B (ref 11) predictions were developed.

Applicable data and data sources are shown in Table 30.

8.1.3 PREDICTION MODEL AND ASSUMPTIONS

This section describes the computer model used for reliability predictions and gives the assumptions made in applying this methodology to the ACT system.

Table 30. *Failure Rates and Data Sources*

Component	MTBF, flight hours	Failure rate per 10^6 flight hours	Data source
Computer	6800	147.0	MTBF guarantee
Act secondary actuator			
Power piston and servo valve		1.6	Reference 8
T valve		10 0	Service data
LVDT—servo valve		7 0	Reference 9
LVDT—power piston		7 0	Reference 9
Solenoid bypass valve		6 0	Service data
Total secondary actuator		31 6	
Inertial reference unit (roll rate and roll angle)		416.7	Vendor MTBF
VYRO accelerometer		7 249	Vendor data
Control column position sensor		11 0	Reference 9
Accelerometers			
Wing—uninhabited area		50 0	Vendor data
Center of gravity—inhabited area		20.0	
Digital air data computer (airspeed, IAS—calibrated, Mach number, angle of attack)		83 3	Vendor data
Discrete switches		0 6	Reference 11
Single hydraulic system loss (assumes either pump will provide adequate pressure)	35 000	28 57	Service data adjusted for added ACT complexity
Loss of all electric power including batteries		0	Based on use of quadruply redundant standby batteries
Independent voter		71 4	Prediction assuming environmental severity factor of 4.0
Secondary actuator mechanical voter		0	Multiple mechanical failures required to cause malfunction
Single-wire segment		0.2	Service data
Connectors			Reference 11
10 pin		0 07	
20 pin		0 14	
200 pin—rack and panel computer connector		3.6	

768-103

8.1.3.1 CARSRA Model

The CARSRA model (ref 6) was used for most ACT predictions. In five cases where the PAS configurations under study were simple enough to be modeled and solved by pure Boolean logic (without truncation), the CARSRA prediction demonstrated sufficient accuracy. Therefore, the CARSRA prediction of the more complex systems was assumed sufficiently accurate to prove compliance with the $< 1 \times 10^{-9}$/FH requirement. However, because CARSRA may only be capable of handling a certain limited kind of logic, Boeing currently is conducting basic research to provide a means for accurate reliability prediction of complex fly-by-wire systems:

- The accuracy limitations of current prediction models and truncation methods are being investigated.
- The logic statements required for both the design and reliability modeling are being evolved as part of the basic design process by direct interaction between the designer and the reliability engineer.
- Computerized methods are being developed to simplify this logic and to accurately predict the probability of undesirable events.

This research should provide a prediction model to accurately handle the many events that can occur in ACT systems. Boeing is also cooperating with Raytheon to adapt the CARE III reliability model to interface with our fault-tree prediction methodology.

8.1.3.2 Assumptions

The following ground rules were established to allow analysis to proceed at the present level of design definition:

- The crucial PAS function shall be isolated from other functions in software and hardware so that common failure modes, which can cause the simultaneous loss of more than one channel, shall be extemely improbable.

- Crucial PAS software shall be so simple that all logic paths can be verified during design and test.

- Single-thread operation shall not be used in normal ACT system operation; i.e., a minimum of two channels is required for successful operation. On this basis, coverage is assumed to be 1.0 (ref 6).

- The PAS system shall be designed to provide no less than degraded, but safe, flight control in the event of a single mechanical disconnect or a jam (including actuator jam) anywhere in the PAS system.

- All channels in the redundant ACT system shall have identical hardware and software to allow for interchangeability and to prevent improper installation.

- If all ac power generation is lost, sufficient battery capacity shall be provided for 30 min of flight.

- One engine failure shall not cause the loss of more than one channel.

- The secondary actuation system shall be designed so that any single actuator will provide sufficient power to drive the active controls. Actuator output is continuously monitored by a mathematical model in each computer. Since four models are available, model reliability is treated as 1.0.

- The PAS system is assumed good (i.e., to have no preexisting failures) at the beginning of each 1 hr flight.

8.1.4 PREDICTION

A reliability trade study was performed to select the simplest configuration that would meet the $<1 \times 10^{-9}$/FH requirement. Four configurations of the crucial quadruple PAS system were analyzed, and three variations in failure rates (or sensors) were considered (fig. 174). Since this prediction required many computer runs and was comparative only, it was not updated to reflect the final failure rates shown in Table 30.

Case	MTBF Sensor	MTBF Computer[g]	MTBF Secondary actuator	Configuration 1	Configuration 2	Configuration 3	Configuration 4
				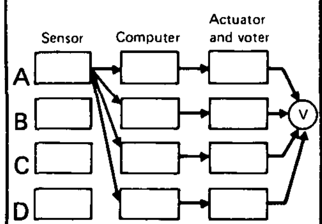	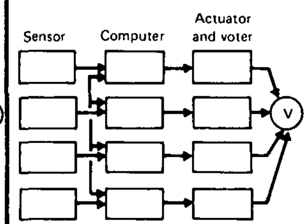	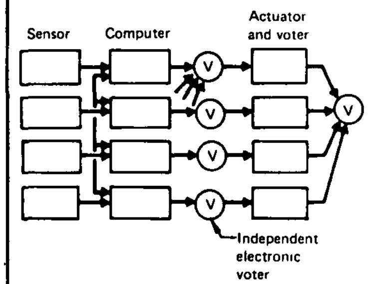	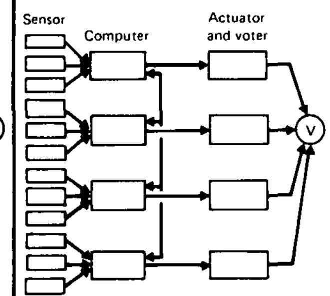
A	Q_A, Q_B, Q_C, Q_D } IRS MTBF 3800 hr	MTBF 4000 hr	4 servo-actuators d)	1.87×10^{-10}	5.92×10^{-10}	5.47×10^{-10}	1.16×10^{-9}
B	Q_A, Q_B, Q_C } IRS MTBF 3800 hr; Q_D = VYRO MTBF = 137 000	MTBF 4000 hr	3 servo-actuators + math model d), e)	9.52×10^{-11}	3.51×10^{-10}	3.4×10^{-10}	9.11×10^{-10}
C	Q_A, Q_B, Q_C, Q_D } VYRO MTBF 137 000	MTBF 4000 hr	3 servo-actuators + math model d), e)	7.56×10^{-11}	8.13×10^{-11}	7.12×10^{-11}	6.41×10^{-10}

Assumptions of analysis:

a) Wiring and connectors $\lambda = 0$
b) Actuator mechanical voter $\lambda = 0$
c) Three hydraulic systems with MTBF = 40 000 each
d) Secondary actuators $\lambda = 31.6 \times 10^{-6}$ hr
e) Math model $\lambda = 0$
f) Independent voter with MTBF = 14 000 hr
g) Software reliability = 1.0

768-103

Figure 174. Four-Channel PAS Reliability Trade Study

In the PAS system, the computers translate sensor data into electric commands to the three electromechanical actuators, which are mechanically force-voted. Actuator force voting is assumed to have reliability of 1.0. Three hydraulic systems provide independent power, one to each of the three actuators. To allow the loss of two out of three hydraulic systems without loss of PAS, each computer has an actuator model so that any single actuator with the mathematical model will provide adequate secondary actuation. The same MTBF for each hydraulic system (40 000 hr) was assumed so as not to exceed the limitations of CARSRA's (ref 6) success configuration table.

The configurations of Figure 174 can be described as:

- Configuration 1—Only pitch rate sensors are regarded as crucial, and these are cross-strapped (hard-wired to each computer) so that the loss of the computer does not cause the loss of a sensor. However, loss of a computer does lose the actuator directly connected to it.

- Configuration 2—Instead of sensor cross-strapping, cross-channel communication between computers enables sensor signals to be interchanged and used, but loss of a computer results in the loss of both the sensor and the actuator directly connected to it.

- Configuration 3—An electronic voter is added between each computer and its actuator. If the computer fails, its associated actuator is not lost because each voter receives and votes on command signals from all four computers. The small impact of the voter is attributable to the low failure rate of the PAS secondary actuators.

- Configuration 4—This is the same as Configuration 2, but airspeed and column force signals are added to provide a more sophisticated control law.

Because of the comparatively low (3800 hr) MTBF of the four inertial reference system (IRS) sensors, Configuration 4A will not meet the reliability design objective of $<1 \times 10^{-9}$/FH probability of failure (fig. 174). This configuration is impractical because, at most, only three IRSs will be installed in the Baseline Configuration.

Cases B and C (fig. 174) show the benefits of using the VYRO (trade name) pitch rate sensors in place of one and four IRSs.

CARSRA predictions for two configurations of three-channel PAS show that neither will meet the crucial PAS objective of $< 1 \times 10^{-9}$ failures/FH (fig. 175); hence, at least four channels are mandatory.

In general, these analyses indicate that:

- Four-channel PAS generally will meet the $< 1 \times 10^{-9}$ failures/FH objective, but three-channel PAS will not.
- The impact on cost of ownership of using four VYROs versus three IRSs plus one VYRO should be studied. Although the cost of the three IRSs will not be charged to ACT because they are part of the Baseline automatic flight control system (AFCS), the impact on reliability might outweigh this advantage.
- Configuration 2 will most simply meet the reliability requirement.

The failure effects analysis (table 31) identified component failures that would cause loss of function and showed which restrictions would have to be imposed on in-flight and dispatch operations.

Using Configuration 2B of Figure 174 and failure rates of Table 30 (including connectors and wiring), the probability of loss of the crucial PAS function is predicted as 3.46×10^{-10}, which is less than 1×10^{-9} failures/FH, so it meets the FAA draft Advisory Circular (ref 8) requirement. The probability of an in-flight schedule change (flight restriction, diversion, air turnback) resulting from a malfunction of ACT components, as defined in Table 31, was calculated for the following scenarios.

- Scenario 1—The schedule changes when some component failures cause one or more of the PAS and flutter mode control (FMC) functions to become inoperable. Malfunction of PAS (short period) is crucial and is not counted as cause for schedule change, but PAS (speed) is critical and is counted.

Requirements	3 actuators + 1 math model		2 actuators + 1 math model	
At least 2 → At least 2 → At least 2 →	Case A: 3 IRS Q sensors 3 computers 3 hardware actuators 1 math model	Case B: 3 VYRO Q sensors 3 computers 3 hardware actuators 1 math model	Case C 3 IRS Q sensors 3 computers 2 hardware actuators 1 math model	Case D 3 VYRO sensors 3 computers 2 hardware actuators 1 math model
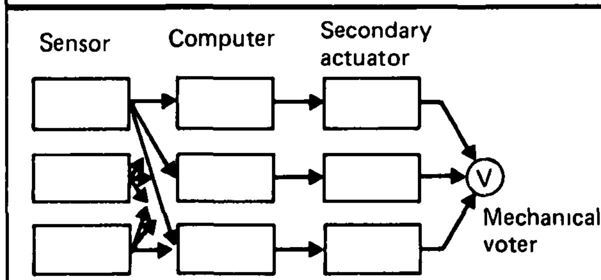 **Configuration 5**	3.95×10^{-7}	1.88×10^{-7}	3.98×10^{-7}	1.91×10^{-7}
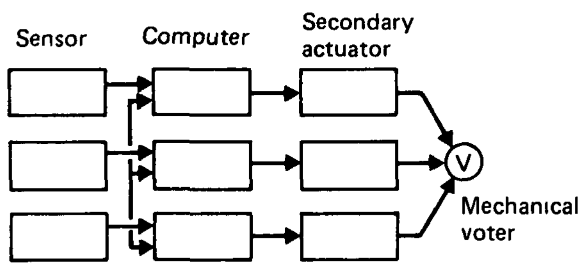 **Configuration 6**	7.89×10^{-7}	1.99×10^{-7}	8.34×10^{-7}	2.44×10^{-7}

768-103

Figure 175. Three-Channel PAS Reliability Trade Study

Table 31. Effects of Failure on In-Flight and Departure Reliability

Case No	Electrical system failures	Hydraulic system failures	Sensor failures	Computer failures	Actuator failures	Failure effects (survivability)								Remarks
							In flight				Dispatch			
						Actuator function loss	Air plane loss	Initiate flight schedule change	Continue changed flight schedule	Continue normal flight schedule	No go	Go with restriction	Go with no restriction	
1		3 channels				PAS and others	√				√			Probability of occurrence is extremely remote
2			3 IRS			PAS and others	√				√			
3			2 IRS + PAS VYRO pitch rate			PAS and others	√				√			
4				3 computers		PAS and others	√				√			
5					3 PAS elevator actuators	PAS and others	√				√			
6	Combination of sensors, computers and actuators that eliminates success path of the PAS system					PAS and others	√				√			
7	Main electrical system failure					Critical actuator functions		√ (divert to nearest air port as soon as possible)			√			Switched to backup batteries in flight
8			2 IRS			Some critical functions		√ (divert to nearest air port as soon as possible)				√		1 failure away from PAS loss
9			1 IRS + PAS VYRO pitch rate			Some critical functions		√ (divert to nearest air port as soon as possible)				√		1 failure away from PAS loss
10			1 CADC			None		√	√			√		1 failure away from PAS (speed) loss
11			2 CADC			PAS (speed) and others		√	√		√			
12			1 FMC accelerometer			None		√	√			√		1 failure away from FMC loss
13			2 FMC accelerometers			FMC loss		√	√			√		
14				1 computer		None		√	√			√		1 failure away from FMC or PAS (speed) loss
15				2 computers		FMC PAS (speed) and others		√	√		√			
16					1 PAS elevator actuator	None		√	√			√		1 failure away from PAS (speed) loss
17					2 PAS elevator actuators	PAS (speed)		√	√		√			
18					FMC actuator (1 electrical or hydraulic channel loss)	None		√	√			√		More study required for FMC actuator
19					FMC actuators (2 electrical or hydraulic channel loss)	FMC		√	√		√			
20		1 channel				None						√		1 failure away from PAS (speed) loss
21		2 channels				PAS and other actuator functions		√ (divert to nearest air port as soon as possible)						
22	Component failures that affect only AAL (except loss of α sensors or stick pusher)					AAL				√	√[a]	√[b]		[a]Complete loss
23	Component failures that affect only WLA (except GLA accelerometer sensors)					WLA				√	√[a]	√[b]		[b]Need 2 channels

768-103

- Scenario II—The schedule changes when a component failure results in only one more component failure being required to produce an inoperable ACT function. Both PAS (short period) and PAS (speed) are considered in the prediction.

The contributions of each subgroup under Scenario I are illustrated in Figure 176 and listed in Table 32. The failure probabilities of components (nearly always single failure) that led to the system being one failure from an ACT shutdown (Scenario II) is shown in Table 33.

Figure 177 shows the probability of complete loss of each critical ACT function. The predicted flight schedule change of 1.39×10^{-3}/FH (table 33) is a good approximation for total ACT if flight restrictions must be imposed when one more component failure would result in loss of function. However, if critical functions are truly fail-safe (i.e., a safe retreat into a restricted flight envelope can be made), an in-flight schedule change of 4.11×10^{-6}/FH (table 32) will be more appropriate.

Four channels are required to meet the $< 1 \times 10^{-9}$/FH failure criterion for the crucial function, and (based on the previously stated assumptions) the PAS configuration selected meets this requirement. However, if PAS should become critical rather than crucial and if safe retreat into a restricted flight envelope becomes possible with the loss of any ACT function, then the level of redundancy required should be decided by a trade between the cost of complexity and the cost of delays and cancellations.

8.2 MAINTAINABILITY

The self-monitoring of the integrated ACT system will greatly improve its maintainability over previous AFCSs. This will correctly isolate 95% of the failures to the offending line replaceable unit (LRU). An "on condition" maintenance concept will be used, with the system condition established automatically at every preflight and at failure detection during flight. This will essentially eliminate the need for scheduled inspections.

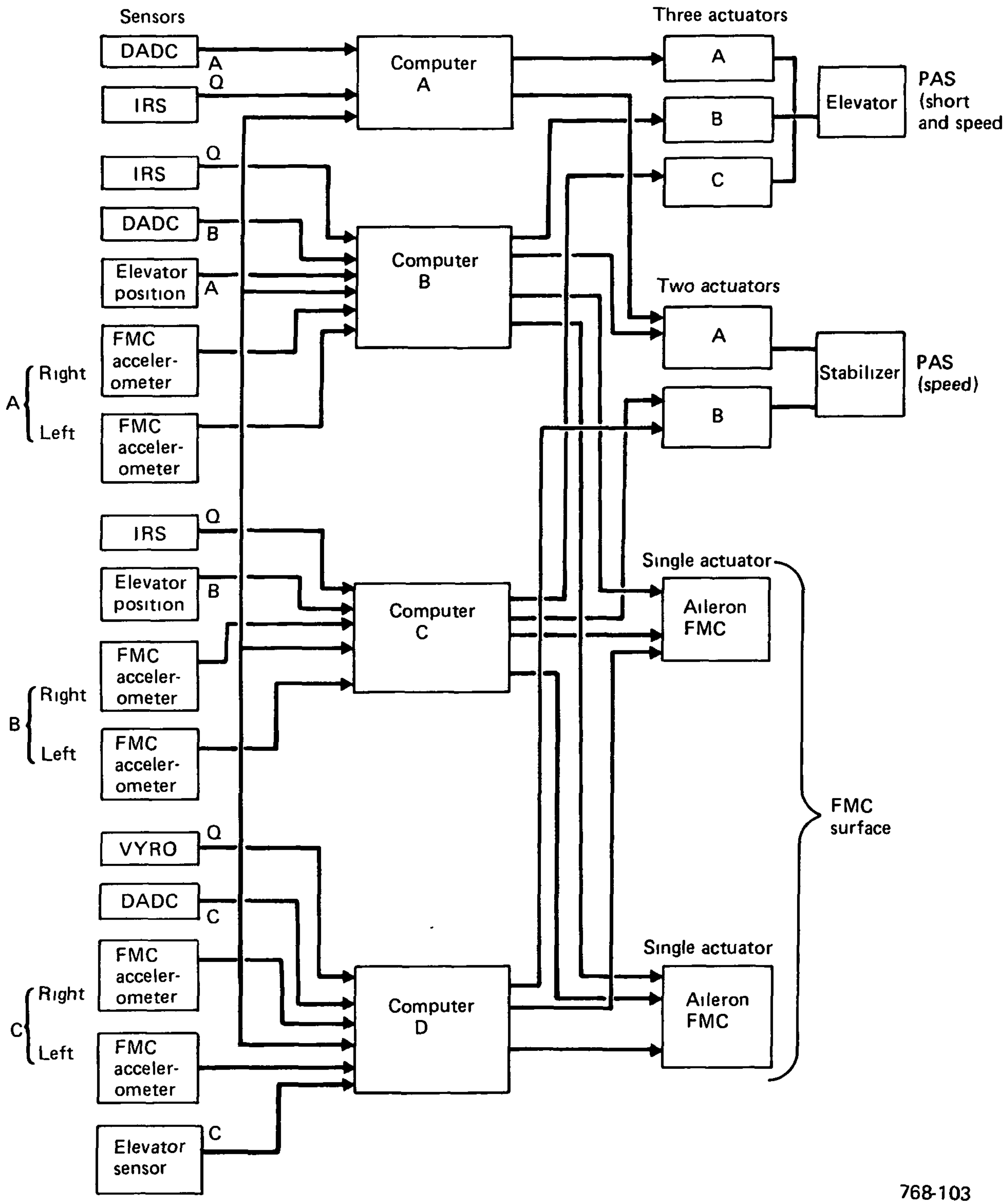

Figure 176. Components Involved in Schedule Change Decisions

Table 32. Probability of Schedule Change Under Scenario I

Components or function	Probability of schedule change
Sensor only	3.94×10^{-8}
Computers only	$1\ 81 \times 10^{-7}$
FMC actuators only	3.6×10^{-6}
Elevator actuators only	$4\ 5 \times 10^{-9}$
Sensor and computer	$1\ 99 \times 10^{-7}$
Actuator and computer	$5\ 36 \times 10^{-8}$
Hydraulic only	$2\ 45 \times 10^{-9}$
Electric power	Negligible
Hydraulics and computers	$3\ 58 \times 10^{-8}$

768-103

Note. The total probability of schedule change in a 1-hr flight is 4.11×10^{-6} (without wiring and connector allowance, this was $3\ 65 \times 10^{-6}$).

Table 33. Probability of Schedule Change Under Scenario II

Component	Maximum number lost without function failure	Probability of maximum number lost
Q sensor (IRS-VYRO)	2	$5\ 36 \times 10^{-7}$
Velocity sensor (DADC)	1	$2\ 55 \times 10^{-4}$
Acceleration sensor (accelerometer)	2	3.26×10^{-4}
Computer	1	$6\ 02 \times 10^{-4}$
Actuator (elevator)[a]	1	1.16×10^{-4}
Hydraulic system	1	$8\ 58 \times 10^{-5}$
Total		$1\ 39 \times 10^{-3}$

768-103

[a]The FMC actuators were excepted from the study, since the system is always one failure from loss of FMC

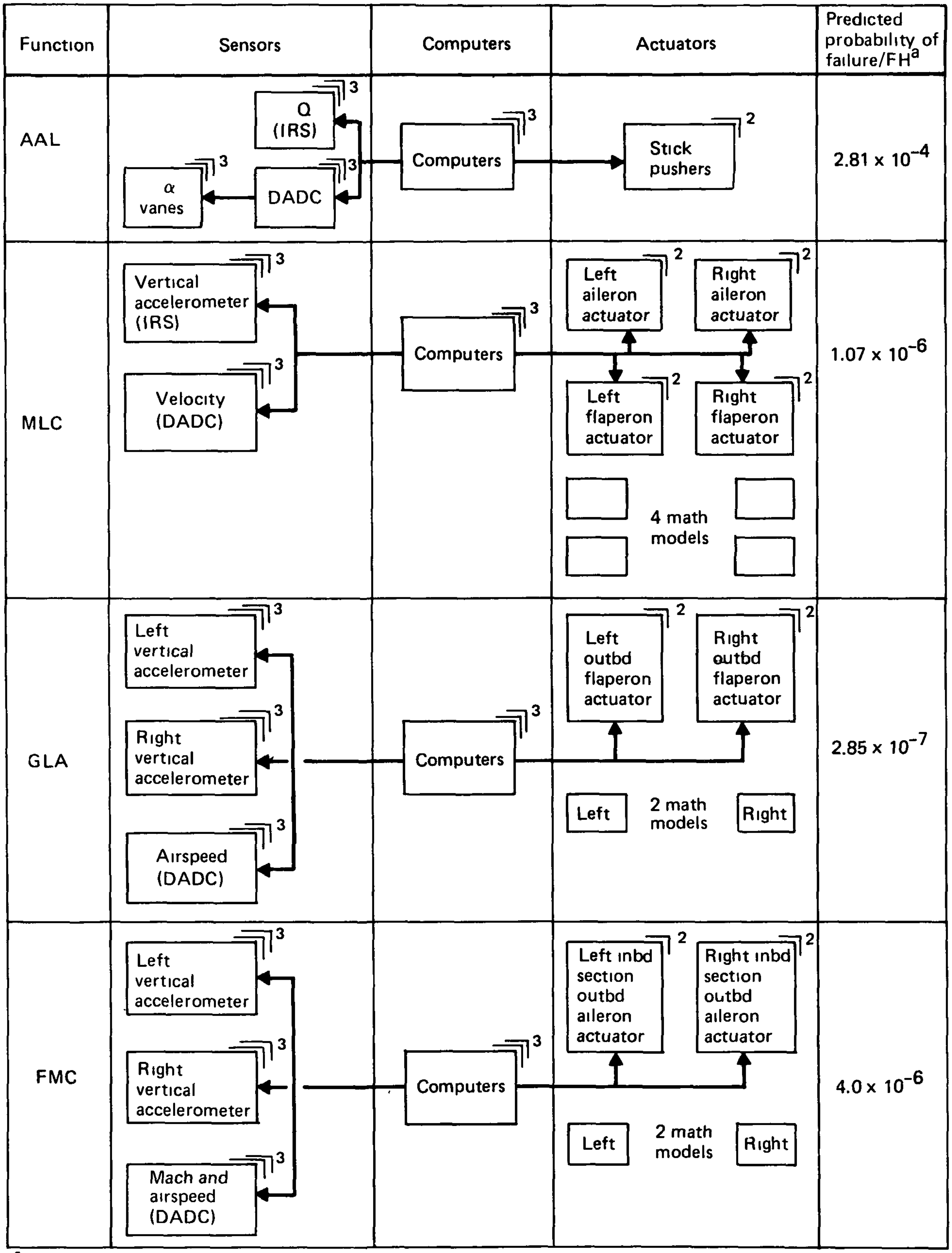

[a]Software reliability assumed equal to 1 0

768-103

Figure 177. Probability of Failure-Critical ACT Functions

8.2.1 REQUIREMENTS AND OBJECTIVES

The maintainability objectives of particular importance to ACT are:

- At least 95% of the failures are to be successfully isolated to the LRU (basic system self-monitoring generally provides this feature without additional built-in equipment).

- Incorrect installation shall be impossible (this is of particular importance to crucial PAS).

- Components that can affect dispatchability shall be replaceable in a time that is compatible with the scheduled reliability requirements.

- The direct maintenance cost for the airplane and its systems shall be $0.56/FH/seat (1977 dollars). This goal, established for Boeing's New Airplane Program for an aircraft similar to the Baseline Configuration, was predicted from service experience data.

8.2.2 MAINTENANCE COST PREDICTION

The incremental maintenance cost per flight hour (based on past experience and recent estimates) is shown in Table 34. Total maintenance cost, which includes direct maintenance cost, maintenance burden, and fringe benefits, is predicted as $4.46/FH. Based on the ground rules of Subsection 8.3.2, the cost of delays and cancellations is estimated as $0.87/FH (table 35). Therefore, the cost for maintenance, delays, and cancellations totals $5.34/FH.

8.3 COST OF OWNERSHIP

Cost-of-ownership analysis identifies the configuration expected to provide the highest return on investment (ROI) to the airline and shows whether it will realize an acceptable profit. This analysis enables present dollar values per flight hour to be calculated for parameters such as weight, drag, fuel burned per flight hour,

Table 34 Prediction of Maintenance Cost per 1000 Flight Hours

Nomenclature	[a] QPA	Reference ASN [b]	Direct [c] maintenance cost—78 $	Total [c] maintenance cost—78 $	Remarks
VYRO	1	N/A	2 64	5 28	Based on workshop experience
Accelerometer—body mounted	6	N/A	96 00	192 00	Based on workshop experience
Accelerometer—wing mounted	6	N/A	240 00	480 00	Based on workshop experience
Computer	4	N/A	940 88	1881 76	Significant component estimate
Preflight and maintenance test panel	1	N/A	137 63	275 26	Significant component estimate
Secondary actuator	9	27-21-675-021	284 65	608 06	727 rudder actuator used as baseline
Actuator for FMC aileron	2	27-21-657-021	63 26	135 13	Based on 727 rudder actuator
Stick pusher pneumatic actuator	1	78-34-008-001	4 40	10 03	Based on 727 thrust reverser actuator
Stick pusher pressure transmitter	2	32 43-556-021	4 04	8 73	Based on 727 pneumatic brake pressure transmitter
Stick pusher solenoid valve	2	30-44-576-201	2 01	4 24	Based on 747 window washer solenoid valve
Stick pusher pneumatic regulator	2	29 03 418-011	21 16	44 39	Based on 727 hydraulic reservoir regulator
Stick pusher pneumatic accumulator	2	32 43-064 011	8 24	17 85	Based on 727 pneumatic brake accumulator
Stick pusher relief valve	2	N/A	0	0	Simple pneumatic relief valve—no maintenance cost
Stick pusher pressure gage	2	32-43-284-031	1 44	3 12	Based on 727 pneumatic brake pressure indicator
Stick pusher pressure switch	2	21-33-522-041	0	0	Based on 727 pressure warning system
Stick pusher dump valve	2	32-43 576-211	12 10	27 33	Based on 727 pneumatic brake control valve
Ni-cad battery	1	N/A	–	170 99	Estimate pro-rated to 0 6649 removal rate
Battery charger	1	24-32-104-011	6 89	15 98	Based on 727
T-R unit	2	24-32-104-011	1 66	3 37	Based on 727
Static inverter	4	24-22-294-011	28 00	58 34	Factor of 10 applied to 747 inverter for continuous duty
Transformer	4	–	0	0	
Delete four elevator control units	-4	27-31-675-051	-172 40	-344 80	Based on United Airlines 747 1977 data
Add additional hydraulic lines and hoses	–	27-31 312-101	10 90	29 16	Based on 727 elevator multiplied by 3
			Total	3,626 22	

768-103

Factor total by 1 28* = $4,641 56 per 1000 flight hours

*Accounts for maintenance costs not covered by LRU reporting

[a] Quantity per aircraft

[b] Boeing identifier

[c] Dollars per 1000 flight hours

Table 35. Component Delay Hours and Cancellations—Initial ACT Configuration

Assigned serial number	Baseline	Initial ACT	QPA[a] factor	Delay, hr (per 1000 departures)	Cancellations (per 1000 departures)
34-12-130-011	DC-10	Active flight control computer	4/2	0 1832	0
27-21-675-021	727	Secondary and FMC + MLC actuators	11/2	0 0259	0 0117
22-41-368-000	727	Preflight and maintenance test panel	1/1	0 0042	0
27-21-280-191	727	ACT hydraulic lines	4/1	0 0379	0
22-35-004-011	DC-10	Accelerometers	13/3	0	0 0265
(27-32) and (32-43)	747/727	Flight envelope limiting system	2/1	0 0668	0
27-31-675-051	747	Delete four elevator PCUs	1/2	-0 0370	0
			Component total	0 281	0 0382

768-103

[a]Quantity of parts per aircraft—QPA factor = $\frac{\text{QPA Initial ACT Configuration}}{\text{QPA Baseline Configuration}}$

maintenance cost, spares inventory cost, and system purchase cost. This avoids the need for intuitive weighting factors (inherent in trade matrices) and removes subjective judgment from the design decision process.

However, four-channel redundancy is dictated for the integrated ACT system by the requirement that the crucial PAS have a failure probability of $< 1 \times 10^{-9}$/FH . As a result, the cost-of-ownership analysis was confined to establishing whether the system will provide an adequate profit and determining what parameters are major cost drivers, rather than studying the ROI effects of potential design simplification.

8.3.1 COST-OF-OWNERSHIP MODEL

The Boeing-developed airline cost-estimating system (ACES) computer program was used in this analysis. For each future year, this program calculates the airline profit or loss that may be expected from the add-on ACT, then calculates the ROI to the airline based on the present equivalent value method. ACES accounts for the expected inflation rate, investment tax credit, depreciation credit, income tax, and operating cost; ACES shows which parameters have the greatest impact on ROI. It also establishes the payback point after which a positive cash flow (profit) to the airline may be expected. Airlines use this important parameter to decide whether to modify an existing fleet, but the payback point is less significant in the purchase of new aircraft.

8.3.2 PARAMETRIC STUDIES

The economic analysis is based on the following cost-of-ownership ground rules that are consistent with those used by Boeing for in-house trade studies:

- Fleet size = 30 aircraft
- Airplane production run = 300 airplanes
- 1978 jet fuel cost = $ 0.1057/ℓ ($0.40/gal)
- Minimum attractive ROI = 15%
- Tax depreciation life = 10 years
- Fleet life = 15 years
- Investment tax credit = 7%
- Cost per delay hour = $1400
- Cost per cancellation = $5100
- Spares holding cost = 10% of spares cost
- Yearly utilization = 2750 hr
- Average trip = 1.25 FH and 863 km (466 nmi)
- Yearly inflation rate = 8%
- Insurance = 0.5% of purchase cost
- All costs = 1978 dollars

Excluding the expense of training, which is covered by the aircraft purchase price, the cost-of-ownership values estimated for Initial ACT Configurations are:

- Cost (to airline) per aircraft of adding ACT to the Baseline Configuration (including recurring and nonrecurring costs) = $300 000 (1978 dollars)

- Fuel saving = 160 kg/FH (352 lb/FH) = 3.3%
- Cost of maintenance and delay/cancellation = $5.34/FH
- Maintenance manual cost per fleet = $21 000
- Test equipment cost per fleet = $22 500

The analysis showed that the airplane would provide a satisfactory incremental ROI of 15.73% using $0.1057/ℓ ($0.40/gal) fuel and the cost estimate listed above. Figure 178 shows the impact on ROI of varying the "best estimate" (nominal) major cost drivers by ±50%. It appears that an ACT incremental purchase cost of much over $300 000 per aircraft will not provide an adequate ROI; however, a fuel cost increase of 50% will greatly improve the attractiveness of the ACT investment. The impact of fuel price is further illustrated in Figure 179, which shows that fuel cost can be expected to dominate the ROI picture.

These factors should be used with caution because each design case must be separately studied to obtain the true ROI.

Tables 36 and 37 show the influence of important economic parameters on airline profit. Generally, fuel price or reduced fuel burned dominates the parameters, accounting for 50% to 70% influence. The influence of Δ first cost and Δ maintenance/delay cost for the "best estimate" ACT aircraft are about equal. Note that investment tax credit and depreciation credit reduce the impact of the first cost by about 45%. Conversely, the assumption of 50% tax on corporate profit reduces ACT profitability potential by 50%.

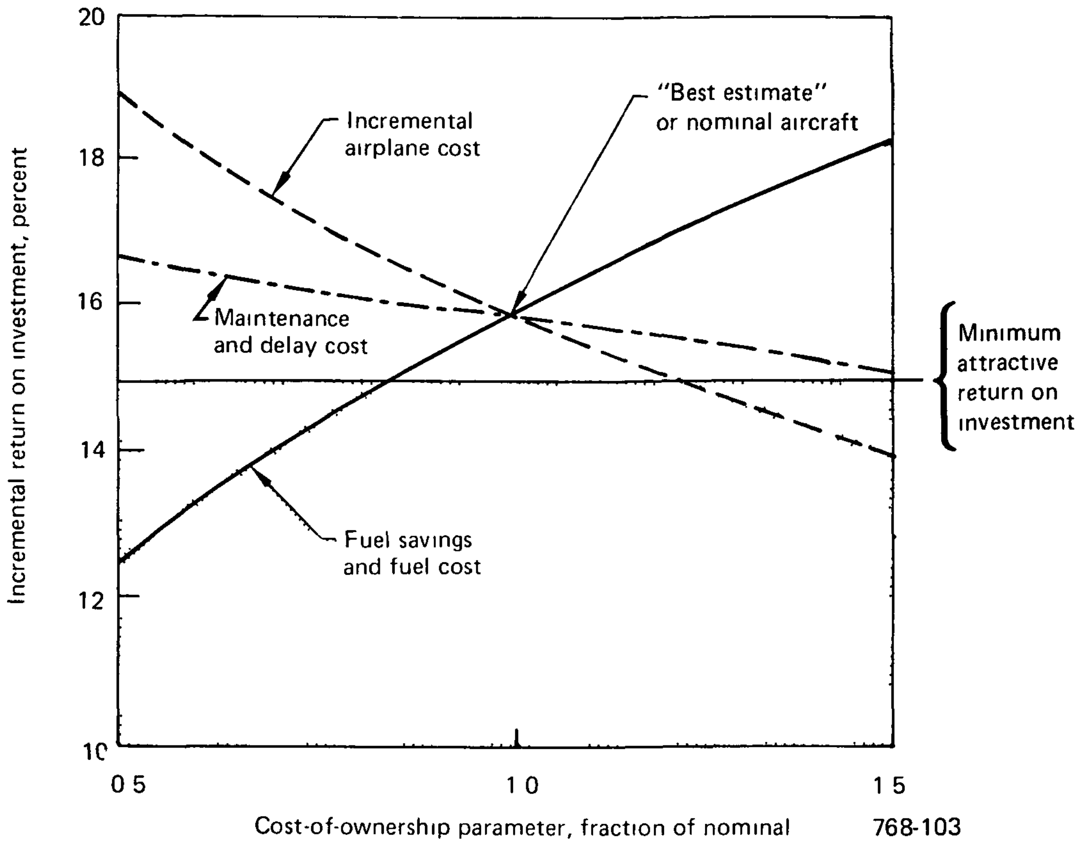

Figure 178. Effect of Changes in Cost Parameters on Incremental Return on Investment

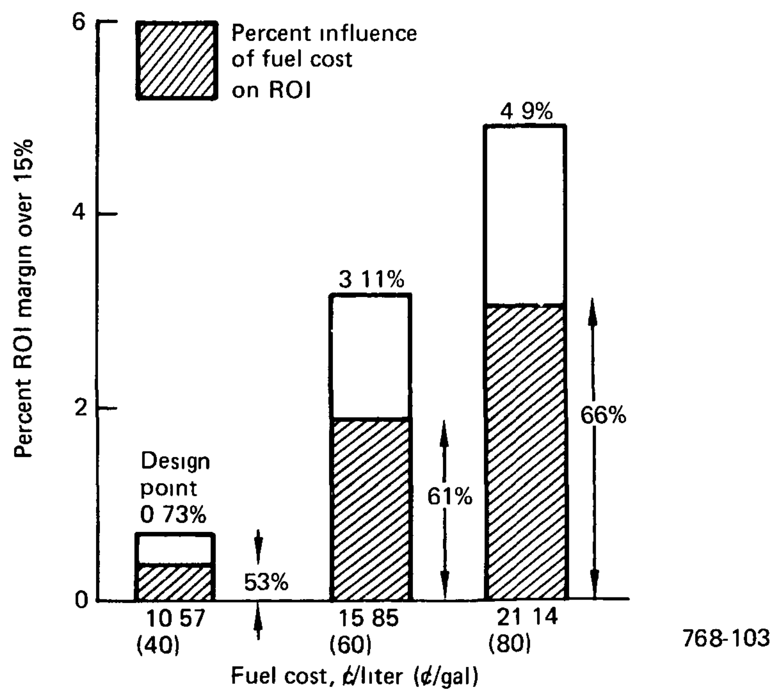

Figure 179. Impact of Fuel Cost on ROI Margin Over 15%

Table 36. *Airline ROI and Payback Point for Varying Significant Economic Parameters*

ACES computer run number	Plus Δ$[a] ACT cost/aircraft	Minus Δ fuel burn/flight hour, kg (lb)	Plus Δ$[a] maintenance and delay cost/flight hour	Payback point, years	ROI to airline	Parameter varied
INV1	100 000	160 (352)	5 34	3 77	20 88	Aircraft Δ first cost from $100 000 to $600 000 at 10 57 ¢/liter (ℓ) (40 ¢/gal) fuel
INV2	200 000	160 (352)	5 34	6 93	17 46	
INV3[b]	300 000	160 (352)	5 34	11.23	15 73	
INV4	400 000	160 (352)	5 34	> 15 0	< 15 0	
INV6	600 000	160 (352)	5.34	> 15 0	< 15 0	
MCS	300 000	160 (352)	2 67	8.99	16 41	Maintenance and delay cost Δ from $2 67 to $10 68/flight hour at 10 57 ¢/ℓ (40¢/gal) fuel
MCS1[b]	300 000	160 (352)	5 34	11.23	15 73	
MCS2	300 000	160 (352)	10 68	> 15.0	< 15 0	
FS40C[b]	300 000	160 (352)	5.34	11.23	15.73	Fuel cost = 10 57 ¢/ ℓ (40 ¢/gal)
FS60C	300 000	160 (352)	5.34	6 04	18.11	15 85 ¢/ ℓ (60 ¢/gal)
FS80C	300 000	160 (352)	5 34	4 42	19 9	21 14 ¢/ℓ (80 ¢/gal)
FS40C[b]	300 000	160 (352)	5 34	11.23	15.73	Percent fuel saving = 3 3% at 10 57 ¢/ℓ
FS80C	300 000	319 32 (704)	5 34	4.42	19 9	6 6% at 10 57 ¢/ℓ

[a]All 1978 dollars

[b]All same data set for best-estimate aircraft

768-103

Table 37. Influence of Cost of Ownership Drivers on ROI

Parameter varied	Influence on ROI, percent[a]		
	Δ$ first cost[b]	Fuel price or percent fuel saved	Δ maintenance cost and spares holding cost
Fuel cost			
10 51¢/liter (ℓ) (40¢/gal)[c]	25	53	22
15.85 ¢/ℓ (60¢/gal)	21	61	18
21.14 ¢/ℓ (80¢/gal)	18	66	16
Δ aircraft cost = \$100 000[b]	11	63	26
Δ aircraft cost = \$200 000[b]	19	57	24
Δ aircraft cost = \$300 000[b, c]	25	53	22
Δ fuel saving, percent			
3.3[c]	25	53	22
6.6	18	66	16
Δ maintenance and delay cost/FH			
\$2.67	14	56	30
\$5.34[c]	25	53	22
\$10.68	19	48	33

768-103

[a] ROI influence calculated after deduction of 50% corporate tax on fuel saving Δ$

[b] Δ$ first cost includes·

(1) Δ$ cost of adding active controls to the airplane, and covers recurring and nonrecurring cost.
(2) First purchase of rotatable spares, test equipment, and maintenance manuals, the sum of these is small compared with (1) above.
(3) Investment tax credit and depreciation credit reduce item (1) by about 45%
(4) Cost of hull insurance, this is small, and less than item (2) above.

[c] Best estimate case—all the same

8.3.3 COST/BENEFITS SUMMARY

Generally the present ACT configuration was selected because the crucial PAS had to meet the $< 1 \times 10^{-9}$/FH failure criterion, which dictated the adoption of the four-channel system regardless of first cost and maintenance cost. If PAS could move to the critical class (i.e., permitting safe retreat inside a restricted flight envelope when failure occurs), a simpler system with lower first cost and maintenance cost might be feasible.

The dominant effect of fuel burned and/or fuel cost on profit potential suggests that significant increases in first cost and maintenance cost would be tolerable, provided that fuel burned decreased comparably.

Therefore, integrated ACT will provide an adequate ROI, even without resizing the airplane and at actual 1978 fuel prices. However, the ROI becomes much more attractive if the aircraft is resized for the Baseline Configuration range and if fuel prices rise faster than the 8% general inflation rate assumed in this analysis.

9.0 CONCLUDING REMARKS AND RECOMMENDATIONS

Page

9.0 CONCLUDING REMARKS AND RECOMMENDATIONS

9.0 CONCLUDING REMARKS AND RECOMMENDATIONS

The principal objective of the IAAC Project is to assess the effects of the integrated application of ACT to a medium-range subsonic transport airplane. As a first step in that study, the Initial ACT Configuration was developed.

Specific conclusions to be drawn from incorporation of active controls in the Initial ACT Configuration development are:

1) Maximum range at constant gross weight and design payload improved by 13%.

2) Block fuel savings from approximately 3% at short range (less than 1000 km [540 nmi]) to better than 6% at ranges above 3000 km (1620 nmi) were shown.

3) The improved operating economics resulting from this performance improvement provide a slightly greater than 15% return on investment (ROI) for the addition of ACT at the assumed fuel price of \$0.106/ℓ (\$0.40/gal). ROI is based on factored cost data and is sensitive to a number of assumptions made in the economic analysis. Sensitivity studies show considerably increased ROI if fuel prices increase at greater than the average inflation rate.

4) Assuming current certification rules and procedures, no serious technical obstacles to achieving the above results have been identified with the exception of software reliability validation to the very high levels required, although considerable control system work remains to be done. The software reliability problem is currently being addressed in other ongoing research programs. Control system development (including acquisition, laboratory test, and, potentially, flight test) of critical ACT system elements must also proceed for ACT to become an integral part of future commercial transports.

To identify the effect of ACT on the configuration and performance, a constant, contemporary level of technology was used throughout in the structure, aerodynamic, and propulsion technologies. For example, because structures and flight controls technologies might interact synergistically, the combination of advanced composites and ACT could result in greater gains than the sum of their individual contributions. Examination of these possibilities is beyond the scope of the present study.

Reliability and maintainability required for commercial operation were considered throughout. Criteria postulated for reliability and degree of dependence upon ACT functions may appear conservative; however, they represent Boeing's engineering judgment of what would be acceptable to the authority certifying airworthiness and to the airline customer.

The performance improvement achieved through ACT was not cycled by resizing the Initial ACT Configuration for constant mission performance. The Final ACT Configuration, which will be developed in a subsequent phase of the IAAC Project, will be mission-sized and should result in significant further improvement in fuel burn and airplane operating costs.

Redesigning an airplane to use ACT results in many complex interactions such as the interaction of loadability, center-of-gravity range, stability and controllability requirements, and landing gear geometry. With the removal or modification of minimum longitudinal stability requirements, high angle-of-attack controllability limits will define minimum longitudinal control power and horizontal tail size. Hydraulic and electric power systems must have reliability and redundancy compatible with the control system requirements. An assessment of ACT without consideration of a fully integrated design could lead to misleading or invalid conclusions.

The configuration development should be continued according to the IAAC Project plan with a wing planform study leading to development of a resized Final ACT Configuration with a wing planform optimized for ACT. Control system development should proceed according to the IAAC Plan (ref 1). These activities should address concerns with hardware and software implementation of the ACT functions and flying qualities characteristics with normal and failed ACT systems under various weather conditions.

Finally, current reliability analysis methods need to be extended to adequately treat redundant digital systems.

10.0 REFERENCES

Page

10.0 REFERENCES

1 Program Plan for Integrated Application of Active Controls (IAAC) Technology to an Advanced Subsonic Transport, NASA CR-3305, Boeing Commercial Airplane Company, 1980.

2 Integrated Application of Active Controls (IAAC) Technology to an Advanced Subsonic Transport Project—Conventional Baseline Configuration Study. NASA CR-159248, Boeing Commercial Airplane Company, June 1980.

3 Fuel Conservation Possibilities for Terminal Area Compatible Aircraft. NASA CR-132608, May 1975.

4 Chalk, C. R., et al.: "Flying Qualities of Piloted Airplanes." Background Information and User Guide for MIL-F-8785(ASG). AFFDL-TR-69-72, August 1969.

5 Federal Aviation Regulations--Part 25. Airworthiness Standards: Transport Category Airplanes. Federal Aviation Administration.

6 Bjurman, B. E., G. M. Jenkins, C. J. Maereliez, K. L. McClellan, and J. E. Templeman. Airborne Advanced Reconfigurable Computer System. NASA CR-145024, 1976.

7 Weight and Balance Data Reporting Forms for Aircraft. MIL-STD-1374 Part 1, March 31, 1972.

8 "Airplane System Design Analysis." Advisory Circular, Federal Aviation Administration, AC-25.1309-X (draft), 1979-80.

9 747 Primary Flight Control Systems Reliability and Maintenance Study. NASA CR-159010, April 1979.

10 Dode, W. W., R. H. Edwards, G. T. Katt, K. L. McClellan, and H. A. Shomber. Flight Control Electronics Reliability/Maintenance Study. NASA-CR-145271, 1977.

11 Reliability Prediction of Electronic Equipment. MIL-HDBK-217B, December 1, 1965.

APPENDIX A—
DESIGN REQUIREMENTS
AND OBJECTIVES

APPENDIX A—
DESIGN REQUIREMENTS
AND OBJECTIVES

APPENDIX A

1.0 GENERAL REQUIREMENTS

Plans for the Integrated Application of Active Controls (IAAC) Project include the development and periodic updating of complete documentation of the design requirements and objectives. Because the resulting detailed documentation is lengthy, and because certain parts are considered proprietary by The Boeing Company, this appendix summarizes the portions specifically affected by the inclusion of Active Controls Technology (ACT) functions.

ACT principally impacts the requirements relating to flight control system design, flying qualities, and—to a lesser extent—structural design and hydraulic and electric power systems. Thus, these topics are included herein.

The most general requirement is that the airplane will be designed to be certifiable under Federal Aviation Regulations (FAR) Part 25 (ref A-1) as a Transport Category Airplane. Design details must recognize the FAR safety and reliability requirements. As it presently exists, FAR 25 may have to be revised or extended to provide adequate, but not unduly restrictive, certification rules for an airplane with ACT functions.

Furthermore, the ACT airplane must be consistent with the Conventional Baseline Configuration in areas such as growth provisions, dispatch reliability, and alternate mission capability, so the costs and benefits of reconfiguring the airplane for ACT can be accurately assessed.

2.0 FLYING QUALITIES

This section summarizes flying-quality criteria related to airframe stability and control; handling qualities, as seen by the pilot through the flight control system; and ride qualities. Flight characteristics and stability and control criteria that impose requirements on the airframe are emphasized even though ACT functions may be used. Operational capabilities and associated flying qualities are summarized in this section, which also provides an overview of how flying-quality criteria are defined.

2.1 OPERATIONAL CAPABILITIES

The ACT aircraft will be flown by conventional piloting techniques. That is, even on approach, attitude and flight-path angle will be controlled by the column, and airspeed by the throttle or speed command selector. The pilot will use only one consistent technique for flying the aircraft, regardless of weight, speed, and other factors. The control system will provide excellent flying qualities in terms of aircraft response, maneuverability, and stabilization. The flight control system will be designed so normal crew reaction to cues produced by failure conditions will result in the appropriate action. The corrective action will not require exceptional piloting skill or strength.

The use of all axis stabilization or command augmentation, or both, is permitted to achieve the basic, normal-mode, control system capabilities.

Autopilot-assist systems, designed to further reduce pilot workload, provide particular operating modes selectable by the pilot. The design may use such modes as autoland, altitude, heading, or speed hold; however, disengagement of a pilot-assist mode will revert the control system to its basic control mode.

Minimum operational margins are defined to provide protection from uncontrollable or unsafe flight conditions during maneuvers and atmospheric disturbances. These margins, which may be provided by ACT functions, fall into four categories:

- Maneuver margins to perform required pullups and turns without buffet or loss of control

- Margin in angle of attack to prevent dangerous loss of lift or control due to atmospheric disturbances

- Margin in speed to preclude dangerous loss of lift or control due to speed variation (either produced by atmospheric disturbances or inadvertent pilot action)

- Margin to maintain desired flight path, even with reasonable speed variations from target speed, and to maintain a required minimum performance margin

2.2 FLYING-QUALITIES DEFINITIONS

2.2.1 FLYING-QUALITY LEVELS

Flying-quality levels are minimum acceptable values expressed in engineering terms such as control authority or response characteristics.

Three levels are:

- Level 1—Flying qualities are clearly adequate for missions within the operational flight envelope. Cooper-Harper pilot rating is 1 to 3.5, or excellent to fair.
- Level 2—Flying qualities are adequate to accomplish the mission, but pilot workload may increase or mission schedule and fuel usage effectiveness may degrade. Cooper-Harper pilot rating is 3.5 to 6.5, or fair to adequate.
- Level 3—Flying qualities allow safe control of the aircraft, but pilot workload is excessive, mission effectiveness is inadequate, or both. The mission can be terminated, and the aircraft can be flown to a suitable airfield for a completed landing. Cooper-Harper pilot rating is 6.5 to 9+, or adequate to minimally safe.

Required flying qualities depend on flight envelope and phase, winds and turbulence, and the failure state of the aircraft.

2.2.2 FLIGHT ENVELOPES AND PHASES

The aircraft may safely fly within operational and design flight envelopes. Operational flight envelopes define the boundaries—in terms of speed, altitude, and load factor—within which the airplane must be capable of operating to accomplish the specified missions. Normal aircraft states require Level 1 flying qualities throughout the operational flight envelopes. Design flight envelopes are boundaries of speed, altitude, and load factor based on aircraft limits rather than mission requirements. Within the design envelope, flying qualities must be at least Level 2 in the absence of critical failures.

The terminal flight phase includes takeoff, approach, go-around, and landing; tasks normally accomplished with gradual maneuvers and requiring accurate flight-path and heading control. The en route flight phase includes climb, cruise, loiter, descent, emergency descent, and emergency deceleration; again, tasks normally accomplished with gradual maneuvers and possibly requiring accurate flight-path control. Either the flying-quality parameters, which are used to specify the level, or their values may vary with flight phase.

2.2.3 CONFIGURATIONS AND LOADING

Configurations denote external shape and internal status such as flap setting, gear position, speed brake deployment, and thrust reverser position. Flying-quality requirements apply to: (1) appropriate configurations for all flight phases associated with the overall design missions, and (2) all permissible weights, loadings, and centers of gravity defined for the appropriate flight phase of the mission.

2.2.4 WINDS AND TURBULENCE

Safe flight will be ensured in the most severe atmospheric environment anticipated in service operation. All terminal-flight-phase tasks must be possible with winds from any heading, including 90 deg crosswind, using normal pilot skill and technique. For aircraft normal states, pilot workload is allowed to increase to Level 2 for high crosswind and turbulence levels with a probability of exceedance (near 10^{-3}/flight hour [FH]). Aircraft safety (Level 3 flying qualities or better) is required for wind/turbulence combinations with exceedance probabilities up to 1×10^{-5}/FH.

Specific capabilities require that a landing with Level 2 flying qualities must be possible in a 30 kn, 90 deg crosswind (measured at an elevation of 15m (50 ft). With an engine or other failure, a landing with Level 2 flying qualities must be possible in a 13 kn crosswind. For flight with critical system failures, the wind/turbulence exceedance probability is reduced to account for the combined probability of failures and wind/turbulence.

The winds and turbulence to be used for design are defined similarly to FAA-RD-74-206. In both low- and high-altitude models, wind and turbulence levels are specified by probability of exceedance.

2.2.5 AIRCRAFT FAILURES

With flight-critical failures, minimum flying-quality requirements are:

	Flying Quality Within:	
Number of Critical Failures	Operational Flight Envelope	Design Flight Envelope
0 (normal aircraft state)	Level 1	Level 2
1	Level 2	Level 3
2 (unless shown to be extremely improbable)	Level 3	Level 3

System and structural reliability will be appropriate for the aircraft to satisfy these minimum requirements and will apply to critical failures for those systems that may have more than one level of redundancy:

- Propulsion
- Flight control
- Hydraulic
- Electric
- Air data
- Active controls

The above requirements also apply to loss of part of the empennage or wing tip.

For normal operation, mission continuation and a safe landing are required after any single failure in a system, including one engine. Flight safety must be maintained after failure of as many as two flight-critical systems. With two engines failed, controllability must be adequate to permit engine restart and/or to achieve a reasonable attitude and airspeed for landing. Loss of part of the empennage or wing tip will be considered equivalent to two critical failures. General system reliability requires that flying-quality Levels 1, 2, and 3 be maintained during 70%, 25%, and 5% respectively, of flight time, which is based on airframe life, mission analysis, and maintenance procedures.

Section 4.0 defines more detailed failures to be considered for design and established reliability objectives for each system.

2.3 GENERAL FLYING-QUALITIES REQUIREMENTS

Tables A-1 through A-4 summarize specific criteria for stability, control, and feel force in ACT and conventional aircraft design. Figure A-1 summarizes the longitudial damping requirements. The requirements at the short-period frequencies are taken from Reference A-2, while the low-frequency (below 0.4 rad/s) requirements are related to in-house simulation experiments done in support of the 1971 United States supersonic transport program. Figure A-2 and A-3 (from ref A-2) show the longitudinal short-period requirements postulated for the airplane, although it is recognized that they may be inadequate or inappropriate for highly augmented transport airplanes.

The aircraft flying qualities must meet all mission requirements and objectives for which the aircraft is designed, and they must not limit aircraft performance. Control forces must be compatible with one-hand operation by the pilot for Level 1 (in the operational flight envelope). In addition, the control force levels, displacements, and sensitivity must not limit maneuver capability or performance of the airplane and must not result in undesirable flying qualities. Any flight condition or task required for the defined operational missions must not allow pilot-induced oscillations. In a stall and post-stall recovery, aircraft motions must be controllable, and recovery must be possible with one engine inoperative.

Crew and passenger ride comfort is not quantitative, but depends on both the airplane and structural motions. Criteria are directed at the structural motion to guide the

Table A-1. Airplane Stability Criteria Summary

Design parameter	Flying quality level 1	Flying quality level 2	Flying quality level 3
Longitudinal			
All flight phase			
Damping	(a)	(a,b)	
Phugoid	$\zeta_P \geqslant 0.04$ [c]	$t_{2x} \geqslant 12$ sec [b]	$t_{2x} \geqslant 6$ sec [b]
$\frac{d\gamma}{dv}$		< 0 deg/kn [d]	$\leqslant 0.06$ deg/kn [d]
Terminal phase			
Short period	(See fig 2 for ω_n versus n/α) [b]		
$\dot{\Theta}$ max/$\dot{\Theta}$ ss	$\leqslant 2.0$ [b]	$\leqslant 3.0$ [b]	No requirement
En route phase			
Short period	(See fig. 3 for ω_n versus n/α) [b]		
$\frac{d\delta e}{dn}$	$\leqslant -2$ deg/g [d]	$\leqslant -1$ deg/g [d]	No requirement
$\dot{\Theta}$ max/$\dot{\Theta}$ ss	$\leqslant 2.5$ [b]	$\leqslant 3.5$ [b]	No requirement
Lateral-direct			
All flight phases			
C_{ℓ_β}	No requirement	< 0 [d]	$\leqslant 0$ [d]
C_{n_β}	No requirement	No requirement	> 0 [c]
Dutch roll	$\omega_n \geqslant 0.8$ rad/s [b]	$\geqslant 0.5$ rad/s [b]	$\geqslant 0.4$ rad/s [d]
	$(\omega_n\zeta) \geqslant 0.16$ rad/s [b]	$\geqslant 0.5$ rad/s [b]	No requirement
	$\zeta \geqslant 0.2$ [b]	$\geqslant 0.08$ [b]	$\geqslant 0.02$ [b]
Spiral mode	$t_{2x} \geqslant 20$ sec [d]	$t_{2x} \geqslant 12$ sec [d]	$t_{2x} \geqslant 4$ sec [b]
			No objectional coupling with roll mode [d]
Roll mode	$\tau_R \leqslant 1.4$ sec [b]	$\leqslant 3$ sec [b]	$\leqslant 6$ sec [b]
Terminal phase			
C_{n_β}	Takeoff tameness	Takeoff tameness [d]	–

768-103

(a) See Figure 1
(b) New criteria for ACT
(c) Modified criteria
(d) Criteria unchanged from the Baseline Configuration

Table A-2. Longitudinal Trim and Control Criteria Summary

Design parameter	Flying quality level		
	1	2	3
All flight phases			
Stall recovery, Θ	-0.08 rad/s^2 recovery	-0.08 rad/s^2 recovery	-0.08 rad/s^2 recovery[a]
Trim limits	–	Trim all loadings and configurations in operational flight envelope with one power failure[b]	–
Retrim	From maximum push or pull[b]	–	–
Terminal phase			
Takeoff	$\dot{\Theta} \geq 5$ deg/s[b]	$\dot{\Theta} \geq 4$ deg/s with $\leq 75\%$ control available or one hydraulic system out[c]	Mistrimmed[b] within green band
Land	–	With any normal cruise trim[b]	With two critical failures[b]
Approach	–	$\ddot{\Theta} \geq 6$ deg/s^2[b] $\Delta\Theta_{1\ sec} \geq 3$ deg[b] $t_{h_{cross}} \leq 1.5$ sec[b]	–
En route phase			
Maneuver (constant speed)	$n_{total} = \frac{L}{W}$ 2.0 to 0.5[c]	1.5 to 0.6[c]	1.25 to 0.75[c]
Dive recovery	–	n = 1.5 with mistrim[b]	n = 1.0 with mistrim and one hydraulic system out[b]

768-103

[a] Modified criteria
[b] New criteria for ACT
[c] Criteria unchanged from the Baseline Configuration

Table A-3. Lateral/Directional Trim and Control Criteria Summary

Design parameter	Flying quality level		
	1	2	3
All flight phases			
Lateral control	–	> rudder control[a]	–
En route phase			
Roll response	$\phi_{4\ sec} \geq 60$ deg[b]	$\phi_{7\ sec} \geq 60$ deg[c]	$\phi_{11\ sec} \geq 60$ deg[b] ARB requirement[a]
Cruise trim $F_P = F_W = 0$	–	No spoilers for engine-out or fuel asymmetry[a]	–
Climb trim $F_P = F_W = 0$	–	For engine-out or fuel asymmetry[a]	–
Terminal phase		Flaps asymmetry[a]	
Trim $F_P = F_W = 0$	–	Engine-out with[a] $\leq$ 2/3 rudder at V_2 and approach[c]	–
Roll response	$\phi_{2.5\ sec} \geq 30$ deg[b]	$\phi_{3\ 2\ sec} \geq 30$	$\phi_{4\ 5\ sec} \geq 30$ deg[a]
Control –	–	–	V_{MCA} with one hydraulic system out[a] Loss of one leading-edge device to 1 3V_S[a] 30-kn crosswind with one hydraulic system out and $\leq$ 2/3 lateral control[a]
Landing control	$\ddot{\psi} \geq 0.08$ rad/s^2[a] Trim full rudder sideslip at 1 3 V_{So} with $\leq$ 2/3 lateral control[a]	No requirement	20-kn crosswind with two hydraulic systems out[a]
Takeoff control	–	Tameness with engine-out at 1.4V_{S1} and $\leq$ 2/3 lateral control available, no rudder[a]	V_{MCG} with one hydraulic system out[a] $\psi = 0$ at V_2 with engine-out and two hydraulic systems out[a]

768-103

[a] Criteria unchanged from the Baseline Configuration

[b] Modified criteria

[c] New criteria for ACT

Table A-4. Feel Force Criteria Summary (for All Flight Phases)

Design parameter	Flying quality level		
	1	2	3
Longitudinal			
Breakout, N (lb)	4.4 to 17.8 (1 to 4)(a)	2.2 to 26.7 (0.5 to 6.0)(a)	0 to 44.5 (0 to 10)(b)
Limits, N (lb)	⩽ 89 (20) for trim of configuration and power changes(c)	⩽ 222 (50) for trim of configuration and power(c) > 222 (50) for n_{limit} > 334 (75) for n_{ult}	⩽ 534 (120) pull(c) ⩽ 400 (90) push(b)
$\frac{F_s}{g}$, N/g (lb)/g	133 to 178 (30 to 40)(a)	89 to 222 (20 to 50)(b) linear(c)	44.5 to 356.0 (10 to 80)
$\frac{F_s}{V}$, N/m·s^{-1} (lb)/(KEAS) for the lesser of 25 m/s (±50 kn) or ±15% speed from trim	0 to −1.44 (0 to −1/6) stable(c)	Linear(c)	No requirement
Lateral			
Breakout, N (lb)	2.2 to 17.8 (0.5 to 4.0)(a)	2.2 to 31.1 (0.5 to 7.0)(b)	0 to 44.5 (0 to 10)(b)
Limits, N (lb)	31.1 to 67.0 (7 to 15)(a)	13.3 to 133.0 (5 to 30)(b)	0 to 267 (0 to 60)(b)
F_w/δ_w	Linear(c)		
Directional			
Breakout, N (lb)	22.2 to 35.6 (5 to 8)(b)	8.9 to 62.3 (2 to 14)(a)	0 to 125 (0 to 28)(b)
Limits, N (lb)	178 to 334 (40 to 75)(c)	89 to 556 (20 to 125)(b)	0 to 800 (0 to 180)(b)

(a) Modified criteria
(b) New criteria for ACT
(c) Criteria unchanged from the Baseline Configuration

768-103

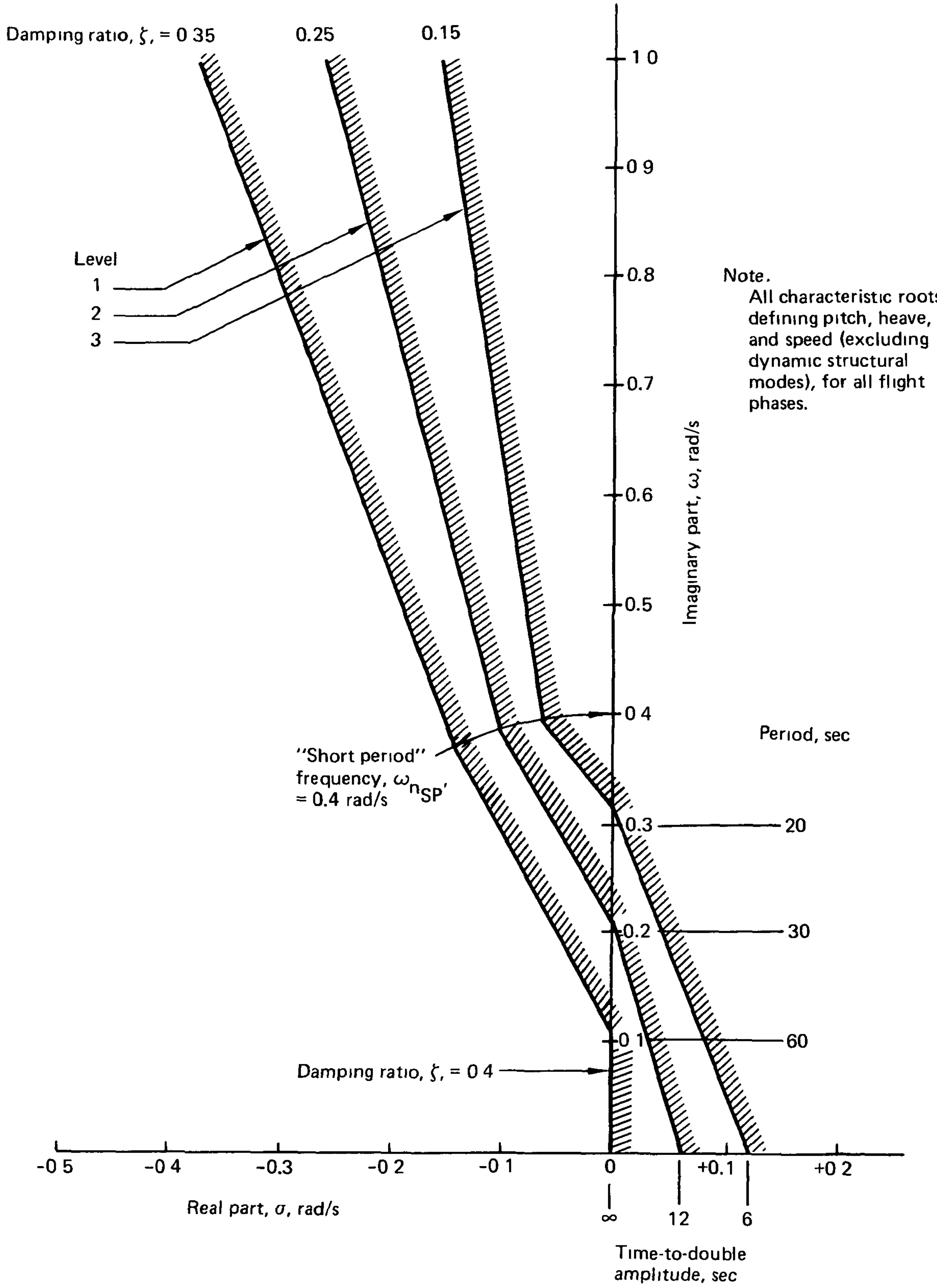

Figure A-1. Longitudinal Damping Requirements

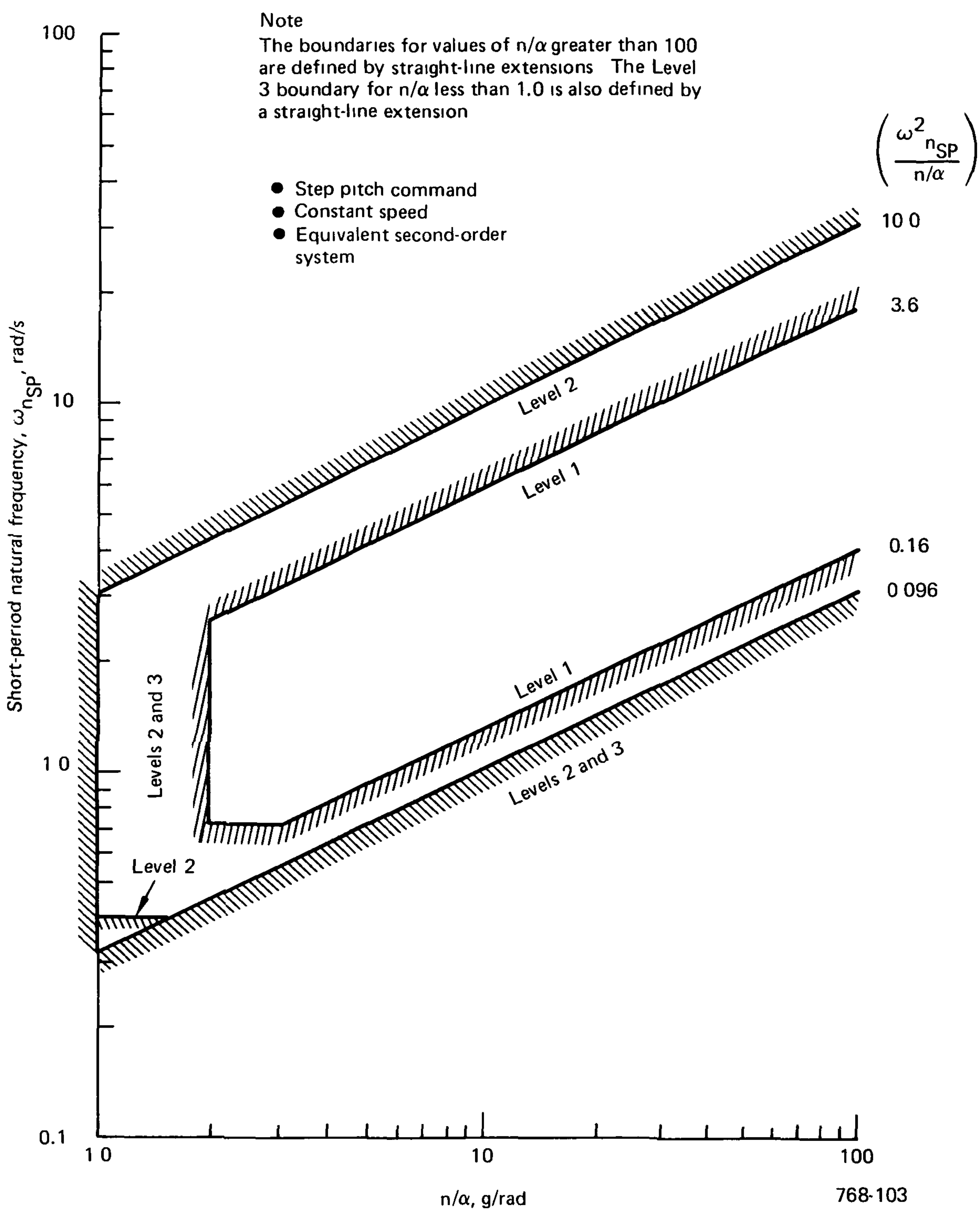

Figure A-2. Short-Period Frequency Requirements (Terminal Flight Phases)

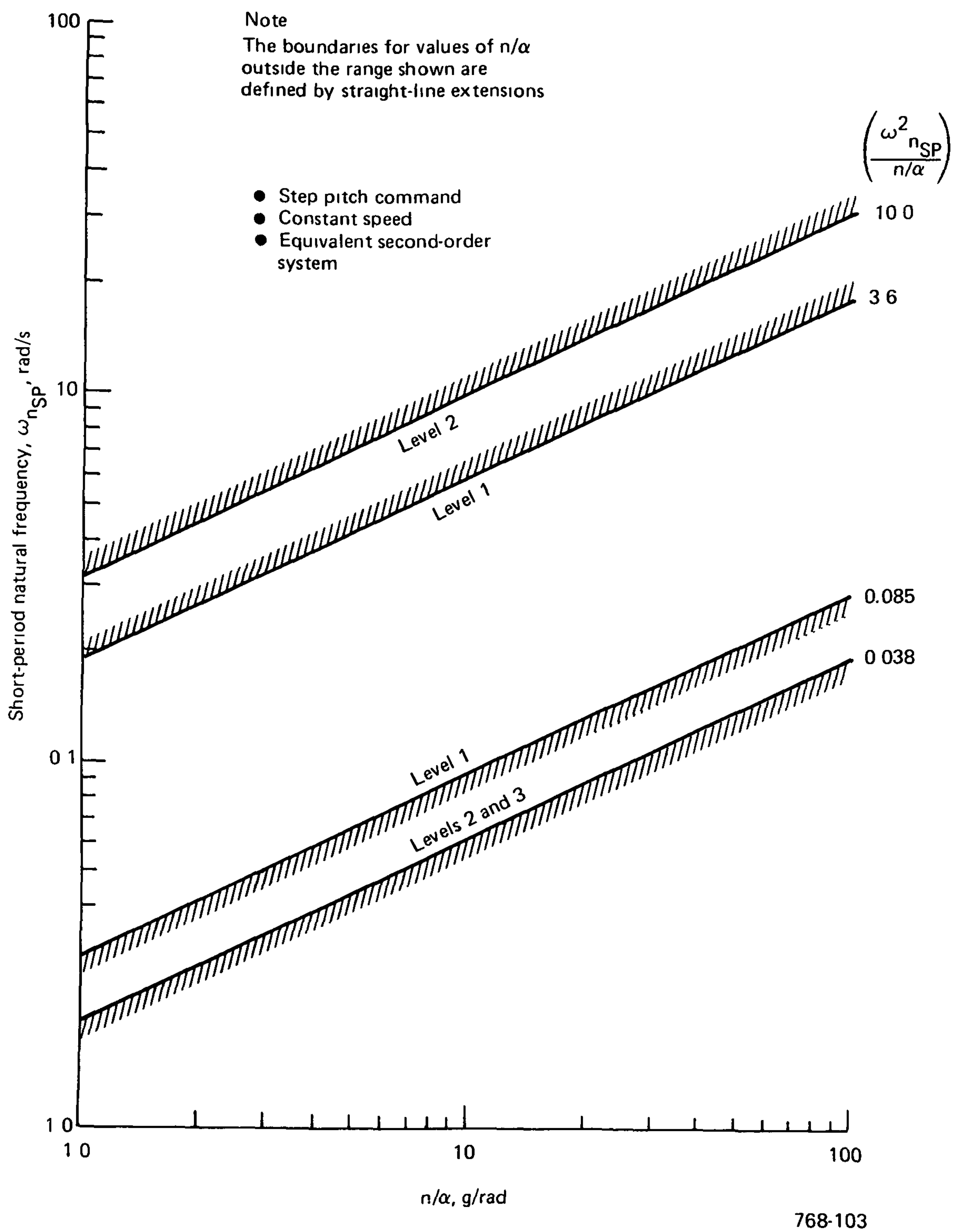

Figure A-3. Short-Period Frequency Requirements (En Route Flight Phases) design of an ACT system so it can achieve acceptable ride qualities for normal operation and for failures affecting ride quality. Three levels of vertical and lateral structural acceleration range from a perception level (1) to a minimum safe level (3) where the crew's ability to perform their tasks is in jeopardy.

3.0 STRUCTURAL DESIGN

The present Federal Aviation Regulations adequately prescribe certification requirements for structural design of airplanes incorporating ACT systems, with the exception of flutter suppression.

Applicable criteria (ref A-1) include:

- FAR 25.335(e)—Design Flap Speeds
- FAR 25.335(f)—Design Drag Device Speeds
- FAR 25.373—Speed Control Devices
- FAR 25.629—Flutter, Deformation, and Fail-Safe Criteria
- FAR 25.671—Control System, General
- FAR 25.672—Stability Augmentation and Automatic and Power-Operated Systems
- FAR 25.1309—Equipment Systems and Installation
- FAR 25.1329—Automatic Pilot System

The wing-load alleviation and flutter mode control systems must be designed to provide safety equivalent to existing designs

3.1 STRENGTH-DESIGN REQUIREMENTS

Current FAR strength-design requirements (ref A-1), summarized in Table A-5, apply to the design of the Initial ACT Airplane. Based on these criteria, structure and ACT systems may be certified separately.

Table A-5. Summary of Strength Design Requirements

System status \ Structure status	Unfailed structure	Failed safe structure
Operational[a,b]	Design to 1 5X (limit load) maneuver and gust	Design to limit load, maneuver and gust
Failed passive[b,c]	Design to limit load, maneuver and gust	Not required
Failed active[b]	Show active failure is extremely improbable so condition need not be considered[d]	Not required

768-103

[a] Account for system nonlinearities at limit load level.
[b] Indicated criteria are the same as for configurations without active controls.
[c] Caution flight crew to loss of system No change to design flight envelope
[d] *Optionally, if system failure is not extremely improbable, show capability* for continued safe flight and landing

3.2 FLUTTER, VIBRATION, DIVERGENCE, AND REVERSAL REQUIREMENTS

Figure A-4 summarizes the flutter analysis and testing criteria established to show flutter stability for IAAC designs. Specific criteria applicable to configurations with automatic flight control systems are included with the requirements of FAR 25.629, 25.671, 25.1309, and 25.672 (ref A-1). In addition, the following supplementary criteria are required.

Flutter Sensitivity to ACT System Performance—If flutter suppression systems are installed, the airplane must also comply with the criteria listed below:

- The airplane must be flutter-free to $1.2V_D/M_D$ when the flutter suppression system is operating:
    - Normally within the limits of a ± 6 dB gain margin in conjunction with a ± 45 deg phase margin

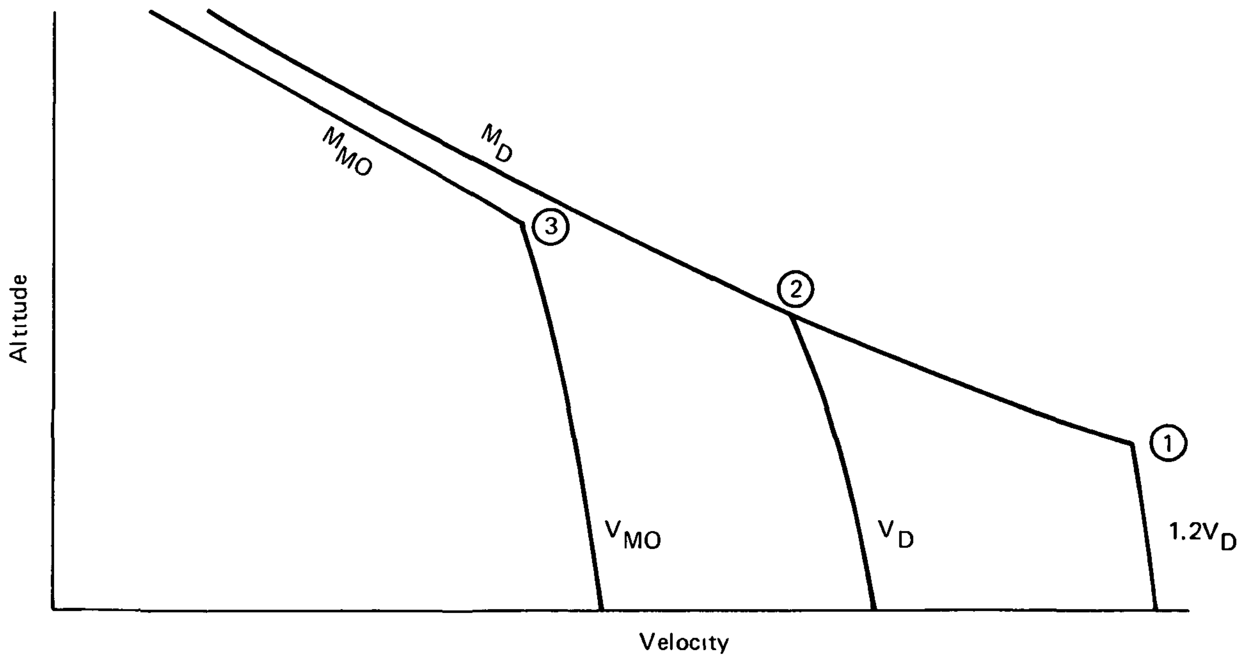

Airplane shall be free from flutter in accordance with criteria below

	Current criteria for conventional airplanes	Criteria for airplane with flutter mode control
1	By analysis and model test to $1.2V_D$	By analysis and model test to $1.2V_D$ with FMC on
2	By flight test to V_D	By analysis and model test to V_D FMC off By flight test to V_D with FMC on
3		By flight test to V_{MO} with FMC off

768-103

Figure A-4. Flutter Criteria for Flutter Mode Control (FMC)

- At nominal phase and gain for sensor-location variations of ±5% of the semispan and ±5% of the local chord

- At nominal phase and gain but with any one hydraulic system off

- The airplane must be flutter-free to V_D/M_D with:

  - The flutter suppression system off

  - The flutter suppression system operating normally within the limits of a ±12 dB gain margin in conjunction with a ±60 deg phase margin

  - Any one or more failures of the flutter suppression system (not shown to be extremely improbable) within the limits of a ±6 dB gain margin in conjunction with a ±45 deg phase margin.

- The airplane must be demonstrated, in flight, to have adequate structural damping up to V_D/M_D, with the flutter suppression system operating normally within the limits of a ±6 dB gain margin.

- The airplane must be demonstrated, in flight, to have adequate structural damping up to V_{MO}/M_{MO} with the flutter suppression system off. A reduced flight placard will be required after a failure of the flutter suppression system. The usual upset margin will be provided between this placard and the speed envelope demonstrated in flight with the flutter suppression system off.

- The flutter suppression system design must:

  - Provide a phase margin of ±180 deg for frequencies greater than twice the frequency of the highest flutter mode being actively suppressed

  - Consider saturation of the system by subjecting the airplane to continuous turbulence of a root mean square (rms) intensity of 4.3 m/s (14 ft/sec)

- Superimpose control function demands on the system response to turbulence, if elements of the primary flight control system are used for flutter suppression

- Provide the pilot with a warning for any system failure that could result in an unsafe condition

- Ensure that the actuator has a natural frequency of response at least three times the frequency limit of the system operational band

- Investigate up to V_{MO}/M_{MO} forced structural vibrations, other than flutter resulting from failures, malfunctions, or adverse conditions in the flutter suppression system

- Installations of ACT functions other than flutter suppression (e.g., maneuver-load alleviation, gust-load alleviation) must not degrade the structural damping to an unacceptable level when operating normally or with any one or more failures not shown to be extremely improbable. Compliance must be shown by:

    - Analysis up to $1.2V_D/M_D$ with the systems operating normally within the limits of a ± 6 dB gain margin in conjunction with a ± 45 deg phase margin

    - Analysis up to V_D/M_D with the systems operating normally within the limits of a ± 12 dB gain margin in conjunction with a ± 60 deg phase margin

    - In-flight demonstration up to V_D/M_D with the systems operating normally within the limits of a ± 6 dB gain margin

    - Investigation of the forced structural vibrations resulting from failures, malfunctions, or adverse conditions in the system up to V_{MO}/M_{MO}

Fail-Safe Structural Requirements—Failure of any principal structural element that complies with fail-safe strength provisions must be considered. With such failures:

- The airplane must be designed to be flutter-free to V_D/M_D with:
  - The flutter suppression system operating normally within the limits of a ±12 dB gain margin in conjunction with a ±60 deg phase margin
  - The flutter suppression system operating at nominal phase and gain but with any one hydraulic system off
- The airplane must be designed to be flutter-free to V_{MO}/M_{MO} with:
  - The flutter suppression system off
  - Any one or more failures of the flutter suppression system (not shown to be extremely improbable) within the limits of a ±6 dB gain margin in conjunction with a ±45 deg phase margin

4.0 FLIGHT CONTROL SYSTEM DESIGN

4.1 DEFINITIONS

4.1.1 FUNCTION CRITICALITY

- Flight crucial—Without that function, an immediate unconditional flight safety hazard exists.
- Flight critical—Without that function, a potential short-term flight safety hazard exists, but can be averted by pilot action with a penalty of flight diversion or a reduced performance envelope, or both.
- Nonflight critical—Loss of the function does not impact flight safety, but the function is considered necessary for the mission and thus may impact the flight plan or dispatch status.

- Dispatch critical—Without that function, an airplane cannot legally be dispatched on a revenue flight.

- Workload/relief—Loss of the function neither impacts flight dispatch status nor flight plan, but the function has convenience value to the crew, or passengers, or both.

4.1.2 FAILURE SURVIVABILITY

These definitions apply only to failure detection for safety reasons where the detected condition directly penalizes performance. Failure detection for purely maintenance purposes is excluded.

- Fail operational/fail-operational—This configuration will withstand at least two independent failures and continue functioning at the required level of performance.

- Fail-operational—This configuration will withstand a single failure and continue functioning at the required level of performance.

- Fail-passive—This configuration will withstand a single probable failure, including its failure transient, without exceeding load or structure limit of the airplane. Subsequently, the control surface will maintain a safe position, and the affected function(s) may no longer be available.

- Fail-safe—In this configuration, a failure or combinations of failures will not cause either transients that exceed airplane structural limits or conditions from which a pilot with average strength and skill cannot easily recover. The control surface will maintain a safe position, and the affected function(s) may no longer be available.

- Significant failure—Those failures must be detected and appropriate action taken for the system to meet the specified safety requirements.

- Latent failures—This is any undetected failure within the system.

- Nuisance alarms—These result when the system cannot function because a failure detector has been tripped by a condition which, if undetected, would not cause a hazard. This includes, but is not limited to, such causes as:

  - Detection of an insignificant failure

  - Detection of a condition that is momentarily out of tolerance, provided the condition does not persist or does not recur frequently

  - Detection of a condition that is close to, but not outside, its specified tolerance

4.2 SYSTEM REQUIREMENTS AND OBJECTIVES

4.2.1 GENERAL SYSTEM DESIGN AND OPERATION

- System Design

  - By definition, the ACT functions will normally operate automatically on a full-time basis within the defined operating envelope under all weather conditions and automatic flight control system (AFCS) operational modes. The system will perform the specified tasks without pilot operation, intervention, or assistance under normal operation.

  - A fault-tolerant control system will be developed for application to ACT to the fullest extent possible, consistent with available technology.

  - The ACT system will include an automatic system test suitable for checkout and practical maintenance of the fault-tolerant ACT system. The level of testing will fault isolate to a much greater confidence level than possible with current commercial transport operational equipment.

- Fly-by-wire techniques will be used wherever benefits may be realized by integrating ACT with primary/secondary flight control surfaces.

- To operate the aerodynamic control surfaces, the components of the ACT system will interface with aircraft flight control systems or will drive dedicated power control units, or both.

- System Operation

  - Operation of the ACT system will impose a minimum workload on the crew. The operational activities will be structured to be highly tolerant of incorrect operation or interpretation by the crew.

  - ACT system/function status will be summarized and caution/warning status displayed at the flight deck.

  - Normal maintenance of ACT functions will require no in-flight action of the crew other than reports of flight squawks.

  - A comprehensive system test will be made possible in the flight deck crew station. Test input will be prevented inflight, but readout status will be available full time upon request.

  - ACT functions that require preflight testing, other than automatic system test, will be kept to a minimum and operable by the flight crew without external assistance.

  - After failures, ACT system will have the capability to reconfigure itself without crew intervention.

4.2.2 ENVIRONMENT

The ACT system will be designed to meet the same environmental requirements as other airplane systems.

The ACT system will be structured to remain operational for, and recover from, faults induced by these transient phenomena:

- Electric power bus normal/abnormal transients
- Sensor signal disagreements
- Lightning strikes
- Hydraulic power transient pressure variations

4.2.3 SAFETY RELIABILITY

The safety reliability goals established for the ACT functions will be based on current regulations in force, the asssessed risks imposed on airplane operation by failures of the ACT system, including the electric and hydraulic supplies.

4.2.4 SCHEDULE RELIABILITY

- The ACT functions deemed dispatch critical, excluding the contributions for electric and hydraulic systems, will contribute no greater than 5% (to be verified [TBV]) of the total airplane delay rate.

- The ACT System will be dispatchable with failures if the system still meets established safety criteria with the failures existing at time of dispatch.

- The schedule delay rate of the ACT system will not be greater than that due to the airplane flight control system. Maintaining the ACT system in dispatch status will not require more maintenance than the flight control system.

4.2.5 CONTROL SURFACES

- The ACT system will use dedicated control surfaces, or primary and secondary flight control surfaces, or both.

- Combining ACT surfaces with conventional flight control surfaces will not degrade airplane performance or generate undesirable characteristics in the primary flight control system. Control surface authorities and rates and the consequences of failures are included in this context.

- Control surface redundancy, which may include sectionalizing conventional flight control surfaces where necessary, will be considered to meet system reliability requirements.

- Control surface authority will provide adequate control power for ACT function commands and for flight control power, wherever such combined functions are used.

- ACT control surface authorities will be limited by mechanical stops. Control authority of individual ACT functions may be electrically limited within the ACT system.

- The control surface rate will be determined by the bandwidth requirements of the ACT function and the size of the control surface.

- Control surface rates of individual ACT functions may be electrically limited within the ACT.

- The control surfaces and hinge structure will be designed interactively with the control design to provide adequate frequency response and control effectiveness.

4.2.6 SYSTEM ARCHITECTURE

- The ACT system will be considered as a single system for design purpose, although the system may perform several distinct functions.

- The basic elements or modules of the ACT system will be sensors, computers, actuators, and man/system interfaces, which may be arranged in any combination or order to perform each defined function.

- Those components, modules, or elements that are necessary for the ACT system performance and that exist as part of other aircraft systems will be an integral part of the ACT system architecture, and therefore will be constrained by the requirements applicable to ACT and other system requirements.

- Design of ACT system will take advantage of fault-tolerant techniques to minimize the level of redundancy required.

4.2.7 FAILURE PROPAGATION/PROTECTION

Failure Propagation—Redundant channels or elements in the ACT system will be arranged so no single failure can affect more than one channel or element unless such an occurrence is shown to be improbable.

ACT equipment will be designed to minimize the effects of malfunction of any equipment or part thereof on the normal operation of other systems interfaced with the ACT system.

Failure Protection—In a single-channel operation, authority and rate limits designed into the system will provide failure protection. The in-flight failure monitor of the ACT system will be designed so no significant failure (i.e., a failure that must be detected to meet the specified safety requirement) will go undetected. The ACT system will incorporate protection against transient loss and failure of primary ac and dc power.

Power Interrupt (Airplane in Flight)—For all isolated short-term power interrupts equal to or less than 20 ms, the system will continue normal operation without tripping any failure monitor or losing any maintenance data. Repeated short-period power transient will be detected, the channel will be disconnected, and the data will be stored for maintenance recall. The system will disconnect the channel when the power interrupt is greater than 20 ms (TBV).

Power Interrupt (Airplane on the Ground)—For long-term interrupt equal to or less than 200 ms (TBV), the system will continue normal operation; when the interrupt is greater than 200 ms, the system will disconnect the channel. Long-term power interrupt will normally only be encountered on the ground during switchover from aircraft power to ground power or vice versa. In this condition, any ground system test in progress will automatically resume without loss of either test sequence or results.

Power Loss—The system will disconnect the channel when the power interrupt is greater than 20 ms (TBV) when the airplane is in flight and greater than 200 ms when the airplane is on the ground.

4.2.8 MAINTENANCE

The ACT system will be maintained strictly "on condition." That is, unless a preflight test indicates that a problem exists or a flight squawk was generated on the previous flights, the ACT system will be assumed operational and available for service.

The maintenance functions are categorized as:

- Through-flight maintenance and service, which will require a total maintenance cycle (fault identification, repair, and system verification) of 25 min (TBV) or less. This function will require only one maintenance crew member to conduct the total maintenance cycle.

- Turnaround maintenance and service including overnight, may require a total maintenance cycle of more than 25 min (TBV). Turnaround maintenance may require more than one maintenance crew member to conduct the total maintenance cycle.

Line Replaceable Unit Fault—The ACT system will automatically identify the faulted mode of operation whenever a faulted LRU or LRU interface is identified. When a particular faulted LRU or LRU interface cannot be identified, the maintenance function will identify the faulted functional group of LRU(s).

The maintenance function will automatically identify the failed LRU and interface the ACT control systems with this success rate:

System Configuration	Success Ratio
Single-channel operation	to be determined (TBD)
Dual-channel operation	TBD
Triple-channel or more	99% (TBV)

The failed LRU will be identified by name in alphanumeric format to avoid potential ambiguities and misinterpretation.

Fault Data Storage—The ACT system will be able to record and store information relative to in-flight fault conditions so it can be accessible for display as part of the ground maintenance operation. The information must enable the line maintenance technician to localize the fault condition to a specific LRU.

Provision will be made for temporary storage within the computers of the identity of all LRU(s) identified in flight as failed. The data storage will be protected from power transient. The failure data will remain in the computers until the failures are repaired and the system functions are verified.

Equipment and Skill Level—Ground testing for through-flight maintenance, which includes verification tests, must be performed by line maintenance personnel using only the equipment normally installed in the airplane with a skill level of a typical maintenance technician.

4.2.9 SYSTEM TESTS

General—To an operator, the ACT system will appear as one system through a system test panel interface, installated in the flight deck for use by either the flight crew for preflight test and inflight display of system operational status, or by the ground crew for maintenance level testing. During routine operation, the flight crew only needs to know of failure conditions affecting flight-critical functions; the maintenance crew must know the existence and location of a malfunction.

The system tests will be implemented in three parts: preflight testing, in-flight testing and monitoring, and maintenance (or postflight testing).

Preflight Test—A preflight readiness test of the ACT functions will verify system performance and warn the crew of any unsafe conditions. An inhibit mechanism will prevent inadvertent test operation while inflight.

The preflight test will have the following characteristics:

- The preflight test will be limited to the minimum dispatch capability of the ACT system.
- The preflight test will detect failures within the system and isolate them to LRU level.
- A semiautomatic capability will be provided for preflight testing. The computer will perform the automatic portion of the test and supply the information to the panel. The information will include test results and manual command information that allow the crew to participate in the preflight test only if required.
- The preflight test will make maximum use of the in-flight monitoring inherent in the system design.
- In keeping with the "on condition" maintenance philosophy, the maintenance burden of preflight test will be minimal, ideally less than 2 min (TBV).

In-flight Testing and Monitoring—Automatic in-flight testing and monitoring will detect and isolate failures during the flight to keep the system configuration operational. All failure information will be processed to determine, if possible, the failed LRU, and all pertinent failure data will be recorded for maintenance recall.

Postflight Testing—The maintenance (or postflight) testing will allow maintenance crews to rapidly determine the total system operational status if clearance of a flight "squawk" is required. With this function, the maintenance crew can locate hard failures within the system and verify proper system operation after maintenance.

The maintenance (or postflight) testing will include a complete checkout—from sensors through servos—of the ACT control system.

The ground crew must be able to initiate the automated system test checkout sequence as part of the ground maintenance operation.

4.2.10 POWER

Electric Power—The ACT system will operate from aircraft power supplied by the aircraft generating system or dedicated backup battery systems. Transients in the power system will not degrade ACT system performance.

Sufficient electric power redundancy will be provided to meet the reliability/safety requirements.

Hydraulic Power—Power for the ACT functions will be supplied by the aircraft's three independent hydraulic systems. Each power-operated ACT function will have sufficient hydraulic power redundancy to meet the reliability/safety goals.

The ability of the airplane to satisfy stability and control and handling qualities criteria will not be degraded by the failure of any single power control component unless the failure can be shown to be improbable. Actuators will be able to produce required deflection at surface rates sufficient to perform critical combined axis/function tasks. Multifunction performance will not be lessened by hydraulic flow rate limits.

4.2.11 SYSTEM INTERFACES

This section covers the constraints imposed upon the ACT system with regard to interaction with other aircraft systems.

Major areas of interfacing are:

- Flight control sensors
- Flight control electronics/computers
- Flight control actuation
- Flight deck systems
- Electric power system
- Hydraulic power system

The ACT equipment will be designed and installed so that operation or malfunction of any equipment will not degrade below acceptable levels the operation of other systems interfacing with the ACT system.

It will be an objective to minimize the interfaces of the ACT configuration consistent with practical implementation and with the reliability/maintainability objectives.

4.3 ACT SYSTEM SENSOR REQUIREMENTS AND OBJECTIVES

4.3.1 REQUIREMENTS

Design–Sensors will be the simplest design necessary to perform required functions. Each sensor will require no more than one excitation or power source and each crucial sensor will be powered by the same emergency/standby power source as its associated computer.

Tracking–Redundant sensors will have the same part number, be collocated, and have the same excitation and loading (to the extent that nulls and gradients are affected), to optimize tracking between sensor output signals. Crucial sensors and their wiring will be physically separated to assure the function surviving an engine burst.

EXCEPTION: Air data sensors, or other sensors located externally on the airframe, will either be protected from handling damage or will be physically separated.

Environment—Sensors will perform their intended function when subjected to all reasonable airplane environment. They will be located to minimize undesired output due to structural deflection or vibration.

4.3.2 OBJECTIVES

Objectives for ACT system sensors are:

- Sensors with no moving parts will be used wherever possible.
- Sensors used by the ACT system will incorporate a self-test capability to facilitate integrated system checking.
- The ACT System and the automatic flight control system will share common sensor self-tests without compromising the integrity of either system.
- Off-the-shelf components with established performance and reliability and with commonality to other system sensors on the baseline airplane will be used wherever possible.
- Dedicated sensors will provide all critical sensor signals. A critical sensor signal may be shared by several functions if the common failure is no more critical than a failure in any one function. Noncritical data may be obtained from shared sensors.

4.4 ACT SYSTEM COMPUTER REQUIREMENTS AND OBJECTIVES

4.4.1 INPUT/OUTPUT INTERFACES

Input/Output—All electronics necessary to interface the ACT system computer with sensors, actuators, and digital data buses will be included in the input/output (I/O).

Display Interfaces—The ACT system computer will interface with the master caution/warning system and the maintenance test panel. Information regarding any failures in the system will be transmitted to the maintenance test panel for the maintenance record. (If flight crew knowledge of the failure is required, it also will be annunciated by the master caution/warning system).

No failure in the maintenance test panel or the master caution/warning system will affect ACT system operation. No failure in the system that is not improbable will cause the maintenance test panel or master caution/warning system to fail.

4.4.2 COMPUTER HARDWARE REQUIREMENTS

The following requirements will be met for computer hardware:

- Computer hardware will meet all environment and temperature requirements for airborne electronic equipment.
- The ACT system computers will be able to self-test and monitor to the extent that a percentage TBD of all ACT control system failures are detected before causing an incorrect output.
- The computer will have a multi-level interrupt capability while minimizing overhead for interrupt processing.
- The computer will use programmable read-only memory (PROM) or read-only memory (ROM) for program storage.

4.4.3 SOFTWARE REQUIREMENTS

Software design will emphasize maintaining visibility of operation and purpose. Each software module will be written so that the purpose of the module and the details of its operation are clear, even though memory requirements may increase or execution speed may be slower.

A top-down approach will be taken for software structuring. Software will be partioned into single-entry, single-exit modules. Control structures used to join modules will be limited primarily to simple catenation, IF-THEN-ELSE branches, N-way branches, and loops.

Errors that could cause simultaneous failure of all computers in a redundant system will be eliminated. This requires tests and analyses to show that software is error free with a confidence factor TBD.

4.4.4 CONTROL LAWS/PROCESSING

The following requirements/objectives will be met in the design of the ACT system control signal processing and computations:

- Control processing authority will allow full active controls operation over the operational flight envelope without control law saturation.

- An objective will be to maximize the flexibility of digital system mechanization by using variable gain scheduling as a function of sensor inputs in tailoring multimode control laws throughout the flight envelope. An additional objective will be to provide a fixed-gain backup mode with minimum safe flying qualities.

4.4.5 REDUNDANCY MANAGEMENT

Redundant channels will be provided for each ACT function to meet the reliability/availability requirements, and all computers will be identical and interchangeable within each ACT subsystem. The ACT computers will meet the following redundancy management requirements:

- Computation, synchronization, or equilization—The ACT computers may be synchronized or equalized so that they eliminate signal drift due to tolerance of the system elements. When the synchronization or equalization schemes are adopted for the ACT system, they will be designed so:

  - The failure (or absence) of one computer unit will not prevent synchronization (or equalization) of other channels.

- The computers will be able to synchronize after power turn on, and resynchronizate after transient power faults or massive transient faults caused by lightning.

- Cross-channel data transmission—Data can be automatically transferred between any two computers.

- Sensor signal selection—The ACT control computers will provide for input signal selection in the redundant channel operation. The signal selector will receive the input from the sensors associated with its own channels and receive the other inputs indirectly or directly from the sensors associated with the other channels. The signal selector will have variations as necessary to handle all types of input signals used in redundant system operation. The signal selection algorithm in conjunction with the signal failure monitor will:

    - Provide outputs that closely track each other so the resulting redundant channel operations are nearly identical

    - Detect and isolate the effects of input signal failures to guarantee the requirement for all signals used in the multichannel operation

    - Reduce "nuisance system failure" caused by signal tolerance and noise

    - Provide smoothing to meet the transient requirement of each ACT function during the process of reconfiguration; placement of the signal selection process in the control laws must be carefully considered

- Automatic start, restart, and reconfiguration—The redundant ACT system will be able to automatically start, restart, and synchronizate after power turn on and automatically restart and synchronizate after transient power failures. The system start, restart and reconfiguration shall not require pilot intervention.

4.4.6 FAILURE DETECTION, ISOLATION, AND REACTION

Failure detection, isolation, and reaction mechanisims will be incorporated as part of the ACT system redundancy management scheme.

- Failure Detection—The ACT system will be able to determine when a failure occurs. The means of detection may be either by hardware, or software, or a combination of both. All detected failures will be stored in the computer's nonvolatile memory for access by the maintenance crew upon request. Failure detection methods will include but not be limited to:

  - Input signal fault monitoring—Input signal fault or out-of-tolerance will be monitored primarily by cross comparison of equivalent signals with other channels. The monitors will be implemented to the greatest extent possible in software but only where necessary in hardware. The monitoring will allow its variables (threshold, time delay, etc.) to be tailored to specific signals being monitored and, where necessary, to the change in the variables with flight conditions. The monitors will be able to discriminate between one failed input out of multi input signals or a difference between two inputs for hardover failures, slow drift failures, oscillating failures, or passive failures.

  All input signals essential for ACT functions will be monitored during multichannel operations. Other types of monitoring, such as reasonableness checks or functional comparison may be used for in-line monitoring during single- and dual-channel operation.

  - Sensor Valid Signal Monitoring—The loss of internally generated sensor valid signals will be used by the failure monitors to supplement sensor monitoring capability. Sensor valid signals will be used for fault isolation in single-channel operation and for system maintenance data.

- Electric Power Monitoring—System computers status information on the aircraft standby electric power will be provided to the ACT system computers for preflight testing. Within the bounds of the ACT system, the ACT control computers will monitor failures of electric power supplies.

For self-testing, the computers will provide full-time hardware monitors and software tests. Software will be tested to detect real-time computing problems.

- The computer will use cross-channel comparison and in-line monitoring techniques for servo actuator monitoring.

- Failure Isolation—The ACT System will be able to automatically isolate failures to the LRU level after failure detection. An objective of the ACT system will be to ensure that failures not detectable to an LRU level at minimum be isolated to a group of units.

As a system concept, failure isolation methods will focus upon system nodal points; i.e., interfaces between sensor and computer and between computer and actuator, as a means of problem isolation to an LRU. Failure isolation will use built-in monitoring and testing features to the greatest extent possible to provide isolation with high confidence.

- Failure Reaction—The ACT system will incorporate a means to automatically react to failures within the system. This will consist of the appropriate decision-making capability required to identify, store, reconfigure or shutdown the active control function/system and to annunciate the system status to the flight crew where degraded operation has become a reality.

  The objective of the system to automatically react to detected failures will be to maximize system survivability and to indicate to the flight crew the most appropriate action to be taken.

4.4.7 COMPUTER SELF-TEST

The ACT control computers will self-test by software and/or hardware as necessary to provide detection of at least 95% of the computer LRU failures. The self-test will be performed independently in each computer and will be conducted wholly or in part during each iteration time frame.

The complete self-test will be conducted within a specified time (TBD) to meet the safety requirements. It will include, but not necessarily be limited to, verification of correct functioning such as power, timing, memory, data/control transmission input/output conversion, and arithmetic processing.

4.5 ACT SYSTEM ACTUATORS

4.5.1 GENERAL

The ACT actuation system will use the latest state-of-the-art actuation control technology to meet the requirements and objectives for each ACT function. The reliability and safety requirements of the ACT system will require multiple-active or monitored channel actuation systems with fault-corrective capability.

4.5.2 ARRANGEMENT

As an objective, all ACT input and feedback signals will be electric. For ACT functions using common flight control surfaces, the input signals will be summed in series with the pilot's control input.

4.5.3 FORCE SYNCHRONIZATION

Redundant actuation, used as necessary to meet the configuration requirements, will meet force synchronization requirements. In addition, differential pressure in ACT series actuators will be limited by a pressure relief valve to allow backdrive during failure conditions.

4.5.4 ACTUATION BANDWIDTH

The actuation bandwidth will be sufficiently higher than the dominant airplane frequencies being controlled to provide the required control.

4.5.5 FAILURE TRANSIENT

As an objective, failure transient will be less than 10% of the actuator authority.

5.0 SYSTEMS

5.1 HYDRAULIC POWER SYSTEM

5.1.1 DEFINITION

The hydraulic power system is defined as the assembly of components and subsystems that perform hydraulic flow generation, flow control, pressure control, temperature control, and flow distribution functions.

5.1.2 SYSTEM REDUNDANCY

The total number of hydraulic power systems and the number supplying each hydraulically powered service shall satisfy the following criteria:

- Compability with the fail-operational requirements for Category IIIb automatic landing plus rollout steering capability and with all engines and hydraulic and electric systems operating when landing is initiated

- Compatibility with the fail-operational requirements for the ACT system functions

5.1.3 PERFORMANCE FOLLOWING FAILURE OF ANY ONE HYDRAULIC SYSTEM

Following the failure of any one hydraulic system, the remaining operational systems will provide sufficient power to retain the following capabilities:

- Flight control system performance that provides flying qualities satisfactory for safe continuation of the flight to the original destination using normal procedures to the greatest extent practical under Category II or better weather minimums.

- Normal control of all wheel brakes, including differential operation for directional control, except that antiskid control in the alternate mode is allowable.

5.1.4 MINIMUM ALLOWABLE PERFORMANCE FOLLOWING MULTIPLE SYSTEM FAILURES

Following any combination of system failures not shown to be extremely improbable, the remaining operational system(s) will provide sufficient power for flight control system performance, which leaves the airplane controllable for flight and landing with appropriate restrictions and the detailed performance specified in Subsection 2.2.5.

5.2 ELECTRIC SYSTEM

5.2.1 SCOPE

The requirements and objectives defined in this section apply to the electric power generation system and to items of electric utilization equipment that are modified by or are peculiar to the airplane incorporating ACT functions.

The electric power generation system includes the airplane primary electric power sources, electric power conversion, energy storage, control, protection, monitoring, indication, and distribution of electric power to all electric utilization equipment.

5.2.2 PRIMARY SOURCE CAPACITY

The primary ac power system will be able to supply the airplane electric loads, including active flight controls and the anticipated standard options to be selected by major airlines, with an allowance for 20% growth with all primary sources operating.

The power system will be designed to enable the airplane to be dispatched with one inoperative engine-driven generator by using the auxiliary power unit (APU) generator to replace the inoperative main generator. Under this condition, the system will be able to supply the airplane electric loads, including the anticipated standard options.

The power system will be designed to enable dispatch with an inoperative APU generator when all engine-driven generators are inoperative.

5.2.3 ESSENTIAL LOADS

The requirements to provide power to the essential loads as defined in FAR 25.1309 will be satisfied.

Power to the essential loads required to maintain flight will not be lost for more than 20 ms as a result of any single failure following dispatch with an inoperative generator.

5.2.4 SYSTEM ISOLATION

The electric power system will satisfy all load system isolation requirements, including those for flight-critical active controls and fail operational autoland.

5.2.5 ADVANCED WIRING

Multiconductor cable (flat and round) using #24 American Wire Gage (AWG) wire with associated terminations or junction boxes, should be used in all areas where the cable is compatible with the environment and where such use would result in a significant weight and/or cost saving without compromising reliability.

Shielded, twisted-pair wiring will be used to interface with ACT components in all lightning exposed areas of the airplane.

5.2.6 SENSITIVE WIRE BUNDLES

Wire bundles associated with flight-crucial and flight-critical active flight control systems should be dedicated to flight controls alone and suitably isolated as required for system redundancy. They will be identified to make them visibly unique as compared to other ship's wire bundles. Such wire bundles will use the minimum number of disconnects required for installation. Each segment will, however, be considered an LRU. All rework will be accomplished in an electric bench environment followed by adequate inspection.

5.2.7 CRITICAL SYSTEM SEPARATION

Separate circuits and buses will be used to supply power to critical multiple-channel systems and critical backup systems so that any single power system failure condition will not cause loss of more than one duplicated channel or system. Where duplicate power inputs are required for equipment, the inputs will be supplied through separate circuits from separate buses.

No immediate action will be required by the crew to maintain operation of critical functions as a result of a single power input failure.

REFERENCES

A-1 Federal Aviation Regulations–Part 25. Airworthiness Standards: Transport Category Airplanes. Federal Aviation Administration.

A-2 Chalk, C. R., et al.: "Flying Qualities of Piloted Airplanes." Background Information and User Guide for MIL-F-8785 (ASG). AFFDL-TR-69-72, August 1969.

APPENDIX B–
AERODYNAMIC DATA BASE

APPENDIX B—
AERODYNAMIC DATA BASE

APPENDIX B

AERODYNAMIC DATA BASE

The aerodynamic data used for flight controls and structural design of the Initial ACT Configuration are organized in this appendix as stability and control and as air loads and hinge moments; however, all data were used by both flight controls and structures technologies. Static aerodynamic force and section and hinge moment estimates are illustrated for controls and longitudinal motion.

STABILITY AND CONTROL

Flaps-down aerodynamic characteristics were based on low-speed wind tunnel data from an early force model of the Baseline Configuration. Corrections were made for the geometric differences between wing, empennage, body, and flaps of the wind tunnel model and the Baseline Configuration. Figure B-1 illustrates estimated pitching moment characteristics of the Baseline Configuration for the critical landing stall recovery. This condition sized the horizontal tail for both the Baseline and Initial ACT Configurations. The tail size difference depends on criteria differences for ACT and the double-hinged elevator effectiveness at stall. Elevator effectiveness, also shown in Figure B-1, was estimated from YC-14 data.

The Initial ACT Configuration's tail-on pitching moment was determined by scaling the tail input and transferring the moment reference. The stall angle of attack is 17 deg. The "T" tail stability contribution deteriorates in the 24 to 30 deg angle-of-attack range as it passes through the wing wake, then increases again above 32 deg.

Transonic test data were obtained at the Boeing Transonic Wind Tunnel (BTWT) facility on an 0.037-scale model of the Baseline Configuration and only required scaling the tail input for the Initial ACT Configuration. Longitudinal stability data are illustrated in Figure B-2 for tail-off and for Baseline Configuration horizontal tail size. Angle of attack for stall warning, $1.2V_S$, and maximum flight altitude are also illustrated in Figure B-2 for the tail-on pitch characteristics. Note the pitchup at about a 7.5 deg angle of attack at M = 0.5; this is predominantly a wing characteristic and is within the design flight envelope to about M = 0.65.

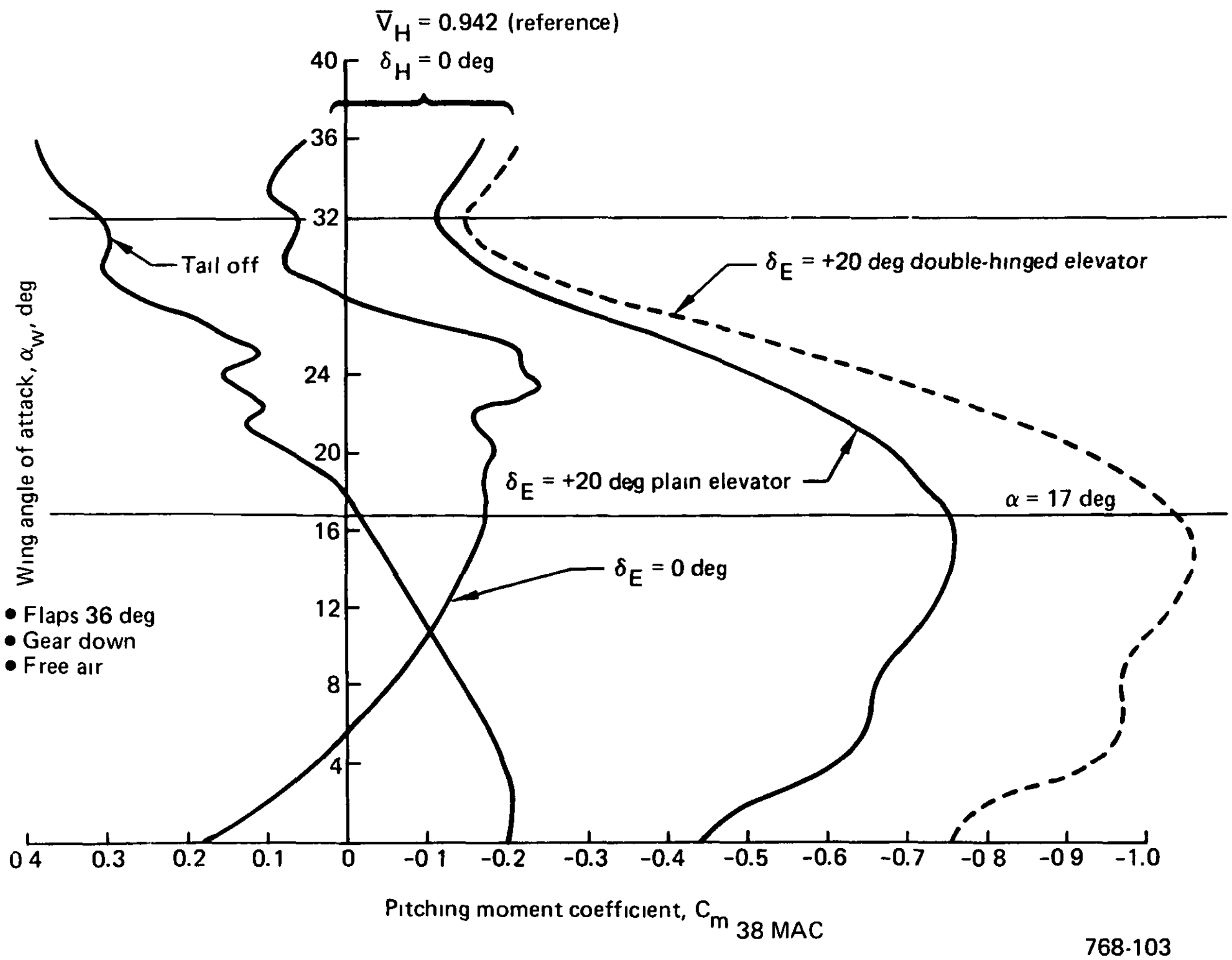

Figure B-1. Landing Pitching Moment With Baseline Tail Size

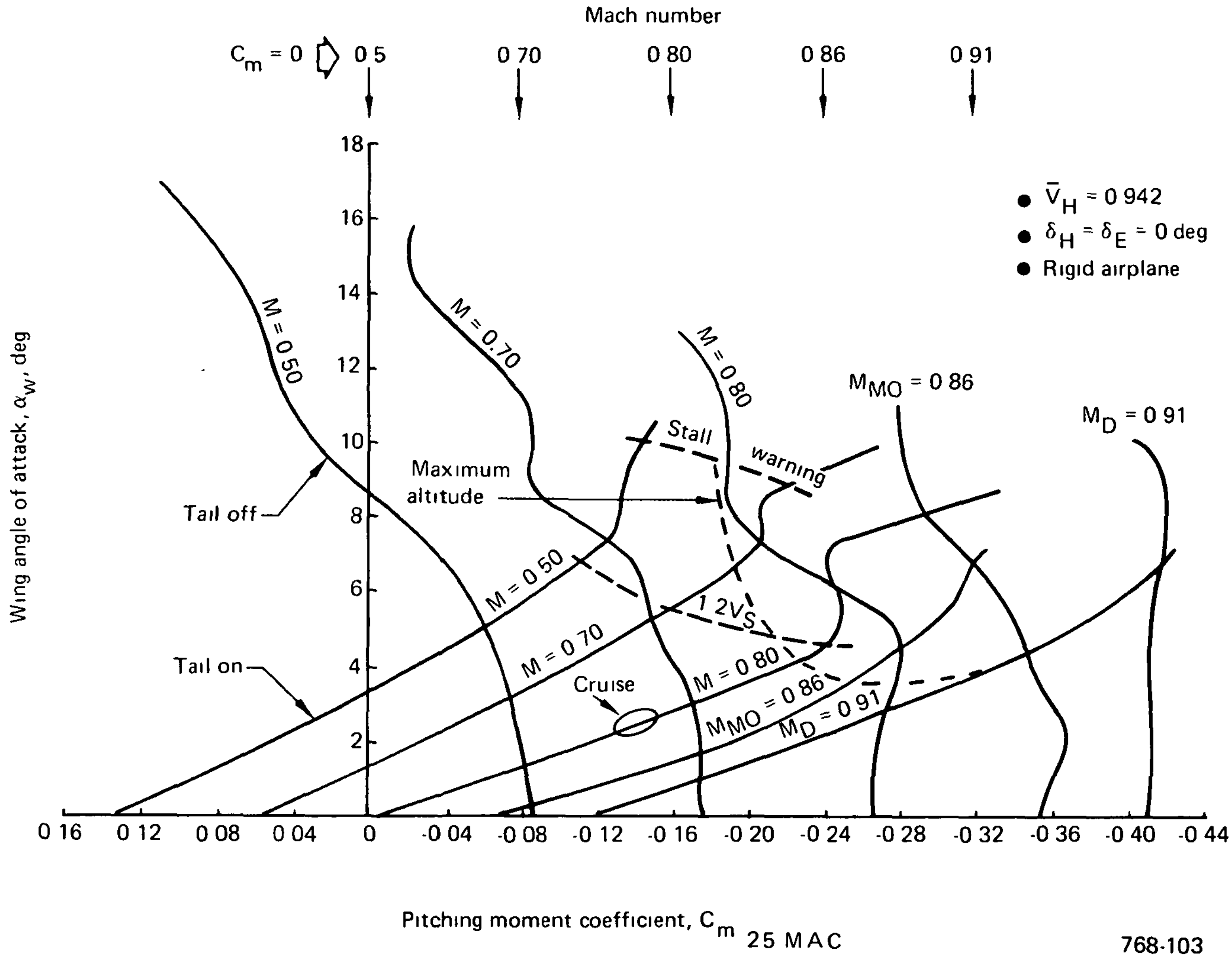

Figure B-2. High-Speed Pitching Moment With Baseline Tail Size

Lateral/directional stability data, also obtained from the BTWT tests, are not shown here because these Baseline and Initial ACT characteristics do not significantly differ and because no new ACT functions were added for the lateral-directional axes. Static lateral and directional stability characteristics are described in Subsection 5.3.3 for the Initial ACT Configuration.

Normalized pitch control effectiveness is shown in Figure B-3 for the stabilizer, plain elevator, and double-hinged elevator. Double-hinged elevator effectiveness was

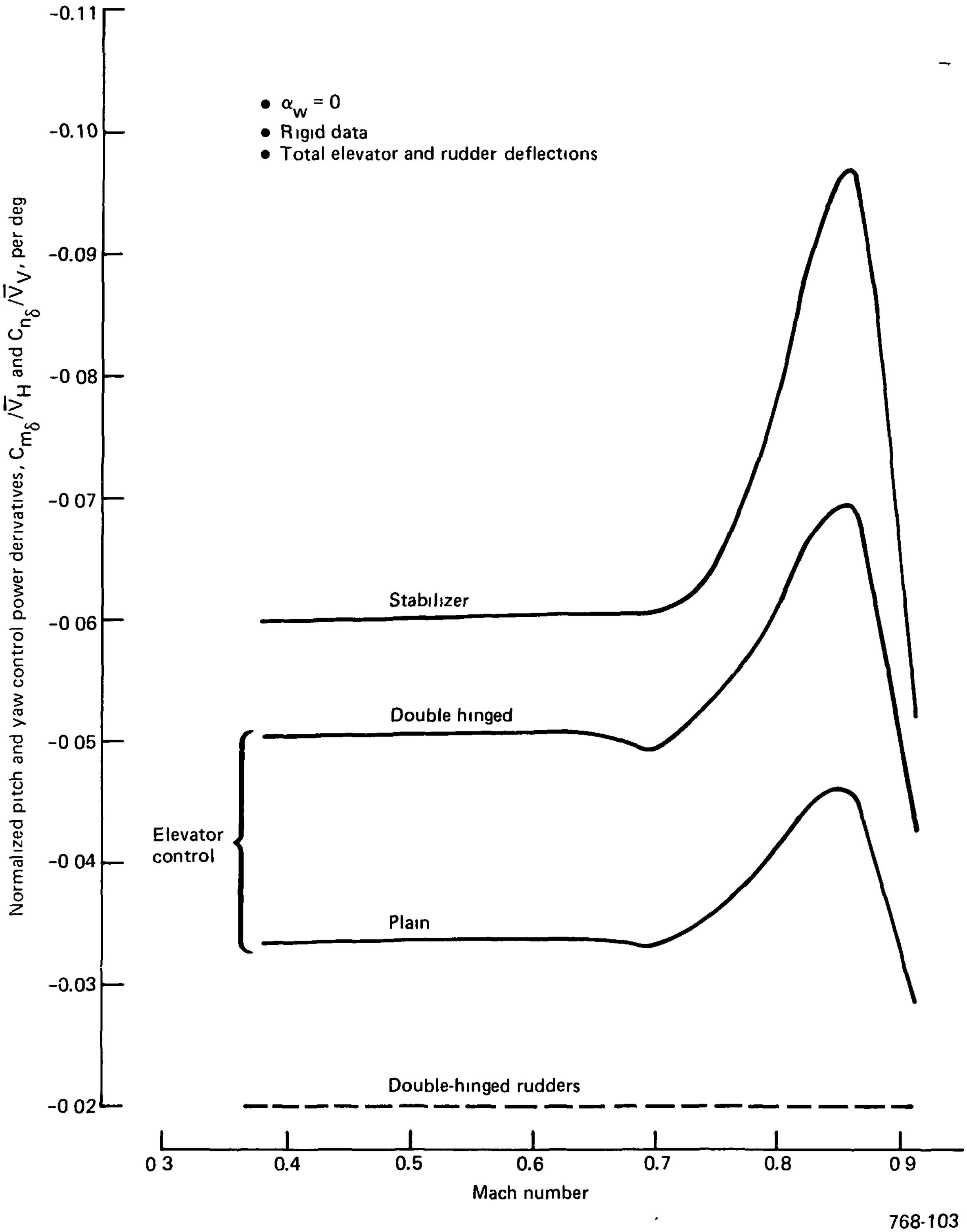

Figure B-3. Pitch and Yaw Control

Lateral/directional stability data, also obtained from the BTWT tests, are not shown here because these Baseline and Initial ACT characteristics do not significantly differ and because no new ACT functions were added for the lateral-directional axes. Static lateral and directional stability characteristics are described in Subsection 5.3.3 for the Initial ACT Configuration.

Normalized pitch control effectiveness is shown in Figure 5-7 for the stabilizer, plain elevator, and double-hinged elevator. Double-hinged elevator effectiveness was estimated from YC-14 data for the Initial ACT Configuration and shows about 50% more effectiveness than the plain elevator. Double-hinged rudder power, estimated from 747SP data by adjusting for vertical planform and volume coefficient, is also shown in Figure B-3. This characteristic is identical for the Baseline and Initial ACT Configurations.

Lateral control effectiveness was obtained on the same tests as the stability data; however, outboard aileron effectiveness was extrapolated to high Mach using 747 test data. Rolling moment is illustrated for the lateral controls in Figure B-4. The Initial ACT Configuration dedicates the inboard third of the outboard aileron to ACT, but requires an additional outboard spoiler panel over the Baseline Configuration to maintain nearly the same total lateral control as the Baseline Configuration. The estimated reduction of outboard aileron effectiveness, shown in Figure B-4, is 40%. The inboard aileron is identical for both configurations.

AIR LOADS

All air loads data presented in this subsection were used for the analysis of static and dynamic loads, flutter, and the dynamic model used for ACT system design. The structural analysis also reflected the basic stability and control characteristics presented in Subsection 7.1. Basic wing section data were obtained from wind tunnel tests. These data characteristics are illustrated in Figures B-5 and B-6. Both the Baseline and Initial ACT wing designs were based on these characteristics. In these figures, the data for the highest Mach No., 0.88, is beyond the lift divergence Mach number.

The Baseline horizontal and vertical tail structures were designed from estimated air load distribution. The Initial ACT horizontal tail structure was designed using

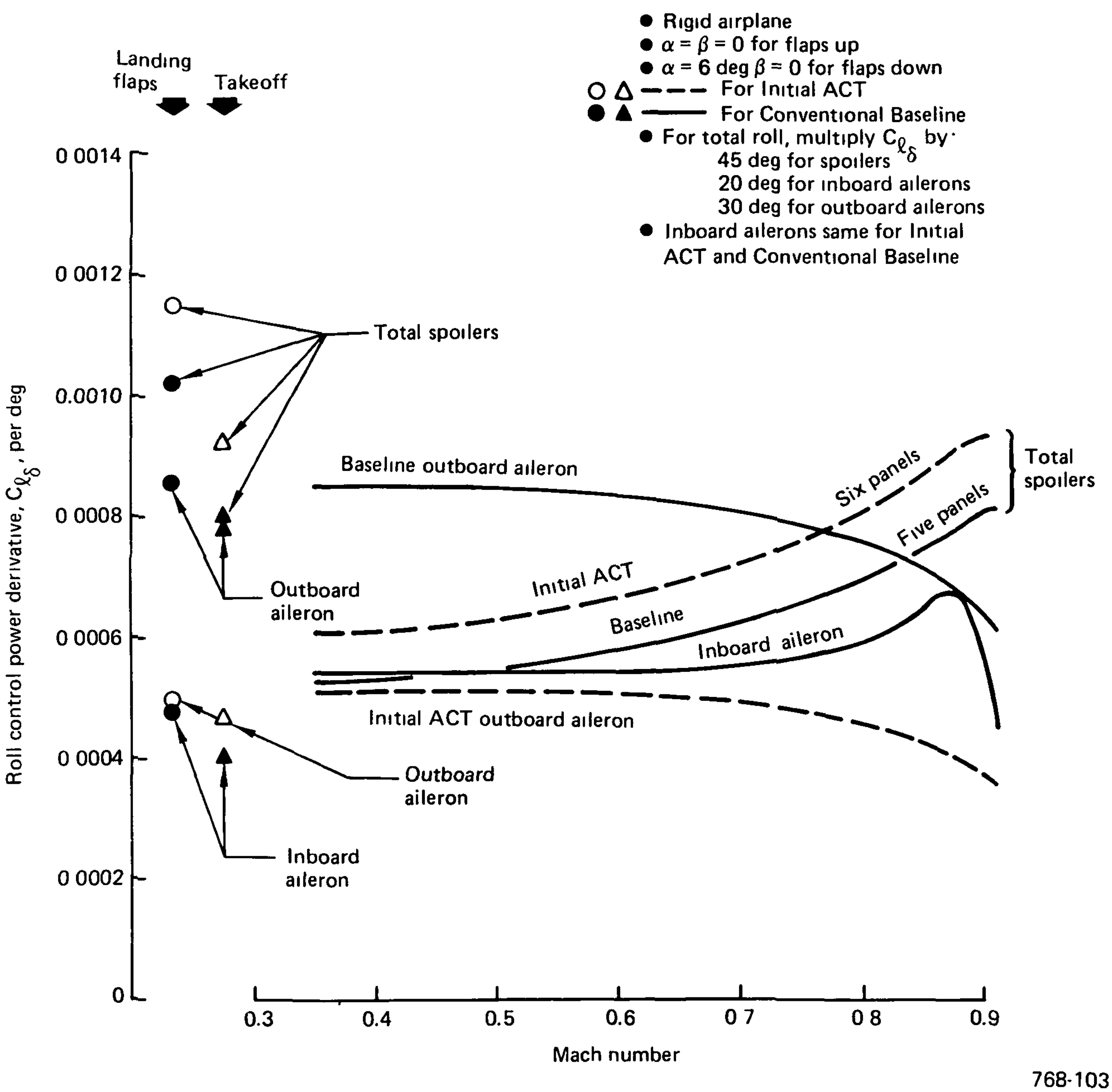

Figure B-4. Roll Control

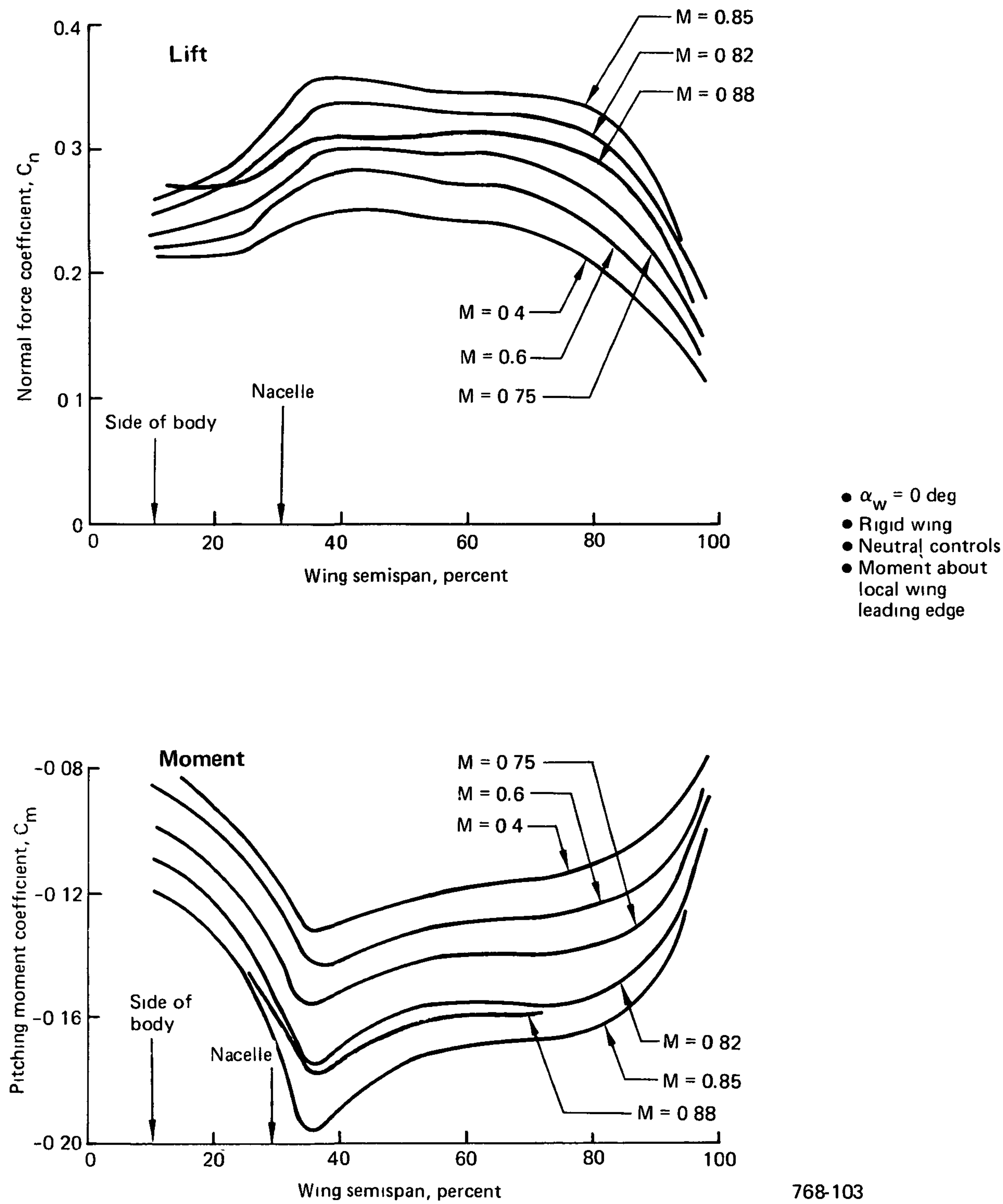

Figure B-5. Wing Section Normal Force and Moment at Zero Alpha

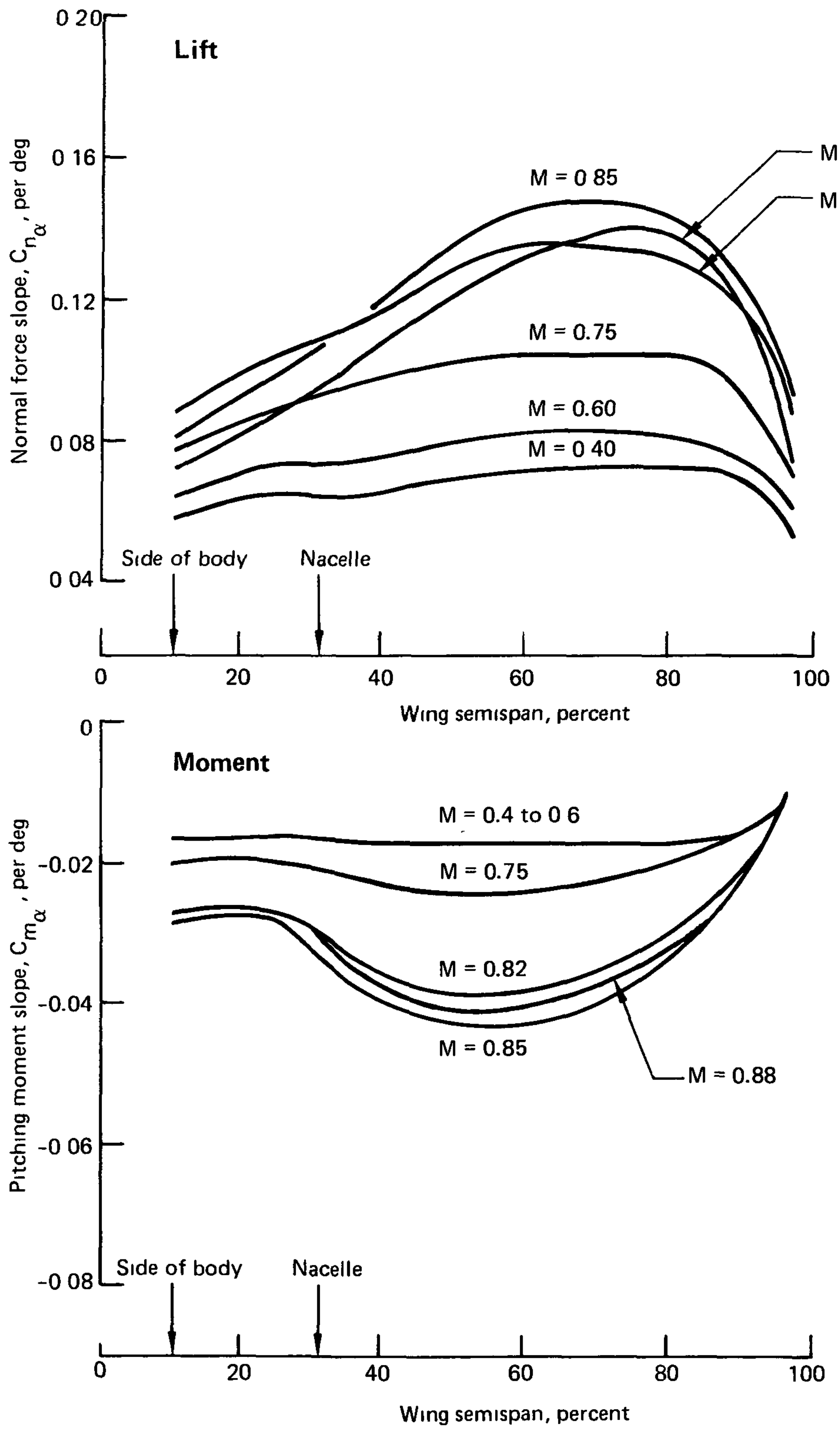

- Rigid wing
- Neutral controls
- Moment about local wing leading edge

768-103

Figure B-6. Wing Section Normal Force and Moment Due to Alpha estimates of double-hinged elevator loads based on YC-14 data. Initial ACT vertical tail airloads are unchanged from the Baseline Configuration.

Estimated outboard aileron section lift and moment data are shown in Figure B-7. These data were derived from wind tunnel tests conducted on the 747 Energy Efficient Transport (EET) Program. The effectiveness of the wing-load alleviation and flutter mode control systems is sensitive to variations in these data that represent one of the least certain portions of the Initial ACT aerodynamic data base. Rigid control effectiveness is defined in Figure B-4 (for rolling moment only), whereas the section data shown in Figure B-7 defines rigid bending and torsion and is used to determine elastic effectiveness for airplane and structural control. The corresponding section data for the inboard flaperon is shown in Figure B-8.

Body and nacelle lift and moment characteristics, as derived from transonic force model tests, are shown in Figures B-9 and B-10, respectively.

HINGE MOMENTS

Figures B-11 through B-13 show estimated hinge moments for all primary control surfaces. These estimates involved adjusting test data derived from the 747 airplane data to the geometry of the Initial ACT Configuration; the double-hinged elevator characteristics were estimated from YC-14 data. At the design conditions that size actuators, control surface hinge moment characteristics are estimated to be accurate within 15%. Variations of this order of magnitude in hinge moments have minor impact on actuator weights and hydraulic system sizing. All hinge moment characteristics, except for the elevators, are identical for the Baseline and Initial ACT Configurations.

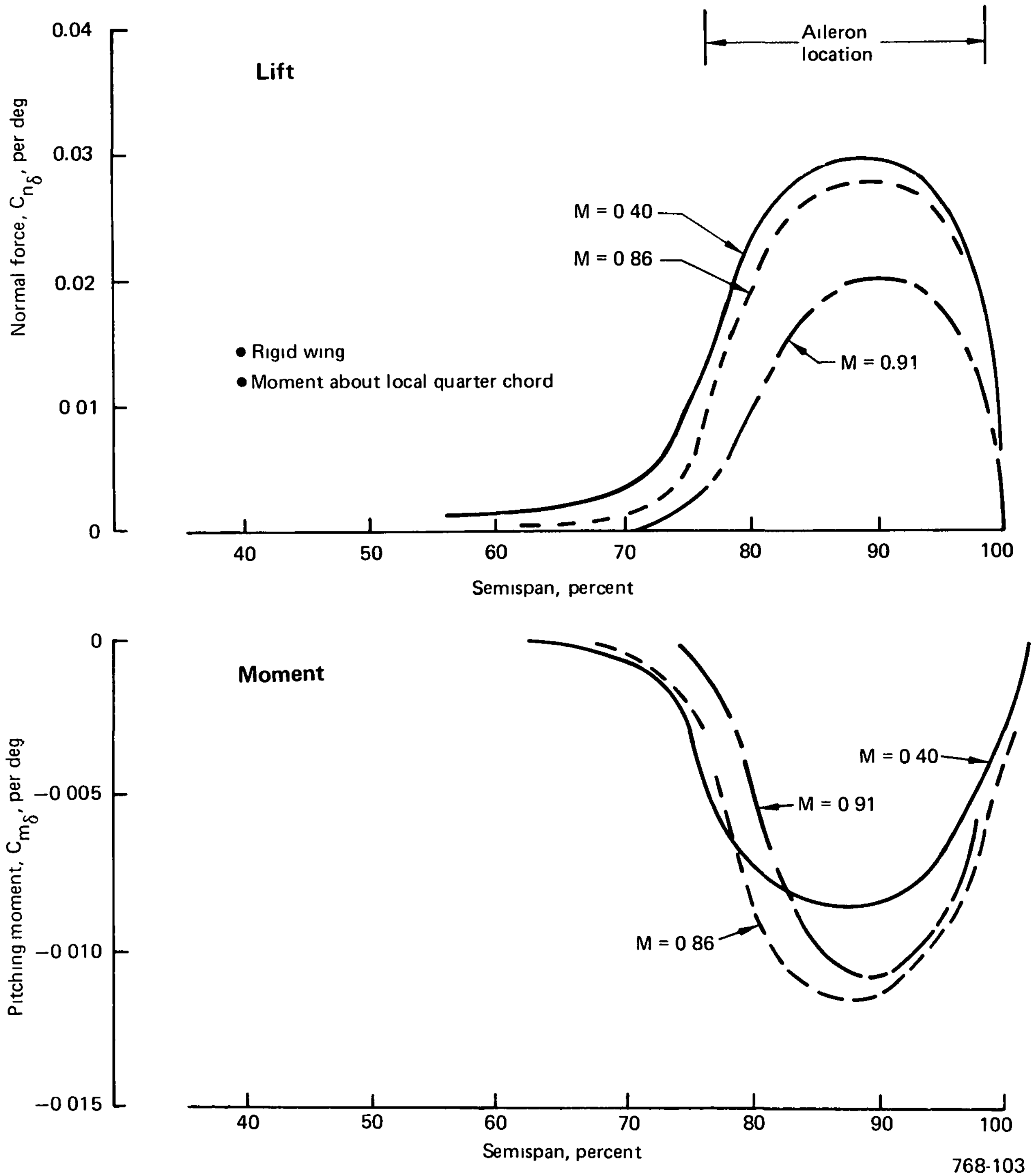

Figure B-7. Outboard Aileron Section Normal Force and Moment Slopes

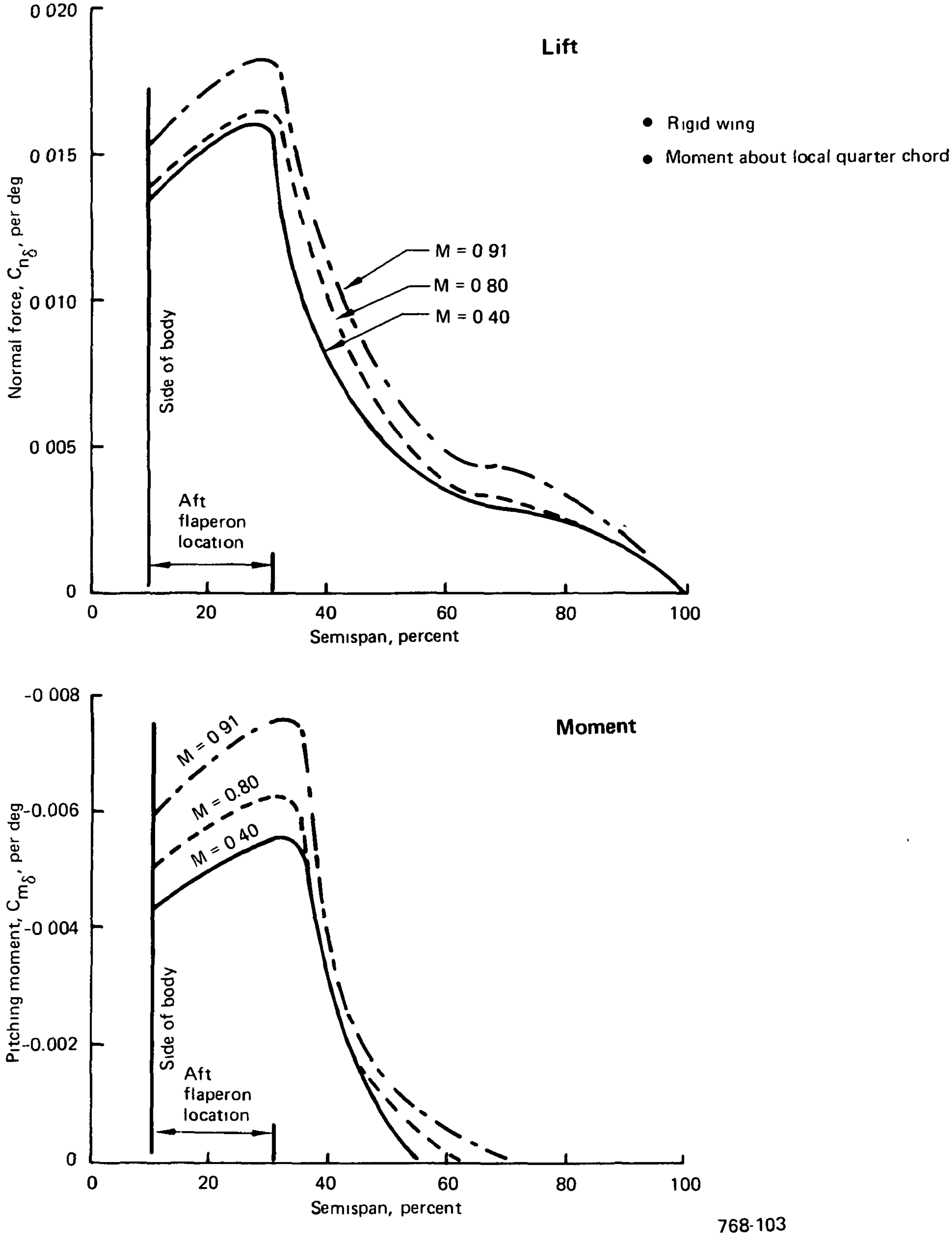

Figure B-8. Inboard Aft Flap Section Normal Force and Moment Slopes

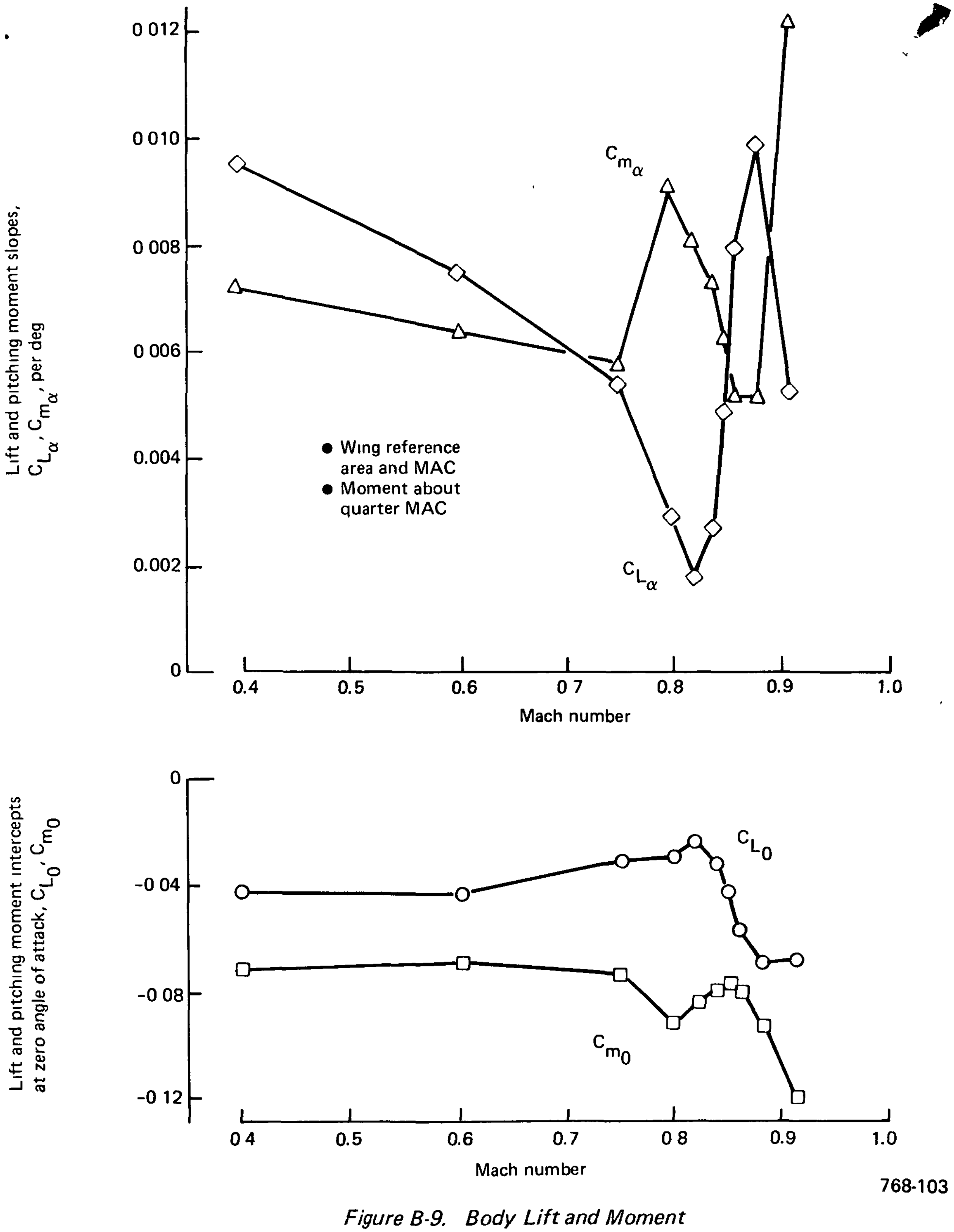

Figure B-9. Body Lift and Moment

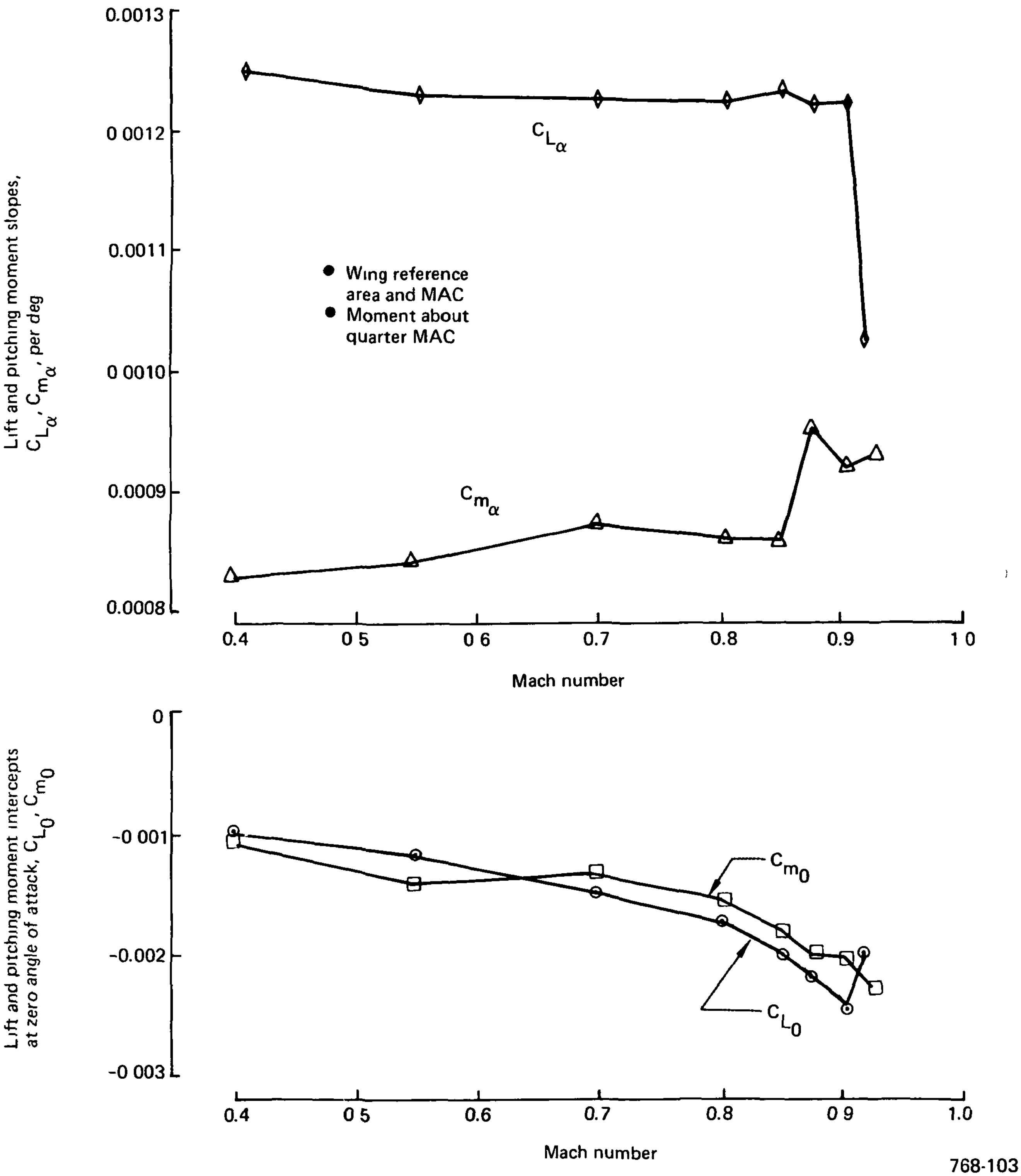

Figure B-10. Nacelle Lift and Moment

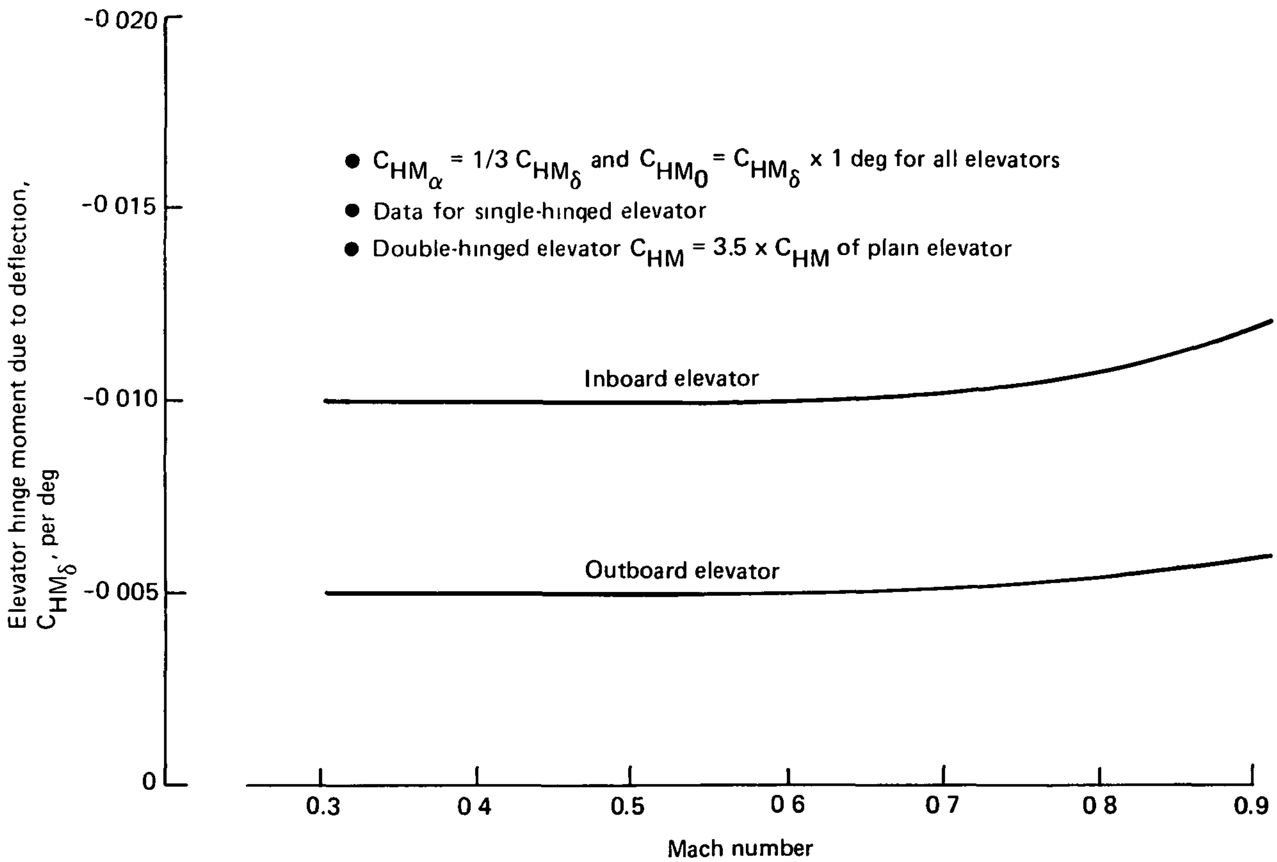

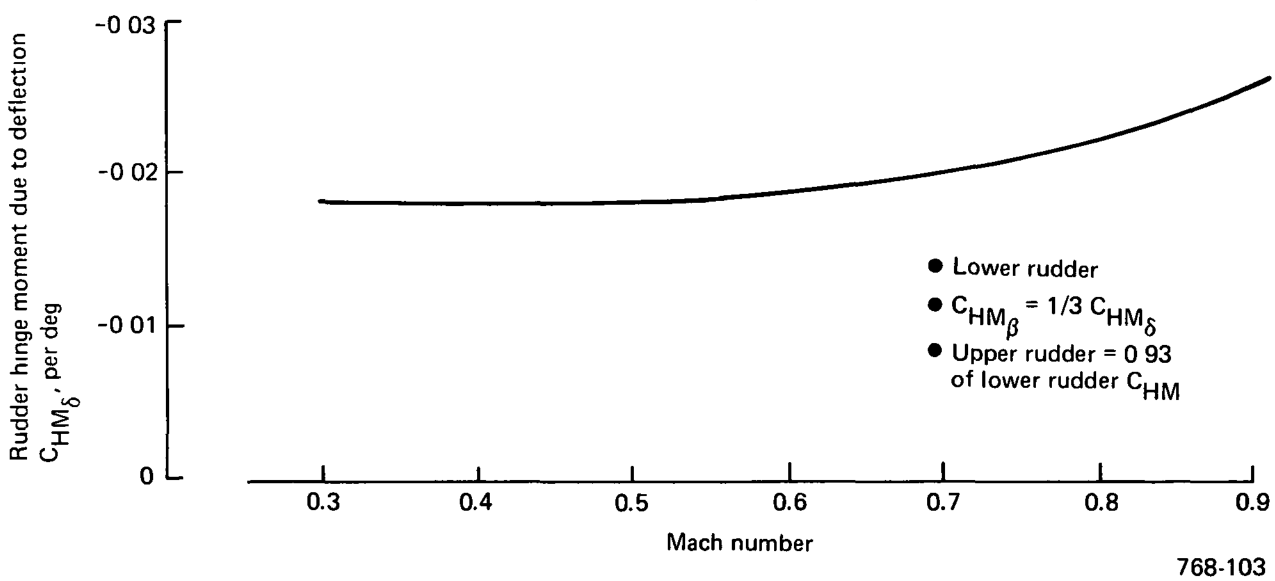

Figure B-11. Elevator and Rudder Hinge Moment

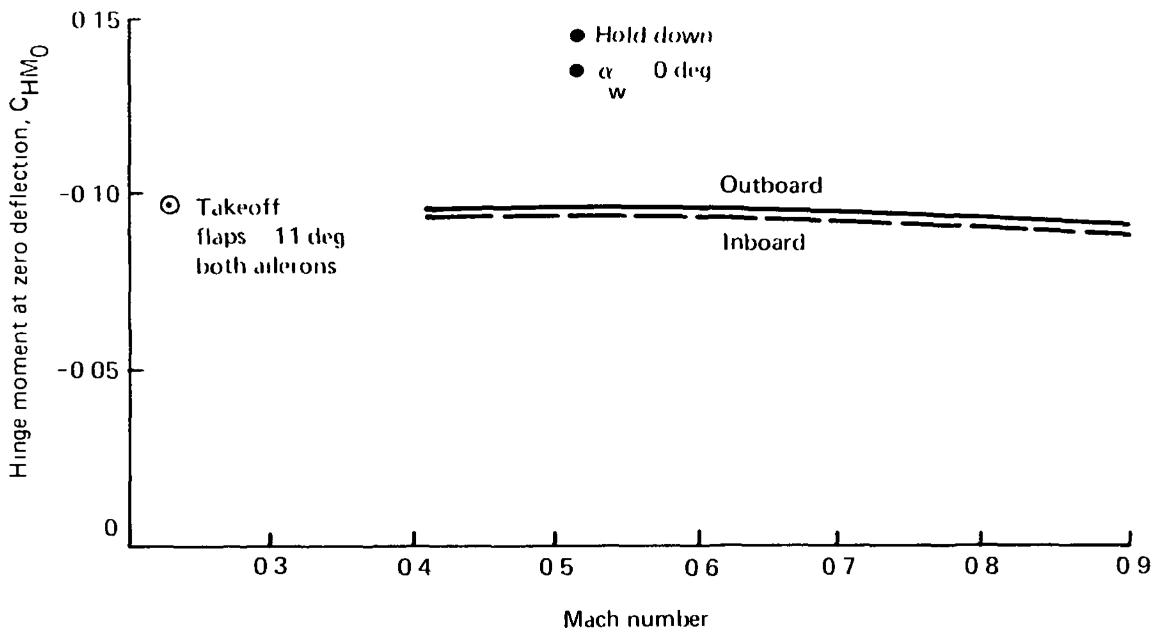

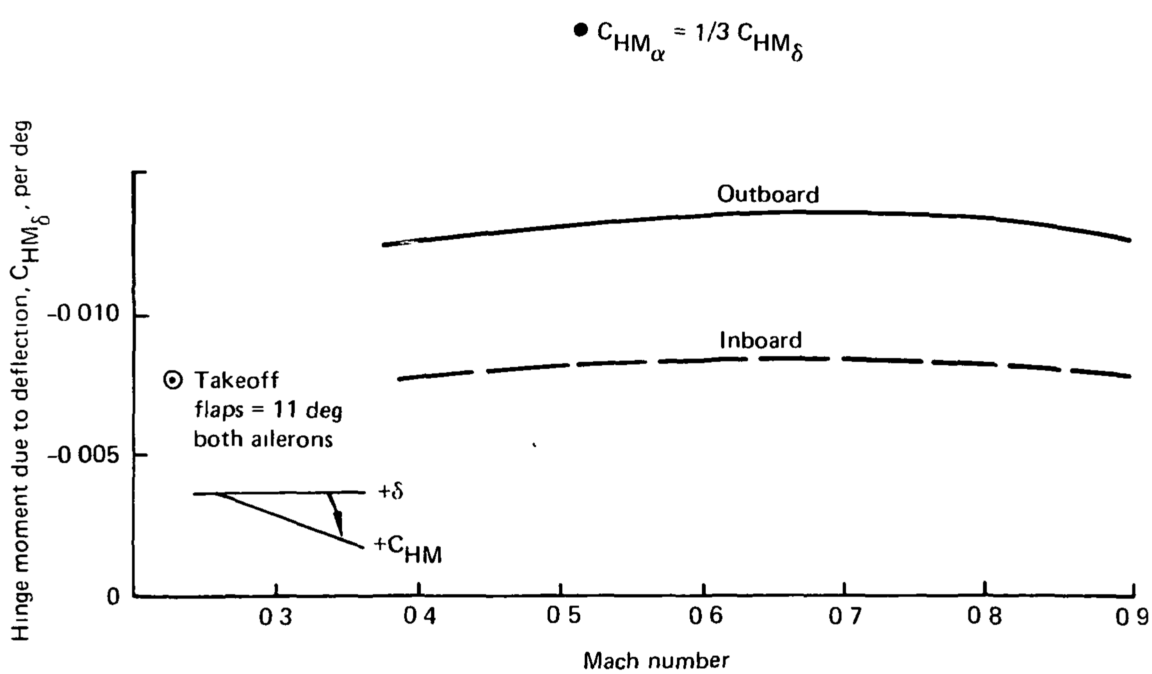

Figure B-12. Aileron Hinge Moment 768-103

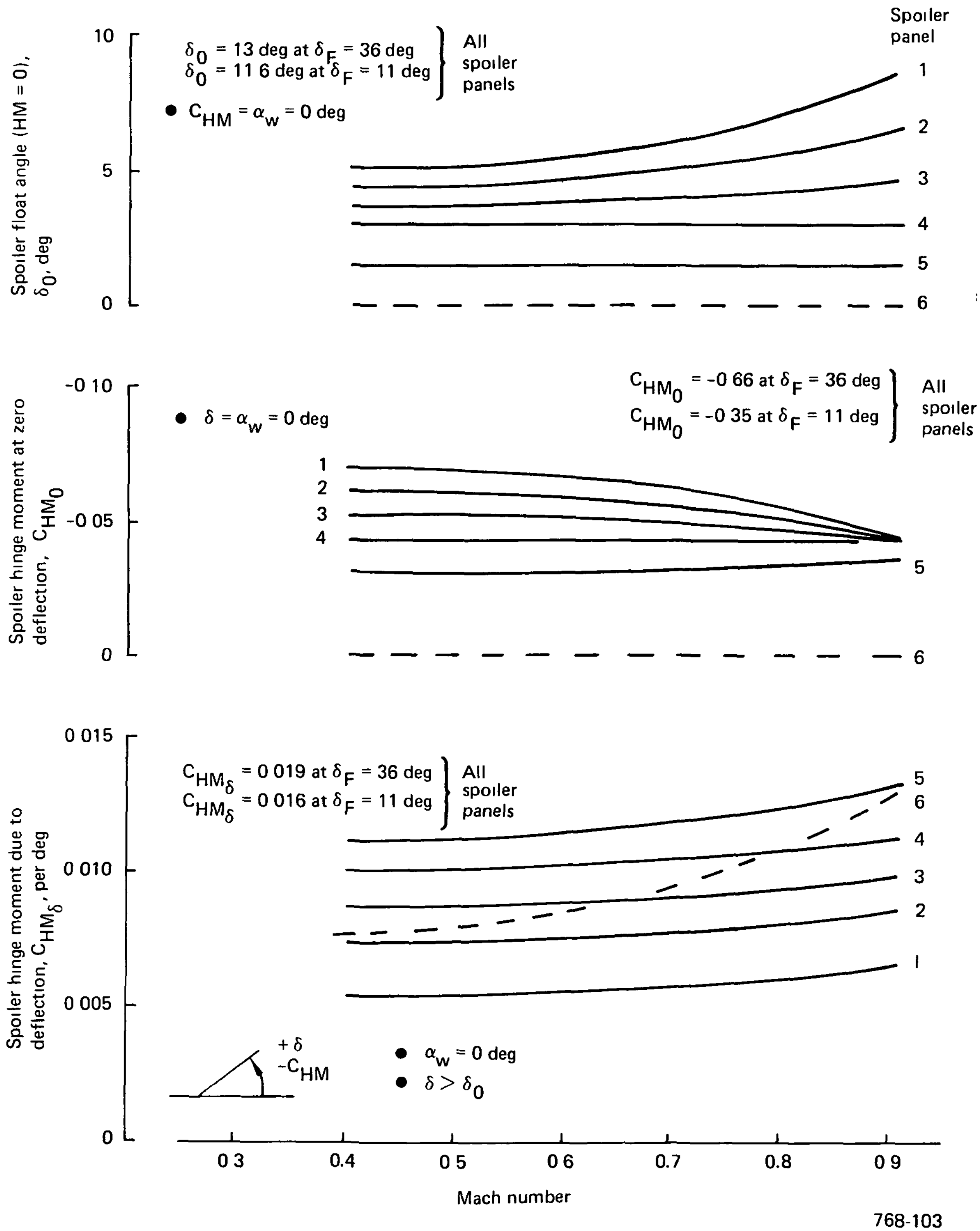

Figure B-13 Spoiler Hinge Moment

1. Report No NASA CR-159249	2 Government Accession No	3. Recipient's Catalog No
4. Title and Subtitle Integrated Application of Active Controls (IAAC) Technology to an Advanced Subsonic Transport Project – Initial ACT Configuration Design Study, Final Report		5. Report Date July 1980
		6. Performing Organization Code
7 Author(s) Boeing Commercial Airplane Company Preliminary Design Department		8. Performing Organization Report No D6-48662
9 Performing Organization Name and Address Boeing Commercial Airplane Company P. O. Box 3707 Seattle, Washington 98124		10 Work Unit No
		11 Contract or Grant No NAS1-14742 & NAS1-15325
12 Sponsoring Agency Name and Address National Aeronautics and Space Administration Washington, D. C. 20546		13. Type of Report and Period Covered Final report August 1978 to September 1979
		14 Sponsoring Agency Code

15 Supplementary Notes

Technical Monitors: D. B. Middleton and R. V. Hood
NASA Langley Research Center

16 Abstract

This report documents the Initial ACT Configuration Design Task of the Integrated Application of Active Controls (IAAC) Technology Project within the Energy Efficient Transport Program. A constrained application of Active Controls Technology (ACT) resulted in significant improvements over a Conventional Baseline Configuration (Baseline) previously established. The configuration uses the same levels of technology, takeoff gross weight, payload, and design requirements/objectives as the Baseline, except for flying qualities, flutter, and ACT. The Baseline wing is moved forward 1.68m. The configuration incorporates pitch-augmented stability (which enabled an approximately 10% aft shift in cruise center of gravity and a 45% reduction in horizontal tail size), lateral/directional-augmented stability, an angle-of-attack limiter, wing-load alleviation, and flutter-mode control. This resulted in a 930-kg reduction in airplane operating empty weight and a 3.6% improvement in cruise efficiency, yielding a 13% range increase. Adjusted to the 3590-km Baseline mission range, this amounts to 6% block-fuel reduction and a 15.7% higher incremental return on investment, using 1978 dollars and fuel cost. Results of the Initial ACT Task indicate that the IAAC Project should proceed to determine further benefits achievable through wing planform changes and advanced technology systems.

17. Key Words (Suggested by Author(s)) Energy Efficient Transport Program, Active Controls Technology, Augmented Stability, Wing-Load Alleviation, Flutter-Mode Control, Angle-of-Attack Limiter, Airplane Design	18 Distribution Statement FEDD Distribution

19 Security Classif (of this report) Unclassified	20 Security Classif (of this page) Unclassified	21 No of Pages 390	22 Price*

*Available: NASA's Industrial Applications Centers